frontiers
RESEARCH TOPICS

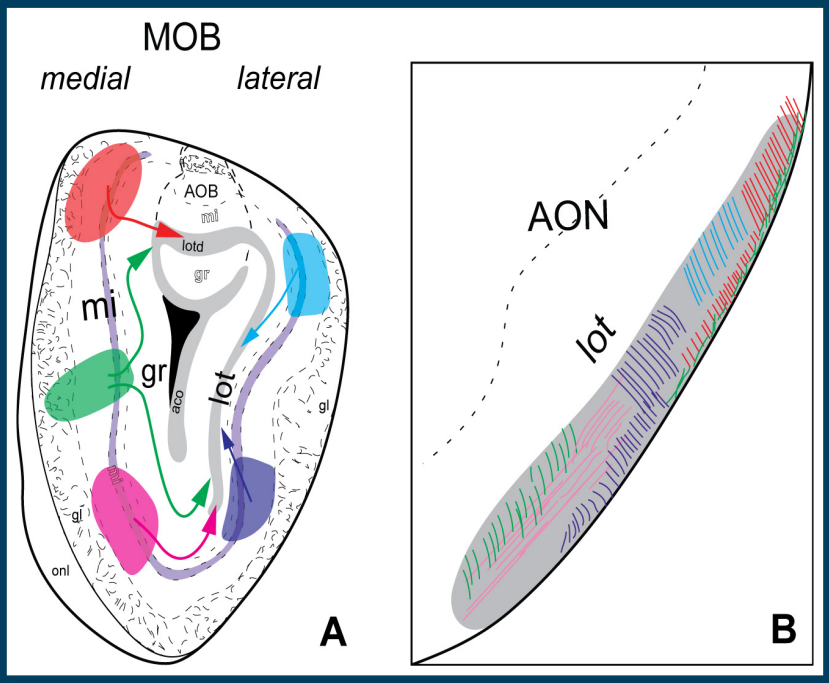

INTERACTIONS BETWEEN THE MAMMALIAN MAIN AND ACCESSORY OLFACTORY SYSTEMS

Topic Editors
Jorge A. Larriva-Sahd and Micheal Baum

frontiers in NEUROANATOMY

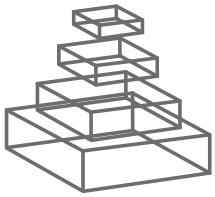

frontiers

ISSN 1664-8714
ISBN 978-2-88919-256-4
DOI 10.3389/978-2-88919-256-4

ABOUT FRONTIERS

Frontiers is more than just an open-access publisher of scholarly articles: it is a pioneering approach to the world of academia, radically improving the way scholarly research is managed. The grand vision of Frontiers is a world where all people have an equal opportunity to seek, share and generate knowledge. Frontiers provides immediate and permanent online open access to all its publications, but this alone is not enough to realize our grand goals.

FRONTIERS JOURNAL SERIES

The Frontiers Journal Series is a multi-tier and interdisciplinary set of open-access, online journals, promising a paradigm shift from the current review, selection and dissemination processes in academic publishing.
All Frontiers journals are driven by researchers for researchers; therefore, they constitute a service to the scholarly community. At the same time, the Frontiers Journal Series operates on a revolutionary invention, the tiered publishing system, initially addressing specific communities of scholars, and gradually climbing up to broader public understanding, thus serving the interests of the lay society, too.

DEDICATION TO QUALITY

Each Frontiers article is a landmark of the highest quality, thanks to genuinely collaborative interactions between authors and review editors, who include some of the world's best academicians. Research must be certified by peers before entering a stream of knowledge that may eventually reach the public - and shape society; therefore, Frontiers only applies the most rigorous and unbiased reviews.
Frontiers revolutionizes research publishing by freely delivering the most outstanding research, evaluated with no bias from both the academic and social point of view.
By applying the most advanced information technologies, Frontiers is catapulting scholarly publishing into a new generation.

WHAT ARE FRONTIERS RESEARCH TOPICS?

Frontiers Research Topics are very popular trademarks of the Frontiers Journals Series: they are collections of at least ten articles, all centered on a particular subject. With their unique mix of varied contributions from Original Research to Review Articles, Frontiers Research Topics unify the most influential researchers, the latest key findings and historical advances in a hot research area!
Find out more on how to host your own Frontiers Research Topic or contribute to one as an author by contacting the Frontiers Editorial Office: researchtopics@frontiersin.org

INTERACTIONS BETWEEN THE MAMMALIAN MAIN AND ACCESSORY OLFACTORY SYSTEMS

Topic Editors:
Jorge A. Larriva-Sahd, Universidad Nacional Autónoma de México, Mexico
Micheal Baum, Boston University, USA

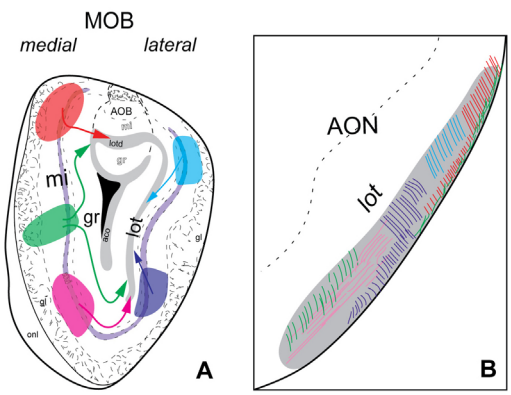

(A) Diagramatic representations of efferent fibers (arrows) from the main olfactory bulb following anterograde tracing injections (shaded in colors). (B) shows positions (dashed) in the lateral olfactory tract (lot) of bulbar efferents following tracer injections showed in (A).

Image taken from: Hintiryan H, Gou L, Zingg B, Yamashita S, Lyden HM, Song MY, Grewal AK, Zhang X, Toga AW and Dong H-W (2012) Comprehensive connectivity of the mouse main olfactory bulb: analysis and online digital atlas. Front. Neuroanat. 6:30. doi: 10.3389/fnana.2012.00030 and Larriva-Sahd J (2012) Cytological organization of the alpha component of the anterior olfactory nucleus and olfactory limbus. Front. Neuroanat. 6:23. doi: 10.3389/fnana.2012.00023

The functional cross-talk and structural interaction between the main and accessory olfactory bulbs is a central problem in mammalian sensory neurobiology. The early supposition that volatile substances and pheromones, most of them hydrosoluble molecules, are exclusively sensed and decoded by the main (MOS) and accessory olfactory systems (AOS), respectively, needs to be revised. In fact, a large number of structural and functional evidences accumulated during the last few decades, suggests that rather than separated entities, the MOS and AOS act synergically, bringing about physiological and behavioural responses. The goal of the present Research Topic was to gather original research studies and revision papers, performed by authoritative research groups that have recently contributed to the broad area of sensory neurobiology. Special attention should is given to contributions addressed to the MOB and AOB cross-talk, involving current developmental, neuroanatomical, and hodological techniques.

Table of Contents

05 ***Interactions Between the Mammalian Main and Accessory Olfactory Systems***
Micheal Baum and Jorge A. Larriva-Sahd

07 ***Postnatal Characterization of Cells in the Accessory Olfactory Bulb of Wild Type and Reeler Mice***
Eduardo Martín-López, Rebeca Corona and Laura López-Mascaraque

15 ***Centrifugal Telencephalic Afferent Connections to the Main and Accessory Olfactory Bulbs***
Alicia Mohedano-Moriano, Carlos de la Rosa-Prieto, Daniel Saiz-Sanchez, Isabel Ubeda-Bañon,Palma Pro-Sistiaga, Miguel de Moya-Pinilla and Alino Martinez-Marcos

25 ***One Nose, One Brain: Contribution of the Main and Accessory Olfactory System to Chemosensation***
Carla Mucignat-Caretta, Marco Redaelli and Antonio Caretta

34 ***Contribution of Pheromones Processed by the Main Olfactory System to Mate Recognition in Female Mammals***
Michael J. Baum

44 ***Sexual Activity Increases the Number of Newborn Cells in the Accessory Olfactory Bulb of Male Rats***
Wendy Portillo, Nancy Unda, Francisco J. Camacho, María Sánchez, Rebeca Corona, Dulce Ma. Arzate, Néstor F. Díaz and Raúl G. Paredes

53 ***Comprehensive Connectivity of the Mouse Main Olfactory Bulb: Analysis and Online Digital Atlas***
Houri Hintiryan, Lin Gou, Brian Zingg, Seita Yamashita, Hannah M. Lyden, Monica Y. Song, Arleen K. Grewal, Xinhai Zhang, Arthur W. Toga and Hong-Wei Dong

69 ***Hypothalamus-Olfactory System Crosstalk: Orexin a Immunostaining in Mice***
Jean Gascuel, Aleth Lemoine, Caroline Rigault, Frédérique Datiche, Alexandre Benani, Luc Penicaud and Laura Lopez-Mascaraque

80 ***Differential Efferent Projections of the Anterior, Posteroventral, and Posterodorsal Subdivisions of the Medial Amygdala in Mice***
Cecília Pardo-Bellver, Bernardita Cádiz-Moretti, Amparo Novejarque, Fernando Martínez-García and Enrique Lanuza

106 ***A Further Analysis of Olfactory Cortex Development***
María Pedraza and Juan A. De Carlos

112 ***Cytological Organization of the Alpha Component of the Anterior Olfactory Nucleus and Olfactory Limbus***
Jorge Larriva-Sahd

134 ***Mutual Influences Between the Main Olfactory and Vomeronasal Systems in Development and Evolution***
Rodrigo Suárez, Diego García-González and Fernando de Castro

148 ***The Main but not the Accessory Olfactory System is Involved in the Processing of Socially Relevant Chemosignals in Ungulates***
Matthieu Keller and Frédéric Lévy

frontiers in
NEUROANATOMY

EDITORIAL
published: 13 June 2014
doi: 10.3389/fnana.2014.00045

Interactions between the mammalian main and accessory olfactory systems

Michael Baum*[1] *and Jorge A. Larriva-Sahd*[2]*

[1] *Department of Biology, Boston University, Boston, MA, USA*
[2] *Departmento de Neurobiología del Desarrollo y Neurofisiología, Instituto de Neurobiología, Universidad Nacional Autónoma de México, Querétaro, Mexico*
**Correspondence: jlsneuro@unam.mx*

Edited and reviewed by:
Javier DeFelipe, Cajal Institute, Spain

Keywords: accessory olfactory system, main olfactory system, ordor, pheromones, sensory interactions

The controversial issue on the independent versus synergic functional role of the vomeronasal and main olfactory systems, motivated the present Research Topic (Larriva-Sahd and Baum, 2014). The resulting 11 studies fall into five broad categories: onto- and phylogenetic, structural, connectional, and integrative or review articles.

Two developmental works deal with the differentiation and distribution of neurons and glia in the main- (MOB), accessory-olfactory (AOB) bulbs, and primary olfactory cortex. The work by Pedraza and De Carlos (2012) presents the pallial and subpallial contributions to the primary olfactory cortex during the prenatal development, whereas Martín-López et al. (2012) describe the ontogenetic development of the MOB and AOB from reeler and wilde mice, with special reference to their laminar organization. In the latter study, cellular distribution over the course of prenatal development is further illustrated by both neuronal and glial markers. The cytological study by Larriva-Sahd (2012) concerns two, poorly-understood bulbar structures: the site of intersection between the MOB and AOB, or olfactory limbus (OL), and the alpha component of the anterior olfactory nucleus (aAON) that underlies the AOB. This work combines silver, and aniline stains, immunocytochemistry, and electron microscopy to define broad cellular organization, cellular types, and the neuropil of the OL and aAON.

The initial dogma regarding VNS and MOS as independent sensory modalities was supported by the dissimilar centripetal distribution of their tributary fibers. However, with the refinement of the tract-tracing techniques numerous sites of central convergence between the two systems have emerged. Three original studies performed in adult mice deal with the connectivity of the MOS and VNS. The paper by Hintiryan et al. (2012) provides a splendid atlas composed of colorful series of sections from brains that had previously been injected with antero-retrograde tracers. These unique specimens permit identification of the axonally linked areas that confirm previous connectional studies. Furthermore, the high resolution afforded by tiny sites of the tracer injections reveals novel interactions between the MOB and AOB with an unexpected detail. The connectional work by Mohedano-Moriano et al. (2012) is complementary in several ways, as it defines the second and third order targets of the MOB and AOB. Since non-sensory recipient areas, especially the nucleus of the diagonal band of Broca, project to both AOB and MOB, the possibility of a simultaneous supra-sensorial modulation of both systems is suggested. In this context (Pardo-Bellver et al., 2012) define the projections of the medial amygdaloid (MA) subdivisions, a nucleus that has been implicated globally in both the behavioral and endocrinological aspects of mammalian reproduction. The highly organized projections to the anterior, posterodorsal, and posteroventral subdivisions of the MA to amygdaloid, bulbar, septal, hypothalamic areas and nuclei, expand the notion that the MA itself is both structurally and functionally compartmentalized. The study by Gascuel et al. (2012) proposes the existence of a system of cells and fibers positive Orexin A-immunoreactivity (O-I) within the hypothalamus, basal forebrain and olfactory bulb itself. Since O-I fibers distribute within and between the hypothalamus and olfactory bulb, therefore author's results support the existence of an orexinergic system possibly associated with the olfactory influences on the diencephalic control of food-intake.

It is now clear that plasticity in the adult nervous system is more common than originally suspected (see Merkle et al., 2014). Notably, the adult MOB and AOB incorporate adult-born neurons to their preexisting circuitry. Rather than a steady generation and incorporation of prospective neurons to the bulbar cortex, this process is highly influenced by the concurring local and environmental demands. The investigation of Portillo et al. (2012) provides cytological and behavioral evidences supporting the notion that sexual experience in rodents enhances incorporation of adult-born cells to the accessory olfactory bulb.

Four review articles present and analyze current concepts of the MOS-AOS interaction. In this framework, the assays by Suárez et al. (2012) and Mucignat-Caretta et al. (2012) present parallel interactions between both systems as a function of species and phylogenetic evolution, respectively. Relevant from the comparative functional perspective is the work by Keller and Lévy (2012) providing direct evidence for the involvement of the main olfactory system in decoding environmental chemosignals from conspecifics. This decoding of socially relevant clues has traditionally been attributed to the AOS, but these authors offer a comprehensive analysis of species differences in this regard. Lastly, the detailed review by one of the Associated Editors of this series (Baum, 2012) emphasizes the structural, connectional and behavioral information relevant for functional interactions between the main and accessory olfactory systems.

REFERENCES

Baum, M. J. (2012). Contribution of pheromones processed by the main olfactory system to mate recognition in female mammals. *Front. Neuroanat*. 6:20. doi: 10.3389/fnana.2012.00020

Gascuel, J., Lemoine, A., Rigault, C., Datiche, F., Benani, A., Penicaud, L., et al. (2012). Hypothalamus-olfactory system crosstalk: orexin A immunostaining in mice. *Front. Neuroanat*. 6:44. doi: 10.3389/fnana.2012.00044

Hintiryan, H., Gou, L., Zingg, B., Yamashita, S., Lyden, H. M., Song, M. Y., et al. (2012). Comprehensive connectivity of the mouse main olfactory bulb: analysis and online digital atlas. *Front. Neuroanat*. 6:30. doi: 10.3389/fnana.2012.00030

Keller, M., and Lévy, F. (2012). The main but not the accessory olfactory system is involved in the processing of socially relevant chemosignals in ungulates. *Front. Neuroanat*. 6:39. doi: 10.3389/fnana.2012.00039

Larriva-Sahd, J. (2012). Cytological organization of the alpha component of the anterior olfactory nucleus and olfactory limbus. *Front. Neuroanat*. 6:23. doi: 10.3389/fnana.2012.00023

Larriva-Sahd, J. A., and Baum, M. (2014). Interactions between the mammalian main and accessory olfactory systems. *Front. Neuroanat*. 8:45. doi: 10.3389/fnana.2014.00045

Martín-López, E., Corona, R., and López-Mascaraque, L. (2012). Postnatal characterization of cells in the accessory olfactory bulb of wild type and reeler mice. *Front. Neuroanat*. 6:15. doi: 10.3389/fnana.2012.00015

Merkle, F. T., Fuentealba, L. C., Sanders, T. A., Magno, T., Kessaris, N., and Alvarez-Buylla, A. (2014). Adult neural stem cells in distinct microdomains generate previously unknown interneuron types. *Nat. Neurosci.* 17, 207–214. doi: 10.1038/nn.3610

Mohedano-Moriano, A., de la Rosa-Prieto, C., Saiz-Sanchez, D., Ubeda-Bañon, I., Pro-Sistiaga, P., de Moya-Pinilla, M., et al. (2012). Centrifugal telencephalic afferent connections to the main and accessory olfactory bulbs. *Front. Neuroanat*. 6:19. doi: 10.3389/fnana.2012.00019

Mucignat-Caretta, C., Redaelli, M., and Caretta, A. (2012). One nose, one brain: contribution of the main and accessory olfactory system to chemosensation. *Front. Neuroanat*. 6:46. doi: 10.3389/fnana.2012.00046

Pardo-Bellver, C., Cádiz-Moretti, B., Novejarque, A., Martínez-García, F., and Lanuza, E. (2012). Differential efferent projections of the anterior, posteroventral, and posterodorsal subdivisions of the medial amygdala in mice. *Front. Neuroanat*. 6:33. doi: 10.3389/fnana.2012.00033

Pedraza, M., and De Carlos, J. A. (2012). A further analysis of olfactory cortex development. *Front. Neuroanat*. 6:35. doi: 10.3389/fnana.2012.00035

Portillo, W., Unda, N., Camacho, F. J., Sánchez, M., Corona, R., Arzate, D. M., et al. (2012). Sexual activity increases the number of newborn cells in the accessory olfactory bulb of male rats. *Front. Neuroanat*. 6:25. doi: 10.3389/fnana.2012.00025

Suárez, R., García-González, D., and de Castro, F. (2012). Mutual influences between the main olfactory and vomeronasal systems in development and evolution. *Front. Neuroanat*. 6:50. doi: 10.3389/fnana.2012.00050

Conflict of Interest Statement: The authors declare that the research was conducted in the absence of any commercial or financial relationships that could be construed as a potential conflict of interest.

Received: 20 February 2014; accepted: 24 May 2014; published online: 13 June 2014.
Citation: Baum M and Larriva-Sahd JA (2014) Interactions between the mammalian main and accessory olfactory systems. Front. Neuroanat. ***8****:45. doi: 10.3389/fnana.2014.00045*
This article was submitted to the journal Frontiers in Neuroanatomy.

frontiers in
NEUROANATOMY

ORIGINAL RESEARCH ARTICLE
published: 22 May 2012
doi: 10.3389/fnana.2012.00015

Postnatal characterization of cells in the accessory olfactory bulb of wild type and reeler mice

Eduardo Martín-López , Rebeca Corona† and Laura López-Mascaraque*

Department of Molecular, Cellular, and Developmental Neurobiology, Instituto Cajal (CSIC), Madrid, Spain

Edited by:
Jorge A. Larriva-Sahd, Universidad Nacional Autónoma de México, México

Reviewed by:
Alino Martinez-Marcos, Universidad de Castilla, Spain
Alfredo Varela-Echavarria, Instituto de Neurobiología - UNAM, México

***Correspondence:**
Laura López-Mascaraque, Instituto Cajal (CSIC), Avenida del Doctor Arce, 37, 28002 Madrid, Spain.
e-mail: mascaraque@cajal.csic.es

†Present Address:
Department of Behavioral and Cognitive Neurobiology, Instituto de Neurobiología (UNAM), Queretaro, Mexico.

Olfaction is the most relevant chemosensory sense of the rodents. General odors are primarily detected by the main olfactory system while most pheromonal signals are received by the accessory olfactory system. The first relay in the brain occurs in the olfactory bulb, which is subdivided in the main and accessory olfactory bulb (MOB/AOB). Given that the cell generation time is different between AOB and MOB, and the cell characterization of AOB remains limited, the goal of this work was first, the definition of the layering of AOB/MOB and second, the determination of cellular phenotypes in the AOB in a time window corresponding to the early postnatal development. Moreover, since reelin (Reln) deficiency has been related to olfactory learning deficits, we analyzed reeler mice. First, we compared the layering between AOB and MOB at early embryonic stages. Then, cell phenotypes were established using specific neuronal and glial markers as well as the Reln adaptor protein Dab1 to analyse differences in both genetic backgrounds. There was no apparent difference in the cell phenotypes among AOB and MOB or between wild type (*wt*) and *reeler* animals. However, a disruption in the granular cell layer of *reeler* with respect to wt mice was observed. In conclusion, the AOB in Reln-deficient mice showed similar neuronal and glial cell types being only affected the organization of granular neurons.

Keywords: main olfactory bulb, reelin, granular cells layering, postnatal development, cell characterization

INTRODUCTION

A wide number of socio-sexual behaviors in mammals depend upon the environment chemosensory signals. In rodents, the olfactory system appears to be the most important for the perception of chemical signals that allows the organism get the information from the environment. Olfaction starts with the direct interaction of the odorant molecules with the olfactory receptors of the sensory neurons that send their axons up to the olfactory bulb, step that constitutes the first relay of the olfactory information to the central nervous system. Olfactory bulb has been divided in two different but complementary systems, the main and accessory olfactory systems. They differ in their anatomy, projections, and function. Sensory receptors of the main olfactory system are a large family of receptors located on the olfactory sensory neurons (OSNs) sited in the main olfactory epithelium and projecting into the main olfactory bulb (MOB). For the accessory olfactory system, the receptors are located in the vomeronasal organ and project to the accessory olfactory bulb (AOB). Both MOB and AOB are an interface between the OSN and higher olfactory centers, and their position in olfaction is often compared to the thalamus in other sensory systems (Shepherd, 2005). These two anatomically distinct olfactory systems were described as functionally distinct, with the main olfactory epithelium detecting volatile odorants and the vomeronasal organ detecting non-volatile pheromones through direct physical contact with the source (Mori et al., 2000). However, OSNs are also sensitive to pheromones present in mouse urine (Restrepo et al., 2004) and the simultaneous presentation of odorants and pheromones to the same animal provoke responses from both MOB and AOB (Luo et al., 2003; Xu et al., 2005). This suggests that these two systems might not be as functionally distinct as was originally thought (Meredith, 1991; Baum and Kelliher, 2009).

Molecular and functional characteristics of these structures have been described (Lopez-Mascaraque and De Castro, 2002; for reviews Blanchart and Lopez-Mascaraque, 2011) but additional information, particularly regarding the AOB development, is still necessary to define the complete form and function of this system. On other hand, it is widely known that layered structures in the brain use Reelin (Reln) as a key molecule for proper neuronal positioning (Honda et al., 2011) and it appears to be relevant during the MOB layering (Wyss et al., 1980; Martin-Lopez et al., 2011). Reln exerts its actions through the Dab1 intracellular adaptor protein (Howell et al., 1997; Rice et al., 1998), molecule which is strongly expressed in the MOB (Martin-Lopez et al., 2011). In addition, Reln acts as detachment signal for chain-migrating neuroblasts which promotes their radial migration into the olfactory bulb (Hack et al., 2002). During OB development, Reln mRNA begins to be expressed at E10 in the mitral cells and it is restricted to mitral and periglomerular cells at postnatal ages (D'Arcangelo et al., 1995; Schiffmann et al., 1997; Alcantara et al., 1998). In the Reln deficient mice (*reeler*), despite alterations in MOB layering (Wyss et al., 1980; Hack et al., 2002), expression patterns of Dab1 is undistinguishable between the MOB of wild type (*wt*) and *reeler* mice (Martin-Lopez et al., 2011). Thus, regardless of

the information known about Reln in the MOB, there is still a lack of information on the effects of this protein on the precise final layering of the AOB.

Consequently, the goals of this work were first, to clarify the layering of AOB from early embryonic stages to late postnatal development and then to compare the AOB/MOB layering. Second, we addressed the spatio-temporal, molecular, and phenotypical characterization of AOB cells comparing *wt* with *reeler* mice during early postnatal development. For this purpose, we characterized the AOB cell populations by using specific markers against mature neurons (MAP2a,b, and NeuN), some periglomerular cells (CB and TH), radial glia (RC2), astrocytes (GFAP), oligodendrocytes (RIP), and molecules involved in layering processes like Reln and its adaptor protein Dab1.

MATERIALS AND METHODS

Wild type C57 (*wt*) and Reln mutant (*reeler*) mice from postnatal stages P0, P3, P7, and P15, were obtained from the Cajal Institute mouse breeding facility. Genotyping of *reeler* mice was performed by PCR analysis of genomic DNA. Experiments were performed in accordance with procedures approved by the Spanish Research Council Bioethics Committee. For animal experimentation, we followed the ethical principles dictated by the European Commission (Directive 2010/63/UE and 86/609/CEE) for use of laboratory animals and Spanish regulation (RD 1201/2003 and ley 32/2007).

NISSL STAINING

Embryonic Nissl staining sagittal sections were obtained from fixed paraformaldehyde thionin-stained sections (Jimenez et al., 2000). Postnatal sagittal sections at 20 µm (see below for Procedure) were stained with acid thionin (pH 4.5) for 1 min and washed with water. Sections were dehydrated with graded ethanol and xylol, and coverslipped with DPX mountant.

IMMUNOHISTOCHEMISTRY

Mice ($n = 5$ per each age and strain) of either sex were deeply anesthetized by hypothermia (P0 and P3) or with i.p. equithesin at lethal dose (P7 and P15) and transcardially perfused with heparinized saline followed by 4% of paraformaldehyde (1 ml/g) in 0.1 M phosphate-buffered (PB). Brains were removed and post-fixed in the same fixative, cryoprotected with 30% sucrose in PB, and sagittally sectioned at 20 µm in a TC1900 cryostat (Leica). Sections were frozen until their use in immunostaining.

Table 1 | List of antibodies.

Primary antibody	Clone	Product company	Dilution	Cell type marked
Calbindin (CB)	300	Swant	1:5000	Localizes D-28k CB which occur in a subset of neurons
Dab1	Polyclonal	Sigma-Aldrich (D1569)	1:1000	A subset of cell types
GFAP	GA5	Chemicon	1:1000	Glial fibrillary acidic protein expressed in astrocytes
Map2a,b	AP20	Chemicon	1:1000	Microtubule associated protein-2 expressed in mature neurons
NeuN	A60	Chemicon	1:1000	Neuronal nuclei protein
RC2	RC2	Hybridoma-Bank	1:500	A 295kDa intermediate filament protein present in radial glial cells
RIP	NS-1	Chemicon	1:1000	Detects non-myelin and myelin oligodendrocytes
Reelin	G10	Chemicon	1:1000	Detects reelin expressed in a subset of neurons
TH	LNC1	Chemicon	1:1000	Detects tyrosine hydroxylase enzyme expressed by dopaminergic neurons

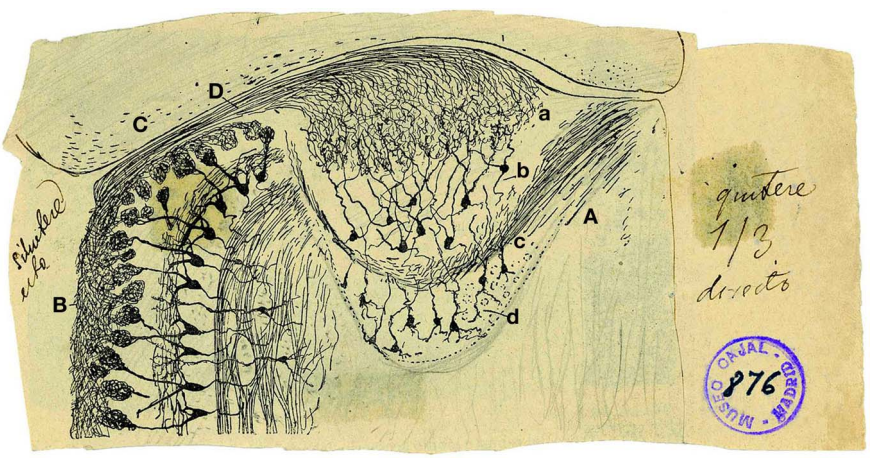

FIGURE 1 | Reproduction of an original Cajal drawing from a Golgi stained horizontal section from 20-days-old mice, showing some morphological features of the accessory and main olfactory bulb. **(A)** Accessory olfactory bulb; **(B)** Main olfactory bulb; **(C)** Cortex; **(D)** Vomeronasal nerve; **(a)** Glomerular layer; **(b)** mitral/tufted layer; **(c)** Plane of the lateral olfactory tract; **(d)** granule cells [Ramon y Cajal (1901)].

Frozen sections were air dried, permeabilized with saline PB (PBS) plus 0.1% TritonX100 (PBST) (Sigma-Aldrich Co.) and by microwave heating in 10 mM citrate buffer, pH 6, for three boiling cycles of 5 min each to unmask the antigen. Unspecific binding of antibodies was blocked with PBST supplemented with 10% normal goat serum (NGS) plus 0.1% bovine serum albumin for 1 h at room temperature (RT) and then incubated overnight at 4°C using specific primary antibodies diluted in PBST plus 1% NGS (**Table 1**). Antibody binding was detected with the following secondary antibodies, diluted 1:1000 in PBST: Alexa 488/568 goat anti-rabbit IgG and Alexa 568 goat anti-mouse IgG (Molecular Probes-Invitrogen). The radial glia antibody (RC2) was detected by incubating 2 h at RT with biotin conjugated goat anti-mouse IgM (Jackson Immunoresearch) and then incubated

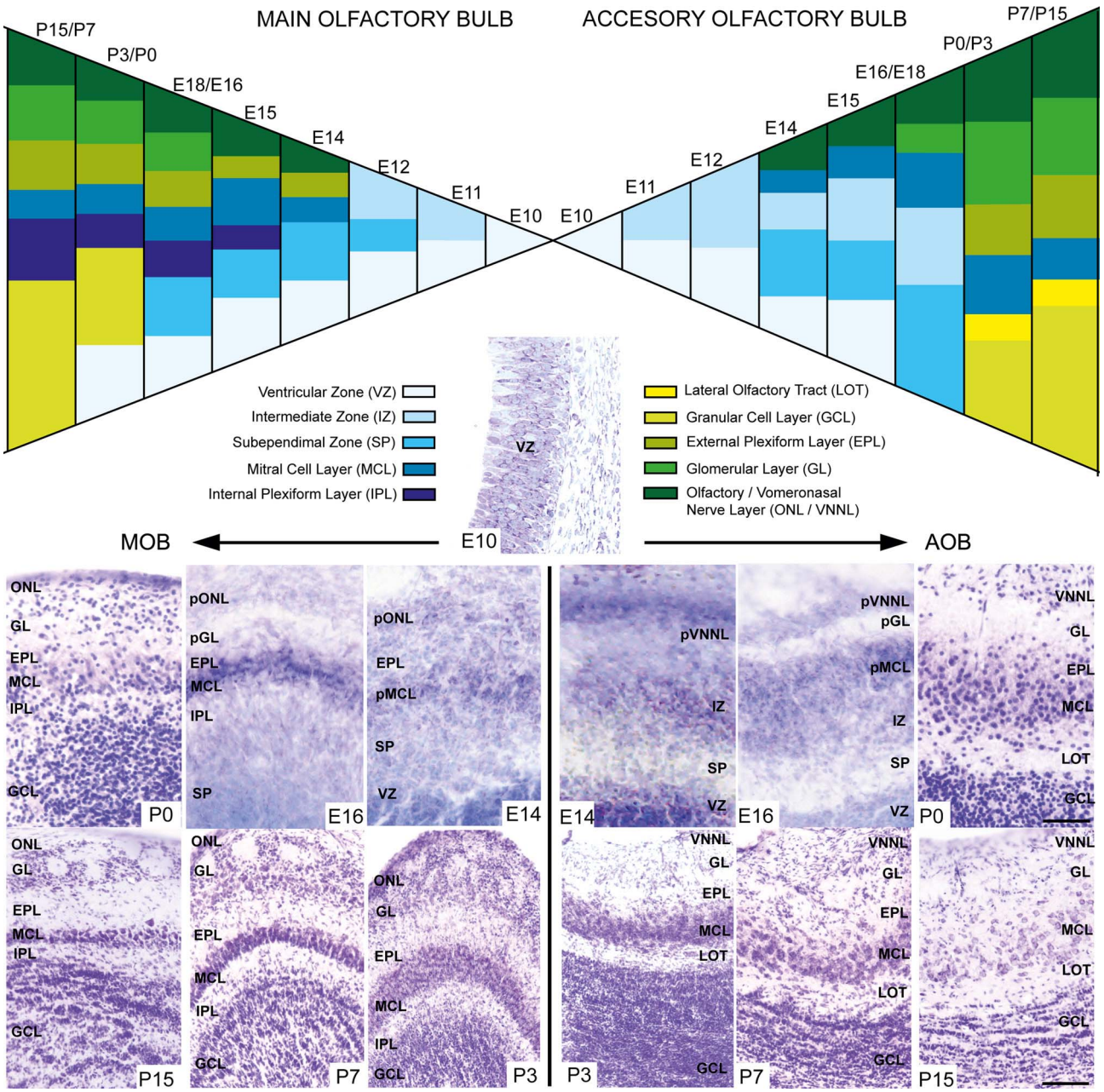

FIGURE 2 | Schematic diagram depicting the developmental layering process in both main and accessory olfactory bulb. Nissl-stained images show the layer disposition in in both AOB and MOB at different embryonic and postnatal ages. VZ, ventricular zone; SEZ, subependimal zone; IZ, intermediate zone; LOT, lateral olfactory tract; GCL, granular cell layer; IPL, internal plexiform layer; MCL, mitral cell layer; pMCL, primitive MCL; EPL, external plexiform layer; GL, glomerular layer; ONL, olfactory nerve layer; VNNL, vomeronasal nerve layer; pONL/pVNNL, primitive ONL/VNNL. (Scale bars: E10–P0: 50 μm; P3–P15: 100 μm).

1 h at RT with Alexa 568 conjugated streptavidin (Molecular Probes-Invitrogen). Nuclei were counterstained with Hoechst (1 μg/ml, Sigma-Aldrich Co). Staining was visualized using a confocal microscope TS5 (Leica).

RESULTS

A BRIEF DESCRIPTION OF THE ACCESSORY OLFACTORY BULB STRUCTURE AND ORGANIZATION

The AOB is a lens-shaped structure, much smaller than the MOB, delimited rostrally and ventrally by the MOB, caudally by the accessory olfactory nucleus and dorsally by the prefrontal cortex. **Figure 1** shows an original drawing by Cajal (Ramon y Cajal, 1901) revealing the structure and layers of both the AOB (**Figure 1A**) and a region of the MOB (**Figure 1B**) in a horizontal section where is included the vomeronasal nerve (**Figure 1D**). Cajal divided the AOB into four layers: the glomerular layer (**Figure 1Aa**, GL), mitral/tufted (**Figure 1Ab**, M/T), lateral olfactory tract (**Figure 1Ac**, LOT), and granule cell layer (**Figure 1Ad**, GCL). This layered structure is similar to MOB although they display some differences previously reviewed (Meisami and Bhatnagar, 1998) and highlighted by Larriva-Sahd (2008).

DEVELOPMENTAL TIMING OF AOB vs. MOB LAYERING

During embryonic brain development, layering of the AOB is slightly different from that of the MOB since cell differentiation occurs at different ages in both structures. To address this issue, we performed a cytoarchitectonic study to compare the formation of the different layers in both AOB and MOB (**Figure 2**). Both bulbs emerged from a neuroepithelium located in the rostral-most part of the telencephalic vesicle (**Figure 2**, E10). One day later (E11) the layering begins when an intermediate zone (IZ) is segregated from the ventricular zone (VZ). Next, a new layer intercalates between VZ and IZ forming the subependimal zone (SP) in the prospective MOB while in the AOB it occurs at E13. Although the first olfactory sensory axons reach the surface of the prospective MOB at E12 (Blanchart et al., 2006, 2008), the primitive olfactory (pONL) and vomeronasal nerve (pVNNL) layers are visible at E13. At E14 in both structures emerges the primitive mitral cell layer (pMCL, **Figure 2**). At E15/16 a prospective glomerular layer becomes evident in both AOB/MOB (pGL, **Figure 2**). From E17 onwards the layering is completed and in the first postnatal days (P0–P3) the granule cell layer becomes thicker and visible in both bulbs. Complete refinement of layering organization is achieved at P7, although periglomerular and granule cells are constantly added to these local circuits in adult brains (Altman, 1969; Lois and Alvarez-Buylla, 1994; Peretto et al., 2001; Oboti et al., 2009).

MOLECULAR CHARACTERIZATION OF THE AOB IN *wt* AND *reeler* POSTNATAL MICE

Since the disabled 1 (Dab1) protein is essential for Reln signaling during brain development and is expressed thorough all MOB layers at early postnatal ages (Martin-Lopez et al., 2011), we analyzed the relationship between the expression of Reln and Dab1 in the AOB of both *wt* and *reeler* mice (**Figure 3**). In the AOB, Reln was markedly expressed in the cytoplasm of mitral and some periglomerular cells at each postnatal ages (**Figures 3A,C,E,G**) as occurs in the MOB (Martin-Lopez et al., 2011). By contrast, Dab1 protein was expressed in most neuronal cells along the AOB layers in both cytoplasm and nuclear cell compartments in both strains (**Figure 3**), although the pattern of protein location changed from P0 to P15. Thus, at P0, strong Dab1 labeling was detected in

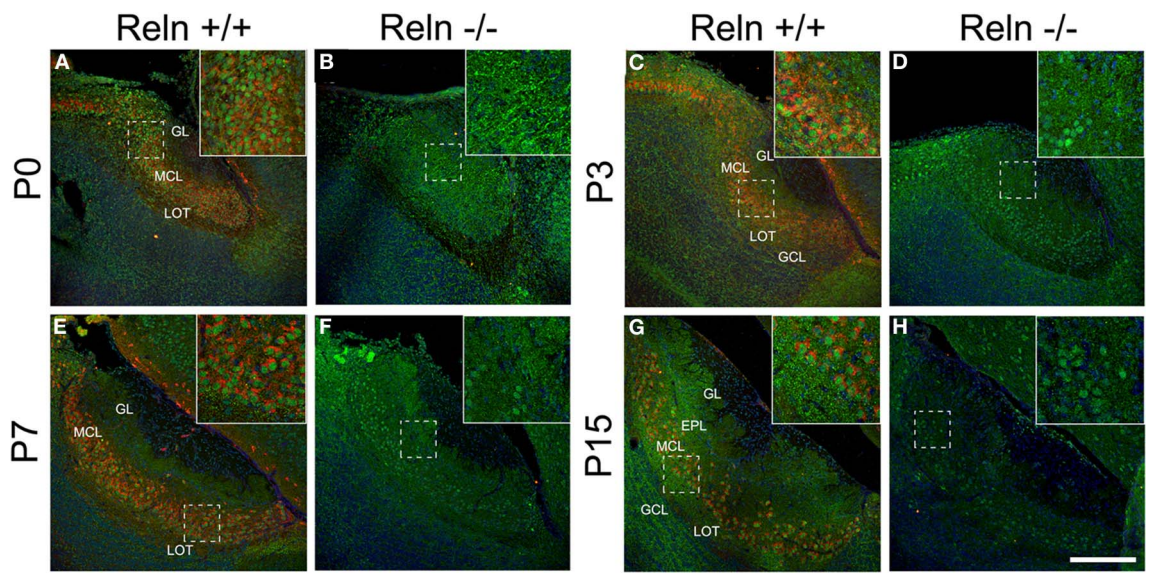

FIGURE 3 | Expression of Reln and its adaptor protein Dab1 in the accessory olfactory bulb of wild type and *reeler* mice. Reln (red) is strongly expressed by mitral and periglomerular cells at P0, P3, P7, and P15 **(A,C,E,G)**. Dab1 expression (green) is mainly located in the nuclei of the MCL and GL cells as well as in the fibers located throughout GL, EPL, IPL, and GCL in both strains **(A–H)**. Nuclei were counterstained with Hoechst (blue). LOT, lateral olfactory tract; GCL, granular cell layer; IPL, internal plexiform layer; MCL, mitral cell layer; EPL, external plexiform layer; GL, glomerular layer (Scale bar: 200 μm).

both nuclei of mitral/periglomerular cells and in thin cellular processes throughout all AOB layers (**Figures 3A,B**). These cellular processes lost the Dab1 expression at P3 (**Figures 3C,D**), while it was maintained as a dotted pattern just in the cell bodies of GCL, MCL, and EPL (**Figures 3E–H**). However, nuclear labeling was intense along all postnatal ages in mitral and periglomerular cells. Dab1 expression pattern was similar between *wt* and *reeler* mice.

Further, we analyzed the neuronal and glial AOB phenotypes and whether the absence of Reln (*reeler*) produced a change in the neurochemical phenotype of those cells. First, we characterized the AOB neuronal phenotypes at different postnatal ages (P0, P3, P7, and P15) by using Map2a,b and NeuN as markers for mature neurons and CB and TH as markers for periglomerular cells (**Figure 4**). Map2a,b protein was strongly expressed in cell bodies and fibers of mature neurons in the GL, EPL, and MCL at all selected ages (**Figures 4A,B,G,H,M,N,S,T**). On the other hand, NeuN was mainly expressed in granular cells in all ages and in many periglomerular cells from P7 (**Figure 4**, NeuN). Thus, at P0–P7, NeuN is expressed in some granular cells, which appeared scattered throughout the GCL in both strains (**Figures 4C,D,I,J,O,P**). At P15, NeuN labeling increases in granular cells that were clustered together in small groups. Those groups were aligned and parallel to the lateral olfactory tract (LOT) in the *wt* (**Figure 4U**, arrows) while this arrangement was disrupted in *reeler* (**Figure 4V**, arrows). Periglomerular cells expressing TH were confined to the edges of the AOB glomeruli at all postnatal ages (**Figure 4**, TH) and no differences were detected between *wt* (**Figures 4E,K,Q,W**) and *reeler* mice (**Figures 4F,L,R,X**). With respect to CB cells just a low expression was present in the AOB (data not shown).

The AOB glial phenotypes were studied using markers for radial glial cells (RC2), astrocytes (GFAP) and oligodendrocytes (RIP). A large number of processes positive for RC2 were observed at P0 along the AOB (**Figures 5A,B**), and then decreased at P3 (**Figures 5G,H**) to be absent at P7–P15 (**Figures 5M,N,S,T**). Moreover, from P3 onwards RC2 protein was also located in stellate shaped-cell bodies throughout all

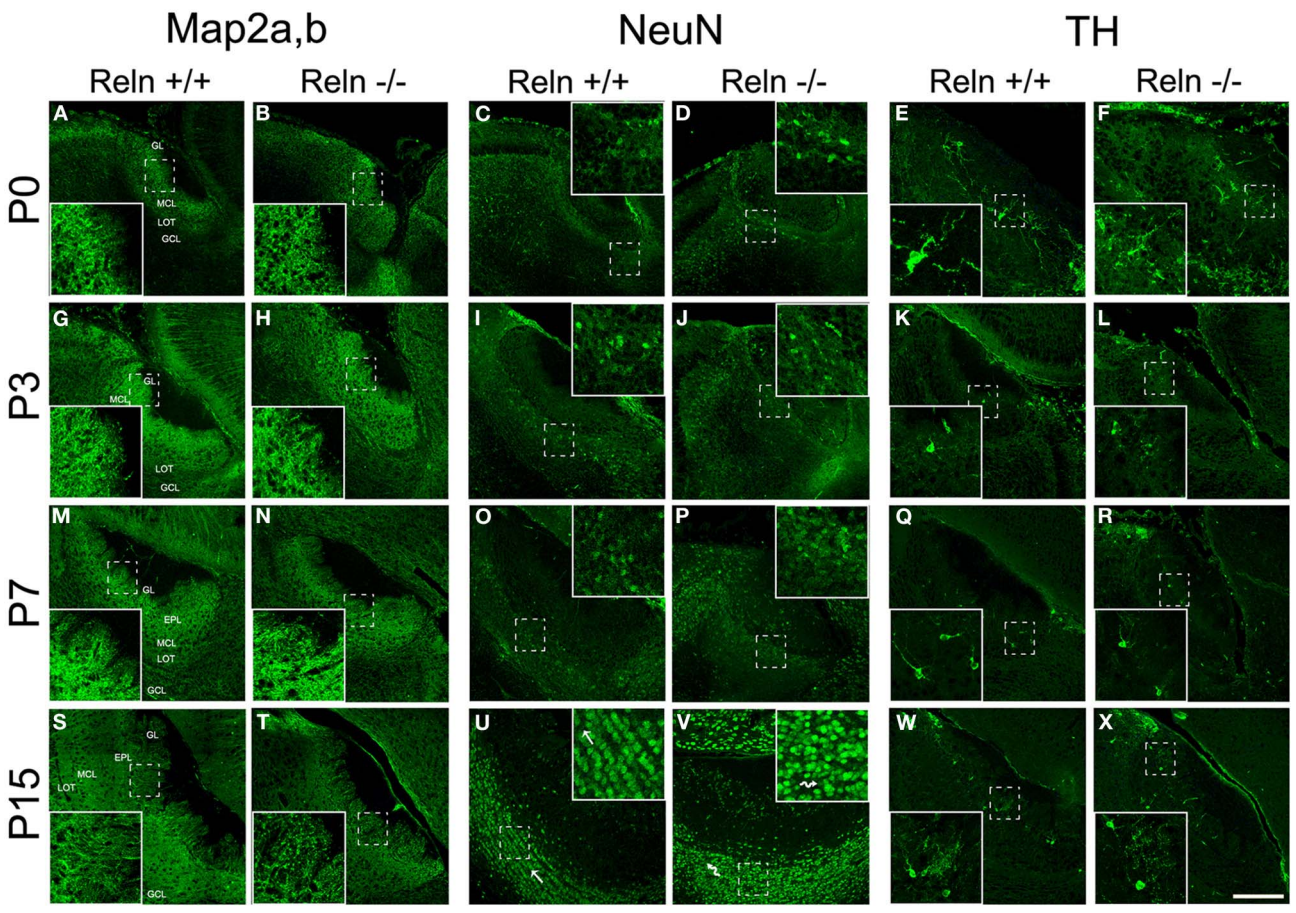

FIGURE 4 | Expression of neuronal markers in the accessory olfactory bulb at P0, P3, P7, and P15. Map2a,b protein is located both in mature neuronal somata and fibers located along the AOB layers **(A,B,G,H,M,N,S,T)**. In the GCL, NeuN is confined to neuronal nuclei and some periglomerular cells **(C,D,I,J,O,P,U,V)**. This labeling reveals a disorganization of granular cells of the AOB in reeler mice respect to wt, most evident at P15 (**U,V** and high magnification images). TH expression is confined to a group of periglomerular cells located around of the glomeruli **(E,F,K,L,Q,R,W,X)**. LOT, lateral olfactory tract; GCL, granular cell layer; IPL, internal plexiform layer; MCL, mitral cell layer; EPL, external plexiform layer; GL, glomerular layer. Images taken from Alexa-568 signal were pseudo-colored in green to enhance the labeling visibility (Scale bar: 200 μm).

AOB layers (**Figures 5G,H,M,N**), although mainly confined to the periglomerular regions at P15 (**Figures 5S,T**). The absence of Reln did not affect the RC2 expression. In relation to the astrocyte marker, in both strains, GFAP expression appeared restricted to the *glia limitans* at P0–P3 (**Figures 5C,D,I,J**). From P7, GFAP labeling extended to the rest of the AOB layers (**Figures 5O,P**) and it was expressed throughout AOB parenchyma at P15 (**Figures 5U,V**). RIP, antibody that recognizes a CNPase specific of oligodendrocytes, showed weak staining in the non-myelin oligodendrocytes at P0–P3 mostly in the LOT region (**Figures 5E,F,K,L**). From P7 the labeling was restricted to both myelin sheets of the LOT (**Figures 5Q,R**) and some myelin fibers crossing the GCL at P15 (**Figures 5W,X** arrows). Labeling of GFAP and RIP was indistinguishable between *wt* and *reeler* mice.

DISCUSSION

The AOB is the CNS structure that receives and integrates the olfactory information from vomeronasal sensory neurons. Since only scattered information is available regarding AOB layering, and because some of it is controversial (Hinds, 1968; Jimenez et al., 2000; Salazar et al., 2006), we first established the prenatal sequence of this process. Then we compared this developmental layer arrangement with that occurring in the MOB. Moreover, we analyzed some molecular features of the AOB as well as the effect of the lack of Reln, defined as a key molecule involved in several developmental processes of the CNS. To study how Reln affects the anatomical characteristics of the AOB, we used *reeler* mutants to study the effects of its functional absence.

In the present study, we schematized the layer development of AOB over the course of the embryonic mouse development. Although the mitral/tufted cell generation in the AOB begins earlier than in MOB (Hinds, 1968; Jimenez et al., 2000), in both structures a homogeneous population of cells surrounding a thick ventricular layer (VZ) was present at E10–E11. However, layer segregation occurs earlier in the MOB than in the AOB (E12–E15). Subsequent developmental changes occurred

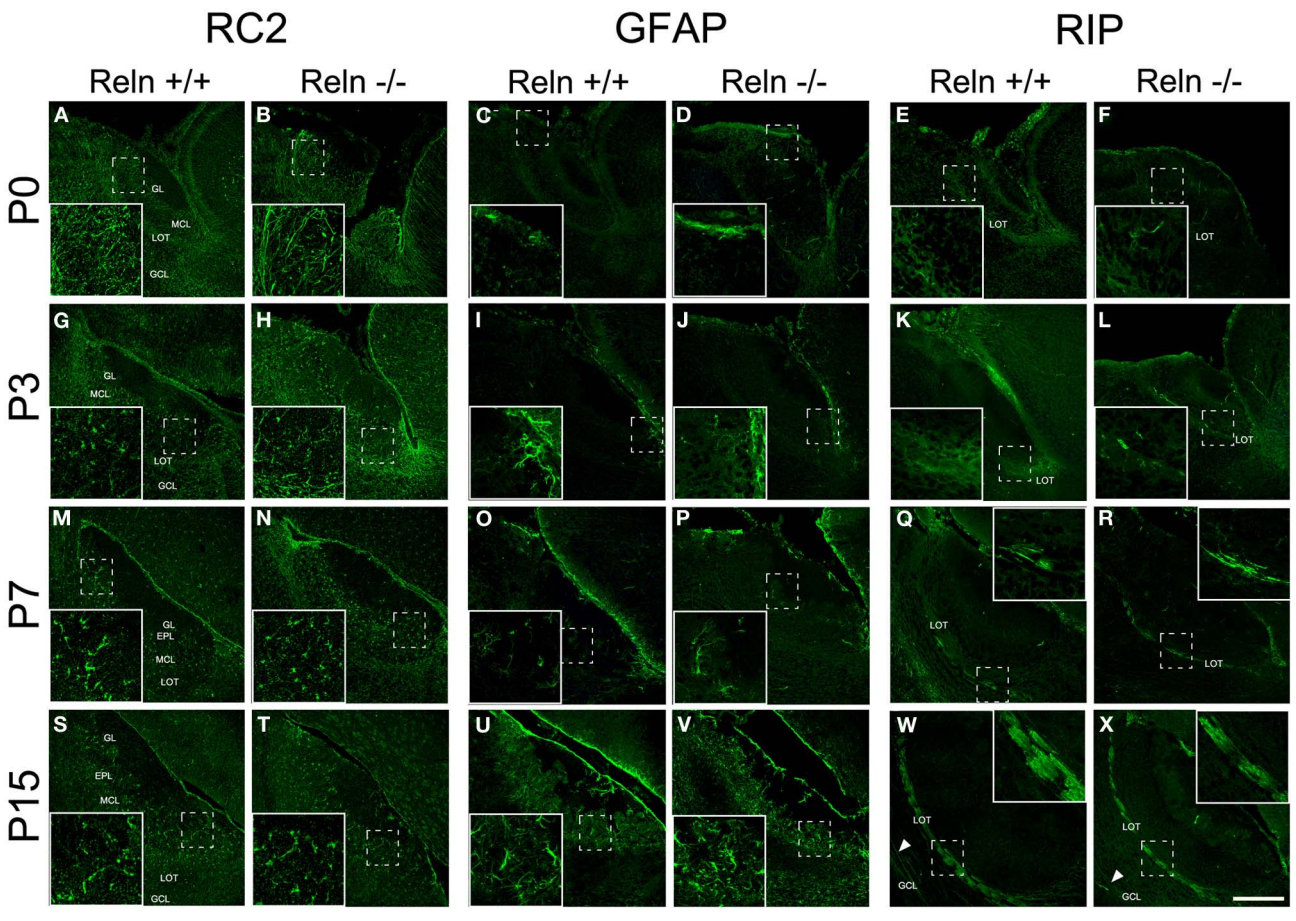

FIGURE 5 | Expression of glial markers in the accessory olfactory bulb at P0, P3, P7, and P15. RC2 immunolabeling is located in radial glia fibers throughout AOB layers at P0–P3 and in few cells with large and thin cellular processes **(A,B,G,H)**. From P7, the labeling is restricted to glial cells without radial process **(M,N,S,T)**. GFAP antibody labels astrocytes restricted to *glia limitans* at P0 and P3 **(C,D,I,J)**. From P7 to P15, GFAP labeling extends to the rest of the AOB layers **(O,P,U,V)**. RIP, an enzyme located in non-myelin oligodendrocytes, is mainly expressed in the LOT regions at P0–P3 **(E,F,K,L)**. From P7 to P15, RIP labeling is restricted to myelin sheaths in the LOT **(Q,R,W,X)** and in some myelin fibers crossing the GCL (**W,X** arrowsheads). LOT, lateral olfactory tract; GCL, granular cell layer; IPL, internal plexiform layer; MCL, mitral cell layer; EPL, external plexiform layer; GL, glomerular layer. Images taken from Alexa-568 signal were pseudo-colored in green to enhance the labeling visibility (Scale bar: 200 μm).

concurrently in both bulbs (Salazar et al., 2006), from poorly defined strata to well-defined layers. Although an external, mitral/tufted cell, internal plexiform, and granule cell layers are evident in the AOB, they are less distinct than in the MOB. These layers were grouped into the external and internal cell layers by Larriva-Sahd (Larriva-Sahd, 2008).

On other hand, Reln is highly expressed in the olfactory system, including the olfactory bulb, vomeronasal organ, and vomeronasal nerves (Ikeda and Terashima, 1997; Alcantara et al., 1998; Teillon et al., 2003). In the OB, the absence of Reln affects the migration of neuroblasts from the rostral migratory stream and the layering of granular cells in the MOB (Hack et al., 2002; Martin-Lopez et al., 2011). This protein is a secreted extracellular matrix component that plays a crucial role in neuroblasts migration and cell settling in the developing brain, particularly for proper formation of laminar structures of mammalian brain (Caviness, Jr., 1976; Hack et al., 2002; Zhao et al., 2004). Our results showed that mice lacking functional Reln did not display significant alteration in the AOB cytoarchitecture, even when the GFAP expression in the hippocampus is altered in *reeler* animals (Zhao et al., 2004). However, we reported a disorganization of granular cells in *reeler*, as occurred in the MOB (Hack et al., 2002; Martin-Lopez et al., 2011), which probably indicates a role of Reln in the organization of the GCL. Similarly, although the AOB and vomeronasal organ showed a high expression of Reln (Teillon et al., 2003) it appears that Reln does not have an axon guidance role in this connection, since there were none differences in the external layers of the AOB between *wt* and *reeler* animals. As a whole, this strongly suggests that Reln does not provide guidance cues to targeting of the vomeronasal axons.

Furthermore, we described some anatomical features of the AOB using several neuronal and glial markers, which showed similar phenotypes to that observed in the MOB (Martin-Lopez et al., 2011). Among the neuronal markers, the expression of calbindin revealed few cells in the postnatal AOB as previously reported (Jia and Halpern, 2003; Kosaka and Kosaka, 2010).

In summary, our data provides new insights into the layering, organization, and the different cellular phenotypes in the AOB. Similar cytoarchitectonic features in the AOB were detected in the AOB and the MOB. Additionally, analysis of Reln mutants (*reeler*) mice revealed a disruption in the organization of granular cells.

ACKNOWLEDGMENTS

The authors are grateful to Sandra Rodriguez for her excellent technical assistance. This work was supported by Research grant BFU2010-15564 from Spanish Ministry of Economy and Competitiveness (MINECO).

REFERENCES

Alcantara, S., Ruiz, M., D'Arcangelo, G., Ezan, F., De, L. L., Curran, T., Sotelo, C., and Soriano, E. (1998). Regional and cellular patterns of reelin mRNA expression in the forebrain of the developing and adult mouse. *J. Neurosci.* 18, 7779–7799.

Altman, J. (1969). Autoradiographic and histological studies of postnatal neurogenesis. IV. Cell proliferation and migration in the anterior forebrain, with special reference to persisting neurogenesis in the olfactory bulb. *J. Comp. Neurol.* 137, 433–457.

Baum, M. J., and Kelliher, K. R. (2009). Complementary roles of the main and accessory olfactory systems in mammalian mate recognition. *Annu. Rev. Physiol.* 71, 141–160.

Blanchart, A., De Carlos, J. A., and Lopez-Mascaraque, L. (2006). Time frame of mitral cell development in the mice olfactory bulb. *J. Comp. Neurol.* 496, 529–543.

Blanchart, A., and Lopez-Mascaraque, L. (2011). From the periphery to the brain: wiring the olfactory system. *Transl. Neurosci.* 2, 293–309.

Blanchart, A., Romaguera, M., Garcia-Verdugo, J. M., De Carlos, J. A., and Lopez-Mascaraque, L. (2008). Synaptogenesis in the mouse olfactory bulb during glomerulus development. *Eur. J. Neurosci.* 27, 2838–2846.

Caviness, V. S. Jr. (1976). Patterns of cell and fiber distribution in the neocortex of the reeler mutant mouse. *J. Comp. Neurol.* 170, 435–447.

D'Arcangelo, G., Miao, G. G., Chen, S. C., Soares, H. D., Morgan, J. I., and Curran, T. (1995). A protein related to extracellular matrix proteins deleted in the mouse mutant reeler. *Nature* 374, 719–723.

Hack, I., Bancila, M., Loulier, K., Carroll, P., and Cremer, H. (2002). Reelin is a detachment signal in tangential chain-migration during postnatal neurogenesis. *Nat. Neurosci.* 5, 939–945.

Hinds, J. W. (1968). Autoradiographic study of histogenesis in the mouse olfactory bulb. I. Time of origin of neurons and neuroglia. *J. Comp. Neurol.* 134, 287–304.

Honda, T., Kobayashi, K., Mikoshiba, K., and Nakajima, K. (2011). Regulation of cortical neuron migration by the Reelin signaling pathway. *Neurochem. Res.* 36, 1270–1279.

Howell, B. W., Hawkes, R., Soriano, P., and Cooper, J. A. (1997). Neuronal position in the developing brain is regulated by mouse disabled-1. *Nature* 389, 733–737.

Ikeda, Y., and Terashima, T. (1997). Expression of reelin, the gene responsible for the reeler mutation, in embryonic development and adulthood in the mouse. *Dev. Dyn.* 210, 157–172.

Jia, C., and Halpern, M. (2003). Calbindin D28K immunoreactive neurons in vomeronasal organ and their projections to the accessory olfactory bulb in the rat. *Brain Res.* 977, 261–269.

Jimenez, D., Garcia, C., De, C. F., Chedotal, A., Sotelo, C., De Carlos, J. A., Valverde, F., and Lopez-Mascaraque, L. (2000). Evidence for intrinsic development of olfactory structures in Pax-6 mutant mice. *J. Comp. Neurol.* 428, 511–526.

Kosaka, T., and Kosaka, K. (2010). Heterogeneity of calbindin-containing neurons in the mouse main olfactory bulb: I. General description. *Neurosci. Res.* 67, 275–292.

Larriva-Sahd, J. (2008). The accessory olfactory bulb in the adult rat: a cytological study of its cell types, neuropil, neuronal modules, and interactions with the main olfactory system. *J. Comp. Neurol.* 510, 309–350.

Lois, C., and Alvarez-Buylla, A. (1994). Long-distance neuronal migration in the adult mammalian brain. *Science* 264, 1145–1148.

Lopez-Mascaraque, L., and De Castro, F. (2002). The olfactory bulb as an independent developmental domain. *Cell Death Differ.* 9, 1279–1286.

Luo, M., Fee, M. S., and Katz, L. C. (2003). Encoding pheromonal signals in the accessory olfactory bulb of behaving mice. *Science* 299, 1196–1201.

Martin-Lopez, E., Blanchart, A., De Carlos, J. A., and Lopez-Mascaraque, L. (2011). Dab1 (disable homolog-1) reelin adaptor protein is overexpressed in the olfactory bulb at early postnatal stages. *PLoS ONE* 6:e26673. doi: 10.1371/journal.pone.0026673

Meisami, E., and Bhatnagar, K. P. (1998). Structure and diversity in mammalian accessory olfactory bulb. *Microsc. Res. Tech.* 43, 476–499.

Meredith, M. (1991). Sensory processing in the main and accessory olfactory systems: comparisons and contrasts. *J. Steroid Biochem. Mol. Biol.* 39, 601–614.

Mori, K., von, C. H., and Yoshihara, Y. (2000). Zonal organization of the mammalian main and accessory olfactory systems. *Philos. Trans. R. Soc. Lond. B Biol. Sci.* 355, 1801–1812.

Oboti, L., Savalli, G., Giachino, C., De, M. S., Panzica, G. C., Fasolo, A., and Peretto, P. (2009). Integration and sensory experience-dependent survival of newly-generated neurons in the accessory olfactory bulb of female mice. *Eur. J. Neurosci.* 29, 679–692.

Peretto, P., Giachino, C., Panzica, G. C., and Fasolo, A. (2001). Sexually dimorphic neurogenesis is topographically matched with the

anterior accessory olfactory bulb of the adult rat. *Cell Tissue Res.* 306, 385–389.

Ramon y Cajal, S. (1901). Textura del lóbulo olfativo accesorio. *Trab. Lab. Invest. Biol.* 1, 141–149.

Restrepo, D., Arellano, J., Oliva, A. M., Schaefer, M. L., and Lin, W. (2004). Emerging views on the distinct but related roles of the main and accessory olfactory systems in responsiveness to chemosensory signals in mice. *Horm. Behav.* 46, 247–256.

Rice, D. S., Sheldon, M., D'Arcangelo, G., Nakajima, K., Goldowitz, D., and Curran, T. (1998). Disabled-1 acts downstream of Reelin in a signaling pathway that controls laminar organization in the mammalian brain. *Development* 125, 3719–3729.

Salazar, I., Sanchez-Quinteiro, P., Cifuentes, J. M., and Fernandez De, T. P. (2006). General organization of the perinatal and adult accessory olfactory bulb in mice. *Anat. Rec. A Discov. Mol. Cell. Evol. Biol.* 288, 1009–1025.

Schiffmann, S. N., Bernier, B., and Goffinet, A. M. (1997). Reelin mRNA expression during mouse brain development. *Eur. J. Neurosci.* 9, 1055–1071.

Shepherd, G. M. (2005). Perception without a thalamus how does olfaction do it? *Neuron* 46, 166–168.

Teillon, S. M., Yiu, G., and Walsh, C. A. (2003). Reelin is expressed in the accessory olfactory system, but is not a guidance cue for vomeronasal axons. *Brain Res. Dev. Brain Res.* 140, 303–307.

Wyss, J. M., Stanfield, B. B., and Cowan, W. M. (1980). Structural abnormalities in the olfactory bulb of the Reeler mouse. *Brain Res.* 188, 566–571.

Xu, F., Schaefer, M., Kida, I., Schafer, J., Liu, N., Rothman, D. L., Hyder, F., Restrepo, D., and Shepherd, G. M. (2005). Simultaneous activation of mouse main and accessory olfactory bulbs by odors or pheromones. *J. Comp. Neurol.* 489, 491–500.

Zhao, S., Chai, X., Forster, E., and Frotscher, M. (2004). Reelin is a positional signal for the lamination of dentate granule cells. *Development* 131, 5117–5125.

Conflict of Interest Statement: The authors declare that the research was conducted in the absence of any commercial or financial relationships that could be construed as a potential conflict of interest.

Received: 13 March 2012; paper pending published: 31 March 2012; accepted: 03 May 2012; published online: 22 May 2012.

Citation: Martín-López E, Corona R and López-Mascaraque L (2012) Postnatal characterization of cells in the accessory olfactory bulb of wild type and reeler mice. Front. Neuroanat. ***6****:15. doi: 10.3389/fnana.2012.00015*

frontiers in
NEUROANATOMY

ORIGINAL RESEARCH ARTICLE
published: 29 May 2012
doi: 10.3389/fnana.2012.00019

Centrifugal telencephalic afferent connections to the main and accessory olfactory bulbs

Alicia Mohedano-Moriano[1], Carlos de la Rosa-Prieto[2], Daniel Saiz-Sanchez[2], Isabel Ubeda-Bañon[2], Palma Pro-Sistiaga[3], Miguel de Moya-Pinilla[2] and Alino Martinez-Marcos[2]*

[1] *Facultad de Medicina de Albacete, Laboratorio de Neuroanatomía Humana, Departamento de Ciencias Médicas, Centro Regional de Investigaciones Biomédicas, Universidad de Castilla-La Mancha, Albacete, Spain*
[2] *Facultad de Medicina de Ciudad Real, Laboratorio de Neuroplasticidad y Neurodegeneración, Departamento de Ciencias Médicas, Centro Regional de Investigaciones Biomédicas, Universidad de Castilla-La Mancha, Ciudad Real, Spain*
[3] *GIP Cyceron, Campus Jules Horowiz, Caen, France*

Edited by:
Micheal Baum, Boston University, USA

Reviewed by:
Kevin R. Kelliher, University of Bridgeport, USA
Ningdong Kang, Washington University in Saint Louis, USA

****Correspondence:***
Alino Martinez-Marcos, Facultad de Medicina de Ciudad Real, Universidad de Castilla-La Mancha, Avda. de Moledores S/N, 13071 Ciudad Real, Spain.
e-mail: alino.martinez@uclm.es

Parallel to the olfactory system, most mammals possess an accessory olfactory or vomeronasal system. The olfactory and vomeronasal epithelia project to the main and accessory olfactory bulbs, which in turn project to adjacent areas of the telencephalon, respectively. New data indicate that projections arising from the main and accessory olfactory bulbs partially converge in the rostral telencephalon and are non-overlapping at caudal telencephalic levels. Therefore, the basal telencephalon should be reclassified in olfactory, vomeronasal, and mixed areas. On the other hand, it has been demonstrated that virtually all olfactory- and vomeronasal-recipient structures send reciprocal projections to the main and accessory olfactory bulbs, respectively. Further, non-chemosensory recipient structures also projects centrifugally to the olfactory bulbs. These feed-back projections appear to be essential modulating processing of chemosensory information. The present work aims at characterizing centrifugal projections to the main and accessory olfactory bulbs arising from olfactory, vomeronasal, mixed, and non-chemosensory recipient telencephalic areas. This issue has been addressed by using tracer injections in the rat and mouse brain. Tracer injections were delivered into the main and accessory olfactory bulbs as well as in olfactory, vomeronasal, mixed, and non-chemosensory recipient telencephalic structures. The results confirm that olfactory- and vomeronasal-recipient structures project to the main and accessory olfactory bulbs, respectively. Interestingly, olfactory (e.g., piriform cortex), vomeronasal (e.g., posteromedial cortical amygdala), mixed (e.g., the anterior medial amygdaloid nucleus), and non-chemosensory-recipient (e.g., the nucleus of the diagonal band) structures project to the main and to the accessory olfactory bulbs thus providing the possibility of simultaneous modulation and interaction of both systems at different stages of chemosensory processing.

Keywords: chemical senses, olfactory system, tract-tracing, vomeronasal system

INTRODUCTION

Two main nasal chemical senses, the olfactory and the vomeronasal systems, have evolved in most vertebrates to detect chemical substances (Taniguchi and Saito, 2011; Ubeda-Banon et al., 2011). In mammals, these systems begin in the olfactory and vomeronasal epithelia that project to the main and accessory olfactory bulbs which in turn send projections to the olfactory and vomeronasal cortices, respectively (Devor, 1976; Skeen and Hall, 1977; Turner et al., 1978; Scott et al., 1980; Kosel et al., 1981; Meyer, 1981; Shammah-Lagnado and Negrao, 1981; Carmichael et al., 1994; Jansen et al., 1998; Mohedano-Moriano et al., 2005; Martinez-Marcos and Halpern, 2006; Gutierrez-Castellanos et al., 2010).

In the 1970's, the observation that secondary olfactory and vomeronasal projections were parallel led to the dual olfactory hypothesis, according to which the olfactory and vomeronasal systems constituted two different parallel anatomical and functional pathways (Winans and Scalia, 1970; Raisman, 1972; Scalia and Winans, 1975). The main olfactory system would be devoted to the perception of airborne chemicals such as odorants, whereas the vomeronasal system would be specialized for the detection of biologically relevant molecules of high molecular weight such as pheromones, which evoke species-specific behavioral and/or physiological responses (Halpern, 1987). The data, however, have demonstrated that this hypothesis is an oversimplification (Halpern and Martinez-Marcos, 2003; Restrepo et al., 2004; Spehr et al., 2006b) since the olfactory and vomeronasal system interact both physiologically (Licht and Meredith, 1987; Peele et al., 2003; Lin et al., 2004; Trinh and Storm, 2004; Xu et al., 2005; Spehr et al., 2006a; Wang et al., 2006; Keller et al., 2009) and

anatomically (Pro-Sistiaga et al., 2007, 2008; Kang et al., 2009, 2011a; Mucignat-Caretta, 2010).

Apart from olfactory- and vomeronasal-recipient areas in the telencephalon, olfactory, and vomeronasal inputs converge in areas classically considered olfactory-recipient (nucleus of the lateral olfactory tract, anterior cortical amygdaloid nucleus, and cortex-amygdala transition zone) or vomeronasal-recipient (ventral anterior amygdala, bed nucleus of the accessory olfactory tract, and anteroventral medial amygdaloid nucleus) (Pro-Sistiaga et al., 2007; Kang et al., 2009, 2011b; Martinez-Marcos, 2009). Further, tertiary olfactory (Ubeda-Banon et al., 2007) and vomeronasal (Ubeda-Banon et al., 2008) projections also converge in the ventral striatum.

In many mammals, the vomeronasal system, in turn, has been demonstrated to be anatomically and functionally dichotomous (Halpern et al., 1998a,b). Two classes of vomeronasal receptor neurons, apically and basally placed in the sensory epithelium, express Gi2α and Goα proteins (Berghard and Buck, 1996; Jia and Halpern, 1996), V1R and V2R vomeronasal receptors (Dulac and Axel, 1995; Herrada and Dulac, 1997; Matsunami and Buck, 1997; Ryba and Tirindelli, 1997), respond to different stimuli (Leinders-Zufall et al., 2000, 2004) and project to the anterior and posterior accessory olfactory bulb (Belluscio et al., 1999; Rodriguez et al., 1999), respectively. The two portions of the accessory olfactory bulb have been demonstrated to show not only convergent (Von Campenhausen and Mori, 2000; Salazar and Brennan, 2001) but differential projections to the vomeronasal amygdala (Martinez-Marcos and Halpern, 1999b; Mohedano-Moriano et al., 2007), which in turn are separately preserved to the hypothalamus (Mohedano-Moriano et al., 2008).

Common traits to all olfactory- and vomeronasal-recipient structures are reciprocal centrifugal projections to the main and accessory olfactory bulbs, respectively. The main olfactory bulb receives afferent connections from a number of olfactory-recipient structures (anterior olfactory nucleus, olfactory tubercle, piriform cortex, nucleus of the lateral olfactory tract, anterior cortical amygdala, posterolateral cortical amygdala, and lateral entorhinal cortex), hippocampus (ventral CA1) as well as from neuromodulatory centers (nucleus of the diagonal band, locus coeruleus, and dorsal raphe nucleus) (Price and Powell, 1970; Raisman, 1972; Barber and Field, 1975; Broadwell and Jacobowitz, 1976; Davis et al., 1978; de Olmos et al., 1978; Macrides et al., 1981; Barber, 1982; Luskin and Price, 1983; Shipley and Adamek, 1984; Zheng et al., 1987; Cenquizca and Swanson, 2007; Matsutani and Yamamoto, 2008; Fletcher and Chen, 2010). Centrifugal inputs have been demonstrated to be essential in the formation of odor-reward associations (Kiselycznyk et al., 2006) as well as to provide inputs to new born cells arriving to the main olfactory bulb (Mouret et al., 2009).

Afferents to the accessory olfactory bulb arise from the vomeronasal-recipient structures (medial amygdaloid nucleus, posteromedial cortical amygdaloid nucleus, bed nucleus of the accessory olfactory tract, and bed nucleus of the stria terminalis), hippocampal formation (ventral subiculum and CA1) as well as from the brainstem (locus coeruleus and dorsal raphe nucleus) (Raisman, 1972; Barber and Field, 1975; Broadwell and Jacobowitz, 1976; Davis et al., 1978; de Olmos et al., 1978; Barber, 1982; Martinez-Marcos and Halpern, 1999a; Cenquizca and Swanson, 2007; de la Rosa-Prieto et al., 2009). Some of these centrifugal afferents (Brennan et al., 1990; Keverne and Brennan, 1996) as well as the addition of new neurons to the accessory olfactory bulb (Oboti et al., 2011) have been demonstrated to be critical for pregnancy block olfactory memory.

As far as we know, the possibility that olfactory-recipient structures project to the accessory olfactory bulb; that vomeronasal-recipient structures project to the main olfactory bulb; or that mixed chemosensory or non-chemosensory structures project to both the main and accessory olfactory bulbs have been not specifically addressed. The aim of this work has been, therefore, to investigate potential interactions between the main and accessory olfactory systems regarding their centrifugal inputs. Further, since most of these projections have been separately investigated in different species in previous reports, we have used both rats and mice in order to have a more complete panorama of centrifugal afferents in rodents.

MATERIALS AND METHODS

EXPERIMENTAL ANIMALS

Adult animals of both sexes were used in the present study: 26 Sprague–Dawley rats and 20 swiss (C57BL) mice. Animals were maintained under veterinary supervision on a 12-h light/dark cycle at 21 ± 2°C with food and drink *ad libitum*. Experimental procedures were carried out according to the guidelines of the European Community Directive 86/609/CEE for the use of laboratory animals and with Spanish law (Real Decreto 1201/2005) under the supervision of the Ethical Committee of Animal Research of the University of Castilla-La Mancha (grant BFU2010-15729).

TRACER INJECTIONS

Animals were anesthetized by an intraperitoneal injection of a combined dose of ketamine hydrochloride (Ketolar, Parke-Davis, Madrid, 1.5 mL/kg, 75 mg/kg) and xylazine (Xilagesic, Calier, Barcelona, 0.5 mL/kg, 10 mg/kg). Eye drops (Lacryvisc, Alcon, Barcelona) were applied to prevent eye ulceration during surgery. The animals were placed in a Kopf (Tujunga, CA) stereotaxic apparatus and the skull trepanned at the intended injection site. Ionophoretic injections of dextran amines conjugated to biotin (BDA), fluorescein (FDA) or tetramethylrhodamine (RDA) (10,000 MW, lysine fixable, Molecular Probes, Eugene, OR) as well as injections of FluoroGold (FG, methanesulfonate hydroxystilbamidine, Biotium, Hayward, CA) were placed in target structures: main olfactory bulb (four rats and two mice), accessory olfactory bulb (eight rats and four mice), piriform cortex (two rats and ten mice), posteromedial cortical amygdaloid nucleus (four rats), medial amygdala (four rats) and ventral CA1 (four rats), and simultaneous injections of dextran amines conjugated to RDA and FDA into the main and accessory olfactory bulbs, respectively (four mice). Only injections centered at the intended injection site and no contaminating neighboring structures were considered. The atlases of rat (Paxinos and Watson, 2007) and mouse (Franklin and Paxinos, 2008) brain were used for this study. Dextran amines (10% in phosphate buffered saline)

and FG (2% saline solution) were delivered from micropipettes (30–80 μm diameter tip) by means of positive current pulses (7/7 s, 2–7 μA, 8–20 min).

PERFUSION, CUTTING, AND TRACER DETECTION

Five to seven days later, animals were anesthetized (as above) and perfused through the ventricle with saline solution followed by 4% paraformaldehyde. The brains were postfixed overnight and cryoprotected with 30% buffered sucrose. Parasagittal (olfactory bulbs) or frontal sections (50 μm) were obtained using a freezing microtome.

For biotinylated dextran-amine detection, endogenous peroxidase activity was quenched by means of 1% H_2O_2 (in 0.05 M Tris buffer saline, pH 7.6, for 30 min). Sections were incubated for 2 h in avidin-biotin complex (ABC elite kit, Vector, Burlingame, CA; diluted at 2% in 0.05 M Tris buffer saline, pH 7.6) and visualized with 0.02% 3,3′-diaminobenzidine (Sigma, St. Louis, MO) diluted in 0.05 M Tris buffer (pH 8.0) with 0.1% ammonium nickel sulfate and 0.01% H_2O_2. Sections were mounted, dried, stained with thionin (Panreac, Barcelona) and coverslipped with DPX (BDH Laboratory, Poole, UK).

For fluorescent tracers, sections were mounted and coverslipped with 30% glycerin in 0.4 M potassium bicarbonate. Analysis was performed under bright-field and epifluorescence microscopy. Contrast and brightness of images were adjusted using Adobe Photoshop (San Jose, CA) 8.0.1 software and arranged and lettered using Canvas 11.0 (Deneba, Miami, FL).

RESULTS

INJECTIONS INTO THE MAIN OLFACTORY BULB

In order to analyze afferent connections to the main olfactory bulb in our own material experiments using FG and dextran amine-labeled RDA were carried out. The pattern of labeling was consistent in the different experiments performed.

Injections of FG yielded a large, poorly defined injection site in the granule cell layer of the main olfactory bulb of rats (as example see case R0207, 7.5 mm from Bregma, **Figure 1A**). As expected, a number of retrogradely labeled cells were observed in the anterior olfactory nucleus (**Figure 1B**), nucleus of the diagonal band (**Figure 1C**), layers 2 and 3 of the rostral piriform cortex (**Figure 1D**), olfactory tubercle (**Figure 1E**), anterior amygdaloid area, and faintly labeled neurons in layers 2 and 3 of the nucleus of the lateral olfactory tract, anterior cortical amygdaloid nucleus, cortex-amygdala transition area, and caudal piriform cortex (**Figure 1F**). Labeled cells were present in the anterodorsal medial amygdaloid nucleus (−1.8 mm from Bregma, **Figure 1G**) and slightly labeled cells were also observed in the posterolateral cortical amygdaloid nucleus (not shown) and lateral entorhinal cortex (**Figure 1H**).

Injections of dextran amine-labeled RDA into the granule cell layer of the main olfactory bulb of rats gave rise a similar pattern of labeling, but a considerably reduced injection site (as example see case R4505, 6.6 mm from Bregma, **Figure 2A**, 7.5 mm from Bregma) and consequently to a scarcer retrograde labeling as compared to FG injections. As in the previous case, labeled cells could be observed in the anterior olfactory nucleus (not shown), nucleus of the diagonal band (**Figure 2B**), rostral piriform cortex (**Figure 2C**), olfactory tubercle (not shown), anterior amygdaloid area, nucleus of the lateral olfactory tract, anterior cortical amygdaloid nucleus, cortex-amygdala transition zone (**Figures 2D,E**), caudal piriform cortex (**Figure 2F**), anterodorsal medial amygdaloid nucleus (−2.0 mm from Bregma, **Figure 2G**), posterolateral cortical amygdaloid nucleus (not show) and lateral entorhinal cortex (**Figure 2H**).

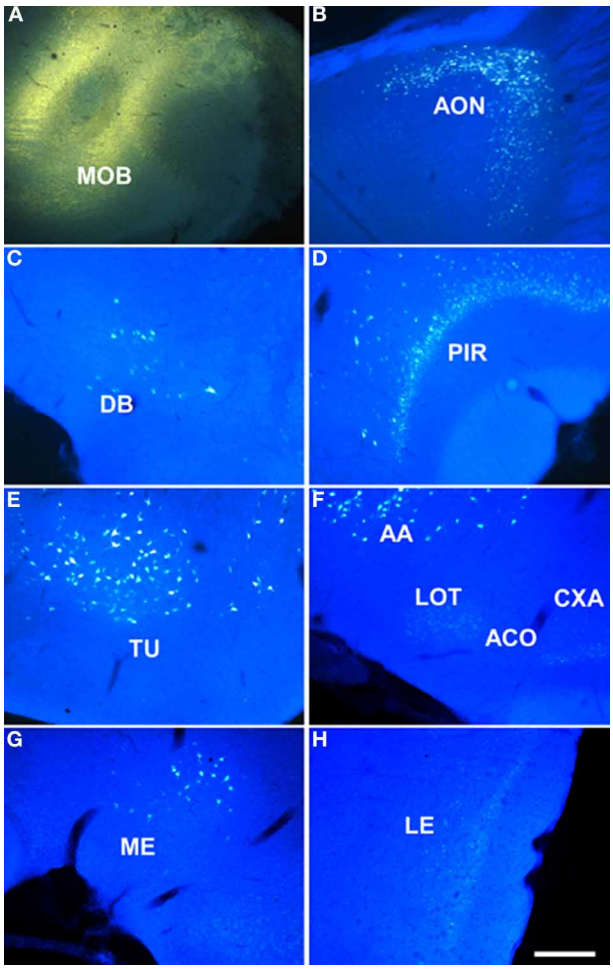

FIGURE 1 | Sagittal (A,B) and coronal sections (C–H) from rostral to caudal levels of the telencephalic hemisphere showing the resulting labeling (B–H) after a FluoroGold injection in the rat main olfactory bulb (A). Abbreviations: AA, anterior amygdala; ACO, anterior cortical amygdala; AON, anterior olfactory nucleus; CXA, cortex-amygdala transition zone; DB, nucleus of the diagonal band; LE, lateral entorhinal cortex; LOT, nucleus of the lateral olfactory tract; ME, medial amygdala; MOB, main olfactory bulb; PIR, piriform cortex; PLCO, posterolateral cortical amygdala; TU, olfactory tubercle. Scale bar for **A**: 1000 μm, **B–H**: 400 μm.

INJECTIONS INTO THE ACCESSORY OLFACTORY BULB

Given the small size of the accessory olfactory bulb, dextran-amines were used as neural tracers. All cases with injections in the accessory olfactory bulb yielded a similar pattern of labeling.

Injections of dextran amine-labeled RDA involving the mitral and granule cell layer of the accessory olfactory bulb of rats

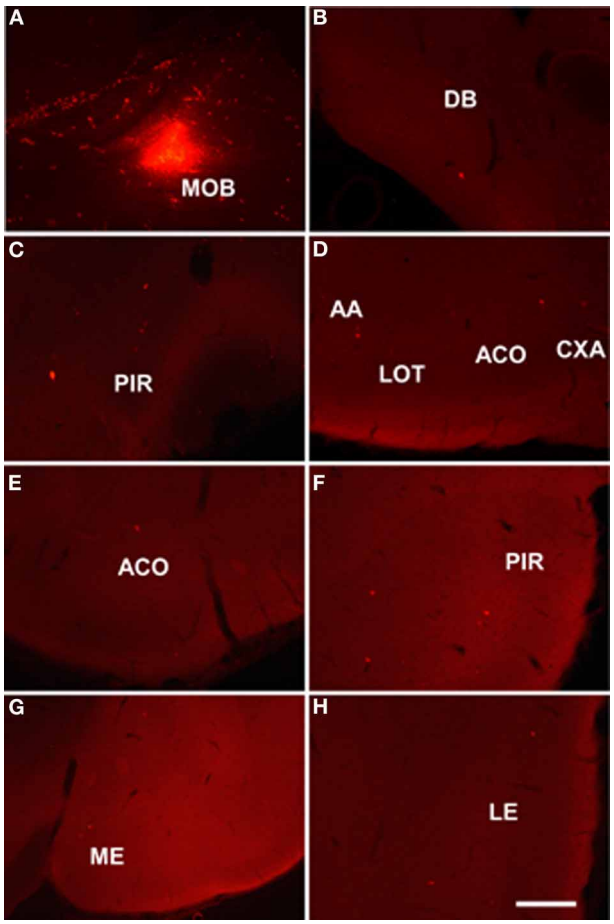

FIGURE 2 | Sagittal (A) and coronal sections (B–H) from rostral to caudal levels of the telencephalic hemisphere showing the resulting labeling (B–H) after a dextran-amine labeled tetramethylrhodamine injection in the rat main olfactory bulb (A). Abbreviations: AA, anterior amygdala; ACO, anterior cortical amygdala; AON, anterior olfactory nucleus; CXA, cortex-amygdala transition zone; DB, nucleus of the diagonal band; LE, lateral entorhinal cortex; LOT, nucleus of the lateral olfactory tract; ME, medial amygdala; MOB, main olfactory bulb; PIR, piriform cortex; PLCO, posterolateral cortical amygdala. Scale bar for **A**: 800 μm, **B–H**: 400 μm.

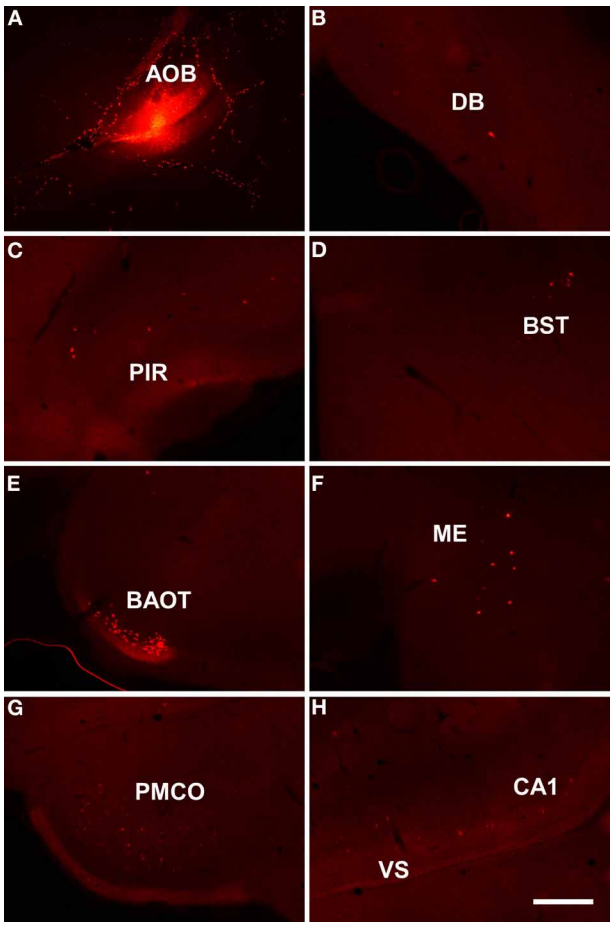

FIGURE 3 | Sagittal (A) and coronal sections (B–H) from rostral to caudal levels of the telencephalic hemisphere showing the resulting labeling (B–H) after a dextran-amine labeled tetramethylrhodamine injection in the rat accessory olfactory bulb (A). Abbreviations: BAOT, bed nucleus of the accessory olfactory tract; BST, bed nucleus of the stria terminalis; CA1, CA1 field of the hippocampus; DB, nucleus of the diagonal band; ME, medial amygdala; PIR, piriform cortex; PMCO, posteromedial cortical amygdala; VS, ventral subiculum. Scale bar for **A**: 800 μm, **B–H**: 400 μm.

(as example see case R8205, 6.2 mm from Bregma, **Figure 3A**) gave rise to scarce retrograde labeled neurons in the nucleus of the diagonal band (**Figure 3B**), rostral pirirform cortex (**Figure 3C**), bed nuclei of the stria terminalis (**Figure 3D**) and accessory olfactory tract (**Figure 3E**), anterodorsal medial amgydaloid nucleus (−1.8 mm from Bregma, **Figure 3F**), posteromedial cortical amygdaloid nucleus (**Figure 3G**), and the ventral portion of the subiculum and CA1 (**Figure 3H**).

It has also to be noted that the dorsal portion of the olfactory tract, through which course centripetal and centrifugal axons to the main olfactory bulb, is situated between the mitral and granule cell layer of the accessory olfactory bulb (Larriva-Sahd, 2008). Accordingly, it cannot rule out the possibility that injections into the accessory olfactory bulb involve these axons. Therefore, anterograde tracing experiments (sections "Injections in the piriform cortex, Injections in the posteromedial cortical amygdala, Injections in the anterodorsal medial amygdaloid nucleus, and Injections in the hippocampal formation") should confirm retrograde tracing results in order to fully discriminate afferent connections either to the main bulb, accessory bulb or both.

INJECTIONS IN THE MAIN AND ACCESSORY OLFACTORY BULBS

In order to compare the centrifugal afferent connections to the main and accessory olfactory bulb, four mice were simultaneously injected with dextran amine-labeled RDA into the main olfactory bulb and dextran amine-labeled FDA into the accessory olfactory bulb. However, these latter injections were not exclusively restricted to the accessory olfactory bulb or affected the dorsal portion of the olfactory tract running through the accessory olfactory bulb. Labeling was consistent to that observed after injections into the main or accessory olfactory bulb in previous experiments.

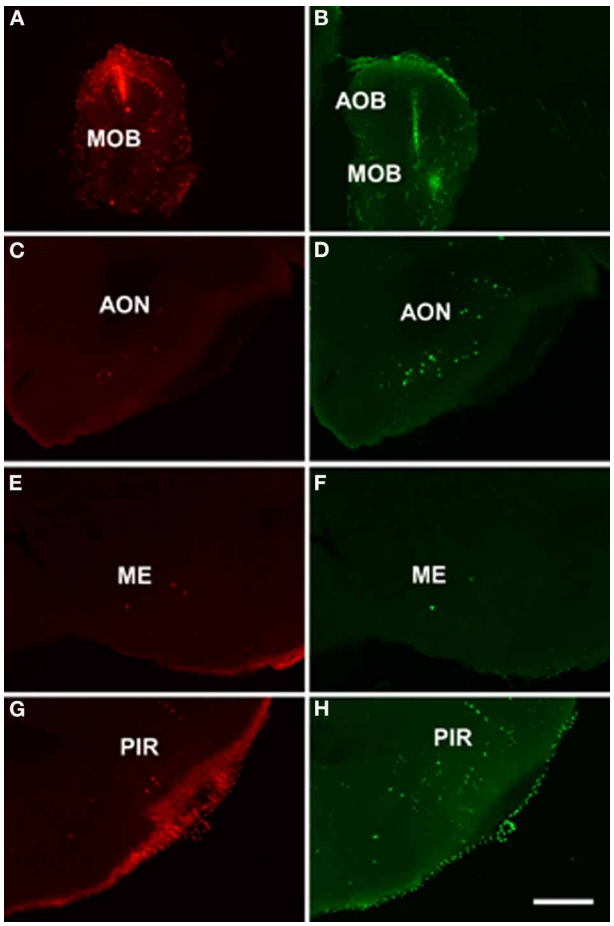

FIGURE 4 | Coronal sections from rostral to caudal levels of the telencephalic hemisphere showing the resulting labeling (C,E,G and D,F,H) after a dextran-amine labeled tetramethylrhodamine injection in the mouse main olfactory bulb (A) and a dextran-amine labeled fluorescein injection in the mouse main and accessory olfactory bulbs (B), respectively. Abbreviations: AOB, accessory olfactory bulb; AON, anterior olfactory nucleus; ME, medial amygdala; MOB, main olfactory bulb; PIR, piriform cortex. Scale bar for **A**, **B**: 800 μm, **C–H**: 400 μm.

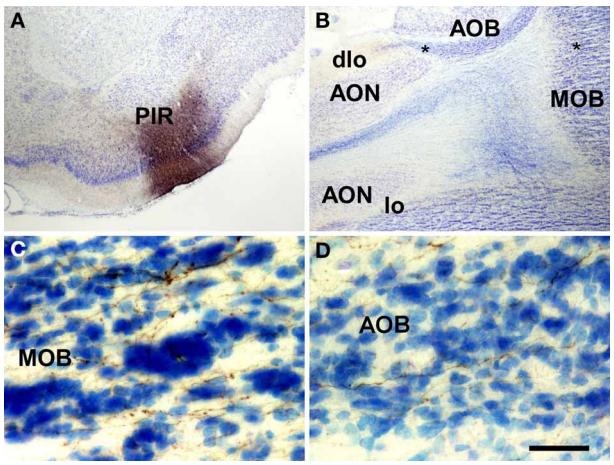

FIGURE 5 | Coronal (A) and sagittal (B–D) sections of the telencephalic hemisphere showing the resulting labeling (B–D) after a biotinylated dextran-amine injection in the rat piriform cortex (A). Asterisks in **B** indicate the approximate location of panels **C** and **D**. Abbreviations: AOB, accessory olfactory bulb; AON, anterior olfactory nucleus; dlo, dorsal lateral olfactory tract; lo, lateral olfactory tract; MOB, main olfactory bulb; PIR, piriform cortex. Scale bar for **A**: 800 μm, **B**: 400 μm, **C,D**: 40 μm.

As example, case RN21312 showed a dextran amine-labeled RDA injection in the main olfactory bulb (4.3 mm from Bregma, **Figure 4A**) and a dextran amine-labeled FDA injection in the accessory olfactory bulb, but that also contaminated the main olfactory bulb (3.5 mm from Bregma, **Figure 4B**). As expected, labeling was present in olfactory and vomeronasal structures such as the anterior olfactory nucleus (**Figures 4C,D**), anterodorsal medial amygdaloid nuelus (−1.0 mm from Bregma, **Figures 4E,F**), and piriform cortex (**Figures 4G,H**).

INJECTIONS IN THE PIRIFORM CORTEX

Injections of biotinylated dextran-amine in the rat piriform cortex gave rise to a similar pattern of labeling (as example see case R10307, −0.2 mm from Bregma, **Figure 5A**) including anterogradely labeled fibers in the ventral and dorsal portions of the lateral olfactory tract (**Figure 5B**). Labeled fibers showing varicosities could be observed throughout the granule cell layer of the main olfactory bulb (**Figure 5C**). A number of labeled fibers were also present in the granule cell layer of the accessory olfactory bulb (**Figure 5D**).

INJECTIONS IN THE POSTEROMEDIAL CORTICAL AMYGDALA

Injections of biotinylated dextran-amine in the rat posteromedial cortical amygdala gave rise to a consistent labeling (as example see case R9207, −4.4 mm from Bregma, **Figure 6A**) with fibers reaching the accessory olfactory bulb where they form a dense plexus of labeled axons showing varicosities in the granule cell layer (**Figure 6B**). A number of labeled beaded axons could also be observed in the granule cell layer of the main olfactory bulb (**Figure 6C**). Labeling was observed in both anterior and posterior portions of the accessory olfactory bulb.

INJECTIONS IN THE ANTERODORSAL MEDIAL AMYGDALOID NUCLEUS

Injections of biotinylated dextran-amine in the rat anterodorsal medial amygdaloid nucleus yielded a similar labeling (as example see case R8305, −1.8 mm from Bregma, **Figure 7A**) including labeled fibers reaching the accessory olfactory bulb where smooth axons could be observed in the mitral cell layer of the accessory olfactory bulb (**Figure 7B**). Labeled fibers were not observed in the granule cell layer of the accessory olfactory bulb or main olfactory bulb.

INJECTIONS IN THE HIPPOCAMPAL FORMATION

Injections of biotinylated dextran-amine in the rat ventral subiculum gave rise to comparable labeling (as example see case R10207, −4.8 mm from Bregma, **Figure 7C**) with labeled fibers reaching the accessory olfactory bulb where fine, beaded axons could be observed in the granule cell layer (**Figure 7D**). Labeled fibers were not observed in the granule cell layer of the main olfactory bulb.

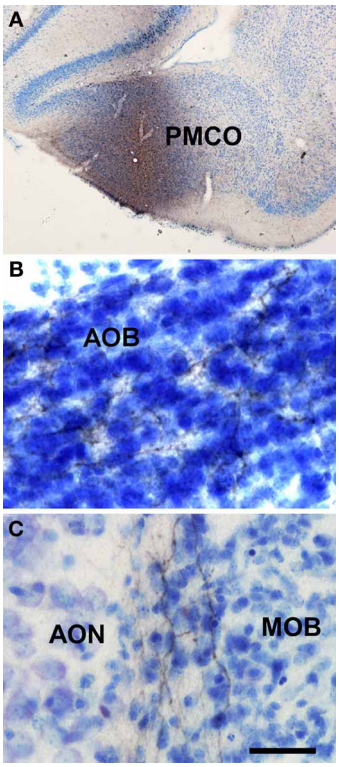

FIGURE 6 | Coronal (A) and sagittal (B,C) sections of the telencephalic hemisphere showing the resulting labeling (B,C) after a biotinylated dextran-amine injection in the rat posteromedial cortical amygdala (A). Abbreviations: AOB, accessory olfactory bulb; AON, anterior olfactory nucleus; MOB, main olfactory bulb; PMCO, posteromedial cortical amygdala. Scale bar for **A**: 800 μm, **B,C**: 40 μm.

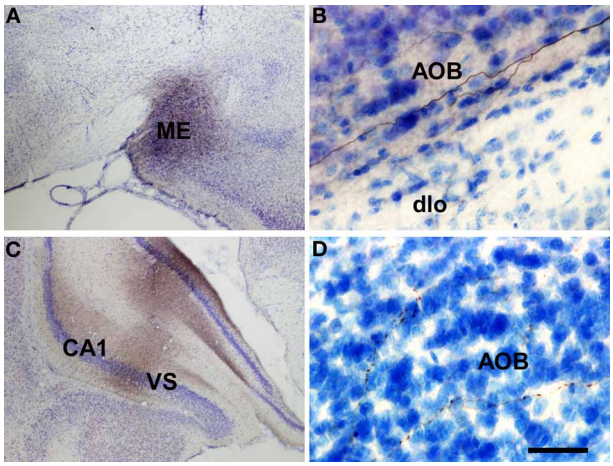

FIGURE 7 | Coronal (A,C) and sagittal (B,D) sections of the telencephalic hemisphere showing the resulting labeling (B,D) after biotinylated dextran-amine injections in the rat anterodorsal medial amygdaloid nucleus (A) and ventral subiculum (C), respectively. Abbreviations: AOB, accessory olfactory bulb; CA1, field CA1 of the hippocampus; dlo, dorsal lateral olfactory tract; ME, medial amygdala; VS, ventral subiculum. Scale bar for **A**: 800 μm, **B,C**: 40 μm.

DISCUSSION

The aim of this work has been to investigate the possibility that olfactory and vomeronasal system can interact anatomically regarding their centrifugal telencephalic afferent connections. Namely, the possibility that olfactory-recipient structures project to the accessory olfactory bulb; that vomeronasal-recipient structures project to the main olfactory bulb; or, that mixed chemosensory or non-chemosensory structures project to both the main and accessory olfactory bulbs.

Our results after retrograde tracing experiments in the main and accessory olfactory bulbs and confirmation anterograde tracing experiments show that, as already reported, olfactory-recipient structures (the anterior olfactory nucleus, the piriform cortex, the cortex-amygdala transition zone, the olfactory tubercle, the nucleus of the lateral olfactory tract, the anterior, anterior cortial and posterolateral cortical amygdalae, and the lateral entorhinal cortex) project back to the main olfactory bulb; and that vomeronasal-recipient structures (the bed nuclei of the stria terminalis and of the accessory olfactory tract and the anterior medial and posteromedial cortical amygdalae) project back to the accessory olfactory bulb. In addition, a pure olfactory-recipient such as the piriform cortex structure also projects to the accessory olfactory bulb; a pure vomeronasal-recipient structure such as the posteromedial cortical amygdaloid nucleus could also project to the main olfactory bulb; a mixed chemosensory-recipient structure such as the anterodorsal medial amygdaloid nucleus project to both the main and accessory olfactory bulb; and, finally, non-chemosensory structures such as the nucleus of the diagonal band project to both bulbs and the ventral subiculum and CA1 project to the accessory olfactory bulb (**Table 1**).

NEUROANATOMICAL REMARKS

In general, our data are in agreement with previous studies regarding the centrifugal telencephalic afferent connections to the main olfactory bulb arising from the anterior olfactory nucleus, piriform cortex, nucleus of the diagonal band, the olfactory tubercle, the nucleus of the lateral olfactory tract, the anterior and posterolateral cortical amygdalae, and the lateral entorhinal cortex (Price and Powell, 1970; Raisman, 1972; Broadwell and Jacobowitz, 1976; Davis et al., 1978; de Olmos et al., 1978; Macrides et al., 1981; Luskin and Price, 1983; Shipley and Adamek, 1984; Matsutani and Yamamoto, 2008).

Similarly, our results confirm previous results in the literature regarding telencephalic centrifugal afferent connections to the accessory olfactory bulb arising from the nucleus of the accessory olfactory tract, bed nucleus of the stria terminalis, and medial and posteromedial cortical amygdalae (Raisman, 1972; Barber and Field, 1975; Broadwell and Jacobowitz, 1976; Davis et al., 1978; de Olmos et al., 1978; Barber, 1982; Martinez-Marcos and Halpern, 1999a; Fan and Luo, 2009). Early reports showed a laminar pattern of afferent connections to the accessory olfactory bulb ending in the granule or internal plexiform layers and originating either in the posteromedial cortical amygdala—and coursing through the stria terminalis—or originating in medial amygdala and bed nucleus of the accessory olfactory tract—and traveling

Table 1 | Summary chart of main results.

Injection site	Retrograde labeling	Anterograde labeling
Main olfactory bulb	Anterior olfactory nucleus Nucleus of the diagonal band Piriform cortex Olfactory tubercle Anterior amygdaloid area Nucleus of the lateral olfactory tract Anterior cortical amygdaloid nucleus Cortex-amygdala transition area Anterodorsal medial amygdaloid nucleus Posterolateral cortical amygdaloid nucleus Lateral entorhinal cortex	
Accessory olfactory bulb	Nucleus of the diagonal band Piriform cortex Bed nucleus of the stria terminalis Bed nucleus of the accessory olfactory tract Anterodorsal medial amygdaloid nucleus Posteromedial cortical amygdaloid nucleus Ventral subiculum and CA1	
Piriform cortex		Granule cell layer of the main olfactory bulb Granule cell layer of the accessory olfactory bulb
Posteromedial cortical amygdaloid nucleus		Granule cell layer of the accessory olfactory bulb Granule cell layer of the main olfactory bulb
Anterodorsal medial amygaloid nucleus		Mitral cell layer of the accessory olfactory bulb
Ventral subiculum		Granule cell layer of the accessory olfactory bulb

through the accessory olfactory tract—respectively (Barber and Field, 1975; Barber, 1982). Later, it has been reported a centrifugal GABAergic projection from the bed nucleus of the stria terminalis to the mitral cell layer and another centrifugal glutamatergic projection from the vomeronasal amygdala to the granule cell layer of the accessory olfactory bulb (Fan and Luo, 2009). Our results are in agreement with previous studies and there are likely at least two centrifugal pathways to the accessory olfactory bulb originating from the bed nucleus of the stria terminalis, bed nucleus of the accessory olfactory bulb and anterodorsal medial amygdala and from the rest of the medial amygdala and posteromedial cortical amygdala.

In addition, our retrograde (**Figures 1**, **2** and **3**) and anterograde (**Figure 5**) tracing experiments demonstrate that the piriform cortex, a pure olfactory-recipient structure, project back to both the main and accessory olfactory bulbs. Since the dorsal portion of the olfactory tract courses between the mitral and granule cell layers of the accessory olfactory bulb, the possibility that axons traveling to the main olfactory bulb were affected in retrograde tracing experiments aimed at the accessory olfactory bulb cannot be discarded (Martinez-Marcos and Halpern, 1999a) (**Figure 3**). Anterograde experiments, however, confirm a projection from the pirifrom cortex to the granule cell layer of the accessory olfactory bulb (**Figure 5**).

Our results after injection centered in the posteromedial cortical amygdaloid nucleus suggest a possible projection from this vomeronasal structure to the main olfactory bulb (**Figure 6**). The fact that retrograde tracing experiments in the main olfactory bulb do not confirm this projection (**Figures 1** and **2**) indicate that further experiments are needed prior to ratify it.

Interestingly, our data after retrograde tracing experiments show that the anterior medial amygdaloid nucleus, which has been reported to be a mixed chemosensory structure (anteroventral division) since it receives both olfactory and vomeronasal inputs (Pro-Sistiaga et al., 2007) critical for sexual behaviors (Kang et al., 2009, 2011b), project back (anterodorsal division) to both the main and accessory olfactory bulbs (**Figures 1**, **2**, **3** and **4**). Our anterograde tracing experiments, however, do not confirm this projection (**Figure 7**). Our interpretation is that this discrepancy is probably due to the fact that the injections in the anterodorsal medial amygdaloid nucleus are not massive enough to fill up the small number of cells in this structure projecting to the bulbs. Therefore, the anterior medial amgydaloid nucleus could be a mixed chemosensory structure not only regarding the afferent but also the efferent connections to the bulbs. The importance of this pathway is supported by behavioral data (Martel and Baum, 2009).

The olfactory bulbs receive a number of non-chemosensory, modulatory centrifugal inputs (Matsutani and Yamamoto, 2008). Namely, our results show a minor telencephalic projection arising from the nucleus of the diagonal band to the main (**Figures 1** and **2**) and accessory (**Figure 3**) bulbs. This projection appears to be cholinergic (Macrides et al., 1981; Zaborszky et al., 1986; Zheng et al., 1987; Kunze et al., 1992) and it has a critical role in olfactory learning (Fletcher and Chen, 2010). In fact, cholinergic inputs from the nucleus of the diagonal band are established

onto dendrites of newly-born granule cells in the olfactory bulbs and are essential for survival of new neurons and olfactory processing (Kiselycznyk et al., 2006; Whitman and Greer, 2007; Mouret et al., 2009).

Finally, our present results (**Figures 3** and **7**) and previous reports (Cenquizca and Swanson, 2007; de la Rosa-Prieto et al., 2009) confirm a projection from the ventral subiculum and CA1 to the granule cell layer of the accessory olfactory bulb. The functional significance of this projection is currently unknown.

CONCLUSION

Our results show an extent anatomical interaction between the olfactory and vomeronasal system regarding their centrifugal connections. Apart from feed-back projections from olfactory- and vomeronasal-recipient structures to the main and accessory olfactory bulbs, respectively, a number of dual connections to both bulbs are presented from olfactory, vomeronasal, mixed, and non-chemosensory structures. Globally, these results further stress the idea of mutual interactions between the olfactory and the vomeronasal systems.

ACKNOWLEDGMENTS

This study was supported by the Spanish Ministry of Science and Innovation-FEDER (BFU2010-15729) and the Autonomous Government of Castilla-La Mancha-FEDER (PEIC11-0045-4490).

REFERENCES

Barber, P. C. (1982). Adjacent laminar terminations of two centrifugal afferent pathways to the accessory olfactory bulb in the mouse. *Brain Res.* 245, 215–221.

Barber, P. C., and Field, P. M. (1975). Autoradiographic demonstration of afferent connections of the accessory olfactory bulb in the mouse. *Brain Res.* 85, 201–203.

Belluscio, L., Koentges, G., Axel, R., and Dulac, C. (1999). A map of pheromone receptor activation in the mammalian brain. *Cell* 97, 209–220.

Berghard, A., and Buck, L. B. (1996). Sensory transduction in vomeronasal neurons: evidence for G alpha o, G alpha i2, and adenylyl cyclase II as major components of a pheromone signaling cascade. *J. Neurosci.* 16, 909–918.

Brennan, P., Kaba, H., and Keverne, E. B. (1990). Olfactory recognition: a simple memory system. *Science* 250, 1223–1226.

Broadwell, R. D., and Jacobowitz, D. M. (1976). Olfactory relationships of the telencephalon and diencephalon in the rabbit. III. The ipsilateral centrifugal fibers to the olfactory bulbar and retrobulbar formations. *J. Comp. Neurol.* 170, 321–345.

Carmichael, S. T., Clugnet, M. C., and Price, J. L. (1994). Central olfactory connections in the macaque monkey. *J. Comp. Neurol.* 346, 403–434.

Cenquizca, L. A., and Swanson, L. W. (2007). Spatial organization of direct hippocampal field CA1 axonal projections to the rest of the cerebral cortex. *Brain Res. Rev.* 56, 1–26.

Davis, B. J., Macrides, F., Youngs, W. M., Schneider, S. P., and Rosene, D. L. (1978). Efferents and centrifugal afferents of the main and accessory olfactory bulbs in the hamster. *Brain Res. Bull.* 3, 59–72.

de la Rosa-Prieto, C., Ubeda-Banon, I., Mohedano-Moriano, A., Pro-Sistiaga, P., Saiz-Sanchez, D., Insausti, R., and Martinez-Marcos, A. (2009). Subicular and CA1 hippocampal projections to the accessory olfactory bulb. *Hippocampus* 19, 124–129.

de Olmos, J., Hardy, H., and Heimer, L. (1978). The afferent connections of the main and the accessory olfactory bulb formations in the rat: an experimental HRP-study. *J. Comp. Neurol.* 181, 213–244.

Devor, M. (1976). Fiber trajectories of olfactory bulb efferents in the hamster. *J. Comp. Neurol.* 166, 31–47.

Dulac, C., and Axel, R. (1995). A novel family of genes encoding putative pheromone receptors in mammals. *Cell* 83, 195–206.

Fan, S., and Luo, M. (2009). The organization of feedback projections in a pathway important for processing pheromonal signals. *Neuroscience* 161, 489–500.

Fletcher, M. L., and Chen, W. R. (2010). Neural correlates of olfactory learning: critical role of centrifugal neuromodulation. *Learn. Mem.* 17, 561–570.

Franklin, K. B. J., and Paxinos, G. (2008). *The Mouse Brain in Stereotaxic Coordinates.* San Diego, CA: Academic Press.

Gutierrez-Castellanos, N., Martinez-Marcos, A., Martinez-Garcia, F., and Lanuza, E. (2010). Chemosensory function of the amygdala. *Vitam. Horm.* 83, 165–196.

Halpern, M. (1987). The organization and function of the vomeronasal system. *Annu. Rev. Neurosci.* 10, 325–362.

Halpern, M., Jia, C., and Shapiro, L. S. (1998a). Segregated pathways in the vomeronasal system. *Microsc. Res. Tech.* 41, 519–529.

Halpern, M., and Martinez-Marcos, A. (2003). Structure and function of the vomeronasal system: an update. *Prog. Neurobiol.* 70, 245–318.

Halpern, M., Shapiro, L. S., and Jia, C. (1998b). Heterogeneity in the accessory olfactory system. *Chem. Senses* 23, 477–481.

Herrada, G., and Dulac, C. (1997). A novel family of putative pheromone receptors in mammals with a topographically organized and sexually dimorphic distribution. *Cell* 90, 763–773.

Jansen, H. T., Iwamoto, G. A., and Jackson, G. L. (1998). Central connections of the ovine olfactory bulb formation identified using wheat germ agglutinin-conjugated horseradish peroxidase. *Brain Res. Bull.* 45, 27–39.

Jia, C., and Halpern, M. (1996). Subclasses of vomeronasal receptor neurons: differential expression of G proteins (Gi alpha 2 and G(o alpha)) and segregated projections to the accessory olfactory bulb. *Brain Res.* 719, 117–128.

Kang, N., Baum, M. J., and Cherry, J. A. (2009). A direct main olfactory bulb projection to the 'vomeronasal' amygdala in female mice selectively responds to volatile pheromones from males. *Eur. J. Neurosci.* 29, 624–634.

Kang, N., Baum, M. J., and Cherry, J. A. (2011a). Different profiles of main and accessory olfactory bulb mitral/tufted cell projections revealed in mice using an anterograde tracer and a whole-mount, flattened cortex preparation. *Chem. Senses* 36, 251–260.

Kang, N., McCarthy, E. A., Cherry, J. A., and Baum, M. J. (2011b). A sex comparison of the anatomy and function of the main olfactory bulb-medial amygdala projection in mice. *Neuroscience* 172, 196–204.

Keller, M., Baum, M. J., Brock, O., Brennan, P. A., and Bakker, J. (2009). The main and the accessory olfactory systems interact in the control of mate recognition and sexual behavior. *Behav. Brain Res.* 200, 268–276.

Keverne, E. B., and Brennan, P. A. (1996). Olfactory recognition memory. *J. Physiol. Paris* 90, 399–401.

Kiselycznyk, C. L., Zhang, S., and Linster, C. (2006). Role of centrifugal projections to the olfactory bulb in olfactory processing. *Learn. Mem.* 13, 575–579.

Kosel, K. C., Van Hoesen, G. W., and West, J. R. (1981). Olfactory bulb projections to the parahippocampal area of the rat. *J. Comp. Neurol.* 198, 467–482.

Kunze, W. A., Shafton, A. D., Kem, R. E., and McKenzie, J. S. (1992). Intracellular responses of olfactory bulb granule cells to stimulating the horizontal diagonal band nucleus. *Neuroscience* 48, 363–369.

Larriva-Sahd, J. (2008). The accessory olfactory bulb in the adult rat: a cytological study of its cell types, neuropil, neuronal modules, and interactions with the main olfactory system. *J. Comp. Neurol.* 510, 309–350.

Leinders-Zufall, T., Brennan, P., Widmayer, P., Chandramani, P., Maul-Pavicic, A., Jager, M., Li, X. H., Breer, H., Zufall, F., and Boehm, T. (2004). MHC class I peptides as chemosensory signals in the vomeronasal organ. *Science* 306, 1033–1037.

Leinders-Zufall, T., Lane, A. P., Puche, A. C., Ma, W., Novotny, M. V., Shipley, M. T., and Zufall, F. (2000). Ultrasensitive pheromone detection by mammalian vomeronasal neurons. *Nature* 405, 792–796.

Licht, G., and Meredith, M. (1987). Convergence of main and accessory olfactory pathways onto single neurons in the hamster amygdala. *Exp. Brain Res.* 69, 7–18.

Lin, W., Arellano, J., Slotnick, B., and Restrepo, D. (2004). Odors detected by mice deficient in cyclic nucleotide-gated channel subunit A2 stimulate the main olfactory system. *J. Neurosci.* 24, 3703–3710.

Luskin, M. B., and Price, J. L. (1983). The topographic organization of associational fibers of the olfactory system in the rat, including centrifugal fibers to the olfactory bulb. *J. Comp. Neurol.* 216, 264–291.

Macrides, F., Davis, B. J., Youngs, W. M., Nadi, N. S., and Margolis, F. L. (1981). Cholinergic and catecholaminergic afferents to the olfactory bulb in the hamster: a neuroanatomical, biochemical, and histochemical investigation. *J. Comp. Neurol.* 203, 495–514.

Martel, K. L., and Baum, M. J. (2009). A centrifugal pathway to the mouse accessory olfactory bulb from the medial amygdala conveys gender-specific volatile pheromonal signals. *Eur. J. Neurosci.* 29, 368–376.

Martinez-Marcos, A. (2009). On the organization of olfactory and vomeronasal cortices. *Prog. Neurobiol.* 87, 21–30.

Martinez-Marcos, A., and Halpern, M. (1999a). Differential centrifugal afferents to the anterior and posterior accessory olfactory bulb. *Neuroreport* 10, 2011–2015.

Martinez-Marcos, A., and Halpern, M. (1999b). Differential projections from the anterior and posterior divisions of the accessory olfactory bulb to the medial amygdala in the opossum, *Monodelphis domestica*. *Eur. J. Neurosci.* 11, 3789–3799.

Martinez-Marcos, A., and Halpern, M. (2006). Efferent connections of the main olfactory bulb in the opossum (*Monodelphis domestica*): a characterization of the olfactory entorhinal cortex in a marsupial. *Neurosci. Lett.* 395, 51–56.

Matsunami, H., and Buck, L. B. (1997). A multigene family encoding a diverse array of putative pheromone receptors in mammals. *Cell* 90, 775–784.

Matsutani, S., and Yamamoto, N. (2008). Centrifugal innervation of the mammalian olfactory bulb. *Anat. Sci. Int.* 83, 218–227.

Meyer, R. P. (1981). Central connections of the olfactory bulb in the American opossum (*Didelphys virginiana*): a light microscopic degeneration study. *Anat. Rec.* 201, 141–156.

Mohedano-Moriano, A., Martinez-Marcos, A., Munoz, M., Arroyo-Jimenez, M. M., Marcos, P., Artacho-Perula, E., Blaizot, X., and Insausti, R. (2005). Reciprocal connections between olfactory structures and the cortex of the rostral superior temporal sulcus in the *Macaca fascicularis* monkey. *Eur. J. Neurosci.* 22, 2503–2518.

Mohedano-Moriano, A., Pro-Sistiaga, P., Ubeda-Banon, I., Crespo, C., Insausti, R., and Martinez-Marcos, A. (2007). Segregated pathways to the vomeronasal amygdala: differential projections from the anterior and posterior divisions of the accessory olfactory bulb. *Eur. J. Neurosci.* 25, 2065–2080.

Mohedano-Moriano, A., Pro-Sistiaga, P., Ubeda-Banon, I., de la Rosa-Prieto, C., Saiz-Sanchez, D., and Martinez-Marcos, A. (2008). V1R and V2R segregated vomeronasal pathways to the hypothalamus. *Neuroreport* 19, 1623–1626.

Mouret, A., Murray, K., and Lledo, P. M. (2009). Centrifugal drive onto local inhibitory interneurons of the olfactory bulb. *Ann. N.Y. Acad. Sci.* 1170, 239–254.

Mucignat-Caretta, C. (2010). The rodent accessory olfactory system. *J. Comp. Physiol. A Neuroethol. Sens. Neural Behav. Physiol.* 196, 767–777.

Oboti, L., Schellino, R., Giachino, C., Chamero, P., Pyrski, M., Leinders-Zufall, T., Zufall, F., Fasolo, A., and Peretto, P. (2011). Newborn interneurons in the accessory olfactory bulb promote mate recognition in female mice. *Front. Neurosci.* 5:113. doi: 10.3389/fnins.2011.00113

Paxinos, G., and Watson, C. (2007). *The Rat Brain in Stereotaxic Coordinates.* Amsterdam: Academic Press.

Peele, P., Salazar, I., Mimmack, M., Keverne, E. B., and Brennan, P. A. (2003). Low molecular weight constituents of male mouse urine mediate the pregnancy block effect and convey information about the identity of the mating male. *Eur. J. Neurosci.* 18, 622–628.

Price, J. L., and Powell, T. P. (1970). An experimental study of the origin and the course of the centrifugal fibres to the olfactory bulb in the rat. *J. Anat.* 107, 215–237.

Pro-Sistiaga, P., Mohedano-Moriano, A., Ubeda-Banon, I., de la Rosa-Prieto, C., Saiz-Sanchez, D., and Martinez-Marcos, A. (2008). Projections of olfactory bulbs to the olfactory and vomeronasal cortices. *Neuroreport* 19, 1541–1544.

Pro-Sistiaga, P., Mohedano-Moriano, A., Ubeda-Banon, I., del Mar Arroyo-Jimenez, M., Marcos, P., Artacho-Perula, E., Crespo, C., Insausti, R., and Martinez-Marcos, A. (2007). Convergence of olfactory and vomeronasal projections in the rat basal telencephalon. *J. Comp. Neurol.* 504, 346–362.

Raisman, G. (1972). An experimental study of the projection of the amygdala to the accessory olfactory bulb and its relationship to the concept of a dual olfactory system. *Exp. Brain Res.* 14, 395–408.

Restrepo, D., Arellano, J., Oliva, A. M., Schaefer, M. L., and Lin, W. (2004). Emerging views on the distinct but related roles of the main and accessory olfactory systems in responsiveness to chemosensory signals in mice. *Horm. Behav.* 46, 247–256.

Rodriguez, I., Feinstein, P., and Mombaerts, P. (1999). Variable patterns of axonal projections of sensory neurons in the mouse vomeronasal system. *Cell* 97, 199–208.

Ryba, N. J., and Tirindelli, R. (1997). A new multigene family of putative pheromone receptors. *Neuron* 19, 371–379.

Salazar, I., and Brennan, P. A. (2001). Retrograde labelling of mitral/tufted cells in the mouse accessory olfactory bulb following local injections of the lipophilic tracer DiI into the vomeronasal amygdala. *Brain Res.* 896, 198–203.

Scalia, F., and Winans, S. S. (1975). The differential projections of the olfactory bulb and accessory olfactory bulb in mammals. *J. Comp. Neurol.* 161, 31–55.

Scott, J. W., McBride, R. L., and Schneider, S. P. (1980). The organization of projections from the olfactory bulb to the piriform cortex and olfactory tubercle in the rat. *J. Comp. Neurol.* 194, 519–534.

Shammah-Lagnado, S. J., and Negrao, N. (1981). Efferent connections of the olfactory bulb in the opossum (Didelphis marsupialis aurita): a Fink-Heimer study. *J. Comp. Neurol.* 201, 51–63.

Shipley, M. T., and Adamek, G. D. (1984). The connections of the mouse olfactory bulb: a study using orthograde and retrograde transport of wheat germ agglutinin conjugated to horseradish peroxidase. *Brain Res. Bull.* 12, 669–688.

Skeen, L. C., and Hall, W. C. (1977). Efferent projections of the main and the accessory olfactory bulb in the tree shrew (*Tupaia glis*). *J. Comp. Neurol.* 172, 1–35.

Spehr, M., Kelliher, K. R., Li, X. H., Boehm, T., Leinders-Zufall, T., and Zufall, F. (2006a). Essential role of the main olfactory system in social recognition of major histocompatibility complex peptide ligands. *J. Neurosci.* 26, 1961–1970.

Spehr, M., Spehr, J., Ukhanov, K., Kelliher, K. R., Leinders-Zufall, T., and Zufall, F. (2006b). Parallel processing of social signals by the mammalian main and accessory olfactory systems. *Cell. Mol. Life Sci.* 63, 1476–1484.

Taniguchi, K., and Saito, S. (2011). Phylogenic outline of the olfactory system in vertebrates. *J. Vet. Med. Sci.* 73, 139–147.

Trinh, K., and Storm, D. R. (2004). Detection of odorants through the main olfactory epithelium and vomeronasal organ of mice. *Nutr. Rev.* 62, S189–S192. discussion S224–S241.

Turner, B. H., Gupta, K. C., and Mishkin, M. (1978). The locus and cytoarchitecture of the projection areas of the olfactory bulb in *Macaca mulatta*. *J. Comp. Neurol.* 177, 381–396.

Ubeda-Banon, I., Novejarque, A., Mohedano-Moriano, A., Pro-Sistiaga, P., de la Rosa-Prieto, C., Insausti, R., Martinez-Garcia, F., Lanuza, E., and Martinez-Marcos, A. (2007). Projections from the posterolateral olfactory amygdala to the ventral striatum: neural basis for reinforcing properties of chemical stimuli. *BMC Neurosci.* 8, 103.

Ubeda-Banon, I., Novejarque, A., Mohedano-Moriano, A., Pro-Sistiaga, P., Insausti, R., Martinez-Garcia, F., Lanuza, E., and Martinez-Marcos, A. (2008). Vomeronasal inputs to the rodent ventral striatum. *Brain Res. Bull.* 75, 467–473.

Ubeda-Banon, I., Pro-Sistiaga, P., Mohedano-Moriano, A., Saiz-Sanchez, D., de la Rosa-Prieto, C., Gutierrez-Castellanos, N., Lanuza, E., Martinez-Garcia, F., and Martinez-Marcos, A. (2011). Cladistic analysis of olfactory and vomeronasal systems. *Front. Neuroanat.* 5:3. doi: 10.3389/fnana.2011.00003

Von Campenhausen, H., and Mori, K. (2000). Convergence of segregated pheromonal pathways from the accessory olfactory bulb to the cortex in the mouse. *Eur. J. Neurosci.* 12, 33–46.

Wang, Z., Balet Sindreu, C., Li, V., Nudelman, A., Chan, G. C., and Storm, D. R. (2006). Pheromone detection in male mice depends on signaling through the type 3 adenylyl cyclase in the main olfactory epithelium. *J. Neurosci.* 26, 7375–7379.

Whitman, M. C., and Greer, C. A. (2007). Synaptic integration of adult-generated olfactory bulb granule cells: basal axodendritic centrifugal input precedes apical dendrodendritic local circuits. *J. Neurosci.* 27, 9951–9961.

Winans, S. S., and Scalia, F. (1970). Amygdaloid nucleus: new afferent input from the vomeronasal organ. *Science* 170, 330–332.

Xu, F., Schaefer, M., Kida, I., Schafer, J., Liu, N., Rothman, D. L., Hyder, F., Restrepo, D., and Shepherd, G. M. (2005). Simultaneous activation of mouse main and accessory olfactory bulbs by odors or pheromones. *J. Comp. Neurol.* 489, 491–500.

Zaborszky, L., Carlsen, J., Brashear, H. R., and Heimer, L. (1986). Cholinergic and GABAergic afferents to the olfactory bulb in the rat with special emphasis on the projection neurons in the nucleus of the horizontal limb of the diagonal band. *J. Comp. Neurol.* 243, 488–509.

Zheng, L. M., Ravel, N., and Jourdan, F. (1987). Topography of centrifugal acetylcholinesterase-positive fibres in the olfactory bulb of the rat: evidence for original projections in atypical glomeruli. *Neuroscience* 23, 1083–1093.

Conflict of Interest Statement: The authors declare that the research was conducted in the absence of any commercial or financial relationships that could be construed as a potential conflict of interest.

Received: 15 April 2012; paper pending published: 02 May 2012; accepted: 12 May 2012; published online: 29 May 2012.

Citation: Mohedano-Moriano A, de la Rosa-Prieto C, Saiz-Sanchez D, Ubeda-Bañon I, Pro-Sistiaga P, de Moya-Pinilla M and Martinez-Marcos A (2012) Centrifugal telencephalic afferent connections to the main and accessory olfactory bulbs. Front. Neuroanat. ***6****:19. doi: 10.3389/fnana.2012.00019*

frontiers in
NEUROANATOMY

REVIEW ARTICLE
published: 09 November 2012
doi: 10.3389/fnana.2012.00046

One nose, one brain: contribution of the main and accessory olfactory system to chemosensation

***Carla Mucignat-Caretta*[1]*, *Marco Redaelli*[1] *and Antonio Caretta*[2]**

[1] *Department of Molecular Medicine, University of Padova, Padova, Italy*
[2] *Department of Pharmaceutical Sciences, University of Parma, Parma, Italy*

Edited by:
Jorge A. Larriva-Sahd, Universidad Nacional Autónoma de México, Mexico

Reviewed by:
Alino Martinez-Marcos, Universidad de Castilla, Spain
Jorge A. Larriva-Sahd, Universidad Nacional Autónoma de México, Mexico

***Correspondence:**
Carla Mucignat-Caretta, Department of Molecular Medicine, University of Padova, Via Marzolo 3, 35131 Padova, Italy.
e-mail: carla.mucignat@unipd.it

The accessory olfactory system is present in most tetrapods. It is involved in the perception of chemical stimuli, being implicated also in the detection of pheromones. However, it is sensitive also to some common odorant molecules, which have no clear implication in intraspecific chemical communication. The accessory olfactory system may complement the main olfactory system and may contribute different perceptual features to the construction of a unitary representation, which merges the different chemosensory qualities. Crosstalk between the main and accessory olfactory systems occurs at different levels of central processing, in brain areas where the inputs from the two systems converge. Interestingly, centrifugal projections from more caudal brain areas are deeply involved in modulating both main and accessory sensory processing. A high degree of interaction between the two systems may be conceived and partial overlapping appears to occur in many functions. Therefore, the central chemosensory projections merge inputs from different organs to obtain a complex chemosensory picture.

Keywords: vomeronasal organ, nose, olfaction, pheromones

INTRODUCTION

Chemical substances originating from the environment stimulate a variety of receptors hosted in the nasobuccal cavity. While taste and trigeminal sensitivity of the mouth are mainly related to evaluation of food, chemical senses of the nose are devoted to evaluation of external stimuli, related to different environmental aspects, including the detection of dangerous substances, food retrieval, and social interactions (Ma, 2007). The chemical senses of mammalian nose include the main olfactory epithelium and the vomeronasal organ (VNO), that are complemented in their functions by the trigeminal afferents and the receptors located in the organ of Masera and in the ganglion of Gruenenberg (**Figure 1**); the function of the last three supports olfaction in detection of molecules (Breer et al., 2006). Complex interactions are now emerging between the main and accessory olfactory systems, both at anatomical and at functional level.

The main olfactory system originates from the olfactory mucosa and projects to the main olfactory bulb (MOB), while the VNO, described by Jacobson in 1813 (Trotier and Doving, 1998) projects to the accessory olfactory bulb (AOB, see **Figure 2**).

The VNO appears as a derived character in tetrapods (Eisthen, 1992): it is present already in aquatic species from the Devonian period, before transition to land (Swaney and Keverne, 2009). Later, it has been lost in some species, including crocodilians, cetaceans, some bats, and primates. The accessory olfactory system may differ in morphology even in closely related species, most probably in relation to functional specialization (for a review, see Salazar and Quinteiro, 2009).

HYPOTHESIS ON THE FUNCTION OF THE ACCESSORY OLFACTORY SYSTEM

Since its first description by Jacobson [translated in Trotier and Doving (1998)], the VNO has been described as a sensory organ, possibly in support of the sense of smell, but its precise role in chemosensation is still poorly understood. The first functional investigation of the accessory olfactory system pointed to a general chemosensation role. One old anatomical study suggested that the VNO, being filled with mucus, should be sensitive to water-borne molecules (Broman, 1920). Electrophysiological recordings preceded any other functional testing, and suggested that the VNO was activated by mechanical stimuli (Adrian, 1955). A similar mechanical sensitivity was reported also for the mammalian main olfactory epithelium, which was found to activate the MOB in response to odorants and also to the airstream pressure (Adrian, 1942). Responses to common odorants were later recorded in the VNO and its target areas in the brain (Tucker, 1963; Meredith and O'Connell, 1979), however, the idea emerged that the VNO could be sensitive to stimuli that included not only low molecular weight volatiles. According to data on the modulation of reproduction in mice and hamsters, it became clear that a direct contact of the snout with the chemical stimulus was mandatory for obtaining a modification of the hormonal milieu, in order to facilitate reproductive responses. For example, a peptide present in the urine of mice was proven to stimulate the anticipation of puberty in female mice via the stimulation of the VNO (Vandenbergh et al., 1975; Mucignat-Caretta et al., 1995), and the female pheromone in vaginal fluid of hamster was demonstrated to be a protein (Singer et al., 1986). This kind of stimuli could hardly be regarded as "volatile," as confirmed by

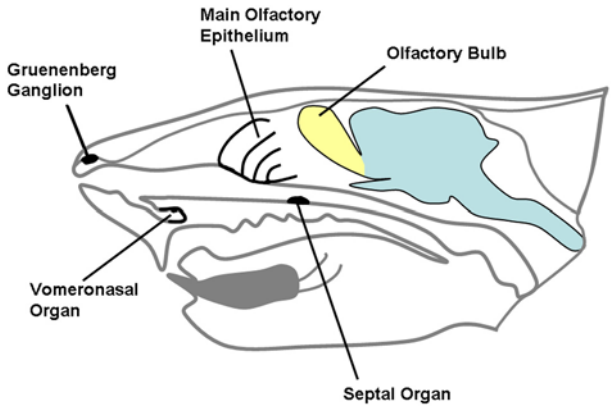

FIGURE 1 | A schematic representation of rodent head in the sagittal plane. The different chemosensory systems of the nasal cavity are indicated.

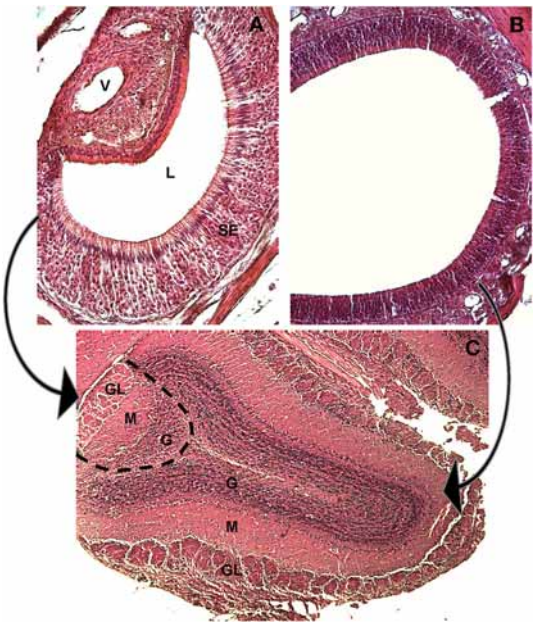

FIGURE 2 | The main and accessory olfactory epithelia of the mouse, and their first central targets, the main and accessory olfactory bulbs. Hematoxylin-eosin staining, mouse at 30 days of age. **(A)** A coronal section of the VNO, medial to the right, lateral to the left, dorsal to the top. The sensory epithelium (SE), the lumen (L) and the vessel (V) are indicated. **(B)** A coronal section of the main olfactory epithelium, dorsal to the upper right. **(C)** A horizontal section through the main and accessory olfactory bulb. The dotted line represents the border between the MOB (to the right) and the AOB (to the left). The arrows indicate the projections from the MOE to the main olfactory bulb (right) and from the VNO to the AOB (left). In both bulbs the main structures are indicated: (GL) glomerular layer, (M) mitral cell layer, (G) granular layer.

the necessity of direct contact of the snout with the pheromonal source, for the induction of pheromonal effects on the neurohormonal system. A major question regarded the type of stimulus that could access to the VNO, because it was not clear that high-molecular weight molecules could be transported inside the VNO lumen. At variance with the main olfactory epithelium, that receives the stimuli only via the airstream flowing through the turbinates, in the VNO an active vascular pumping mechanism allows large molecules dissolved in liquid to reach the organ (Meredith and O'Connell, 1979). By sucking up the liquid, large molecules or even particles are able to reach the VNO lumen (Wysocki et al., 1980; Mucignat-Caretta, 2010). Therefore, at least in some instances, the stimuli that activate the VNO are chemically different from those that activate the main olfactory system.

Lesion studies suggested a role for the accessory olfactory system in the modulation of reproductive physiology induced by pheromones: this is possible because the accessory olfactory system directly projects to the hypothalamus. However, a misunderstanding arose during the seventies, when several papers correctly pointed out that the VNO is connected with specific nuclei in the amygdala (Winans and Scalia, 1970; Scalia and Winans, 1975), and that information from the amygdala could modulate back the activity in the AOB, thus depicting an interactive circuit for the processing of inputs from the VNO (Raisman, 1972). Herein, the concept of a dual olfactory system emerged, with the main olfactory system devoted to the conscious perception of volatile odorants, due to its cortical projections, and the accessory olfactory system devoted to pheromones perception, due to its subcortical connections. Later on, this concept has been misinterpreted as an absolute specialization, and several studies assumed that information processing in the main and accessory olfactory system pertained to two different classes of stimuli, general odorants and pheromones, respectively. This is apparently not the case, since it is clear now that both systems are able to respond to either class of molecules, and that their central projections are heavily interconnected (Pro-Sistiaga et al., 2007), as summarized below.

Olfactory function during development

A possible distinction in the function of the main and accessory olfactory systems concerns their role in the first days of life. Immature newborns, like murine rodents, depend on tactile and olfactory stimuli for their survival. Several studies indicated that the main olfactory system is functional at birth, being involved in the pup's perception of the dam's pheromones (Teicher et al., 1980; Greer et al., 1982). In rabbit, the mammary pheromone is detected only by the main olfactory system (Charra et al., 2012), and in rat at least half of the main olfactory mucosa must be functional in order to drive the pup to the nipple (Kawagishi et al., 2009). Also cognitive functions related to olfaction are functional at birth. Olfactory learning in rodents is facilitated immediately after birth, in order to provide strong association among stimuli essential for survival (Miller and Spear, 2008). Processing of main olfactory signals, related to associative learning, is dependent upon the dense serotonergic innervation of the MOB mitral cells, that can be detected after birth (McLean et al., 1995). Olfactory learning is particularly facilitated during nursing, from feeding throughout the postprandial period: during this time, newborns easily learn associations between odors and other stimuli in order to acquire the characteristics of their familiar environment (Serra et al., 2009). However,

the features of neonate olfactory learning are different from those of adults, suggesting a high degree of specialization in olfactory processing in the post partum period: for example, facilitation for learning of olfactory associations is accompanied by an increased difficulty in learning aversions during the first week, while the adult pattern of events emerges during the second postnatal week, in coincidence with the termination of the corticosterone hyporesponsive period (Moriceau et al., 2006). In the olfactory bulb, the refinement of electrical activity follows a three stage process: an immature period until day 11 of extrauterine life, a transition period until day 17 and a mature period thereafter (Sugai et al., 2005). A similar shift in activation pattern, revealed by c-Fos immunohistochemistry, has been detected in the rat piriform cortex (Illig, 2007). The modifications in olfactory processing in these two olfactory areas parallel neuro-hormonal and behavioral maturation. The responses to the same chemosignal, in fact, change during development of the receiver, as the hedonic value of male mice pheromones changes from infancy to puberty and adult age (Mucignat-Caretta et al., 1998).

The role of the accessory olfactory system during the first postnatal days is less clear than the role of the main olfactory system. The VNO is electrically active *in utero* (Mendoza and Szabo, 1988), but its functional role in the newborn is still obscure, albeit its structural characteristics suggest an advanced stage of functional maturation at birth (Coppola and O'Connell, 1989). Conceivably, in the first days of life, the main olfactory system has a major role in pup survival. However, recent evidence confirms that in mice the vomeronasal duct is open at birth and the sensory neurons do release neurotransmitter in the AOB already one day after birth; moreover, the precise connectivity of incoming axons is modulated by the exposure to pheromonal cues in the first postnatal days (Hovis et al., 2012). Contrary to previous data, this paper suggests a deeper involvement of the accessory olfactory system in chemosensory processing during the first postnatal days.

Likewise, the mother uses the olfactory system to discriminate its newborn. Apparently, the main role in the discrimination of the individual odor of each pup pertains to the main olfactory system (Keller and Lévy, 2012). Profound modifications in the synaptic circuits of the MOB take place at parturition, so that the mother learns her own pup odor, and shifts its behavior from aversion, as present in the virgin female, to maternal care (Lévy and Keller, 2009). However, maternal behavior onset benefits from both main and accessory olfactory information. In fact, the detection of dodecyl propionate, a pheromone produced by the rat pup preputial gland, is mediated by the VNO, thus triggering anogenital licking in the dam, a behavior necessary for the pup's survival (Brouette-Lahlou et al., 1999). Therefore, both the main and accessory olfactory systems are involved in mother-pup interactions.

FUNCTIONAL OVERLAPPING OF MAIN AND ACCESSORY OLFACTORY SYSTEMS IN RESPONSE TO COMMON VOLATILES AND SOCIAL ODORS OR PHEROMONES

Chemosensation mediates many aspects of social interactions in mammals not only during infancy but also afterwards, including sexual, territorial, and aggressive behaviors. The molecules that are involved in such interactions are not completely known, as well as their receptors. Different types of chemosensory receptors are present in the various receptors organs of the nose. They include the main olfactory epithelium, the VNO, the septal organ, and the Gruenenberg ganglion. The sensory neurons in these organs host various types of receptor molecules: olfactory receptors, V1R, the first class of vomeronasal receptors, V2Rs, the second class of vomeronasal receptors, trace-amine-associated receptors, formyl-peptide receptors, and guanylil-cyclase D receptors (for a review, see Fleischer et al., 2009).

The key distinction between main and accessory olfactory system led to the idea of a functional specialization of the two systems. However, from early studies it was clear that VNO stimulation did not coincide with pheromonal stimulation, since some pheromones could stimulate also the main olfactory epithelium (Meredith, 1998). The two systems instead differ in their projections to different amygdala nuclei, being the VNO linked to activation of medial amygdala (Samuelsen and Meredith, 2009), which in turn affects the luteinizing-hormone releasing hormone (LHRH) release from the hypothalamus. LHRH is released in female rodents after male chemostimulation of the accessory, not the main, olfactory system (Meredith, 1991), and involves long-term effects via the vomeronasal amygdala (Mucignat-Caretta et al., 2006). On the other hand, in both the main and accessory olfactory system vasopressin neurons are present to facilitate the social odor identification (Wacker et al., 2011): hence, the main olfactory system is mainly involved in learning and recognition of social odors for discrimination of individuals, pups, mates, or conspecifics (Sanchez-Andrade and Kendrick, 2009), while the accessory olfactory system may activate also the neurohormonal pathway. The sexual dimorphism of accessory olfactory system and the presence therein of steroid receptors support its involvement in reproductive/neuroendocrine modulation (Guillamon and Segovia, 1997). In turn, sociosexual interactions like mating may influence the rate of cell differentiation in the accessory, but not in the MOB (Corona et al., 2011).

Apparently, both the main and accessory olfactory system work together to allow successful social interactions: the first approach to airborne chemicals may be mediated by the main olfactory system, that in case of detection of interesting stimuli may trigger the active exploratory behavior, that is necessary for VNO pump activation (O'Connell and Meredith, 1984; Keverne, 2004).

VARIOUS TYPES OF STIMULI MAY ACTIVATE THE ACCESSORY OLFACTORY SYSTEM

The VNO handles different types of meaningful stimuli; however, stimulus processing appears more selective in the VNO, compared to the main olfactory epithelium (Luo and Katz, 2004). Chemical signals related to strain and individuals are encoded by populations of VNO neurons, while some cells respond to gender-specific cues (He et al., 2008). The VNO is also involved in the perception of alarm pheromones (Kiyokawa et al., 2007), a function it shares with the Gruenenberg ganglion (Brechbühl et al., 2008), and participates in the perception of predator

chemosignals (Masini et al., 2010). The VNO may mediate also the behavioral reactions to non-pheromonal chemicals (Inagaki et al., 2010).

Vomeronasal neurons respond to known low-molecular weight urinary molecules (Del Punta et al., 2002) and volatile pheromones (Leinders-Zufall et al., 2000), mainly by activating V1 receptors (Boschat et al., 2002). However, vomeronasal neurons respond also to non-volatile chemosignals, like sulfated steroids (Nodari et al., 2008) and proteins, for example lipocalins like alpha-2U (Krieger et al., 1999) or peptides excreted by exocrine glands (Kimoto et al., 2005; Taha et al., 2009) or related to MHC (Leinders-Zufall et al., 2004). A class of VNO receptor cells express formyl-peptide receptors, which may respond to peptides from bacteria or related to the immune system (Liberles et al., 2009; Rivière et al., 2009). Some of the non-volatile chemosignals appear intrinsically attractive and may act as unconditioned stimuli for associated odorants (Martínez-Ricós et al., 2008).

Different populations of VNO receptors mediate responses to volatile pheromones and to proteins that are, respectively, perceived from cells bearing V1Rs, located in the apical part of the VNO mucosa, and from basal neurons, expressing V2Rs (Krieger et al., 1999). Complex mixtures involved in intraspecific communication, like urine, differentially activate various populations of receptors in the AOB (Dudley and Moss, 1999). Moreover, some cells in the apical layer of the VNO have been shown to express odorant receptors and project to the anterior AOB: they may sustain the responsivity of VNO/AOB to common odorants, in addition to cells expressing the vomeronasal receptors (Lévai et al., 2006).

Therefore, the VNO appears to be involved in the perception of different chemical stimuli, which may selectively activate various cells.

DIFFERENT TYPES OF STIMULI INDUCE VARIOUS RESPONSES IN THE ACCESSORY OLFACTORY SYSTEM

VNO cells activity was firstly recorded in response to general odorants and also to volatile molecules that act as pheromones (Tucker, 1963; Meredith and O'Connell, 1979). Later on, the activity of the rodent VNO was investigated mainly by studying the responsiveness to putative pheromones, either volatiles or not (for a review, see Bigiani et al., 2005). The electrical activity induced by odorants was in general less studied, on the assumption that the main role of the VNO should be in the perception of pheromones. It is now clear that this assumption is an oversimplification of both the role of the VNO and of the signaling function of pheromones or social odors in intraspecific chemical communication.

In mice, the exposure to urinary odors leads to the activation of the VNO and the AOB, which respond differently from the main olfactory system. The responses to urinary stimuli appear to be mediated in VNO receptors by inositol-trisphosphate, while most olfactory receptors act via the cAMP cascade (Thompson et al., 2004). Different cells in rat and mouse VNO are selective for the urinary stimuli originated from each gender (Inamura et al., 1999; Holy et al., 2000). In fact, while main olfactory receptors are broadly tuned, the VNO neurons show high response selectivity: each pheromone activates a small subset of receptors that then converge on the AOB, in order to provide complex information already at the first step of central processing (Luo and Katz, 2004). At variance to the main olfactory system, in which cells expressing a single receptor converge to one glomerulus, VNO neurons expressing one specific receptor projects to different glomeruli, located nearby. In this way, each AOB glomerulus processes information coming from different receptors (Belluscio et al., 1999). In addition, single glomeruli and mitral cells receive inputs from different, but related V1R receptors, thus integrating information from various receptors (Wagner et al., 2006). The morphology of vomeronasal axons, which branch several times before reaching their glomerular targets, support divergent projections to different glomeruli (Larriva-Sahd, 2008).

The processing of VNO inputs in the AOB was initially compared to olfactory processing in the MOB, since both bulbs circuitry share some basic characteristics: the output cells are activated by peripheral receptors and in turn activate granule cells via dendrodendritic synapses, the mitral-to-granule synapse is glutamatergic, while the granule-to-mitral is GABA-ergic (Jia et al., 1999). However, the membrane responses of output cells in the AOB were found to differ from those in the MOB, so that the information processing in both bulbs appear more different than previously reported. Output cells in the AOB can be classified in three groups, according to their responses, and can be activated to amplify responses to long-lasting signals while depressing responses to short-lived stimuli (Zibman et al., 2011).

Both the main and accessory olfactory bulb may respond simultaneously to both odors and pheromones: volatile pheromones may strongly activate both bulbs. However, in the presence of complex mixtures of pheromones, like in the exposure to natural urine, the activation is more pronounced in the AOB than in the MOB, where the activation is limited to some regions, suggesting a different selectivity of the two systems (Xu et al., 2005).

Neurons in the AOB respond differentially to urinary pheromones (Guo et al., 1997), according to the gender of the donor and of the recipient: the AOB mitral and granule cells are more active in responding to opposite-sex urinary volatiles; these same stimuli concurrently activate discrete clusters of MOB glomeruli, in both males and females (Martel and Baum, 2007; Baum, 2012). However, the activation of the accessory olfactory system is not mandatory to discriminate the urine derived from males or females with different hormonal status, and does not prevent the expression of male sexual behavior. The AOB appears indeed important for coding the incentive value of opposite-gender urinary volatiles (Jakupovic et al., 2008). Apparently, the processing of pheromonal inputs, mediated via the accessory olfactory system, acts in females to suppress the male-typical courtship behavior, through gender-specific connections in the amygdala and hypothalamus (Baum, 2009).

Both the main and accessory olfactory system processing of social chemosignals are influenced by the hormonal status, including steroid and non-steroid hormones, which modulate

the responses to chemical cues. This modulation involves behavioral modifications, by enhancing investigation, or neural mechanisms that enhance the responsivity of both the main and of the accessory olfactory bulb to the specific chemosignals, to provide concurrent stimulation that enhances the probability of mating in the most favorable conditions (Moffatt, 2003). Therefore, the main and accessory olfactory systems simultaneously process complex chemosensory stimuli according to the neurohormonal status of the receiver.

CONVERGENCE OF MAIN AND ACCESSORY OLFACTORY INPUTS WITHIN THE BRAIN

The abovementioned studies show that both the main and accessory olfactory systems process similar stimuli, but their involvement appears slightly different in inducing various effects. Therefore, it is important to understand how, when and where the two systems integrate their respective information.

The central olfactory projection areas were initially investigated by functional studies that revealed several brain areas connected to the processing of olfactory inputs (Powell et al., 1965).

Anatomical tracing studies revealed that the main olfactory epithelium and the VNO projected to the main and accessory olfactory bulb, respectively (Barber and Raisman, 1974).

The processing of odorant information flows then from the MOB, where the single mitral cells are activated by few odorants, to the anterior olfactory nucleus, where neurons show a broader responsiveness, and where responses to mixtures often exceed the responses to the single components (Lei et al., 2006). In the MOB, the axons of cells expressing the same receptor do converge to couples of glomeruli, defining a stereotyped map. In the piriform cortex, however, no spatial map can be recognized for mapping odorant identity (Choi et al., 2011). This is due to a different wiring of homotypic mitral/tufted cells (Ghosh et al., 2011), which project diffusely from MOB to the piriform cortex (Miyamichi et al., 2011; Sosulski et al., 2011).

The segregation of vomeronasal inputs starts at the peripheral level: V1R receptors are hosted in the more superficial layer of the vomeronasal epithelium, and V2R neurons are located deeper; the afferents remain segregated by projecting to the anterior and posterior AOB, respectively (Bigiani et al., 2005; Tirindelli et al., 2009). A certain degree of separation remains also in the downstream projection areas, since the anterior AOB is connected to the bed nucleus of the stria terminalis, and the posterior AOB projects to the dorsal anterior amygdala, and remains in part segregated also in the hypothalamus (Mohedano-Moriano et al., 2008). The amygdala is involved in the modulation of fear and anxiety behavior as well as intraspecific reproductive and aggressive behavior (Martínez-García et al., 2008); it receives inputs directly from the AOB, and is involved in the perception of sexual pheromones, giving them an innate attractivity, independently from the activation of the reward system in the ventral tegmental area. In turn, the amygdala project to the striatal olfactory tubercle and Islands of Calleja, which are presumably involved in pheromonal communication (Lanuza et al., 2008). The cortex is a site of convergence of segregated VNO pathways, since no segregation has been detected in accessory olfactory cortical areas, including the bed nucleus of the accessory olfactory tract, the medial amygdaloid nucleus, the posteromedial cortical amygdaloid nucleus, and the bed nucleus of the stria terminalis (Von Campenhausen and Mori, 2000).

The interaction between the main and the accessory olfactory systems may initiate already at the first stages of central processing. The AOB receives all chemosensory inputs from the VNO. However, the principal cells of the AOB and the bulbar interstitial neurons, hosted in the most rostral portion of the AOB, allocate efferent fibers originating from the MOB, as demostrated by terminal degeneration in the AOB after MOB lesions, being thus the first documented site of convergence of main and accessory olfactory inputs (Larriva-Sahd, 2008).

The crosstalk between the main and the accessory olfactory system proceeds also in the subsequent stations: single neurons in the amygdala may receive inputs from both systems (Licht and Meredith, 1987), and the medial amygdala, which is a target for AOB projection neurons, also receives inputs from the MOB in its more superficial laminae (Kang et al., 2009).

Apparently, the interconnection of the main and accessory olfactory system delineates also areas in which the systems do overlap, including the anterior medial amygdala and the stria terminalis. The two systems converge also in classical olfactory areas, including the nucleus of the lateral olfactory tract, the anterior cortical amygdaloid nucleus, and the transition between amygdala and cortex, but also in previously considered exclusive vomeronasal-receiving areas, including the ventral anterior amygdala, the bed nucleus of the accessory olfactory tract, and the anteroventral medial amygdaloid nucleus. In other areas, however, the main and accessory olfactory inputs remain segregated, for example in the posteromedial and posterolateral cortical amygdala: consequently, a functional distinction between olfactory, vomeronasal and mixed chemosensory areas has been proposed (Pro-Sistiaga et al., 2007, see **Figure 3**).

The centrifugal pathways, which send back information to the various areas, play a great role in the processing of chemosensory inputs (Mohedano-Moriano et al., 2012). Ideally, the schema of vomeronasal projections follows a simple three-step process from VNO to AOB and hypothalamus, supporting the modulatory role for reproductive processes. The AOB receives inputs from neurons hosting estrogen receptors therefore, a modulation of incoming stimuli is present already at the level of the AOB, according to the hormonal status. Actually, the bed nucleus of the stria terminalis sends GABAergic axons to the AOB mitral cells, while the vomeronasal amygdala sends glutamatergic inputs to the AOB granule cells (Fan and Luo, 2009). Also the olfactory-recipient medial amygdala has been proposed to send back information to the AOB (Martel and Baum, 2009). Moreover, the entorhinal cortex receives afferents from the MOB and in turn sends to the hippocampus that projects back from the CA1 field and the ventral

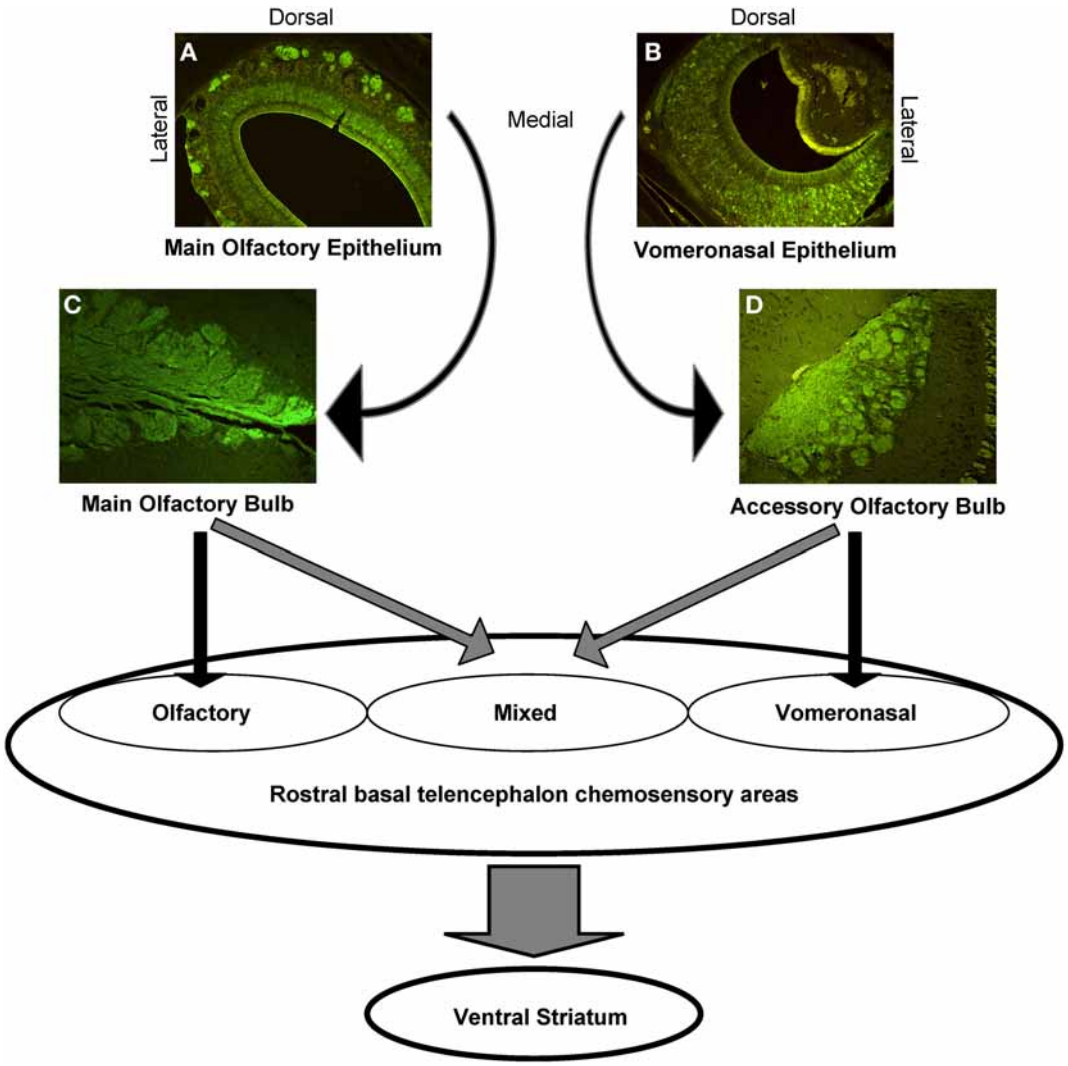

FIGURE 3 | Schematic representation of the central connections of the main and accessory olfactory systems. The photomicrographs show the anti-Olfactory Marker Protein immunoreactivity, that highlights the main olfactory neurons and nerves **(A)**, and the glomeruli in the MOE **(C)**; the VNO sensory neurons **(B)**, and the AOB glomeruli **(D)**.

subiculum, to the AOB, suggesting a possible involvement of memory-related areas in AOB processing (de la Rosa-Prieto et al., 2009).

Thus, the primary projections to the main and accessory olfactory bulb remain separated, while the secondary projections to the rostral basal telencephalon and the tertiary projections to the ventral striatum widely overlap (Martinez-Marcos, 2009).

CONCLUSIONS

Social interactions in numerous species of mammals are mediated by a variety of different chemical stimuli, which are concurrently perceived by the main and accessory olfactory system. Both systems may process similar chemosignals, and participate in managing the reproductive behavior, from mate identification to pup care (Keller et al., 2009). Both systems are possibly involved in the detection of biologically relevant odors, by processing them in parallel and contributing to the different neurohormonal responses at various degrees (Restrepo et al., 2004; Spehr et al., 2006). A possible complementary function may be foreseen for the two systems, with the main olfactory system involved in detection of substances at a distance, and the vomeronasal system having a more specific role in active exploration of relevant stimuli (Martínez-García et al., 2009).

In every instance, the cross-talk between the main and the accessory olfactory systems from the early stages of central processing, as demonstrated by the anatomical connections, supports the idea that both systems participate in the construction of an unitary chemosensory perception.

ACKNOWLEDGMENTS

This paper was supported by the SNIFFER EU grant no. 285203 to Carla Mucignat-Caretta.

REFERENCES

Adrian, E. D. (1942). Olfactory reactions in the brain of the hedgehog. *J. Physiol. (Lond.)* 100, 459–473.

Adrian, E. D. (1955). Synchronised activity in the vomero-nasal nerves with a note on the function of the organ of Jacobsen. *Pflugers Arch.* 260, 188–192.

Barber, P. C., and Raisman, G. (1974). An autoradiographic investigation of the projection of the vomeronasal organ to the accessory olfactory bulb in the mouse. *Brain Res.* 81, 21–30.

Baum, M. J. (2009). Sexual differentiation of pheromone processing: links to male-typical mating behavior and partner preference. *Horm. Behav.* 55, 579–588.

Baum, M. J. (2012). Contribution of pheromones processed by the main olfactory system to mate recognition in female mammals. *Front. Neuroanat.* 6:20. doi: 10.3389/fnana.2012.00020

Belluscio, L., Koentges, G., Axel, R., and Dulac, C. (1999). A map of pheromone receptor activation in the mammalian brain. *Cell* 97, 209–220.

Bigiani, A., Mucignat-Caretta, C., Montani, G., and Tirindelli, R. (2005). Pheromone reception in mammals. *Rev. Physiol. Biochem. Pharmacol.* 154, 1–35.

Boschat, C., Pelofi, C., Randin, O., Roppolo, D., Luescher, C., Broillet, M. C., et al. (2002). Pheromone detection mediated by a V1r vomeronasal receptor. *Nat. Neurosci.* 5, 1261–1262.

Brechbühl, J., Klaey, M., and Broillet, M. C. (2008). Grueneberg ganglion cells mediate alarm pheromone detection in mice. *Science* 321, 1092–1095.

Breer, H., Fleischer, J., and Strotmann, J. (2006). The sense of smell: multiple olfactory subsystems. *Cell. Mol. Life Sci.* 63, 1465–1475.

Broman, I. (1920). Das organon vomero-nasale jacobsoni-ein wassergeruchsorgan! *Anat. Hefte* 174, 137–191.

Brouette-Lahlou, I., Godinot, F., and Vernet-Maury, E. (1999). The mother rat's vomeronasal organ is involved in detection of dodecyl propionate, the pup's preputial gland pheromone. *Physiol. Behav.* 66, 427–436.

Charra, R., Datiche, F., Casthano, A., Gigot, V., Schaal, B., and Coureaud, G. (2012). Brain processing of the mammary pheromone in newborn rabbits. *Behav. Brain Res.* 226, 179–188.

Choi, G. B., Stettler, D. D., Kallman, B. R., Bhaskar, S. T., Fleischmann, A., and Axel, R. (2011). Driving opposing behaviors with ensembles of piriform neurons. *Cell* 146, 1004–1015.

Coppola, D. M., and O'Connell, R. J. (1989). Stimulus access to olfactory and vomeronasal receptors *in utero*. *Neurosci. Lett.* 106, 241–248.

Corona, R., Larriva-Sahd, J., and Paredes, R. G. (2011). Paced-mating increases the number of adult new born cells in the internal cellular (granular) layer of the accessory olfactory bulb. *PLoS ONE* 6:e19380. doi: 10.1371/journal.pone.0019380

de la Rosa-Prieto, C., Ubeda-Banon, I., Mohedano-Moriano, A., Pro-Sistiaga, P., Saiz-Sanchez, D., Insausti, R., et al. (2009). Subicular and CA1 hippocampal projections to the accessory olfactory bulb. *Hippocampus* 19, 124–129.

Del Punta, K., Leinders-Zufall, T., Rodriguez, I., Jukam, D., Wysocki, C. J., Ogawa, S., et al. (2002). Deficient pheromone responses in mice lacking a cluster of vomeronasal receptor genes. *Nature* 419, 70–74.

Dudley, C. A., and Moss, R. L. (1999). Activation of an anatomically distinct subpopulation of accessory olfactory bulb neurons by chemosensory stimulation. *Neuroscience* 91, 1549–1556.

Eisthen, H. L. (1992). Phylogeny of the vomeronasal system and of receptor cell types in the olfactory and vomeronasal epithelia of vertebrates. *Microsc. Res. Tech.* 23, 1–21.

Fan, S., and Luo, M. (2009). The organization of feedback projections in a pathway important for processing pheromonal signals. *Neuroscience* 161, 489–500.

Fleischer, J., Breer, H., and Strotmann, J. (2009). Mammalian olfactory receptors. *Front. Cell. Neurosci.* 3:9. doi: 10.3389/neuro.03.009.2009

Ghosh, S., Larson, S. D., Hefzi, H., Marnoy, Z., Cutforth, T., Dokka, K., et al. (2011). Sensory maps in the olfactory cortex defined by long-range viral tracing of single neurons. *Nature* 472, 217–220.

Greer, C. A., Stewart, W. B., Teicher, M. H., and Shepherd, G. M. (1982). Functional development of the olfactory bulb and a unique glomerular complex in the neonatal rat. *J. Neurosci.* 2, 1744–1759.

Guillamon, A., and Segovia, S. (1997). Sex differences in the vomeronasal system. *Brain Res. Bull.* 44, 377–382.

Guo, J., Zhou, A., and Moss, R. L. (1997). Urine and urine-derive compounds induce c-fos mRNA expression in accessory olfactory bulb. *Neuroreport* 8, 1679–1683.

He, J., Ma, L., Kim, S. S., Nakai, J., and Yu, C. R. (2008). Encoding gender and individual information in the mouse vomeronasal organ. *Science* 320, 535–538.

Holy, T. E., Dulac, C., and Meister, M. (2000). Responses of vomeronasal neurons to naural stimuli. *Science* 289, 1569–1572.

Hovis, K. R., Ramnath, R., Dahlen, J. E., Romanova, A. L., Larocca, G., Bier, M. E., et al. (2012). Activity regulates functional connectivity from the vomeronasal organ to the accessory olfactory bulb. *J. Neurosci.* 32, 7907–7916.

Illig, K. R. (2007). Developmental changes in odor-evoked activity in rat piriform cortex. *Neuroscience* 145, 370–376.

Inagaki, H., Taniguchi, M., Muramoto, K., Kaba, H., Takeuchi, Y., and Mori, Y. (2010). The effect of vapor of propylene glycol on rats. *Chem. Senses* 35, 221–228.

Inamura, K., Matsumoto, Y., Kashiwayanagi, M., and Kurihara, K. (1999). Laminar distribution of pheromone-receptive neurons in rat vomeronasal epithelium. *J. Physiol.* 517, 731–739.

Jakupovic, J., Kang, N., and Baum, M. J. (2008). Effect of bilateral accessory olfactory bulb lesions on volatile urinary odor discrimination and investigation as well as mating behavior in male mice. *Physiol. Behav.* 93, 467–473.

Jia, C., Chen, W. R., and Shepherd, G. M. (1999). Synaptic organization and neurotransmitters in the rat accessory olfactory bulb. *J. Neurophysiol.* 81, 345–355.

Kang, N., Baum, M. J., and Cherry, J. A. (2009). A direct main olfactory bulb projection to the 'vomeronasal' amygdala in female mice selectively responds to volatile pheromones from males. *Eur. J. Neurosci.* 29, 624–634.

Kawagishi, K., Yokouchi, K., Fukushima, N., Sakamoto, M., Sumitomo, N., and Morizumi, T. (2009). Determination of functionally essential neuronal population of the olfactory epithelium for nipple search and subsequent suckling behavior in newborn rats. *Brain Res.* 1276, 50–57.

Keller, M., and Lévy, F. (2012). The main but not the accessory olfactory system is involved in the processing of socially relevant chemosignals in ungulates. *Front. Neuroanat.* 6:39. doi: 10.3389/fnana.2012.00039

Keller, M., Baum, M. J., Brock, O., Brennan, P. A., and Bakker, J. (2009). The main and the accessory olfactory systems interact in the control of mate recognition and sexual behavior. *Behav. Brain Res.* 200, 268–276.

Keverne, E. B. (2004). Importance of olfactory and vomeronasal systems for male sexual function. *Physiol. Behav.* 83, 177–187.

Kimoto, H., Haga, S., Sato, K., and Touhara, K. (2005). Sex-specific peptides from exocrine glands stimulate mouse vomeronasal sensory neurons. *Nature* 437, 898–901.

Kiyokawa, Y., Kikusui, T., Takeuchi, Y., and Mori, Y. (2007). Removal of the vomeronasal organ blocks the stress-induced hyperthermia response to alarm pheromone in male rats. *Chem. Senses* 32, 57–64.

Krieger, J., Schmitt, A., Löbel, D., Gudermann, T., Schultz, G., Breer, H., et al. (1999). Selective activation of G protein subtypes in the vomeronasal organ upon stimulation with urine-derived compounds. *J. Biol. Chem.* 274, 4655–4662.

Lanuza, E., Novejarque, A., Martínez-Ricós, J., Martínez-Hernández, J., Agustín-Pavón, C., and Martínez-García, F. (2008). Sexual pheromones and the evolution of the reward system of the brain: the chemosensory function of the amygdala. *Brain Res. Bull.* 75, 460–466.

Larriva-Sahd, J. (2008). The accessory olfactory bulb in the adult rat: a cytological study of its cell types, neuropil, neuronal modules, and interactions with the main olfactory system. *J. Comp. Neurol.* 510, 309–350.

Lei, H., Mooney, R., and Katz, L. C. (2006). Synaptic integration of olfactory information in mouse anterior olfactory nucleus. *J. Neurosci.* 26, 12023–12032.

Leinders-Zufall, T., Brennan, P., Wildmayer, P., Chandramani, P. S., Maul-Pavicic, A., Jaeger, M., et al. (2004). MHC class I peptides as chemosensory signals in the vomeronasal organ. *Science* 306, 1033–1037.

Leinders-Zufall, T., Lane, A. P., Puche, A. C., Ma, W., Novotny, M. V., Shipley, M. T., et al. (2000). Ultrasensitive pheromone detection by mammalian vomeronasal neurons. *Nature* 405, 792–796.

Lévai, O., Feistel, T., Breer, H., and Strotmann, J. (2006). Cells in the vomeronasal organ express odorant receptors but project to the accessory olfactory bulb. *J. Comp. Neurol.* 498, 476–490.

Lévy, F., and Keller, M. (2009). Olfactory mediation of maternal behavior in selected mammalian species. *Behav. Brain Res.* 200, 336–345.

Liberles, S. D., Horowitz, L. F., Kuang, D., Contos, J. J., Wilson, K. L., Siltberg-Liberles, J., et al. (2009). Formyl peptide receptors are candidate chemosensory receptors in the vomeronasal organ. *Proc. Natl. Acad. Sci. U.S.A.* 106, 9842–9847.

Licht, G., and Meredith, M. (1987). Convergence of main and accessory olfactory pathways onto single neurons in the hamster amygdala. *Exp. Brain Res.* 69, 7–18.

Luo, M., and Katz, L. C. (2004). Encoding pheromonal signals in the mammalian vomeronasal system. *Curr. Opin. Neurobiol.* 14, 428–434.

Ma, M. (2007). Encoding olfactory signals via multiple chemosensory systems. *Crit. Rev. Biochem. Mol. Biol.* 42, 463–480.

Martel, K. L., and Baum, M. J. (2007). Sexually dimorphic activation of the accessory, but not the main, olfactory bulb in mice by urinary volatiles. *Eur. J. Neurosci.* 26, 463–475.

Martel, K. L., and Baum, M. J. (2009). A centrifugal pathway to the mouse accessory olfactory bulb from the medial amygdala conveys gender-specific volatile pheromonal signals. *Eur. J. Neurosci.* 29, 368–376.

Martínez-García, F., Martínez-Ricós, J., Agustín-Pavón, C., Martínez-Hernández, J., Novejarque, A., and Lanuza, E. (2009). Refining the dual olfactory hypothesis: pheromone reward and odour experience. *Behav. Brain Res.* 200, 277–286.

Martínez-García, F., Novejarque, A., and Lanuza, E. (2008). Two interconnected functional systems in the amygdala of amniote vertebrates. *Brain Res. Bull.* 75, 206–213.

Martinez-Marcos, A. (2009). On the organization of olfactory and vomeronasal cortices. *Prog. Neurobiol.* 87, 21–30.

Martínez-Ricós, J., Agustín-Pavón, C., Lanuza, E., and Martínez-García, F. (2008). Role of the vomeronasal system in intersexual attraction in female mice. *Neuroscience* 153, 383–395.

Masini, C. V., Garcia, R. J., Sasse, S. K., Nyhuis, T. J., Day, H. E., and Campeau, S. (2010). Accessory and main olfactory systems influences on predator odor-induced behavioral and endocrine stress responses in rats. *Behav. Brain Res.* 207, 70–77.

McLean, J. H., Darby-King, A., and Paterno, G. D. (1995). Localization of 5-HT2A receptor mRNA by in situ hybridization in the olfactory bulb of the postnatal rat. *J. Comp. Neurol.* 353, 371–378.

Mendoza, A. S., and Szabo, K. (1988). Developmental studies on the rat vomeronasal organ: vascular pattern and neuroepithelial differentiation. II. Electron microscopy. *Dev. Brain Res.* 39, 259–268.

Meredith, M. (1991). Sensory processing in the main and accessory olfactory systems: comparisons and contrasts. *J. Steroid Biochem. Mol. Biol.* 39, 601–614.

Meredith, M. (1998). Vomeronasal function. *Chem. Senses* 23, 463–466.

Meredith, M., and O'Connell, R. J. (1979). Efferent control of stimulus access to the hamster vomeronasal organ. *J. Physiol.* 286, 301–316.

Miller, S. S., and Spear, N. E. (2008). Olfactory learning in the rat neonate soon after birth. *Dev. Psychobiol.* 50, 554–565.

Miyamichi, K., Amat, F., Moussavi, F., Wang, C., Wickersham, I., Wall, N. R., et al. (2011). Cortical representations of olfactory input by trans-synaptic tracing. *Nature* 472, 191–196.

Moffatt, C. A. (2003). Steroid hormone modulation of olfactory processing in the context of socio-sexual behaviors in rodents and humans. *Brain Res. Brain Res. Rev.* 43, 192–206.

Mohedano-Moriano, A., de la Rosa-Prieto, C., Saiz-Sanchez, D., Ubeda-Bañon, I., Pro-Sistiaga, P., de Moya-Pinilla, M., et al. (2012). Centrifugal telencephalic afferent connections to the main and accessory olfactory bulbs. *Front. Neuroanat.* 6:19. doi: 10.3389/fnana.2012.00019

Mohedano-Moriano, A., Pro-Sistiaga, P., Ubeda-Bañon, I., de la Rosa-Prieto, C., Saiz-Sanchez, D., and Martinez-Marcos, A. (2008). V1R and V2R segregated vomeronasal pathways to the hypothalamus. *Neuroreport* 19, 1623–1626.

Moriceau, S., Wilson, D. A., Levine, S., and Sullivan, R. M. (2006). Dual circuitry for odor-shock conditioning during infancy: corticosterone switches between fear and attraction via amygdala. *J. Neurosci.* 26, 6737–6748.

Mucignat-Caretta, C. (2010). The rodent accessory olfactory system. *J. Comp. Physiol. A* 196, 767–777.

Mucignat-Caretta, C., Caretta, A., and Baldini, E. (1998). Protein-bound male urinary pheromones: differential responses according to age and gender. *Chem. Senses* 23, 67–70.

Mucignat-Caretta, C., Caretta, A., and Cavaggioni, A. (1995). Acceleration of puberty onset in female mice by male urinary proteins. *J. Physiol.* 486, 517–522.

Mucignat-Caretta, C., Colivicchi, M. A., Fattori, M., Ballini, C., Bianchi, L., Gabai, G., et al. (2006). Species-specific chemosignals evoke delayed excitation of the vomeronasal amygdala in freely-moving female rats. *J. Neurochem.* 99, 881–891.

Nodari, F., Hsu, F. F., Fu, X., Holekamp, T. F., Kao, L. F., Turk, J., et al. (2008). Sulfated steroids as natural ligands of mouse pheromone-sensing neurons. *J. Neurosci.* 28, 6407–6418.

O'Connell, R. J., and Meredith, M. (1984). Effects of volatile and non-volatile chemical signals on male sex behaviors mediated by the main and accessory olfactory systems. *Behav. Neurosci.* 98, 1083–1093.

Powell, T. P. S., Cowan, W. M., and Raisman, G. (1965). The central olfactory connexions. *J. Anat.* 99, 791–813.

Pro-Sistiaga, P., Mohedano-Moriano, A., Ubeda-Bañon, I., Del Mar Arroyo-Jimenez, M., Marcos, P., Artacho-Pérula, E., et al. (2007). Convergence of olfactory and vomeronasal projections in the rat basal telencephalon. *J. Comp. Neurol.* 504, 346–362.

Raisman, G. (1972). An experimental study of the projection of the amygdala to the accessory olfactory bulb and its relationship to the concept of a dual olfactory system. *Exp. Brain Res.* 14, 395–408.

Restrepo, D., Arellano, J., Oliva, A. M., Schaefer, M. L., and Lin, W. (2004). Emerging views on the distinct but related roles of the main and accessory olfactory systems in responsiveness to chemosensory signals in mice. *Horm. Behav.* 46, 247–256.

Rivière, S., Challet, L., Fluegge, D., Spehr, M., and Rodriguez, I. (2009). Formyl peptide receptor-like proteins are a novel family of vomeronasal chemosensors. *Nature* 459, 574–577.

Salazar, I., and Quinteiro, P. S. (2009). The risk of extrapolation in neuroanatomy: the case of the mammalian vomeronasal system. *Front. Neuroanat.* 3:22. doi: 10.3389/neuro.05.022.2009

Samuelsen, C. L., and Meredith, M. (2009). The vomeronasal organ is required for the male mouse medial amygdala response to chemical-communication signals, as assessed by immediate early gene expression. *Neuroscience* 164, 1468–1476.

Sanchez-Andrade, G., and Kendrick, K. M. (2009). The main olfactory system and social learning in mammals. *Behav. Brain Res.* 200, 323–335.

Scalia, F., and Winans, S. (1975). The differential projections of the olfactory bulb and accessory olfactory bulb in mammals. *J. Comp. Neurol.* 161, 31–56.

Serra, J., Ferreira, G., Mirabito, L., Lévy, F., and Nowak, R. (2009). Post-oral and perioral stimulations during nursing enhance appetitive olfactory memory in neonatal rabbits. *Chem. Senses* 34, 405–413.

Singer, A. G., Macrides, F., Clancy, A. N., and Agosta, W. C. (1986). Purification and analysis of a proteinaceous aphrodisiac pheromone from hamster vaginal discharge. *J. Biol. Chem.* 261, 13323–13326.

Sosulski, D. L., Bloom, M. L., Cutforth, T., Axel, R., and Datta, S. R. (2011). Distinct representations of olfactory information in different cortical centres. *Nature* 472, 213–216.

Spehr, M., Spehr, J., Ukhanov, K., Kelliher, K. R., Leinders-Zufall, T., and Zufall, F. (2006). Parallel processing of social signals by the mammalian main and accessoryolfactory systems. *Cell. Mol. Life Sci.* 63, 1476–1484.

Sugai, T., Miyazawa, T., Yoshimura, H., and Onoda, N. (2005). Developmental changes in oscillatory and slow responses of the rat accessory olfactory bulb. *Neuroscience* 134, 605–616.

Swaney, W. T., and Keverne, E. B. (2009). The evolution of pheromonal communication. *Behav. Brain Res.* 200, 239–247.

Taha, M., McMillon, R., Napier, A., and Wekesa, K. S. (2009). Extracts from salivary glands stimulate aggression and inositol-1, 4, 5-triphosphate (IP3) production in the vomeronasal organ of mice. *Physiol. Behav.* 98, 147–155.

Teicher, M. H., Stewart, W. B., Kauer, J. S., and Shepherd, G. M. (1980). Suckling pheromone stimulation of a modified glomerular region in the developing rat olfactory bulb revealed by the 2-deoxyglucose method. *Brain Res.* 194, 530–535.

Thompson, R. N., Robertson, B. K., Napier, A., and Wekesa, K. S. (2004). Sex-specific responses to urinary chemicals by the mouse vomeronasal organ. *Chem. Senses* 29, 749–754.

Tirindelli, R., Dibattista, M., Pifferi, S., and Menini, A. (2009). From pheromones to behavior. *Physiol. Rev.* 80, 921–956.

Trotier, D., and Doving, K. B. (1998). "Anatomical description of a new organ in the nose of the domesticated animals" by Ludvig Jacobson (1813). *Chem. Senses* 23, 743–754.

Tucker, D. (1963). "Olfactory vomeronasal and trigeminal receptor responses to odorants," in *Olfaction and Taste*, ed Y. Zotterman (New York, NY: Macmillan), 45–69.

Vandenbergh, J. G., Whitsett, J. M., and Lombardi, J. R. (1975). Partial isolation of a pheromone accelerating puberty in female mice. *J. Reprod. Fertil.* 43, 515–523.

Von Campenhausen, H., and Mori, K. (2000). Convergence of segregated pheromonal pathways from the accessory olfactory bulb to the cortex in the mouse. *Eur. J. Neurosci.* 12, 33–46.

Wacker, D. W., Engelmann, M., Tobin, V. A., Meddle, S. L., and Ludwig, M. (2011). Vasopressin and social odor processing in the olfactory bulb and anterior olfactory nucleus. *Ann. N.Y. Acad. Sci.* 1220, 106–116.

Wagner, S., Gresser, A. L., Torello, A. T., and Dulac, C. (2006). A multireceptor genetic approach uncovers an ordered integration of VNO sensory inputs in the accessory olfactory bulb. *Neuron* 50, 697–709.

Winans, S. S., and Scalia, F. (1970). Amygdaloid nucleus: new afferent input from the vomeronasal organ. *Science* 170, 330–332.

Wysocki, C. J., Wellington, J. L., and Beauchamp, G. K. (1980). Access of urinary nonvolatiles to the mammalian vomeronasal organ. *Science* 207, 781–783.

Xu, F., Schaefer, M., Kida, I., Schafer, J., Liu, N., Rothman, D. L., et al. (2005). Simultaneous activation of mouse main and accessory olfactory bulbs by odors or pheromones. *J. Comp. Neurol.* 489, 491–500.

Zibman, S., Shpak, G., and Wagner, S. (2011). Distinct intrinsic membrane properties determine differential information processing between main and accessory olfactory bulb mitral cells. *Neuroscience* 189, 51–67.

Conflict of Interest Statement: The authors declare that the research was conducted in the absence of any commercial or financial relationships that could be construed as a potential conflict of interest.

Received: 17 April 2012; accepted: 22 October 2012; published online: 09 November 2012.

Citation: Mucignat-Caretta C, Redaelli M and Caretta A (2012) One nose, one brain: contribution of the main and accessory olfactory system to chemosensation. Front. Neuroanat. ***6****:46. doi: 10.3389/fnana.2012.00046*

frontiers in
NEUROANATOMY

REVIEW ARTICLE
published: 05 June 2012
doi: 10.3389/fnana.2012.00020

Contribution of pheromones processed by the main olfactory system to mate recognition in female mammals

Michael J. Baum*

Department of Biology, Boston University, Boston, MA, USA

Edited by:
Jorge A. Larriva-Sahd, Universidad Nacional Autónoma de México, Mexico

Reviewed by:
Jianzheng Zheng, University of New Mexico, USA
Raúl G. Paredes, National University of Mexico, Mexico

****Correspondence:***
Michael J. Baum, Department of Biology, Boston University, 5 Cummington St., Boston, MA 02215, USA.
e-mail: baum@bu.edu

Until recently it was widely believed that the ability of female mammals (with the likely exception of women) to identify and seek out a male breeding partner relied on the detection of non-volatile male pheromones by the female's vomeronasal organ (VNO) and their subsequent processing by a neural circuit that includes the accessory olfactory bulb (AOB), vomeronasal amygdala, and hypothalamus. Emperical data are reviewed in this paper that demonstrate the detection of volatile pheromones by the main olfactory epithelium (MOE) of female mice which, in turn, leads to the activation of a population of glomeruli and abutting mitral cells in the main olfactory bulb (MOB). Anatomical results along with functional neuroanatomical data demonstrate that some of these MOB mitral cells project to the vomeronasal amygdala. These particular MOB mitral cells were selectively activated (i.e., expressed Fos protein) by exposure to male as opposed to female urinary volatiles. A similar selectivity to opposite sex urinary volatiles was also seen in mitral cells of the AOB of female mice. Behavioral data from female mouse, ferret, and human are reviewed that implicate the main olfactory system, in some cases interacting with the accessory olfactory system, in mate recognition.

Keywords: mouse, ferret, human, vomeronasal organ, hypothalamus

INTRODUCTION

Mice preferentially use olfactory as opposed to visual or auditory signals to locate potential mates (Brennan and Zufall, 2006). Pheromonal cues emitted from males' tear glands and/or preputial glands (excreted in urine) are thought to signal his presence, thereby attracting the female whereupon a pheromone-induced facilitation of lordosis behavior occurs in response to the flank palpation provided by the male's mounting behavior. Mice of both sexes possess two detection systems for environmental odors. (1) The vomeronasal organ (VNO) has traditionally been considered to be the murine "pheromone detection system" (Tirindelli et al., 2009). VNO receptors located in the roof of the mouth extend axons to glomeruli located in the accessory olfactory bulb (AOB) where they synapse onto the dendrites of AOB mitral cells which extend axons to the medial amygdala (MeA; part of the "vomeronasal amygdala") (Kevetter and Winans, 1981a). Neurons in the MeA project, in turn, to hypothalamic targets including the bed nucleus of the stria terminalis (BNST), the medial preoptic area (mPOA), and the ventromedial hypothalamus (VMH). These brain areas are included in circuits that control females' proceptive (approach) and receptive (lordosis) behaviors (Blaustein and Erskine, 2002). (2) The main olfactory epithelium (MOE) has traditionally been thought to be the detection system for all non-pheromonal odorants present in the environment (Xu et al., 2000). Olfactory receptor neurons in the MOE extend axons to glomeruli located on the surface of the main olfactory bulb (MOB) where they synapse with dendrites of mitral cells that project extensively to diffuse target sites in the olfactory tubercle and in the anterior as well as the posterior piriform cortex (Sosulski et al., 2011). An early study (Kevetter and Winans, 1981b) demonstrated that a subset of MOB mitral cells also project to cortical amygdaloid nuclei ("olfactory amygdala"); however, more recent studies (Pro-Sistiaga et al., 2007; Kang et al., 2009; Thompson et al., 2012) show that there is a subpopulation of MOB mitral cells that project directly to the MeA ("vomeronasal amygdala"). This review summarizes the neuroanatomical and functional/behavioral experiments that established the existence of this latter MOB projection pathway and its role in the detection of volatile male pheromones in female mice. I will also review studies that point to a central role of the main olfactory system in the processing of pheromonal cues leading to mate recognition in female pigs and ferrets, and I will end by summarizing current evidence of the possible contribution of a putative male signaling pheromone to heterosexual attraction in women.

INTERACTIVE ROLES OF THE MOE AND VNO IN MATE RECOGNITION AND SEXUAL BEHAVIOR IN FEMALE MICE

Kimchi and co-workers (Kimchi et al., 2007) reported that female mice with a null mutation of the Trp2C gene (initially reported to cause a total elimination of VNO function) failed to discriminate male from female conspecifics (Trp2C mutant females reportedly directed mounting behavior indiscriminately toward a castrated male and an estrous female). However, several other studies showed that surgical VNO destruction failed to disrupt the ability of female mice to discriminate body and/or urinary odors

of male vs female or of testes-intact vs castrate male specifics (Lloyd-Thomas and Keverne, 1982; Keller et al., 2006b; Martel and Baum, 2009a). The Kimchi et al. study can be criticized on two grounds. First, it seems likely that some VNO neurons remain functional even after the Trp2C channel is knocked out: thus pregnancy block in response to pheromones from a strange (non-mating) male was retained in Trp2C female mice (Kelliher et al., 2006) even though surgical VNO removal has been shown to eliminate the pregnancy block otherwise induced in recently mated female mice that are exposed to urinary odors from a strange (non-mating) male (Lloyd-Thomas and Keverne, 1982). A recent study (Kim et al., 2011) showed that calcium activated chloride currents may also generate action potentials in murine VNO neurons. Second, Kimchi and co-workers (Kimchi et al., 2007) never directly assessed the ability of their Trp2C null mutant females to discriminate between pheromonal cues derived from male vs female conspecifics; instead females' motivation to direct mounts toward a castrated male vs an estrous female was assessed. By itself, this does not constitute a rigorous assessment of females' female-typical sexual motivation or of its signaling by sex-specific pheromonal cues. Systematic analysis of olfactory preferences in female mice (Keller et al., 2006b; Martel and Baum, 2009a) showed that surgical VNO destruction eliminated females' preference to investigate male vs female non-volatile urinary odors without disrupting their preference to approach volatile odor cues from a male. VNO destruction also dramatically reduced the capacity of female mice, when tested while in estrus, to display lordosis in response to the receipt of mounts from a male. A similar disruption of lordosis was seen in female mice given bilateral lesions of the AOB (Martel and Baum, 2009a). Likewise, in estrous female rats VNO lesions (Rajendren et al., 1990) as well as AOB lesions (Dudley and Moss, 1994) significantly reduced the expression of lordosis behavior. Further evidence of VNO involvement in the control of lordosis in mice comes from the work of Haga et al. (2010) who identified a pheromone secreted in male tears (exocrine gland-secreted pepide; ESP1). These workers showed that ESP1 stimulated immediate early gene expression in the female's VNO, after being detected by Vmn2r116 receptor. Further behavioral studies showed that application of ESP1 to WT females in estrus enhanced their lordosis behavior; however, no such facilitation was seen in females in which the Vmn24116 receptor was knocked out.

Several studies (Edwards and Burge, 1973; Keller et al., 2006a) showed that zinc sulfate lesions of the MOE eliminated the capacity of female mice to show a preference for volatile body odors emitted from male vs female or from testes-intact male vs castrated male conspecifics. These investigators also reported significant reductions in females' lordosis capacity after MOE lesions. Thus both the accessory and main olfactory inputs to the MeA may mediate the pheromonal facilitation of lordosis capacity in female mice. Results of a recent study (DiBenedictis et al., 2012) showed that bilateral lesions of the MeA (like lesions of the VNO, MOE, or AOB) also significantly diminished lordosis in ovariectomized females following priming with ovarian hormones. Thus central disruption of pheromonal inputs (e.g., ESP-1 males' tears; other yet to be determined male urinary volatiles) that are initially detected by either the VNO or the MOE are potentially as disruptive to the display of females' lordosis behavior as eliminating the ovarian sex hormones (e.g., after ovariectomy).

Early studies using female mice showed that females placed on soiled male bedding showed an increase in Fos and/or EGR-1 expression in VNO sensory neurons (Halem et al., 1999, 2001; Kimoto et al., 2005) as well as in central target sites of these neurons including the AOB, the vomeronasal amygdala and hypothalamic regions including the BNST and VMH. These results have recently (Isogai et al., 2011) been confirmed and extended. In so far as subjects used in these studies had direct nasal contact with pheromones deposited in soiled bedding, it seems likely that the VNO played a central role in the pheromone detection Other early studies (Schaefer et al., 2001, 2002) showed, however, that urinary volatiles from male mice of different major histocompatibility complex (MHC) genotypes elicited significantly different profiles of MOB glomerular activation in females, as indexed by odor-induced expression of Fos in periglomerular cells surrounding activated glomeruli. The pheromone-activated glomeruli were concentrated in the ventral portion of the MOB. Numerous studies (Boehm and Zufall, 2006; Spehr et al., 2006) conducted over the past 30 years have shown that volatile MHC molecules as well as small peptide ligands for these molecules, contribute to individual mate recognition and mate choice in female mice. The detection of these individual MHC odortypes likely occurs after their detection by the MOE, since female mice from which the VNO was removed continued to successfully discriminate urinary volatiles from males of two MHC haplotypes (Wysocki et al., 2004). It is not known which of the ∼1000 different classical olfactory receptor genes (Buck and Axel, 1991) expressed in the MOE detect MHC molecules. A second family of receptors (trace amine-associated receptors; TAARs) was recently found to be expressed in the MOE of mice (Liberles and Buck, 2006). These investigators also showed that trimethylamine is elevated in the urine of male vs female mice and is bound by mTAAR5-expressing cells. Liberles and Buck (2006) raised the possibility that trimethylamine, which like methylthio methanethiol (MTMT; see below) is a volatile component of male mouse urine, may serve as a signaling pheromone to attract males to female conspecifics. Other recent work (Lin et al., 2007) showed that many of the pheromone-responsive glomeruli in the MOB of both sexes are innervated by axons whose cell bodies in the MOE express the transient receptor potential channel M5 (TRPM5). It is not known whether TRPM5 expression occurs in subsets of MOE receptor neurons that express classical olfactory receptor proteins, TAARs, or both types of receptors. Electrophysiological recording from mitral cells in the ventral MOB of female mice revealed that a subset of these neurons were activated by male urinary volatiles (Lin et al., 2005). These same neurons in the female MOB were also reliably activated by MTMT which was also found to attract sexually experienced female mice in behavioral tests. In another study (Xu et al., 2005) functional magnetic resonance imaging (fMRI) was used to reveal glomerular activation in both the MOB and AOB of female mice in response to male urinary volatiles, with the MOB activation occurring slightly earlier than

that in AOB. Slotnick and colleagues (Slotnick et al., 2010) suggested that the VNO responses to volatile pheromones typically are preceded by MOE detection which then leads the animal to make the nasal contact with a non-volatile pheromone, leading to VNO activation. Early work (Luo et al., 2003) showed used *in vivo* recordings from the mouse AOB in which neuronal activation was only seen after direct nasal contact with pheromonal stimuli.

The observation (Xu et al., 2005) that AOB activation (indexed by fMRI) occurred in response to urinary volatiles, which are thought to be detected solely by the MOE as opposed to the VNO, was surprising. However, this outcome was confirmed and extended by a study (Martel and Baum, 2007) which compared the ability of urinary volatiles from male vs female mice to activate MOB glomeruli (indexed by Fos expression in the periglomerular cells) and augment Fos expression in AOB mitral and granule cells as well as in targets of VNO olfactory input in the vomeronasal amygdala and hypothalamus of gonadectomized (non-hormone treated) male and female mice. As predicted from the outcome of several above-mentioned studies, both male and female urinary volatiles activated multiple glomeruli located in the ventral MOB of both male and female subjects; the distribution of these activated glomeruli, while overlapping, was distinct in mice of both sexes exposed to male vs female urinary volatiles. In contrast to the MOB, only opposite-sex urinary volatiles stimulated Fos expression in mitral and granule cells of the AOB of each sex (i.e., female subjects showed AOB Fos responses to male urinary volatiles whereas male subjects showed AOB Fos responses to urinary volatiles from estrous females). In female subjects the selective Fos responsiveness of the AOB to male urinary volatiles extended to other forebrain targets of pheromone processing, including the vomeronasal amygdala and hypothalamus. By contrast, in male subjects exposure to either female or male urinary volatiles stimulated Fos expression in forebrain regions including the vomeronasal amygdala and hypothalamus. It is noteworthy that all of the MOB, AOB, and other forebrain Fos responses to urinary volatiles were absent in groups of gonadectomized female and male mice that 4 days earlier had received intranasal infusions of the toxic compound, zinc sulfate, which killed MOE sensory neurons. Zinc sulfate lesions of the MOE did not attenuate the ability of direct nasal contact with male urine to augment Fos expression in AOB mitral and/or granule cells. These results suggest that all observed Fos responses to urinary volatiles resulted from their detection by MOE, as opposed to VNO sensory neurons, and that there exists an input pathway whereby main olfactory signals reach the AOB.

Studies (Pro-Sistiaga et al., 2007; Kang et al., 2009) from rat and mouse point to the existence of a population of MOB mitral cells that extend axons directly to portions of the "vomeronasal (MeA) amygdala." These mitral cells are separate from the population of MOB mitral cells, described in the classic paper of Kevetter and Winans (1981b), which target subdivisions of the "olfactory amygdala," including the anterior cortical amygdala. In studies using female mice (Kang et al., 2009) dual labeling of the MOB (PHA-L) and AOB (Fluoro-Ruby) with anterograde tracers led to labeling of abutting superficial laminae of the ipsilateral MeA and MePD. In additional females, injection of the retrograde tracer, Cholera Toxin B (CTb) into the MeA led to retrograde labeling of a large number of AOB mitral cells as well as a restricted population of mitral cells located in the ventral and medial subdivisions of the MOB. In a functional study (Kang et al., 2009) exposure of ovariectomized, hormone-primed female mice to urinary volatiles from male, but not from female mice, significantly augmented the population of MeA projecting MOB mitral cells that co-expressed Fos protein. More recently, Thompson et al. (2012) found using both male and female mice that MOB glomeruli which receive synaptic inputs from MOE olfactory sensory neurons that express the cation channel TRPM5 (and which are thought to respond selectively to several different pheromones) are more likely to be innervated by an apical dendrite from MOB mitral cells that extend axons to the vomeronasal amgydala (MeA), although this overlap was not complete. Finally, evidence of a direct projection pathway of MOB mitral cells to the granule cells of the adjacent (ipsilateral) AOB has been provided in male rats (Larriva-Sahd, 2008).

We asked whether the MOB-MeA projection pathway passes information about male urinary volatiles on to the AOB, thereby accounting for our previous observation (Martel and Baum, 2007) that opposite-sex urinary volatiles (detected by the MOE, and not the VNO) augmented Fos expression in AOB mitral and granule cells? An anatomical study (Fan and Luo, 2009) used an anterograde tracer to show that axons extend from MeA neurons to innervate granule cells in the ipsilateral AOB of mice. We found (Martel and Baum, 2009b) that exposure to male, but not female, urinary volatiles stimulated the expression of Fos in the cell bodies of MeA neurons that were co-labeled with CTb which had been injected 1 week earlier into the ipsilateral AOB. As in our previous study (Martel and Baum, 2007) exposure to male, but not to female, urinary volatiles stimulated Fos expression in several brain regions, including the vomeronasal amygdala and several hypothalamic regions including the BNST, MPA, and VMH. Taken together, these data raised the possibility that opposite-sex (male) urinary volatiles are detected in the MOE by sensory neurons that express TRPM5. These neurons convey their inputs to a subset of MOB glomeruli where information about "maleness" is transferred directly to a subset of MOB mitral cells that target the MeA. The intregration of these main olfactory inputs and signaling from ovarian hormones (estradiol and progesterone) likely occurs in the posterior dorsal portion of the MeA, as indicated by our recent finding (DiBenedictis et al., 2012) that bilateral lesions of the caudal (PD), but not the rostral, subdivision of the MeA disrupted the preference of estrous females to approach urinary volatiles from testes-intact vs castrated male mice.

It is widely agreed that even in the absence of previous nasal contact with male pheromonal cues, adult female mice are inherently motivated to investigate/make nasal contact with non-volatile urinary pheromones deposited by testes-intact adult males (Ramm et al., 2008). The attraction has been attributed to the presence of a particular major urinary protein (MUP), named darcin (Roberts et al., 2010), which is excreted in male mouse urine. This female-typical preference for male urine/darcin is hard wired, and likely depends on the absence of sex steroid signaling around the time of females' birth (which contrasts with an

organizational action of perinatal testosterone and/or estrogenic metabolites of testosterone in the developing male hypothalamus) coupled with the later presence in females of estradiol signaling over a prepubertal period (P15-P25); (Brock et al., 2010, 2011). The strongest preference for male odors is expressed in adult cycling females on the night of proestrus, thanks to the central "activational" actions of estradiol and progesterone in the projection circuit that processes pheromonal cues. Additional studies (Ramm et al., 2008; Martinez-Garcia et al., 2009) suggested that female mice which had never had nasal contact or mating experience with a male showed no preference to seek out airborn urinary volatiles from male vs female conspecifics. By contrast, a robust preference for airborn (volatile) scents from males (vs castrated males or females) was seen in female mice that previously had experienced nasal contact with male urine or had mated with a male. This preference was strongest for volatile body odors from socially dominant males, provided females had previously had direct nasal access with the suite of odors deposited on cage bedding by dominant males (Mak et al., 2007; Veyrac et al., 2011). As already stated, female mice were strongly attracted to the volatile component of male urine, MTMT (Lin et al., 2005), a behavioral effect that was correlated with the ability of MTMT to augment electrical activity of MOB mitral cells in female mice. All of the females used in that study had received prior mating experience with males, thus it is not known whether naïve females which had not previously received either mating experience or nasal contact with male body parts/male urine would have been attracted to the putative volatile male urinary pheromone. Martinez-Ricos et al. (2007) also reported that nasal contact with soiled male bedding reliably served as a stimulus that established a learned conditioned place preference (CCP) response in female mice whereas access to volatiles emitted from soiled male bedding failed to establish a CCP. In this latter study, as in the other studies (Martinez-Ricos et al., 2008) that reported an absence of female preference for male vs female or male vs castrated male urinary or body volatile odorants the female subjects had been kept in a separate colony room from males beginning at the age of weaning. In these particular studies odor "naïve" female subjects were given behavioral tests in adulthood while ovary intact and at an unspecified stage of the estrous cycle. In another study (Ramm et al., 2008) female mice derived from wild caught parents were carefully prevented from experiencing contact with male body odorants until adulthood. In the absence of direct nasal experience with urine from a particular male, these females showed no preference to approach male vs female urinary volatiles. After nasal experience with a specific male, females later preferred to approach male vs female urinary odors, provided the male odor presented was from a specific male. Finally, Ramm et al. (2008) reported that they exposed all of their subjects to soiled bedding from an unfamiliar male for three consecutive days in order to bring their ovary-intact females into proestrous/estrous at the time their preference for male vs female urinary volatiles was assessed. No direct confirmation of the successful induction of proestrus/estrus (using vaginal smears) was carried out in this study, thus it remains a matter of speculation as to whether odor preferences were actually made while females were in an optimal hormonal condition to show a male-directed preference. Also, it is hard to argue that the subjects in this study were odor "naïve" given that direct nasal contact with soiled male bedding was reportedly used to bring all females in to proestrus/estrus at the time of testing.

In two recent studies (Martel and Baum, 2009a; DiBenedictis et al., 2012) my colleagues and I examined the preference of young adult female Swiss-Webster mice to approach volatile urinary odors from testes intact males vs either estrous females or castrated males. Although our females may have previously been exposed to volatile male body odors in the colony room, they had never had direct nasal access to such male odorants, nor had they had any mating experience prior to these studies. In both studies such naïve female subjects showed a significant preference to investigate volatile urinary odors from testes intact males vs estrous females (Martel and Baum, 2009a) or from testes intact males vs castrated males (DiBenedictis et al., 2012). In the former study the female subjects had been ovariectomized and treated chronically with a s.c. Silastic capsule releasing estradiol at the time odor preference was assessed. In the latter study, the female subjects had been ovariectomized, treated chronically with a s.c. Silastic capsule releasing estradiol, and given a s.c. injection progesterone 3–6 h prior to the assessment of odor preference. Thus in both of our studies male odor "naïve" females (no prior nasal contact with male odors) showed a preference to investigate male urinary volatiles—findings that conflict with previous reports (Ramm et al., 2008; Martinez-Garcia et al., 2009) that female mice require prior nasal contact with male body or urinary odors in order for male urinary volatiles associated with non-volatiles (presumably detected by the female's VNO-AOB-accessory olfactory system). The absence of a preference for male urinary volatiles in the absence of previous nasal contact with male urine may reflect the non-estrous status at the time of behavioral testing in a large proportion of the ovary-intact females used in those previous experiments. It will be important in future studies to systematically assess the role of ovarian hormones in the expression of females' preference for male urinary (or general body) volatile odorants. The suggestion (Martinez-Garcia et al., 2009) that female mice attend to male urinary volatiles and find them rewarding only after a conditioning process in which these odors are paired with VNO detection of non-volatile male odorants that are processed via a hard-wired straight line pathway to the hypothalamus via the medial amygdala (Choi et al., 2005) is an attractive one. Indeed, there are several lines of neuroanatomical data that indirectly support this proposed mechanism. Thus inputs from the VNO are passed directly on to the AOB which, in turn, directly targets the MeA, followed by the hypothalamus with little or no input to higher olfactory cortical structures (Kevetter and Winans, 1981a; Kang et al., 2009). By contrast, MOB mitral cells that target the MeA invariably extend axon collaterals into the far reaches of anterior and posterior piriform cortex (Kang et al., 2011). The intermingling of AOB and MOB inputs to the MeA, combined with parallel cortical processing of MOB inputs to the MeA may provide a substrate for the type of olfactory learning proposed by others (Ramm et al., 2008; Martinez-Garcia et al., 2009). It may also be, however, that ovarian hormones somehow obviate the need for this learning, leading females to express a preference for

volatile male urinary odors in the absence of prior direct nasal contact with male urine. More research is needed to answer this question.

EARLY EVIDENCE THAT FEMALE PIGS AND FERRETS USE THE MAIN OLFACTORY SYSTEM TO IDENTIFY OPPOSITE-SEX MATING PARTNERS

The early work of Signoret and co-workers (Signoret, 1967, 1970) showed that female sows, when in estrus, were strongly attracted to the odor of androstenone, which is excreted in the saliva of boars that are in breeding condition. Androstenone both attracted estrous sows and facilitated their receptive, "standing" behavior when pressure was applied to the back by a mounting male. Dorries and coworkers showed that females detect low concentrations of androstenone more readily than male pigs (Dorries et al., 1995), and that the occlusion of the VNO ducts in female pigs failed to disrupt their detection/motivation to approach this odor (Dorries et al., 1997). These results suggested that the detection and processing of the volatile male steroid, androstenone, by the main as opposed to the accessory olfactory system was responsible for its actions as both a signaling and a releaser pheromone in the female pig. To date, nobody has directly tested this hypothesis in the pig.

Several studies from my laboratory established an obligatory role of the main, as opposed to the accessory system, in the detection of male pheromones that are required for females' sexual attraction to males. In the absence of prior mating experience, female ferrets that had been ovariectomized and treated in adulthood with estradiol preferred to approach volatile odors emitted from a breeding male vs and an estrous female that was anesthetized/placed in the goal boxes of an air-tight Y maze (Kelliher and Baum, 2001, 2002). The composition of volatiles emitted from anal scent gland secretions as well as urine is different in the two sexes (Zhang et al., 2005); presumably the female ferrets used in our behavioral experiments were responding to some combination of these volatile odorants. Female's preference for male volatiles persisted when the stimulus animals had previously had their anal scent glands surgically removed (Cloe et al., 2004), implying that other excretions (e.g., urine) emit volatiles that are sufficient to signal ferrets' sex to conspecifics. When we began studying mechanisms controlling mate recognition in ferrets there was controversy about the existence of a functional VNO/AOB in ferret of either sex (Weiler et al., 1999). We confirmed the existence of a VNO in both male and female ferrets (Kelliher et al., 2001) and identified the projection target of VNO sensory neurons by identifying a small AOB located in the medial MOB that was selectively stained by soybean agglutinin—horseradish peroxidase. In a subsequent study (Woodley et al., 2004) surgical removal of the VNO from ovariectomized, estradiol-primed female ferrets failed to diminish their preference to approach volatile body odors emitted from an anesthetized male as opposed to an estrous stimulus female in Y maze tests. Likewise, following VNO removal female ferrets retained their ability to discriminate between odors released from either anal scent gland secretions or urine of male vs female ferrets, although the preference of VNO lesioned females to show prolonged nasal investigation of either 1-day-old male urine spots or blocks of wood previously soiled by a male ferret was lower than in sham-operated controls. We interpreted these findings to mean that VNO/accessory olfactory inputs in female ferrets, as in female mice (Martel and Baum, 2009a), function to maintain females in close proximity to non-volatile male pheromones previously deposited in the environment. Such VNO function may be important for ferrets living in the wild, in which the two sexes live apart except for the period of several weeks when the two sexes seek each other out/mate as the annual breeding season occurs in response to lengthening photoperiod (Moors and Lavers, 1981).

The persistence of female ferrets' ability to identify and approach male volatile odorants even after removal of the VNO implies that the main olfactory system plays a central role in mate recognition in this species. Two additional studies further support this view. First (Woodley and Baum, 2004), exposure to volatiles emitted from male and estrous female anal scent gland secretions led to the differential activation of glomeruli (indexed by the upreglation of Fos expression in periglomerular inter neurons) located mainly in the ventral MOB of estrous female ferrets, and the degree of activation by male anal scent gland odorants was not appreciably diminished after ovariectomy. The different profiles of MOB glomerular activation induced by volatile male and female anal scent gland odorants also occurred in male subjects; at the level of the MOB the glomerular responses to the same odors (e.g., male anal scent gland volatiles) was very similar in the two sexes. Earlier studies (Wersinger and Baum, 1997; Kelliher et al., 1998) suggested that the ability of male body odors to activate (stimulate Fos expression) the hypothalamus of male and female ferrets differs, an observation that correlates with the profound sex difference in the motivation of breeding ferrets to seek out volatile (and non-volatile) body odors from males. A second study (Kelliher and Baum, 2001) definitively implicated the main olfactory system in the detection/processing of volatile odors needed for heterosexual mate recognition. Estrous female ferrets were made permanently anosmic by infusing dental impression cement into both nares, thereby occluding the MOE. Anosmia was confirmed by showing that females given intra nares dental cement could not learn to use peppermint as a discriminative stimulus to locate food in Y maze tests. Also, following sacrifice at the end of the study, minimal Fos expression was seen in the mitral or granule cell layers of the MOB of anosmic females (no such reduction was seen in the AOB), and there was little periglomerlar expression of tyrosine hydoxylase in these animals. When confronted with a choice between volatile body odors from an anesthetized male vs estrous female, sham-occluded control female showed a strong preference to approach the male odors whereas no preference was seen in nares-occluded females. This was not surprising, given that only odor cues were available to allow anosmic females to make a choice (and they couldn't smell). The absence of a preference for males among anosmic females was more surprising in additional tests in which the sight and sound of male vs female stimulus animals was also available (male ferrets are twice as large as females; the two sexes also may emit different audible sounds). When confronted with a male in a small compartment, estrous females mated normally, even when they were anosmic. However, when

subsequently retested for approach behaviors in the Y-maze, nares occluded (anosmic) females continued showing no preference to approach the male vs female stimulus animals, even when a brief behavioral interaction was allowed between the subject and the stimulus ferrets at the end of each Y-maze trial. These data showed that selective occlusion of the MOE (while apparently avoiding any disruption of VNO signaling) eliminated the capacity of estrous female ferrets to identify an appropriate male mating partner. Considered together with the demonstration (Woodley et al., 2004) that VNO removal failed to disrupt this capacity in female ferrets, these data establish the obligatory role of the MOE/main olfactory pathway in mate recognition in ferrets. As already explained, this outcome pointed to a similar mechanism that was subsequently found to be operative in female mice.

IMPLICATIONS OF THE ANIMAL DATA FOR A ROLE OF THE MAIN OLFACTORY SYSTEM IN MATE RECOGNITION/ PSYCHOSEXUAL FUNCTION IN WOMEN

There has been considerable controversy over the years about whether higher primates, including humans, communicate using pheromones (Wysocki and Preti, 2004). An early claim (Michael and Keverne, 1968) that sexual arousal/mating performance in male rhesus monkeys depended solely on the actions of "copulins," pheromones produced by the vagina of estradiol-primed females, was disputed (Goldfoot et al., 1978). However, the possibility remains that volatile odors emitted from the vagina modulate the motivation of male rhesus monkeys to approach females, depending on the phase of the female's menstrual cycle. There is also evidence (Baum et al., 1976, 1977) that progesterone reduces males' interest in females by counteracting the stimulatory action of estradiol on the vaginal production of pheromonal cues that signal attraction. However, results of other studies (Baum et al., 1978) showed that female stumptail monkeys would continue to be attractive to male conspecifics after all ovarian and adrenal steroids hormones were removed by combined ovariectomy and adrenalectomy. The same is true of post-menopausal women, who continue to be attractive to male partners, essentially in the absence of circulating sex hormones. Disagreement about whether pheromonal communication occurs in humans was further fueled by the belief that pheromonal communication in lower mammals depends solely on the existence of a functional VNO-accessory olfactory system. Genetic evidence (Kouros-Mehr et al., 2001) shows that VNO receptor genes in humans are non-functional, pseudogenes while anatomical experiments (Trotier et al., 2000) have shown that adult humans lack a functional VNO with sensory neurons that establish connections with an AOB (Meisami and Bhatnagar, 1998). The apparent absence of a functional VNO in humans led many skeptics to believe that the human lacks the detectors/circuits required for pheromonal communication. However, the results of many animal studies reviewed, above, suggest that this conclusion is unwarranted. Between-sex pheromonal communication clearly occurs in mice and ferrets after removal of the VNO. Thus the animal literature does not rule out the possibility of pheromonal communication in species such as humans which lack a functional VNO.

There are several examples in the literature of apparent male pheromonal actions in women. These include the ability of male underarm volatiles, when applied to the lips of women subjects, to accelerate the next LH pulse and improve mood ratings (Preti et al., 2003). A related example of human male pheromonal communication is the report (Jacob et al., 2002b) that women preferred to smell underarm odors of men that shared paternally inherited MHC alleles when them. This outcome is consistent with the report (Helgason et al., 2008) that women's fertility was highest when they mated with men who were third or fourth cousins. Thus in women, as in female mice (Barnard and Fitzsimons, 1989), reproductive success is maximized by breeding with distant relatives as opposed to totally unrelated males. Putative pheromonal cues from women may also influence neuroendocrine and behavioral functions in other women. Thus, Stern and McClintock (1998) reported that underarm odorants collected from women at different stages of the menstrual cycle advanced or delayed the timing of the preovulatory surge of luteinizing hormone in cycling female subjects. McClintock's group (Spencer et al., 2004) also reported that odorants collected from lactating women and their breast feeding infants augmented sexual motivation in women who smelled these odorants. These different examples of human pheromonal communication involve several classes of pheromones including primers, signalers, and releasers (McClintock, 2002). The mechanism whereby women (like female mice) identify the ideal mate may involve pheromonal communication mediated by the main olfactory system.

As already reviewed, the volatile steroid, androstenone, is a pheromone emitted from the saliva of male pigs which both signals the presence of a male in breeding condition and releases sexual activity, including approach and a receptive posture, in females. An evolving body of literature suggests that another, structurally related steroid, androstadienone (AND) is produced in underarms of men which may act as a pheromone that signals males' reproductive status to women. Polymorphisms in the olfactory receptor protein, OR7D4, were associated with variations among individual humans in their ability to detect AND and in their ratings of its pleasantness (Keller et al., 2007). There was no distinction between men and women in the number of people who reported being unable to smell AND or androstenone in this study; however, in previous report (Dorries et al., 1989) the ability to detect androstenone was more likely to diminish in boys than in girls after the age of puberty. An additional study (Zhuang et al., 2009) showed that there is considerable variation in OR7D4 sequences among old world monkeys and great apes, a result that is perhaps not surprising given the variation in sequence seen among humans. Despite the lack of uniformity in the expression of MOE olfactory receptor proteins that are capable of detecting AND, there are several studies suggesting that AND may attract women to men or attract gay men to other gay men. In a systematic comparison of rated preferences for different underarm odors, heterosexual women preferred the smell of underarm odors from heterosexual as opposed to gay men while gay men preferred underarm odors of other gay men (Martins et al., 2005). The authors raised the possibility that differences in the preference for the putative male underarm pheromone, AND,

may underlie this profile of preferences, although this was not tested directly. A series of studies from Savic and co-workers used PET scanning to compare the profile of hypothalamic activation induced by application of AND to the upper lip of straight vs gay men and women as well as transgender persons. In an initial study (Savic et al., 2001) AND was found to induce hypothalamic activation in heterosexual women, but not in men. Gay men were subsequently found to show hypothalamic activation in response to AND that resembled that seen in heterosexual women (Savic et al., 2005); lesbian women failed to show hypothalamic PET responses to AND (Berglund et al., 2006), and in this respect resembled heterosexual men. In another study (Berglund et al., 2008) 46 XY male to female transsexuals showed a significant hypothalamic PET response to AND that resembled the response seen in heterosexual women. The transsexual subjects used in that study stated that they had never received exogenous ovarian hormones in conjunction with their transition from male to female gender identity and role. This raises the question of whether fetal, organizational actions of testosterone in the male, as opposed to adult, activation effects of sex hormones, account for the observed sex differences in the AND-induced PET signal in the hypothalamus. Finally, in another study from the Savic group (Ciumas et al., 2009) significant AND-induced PET activation in the hypothalamus was seen in women with congenital adrenal hyperplasia and in whom fetal testosterone signaling was very likely higher than in the normal control women. This outcome calls into question the possible role of different fetal sex hormone signaling as the determinants of the reported sex differences/sexual orientation/gender identity effects on hypothalamic responses to AND. More research will be needed to resolve this issue. There is also a lingering question from these studies about the very high, potentially non-physiological, concentration of AND that was applied to subjects' upper lip.

Several studies have assessed the ability of AND to affect neuroendocrine as well as psychological functions related to mate recognition among women. Thus application of AND to the upper lip of heterosexual women significantly augmented salivary levels of cortisol (Wyart et al., 2007). Surprisingly, this effect of AND on cortisol secretion was correlated with a reported increase in sexual arousal while viewing an erotic film and with a reduction in the negative mood otherwise seen in a control condition. In another study (Cornwell et al., 2004) heterosexual women were asked to rate men's faces for potential long vs short term relationships, and while viewing the respective types of male face they were asked to rate the pleasantness of a series of 5 different odorants, including AND. There was a significant correlation between women's rating of men's faces for long-term relationships and positive pleasantness ratings of AND. The authors argued that visual and olfactory (AND) cues interact to signal male reliability for long term romantic relationships. Another study (Saxton et al., 2008) studied the possible interaction between visual and cognitive attributes of men and AND signaling on womens' ratings of male attractiveness in three different speed dating events. AND dissolved in a masking odor, clove oil, was applied to the upper lip as had been done in some earlier studies (Jacob and McClintock, 2000; Jacob et al., 2002a) which sought to avoid any conscious perception of the presence of AND when it was presented. Application of AND, as opposed to clove oil alone or water, caused women (whose sexual orientation was not explicitly determined, although most were presumably heterosexual) to give men they encountered in two of the three speed dating events significantly higher attractiveness ratings. While not a uniformly positive outcome, these results further point to a possible AND-dependent facilitation of the effects of visual and other cognitive cues on women's perception of men as attractive romantic partners. A somewhat different outcome was obtained in another recent study (Parma et al., 2012) in which eye movements of heterosexual women were monitored while they viewed male or female faces or several different inanimate objects. Women that were studied during the preovulatory, follicular (potentially fertile) phase of the menstrual cycle showed maximal attention (viewing time) directed toward female faces (vs male faces or inanimate objects), regardless of whether AND (dissolved in clove oil) or clove oil alone (control) was applied to the upper lip. By contrast, women studied during their luteal phase (low conception risk) preferred to watch female faces, provided they had received AND on the upper lip prior to the test. The authors argued that AND enhances intrasex competition for mates, although their case would have been stronger had they found that the ability of AND to focus women's attention on potential competitors was highest during the fertile phase of the menstrual cycle.

CONCLUSION

Over the past decade numerous papers using several different mammalian species have established an essential role for the MOE-MOB-main olfactory circuit in the detection and processing of male pheromonal cues that signal potential reproductive partners. In this review we have centered on the mouse, pig, and ferret as representative species in which this role of the main olfactory system in females' mate recognition clearly occurs. There is also some evidence for a similar role of the main olfactory system in the female hamster, another frequently used animal for studies of pheromone effects on mate recognition. Surgical destruction of the VNO in female hamsters failed to disrupt the ability to discriminate flank odors from individual male hamsters nor did VNO removal disrupt females' preference to investigate male as opposed to female odors (Petrulis et al., 1999; Johnston and Peng, 2000). To my knowledge, nobody has assessed the effects of MOE lesions on the preference of female hamsters for male vs female pheromones. Thus evidence of a definitive role of the main olfactory system in mate recognition in female hamsters is not yet forthcoming. The same is true of the female rat. Future studies, perhaps best carried out using mice, need to address several central questions: Is there a contribution of experience (either nasal contact with male non-volatile pheromones or mating experience itself) to the establishment of females' preference to seek out volatile male pheromones and what, if any, releaser function might such volatile male pheromones have on the expression of females' mating behavior? Are local circuits in the MOB and AOB of female mice differentially tuned to respond to male pheromones (either volatile or non-volatile pheromones, respectively) as opposed to semiochemicals from other females or from young pups? If so, is there a role of

prepubertal ovarian hormones in the organization of female-typical responses to pheromones that are detected by the main and/or accessory olfactory systems? Finally, further, definitive, experiments are needed to determine whether the putative human male pheromone, AND, facilitates the attractivity of potential male sexual partners to women. A further analysis of the circuits that are activated by AND in men and women await the development of *in vivo* imaging methods with better resolution of amygdaloid and hypothalamic circuits than is possible with either PET or fMRI.

REFERENCES

Barnard, C. J., and Fitzsimons, J. (1989). Kin recognition and mate choice in mice: fitness consequences of mating with kin. *Anim. Behav.* 38, 35–40.

Baum, M. J., Everitt, B. J., Herbert, J., Keverne, E. B., and de Greef, W. J. (1976). Reduction of sexual interaction in rhesus monkeys by a vaginal action of progesterone. *Nature* 263, 606–608.

Baum, M. J., Keverne, E. B., Everitt, B. J., Herbert, J., and de Greef, W. J. (1977). Effects of progesterone and estradiol on sexual attractivity of female rhesus monkeys. *Physiol. Behav.* 18, 659–670.

Baum, M. J., Slob, A. K., de Jong, F. H., and Westbroek, D. L. (1978). Persistence of sexual behavior in ovariectomized stumptail macaques following dexamethasone treatment or adrenalectomy. *Horm. Behav.* 11, 323–347.

Berglund, H., Lindstrom, P., Dhejne-Helmy, C., and Savic, I. (2008). Male-to-female transsexuals show sex-atypical hypothalamus activation when smelling odorous steroids. *Cereb. Cortex* 18, 1900–1908.

Berglund, H., Lindstrom, P., and Savic, I. (2006). Brain response to putative pheromones in lesbian women. *Proc. Natl. Acad. Sci. U.S.A.* 103, 8269–8274.

Blaustein, J. D., and Erskine, M. S. (2002). "Feminine sexual behavior: cellular integration of hormonal and afferent information in the rodent brain," in *Hormones and Behavior,* eds D. W. Pfaff, A. P. Arnold, and E. Al (New York, NY: Academic Press), 139–214.

Boehm, T., and Zufall, F. (2006). MHC peptides and the sensory evaluation of genotype. *Trends Neurosci.* 29, 100–107.

Brennan, P. A., and Zufall, F. (2006). Pheromonal communication in vertebrates. *Nature* 444, 308–315.

Brock, O., Baum, M. J., and Bakker, J. (2011). The development of female sexual behavior requires prepubertal estradiol. *J. Neurosci.* 31, 5574–5578.

Brock, O., Douhard, Q., Baum, M. J., and Bakker, J. (2010). Reduced prepubertal expression of progesterone receptor in the hypothalamus of female aromatase knockout mice. *Endocrinology* 151, 1814–1821.

Buck, L., and Axel, R. (1991). A novel multigene family may encode odorant receptors: a molecular basis for odor recognition. *Cell* 65, 175–187.

Choi, G. B., Dong, H. W., Murphy, A. J., Valenzuela, D. M., Yancopoulos, G. D., Swanson, L. W., and Anderson, D. J. (2005). Lhx6 delineates a pathway mediating innate reproductive behaviors from the amygdala to the hypothalamus. *Neuron* 46, 647–660.

Ciumas, C., Linden Hirschberg, A., and Savic, I. (2009). High fetal testosterone and sexually dimorphic cerebral networks in females. *Cereb. Cortex* 19, 1167–1174.

Cloe, A. L., Woodley, S. K., Waters, P., Zhou, H., and Baum, M. J. (2004). Contribution of anal scent gland and urinary odorants to mate recognition in the ferret. *Physiol. Behav.* 82, 871–875.

Cornwell, R. E., Boothroyd, L., Burt, D. M., Feinberg, D. R., Jones, B. C., Little, A. C., Pitman, R., Whiten, S., and Perrett, D. I. (2004). Concordant preferences for opposite-sex signals? Human pheromones and facial characteristics. *Proc. Biol. Sci.* 271, 635–640.

DiBenedictis, B. T., Ingraham, K. L., Baum, M. J., and Cherry, J. A. (2012). Disruption of urinary odor preference and lordosis behavior in female mice given lesions of the medial amygdala. *Physiol. Behav.* 105, 554–559.

Dorries, K. M., Adkins-Regan, E., and Halpern, B. P. (1995). Olfactory sensitivity to the pheromone, androstenone, is sexually dimorphic in the pig. *Physiol. Behav.* 57, 255–259.

Dorries, K. M., Adkins-Regan, E., and Halpern, B. P. (1997). Sensitivity and behavioral responses to the pheromone androstenone are not mediated by the vomeronasal organ in domestic pigs. *Brain. Behav. Evol.* 49, 53–62.

Dorries, K. M., Schmidt, H. J., Beauchamp, G. K., and Wysocki, C. J. (1989). Changes in sensitivity to the odor of androstenone during adolescence. *Dev. Psychobiol.* 22, 423–435.

Dudley, C. A., and Moss, R. L. (1994). Lesions of the accessory olfactory bulb decrease lordotic responsiveness and reduce mating-induced c-fos expression in the accessory olfactory system. *Brain Res.* 642, 29–37.

Edwards, D. A., and Burge, K. G. (1973). Olfactory control of the sexual behavior of male and female mice. *Physiol. Behav.* 11, 867–872.

Fan, S., and Luo, M. (2009). The organization of feedback projections in a pathway important for processing pheromonal signals. *Neuroscience* 161, 489–500.

Goldfoot, D. A., Essock-Vitale, S. M., Asa, C. S., Thornton, J. E., and Leshner, A. I. (1978). Anosmia in male rhesus monkeys does not alter copulatory activity with cycling females. *Science* 199, 1095–1096.

Haga, S., Hattori, T., Sato, T., Sato, K., Matsuda, S., Kobayakawa, R., Sakano, H., Yoshihara, Y., Kikusui, T., and Touhara, K. (2010). The male mouse pheromone ESP1 enhances female sexual receptive behaviour through a specific vomeronasal receptor. *Nature* 466, 118–122.

Halem, H. A., Baum, M. J., and Cherry, J. A. (2001). Sex difference and steroid modulation of pheromone-induced immediate early genes in the two zones of the mouse accessory olfactory system. *J. Neurosci.* 21, 2474–2480.

Halem, H. A., Cherry, J. A., and Baum, M. J. (1999). Vomeronasal neuroepithelium and forebrain Fos responses to male pheromones in male and female mice. *J. Neurobiol.* 39, 249–263.

Helgason, A., Palsson, S., Gudbjartsson, D. F., Kristjansson, T., and Stefansson, K. (2008). An association between the kinship and fertility of human couples. *Science* 319, 813–816.

Isogai, Y., Si, S., Pont-Lezica, L., Tan, T., Kapoor, V., Murthy, V. N., and Dulac, C. (2011). Molecular organization of vomeronasal chemoreception. *Nature* 478, 241–245.

Jacob, S., Garcia, S., Hayreh, D., and McClintock, M. K. (2002a). Psychological effects of musky compounds: comparison of androstadienone with androstenol and muscone. *Horm. Behav.* 42, 274–283.

Jacob, S., and McClintock, M. K. (2000). Psychological state and mood effects of steroidal chemosignals in women and men. *Horm. Behav.* 37, 57–78.

Jacob, S., McClintock, M. K., Zelano, B., and Ober, C. (2002b). Paternally inherited HLA alleles are associated with women's choice of male odor. *Nat. Genet.* 30, 175–179.

Johnston, R. E., and Peng, M. (2000). The vomeronasal organ is involved in discrimination of individual odors by males but not by females in golden hamsters. *Physiol. Behav.* 70, 537–549.

Kang, N., Baum, M. J., and Cherry, J. A. (2009). A direct main olfactory bulb projection to the 'vomeronasal' amygdala in female mice selectively responds to volatile pheromones from males. *Eur. J. Neurosci.* 29, 624–634.

Kang, N., Baum, M. J., and Cherry, J. A. (2011). Different profiles of main and accessory olfactory bulb mitral/tufted cell projections revealed in mice using an anterograde tracer and a whole-mount, flattened cortex preparation. *Chem. Senses* 36, 251–260.

Keller, A., Zhuang, H., Chi, Q., Vosshall, L. B., and Matsunami, H. (2007). Genetic variation in a human odorant receptor alters odour perception. *Nature* 449, 468–472.

Keller, M., Douhard, Q., Baum, M. J., and Bakker, J. (2006a). Destruction of the main olfactory epithelium reduces female sexual behavior and olfactory investigation in female mice. *Chem. Senses* 31, 315–323.

Keller, M., Pierman, S., Douhard, Q., Baum, M. J., and Bakker, J. (2006b). The vomeronasal organ is required for the expression of lordosis behaviour, but not sex discrimination in female mice. *Eur. J. Neurosci.* 23, 521–530.

Kelliher, K., and Baum, M. (2002). Effect of sex steroids and coital experience on ferrets' preference for the smell, sight and sound of conspecifics. *Physiol. Behav.* 76, 1–7.

Kelliher, K. R., and Baum, M. J. (2001). Nares occlusion eliminates heterosexual partner selection without disrupting coitus in ferrets of both sexes. *J. Neurosci.* 21, 5832–5840.

Kelliher, K. R., Baum, M. J., and Meredith, M. (2001). The ferret's

vomeronasal organ and accessory olfactory bulb: effect of hormone manipulation in adult males and females. *Anat. Rec.* 263, 280–288.

Kelliher, K. R., Chang, Y. M., Wersinger, S. R., and Baum, M. J. (1998). Sex difference and testosterone modulation of pheromone-induced NeuronalFos in the Ferret's main olfactory bulb and hypothalamus. *Biol. Reprod.* 59, 1454–1463.

Kelliher, K. R., Spehr, M., Li, X. H., Zufall, F., and Leinders-Zufall, T. (2006). Pheromonal recognition memory induced by TRPC2-independent vomeronasal sensing. *Eur. J. Neurosci.* 23, 3385–3390.

Kevetter, G. A., and Winans, S. S. (1981a). Connections of the corticomedial amygdala in the golden hamster. I. Efferents of the "vomeronasal amygdala". *J. Comp. Neurol.* 197, 81–98.

Kevetter, G. A., and Winans, S. S. (1981b). Connections of the corticomedial amygdala in the golden hamster. II. Efferents of the "olfactory amygdala". *J. Comp. Neurol.* 197, 99–111.

Kim, S., Ma, L., and Yu, C. R. (2011). Requirement of calcium-activated chloride channels in the activation of mouse vomeronasal neurons. *Nat. Commun.* 2, 365.

Kimchi, T., Xu, J., and Dulac, C. (2007). A functional circuit underlying male sexual behaviour in the female mouse brain. *Nature* 448, 1009–1014.

Kimoto, H., Haga, S., Sato, K., and Touhara, K. (2005). Sex-specific peptides from exocrine glands stimulate mouse vomeronasal sensory neurons. *Nature* 437, 898–901.

Kouros-Mehr, H., Pintchovski, S., Melnyk, J., Chen, Y. J., Friedman, C., Trask, B., and Shizuya, H. (2001). Identification of non-functional human VNO receptor genes provides evidence for vestigiality of the human VNO. *Chem. Senses* 26, 1167–1174.

Larriva-Sahd, J. (2008). The accessory olfactory bulb in the adult rat: a cytological study of its cell types, neuropil, neuronal modules, and interactions with the main olfactory system. *J. Comp. Neurol.* 510, 309–350.

Liberles, S. D., and Buck, L. B. (2006). A second class of chemosensory receptors in the olfactory epithelium. *Nature* 442, 645–650.

Lin, D. Y., Zhang, S. Z., Block, E., and Katz, L. C. (2005). Encoding social signals in the mouse main olfactory bulb. *Nature* 434, 470–477.

Lin, W., Margolskee, R., Donnert, G., Hell, S. W., and Restrepo, D. (2007). Olfactory neurons expressing transient receptor potential channel M5 (TRPM5) are involved in sensing semiochemicals. *Proc. Natl. Acad. Sci. U.S.A.* 104, 2471–2476.

Lloyd-Thomas, A., and Keverne, E. B. (1982). Role of the brain and accessory olfactory system in the block to pregnancy in mice. *Neuroscience* 7, 907–913.

Luo, M., Fee, M. S., and Katz, L. C. (2003). Encoding pheromonal signals in the accessory olfactory bulb of behaving mice. *Science* 299, 1196–1201.

Mak, G. K., Enwere, E. K., Gregg, C., Pakarainen, T., Poutanen, M., Huhtaniemi, I., and Weiss, S. (2007). Male pheromone-stimulated neurogenesis in the adult female brain: possible role in mating behavior. *Nat. Neurosci.* 10, 1003–1011.

Martel, K. L., and Baum, M. J. (2007). Sexually dimorphic activation of the accessory, but not the main, olfactory bulb in mice by urinary volatiles. *Eur. J. Neurosci.* 26, 463–475.

Martel, K. L., and Baum, M. J. (2009a). Adult testosterone treatment but not surgical disruption of vomeronasal function augments male-typical sexual behavior in female mice. *J. Neurosci.* 29, 7658–7666.

Martel, K. L., and Baum, M. J. (2009b). A centrifugal pathway to the mouse accessory olfactory bulb from the medial amygdala conveys gender-specific volatile pheromonal signals. *Eur. J. Neurosci.* 29, 368–376.

Martinez-Garcia, F., Martinez-Ricos, J., Agustin-Pavon, C., Martinez-Hernandez, J., Novejarque, A., and Lanuza, E. (2009). Refining the dual olfactory hypothesis: pheromone reward and odour experience. *Behav. Brain Res.* 200, 277–286.

Martinez-Ricos, J., Agustin-Pavon, C., Lanuza, E., and Martinez-Garcia, F. (2007). Intraspecific communication through chemical signals in female mice: reinforcing properties of involatile male sexual pheromones. *Chem. Senses* 32, 139–148.

Martinez-Ricos, J., Agustin-Pavon, C., Lanuza, E., and Martinez-Garcia, F. (2008). Role of the vomeronasal system in intersexual attraction in female mice. *Neuroscience* 153, 383–395.

Martins, Y., Preti, G., Crabtree, C. R., Runyan, T., Vainius, A. A., and Wysocki, C. J. (2005). Preference for human body odors is influenced by gender and sexual orientation. *Psychol. Sci.* 16, 694–701.

McClintock, M. K. (2002). "Pheromones, odors, and vasanas: the neuroendocrinology of social chemosignals in humans and animals," in *Hormones, Brain and Behavior,* eds D. W. Pfaff, A. P. Arnold, A. M. Etgen, S. E. Fahrbach, and R. T. Rubin (San Diego, CA: Elsevier), 797–870.

Meisami, E., and Bhatnagar, K. P. (1998). Structure and diversity in mammalian accessory olfactory bulb. *Microsc. Res. Tech.* 43, 476–499.

Michael, R. P., and Keverne, E. B. (1968). Pheromones in the communication of sexual status in primates. *Nature* 218, 746–749.

Moors, L. M., and Lavers, R. B. (1981). Movements and home range of ferrets at the Pukepuke lagoon, New Zealand. *N.Z. J. Zool.* 8, 413–423.

Parma, V., Tirindelli, R., Bisazza, A., Massaccesi, S., and Castiello, U. (2012). Subliminally perceived odours modulate female intrasexual competition: an eye movement study. *PLoS ONE* 7:e30645. doi: 10.1371/journal.pone.0030645

Petrulis, A., Peng, M., and Johnston, R. E. (1999). Effects of vomeronasal organ removal on individual odor discrimination, sex-odor preference, and scent marking by female hamsters. *Physiol. Behav.* 66, 73–83.

Preti, G., Wysocki, C. J., Barnhart, K. T., Sondheimer, S. J., and Leyden, J. J. (2003). Male axillary extracts contain pheromones that affect pulsatile secretion of luteinizing hormone and mood in women recipients. *Biol. Reprod.* 68, 2107–2113.

Pro-Sistiaga, P., Mohedano-Moriano, A., Ubeda-Banon, I., del Mar Arroyo-Jimenez, M., Marcos, P., Artacho-Perula, E., Crespo, C., Insausti, R., and Martinez-Marcos, A. (2007). Convergence of olfactory and vomeronasal projections in the rat basal telencephalon. *J. Comp. Neurol.* 504, 346–362.

Rajendren, G., Dudley, C. A., and Moss, R. L. (1990). Role of the vomeronasal organ in the male-induced enhancement of sexual receptivity in female rats. *Neuroendocrinology* 52, 368–372.

Ramm, S. A., Cheetham, S. A., and Hurst, J. L. (2008). Encoding choosiness: female attraction requires prior physical contact with individual male scents in mice. *Proc. Biol. Sci.* 275, 1727–1735.

Roberts, S. A., Simpson, D. M., Armstrong, S. D., Davidson, A. J., Robertson, D. H., McLean, L., Beynon, R. J., and Hurst, J. L. (2010). Darcin: a male pheromone that stimulates female memory and sexual attraction to an individual male's odour. *BMC Biol.* 8, 75.

Savic, I., Berglund, H., Gulyas, B., and Roland, P. (2001). Smelling of odorous sex hormone-like compounds causes sex-differentiated hypothalamic activations in humans. *Neuron* 31, 661–668.

Savic, I., Berglund, H., and Lindstrom, P. (2005). Brain response to putative pheromones in homosexual men. *Proc. Natl. Acad. Sci. U.S.A.* 102, 7356–7361.

Saxton, T. K., Lyndon, A., Little, A. C., and Roberts, S. C. (2008). Evidence that androstadienone, a putative human chemosignal, modulates women's attributions of men's attractiveness. *Horm. Behav.* 54, 597–601.

Schaefer, M. L., Yamazaki, K., Osada, K., Restrepo, D., and Beauchamp, G. K. (2002). Olfactory fingerprints for major histocompatibility complex-determined body odors II: relationship among odor maps, genetics, odor composition, and behavior. *J. Neurosci.* 22, 9513–9521.

Schaefer, M. L., Young, D. A., and Restrepo, D. (2001). Olfactory fingerprints for major histocompatibility complex-determined body odors. *J. Neurosci.* 21, 2481–2487.

Signoret, J. P. (1967). Attraction de la femelle en oestrus par le male chez les porcins. *Rev. Comp. Anim.* 4, 10–22.

Signoret, J. P. (1970). Reproductive behaviour of pigs. *J. Reprod. Fertil. Suppl.* (Suppl. 11), 105–117.

Slotnick, B., Restrepo, D., Schellinck, H., Archbold, G., Price, S., and Lin, W. (2010). Accessory olfactory bulb function is modulated by input from the main olfactory epithelium. *Eur. J. Neurosci.* 31, 1108–1116.

Sosulski, D. L., Bloom, M. L., Cutforth, T., Axel, R., and Datta, S. R. (2011). Distinct representations of olfactory information in different cortical centres. *Nature* 472, 213–216.

Spehr, M., Kelliher, K. R., Li, X. H., Boehm, T., Leinders-Zufall, T., and Zufall, F. (2006). Essential role of the main olfactory system in social recognition of major histocompatibility complex peptide ligands. *J. Neurosci.* 26, 1961–1970.

Spencer, N. A., McClintock, M. K., Sellergren, S. A., Bullivant, S., Jacob, S., and Mennella, J. A. (2004). Social chemosignals from breastfeeding women increase sexual motivation. *Horm. Behav.* 46, 362–370.

Stern, K., and McClintock, M. K. (1998). Regulation of ovulation by human pheromones. *Nature* 392, 177–179.

Thompson, J. A., Salcedo, E., Restrepo, D., and Finger, T. E. (2012). Second order input to the medial amygdala from olfactory sensory neurons expressing the transduction channel TRPM5. *J. Comp. Neurol.* 520, 1819–1830.

Tirindelli, R., Dibattista, M., Pifferi, S., and Menini, A. (2009). From pheromones to behavior. *Physiol. Rev.* 89, 921–956.

Trotier, D., Eloit, C., Wassef, M., Talmain, G., Bensimon, J., Doving, K., and Ferrand, J. (2000). The vomeronasal cavity in adult humans. *Chem. Senses* 25, 369–380.

Veyrac, A., Wang, G., Baum, M. J., and Bakker, J. (2011). The main and accessory olfactory systems of female mice are activated differentially by dominant versus subordinate male urinary odors. *Brain Res.* 1402, 20–29.

Weiler, E., Apfelbach, R., and Farbman, A. I. (1999). The vomeronasal organ of the male ferret. *Chem. Senses* 24, 127–136.

Wersinger, S. R., and Baum, M. J. (1997). Sexually dimorphic processing of somatosensory and chemosensory inputs to forebrain luteinizing hormone-releasing hormone neurons in mated ferrets. *Endocrinology* 138, 1121–1129.

Woodley, S. K., and Baum, M. J. (2004). Differential activation of glomeruli in the ferret's main olfactory bulb by anal scent gland odours from males and females: an early step in mate identification. *Eur. J. Neurosci.* 20, 1025–1032.

Woodley, S. K., Cloe, A. L., Waters, P., and Baum, M. J. (2004). Effects of vomeronasal organ removal on olfactory sex discrimination and odor preferences of female ferrets. *Chem. Senses* 29, 659–669.

Wyart, C., Webster, W. W., Chen, J. H., Wilson, S. R., McClary, A., Khan, R. M., and Sobel, N. (2007). Smelling a single component of male sweat alters levels of cortisol in women. *J. Neurosci.* 27, 1261–1265.

Wysocki, C. J., and Preti, G. (2004). Facts, fallacies, fears, and frustrations with human pheromones. *Anat. Rec. A Discov. Mol. Cell. Evol. Biol.* 281, 1201–1211.

Wysocki, C. J., Yamazaki, K., Curran, M., Wysocki, L. M., and Beauchamp, G. K. (2004). Mice (*Mus musculus*) lacking a vomeronasal organ can discriminate MHC-determined odortypes. *Horm. Behav.* 46, 241–246.

Xu, F., Greer, C. A., and Shepherd, G. M. (2000). Odor maps in the olfactory bulb. *J. Comp. Neurol.* 422, 489–495.

Xu, F., Schaefer, M., Kida, I., Schafer, J., Liu, N., Rothman, D. L., Hyder, F., Restrepo, D., and Shepherd, G. M. (2005). Simultaneous activation of mouse main and accessory olfactory bulbs by odors or pheromones. *J. Comp. Neurol.* 489, 491–500.

Zhang, J. X., Soini, H. A., Bruce, K. E., Wiesler, D., Woodley, S. K., Baum, M. J., and Novotny, M. V. (2005). Putative chemosignals of the ferret (*Mustela furo*) associated with individual and gender recognition. *Chem. Senses* 30, 727–737.

Zhuang, H., Chien, M. S., and Matsunami, H. (2009). Dynamic functional evolution of an odorant receptor for sex-steroid-derived odors in primates. *Proc. Natl. Acad. Sci. U.S.A.* 106, 21247–21251.

Conflict of Interest Statement: The author declares that the research was conducted in the absence of any commercial or financial relationships that could be construed as a potential conflict of interest.

Received: 17 April 2012; accepted: 19 May 2012; published online: 05 June 2012.

*Citation: Baum MJ (2012) Contribution of pheromones processed by the main olfactory system to mate recognition in female mammals. Front. Neuroanat. **6**:20. doi: 10.3389/fnana.2012.00020*

frontiers in
NEUROANATOMY

ORIGINAL RESEARCH ARTICLE
published: 06 July 2012
doi: 10.3389/fnana.2012.00025

Sexual activity increases the number of newborn cells in the accessory olfactory bulb of male rats

Wendy Portillo[1], Nancy Unda[1], Francisco J. Camacho[1], María Sánchez[1], Rebeca Corona[1], Dulce Ma. Arzate[1], Néstor F. Díaz[2] and Raúl G. Paredes[1]*

[1] Instituto de Neurobiología, Universidad Nacional Autónoma de México, Querétaro, México
[2] Instituto Nacional de Perinatología, D.F., México

Edited by:
Micheal Baum, Boston University, USA

Reviewed by:
Jianzheng Zheng, University of New Mexico, USA
Matthieu Keller, Centre National de la Recherche Scientifique, France

***Correspondence:**
Raúl G. Paredes, Instituto de Neurobiología, Universidad Nacional Autónoma de México, Apartado Postal 1-1141, Querétaro, Qro 76001, México.
e-mail: rparedes@unam.mx

In rodents, sexual behavior depends on the adequate detection of sexually relevant stimuli. The olfactory bulb (OB) is a region of the adult mammalian brain undergoing constant cell renewal by continuous integration of new granular and periglomerular neurons in the accessory (AOB) and main (MOB) olfactory bulbs. The proliferation, migration, survival, maturation, and integration of these new cells to the OB depend on the stimulus that the subjects received. We have previously shown that 15 days after females control (paced) the sexual interaction an increase in the number of cells is observed in the AOB. No changes are observed in the number of cells when females are not allowed to control the sexual interaction. In the present study we investigated if in male rats sexual behavior increases the number of new cells in the OB. Male rats were divided in five groups: (1) males that did not receive any sexual stimulation, (2) males that were exposed to female odors, (3) males that mated for 1 h and could not pace their sexual interaction, (4) males that paced their sexual interaction and ejaculated one time and (5) males that paced their sexual interaction and ejaculated three times. All males received three injections of the DNA synthesis marker bromodeoxyuridine at 1h intervals, starting 1 h before the beginning of the behavioral test. Fifteen days later, males were sacrificed and the brains were processed to identify new cells and to evaluate if they differentiated into neurons. The number of newborn cells increased in the granular cell layer (GrCL; also known as the internal cell layer) of the AOB in males that ejaculated one or three times controlling (paced) the rate of the sexual interaction. Some of these new cells were identified as neurons. In contrast, no significant differences were found in the mitral cell layer (also known as the external cell layer) and glomerular cell layer (GlCL) of the AOB. In addition, no significant differences were found between groups in the MOB in any of the layers analyzed. Our results indicate that sexual behavior in male rats increases neurogenesis in the GrCL of the AOB when they control the rate of the sexual interaction.

Keywords: sexual behavior, neurogenesis, accessory olfactory bulb and main olfactory bulb

INTRODUCTION

In rodents, male sexual behavior relies on the male's ability to identify a conspecific and to determine if she is sexually receptive. Sexually active females and males emit many kinds of stimuli that affect several sensory modalities to attract the opposite sex. Several studies have demonstrated that olfactory cues are crucial for the appropriate selection of a sexual partner in rodents (Curtis et al., 2001; Brennan and Kendrick, 2006; Baum and Kelliher, 2009).

The accessory and the main olfactory systems are functionally and anatomically interrelated. Thus, the main olfactory system can respond to odors that effectively activate the accessory olfactory system and neurons in the vomeronasal organ can be activated by volatile and non volatile odorants (Trinh and Storm, 2003; Xu et al., 2005; Levai et al., 2006; Spehr et al., 2006). Both systems respond sequentially to sexually relevant cues, responsible for social responses to chemical signals from conspecifics (Xu et al., 2005; Martel and Baum, 2007; Jakupovic et al., 2008; Slotnick et al., 2010). There are, in fact two sites of interaction between the main (MOB) and accessory (AOB) olfactory bulb (OB) namely, interstitial neurons of the bulbi (INBs) and the main accessory cells (MAC) (Larriva-Sahd, 2008).

In male rats, mating activates the granular (GrCL; also known as the internal) and mitral (MCL; also known as the external) cell layers of the AOB as evaluated by expression of the immediate early gene cFos (Kondo et al., 2003). Surgical removal of the vomeronasal organ decreases basal as well as mating induced cFos in the GrCL (Kondo et al., 2003). Sexually experienced male rats with lesions of the vomeronasal organ show an increase in the number of mounts and a longer intromission and ejaculation latency (Saito and Moltz, 1986; Kondo et al., 2003). Sexually naive male rats with lesions of the vomeronasal organ also show longer intromission and ejaculation latencies and higher number of intromissions (Saito and Moltz, 1986). On the other hand, in sexually experienced male rats, olfactory preference for sexually active females is impaired by lesions of the olfactory epithelium

(Dhungel et al., 2011). These lesions decrease intromission frequency and increase ejaculation and mount latency (Dhungel et al., 2011). These studies clearly indicate that the olfactory systems play a crucial role in the modulation of male sexual behavior.

The OB is a region where new neurons are continuously added during adult life (Alvarez-Buylla and Garcia-Verdugo, 2002). The new cells originate in the subventricular zone, which contains neuronal stem cells that generate neuroblasts (Reynolds and Weiss, 1992; Lois et al., 1996). The neuroblasts travel along the rostral migratory stream toward the OB using tangential chain migration (Lois et al., 1996; Peretto et al., 1997). Once they reach the OB the immature cells detach from the migratory stream and migrate radially toward different layers of the MOB and AOB (Peretto et al., 2001; Belluzzi et al., 2003; Carleton et al., 2003; Curtis et al., 2007; Oboti et al., 2009). Approximately 95% of the new neurons differentiate into GABAergic granular interneurons (Lledo and Saghatelyan, 2005; Bagley et al., 2007). A minority become GABAergic periglomerular interneurons (Bagley et al., 2007; Batista-Brito et al., 2008; Whitman and Greer, 2009; Ming and Song, 2011). Petreanu and Alvarez-Buylla (2002) describe five stages in the differentiation of adult born granular cells in mice. In stage 1 (days 2–7) cells migrate to the rostral migratory stream, in stage 2 (days 5–9) the new cells initiate radial migration to the OB. In stage 3 (days 9–13) they reach their final position, in stage 4 (days 11–22) the new cells develop dendrite arbors, and finally in stage 5 (days 21–42) the new granular cells show a mature morphology (Petreanu and Alvarez-Buylla, 2002). Between 15 and 45 days after birth, approximately 50% of the newly generated granule cells die and the other half is integrated in the OB.

The survival of the new cells depends on the level of activity that they received (Petreanu and Alvarez-Buylla, 2002; Winner et al., 2002). For example, it has been demonstrated that in male mice the prolonged exposure (40 days) to an odor enriched environment increases the number of new cells in the glomerular cell layer (GlCL) of the MOB facilitating odor discrimination (Rochefort et al., 2002; Rochefort and Lledo, 2005). Sexually relevant odors also increase neurogenesis in the OB (Mak et al., 2007; Larsen et al., 2008; Oboti et al., 2009). Exposure of female mice for seven days to pheromones from a dominant, but not from a subordinate male, induced an increase in the number of new cells in the subventricular zone and dentate gyrus. This increase in the number of new cells had functional relevance because females exposed to soiled bedding from dominant males showed a clear preference for these males instead of subordinate males. This preference was eliminated if the females were treated with a mitotic inhibitor in order to prevent neurogenesis (Mak et al., 2007). The new cells that are integrated into the OB express cFos in response to estrous female odors and mating stimulation in male hamsters (Huang and Bittman, 2002). Taken together, these studies suggest that the new cells that reach the OBs can participate in the processing of socio-sexual relevant signals.

Sexual behavior also induces cell proliferation and neurogenesis. Males that mated once or several times show an increase in cell proliferation and neurogenesis in the dentate gyrus of the hippocampus. No changes were observed in those males only exposed to receptive females (Leuner et al., 2010). Our laboratory was the first to demonstrate that sexual stimulation in females increases the number of new cells in the OB. Female rats that paced the sexual interaction showed an increase in the number of new cells that reach the GrCL of the AOB 15 days after mating. No significant differences were found in the number of new cells in GlCL, or MCL of the AOB. Nor were any significant differences found in the cell layers of the MOB (Corona et al., 2011b). The aim of the present study was to evaluate if sexual behavior in male rats increases the number of new cells that reach the OB and if those new cells differentiate into neurons. We evaluated the number of new cells in the OB 15 days after sexual stimulation because at this time more new cells arrive to the layers of the OB and develop spines (Petreanu and Alvarez-Buylla, 2002; Winner et al., 2002).

For this purpose the following groups were included: (1) control males, that did not receive any sexual stimulation, (2) males exposed for 1 h to a sexually receptive female, (3) males that mated for 1 h in a setting where they were not able to pace the sexual interaction, (4) males that paced their sexual interaction with a receptive female until they ejaculated once and (5) males that paced their sexual interaction until they ejaculated three times. We predicted that those males that control the rate (pace) of the sexual interaction would have a higher number of new cells in the GrCL but not in the MCL or GlCL layer of the AOB. In addition, since no changes were observed in the MOB when females paced the sexual interaction we did not expect differences in any of the layers of the MOB. We also evaluated if some of the new cells differentiate into neurons.

METHODS

ANIMALS

Sexually naive male Wistar rats (250–350 g) were obtained from the local breeding colony at the Instituto de Neurobiología de la Universidad Nacional Autónoma de México. Subjects were maintained in a room with controlled temperature (25 °C) and humidity and under a reverse dark-light cycle (12–12 h). Standard laboratory rat chow and water were available ad libitum. Sexually experienced female Wistar rats (200–300 g) were used as stimulus. They were gonadectomized and brought into estrous by hormone treatment with 25 μg/rat of estradiol benzoate (Sigma) 48 h before and with 1mg/rat of progesterone (Aldrich) 4 h before the mating test (Gonzalez-Flores et al., 2004; Arzate et al., 2011; Corona et al., 2011a). In order to acquire sexual experience males mated in a condition where they were allow to pace the sexual interaction with sexually receptive females in three 30 min tests, one test per week. Only those males that ejaculated in each test were included in the experiment. All experiments were carried out in accordance with the "Reglamento de la Ley General de Salud en Materia de Investigación para la Salud" of the Mexican Health Ministry.

APPARATUS

The behavioral tests were performed in clear acrylic cages (40 × 60 × 40 cm), with fresh sawdust covering the cage floor.

EXPERIMENTAL DESIGN

Groups

Males were randomly divided into five groups ($N = 7$ each) as follows: group (1) males were placed for 1 h in a clean mating cage without sexual or olfactory stimulation (control, C); group (2) males were exposed for 1 h to female odors (EXP). They were placed in a mating cage divided in two equal compartments by an acrylic screen with 1 mm diameter holes. The experimental male was placed on one side of the cage and the sexually receptive female on the opposite side; in this way, males were able to smell, see and hear the stimulus female without physical contact; group (3) males mated for 1 h in a setting where they were not able to pace the sexual interaction (NP). In this group the mating cage was divided by a removal clear screen with a small hole at the bottom that allowed the female, but not the male, to move freely from one side of the cage to the other. In this condition the male is not able to pace the sexual interaction; group (4) males paced their sexual interaction with a receptive female until they ejaculated one time (1E); group (5) males paced their sexual interaction until they ejaculated three times (3E), see **Figure 1**. Each male always mated with the same female to avoid possible effects of female novelty on the number of new cells.

SEXUAL BEHAVIOR PARAMETERS

In the sexual behavioral tests, the following parameters were recorded: number of mounts (M), intromissions (I), and ejaculations (E); the latency to first M, I, and E; the post ejaculatory interval (PEI) and the inter-intromission interval (III, ejaculation latency/number of intromission before ejaculation).

BrdU ADMINISTRATION

On day 0 of the experiment, males were injected intraperitoneally three times with the DNA synthesis marker 5′-bromo-2-deoxyuridine (BrdU; Sigma, dissolved in saline solution). They were injected: (1) 1 h before the test, (2) immediately after the behavioral test and (3) 1 h after the test. This procedure allows labeling of the new cells synthesized around the time of the behavioral test. Each BrdU administration was 100 mg/kg which means that each male received a total of 300 mg/kg of the DNA synthesis marker (**Figure 1**).

Fifteen days after BrdU administration, all males were injected with a lethal dose of sodium pentobarbital (100 mg/kg). They were perfused with 0.1 M phosphate-buffered solution (PBS, pH 7.4) followed by 4% paraformaldehyde in 0.1 M PBS. The brains were removed from the skull and postfixed in 4% paraformaldehyde for 1 h before they were placed in 30% sucrose dissolved in 0.1 M PBS solution for cryoprotection. The two brain hemispheres were separated and the right half was sliced in the sagittal plane at 35 μm using a sledge microtome. Brain slices were divided in two series; one was processed for immunohistochemistry and the other for immunofluorescence.

IMMUNOCHEMISTRY

Brain slices were processed as previously reported (Corona et al., 2011b). Briefly, free-floating sections were incubated for at least 16 h at 4°C in primary antibody mouse monoclonal anti-BrdU (1:2,000; BD Bioscience). Later, primary antibody was removed by rinsing and the tissue was incubated for 2 h at room temperature with the secondary antibody biotinylated goat anti-mouse IgG (1:500; Vector laboratories). Brain sections were then rinsed and incubated in Avidin Biotin Complex (AB elite kit; Vector Laboratories) for 90 min at room temperature. Brain sections were rinsed and revealed with the chromogen solution nickel chloride-3,3′-diaminobenzidine (DAB; Vector Laboratories) and H_2O_2. Finally, the reactions were stopped by washing the slices in buffer solution. The brain slices were mounted onto

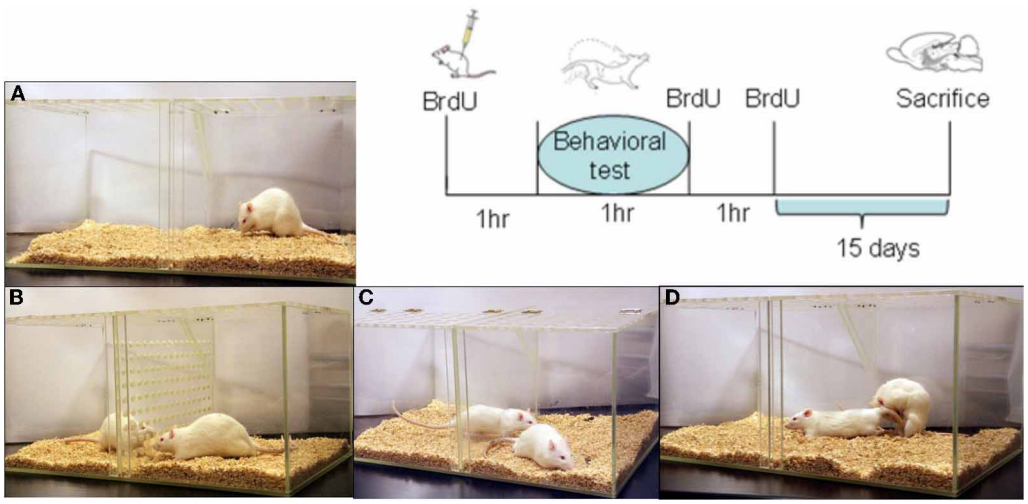

FIGURE 1 | Representation of the different groups (A–D) and sequence of BrdU injections for all subjects. The control group **(A)** was placed in the mating cage for 1 h; in group **(B)** males were exposed without physical contact to a sexually receptive female; in group **(C)** the males mated but could not control the rate of the sexual interaction, while males in group **(D)** were allowed to pace the sexual interaction until 1 ejaculation or until 3 ejaculations. BrdU treatment (100 mg/kg per injection; 3 injections) was administered 1 h before the behavioral test (day 0), at the end of the test, and 1 h after the test. Subjects were sacrificed 15 days after the behavioral test.

gelatin-coated slides and cover slipped using permount. For each animal, three sections were analyzed, and the average was used for statistical analysis. The OB was reconstructed using microphotographs (10×) taken in a light microscope (Olympus BX60) connected to a motorized slide (Prior ProScan) and analyzed by Image Pro software. Sagittal brain sections were selected at the level of the AOB and MOB; we analyzed the GrCL, MCL, and GlCL layers (**Figure 2A**). The area of interest was delimited on the AOB by three circles of 200 μm diameter and in the MOB by 400 μm diameter circles placed in the rostral medial region. We chose these locations because we and other groups have evaluate neurogenesis process in this region (Bagley et al., 2007; Whitman and Greer, 2009; Corona et al., 2011b), and cells in these areas are activated during the processing of relevant odors (Keller et al., 2006). Data were expressed as the number of new cells per area in order to compare with our previous studies in female rats and in accordance with reports that evaluate the neurogenesis process in the OB (Alonso et al., 2006; Mouret et al., 2008; Honda et al., 2009; Mouret et al., 2009; Corona et al., 2011b).

IMMUNOFLUORESCENCE

In order to evaluate if the new cells (BrdU positive) differentiate into neuron lineage we measured immunofluorescence of neuronal nuclei. For this analysis we processed brains only from C, 1E, and 3E groups, because 1E and 3E groups showed an increased in the number of new cells in comparison to control males. As we already described (Corona et al., 2011b) sagittal brain sections were incubated for two nights at 4°C with the primary antibodies, rat monoclonal anti-BrdU (1:800; AbD serotec) and mouse monoclonal Neuronal Nuclei antibody (NeuN) to label mature neurons (1:250; CHEMICON). Later the samples were incubated with the secondary antibodies, anti-rat IgG Alexa Fluor 488 (1:1000; Invitrogen) and anti-mouse IgG Alexa Fluor 568 (1:1,000; Invitrogen), respectively. At the end of the procedure the brain sections were mounted and cover slipped using Aqua Poly/Mount (Polysciences, Inc.). At least three sections of three animals in each group were evaluated and the average of the sections per male were analyzed. Olfactory bulb reconstruction was made at 20× using a fluorescence lamp. Image-Pro software was used to merge photographs of the BrdU and NeuN positive cells. In order to verify the double labeled cells, the images were acquired in a LSM 510 Meta confocal microscope (Carl Zeiss, Germany) using a plan-neofluar 20× objective (N.A. 0.50, Zeiss), to detect Alexa 488 with Argon Laser in 488 nm wavelength and Alexa 568 was detected with DPSS Laser 561 nm wavelength fluorescence in a sequential fashion. To establish co-expression of the markers used, merged images were generated (**Figure 4**). The examiner was unaware of the groups of the slices.

STATISTICS

Data from sexual behavior were not normally distributed and therefore were analyzed by a Kruskal-Wallis test followed by Student Newman-Keuls test. Data from the number of BrdU immunoreactive cells and number of BrdU/NeuN immunofluorescence cells were normally distributed and therefore analyzed by One-Way analysis of variance (ANOVA) for each layer. In case of significant effects *post hoc* comparisons were performed with Fisher's least significant difference test.

RESULTS

SEXUAL BEHAVIOR

During the three training tests to obtain sexual experience no significant differences between groups were observed in any of the parameters analyzed (data not shown). In the sexual behavior test performed when BrdU was injected we found a significant difference in the number of intromissions (K-W test: $\chi^2 = 6.75$,

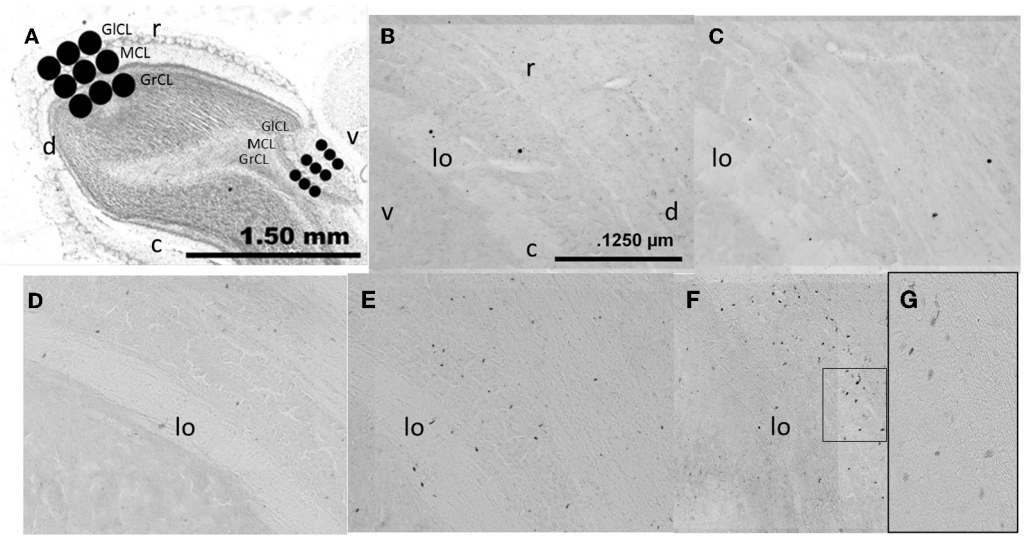

FIGURE 2 | Photomicrographs showing the layers analyzed in the sagittal (A) plane in the AOB and MOB, glomerular cell layer (GlCL), mitral cell layer (MCL), and granular cell layer (GrCL). Representative photomicrographs (10×) showing BrdU positive cells in the GrCL of the AOB in control **(B)**, exposed **(C)**, non-paced **(D)**, 1 ejaculation **(E)** and 3 ejaculation **(F)** groups. A 40× magnification of the 3 ejaculation group is shown in **(G)**. lo, lateral olfactory tract; r, rostral; c, caudal; d, dorsal and v, ventral.

$P = 0.034$). The *Post hoc* test revealed that the 1E and 3E groups displayed a higher number of intromissions than the NP group. Significant differences were also found in III (K-W test: $\chi^2 = 7.22$, $P = 0.027$), the NP group had a longer III than 1E and 3E groups. Although the 3E and 1E groups had a higher number of M that NP males, this difference was not statistically different (K-W test: $\chi^2 = 5.8$, $P = 0.054$). As well, in the other parameters no significant differences were found: latency to the first M (K-W test: $\chi^2 = 0.5$, $P = 0.79$), I (K-W test: $\chi^2 = 0.9$, $P = 0.65$), E (K-W test: $\chi^2 = 0.36$, $P = 0.83$), and PEI (K-W test: $\chi^2 = 4.4$, $P = 0.11$) **Table 1**.

BrdU POSITIVE CELLS

AOB

Our data showed significant differences between groups in the number of new cells in the GrCL [$F_{(4, 34)} = 11.64$, $P < 0.001$]. *Post hoc* tests revealed an increase in the number of new cells in the 3E group compared to all other groups. We also found significantly more new cells in the 1E group than in groups C and NP.

No significant differences between groups were found in the number of new cells in the MCL [$F_{(4, 23)} = 0.52$, $P = 0.72$], nor did we find any significant differences in the GlCL [$F_{(4, 34)} = 0.51$, $P = 0.74$] (**Figures 2B–G** and **3A**).

MOB

No significant differences were found between groups in the number of new cells in the GlCL [$F_{(4, 34)} = 1.85$, $P = 0.15$]; MCL [$F_{(4, 34)} = 0.39$, $P = 0.82$] or GrCL [$F_{(4, 34)} = 1.49$, $P = 0.23$] (**Figure 3B**).

We also evaluated the number of new cells in the coronal plane in the AOB and MOB to determinate if the results vary depending on the type of section. In the AOB, identical results were found, that is a significant greater number of BrdU positive cells in the GrCL in the 3E group compared to all other groups. A significant increase in the 1E group as compared to the C, EXP, and NP groups was also observed. No significant differences were found in the GlCL and ML (data not shown). In the MOB, as well as the sagittal sections, no significant differences were found in the coronal GlCL and MCL. However in the coronal GrCL we found that the 3E group integrates more cells than the 1E and control group (data not shown). This difference could be a spurious effect since the difference is marginal ($P = 0.04$) and has not been observed in females. Thus, in general the results did not depend on the type of section.

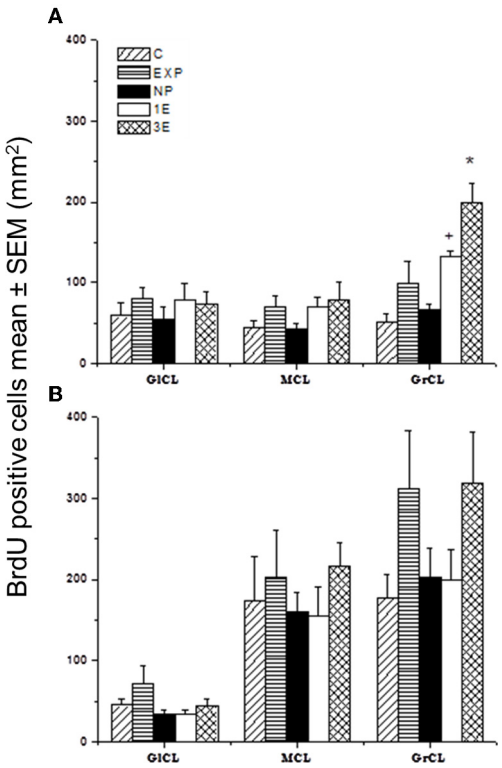

FIGURE 3 | Number of BrdU positive cells in the sagittal plane in the accessory olfactory bulb (AOB; A) and main olfactory bulb (MOB; B) in control (C), exposed (EXP), non-paced (NP), 1 ejaculation (1E), and 3 ejaculation (3E) groups. The areas analyzed were the glomerular (GlCL), mitral (MCL) and granular cell layer (GrCL). Data are expressed as mean ± SEM. $N = 7$.
*Different from all other groups in the same layer. $P < 0.05$.
+Different from C and NP in the same layer. $P < 0.05$.

Table 1 | Sexual behavior parameters in the different groups; no pacing (NP), one ejaculation (1E), and three ejaculations (3E).

	NP	1E	3E
Number			
Mounts	6 ± 1	14.3 ± 3.2	8.1 ± 1.3
Intromissions	11 ± 1.2	20.4 ± 2.3*	18.7 ± 3*
Ejaculations	3.4 ± 0.2	1	3
Latencies (sec)			
Mounts	94.3 ± 25.3	183.1 ± 82.6	122.1 ± 40
Intromissions	103.6 ± 26.7	223.28 ± 95.9	154.1 ± 44.3
Ejaculations	937.9 ± 85.8	905.6 ± 189.2	903.9 ± 186
IPE	417.9 ± 36.6	356 ± 13.2	416.7 ± 21.3
III (sec)	94.7 ± 19.3	45.4 ± 9.3*	49.5 ± 8.1*

Data are expressed as mean ± SEM. N = 7 per group.
** Different from NP. P < 0.05.*

BrdU/NeuN positive cells

We quantified the number of new cells that expressed the marker of neuronal differentiation (BrdU/NeuN positives) in the GrCL in the C, 1E, and 3E groups because only between them we found significant differences in the number of new cells. Our data showed significant differences in the number of BrdU/NeuN positive cells [$F_{(2, 8)} = 9.0$, $P = 0.02$]. The *post hoc* test showed that the 3E group had more BrdU/NeuN positive cells per mm^2 (BrdU positive cells 155.7 ± 20, BrdU/NeuN positive cells 69 ± 8, 44%) than the C (BrdU positive cells 51.3 ± 30.7, BrdU/NeuN positive cells 26.5 ± 9.2, 52%) and 1E groups (BrdU positive cells 106.2 ± 22, BrdU/NeuN positive cells 33.6 ± 4.7, 32%). In order to verify the colocalization of the double-labeled BrdU/NeuN cells we obtained 20× photomicrographs using a confocal microscope

(Zeiss LSM 510) in the GrCL of the AOB, two sagittal slices from three randomly chosen subjects from the C, 1E and 3E groups were analyzed (**Figure 4**).

DISCUSSION

As expected, our data indicate that those males that ejaculated in a condition where they controlled the rate of sexual stimulation (paced mating) have a higher number of new cells in the GrCL of the AOB, regardless whether they ejaculated one or three times. We also showed that around 40% of these new cells differentiate into neurons within 15 days after mating and BrdU administration. Our results indicate that the increase in the number of new cells in the GrCL of the AOB depends on the ability to pace the sexual interaction more than on the number of ejaculations itself. The group of males not allowed to pace the sexual interaction ejaculated a mean of 3.4 times during the 1 h test (NP group) but did not show an increase in the number of new cells. Thus, paced genital stimulation appears to be fundamental to potentiate neurogenesis in the GrCL of the AOB in the adult male rat. The genital stimulation that the male receives during paced and non-paced mating is quantitatively and qualitatively different. Males that mate in a setting where they control (pace) the sexual interaction display a higher number of intromissions, longer intromission duration and a shorter inter-intromission interval in comparison to males not able to control the sexual interaction. Thus penile stimulation during intromissions is higher in those males that pace the sexual interaction (Erskine, 1989). The results of the present study further support this contention: males that paced the sexual interaction (1E and 3E) displayed a higher number of intromissions and had a shorter inter-intromission interval than the group unable to pace the sexual interaction (NP).

Another difference between paced and non-paced mating is the rewarding value of the sexual interaction. Sexual stimulation induces a reward state only if subjects, males or females, pace the sexual interaction (Martinez and Paredes, 2001; Camacho et al., 2009). This reward state is mediated by opioids since administration of the opioid antagonist naloxone, blocks the rewarding effects induced by sexual behavior in both males and females (Agmo and Gomez, 1993; Paredes and Martinez, 2001). Based on these and other observations it has been postulated that opioids are release during sexual behavior thereby reducing the aversive consequences of repeated sexual stimulation and enabling the eventual development of a reward or positive affective state (Agmo and Gomez, 1993; Paredes, 2009, 2010). Interestingly, opioids are also involved in the proliferation and survival of the new cells in the subventricular zone (Sargeant et al., 2008). Morphine treatment increased the number of new cells [detected by (3H) thymidine up take] in the subventricular zone of adult male rats (Messing et al., 1979; Miller et al., 1982). Furthermore, activation of the δ opioid receptor induced neuronal differentiation of brain stem cells, and the blockade of this opioid receptor induced astrogliosis (Narita et al., 2006). Therefore, endogenous opioid release during paced mating could be involved in the higher number of new neurons observed in the AOB.

Similar arguments could be presented for other neuromodulators. For example, oxytocin is also involved in the reward aspects of sexual interaction in females. Moreover, oxytocin release increases in the hypothalamic paraventricular nucleus of those females that pace the sexual interaction (Nyuyki et al., 2011). Additionally, oxytocin increases proliferation and adult neurogenesis in the ventral dentate gyrus of the hippocampus (Leuner et al., 2012). Further studies need to directly assess if blockade of either opioids or oxytocin during sexual behavior interferes with the increase of new neurons in the AOB.

It has been demonstrated that sexual stimulation activates neurons in the AOB. For example, Binns and Brennan demonstrated

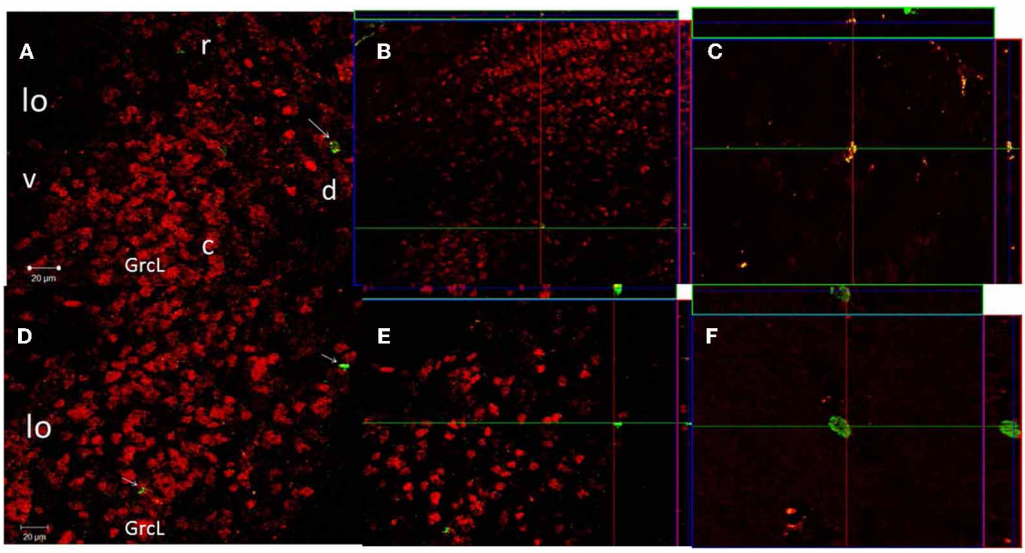

FIGURE 4 | Confocal images of cells in the GrCL of the AOB double-labeled with NeuN (red) and BrdU (green), taken at 20× magnification. Projection and orthogonal plane in control **(A–C)**, and 3E **(D–F)** groups. The images were rotated in orthogonal planes to verify double labeling throughout its extent **(B,E)**. Photomicrographs C and F were taken at 63× magnification. r, rostral; c, caudal; d, dorsal and v, ventral.

that mating in female mice induces a significant change in baseline activity in local field potential (LFP) in the granular cells of the AOB, resulting in significantly higher baseline LFP power in the frequency bands related to sensory perception and long-range interaction between brain regions (Binns and Brennan, 2005). Vaginal stimulation in females during proestrous-estrous also induces an increase in the firing rate in cells of the mitral cell layer of the MOB (Guevara-Guzman et al., 1997). In the same study, an increase in the number of cells that express cFos was reported in the GrCL of the AOB and in the GlCL and external plexiform layers of the MOB in proestrous-estrous females after vaginal stimulation (Guevara-Guzman et al., 1997).

Changes in olfactory function after exposure to relevant chemosensory cues and sexual stimulation are also observed in males. Subjects exposed to soiled estrous bedding showed an increase in the number of granular cells that express the immediate early gene, activity-regulated cytoskeleton-associated protein (ARC) in the MOB. Mating caused an even greater increase in the number of ARC-expressing granular cells in the MOB and in the AOB (Matsuoka et al., 2002). Moreover, in male rats genital stimulation increased the number of cells that express cFos in the medial amygdala and in the GrCL and MCL layers of the AOB (Kondo et al., 2003). Thus, genital stimulation can modify the activity of the OB, and this stimulation can be fundamental to increase the number of new cells that arrive to the AOB.

In the present study no changes in the number of new cells were observed in the group exposed to a sexually receptive female. This observation is at variance with reports showing that scent-rich environments and sexually-relevant odors induce an increase in the number of new cells in the OB (Mak et al., 2007; Larsen et al., 2008; Oboti et al., 2009). However, in those studies experimental animals were continuously exposed to the odors for at least two days, whereas in our experiment the males were exposed to the female odors for only 1 h. It has been proposed that short term exposure to odorants does not increase the survival of new cells, instead their survival requires the discrimination, association, and formation of olfactory memory (Alonso et al., 2006; Mouret et al., 2008; Lazarini and Lledo, 2011). It is also possible that acute or chronic exposure to sexually relevant odors might have a different effect on OB neurogenesis, but in the present experiment the induction of new cells by mating does not appear to be associated with female odors. Further support for this contention comes from a recent study where females allowed to pace the sexual interaction showed an increase in the number of new cells in the GrCL of the AOB, while females exposed to sexually experienced males did not show changes in the number of cells in the this layer (Corona et al., 2011b). Similar observations have been described in the hippocampus after sexual behavior in males. Subjects exposed to a sexually receptive female, with whom they could copulate for 14 days had more neurons in the dentate gyrus than those males exposed to non-receptive females (Leuner et al., 2010). In this case males were mated in a conditioned where they controlled the sexual interaction. Thus, pacing the sexual interaction induces genital stimulation and reward value that are quantitatively and qualitatively different from non paced mating. These differences can modulate the number of new cells.

No significant differences in the number of new cells were found in the MOB and in the GlCL and MCL of the AOB. It has been demonstrated in mice that, while the number of new cells that reach the GrCL of the AOB is maximum 7 days after BrdU administration, the new granular cells in the MOB reach their maximum levels 15 days after the administration of the DNA synthesis marker (Oboti et al., 2009). Also, the majority of the new cells that reach the OB differentiate into granular cells and only a rare proportion migrate into the glomerular layer reaching their maximum level 1 month after BrdU administration (Petreanu and Alvarez-Buylla, 2002; Winner et al., 2002). Future studies are been planned to evaluate proliferation in the SVZ and RMS 2 days after mating and neurogenesis in the OB 45 days after sexual stimulation and determine if some cells integrate in the MOB or other layers of the AOB.

ACKNOWLEDGMENTS

We thank Elsa Nydia Hernández, Leonor Casanova, Omar González, Ramón Martínez, Nancy Lorena Ortíz, Ma. De Lourdes Lara, Martín García, Laura Sánchez and Javier Valles for their excellent technical assistance. This research was supported by CONACyT grants152872 (Wendy Portillo), 167101 (Raúl G. Paredes), 140917 (Néstor F. Díaz), 130627 (Néstor F. Díaz); DGAPA IN200512 (Raúl G. Paredes) and IA200911 (Wendy Portillo).

REFERENCES

Agmo, A., and Gomez, M. (1993). Sexual reinforcement is blocked by infusion of naloxone into the medial preoptic area. *Behav. Neurosci.* 107, 812–818.

Alonso, M., Viollet, C., Gabellec, M. M., Meas-Yedid, V., Olivo-Marin, J. C., and Lledo, P. M. (2006). Olfactory discrimination learning increases the survival of adult-born neurons in the olfactory bulb. *J. Neurosci.* 26, 10508–10513.

Alvarez-Buylla, A., and Garcia-Verdugo, J. M. (2002). Neurogenesis in adult subventricular zone. *J. Neurosci.* 22, 629–634.

Arzate, D. M., Portillo, W., Rodriguez, C., Corona, R., and Paredes, R. G. (2011). Extended paced mating tests induces conditioned place preference without affecting sexual arousal. *Horm. Behav.* 59, 674–680.

Bagley, J., Larocca, G., Jimenez, D. A., and Urban, N. N. (2007). Adult neurogenesis and specific replacement of interneuron subtypes in the mouse main olfactory bulb. *BMC Neurosci.* 8, 92.

Batista-Brito, R., Close, J., Machold, R., and Fishell, G. (2008). The distinct temporal origins of olfactory bulb interneuron subtypes. *J. Neurosci.* 28, 3966–3975.

Baum, M. J., and Kelliher, K. R. (2009). Complementary roles of the main and accessory olfactory systems in mammalian mate recognition. *Annu. Rev. Physiol.* 71, 141–160.

Belluzzi, O., Benedusi, M., Ackman, J., and Loturco, J. J. (2003). Electrophysiological differentiation of new neurons in the olfactory bulb. *J. Neurosci.* 23, 10411–10418.

Binns, K. E., and Brennan, P. A. (2005). Changes in electrophysiological activity in the accessory olfactory bulb and medial amygdala associated with mate recognition in mice. *Eur. J. Neurosci.* 21, 2529–2537.

Brennan, P. A., and Kendrick, K. M. (2006). Mammalian social odours: attraction and individual recognition. *Philos. Trans. R. Soc. Lond. B Biol. Sci.* 361, 2061–2078.

Camacho, F. J., Portillo, W., Quintero-Enriquez, O., and Paredes, R. G. (2009). Reward value of intromissions and morphine in male rats evaluated by conditioned place preference. *Physiol. Behav.* 98, 602–607.

Carleton, A., Petreanu, L. T., Lansford, R., Alvarez-Buylla, A., and Lledo, P. M. (2003). Becoming a new neuron in the adult olfactory bulb. *Nat. Neurosci.* 6, 507–518.

Corona, R., Camacho, F. J., Garcia-Horsman, P., Guerrero, A., Ogando, A., and Paredes, R. G. (2011a). Different doses of estradiol benzoate induce conditioned place preference after paced mating. *Horm. Behav.* 60, 264–268.

Corona, R., Larriva-Sahd, J., and Paredes, R. G. (2011b). Paced-mating increases the number of adult new born cells in the internal cellular (granular) layer of the accessory olfactory bulb. *PLoS ONE* 6:e19380. doi: 10.1371/journal.pone.0019380

Curtis, J. T., Liu, Y., and Wang, Z. (2001). Lesions of the vomeronasal organ disrupt mating-induced pair bonding in female prairie voles (Microtus ochrogaster). *Brain Res.* 901, 167–174.

Curtis, M. A., Kam, M., Nannmark, U., Anderson, M. F., Axell, M. Z., Wikkelso, C., Holtas, S., Van Roon-Mom, W. M., Bjork-Eriksson, T., Nordborg, C., Frisen, J., Dragunow, M., Faull, R. L., and Eriksson, P. S. (2007). Human neuroblasts migrate to the olfactory bulb via a lateral ventricular extension. *Science* 315, 1243–1249.

Dhungel, S., Masaoka, M., Rai, D., Kondo, Y., and Sakuma, Y. (2011). Both olfactory epithelial and vomeronasal inputs are essential for activation of the medial amygdala and preoptic neurons of male rats. *Neuroscience* 199, 225–234.

Erskine, M. S. (1989). Solicitation behavior in the estrous female rat: a review. *Horm. Behav.* 23, 473–502.

Gonzalez-Flores, O., Camacho, F. J., Dominguez-Salazar, E., Ramirez-Orduna, J. M., Beyer, C., and Paredes, R. G. (2004). Progestins and place preference conditioning after paced mating. *Horm. Behav.* 46, 151–157.

Guevara-Guzman, R., Barrera-Mera, B., and Weiss, M. L. (1997). Effect of the estrous cycle on olfactory bulb response to vaginocervical stimulation in the rat: results from electrophysiology and Fos immunocytochemistry experiments. *Brain Res. Bull.* 44, 141–149.

Honda, N., Sakamoto, H., Inamura, K., and Kashiwayanagi, M. (2009). Age-dependent spatial distribution of bromodeoxyuridine-immunoreactive cells in the main olfactory bulb. *Biol. Pharm. Bull.* 32, 627–630.

Huang, L., and Bittman, E. L. (2002). Olfactory bulb cells generated in adult male golden hamsters are specifically activated by exposure to estrous females. *Horm. Behav.* 41, 343–350.

Jakupovic, J., Kang, N., and Baum, M. J. (2008). Effect of bilateral accessory olfactory bulb lesions on volatile urinary odor discrimination and investigation as well as mating behavior in male mice. *Physiol. Behav.* 93, 467–473.

Keller, M., Douhard, Q., Baum, M. J., and Bakker, J. (2006). Sexual experience does not compensate for the disruptive effects of zinc sulfate–lesioning of the main olfactory epithelium on sexual behavior in male mice. *Chem. Senses* 31, 753–762.

Kondo, Y., Sudo, T., Tomihara, K., and Sakuma, Y. (2003). Activation of accessory olfactory bulb neurons during copulatory behavior after deprivation of vomeronasal inputs in male rats. *Brain Res.* 962, 232–236.

Larriva-Sahd, J. (2008). The accessory olfactory bulb in the adult rat: a cytological study of its cell types, neuropil, neuronal modules, and interactions with the main olfactory system. *J. Comp. Neurol.* 510, 309–350.

Larsen, C. M., Kokay, I. C., and Grattan, D. R. (2008). Male pheromones initiate prolactin-induced neurogenesis and advance maternal behavior in female mice. *Horm. Behav.* 53, 509–517.

Lazarini, F., and Lledo, P. M. (2011). Is adult neurogenesis essential for olfaction? *Trends Neurosci.* 34, 20–30.

Leuner, B., Caponiti, J. M., and Gould, E. (2012). Oxytocin stimulates adult neurogenesis even under conditions of stress and elevated glucocorticoids. *Hippocampus* 22, 861–868.

Leuner, B., Glasper, E. R., and Gould, E. (2010). Sexual experience promotes adult neurogenesis in the hippocampus despite an initial elevation in stress hormones. *PLoS ONE* 5:e11597. doi: 10.1371/journal.pone.0011597

Levai, O., Feistel, T., Breer, H., and Strotmann, J. (2006). Cells in the vomeronasal organ express odorant receptors but project to the accessory olfactory bulb. *J. Comp. Neurol.* 498, 476–490.

Lledo, P. M., and Saghatelyan, A. (2005). Integrating new neurons into the adult olfactory bulb: joining the network, life-death decisions, and the effects of sensory experience. *Trends Neurosci.* 28, 248–254.

Lois, C., Garcia-Verdugo, J. M., and Alvarez-Buylla, A. (1996). Chain migration of neuronal precursors. *Science* 271, 978–981.

Mak, G. K., Enwere, E. K., Gregg, C., Pakarainen, T., Poutanen, M., Huhtaniemi, I., and Weiss, S. (2007). Male pheromone-stimulated neurogenesis in the adult female brain: possible role in mating behavior. *Nat. Neurosci.* 10, 1003–1011.

Martel, K. L., and Baum, M. J. (2007). Sexually dimorphic activation of the accessory, but not the main, olfactory bulb in mice by urinary volatiles. *Eur. J. Neurosci.* 26, 463–475.

Martinez, I., and Paredes, R. G. (2001). Only self-paced mating is rewarding in rats of both sexes. *Horm. Behav.* 40, 510–517.

Matsuoka, M., Yoshida-Matsuoka, J., Sugiura, H., Yamagata, K., Ichikawa, M., and Norita, M. (2002). Mating behavior induces differential Arc expression in the main and accessory olfactory bulbs of adult rats. *Neurosci. Lett.* 335, 111–114.

Messing, R. B., Dodge, C., Waymire, J. C., Lynch, G. S., and Deadwyler, S. A. (1979). Morphine induced increases in the incorporation of 3H-thymidine into brain striatal DNA. *Brain Res. Bull.* 4, 615–619.

Miller, C. R., O'steen, W. K., and Deadwyler, S. A. (1982). Effect of morphine on 3H-thymidine incorporation in the subependyma of the rat: an autoradiographic study. *J. Comp. Neurol.* 208, 209–214.

Ming, G. L., and Song, H. (2011). Adult neurogenesis in the mammalian brain: significant answers and significant questions. *Neuron* 70, 687–702.

Mouret, A., Gheusi, G., Gabellec, M. M., De Chaumont, F., Olivo-Marin, J. C., and Lledo, P. M. (2008). Learning and survival of newly generated neurons: when time matters. *J. Neurosci.* 28, 11511–11516.

Mouret, A., Lepousez, G., Gras, J., Gabellec, M. M., and Lledo, P. M. (2009). Turnover of newborn olfactory bulb neurons optimizes olfaction. *J. Neurosci.* 29, 12302–12314.

Narita, M., Kuzumaki, N., Miyatake, M., Sato, F., Wachi, H., Seyama, Y., and Suzuki, T. (2006). Role of delta-opioid receptor function in neurogenesis and neuroprotection. *J. Neurochem.* 97, 1494–1505.

Nyuyki, K. D., Waldherr, M., Baeuml, S., and Neumann, I. D. (2011). Yes, I am ready now: differential effects of paced versus unpaced mating on anxiety and central oxytocin release in female rats. *PLoS ONE* 6:e23599. doi: 10.1371/journal.pone.0023599

Oboti, L., Savalli, G., Giachino, C., De Marchis, S., Panzica, G. C., Fasolo, A., and Peretto, P. (2009). Integration and sensory experience-dependent survival of newly-generated neurons in the accessory olfactory bulb of female mice. *Eur. J. Neurosci.* 29, 679–692.

Paredes, R. G. (2009). Evaluating the neurobiology of sexual reward. *ILAR J.* 50, 15–27.

Paredes, R. G. (2010). Hormones and sexual reward. *Vitam. Horm.* 82, 241–262.

Paredes, R. G., and Martinez, I. (2001). Naloxone blocks place preference conditioning after paced mating in female rats. *Behav. Neurosci.* 115, 1363–1367.

Peretto, P., Giachino, C., Panzica, G. C., and Fasolo, A. (2001). Sexually dimorphic neurogenesis is topographically matched with the anterior accessory olfactory bulb of the adult rat. *Cell Tissue Res.* 306, 385–389.

Peretto, P., Merighi, A., Fasolo, A., and Bonfanti, L. (1997). Glial tubes in the rostral migratory stream of the adult rat. *Brain Res. Bull.* 42, 9–21.

Petreanu, L., and Alvarez-Buylla, A. (2002). Maturation and death of adult-born olfactory bulb granule neurons: role of olfaction. *J. Neurosci.* 22, 6106–6113.

Reynolds, B. A., and Weiss, S. (1992). Generation of neurons and astrocytes from isolated cells of the adult mammalian central nervous system. *Science* 255, 1707–1710.

Rochefort, C., Gheusi, G., Vincent, J. D., and Lledo, P. M. (2002). Enriched odor exposure increases the number of newborn neurons in the adult olfactory bulb and improves odor memory. *J. Neurosci.* 22, 2679–2689.

Rochefort, C., and Lledo, P. M. (2005). Short-term survival of newborn neurons in the adult olfactory bulb after exposure to a complex odor environment. *Eur. J. Neurosci.* 22, 2863–2870.

Saito, T. R., and Moltz, H. (1986). Copulatory behavior of sexually naive and sexually experienced male rats following removal of the vomeronasal organ. *Physiol. Behav.* 37, 507–510.

Sargeant, T. J., Miller, J. H., and Day, D. J. (2008). Opioidergic regulation of astroglial/neuronal proliferation: where are we now? *J. Neurochem.* 107, 883–897.

Slotnick, B., Restrepo, D., Schellinck, H., Archbold, G., Price, S., and Lin, W. (2010). Accessory olfactory bulb function is modulated by input from the main olfactory epithelium. *Eur. J. Neurosci.* 31, 1108–1116.

Spehr, M., Kelliher, K. R., Li, X. H., Boehm, T., Leinders-Zufall, T.,

and Zufall, F. (2006). Essential role of the main olfactory system in social recognition of major histocompatibility complex peptide ligands. *J. Neurosci.* 26, 1961–1970.

Trinh, K., and Storm, D. R. (2003). Vomeronasal organ detects odorants in absence of signaling through main olfactory epithelium. *Nat. Neurosci.* 6, 519–525.

Whitman, M. C., and Greer, C. A. (2009). Adult neurogenesis and the olfactory system. *Prog. Neurobiol.* 89, 162–175.

Winner, B., Cooper-Kuhn, C. M., Aigner, R., Winkler, J., and Kuhn, H. G. (2002). Long-term survival and cell death of newly generated neurons in the adult rat olfactory bulb. *Eur. J. Neurosci.* 16, 1681–1689.

Xu, F., Schaefer, M., Kida, I., Schafer, J., Liu, N., Rothman, D. L., Hyder, F., Restrepo, D., and Shepherd, G. M. (2005). Simultaneous activation of mouse main and accessory olfactory bulbs by odors or pheromones. *J. Comp. Neurol.* 489, 491–500.

Conflict of Interest Statement: The authors declare that the research was conducted in the absence of any commercial or financial relationships that could be construed as a potential conflict of interest.

Received: 20 April 2012; accepted: 20 June 2012; published online: 06 July 2012.

Citation: Portillo W, Unda N, Camacho FJ, Sánchez M, Corona R, Arzate DM, Díaz NF and Paredes RG (2012) Sexual activity increases the number of newborn cells in the accessory olfactory bulb of male rats. Front. Neuroanat. ***6****:25. doi: 10.3389/fnana. 2012.00025*

frontiers in
NEUROANATOMY

ORIGINAL RESEARCH ARTICLE
published: 07 August 2012
doi: 10.3389/fnana.2012.00030

Comprehensive connectivity of the mouse main olfactory bulb: analysis and online digital atlas

Houri Hintiryan, Lin Gou, Brian Zingg, Seita Yamashita, Hannah M. Lyden, Monica Y. Song, Arleen K. Grewal, Xinhai Zhang, Arthur W. Toga and Hong-Wei Dong*

Laboratory of Neuro Imaging, Department of Neurology, David Geffen School of Medicine, University of California, Los Angeles, Los Angeles, CA, USA

Edited by:
Jorge A. Larriva-Sahd, Universidad Nacional Autónoma de México, Mexico

Reviewed by:
Marco Aurelio M. Freire, Edmond and Lily Safra International Institute for Neurosciences of Natal, Brazil
Juan Andrés De Carlos, Instituto Cajal (Consejo Superior de Investigaciones Científicas), Spain

***Correspondence:**
Hong-Wei Dong, Laboratory of Neuro Imaging, Department of Neurology, David Geffen School of Medicine, University of California, Los Angeles, 635 Charles E. Young Drive South, Suite 225, Los Angeles, CA 90095-7334, USA.
e-mail: hongwei.dong@loni.ucla.edu

We introduce the first open resource for mouse olfactory connectivity data produced as part of the Mouse Connectome Project (MCP) at UCLA. The MCP aims to assemble a whole-brain connectivity atlas for the C57Bl/6J mouse using a double coinjection tracing method. Each coinjection consists of one anterograde and one retrograde tracer, which affords the advantage of simultaneously identifying efferent and afferent pathways and directly identifying reciprocal connectivity of injection sites. The systematic application of double coinjections potentially reveals interaction stations between injections and allows for the study of connectivity at the network level. To facilitate use of the data, raw images are made publicly accessible through our online interactive visualization tool, the iConnectome, where users can view and annotate the high-resolution, multi-fluorescent connectivity data (www.MouseConnectome.org). Systematic double coinjections were made into different regions of the main olfactory bulb (MOB) and data from 18 MOB cases (~72 pathways; 36 efferent/36 afferent) currently are available to view in iConnectome within their corresponding atlas level and their own bright-field cytoarchitectural background. Additional MOB injections and injections of the accessory olfactory bulb (AOB), anterior olfactory nucleus (AON), and other olfactory cortical areas gradually will be made available. Analysis of connections from different regions of the MOB revealed a novel, topographically arranged MOB projection roadmap, demonstrated disparate MOB connectivity with anterior versus posterior piriform cortical area (PIR), and exposed some novel aspects of well-established cortical olfactory projections.

Keywords: main olfactory bulb, piriform cortical area, lateral olfactory tract, online digital atlas, connectome, neural tract tracing

Abbreviations: AAA, anterior amygdalar area; ACAd, anterior cingulate area, dorsal part; *aco*, anterior commissure, olfactory limb; AMd, anteromedial thalamic nucleus, dorsal part; AOB, accessory olfactory bulb; AON, anterior olfactory nucleus; AONd, anterior olfactory nucleus, dorsal part; AONe, anterior olfactory nucleus, external part; AONm, anterior olfactory nucleus, medial part; AONpv, anterior olfactory nucleus, posteroventral part; ARA, allen reference atlas; BA, bed nucleus of accessory olfactory tract; BDA, biotinylated dextran amine; BST, bed nuclei of stria terminalis; COAa, cortical amygdalar area, anterior part; COApl, cortical amygdalar area, posterior part, lateral zone; COApm, cortical amygdalar area, posterior part, medial zone; CTb, cholera toxin subunit b; DP, dorsal peduncular area; ENT, entorhinal area; ENTl, entorhinal area, lateral part; ENTm, entorhinal area, medial part; FG, Fluorogold; gr, granule cell; *int*, internal capsule; *lot*, lateral olfactory tract; *lotd*, lateral olfactory tract, dorsal part; MA, magnocellular nucleus; MCP, mouse connectome project; MEAav, medial amygdalar area, anteroventral part; mi, mitral cell; MOB, main olfactory bulb; MOBgl, main olfactory bulb, glomerular layer; MOBgr, main olfactory bulb, granule layer; MOBipl, main olfactory bulb, inner plexiform layer; MOBmi, main olfactory bulb, mitral layer; MOBopl, main olfactory bulb, outer plexiform layer; MOp, primary motor area; NLOT, nucleus of the lateral olfactory tract; NT, NeuroTrace®; OSN, olfactory sensory neuron; OT, olfactory tubercle; OTl, olfactory tubercle, lateral part; OTm, olfactory tubercle, medial part; PAA, piriform-amygdalar area; PHAL, *Phaseolus vulgaris-leucoagglutinin*; PIR, piriform area; PIRa, piriform area, anterior part; PIR-OT, piriform-olfactory tubercle junction; PIRp, piriform area, posterior part; py, pyramidal cell; RT, reticular nucleus of the thalamus; SSp, primary somatosensory area; SSs, supplemental somatosensory area; tf, tufted cell; TR, postpiriform transition area; TTd, taenia tecta, dorsal part; TTv, taenia tecta, ventral part; VISC, visceral area; VNO, vomeronasal organ.

INTRODUCTION

In his pioneering work, Ramon y Cajal (1904) elegantly illustrated the cytoarchitecture of the main olfactory bulb (MOB) and its general pathways to cortical destinations using the Golgi stain. Since then, olfactory pathways have been thoroughly examined using more advanced techniques, ranging from circuit tracers to cell-type specific viral tracers (Cragg, 1961; Powell et al., 1965; Price, 1973; Scalia and Winans, 1975; Shipley and Adamek, 1984; Pro-Sistiaga et al., 2007; Yan et al., 2008; Nagayama et al., 2010; Miyamichi et al., 2011; Sosulski et al., 2011; for reviews see Haberly, 2001; Friedrich, 2011). Technological advancements also have improved presentation of neuroconnectivity data. High cost and space limitations typically allow publication of figures depicting connectivity that is of most interest, precluding presentation of the majority of the data. Unfortunately, this provides only a partial view of the whole picture. Presently, advanced imaging equipment and computer technology have revolutionized neuroanatomy such that whole-brain high-resolution images can be acquired and made publicly accessible for world-wide use (Dong, 2007; Jones et al., 2011). At the forefront of this new neuroanatomy era is the iConnecome, where systematically accumulated multi-fluorescent

connectivity data can be accessed (www.MouseConnectome.org). Whole-brain coronal sections starting from rostral regions of the olfactory bulb and extending to the caudal regions of the hindbrain are available for each case. For example, olfactory cortical projections from the MOB and accessory olfactory bulbs (AOBs) extend long distances reaching the caudal ends of the entorhinal cortical area (ENT) (**Figures 1A–E**). Coronal sections with all of the labeling from each injection site are available in iConnectome and provide a comprehensive view of connections associated with each injected structure (**Figure 1E**).

CIRCUIT TRACING APPROACH

The Mouse Connectome Project (MCP) at UCLA aims to generate a connectivity map of the mouse brain using a double coinjection tracing strategy, which was first reported for studying neuronal connectivity in the rat (Thompson and Swanson, 2010). Each of the two non-overlapping coinjections consists of one anterograde and one retrograde tracer. *Phaseolus vulgaris-leucoagglutinin* (PHAL: anterograde: green) is coinjected with cholera toxin subunit b (CTb: retrograde: magenta) while biotinylated dextran amine (BDA: anterograde: red) is coinjected with Fluorogold (FG: retrograde: gold)

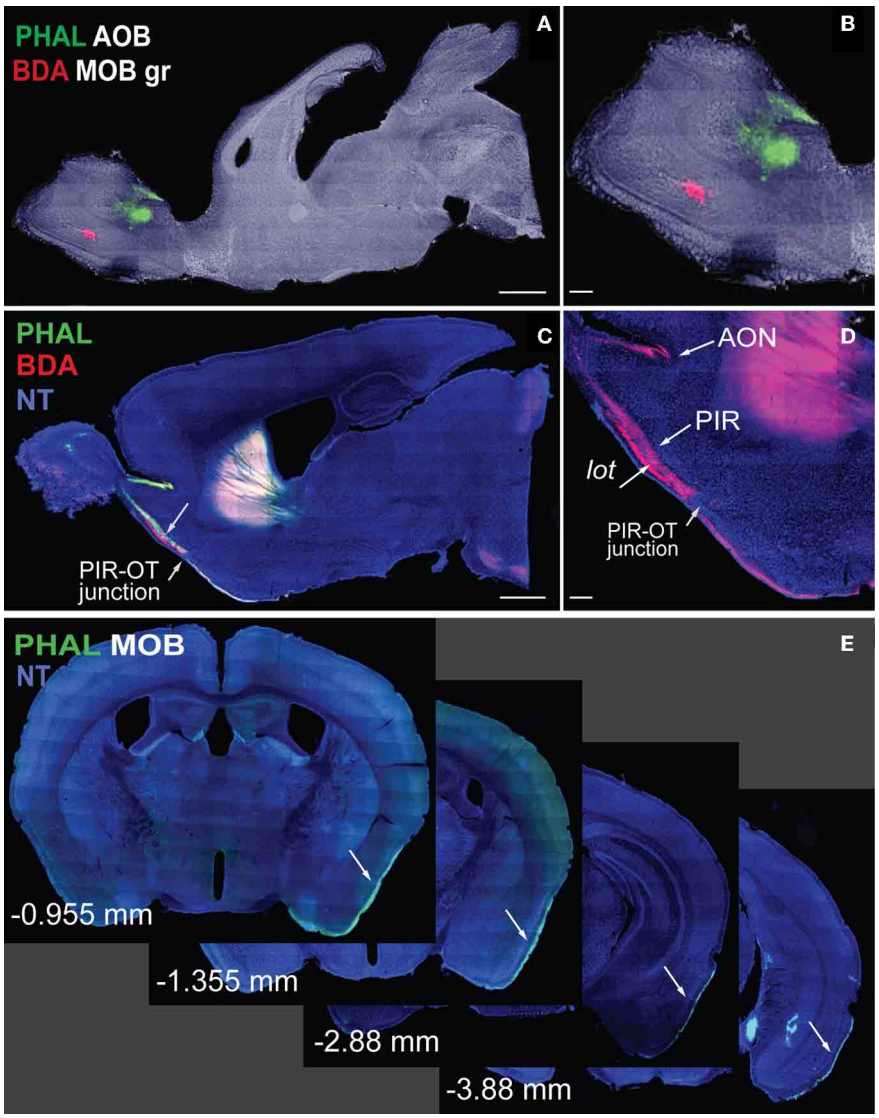

FIGURE 1 | Sagittal images of anterograde tracers *Phaseolus vulgaris-leucoagglutinin* (PHAL; green) and biotinylated dextran amine (BDA; red) injections in MOB (A, magnified in B). Fibers originating from MOB injections travel long distances across cortical olfactory areas **(C)**. Magnified image of fibers in **(D)** shows BDA fibers in AON, PIR, and *lot*. Note the decrease in BDA axons across the PIR-OT junction **(C,D)**. Whole-brain coronal sections of PHAL fibers from MOB traveling from rostral to caudal regions of the brain (**E**; −0.955 to −3.88 mm from bregma). *Case numbers SW101215-02A **(A)**; SW101213-01A **(E)***. Scale bar, 1 mm **(A,C)**; 200 μm **(B,D)**. Abbreviations: MOB, main olfactory bulb; MOBgr, MOB granule layer; AOB, accessory olfactory bulb; PIR, piriform cortical area; OT, olfactory tubercle; AON, anterior olfactory nucleus; PHAL, *Phaseolus vulgaris-leucoagglutinin*; BDA, biotinylated dextran amine; NT, neurotrace blue.

(**Figure 2A**). These double coinjections allow concurrent examination of input and output pathways from each injection and yield four times the amount of data collected from classic single tracer injections, reducing cost, processing time, and number of animals used. Coinjections also expose topographically distinct connectional patterns associated with the two injections within the same brain (**Figure 2B**), increasing the precision of a connectome map. Further, unlike MacroConnectomes that utilize *in vivo* diffusion tractography imaging to map fiber tracts (Behrens and Sporns, 2012; Cammoun et al., 2012; Van Essen et al., 2012) and MicroConnectomes (or synaptomes) (Lichtman et al., 2008; Micheva et al., 2010; Bock et al., 2011; Briggman et al., 2011) that map local circuits or synaptic connectivity at single neuron level, our approach concurrently reveals long projection pathways (**Figures 2C,H–K**) and inter-regional connectivity (**Figures 2H–K**). These inter-regional connections can be recurrent (reciprocal) connections (**Figures 2C,F**) and/or interaction stations (**Figure 2G**). Reciprocal connections between the injection sites and other structures are indicated by overlapping PHAL-labeled terminals and CTb-labeled neurons (**Figures 2C,F**) or by BDA terminals overlapping with FG-labeled neurons. Potential interaction stations between injection sites are demonstrated by PHAL-fiber innervation of FG-labeled neurons (**Figure 2G**) or BDA innervation of CTb-labeled neurons.

Inter-regional synaptic connectivity is confirmed by cross validation of the data. For example, PHAL injections in the primary somatosensory cortical area (SSp; **Figure 2H**) label fibers and terminal boutons in the primary motor area (MOp; **Figure 2I**) suggesting a synaptic connection with that region. A FG injection in the same MOp region that contains the PHAL terminals (**Figure 2K**) layer-specifically back-labels neurons in the SSp (**Figure 2J**) where the PHAL injection was made. This confirms the MOp and SSp inter-regional synaptic connection and also reveals the specific SSp layers that project to the MOp.

Sections containing the injection site are exposed to reveal fibers, which make the infusions look large (**Figure 2C**). However, injection sizes typically range from 300–500 μm in diameter (**Figures 2D,E**) and more confined injections with 200 μm diameters are made when smaller nuclei are targeted.

THE ICONNECTOME, AN ONLINE DIGITAL CONNECTIVITY ATLAS

The iConnectome is an interactive visualization tool for our whole-brain, high-resolution connectivity data. For each case, up to four fluorescent channels, each corresponding to a tracer, can be viewed and adjusted for brightness and contrast to reveal labeling of interest (**Figure 3A**). PHAL is represented in the green channel (**Figure 3A**, upper right and lower left panels), CTb in magenta (**Figure 3A**, lower panels), BDA in red (**Figure 3A**, upper left), and FG in yellow (**Figure 3A**, upper right). Up to four different cases (approximately 16 pathways) can be viewed simultaneously (**Figure 3A**). Windows can be synchronized such that any action performed in the master viewport is mirrored in the slave window(s) allowing comparison of labeling patterns from different cases.

The purpose of this publicly accessible connectivity data is to help neuroscientists generate testable hypotheses regarding finer scale brain circuitry, brain function, behavior, and disease. Two features that ease the analysis of the connectivity data are available in iConnectome. The first is a channel that allows each section to be viewed within its own bright-field Nissl cytoarchitectural background (**Figures 3B,C,G**). Previously, this has not been attainable due to technical constraints and consequently adjacent sections commonly have been used as Nissl references. The bright-field background of the same section enables more precise identification of labeling in distinguishable nuclei, decreasing the margin of error in analysis. The second feature is a sixth channel that represents the section's corresponding Allen Reference Atlas (ARA; Dong, 2007) level, which also aids in the annotation of the data (**Figures 3D–F**).

For each case, a thumbnail widget containing representative images also is available. The widget can be accessed by clicking on the magnifying glass icon next to each case number (**Figure 3H**). This feature provides an overview of the labeling for the case, but more importantly, displays the actual injection site size. As aforementioned, injection sites are over exposed to reveal finer labeling present in the section (**Figure 2C**), which enlarges the infusion area and misrepresents the injection size.

Currently, the iConnectome features 63 cases, 18 of which contain MOB injections that trace approximately 35 efferent and 20 afferent pathways across the entire brain. Eventually, injections made into the AOB, anterior olfactory nucleus (AON), and other cortical olfactory areas also will be available.

RESULTS

Analysis of injections made into the mitral cell (MOBmi) and granule (MOBgr) layers of the MOB and into the piriform cortical area (PIR) revealed novel topographic MOB projections to and within the *lot*, demonstrated different MOB connections with the anterior versus posterior PIR, and exposed novel characteristics of well-established cortical olfactory projections.

PROJECTION ROADMAP OF THE MOB: ROUTE PREFERENCES OF LATERAL VERSUS MEDIAL MOB MITRAL CELLS

Double coinjections were made into the (1) dorsal, (2) middle, or (3) ventral MOBmi along the dorsal-ventral axis and into *medial* or *lateral* regions along the medial-lateral axis (**Figures 4A,C**, **5A**, **6A1,A2,B1,B2,C1**).

Regardless of their origin along the dorsal-ventral axis, axons from the *lateral* MOB course through the granule layer headed toward the *lot*, the main route from the olfactory bulb to olfactory cortical areas (Gloor, 1997) (**Figures 4A,C**, **5A**). Within the *lot*, axons from the dorsal *lateral* region travel roughly in dorsal intermediate parts of the tract, while axons from the ventral *lateral* MOBmi travel roughly in the ventral intermediate portion (**Figures 4B,D**, **5B**) before arborizing in the AON and PIR.

Axons from the *medial* MOB take different routes to join the *lot* depending on their origin along the dorsal-ventral axis. Those from dorsal *medial* MOBmi (**Figure 6A1**) travel through the dorsal limb of the *lot* (*lotd*; **Figure 6A2**) and through a distinct

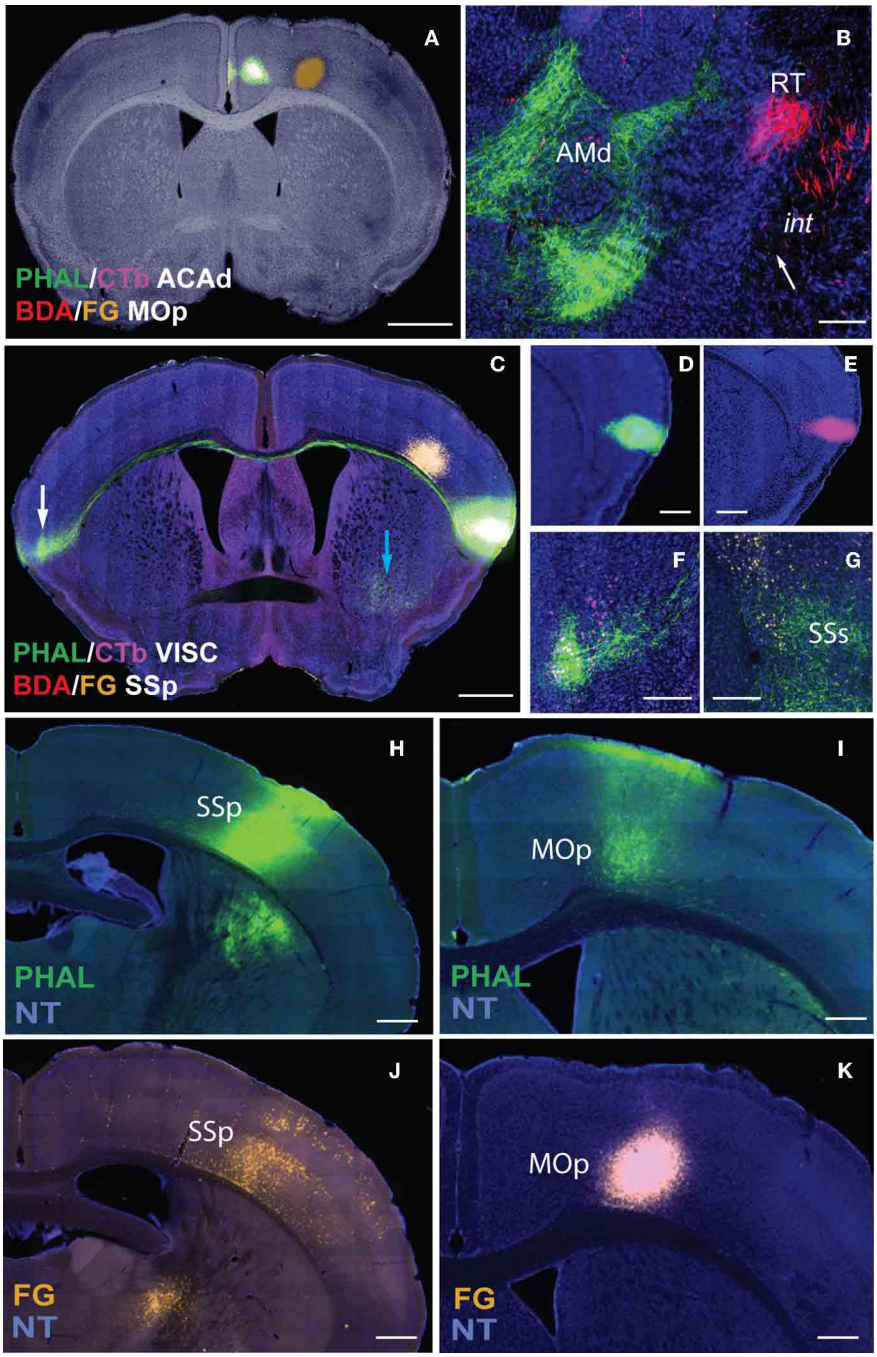

FIGURE 2 | Non-overlapping double coinjections of PHAL/CTb in ACAd and BDA in MOp on bright-field Nissl background (A) directly reveal topography in both gray (AMd and RT) and white matter (*int*; B). White arrow indicates PHAL fibers (as dots) traveling ventral to BDA fibers in *int* **(B)**. Injections **(C–E)** also reveal long projections pathways as demonstrated by PHAL fibers from the VISC crossing the corpus callosum and terminating in the contralateral mirror VISC area also labeled with CTb neurons (**C**; white arrow magnified in **F**). Overlapping PHAL and CTb **(C,F)** labeling suggests reciprocal connectivity between the mirrored structures. Image with the VISC and SSp injections in **(C)** is exposed to reveal fine fibers (blue and white arrows) that would otherwise not be visible if adjusted for the injection. Although PHAL and CTb injections look large, their actual size is ~300 μm in diameter **(D,E)**. Possible interaction stations between the two injections sites **(C)** is indicated by PHAL fibers from VISC overlapping with FG back-labeled neurons from SSp within the supplementary somatosensory area (SSs) suggesting a VISC→SSs→SSp connectivity chain. Inter-regional connectivity is corroborated by cross validation of data **(H–K)**. PHAL injection in SSp **(H)** labels terminals in MOp **(I)**. FG injection in the same MOp site as PHAL-labeled terminals **(K)** layer-specifically back-labels neurons in SSp **(J)**, precisely in SSp PHAL injection area **(H)**. Scale bar, 1 mm **(A,C)**; 200 μm **(B,D–G)**; 500 μm **(H–K)**. *Case numbers SW110323-02A **(A,B)**; SW101014-04A **(C–G)**; SW110419-03A **(H,I)**; SW110323-02A **(J,K)**.* Abbreviations: VISC, visceral area; SSp, primary somatosensory area; SSs, supplemental somatosensory area; MOp, primary motor area; AMd, dorsal anteromedial thalamic nucleus; RT, reticular nucleus of thalamus; int, internal capsule.

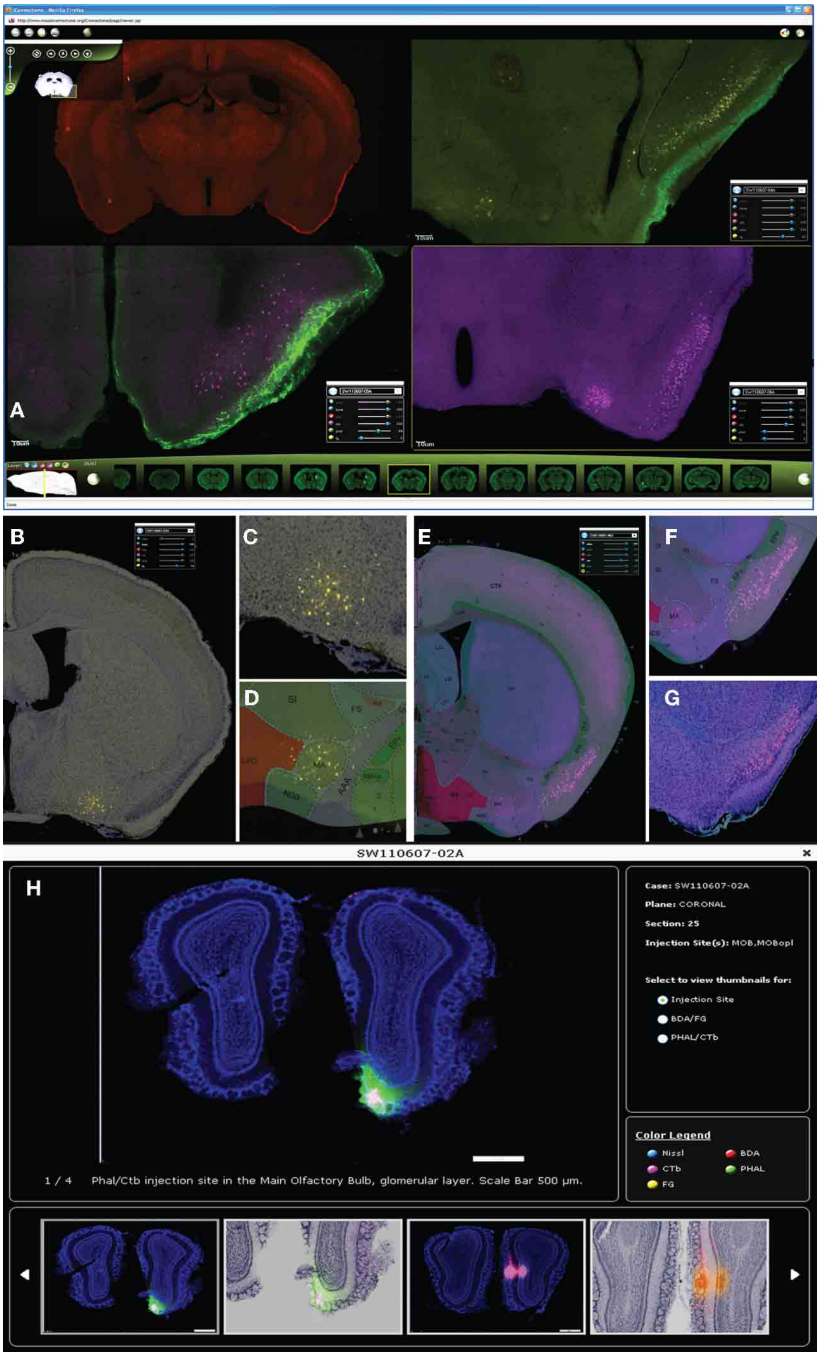

FIGURE 3 | Up to four cases can be viewed simultaneously in iConnectome for ease of comparing labeling from different cases (A). The four fluorescent tracers can be viewed per case: BDA in the red channel (upper left); PHAL in green (upper right, lower left); CTb in magenta (lower panels), and FG in yellow (upper right). Each tracer can be viewed either on their own bright-field Nissl background **(B,C,G)** or on their corresponding ARA level **(D–F)**. Back-labeled FG neurons in MA **(B)** are magnified in **(C)** and are clearly registered onto the MA nucleus on ARA **(D)**. ARA background shows CTb back-labeled neurons in the pyramidal layer of PIR **(E)**, magnified in **(F)**. Location of neurons in layer II of PIR clearly is also seen on bright-field Nissl **(G)**. The thumbnail widget containing representative images of actual injection site size **(H)**. Thumbnails containing interesting patterns of labeling from each tracer for each case can also be found in the widget.

dorsolateral and lateral region of the *lot* (**Figures 6A3**,**A4**). From the ventral *medial* MOBmi, axons travel ventrolaterally across the MOB toward the *lot* (**Figures 6B1,B2,B2'**) and extend caudally roughly through the ventromedial *lot* (**Figures 6B3–B5**). Axons from the middle *medial* MOBmi (**Figure 6C1**) travel either dorsally via the *lotd* or go ventrolaterally toward the *lot* (**Figure 6C2**). Axons from the *lotd* occupy the dorsolateral or lateral edge of the *lot*, while axons traveling ventrolaterally

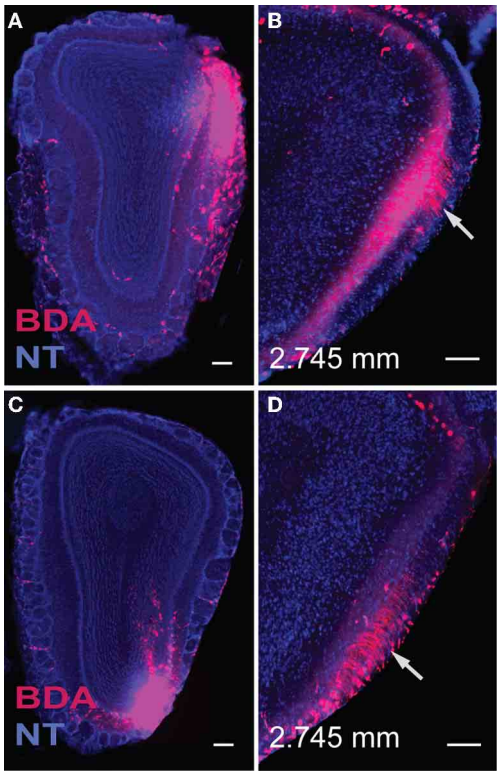

FIGURE 4 | Injections in the dorsal (A) and ventral (C) *lateral* MOB result in axons traveling directly toward the *lot* located on the same side. Within the *lot*, fibers from the dorsal *lateral* MOBmi travel predominantly in dorsal parts of the *lot* **(B)**, while those from ventral *lateral* regions remain primarily in ventral *lot* **(D)** as they travel caudally toward their olfactory cortical destinations. Sections containing the *lot* are at the same level, approximately 2.745 mm anterior from bregma **(B,D)**. Scale bar, 200 μm. *Case numbers SW110608-05A **(A,B)**, SW110607-03A **(C,D)**.*

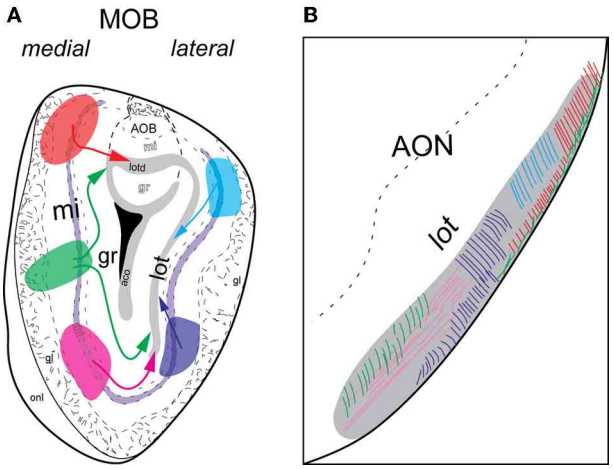

FIGURE 5 | Schematic of *lateral* and *medial* MOB projections to *lot*. Colors of injections in **(A)** and *lot* fibers in **(B)** are linked. Axons from dorsal (blue) or ventral (purple) *lateral* MOB travel directly toward the *lot* on the same side **(A)** and remain approximately in the dorsal and ventral *lot*, respectively **(B)**. Fibers from dorsal *medial* MOB (orange) travel through the *lotd*, while those from ventral *medial* MOB (pink) take a ventrolateral route. Fibers originating from the middle *medial* MOB (green) travel either through the *lotd* or ventrolaterally toward *lot*. Within the *lot*, dorsal *medial* MOB fibers stay restricted roughly within the lateral or dorsolateral region. Axons from ventral *medial* MOB remain approximately in ventromedial region and those from middle *medial* MOB travel through either dorsolateral or ventromedial *lot*. Abbreviations: AOB, accessory olfactory bulb; AON, anterior olfactory nucleus; lot, lateral olfactory tract; lotd, dorsal limb of lot.

occupy more ventromedial parts (**Figures 6C3,C4**; see **Figure 5** for schematic).

DIFFERENTIAL CONNECTIVITY PATTERNS OF THE ANTERIOR VERSUS POSTERIOR PIR

Injections made into the MOBgr revealed unique connections of the MOB with the anterior and posterior PIR. FG injections encompassed within the dorsal deep MOBgr (**Figure 7A**) result in back-labeled neurons both in the posterior PIR (PIRp) and magnocellular nucleus (MA; **Figure 7B**). FG injections in the MOBmi that encroach slightly onto the superficial granular layer (**Figure 7C**) label neurons only in the MA, not the PIRp (**Figure 7D**). This suggests that the MA projects to both MOBgr and MOBmi, but that the PIRp projects only to the deep MOBgr. Corroborating this connection, PHAL/CTb injections in the PIRp (**Figure 7E**) result in labeled terminals solely in the deep MOBgr (**Figure 7F**), a pattern that is preserved in posterior MOBgr regions (**Figures 7G,H**). PIRp CTb injections confirm that cells in the entire MOBmi project back to the PIRp (**Figures 7F–H**). Together, the data suggest a connection chain from the MOBmi→PIRp→deep MOBgr. PHAL injections in the anterior PIR (PIRa) specifically innervate the superficial MOBgr layers and the MOBmi (**Figures 7I,J,M–P**). This pattern also is preserved in more posterior regions of the MOB (**Figures 7K,L**) and suggests a neural chain from MOBmi→PIRa→MOBmi/superficial MOBgr. Combined, these results demonstrate that (a) the MOBgr can be stratified into superficial and deep layers and (b) the PIRa and PIRp show differential connectivity patterns to the MOB, namely that the PIRa projects to the superficial MOBgr and MOBmi, while PIRp projects to deep MOBgr and avoids the MOBmi (**Figure 8**). This distinct connectivity of the PIRa and PIRp possibly has important implications for their roles in MOB activation (see "Discussion").

Differential PIRa and PIRp connectivity is substantiated by FG injections in the *medial* and *lateral* MOBmi that back-label neurons only in the PIRa and not PIRp (**Figures 9A–F**). This pattern holds true regardless of the dorsal-ventral position of the MOB injections (data not shown). Our data also suggests that PIRa receives more inputs from MOBmi than the PIRp. From a sagittal view, MOB fiber ramifications decrease as they progress from PIRa to PIRp (**Figures 9G–I**).

A rough topography within PIRa also exists where more dorsal neurons project to dorsal MOBmi and more ventral PIRa neurons project to ventral MOBmi (**Figures 9B,E**). This coarse organization is observed more clearly when CTb and FG are double injected in the dorsal and ventral MOBmi, respectively (**Figures 9J,K**). CTb neurons roughly cluster in more dorsal parts of the PIRa, while FG neurons occupy more ventral regions (**Figures 9L,M**).

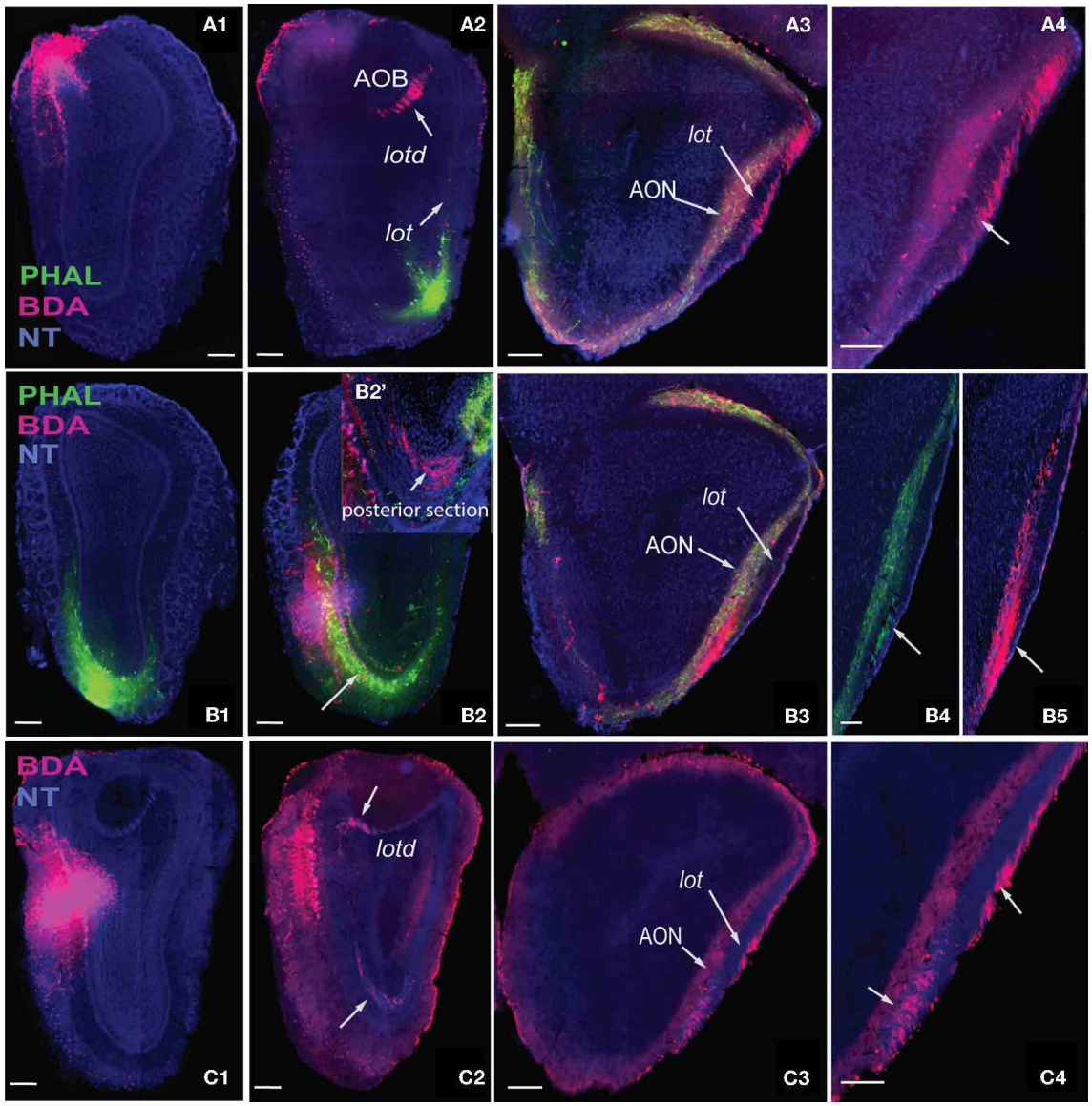

FIGURE 6 | Axons from the dorsal *medial* MOB (A1) travel through *lotd* (A2) to *lot* and travel along the dorsolateral edge within the *lot* (A3,A4). Ventral *medial* MOB axons **(B1,B2)** travel ventrolaterally toward *lot* **(B2,B2')** and within the ventromedial parts of *lot* **(B3–B5)**. **B2'** is one section posterior to section in **B2**. Axons from middle *medial* MOB **(C1)** cross over either through the *lotd* or ventrolaterally toward the *lot* **(C2)** and travel either through its dorsolateral or ventromedial parts **(C3,C4)**. Scale bar, 200 μm. *Case numbers SW101213-01A **(A)**, SW101215-01A **(B)**, SW100302-01A **(C)**.*

MOB CORTICAL PROJECTIONS

Double coinjections were made into the dorsal *medial* (BDA; **Figure 6A1**) and ventral *lateral* (PHAL; **Figure 6A2**) MOBmi and fibers from the rostral to caudal regions of the brain were examined. Regardless of their origin, all axons extensively arborize along the molecular Ia sublayer of the olfactory cortex without any spatial topographic specificity. From the *lot*, fibers from dorsal *medial* and ventral *lateral* MOBmi first arborize in the AON, extending across its external, dorsal, lateral, and posterior ventral divisions (**Figures 10A**, **11A**). Caudally, fibers continue into the Ia layer of the PIR, dorsal/ventral taenia tecta (TTd, TTv), but do not project as far mediodorsal as the dorsal peduncular area (DP; **Figures 10B**, **11B**). Axons densely ramify at the juncture between the PIR and the olfactory tubercle (OT; **Figures 10C**, **11C**). Several cases substantiate this PIR-OT junction labeling where it appears that axons from different parts of the MOB, including the MOBmi and glomerular layer (MOBgl; **Figures 12A,E,F**), extend into layer II and wrap around pyramidal OT neurons (**Figures 12B–D,G–I**).

Fibers continue caudally and terminate in the lateral OT, avoiding its medial portion across the rostral-caudal extent of the structure (**Figures 10D**, **11D**). PHAL and BDA MOBmi axons also terminate in the anterior amygdalar area (AAA; **Figures 10E**, **11E**), nucleus of the olfactory tract (NLOT;

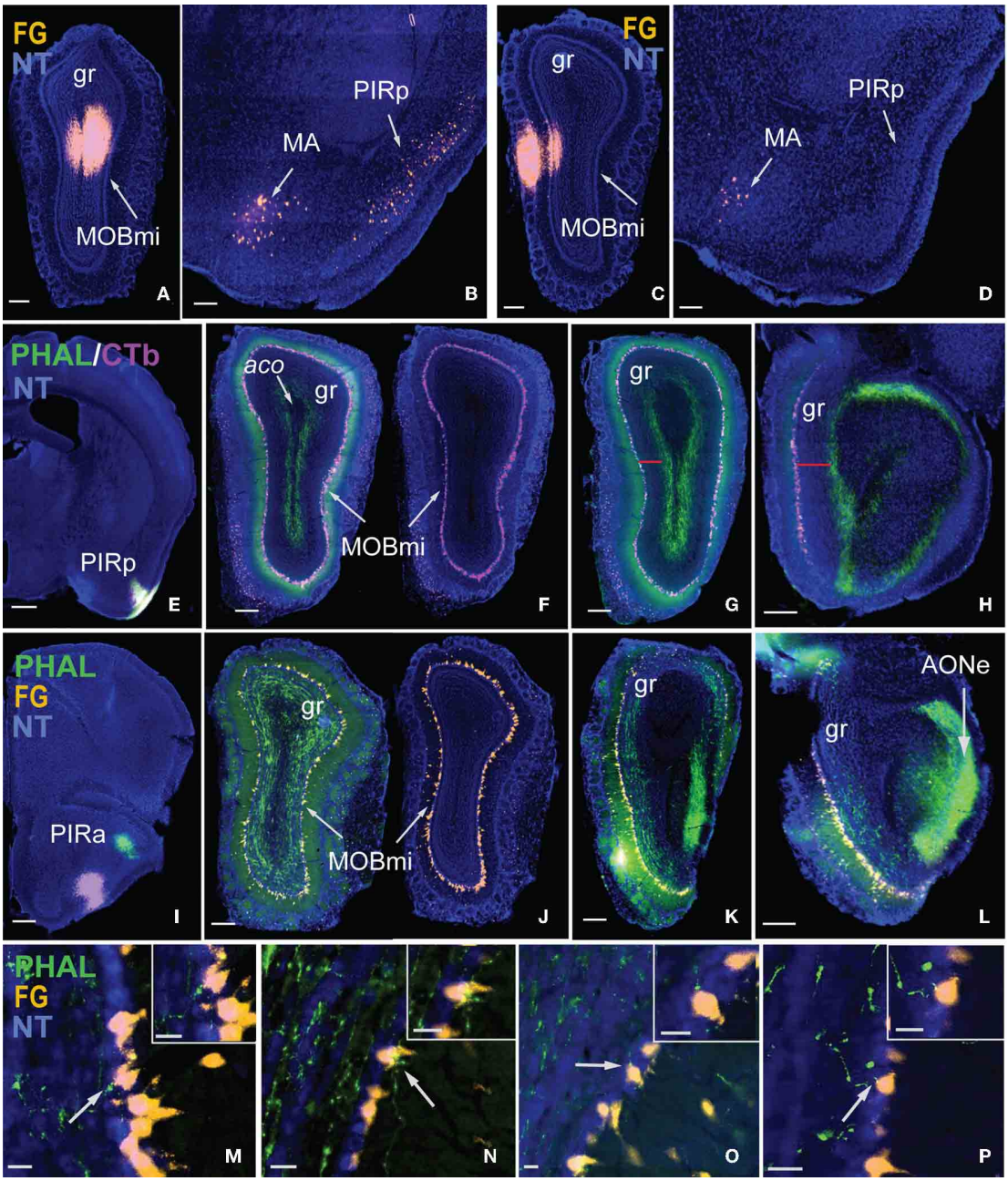

FIGURE 7 | Stratification of MOBgr and differential connectivity patterns of PIRa and PIRp with MOB. Injections in deep MOBgr **(A)** retrogradely label neurons in both MA and PIRp **(B)**, while injections in MOBmi **(C)** label only MA neurons and not PIRp **(D)**. PHAL injections into PIRp **(E)** label axons only in deep MOBgr **(F)**, a pattern that is preserved in posterior sections **(G,H)**. Note the distance from CTb labeled mitral cells and PHAL labeled fibers in **G,H** indicated by a red bar. PIRa projects to MOBmi and more superficial MOBgr **(I,J)**, which is also apparent in posterior MOBgr **(K,L)**. Note the distance between FG labeled mitral cells and PHAL labeled fibers. **(M–P)** are magnified images from **(J)** showing PHAL-labeled terminal boutons from PIRa contacting FG-labeled mitral cells. White arrows indicate magnified cells in top right corner of image. Scale bar 200 μm **(A–D,F–L)**; 500 μm **(E)**; 20 μm **(M–P)**. *Case numbers SW101215-05A **(A,B)**, SW110607-05A **(C,D)**; SW110403-01A **(E–H)**, SW110616-04A **(I–L)**.* Abbreviations: MA, magnocellular nucleus; PIRp, posterior piriform area; PIRa, anterior piriform area; aco, anterior commissure olfactory limb; MOBmi, MOB mitral cell layer; gr, granule layer of MOB; AONe, external anterior olfactory nucleus.

(**Figures 10F**, **11F**), bed nucleus of accessory olfactory tract (BA; **Figures 10G**, **11G**), anterior cortical amygdalar area (COAa; **Figures 10F–H**, **11F–H**), posterior lateral COA (COApl; **Figures 10G–I**, **11G–I**), anterior ventral part of the medial amygdalar nucleus (MEAav; **Figures 10H**, **11H**), piriform-amygdalar area (PAA; **Figures 10H,I**, **11H,I**), and postpiriform transition area (TR; **Figures 10I**, **11I**). Terminal boutons are not present in the posterior medial COA (COApm; **Figures 10I**, **11I**).

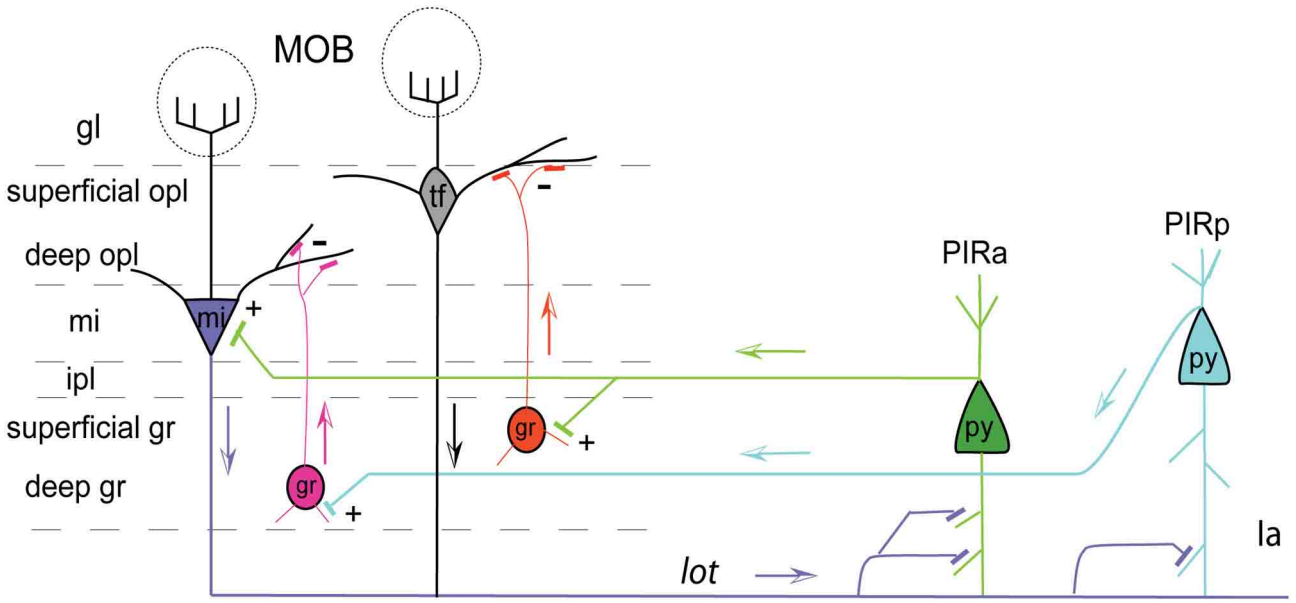

FIGURE 8 | Pyramidal cells of PIRa (green) send excitatory projections (indicated by +) to MOB mitral cells (mi; purple). PIRa (green) also directly projects to superficial MOB granule cells (gr; orange), which in turn inhibit (indicated by –) tufted cells (tf) in the superficial outer plexiform layer (opl). Pyramidal cells of PIRp (teal) project only to deep granule cells (gr; pink), which inhibit mi cells. Axons from MOB mi cells (mi; purple), through the *lot*, project more densely to PIRa compared to PIRp indicated by more synaptic connections. Apical dendrites of PIRa (py; green) and PIRp (py; teal) pyramidal neurons form connections with MOB mi projecting axons traveling within layer Ia. Arrows indicate flow of direction. Abbreviations: gl, glomerular layer; opl, outer plexiform layer; mi, mitral cell layer; ipl, inner plexiform layer; gr, granule layer; Ia, molecular layer 1a.

Similarly, arborizations are observed in the Ia layer of the lateral entorhinal cortical area (ENTl), but not the medial ENT (ENTm; **Figures 10J**, **11J**).

The number of axons progressively decreases not only as they project medially, but also caudally. For example, massive axons in the AON and PIR dramatically decrease in number after the PIR-OT juncture (**Figures 10C,D**, **11C,D**), an observation that is more evident in sagittal sections (**Figure 1C**).

DISCUSSION

MOB PROJECTION ROADMAP

An important question in the olfactory field is whether the exquisite spatial arrangement of olfactory sensory neuron (OSN) inputs to olfactory bulb glomeruli is preserved in connections to higher brain regions (Isaacson, 2010). In rodents, each OSN class expresses a unique odorant receptor set and has projections to two glomeruli that are located in symmetrical positions of the olfactory bulb: one on the medial and the other on the lateral side (Ressler et al., 1994; Vassar et al., 1994; Mombaerts et al., 1996). As a consequence of this topography, each olfactory receptor, and the odors that activate it, is represented in the olfactory bulb as a pattern of activated glomeruli. Imaging experiments have validated that different odorants elicit distinct patterns of glomerular activity (Rubin and Katz, 1999). Each of these symmetrically located glomeruli receives input from mitral cells located in the same symmetric positions and evidence suggests existence of organized projections from glomeruli to AON (Franks et al., 2011). Predicated on this organization, we purported that symmetrically located mitral cells in the *medial* and *lateral* regions of the MOB would have similar projection patterns, while those located in different positions along the dorsal-ventral axis would differ. Our projection roadmap of the MOB supports this claim. Once within the *lot*, fibers from the dorsal *medial* and *lateral* MOB travel roughly within the dorsal region of the tract, while those in the ventral *medial* and *lateral* travel approximately in its ventral portion (**Figures 4, 5**, and **6**). Therefore, within the *lot*, positions of axons from symmetrical *medial* and *lateral* MOB locations are topographically similar, while positions of *lot* axons from dorsal and ventral MOB locations differ. Support for this dorsal/ventral *lot* stratification is provided by differential expression of molecular markers within the fiber tract (Inaki et al., 2004). Our data did not show spatial arrangements from *lot* to layer Ia of olfactory cortical areas, which is consistent with the majority of reports in the literature (Ghosh et al., 2011; Kang et al., 2011a; Sosulski et al., 2011), although some evidence suggests that the OT preferentially receives more inputs from the dorsal MOB exists (Haberly and Price, 1977).

The olfactory pathways have been studied extensively over the last several decades (for reviews see Gloor, 1997; Haberly, 2001). Consistent with the literature, our data show that axons arising from different parts of the MOB generate axonal projections to other olfactory cortical areas including the AON, TTd, TTv, PIR, MEA, COA, and ENT as well as to the OT, which forms part of the ventral striatum. Generally, MOB projections stay restricted to the lateral division of structures i.e., the lateral OT, COApl, and ENTl, avoiding the medial OT, COApm, and ENTm. Unlike most cortical projecting MOB axons that remain restricted in the

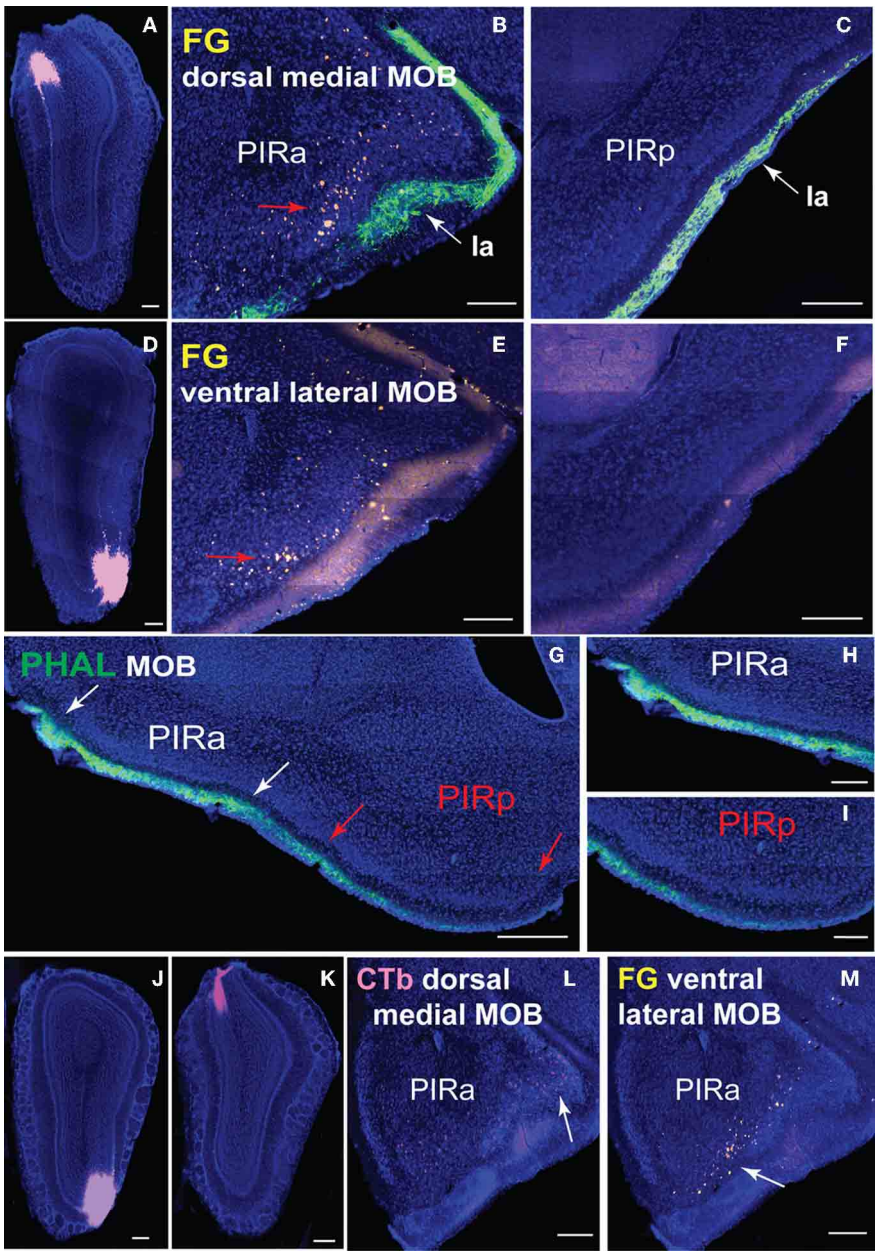

FIGURE 9 | Connectional differences between PIRa and PIRp. FG injections in dorsal *medial* **(A)** and ventral *lateral* **(D)** MOBmi back-label neurons in PIRa **(B,E)**, but not in PIRp **(C,F)**. Layer Ia of PIR, labeled with PHAL (see **Figure 6A2** for PHAL injection), appears to get thinner in width from PIRa to PIRp (**B,C,E–I**). Input to PIRa and PIRp is also different as MOB projects more densely to PIRa compared to PIRp **(G–I)**. PIRa between white arrows **(G)** is magnified in **(H)**, while PIRp in between red arrows **(G)** is magnified in (**I**; see **Figures 1A,B** for PHAL injection). Topographic arrangement of neurons in PIRa (red arrows in **B,E**) are more clearly observed when FG and CTb are double injected in dorsal versus ventral MOBmi, respectively **(J,K)**. Dorsal MOBmi projecting CTb neurons occupy more dorsal regions of PIRa **(L)**, while ventral projecting neurons are in more ventral parts of PIRa **(M)**. Scale bar, 200 μm; 500 μm **(G)**. *Case numbers SW101213-01A **(A–C)**, SW101215-03A **(D–F)**, SW101215-02A **(G–I)**, SW110607-03A **(J–M)**.*

molecular Ia layer, MOB axons from all regions generate terminals in the junction between the PIR and OT while the axons surround the OT layer II pyramidal neurons. This suggests that unlike pyramidal neurons in other olfactory cortical areas that receive MOB inputs via the distal portion of their apical dendrites, MOB axons potentially form direct connections onto somas and/or dendrites of OT neurons.

Finally, the amount of MOB axons progressively decreases as they project medially and caudally. The massive number of axons in the AON and PIR dramatically decrease as they reach the OT. They decrease even further in more caudal structures like COA and ENT. This is observed on both coronal and sagittal sections and across several cases. There are two possible explanations for this phenomenon: (1) not all axons travel the entire course. Some

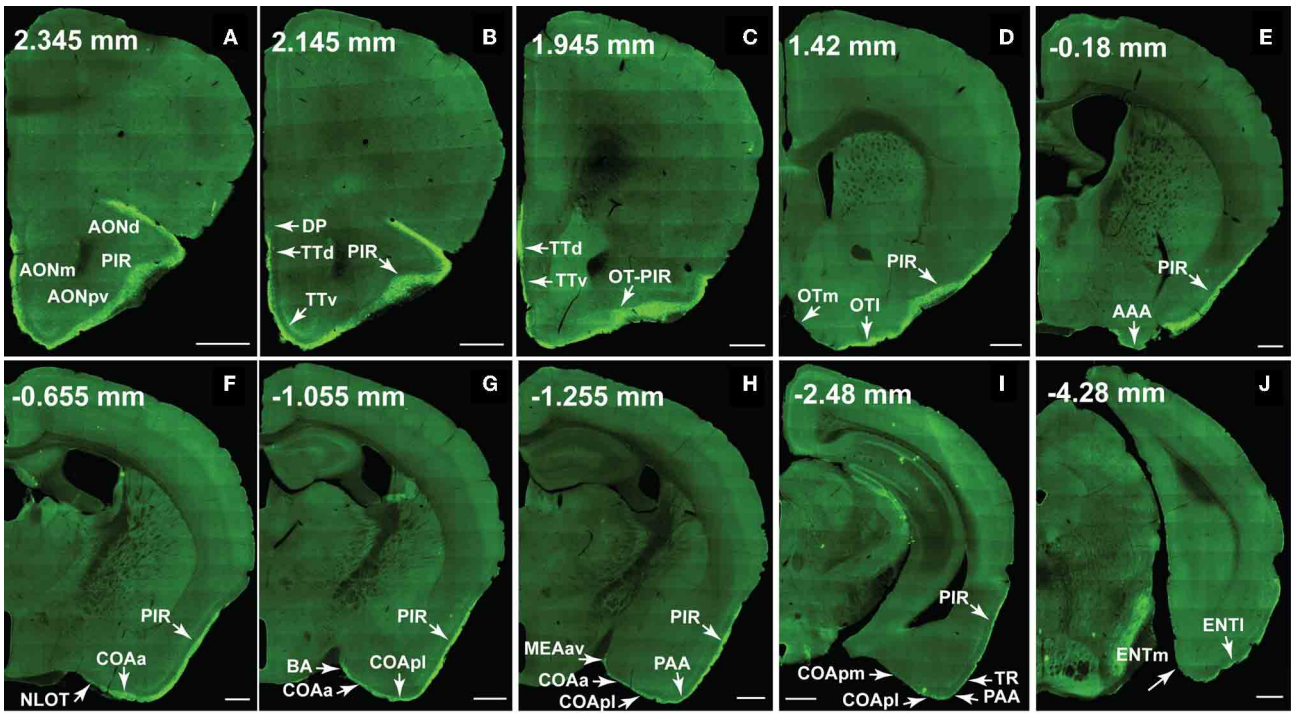

FIGURE 10 | The ventral *lateral* MOB projects to olfactory cortical structures from the AON to the ENT (2.345 to –4.28 mm from bregma). Axons ramify in AONd, AONm, AONpv **(A)**, TTd, TTv **(B,C)**, PIR **(A–I)**, OTl **(D)**, AAA **(E)**, NLOT **(F)**, COAa **(F–H)**, COApl **(G–I)**, BA **(G)**, MEAav **(H)**, PAA **(H,I)**, TR **(I)**, and ENTl **(J)** without any spatial topography. The DP, OTm, COApm, and ENTm do not receive inputs from the ventral *lateral* MOBmi (**B,D,I,J**). The PIR-OT junction contains dense labeling **(C)**, where the fibers appear to wrap around layer II pyramidal neurons in OTl (**Figures 12H,I**). Axon numbers appear to decrease as they travel medially **(B–J)** and caudally **(A–J)**. Differences between projection patterns from the ventral *lateral* and dorsal *medial* MOBmi were not detected (see **Figure 11**). *Case number SW101213-01A.* Scale bar, 500 μm. Abbreviations: AONd, dorsal anterior olfactory nucleus; AONm, medial AON; AONpv, posterior ventral AON; TTd, dorsal taenia tecta; TTv, ventral TT; PIR, piriform area; OTl, lateral olfactory tubercle; OTm, medial OT; AAA, anterior amygdalar area; NLOT, nucleus of lateral olfactory tract; COAa, anterior cortical amygdalar area; COApm, posterior medial COA; BA, bed nucleus of accessory olfactory tract; MEAav, anterior ventral medial amygdalar nucleus; PAA, piriform-amygdalar area; TR, postpiriform transition area; ENTl, lateral entorhinal area; ENTm, medial ENT.

axons may terminate specifically in the PIR or COA, while others extend all the way to ENTl or (2) the axons do extend through the entire course, but generate less collaterals and arborizations toward the caudal end of the brain. This question can be investigated by genetically labeling individual neurons in the MOB and examining the morphological details of their long axonal projections.

MOB PROJECTIONS TO THE PIR AND OTHER CORTICAL AREAS

There is contradictory information regarding MOB inputs to the PIR. Earlier reports assert that afferents from olfactory bulb synapse primarily onto neurons in the PIRa and only send lighter, more distributed inputs to PIRp (Haberly and Price, 1978; Shipley and Adamek, 1984; Haberly, 2001). In contrast, genetic tracing methods have reported that axons from individual glomeruli project diffusely to the entire PIR without apparent spatial preference (Sosulski et al., 2011). A possible explanation for these contradictory observations is that flattened hemi-brain preparations were used for some studies (Sosulski et al., 2011), while coronal sections were used in others. While a flattened hemi-brain preparation facilitates the observation of the axonal arborizations on the tangential plane, coronal sections reveal the entire scope of axonal ramifications.

Based on our data from coronal sections, distinct projection patterns from the MOBmi to PIRa versus PIRp are not evident. However, progressing from PIRa to PIRp, layer Ia appears to get thinner in width while the Ib thickens (**Figures 9B,C,E–G**). If this truly is the case and since Ia is the specific layer in which ramifications from MOB projections occur, this suggests that PIRa receives more inputs from the MOB compared to PIRp. Although differences in axon numbers are not discernible from the coronal plane, it is clear from sagittal sections that MOB fibers decrease as they travel from PIRa to PIRp (**Figures 9G–I**). Such patterns (i.e., number of MOB axons and layer width) potentially have implications for the connections formed between the MOB and these structures. It is possible that MOB axons form synaptic connections along the entire length of dendrites of AON and PIRa pyramidal neurons given their thicker and more densely populated Ia layer. In contrast, in the PIRp, COA, and ENT, potentially only pyramidal neurons with long apical dendrites that reach the outermost regions of a relatively thinner Ia can receive input from the far fewer MOB axons traveling through these areas. In fact, it

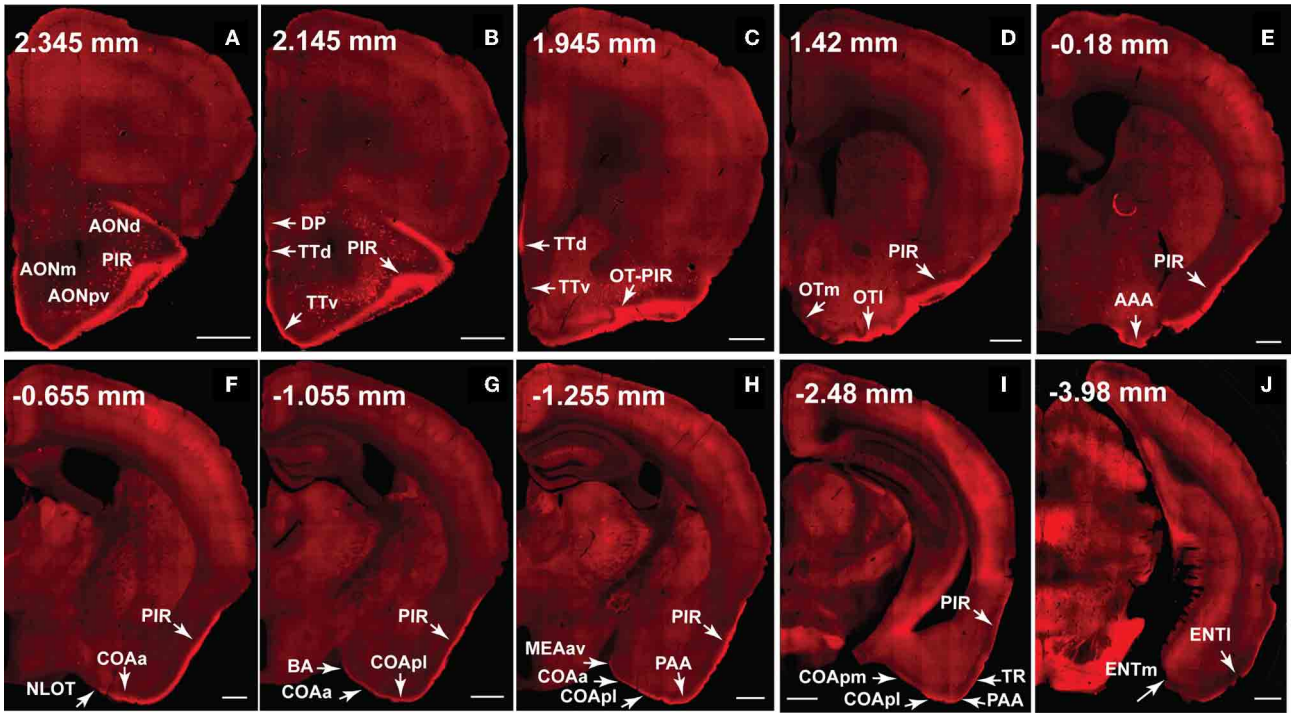

FIGURE 11 | The dorsal *medial* MOB projects to olfactory cortical structures from the AON to the ENT (2.345 to –3.98 mm from bregma). Axons ramify in AONd, AONm, AONpv **(A)**, TTd, TTv **(B,C)**, PIR **(A–I)**, OTl **(D)**, AAA **(E)**, NLOT **(F)**, COAa **(F–H)**, COApl **(G–I)**, BA **(G)**, MEAav **(H)**, PAA **(H,I)**, TR **(I)**, and ENTl **(J)** without any spatial topography. The DP, OTm, COApm, and ENTm do not receive inputs from the dorsal *medial* MOBmi **(B,D,I,J)**. The PIR-OT junction contains dense labeling **(C)**, where the fibers appear to wrap around layer II pyramidal neurons in OTl **(Figures 12H,I)**. Axon numbers appear to decrease as they travel medially **(B–J)** and caudally **(A–J)**. Differences between projection patterns from the dorsal *medial* and ventral *lateral* MOBmi were not detected (see **Figure 10**). *Case number SW101213-01A.* Scale bar, 500 μm. Abbreviations: AONd, dorsal anterior olfactory nucleus; AONm, medial AON; AONpv, posterior ventral AON; TTd, dorsal taenia tecta; TTv, ventral TT; PIR, piriform area; OTl, lateral olfactory tubercle; OTm, medial OT; AAA, anterior amygdalar area; NLOT, nucleus of lateral olfactory tract; COAa, anterior cortical amygdalar area; COApm, posterior medial COA; BA, bed nucleus of accessory olfactory tract; MEAav, anterior ventral medial amygdalar nucleus; PAA, piriform-amygdalar area; TR, postpiriform transition area; ENTl, lateral entorhinal area; ENTm, medial ENT.

is reported that the ratio of associative layer Ib to afferent Ia inputs is higher in more posterior regions of the PIR (Haberly, 1998).

The anatomical similarities between the AON and PIRa (**Figures 1C,D**) may be important for understanding how olfactory information is processed. The two structures can serve as the first association relay station between the MOB and caudal olfactory cortex. The AON is critical for synchronizing and integrating olfactory information from both sides of the bulb (Yan et al., 2008), while PIRa neurons encode sensory features of olfactory cues and relay this information rostrocaudally along the olfactory cortex (Haberly, 2001; Calu et al., 2007; Roesch et al., 2007). This information could be processed further in the second association area, the PIRp, which integrates olfactory information with inputs from the amygdala, entorhinal, medial prefrontal, orbitofrontal, and insular cortices that process multimodal and associative information (Johnson et al., 2000; Haberly, 2001). Functional data also suggests that PIRp neurons are involved in higher order processing compared to the PIRa. For example, the PIRp processes the predictive value of olfactory cues, implicating its involvement in associative olfactory learning (Calu et al., 2007; Roesch et al., 2007). This also is demonstrated in humans where PIRp, rather than the PIRa, generates olfactory predictive codes to augment olfactory perception based on previous experience (Zelano et al., 2011), which is important for orienting selective attention toward an odor of interest and away from an odor of no interest upon subsequent exposures. Since the PIRp projects directly to the deep MOBgr it may then indirectly inhibit further outputs from mitral cells to olfactory cortices (discussed below).

DISTINCT PIR PROJECTIONS TO MOB

It is reported that the PIR receives direct mitral cell input representing glomeruli from different regions of the olfactory bulb with no apparent spatial organization (Miyamichi et al., 2011). Our data support this result since CTb injected into the PIR non-preferentially back-labels mitral cells throughout the entire bulb (**Figure 7F**). Although MOB efferents suggest no topographic connectivity with the PIR, distinct connectional patterns are exposed when examining projections from the PIR to the MOBmi. Inputs to MOBmi show that while the PIRa projects to the MOBmi and to the superficial MOBgr, PIRp projects only to the deep MOBgr. In the basic organization of the olfactory system, GABAergic granule cells via dendrodendritic synapses (Gloor, 1997) act to inhibit the glutamatergic mitral or tufted cells (tfs), whose activation is the principal

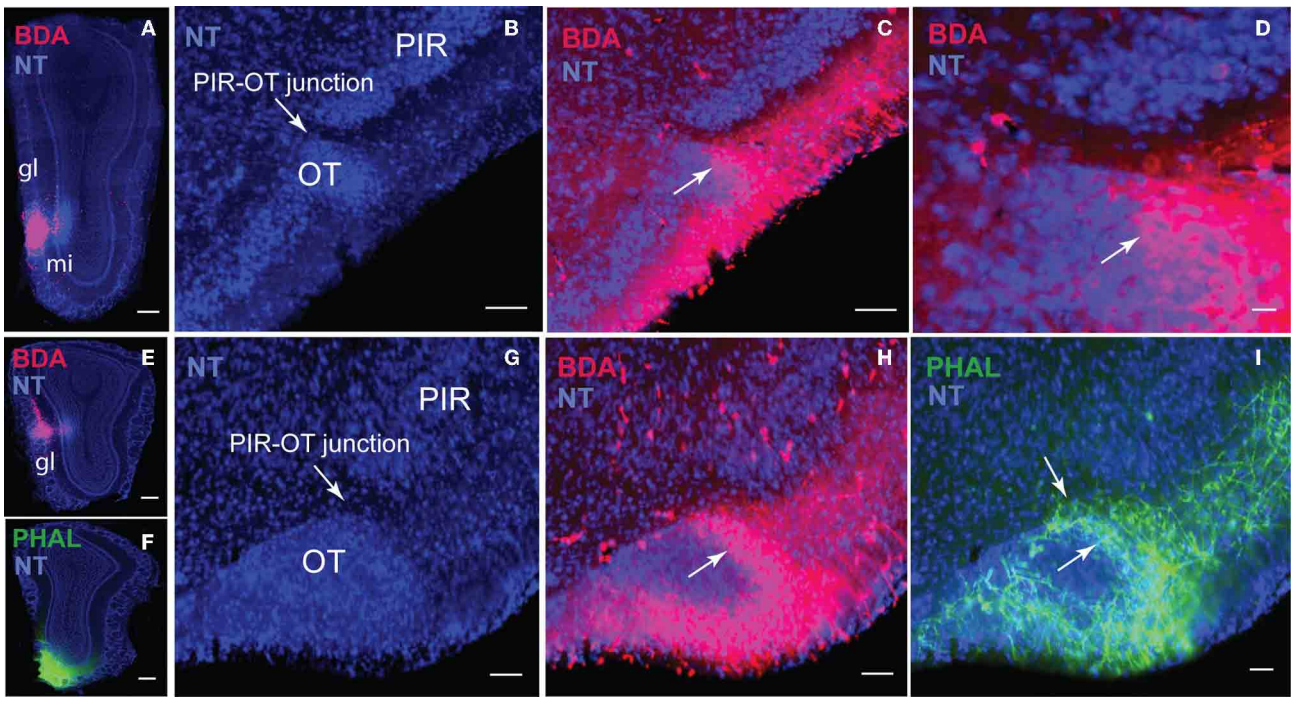

FIGURE 12 | Dense projections from different regions of the MOB including the MOBgl and MOBmi (A,E,F) to the junction between the PIR and OT (B–D,G–I). (C) is magnified in **(D)** to demonstrate how axons wrap around pyramidal OT neurons **(H,I)**. Scale bar, 100 μm; 20 μm **(D)**. *Case numbers SW101213-04A **(A–D)**; SW110607-02A **(E–I)***. Abbreviations: gl, glomerular layer of MOB; mi, mitral cell layer of MOB; PIR-OT, piriform-olfactory tubercle junction.

means of mediating output control of the olfactory bulb. This MOBgr stratification (deep versus superficial layers) is supported by data demonstrating that granule cells segregate into at least three different subpopulations based on morphological and molecular criteria. Deep granule cells have their dendritic arbors restricted to the deep outer plexiform layer (opl) where they are believed to synapse predominately with mitral cell secondary dendrites. In contrast, superficial granule cells arborize in the superficial opl where they synapse with tf dendrites (for review see Shepherd et al., 2007). Together with our data, this suggests that the PIRa possibly provides direct excitatory inputs to the MOBmi (MOBmi→PIRa→MOBmi), while its inputs to the superficial MOBgr cells provide an indirect inhibitory feedback control of MOBtf cells (MOBmi/tf→PIRa→superficial MOBgr→MOBtf). On the other hand, PIRp could indirectly inhibit the MOBmi cells via its projections to deep granule cells (MOBmi→PIRp→deep MOBgr→MOBmi; see **Figure 8** for schematic).

Our data also revealed a coarse topography within PIRa where more dorsal PIRa neurons tend to project to dorsal MOBmi, while more ventral PIRa neurons project to more ventral MOBmi. This is observed more clearly in a case where CTb and FG were double injected in the dorsal and ventral MOBmi, respectively, in the same animal. CTb neurons clustered in more dorsal parts of the PIRa, while FG roughly occupied more ventral regions. It should be noted that based on the data at hand, a clear boundary between the PIRa and PIRp or dorsal and ventral PIRa cannot be defined. Setting hard boundaries would require a more comprehensive examination of PIR connectivity, which will be performed in the future.

MOB PROJECTIONS TO CLASSIC ACCESSORY OLFACTORY STRUCTURES

The rodent olfactory system consists of two parallel chemosensory systems: the vomeronasal (VNO) or "accessory olfactory" and main olfactory systems. Classically, the VNO is thought to process non-volatile pheromones that lead to stereotyped endocrinological responses like aggression, acceleration or suppression of estrus, and pregnancy block (for review see Halpern, 1987). Primary projections of the AOB critical for pheromone processing include the BA, MEAa, MEApd, MEApv, COApm, and bed nuclei of stria terminalis (BST; principle nucleus) (Halpern, 1987; Simerly, 1990; Gloor, 1997). The main olfactory system primarily processes more complex, volatile chemosensory cues that are modifiable through experience (Halpern, 1987) and involve MOB projections to the AON, OT, and ENT (Gloor, 1997; Haberly, 2001). This strict segregation of the VNO and MOB systems has been challenged as research has shown pheromone activation of the MOB and MOB projections to more classic accessory structures like BA and MEAa, MEApd (Martínez-García et al., 1991; Pro-Sistiaga et al., 2007; Kang et al., 2011a,b). Our data also show MOBmi projections to BA and MEAav lending support for the possibility that the classic views of the main and accessory olfactory systems require modification. Fortifying this view is data showing prototypal olfactory recipients such as NLOT, COAa, and PAA also receive significant inputs from the AOB (Pro-Sistiaga

et al., 2007). Thus, the MEAav, BA, NLOT, COAa, and PAA may form a third "integrated" category of the olfactory system, which receives and processes converged information from both AOB and MOB. Evidence for complementary roles for the main and AOBs substantiates this possibility of integrated VNO and MOB systems (Martínez-García et al., 2009).

CONCLUDING COMMENTS

We provide the first open resource for olfactory pathways, which gradually will be expanded to include structures from the entire olfactory system. This connectivity database will generate testable hypothesis for studying the olfactory system and its interactions with structures such as the amygdala, hippocampus, medial prefrontal cortical area, and thalamus.

Our data showed topographically organized projection patterns of the *medial* MOBmi. Similar to reports in the literature, there was no clear spatially topographic projection from the MOB to PIR. However, we did find that axons from the MOB project more densely to PIRa than to PIRp. Further, we showed a clear topographic projection from the PIRa and PIRp to the MOB. This evidence suggests that the PIRa possibly provides direct excitatory inputs to the MOBmi, while its inputs to the superficial MOBgr cells provide an indirect inhibitory feedback control of MOBtf cells. It also suggests that the PIRp inhibits MOBmi via it projections to deep MOBgr cells. This hypothesis can be further tested and may shed light on the mechanisms underlying olfactory related behaviors.

MATERIALS AND METHODS

SUBJECTS AND HUSBANDRY

Data from 17 eight-week old male C57Bl/6J mice from Jackson Laboratories were used. They were housed in pairs in a temperature (21–22°C), humidity (51%), and light controlled (12 h light:12 h dark cycle with lights on at 6:00 am and off at 6:00 pm) vivarium. Mice were allowed 1 week to adapt to their living conditions before surgery. Experiments were conducted according to the standards set by the National Institutes of Health Guide for the Care and Use of Laboratory Animals and the institutional guidelines of the University of California, Los Angeles.

SURGERIES

To comprehensively examine MOB connectivity patterns, double coinjections were made into the (1) dorsal, (2) middle, or (3) ventral MOBmi along the dorsal-ventral axis and into *medial* and *lateral* regions along the medial-lateral axis. Injections also were made into the MOBgr and PIR (coordinates for each injection are available at www.MouseConnectome.org. Mice were initially anesthetized in an induction chamber primed with isoflurane and subsequently mounted to the stereotaxic apparatus where they were maintained under anesthetic state [2.5 gas mixture with oxygen (0.5 L/min) and nitrogen (1 L/min)]. PHAL/CTb and BDA/FG infusions were delivered iontophoretically using glass micropipettes (O.D. ~15–20 μm). A positive 5 μAmp, 7 s alternating current was delivered for 10 min. The analgesic buprenorphine was administered the day of and day following surgeries (0.05 mg/kg). Animals were sacrificed with an overdose injection of pentobarbital (6 mg/kg) 7 days following surgeries.

TRACERS

PHAL (2.5%; Vector Laboratories) was coinjected with CTb (647 conjugate, 0.25%; Invitrogen), while BDA (FluoroRuby, 5%; Invitrogen) and FG (1%; Fluorochrome, LLC) were injected in combination.

TISSUE PREPARATION

Each animal was transcardially perfused with approximately 50 ml of 0.9% NaCl followed by 50 ml of 4% paraformaldehyde solution (PFA; pH 9.5) following an overdose injection of sodium pentobarbital. Brains were post-fixed in 4% PFA for 24–48 h at 4°C after which they were embedded in 3% Type I-B agarose and sectioned into four series of coronal sections at 50 μm thickness.

IMMUNOFLUORESCENCE STAINING

One of four series was stained for PHAL using the free-floating method. Briefly, sections were transferred to a blocking solution (normal donkey serum and Triton X) for one hour. Following three 5 min rinses, sections were incubated with 1:1000 concentration of rabbit anti-PHAL antibody for 48–72 h at 4°C along with donkey serum and Triton. Sections were rinsed three times in KPBS and then soaked for 3 h in the secondary antibody solution (1:500 concentration of anti-rabbit IgG conjugated with Alexa Fluor® 488). Sections were counterstained with the fluorescent Nissl stain NeuroTrace® 435/455 (NT; 1:1000), mounted, and coverslipped using 65% glycerol.

IMAGING AND POST-ACQUISITION PROCESSING

Sections were imaged using an Olympus VS110 virtual slide scanner. Each image was flipped to the correct left-right orientation, matched to the nearest ARA (Dong, 2007) atlas level, and converted to tiff format prior to being registered (discussed below). Following registration and registration refinement, the fluorescent Nissl was converted to bright-field and each image for each channel (PHAL, CTb, BDA, FG, and NT) manually was adjusted for brightness and contrast to maximize labeling visibility and quality in iConnectome. Following final modifications (i.e., skewness, angles, preparation of images for thumbnail widget) and pyramidal tiff conversions, images were published to iConnectome.

Distracting artifacts from BDA that may have been mistaken for labeling were removed from the images. Labeling (axons, boutons, neurons) for the images was not manipulated and all original raw images are available on iConnectome.

SEMI-AUTOMATED IMAGE REGISTRATION

To ease analysis of the connectivity data, each section was registered onto its corresponding ARA atlas level (**Figures 3D–F**). A combination of automatic and manual registration steps was used to resample, align, and co-register the acquired brain images with the ARA atlas image. Each individual image was manually matched to its closest corresponding ARA atlas level and the information was manually inserted into a registration table. Although manual, this reduces the 2D registration variability and improves registration accuracy versus using a fully automated registration algorithm purely based on fiducial markers like the Allen Brain Atlas.

A 2D diffeomorphic demons algorithm (Vercauteren et al., 2009) was used for image registration. Affine registration was chosen to minimize distortion to preserve axonal morphology. The deformation matrix resulting from the registration process was applied on the original resolution images to attain high-resolution warped images. The algorithm was implemented in Matlab and standalone binaries were generated using Matlab compiler. The Laboratory of Neuro Imaging (LONI) pipeline was used for parallel execution of registration of multiple cases.

ACKNOWLEDGMENTS

We would like to thank Larry W. Swanson and Harvey Karten for advising this project. This work was supported by NIH/NIMH, MH094360-01A1 (Hong-Wei Dong) and P41 Supplement (3P41RR013642-12S3).

REFERENCES

Behrens, T. E., and Sporns, O. (2012). Human connectomics. *Curr. Opin. Neurobiol.* 22, 144–153.

Bock, D. D., Lee, W. C., Kerlin, A. M., Andermann, M. L., Hood, G., Wetzel, A. W., Yurgenson, S., Soucy, E. R., Kim, H. S., and Reid, R. C. (2011). Network anatomy and *in vivo* physiology of visual cortical neurons. *Nature* 471, 177–182.

Briggman, K. L., Helmstaedter, M., and Denk, W. (2011). Wiring specificity in the direction-selectivity circuit of the retina. *Nature* 471, 183–188.

Cajal, S. R. (1904). *Textura del Sistema Nervioso del Hombre y de los Vertebrados.* Madrid: Moya, 611–1209.

Calu, D. J., Roesch, M. R., Stalnaker, T. A., and Schoenbaum, G. (2007). Associative encoding in posterior piriform cortex during odor discrimination and reversal learning. *Cereb. Cortex* 17, 1342–1349.

Cammoun, L., Gigandet, X., Meskaldji, D., Thiran, J. P., Sporns, O., Do, K. Q., Maeder, P., Meuli, R., and Hagmann, P. (2012). Mapping the human connectome at multiple scales with diffusion spectrum MRI. *J. Neurosci. Methods* 203, 386–397.

Cragg, B. G. (1961). Olfactory and other afferent connections of the hippocampus in the rabbit, rat, and cat. *Exp. Neurol.* 3, 588–600.

Dong, H. W. (2007). *Allen Reference Atlas: A Digital Color Brain Atlas of the C57BL/6J Male Mouse.* Hoboken, NJ: Wiley.

Franks, K. M., Russo, M. J., Sosulski, D. L., Mulligan, A. A., Siegelbaum, S. A., and Axel, R. (2011). Recurrent circuitry dynamically shapes the activation of piriform cortex. *Neuron* 72, 49–56.

Friedrich, R. W. (2011). Olfactory neuroscience: beyond the bulb. *Curr. Biol.* 21, R438–R440.

Ghosh, S., Larson, S. D., Hefzi, H., Marnoy, Z., Cutforth, T., Dokka, K., and Baldwin, K. K. (2011). Sensory maps in the olfactory cortex defined by long-range viral tracing of single neurons. *Nature* 472, 217–220.

Gloor, P. (1997). "The olfactory system," in *The Temporal Lobe and Limbic System*, (New York, NY: Oxford University Press), 273–323.

Haberly, L. B. (1998). "Olfactory cortex," in *The Synaptic Organization of the Brain*, ed G. M. Shepherd (New York, NY: Oxford University Press), 377–416.

Haberly, L. B. (2001). Parallel-distributed processing in olfactory cortex: new insights from morphological and physiological analysis of neuronal circuitry. *Chem. Senses* 26, 551–576.

Haberly, L. B., and Price, J. L. (1977). The axonal projection patterns of the mitral and tufted cells of the olfactory bulb in the rat. *Brain Res.* 129, 152–157.

Haberly, L. B., and Price, J. L. (1978). Association and commissural fiber systems of the olfactory cortex of the rat. II. Systems originating in the olfactory peduncle. *J. Comp. Neurol.* 181, 781–807.

Halpern, M. (1987). The organization and function of the vomeronasal system. *Annu. Rev. Neurosci.* 10, 325–362.

Inaki, K., Nishimura, S., Nakashiba, T., Itohara, S., and Yoshihara, Y. (2004). Laminar organization of the developing lateral olfactory tract revealed by differential expression of cell recognition molecules. *J. Comp. Neurol.* 479, 243–256.

Isaacson, J. S. (2010). Odor representations in mammalian cortical circuits. *Curr. Opin. Neurobiol.* 20, 328–331.

Johnson, D. M., Illig, K. R., Behan, M., and Haberly, L. B. (2000). New features of connectivity in piriform cortex visualized by intracellular injection of pyramidal cells suggest that "primary" olfactory cortex functions like "association" cortex in other sensory systems. *J. Neurosci.* 20, 6974–6982.

Jones, E. G., Stone, J. M., and Karten, H. J. (2011). High-resolution digital brain atlases: a Hubble telescope for the brain. *Ann. N.Y. Acad. Sci.* 1225(Suppl. 1), E147–E159.

Kang, N., Baum, M. J., and Cherry, J. A. (2011a). Different profiles of main and accessory olfactory bulb mitral/tufted cell projections revealed in mice using an anterograde tracer and a whole-mount, flattened cortex preparation. *Chem. Senses* 36, 251–260.

Kang, N., McCarthy, E. A., Cherry, J. A., and Baum, M. J. (2011b). A sex comparison of the anatomy and function of the main olfactory bulb-medial amygdala projection in mice. *Neuroscience* 172, 196–204.

Lichtman, J. W., Livet, J., and Sanes, J. R. (2008). A technicolour approach to the connectome. *Nat. Rev. Neurosci.* 9, 417–422.

Martínez-García, F., Martínez-Ricós, J., Augustín-Pavón, C., Martínez-Hernández, J., Novejarque, A., and Lanuza, E. (2009). Refining the dual olfactory hypothesis: pheromone reward and odour experience. *Behav. Brain Res.* 200, 277–286.

Martínez-García, F., Olucha, F. E., Teruel, V., Lorente, M. J., and Schwerdtfeger, W. K. (1991). Afferent and efferent connections of the olfactory bulbs in the lizard *Podarcis hispanica*. *J. Comp. Neurol.* 305, 337–347.

Micheva, K. D., O'Rourke, N., Busse, B., and Smith, S. J. (2010). Array tomography: high-resolution three-dimensional immunofluorescence. *Cold Spring Harb. Protoc.* doi: 10.1101/pdb.top89. [Epub ahead of print].

Miyamichi, K., Amat, F., Moussavi, F., Wang, C., Wickersham, I., Wall, N. R., Taniguchi, H., Tasic, B., Huang, Z. J., He, Z., Callaway, E. M., Horowitz, M. A., and Luo, L. (2011). Cortical representations of olfactory input by trans-synaptic tracing. *Nature* 472, 191–196.

Mombaerts, P., Wang, F., Dulac, C., Chao, S. K., Nemes, A., Mendelsohn, M., Edmondson, J., and Axel, R. (1996). Visualizing an olfactory sensory map. *Cell* 87, 675–686.

Nagayama, S., Enerva, A., Fletcher, M. L., Masurkar, A. V., Igarashi, K. M., Mori, K., and Chen, W. R. (2010). Differential axonal projection of mitral and tufted cells in the mouse main olfactory system. *Front. Neural Circuits* 4:120. doi: 10.3389/fncir.2010.00120

Powell, T. P., Cowan, W. M., and Raisman, G. (1965). The central olfactory connexions. *J. Anat.* 99, 791–813.

Price, J. L. (1973). An autoradiographic study of complementary laminar patterns of termination of afferent fibers to the olfactory cortex. *J. Comp. Neurol.* 150, 87–108.

Pro-Sistiaga, P., Mohedano-Moriano, A., Ubeda-Banon, I., Del Mar Arroyo-Jimenez, M., Marcos, P., Artacho-Pérula, E., Crespo, C., Insausti, R., and Martinez-Marcos, A. (2007). Convergence of olfactory and vomeronasal projections in the rat basal telencephalon. *J. Comp. Neurol.* 504, 346–362.

Ressler, K. J., Sullivan, S. L., and Buck, L. B. (1994). Information coding in the olfactory system: evidence for a stereotyped and highly organized epitope map in the olfactory bulb. *Cell* 79, 1245–1255.

Roesch, M. R., Stalnaker, T. A., and Schoenbaum, G. (2007). Associative encoding in anterior piriform cortex versus orbitofrontal cortex during odor discrimination and reversal learning. *Cereb. Cortex* 17, 643–652.

Rubin, B. D., and Katz, L. C. (1999). Optical imaging of odorant representations in the mammalian olfactory bulb. *Neuron* 23, 499–511.

Scalia, F., and Winans, S. S. (1975). The differential projections of the olfactory bulb and accessory olfactory bulb in mammals. *J. Comp. Neurol.* 161, 31–55.

Shepherd, G. M., Chen, W. R., Willhite, D., Migliore, M., and Greer, C. A. (2007). The olfactory granule cell: from classical enigma to central role in olfactory processing. *Brain Res. Rev.* 55, 373–382.

Shipley, M. T., and Adamek, G. D. (1984). The connections of the mouse olfactory bulb: a study using orthograde and retrograde transport of wheat germ agglutinin conjugated to horseradish peroxidase. *Brain Res. Bull.* 12, 669–688.

Simerly, R. B. (1990). Hormonal control of neuropeptide gene

expression in sexually dimorphic olfactory pathways. *Trends Neurosci.* 13, 104–110.

Sosulski, D. L., Bloom, M. L., Cutforth, T., Axel, R., and Datta, S. R. (2011). Distinct representations of olfactory information in different cortical centres. *Nature* 472, 213–216.

Thompson, R. H., and Swanson, L. W. (2010). Hypothesis-driven structural connectivity analysis supports network over hierarchical model of brain architecture. *Proc. Natl. Acad. Sci. U.S.A.* 107, 15235–15239.

Van Essen, D. C., Ugurbil, K., Auerbach, E., Barch, D., Behrens, T. E. J., Bucholz, R., Chang, A., Chen, L., Corbetta, M., Curtiss, S. W., Della Penna, S., Feinberg, D., Glasser, M. F., Harel, N., Heath, A. C., Larson-Prior, L., Marcus, D., Michalareas, G., Moeller, S., Oostenveld, R., Petersen, S. E., Prior, F., Schlaggar, B. L., Smith, S. M., Snyder, A. Z., Xu, J., and Yacoub, E. (2012). The human connectome project: a data acquisition perspective. *Neuroimage*. doi: 10.1016/j.neuroimage.2012.02.018. [Epub ahead of print].

Vassar, R., Chao, S. K., Sitcheran, R., Nunez, J. M., Vosshall, L. B., and Axel, R. (1994). Topographic organization of sensory projections to the olfactory bulb. *Cell* 79, 981–991.

Vercauteren, T., Pennec, X., Perchant, A., and Ayache, N. (2009). Diffeomorphic demons: efficient non-parametric image registration. *Neuroimage* 45, S61–S72.

Yan, Z., Tan, J., Qin, C., Lu, Y., Ding, C., and Luo, M. (2008). Precise circuitry links bilaterally symmetric olfactory maps. *Neuron* 58, 613–624.

Zelano, C., Mohanty, A., and Gottfried, J. A. (2011). Olfactory predictive codes and stimulus templates in piriform cortex. *Neuron* 72, 178–187.

Conflict of Interest Statement: The authors declare that the research was conducted in the absence of any commercial or financial relationships that could be construed as a potential conflict of interest.

Received: 09 May 2012; paper pending published: 26 May 2012; accepted: 19 July 2012; published online: 07 August 2012.

*Citation: Hintiryan H, Gou L, Zingg B, Yamashita S, Lyden HM, Song MY, Grewal AK, Zhang X, Toga AW and Dong H-W (2012) Comprehensive connectivity of the mouse main olfactory bulb: analysis and online digital atlas. Front. Neuroanat. **6**:30. doi: 10.3389/fnana.2012.00030*

frontiers in
NEUROANATOMY

ORIGINAL RESEARCH ARTICLE
published: 08 November 2012
doi: 10.3389/fnana.2012.00044

Hypothalamus-olfactory system crosstalk: orexin A immunostaining in mice

Jean Gascuel*[1,2,3,4]*, Aleth Lemoine*[2,3,4]*, Caroline Rigault*[2,3,4]*, Frédérique Datiche*[2,3,4]*, Alexandre Benani*[2,3,4]*, Luc Penicaud*[2,3,4]*and Laura Lopez-Mascaraque*[1]*

[1] *Instituto Cajal, CSIC, Avda del Doctor Arce, Madrid, Spain*
[2] *CNRS UMR 6265, Centre des Sciences du Goût et de l'Alimentation, Dijon, France*
[3] *Institut National de la Recherche Agronomique UMR 1324, Centre des Sciences du Goût et de l'Alimentation, Dijon, France*
[4] *Université de Bourgogne UMR CSGA, Centre des Sciences du Goût et de l'Alimentation, Dijon, France*

Edited by:
Jorge A. Larriva-Sahd, Universidad Nacional Autónoma de México, Mexico

Reviewed by:
Guy Elston, Centre for Cognitive Neuroscience, Australia
Jorge A. Larriva-Sahd, Universidad Nacional Autónoma de México, Mexico
Alfredo Varela-Echavarria, Universidad Nacional Autónoma de México, Mexico

****Correspondence:***
Laura Lopez-Mascaraque, Instituto Cajal, Avda del Doctor Arce 37, 28002 Madrid, Spain.
e-mail: mascaraque@cajal.csic.es

It is well known that olfaction influences food intake, and conversely, that an individual's nutritional status modulates olfactory sensitivity. However, what is still poorly understood is the neuronal correlate of this relationship, as well as the connections between the olfactory bulb and the hypothalamus. The goal of this report is to analyze the relationship between the olfactory bulb and hypothalamus, focusing on orexin A immunostaining, a hypothalamic neuropeptide that is thought to play a role in states of sleep/wakefulness. Interestingly, orexin A has also been described as a food intake stimulator. Such an effect may be due in part to the stimulation of the olfactory bulbar pathway. In rats, orexin positive cells are concentrated strictly in the lateral hypothalamus, while their projections invade nearly the entire brain including the olfactory system. Therefore, orexin appears to be a good candidate to play a pivotal role in connecting olfactory and hypothalamic pathways. So far, orexin has been described in rats, however, there is still a lack of information concerning its expression in the brains of adult and developing mice. In this context, we revisited the orexin A pattern in adult and developing mice using immunohistological methods and confocal microscopy. Besides minor differences, orexin A immunostaining in mice shares many features with those observed in rats. In the olfactory bulb, even though there are few orexin projections, they reach all the different layers of the olfactory bulb. In contrast to the presence of orexin projections in the main olfactory bulb, almost none have been found in the accessory olfactory bulb. The developmental expression of orexin A supports the hypothesis that orexin expression only appears post-natally.

Keywords: orexin A, olfactory system, hypothalamus, food intake behavior, AOB, MOB, immunocytology

INTRODUCTION

Everyone at some point in their lives has been astonished by the influence that feeding has on olfactory sensitivity, particularly in the perception of food-associated odorants. This suggests that one of the first ways in which the brain regulates food intake behavior is by modulating the perception of the food odorant itself. Indeed, such change in sensory perception has been defined as alliesthesia (Cabanac and Duclaux, 1973; Duclaux et al., 1973) and sensory specific satiety (SSS; Yeomans, 2006). At the most peripheral level – the olfactory epithelium (OE) – many neuropeptides and metabolic hormones such as Gonadotropin-Releasing Hormone (GnRH), Neuronal Peptide Y (NPY), leptin, adiponectin, and orexins are thought to modulate the sensitivity of olfactory sensory neurons in different species. For instance, in lower vertebrates, LHRH/GnRH, released by the nervus terminalis (NT) at the OE level (Wirsig-Wiechmann, 1993; Oka, 1997), modulates olfactory neuronal sensitivity (Kawai et al., 2009) reducing evoked responses to food odorant cues during the reproductive period in Axolotl. This allows the olfactory system to be available predominantly for odorants involved in mating (Mousley et al., 2006). In contrast, NPY, an orexigenic neuropeptide, is also released producing

Abbreviations: 3V, third ventricle; Aci, anterior commissure intrabulbar; AHA, anterior hypothal. area; AOB, accessory olfactory bulb; AOM, anterior olfactory nucleus anterior; AOP, anterior olfactory nucleus posterior; APTD, anterior pretectal nucleus dors.; Arc, arcuate nucleus; CCK, cholecystokinin; D3V, dorsal third ventricle; DG, dentate gyrus; DLG, dorsal lateral geniculate; DM, dorso medi hypothal. nu.; DTT, dorsal tenia tecta; E/OV, ependy/olfactory ventricle; EPl, external plexiform layer; fr, fasciculus retroflexus; Gl, glomerular level; GlA, glomerular layer of the accessory olfactory bulb; GnRH, gonadotropin-releasing hormone; GrA, granular cell layer of the accessory olfactory bulb; GrO, granular cell layer; Hb, habenular nucleus; Ipl, internal plexiform layer; LA, lateroant. hypothal. nu.; LH, lateral hypothalamus; LPMR, lat. post. thal. nu.; MD, medio dorsal thalamus nucleus; Me, med amygdala; ME, median eminence; Mi, mitral cell layer; MiA, mitral cell layer of the accessory olfactory bulb; MOB, main olfactory bulb; MPA, med. preoptic area nu.; NPY, neuropeptide Y; OE, olfactory epithelium; OB, olfactory bulb; OPT, olivary pretectal nucleus; opt, optical nerve; PaAP, pa. anterior parvicell. Pt. pc, post commissure; PF, para fascicular thalamus nucleus; Pir, piriform cortex; PLCo, postlat cx amygdale nu.; PMV, premammill. nu. ventral; Po, post. thal. nu.; PV, paraventricular thalamic nucleus; PVP, paraventricular thalamic nucleus post; SCh, suprachiasmatic nu.; SCO, sub commissural organ; SSS, sensory specific satiety; TS, triangular septal nucleus; VIP, vasoactive intestinal peptide; VLG, ventral lateral geniculate; VMH, ventral hypothalamic nu.; VPL, ventro postero lateral; VPM, ventro postero med. thal.; VTT, ventral tenia tecta.

an inverse effect in the OE, i.e., causing an increase in sensitivity to food odorants (Mousley et al., 2006). In mammals, hormonal mechanisms have also been shown to modulate the sensitivity of the olfactory system. Leptin – a hormone produced by adipocytes in proportion to the fat content, and involved in modulation of the neuronal network linked to energy balance (Friedman, 2002; Pinto et al., 2004) – is present in the OE and has a modulatory effect on olfactory sensory neurons (Savigner et al., 2009). Similarly, adiponectin receptors 1 (receptor for adiponectin, a hormone involved in glucose and lipid metabolism) are expressed by mature sensory neurons (Hass et al., 2008), suggesting that this peptide is also able to modulate olfactory responses.

At the central level, many hormones and neuropeptides such as vasoactive intestinal peptide (VIP, Garcia-Llanes et al., 2003), cholecystokinin (CCK, Tanganelli et al., 2001), NPY (Matsutani et al., 1988), LHRH/GnRH (Apelbaum et al., 2005), and insulin (Fadool et al., 2011) may modulate olfactory processing. However, besides such hormonal mechanisms, a body of data (Doucette et al., 2007; Doucette and Restrepo, 2008; Fletcher and Chen, 2010) suggests the existence of a neuronal centrifugal modulation of olfactory bulb (OB) activity in different tasks, including the modulation of olfactory sensitivity toward food odorants (Pager et al., 1972; Pager, 1978; Royet et al., 1983). Different pathways (**Figure 1**), which are known to connect hypothalamic nuclei with olfactory centers, could be the neuroanatomical substrates accounting for the observations reported by Pager (1978). Among these, the "orexin/hcrt neurones" appear to be a likely candidate. Indeed, orexin/hypocretin (hcrt), a neuropeptide involved in sleep/wake regulation (Sakurai et al., 1998, 2010; Sakurai and Mieda, 2011), is also involved in feeding behavior (Horvath and Gao, 2005). Many studies have demonstrated that it could act by modulating olfactory sensitivity according to satiety (Aimé et al., 2007; Julliard et al., 2007; Prud'homme et al., 2009, for review: Palouzier-Paulignan et al., 2012). The cytological, connectional (Hahn and Swanson, 2010, 2012), immunohistological, and molecular (Peyron et al., 1998; Sakurai et al., 2005; Swanson et al., 2005) characterization of the lateral hypothalamus (LH) has already been performed. These studies suggest the existence of a functional loop between olfactory centers and the hypothalamus, which could explain the modulation of olfaction depending on energy balance. Unfortunately, inputs that project to orexin neurons have been shown in mice (Sakurai et al., 2005), while the LH orexin neuron projections to the OB have been shown in rats (Peyron et al., 1998; Nambu et al., 1999). Showing the existence of synaptic output from LH orexin neurons to the OB is a prerequisite to validate the reality of this loop in mice. Owing to the fact that the orexin immunostaining pattern presents variations amongst rodents, for instance between rats and hamsters (Nixon and Smale, 2007), the first preliminary step toward the validation of the putative loop between the LH and the OB was to validate data in mice obtained previously in rats (Peyron et al., 1998; Nambu et al., 1999). The aim of this study being established, future studies will address the question of connectivity through a trans-synaptic tracer experiment in order to draw the exact circuitry between OB and hypothalamus.

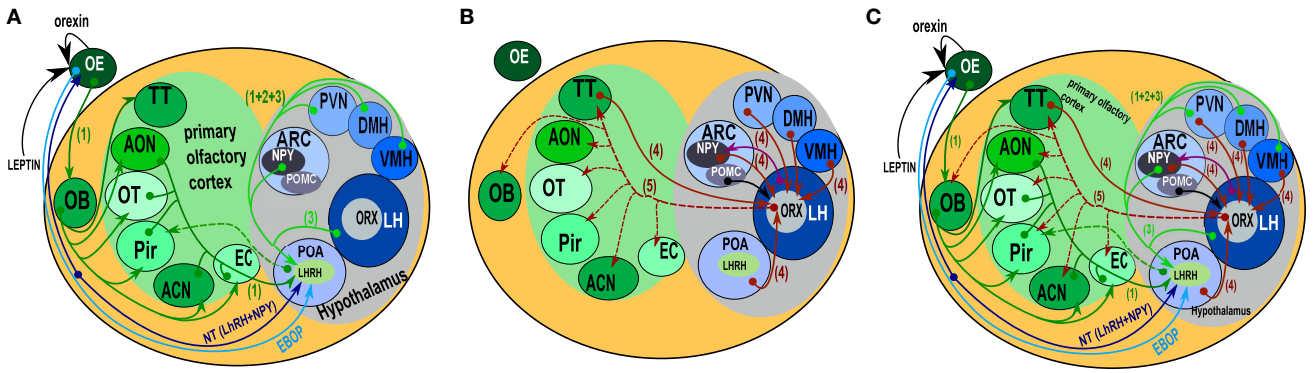

FIGURE 1 | Schematic representation of the "connectome" between the olfactory system and the hypothalamus. (A) Paracrine, extrabulbar connection, and afferents to LHRH/GnRH hypothalamic neurons. Orexin and leptin could modulate olfactory neuron sensitivity by paracrine action. The EBOP (Extra Bulbar Olfactory Pathway) is made up of sensory neurons that project directly to the POA in the hypothalamus. However, this pathway has only been identified in lower vertebrates. In contrast, the Nervus Terminalis is known in mammals and humans. This complex structure, which projects both to the olfactory epithelium and the POA, is thought to play a bidirectional modulatory role. LHRH/GnRH neurons get afferents from nearly all the areas of the olfactory system (including the OB), and from the most important hypothalamic structures involved in the regulation of food intake behavior (1, 2). However, no direct output onto olfactory structures has been evidenced. **(B)** Afferents onto orexin neurons (4). Orexin neurons received input from nearly all of the hypothalamic areas. Interestingly, they also received input from the Tenia Tecta (TT) of the olfactory cortex. From the arcuate nucleus, both POMC and NPY (6) neurons project onto orexin neurons. Both the input and output (Peyron et al., 1998) of orexin neurons are represented. Output data are only from rats, but they provided evidence of a putative output from orexin neurons onto the olfactory structures and input from the TT of the olfactory cortex onto orexin neurons. **(C)** This synthetic representation, even though incomplete, reveals the complexity of the putative interactions between olfaction and hypothalamic areas. (1 = Yoon et al., 2005; 2 = Boehm et al., 2005; 3, 6 = Yoshida et al., 2006; 4 = Sakurai et al., 2005; 5 = Peyron et al., 1998; 6 = Elias et al., 1998). ACN, amygdaloïd cortical nucleus; AON, anterior olfactory nucleus; ARC, arcuate nucleus; DMH, dorso medial nucleus of the hypothalamus; EBOP, extra bulbar olfactory pathway; EC, entorhinal cortex; LH, lateral hypothalamus; NT, nervus terminalis; OB, olfactory bulb; OE, olfactory epithelium; OT, olfactory tubercle; Pir, cortex piriform; POA, preoptic area; PVN, paraventricular nucleus of the hypothalamus; TT, tenia tecta; VMH, ventro medial nucleus of the hypothalamus.

MATERIALS AND METHODS

ANIMALS

C57 mice were raised at the Cajal Institute mouse-breeding facility. All procedures followed the guidelines for animal care of the European Community Council (86/609/CEE), and were approved by the Bioethical Committee of the Spanish National Research Council (CSIC). The animals were kept under a constant 12–12 h dark-light cycle (light on at 07:00am). The day the vaginal plug was detected was designated as embryonic day 0 (E0). The mice were killed by hypothermia (embryos and P3) or with i.p. equithesin at a sub-lethal dose (3 mL/kg body weight; from P3 to adult) systematically at the same time of the diurnal cycle (04:00pm).

IMMUNOHISTOCHEMISTRY

After anesthesia, the mice were transcardially perfused with 4% paraformaldehyde (PF) in 0.1 M phosphate buffer (PB, pH 7.2). The brains were then post-fixed in PF for 2 h at 4°C, and coronal vibratome sections were obtained at 70 μm. One out of three sections was used for immunocytochemistry. Unspecific binding of antibodies was blocked by three washes in NGS 10% in Tris buffered saline with 5% Tween (TBS-T), followed by overnight incubation using primary rabbit anti-orexin A (Millipore AB3098; Sakurai et al., 1998) and diluted to 1:1000 in the buffer. Antibody binding was detected with the secondary antibody goat Anti-rabbit Alexa 488 (Invitrogen A11001) diluted to 1:700 during 2 h at room temperature. Sections were then washed three times in TBS-T. Nuclei were counterstained with Hoechst (1 μg/ml, Sigma-Aldrich Co.). The control consisted of substituting the primary antibody by an orexin B antibody, followed by the same immunohistological protocol just described.

MICROSCOPY AND IMAGE PROCESSING

Optical sections were acquired using a Leica SP5 confocal microscope, 10× objectives HPC PL Apo CS dry UV, at a resolution of 1024 × 1024, without zoom magnification. The voxel size was 1.51 × 1.51 × 5.32. Whole coronal sections of the brains were reconstructed by doing XY mosaics using Leica software. For each XY position, six to seven optical sections were acquired in Z. Projections were made with a "Max intensity" algorithm using FIJI (an ImageJ plug-in). Relative quantification of orexin fibers was determined after thresholding the image in order to differentiate the neurite profile from the background. The measurements give values in percentage of surface area, thus expressing the density of orexin fibers per unit of area.

TISSUE DISSECTION AND RNA EXTRACTION AND PROCESSING

After decapitation, embryo (E17) and newborn (P3) brains were rapidly dissected on ice. For adult males and 11-day-old mice (P11) the hypothalamus and cerebellum were quickly microdissected on ice systematically at the same time of the diurnal cycle (between 02:00 and 04:00pm). Liver tissue was also isolated from each animal. All of the collected tissues were immediately frozen in liquid nitrogen and stored at −80°C. Total RNA was extracted using the RNeasy Mini Kit (Qiagen). Possible DNA contaminants in the RNA preparation were eliminated by treatment with DNAse I (Qiagen). RNA quality was assessed with the Experion electrophoresis system (Bio-Rad) and the Experion RNA StdSens Analysis Kit (Bio-Rad). Total RNA concentration was determined using the Nanodrop spectrophotometer (Thermo Scientific).

REAL-TIME PCR ANALYSIS

Reverse transcription was performed with 500 ng of total RNAs, using the High-Capacity RNA-to-cDNA Master Mix (Applied Biosystem). For qPCR, the Fast SYBR Green Master Mix (Applied Biosystems) was used. Each reaction contained 1 μl of cDNA diluted 1:10 and 200 nM of gene specific intron-spanning primers. The sequences of the primers used for *prepro-orexin (Ppox)* amplification were 5′-GGCACCATGAACTTTCCTTC-3′ and 5′-GACAGCAGTCGGGCAGAG-3′. TATA box binding protein (Tbp) RNA expression was used as an endogenous control. The sequences of the primers were 5′-GGGAGAATCATGGACCAGAA-3′ and 5′-CCGTAAGGCATCAT TGGACT-3′. Real-time PCR reactions were performed on a StepOne Plus thermocycler (Applied Biosystems). PCR conditions were 20 s at 95°C, followed by 40 cycles of 3 s at 95°C and 30 s at 60°C. Relative quantitation of gene expression (RQ) was based on the $\Delta\Delta C_t$ method.

RESULTS

OREXIN IN ADULT MICE

We analyzed orexin A staining all along the antero-posterior axis of the mouse brains by immunohistochemistry. We selected confocal coronal sections, from the OB to the cerebellum, to perform a semi-quantitative evaluation of orexin A staining (**Table 1**), and compared the results with rat orexin staining (Peyron et al., 1998). For each brain area reported in **Table 1**, we quantified the percentage of orexin fibers (see "Materials and Methods"). Our data revealed that in mice, the orexin A immunostaining was as follows:(i) the localization of orexin A neuronal cell bodies in the LH (ii) a wide distribution of orexin A fibers in all brain areas except the cerebellum and caudate putamen, (iii) a strong presence of orexin A fibers in the thalamus and the hypothalamus. Therefore, the mouse orexin A pattern is similar to that in rats, even though there are some minor differences.

In the mouse, the **thalamic area** appeared to be heavily orexin A labeled (**Figure 2**) at the level of the parafascicular thalamic nucleus (PF; **Figure 2C**), the paraventricular nuclei (PV; **Figures 2A** and **3B**), the subcommissural organ (SCO; **Figure 2B**), the central medial, and mediodorsal (MD) thalamic nuclei (**Figure 2A**). Nevertheless, the immunostaining was not homogeneous throughout the whole thalamus. It appeared faintly stained in epithalamic areas: such as the lateral and medial habenular nucleus (Hb, **Figure 2A**), the olivary pretectal nucleus (OPT, **Figure 2C**) and the antero-pretectal-dorsal nucleus (APTD, **Figure 2C**). At the geniculate nucleus level, there was no orexin A in the dorso-lateral geniculate nucleus (DLG; **Figure 2D**), while the ventral lateral geniculate nucleus (VLG) was strongly stained (**Figure 2D**). There was almost no staining in the ventro lateral thalamus, the ventro-postero-lateral (VPL) and ventro-postero-medial thalamic nuclei (VPM; **Figure 2D**).

At **hippocampus level,** the staining was discrete and mostly located in CA1 and CA2. CA3 was consistently less stained than CA1 or CA2 (**Figure 2E**). The dentate gyrus was poorly labeled by orexin A staining (**Figures 2A–C**). The triangular septal nucleus

Table 1 | Semi-quantitative estimation of the density of presence in different brain areas.

AMYGDALE		
AHiAL	Amygdalohippocampal area, anterolateral part	$0.01 < X < 0.49$
BLA	Basolateral amygdaloid nucleus, anterior part	$0.01 < X < 0.49$
BLP	Basolateral amygdaloid nucleus, posterior part	$0.01 < X < 0.49$
BLV	Basolateral amygdaloid nucleus, ventral part	$0.01 < X < 0.49$
BMA	Basomedial amygdaloid nucleus, anterior part	$0.49 < X < 0.99$
BMP	Basomedial amygdaloid nucleus, posterior part	$0.01 < X < 0.49$
ASt	Amygdalostriatal transition area	$0.01 < X < 0.49$
CeC	Central amygdaloid nucleus, capsular part	$0.49 < X < 0.99$
CeL	Central amygdaloid nucleus, lateral division	$0.49 < X < 0.99$
LaVL	Lateral amygdaloid nucleus, ventrolateral part	$0.01 < X < 0.49$
LaVM	Lateral amygdaloid nucleus, ventromedial part	$0.01 < X < 0.49$
MeAD	Medial amygdaloid nucleus, anterodorsal	$X > 1$
MeAV	Medial amygdaloid nucleus, anteroventral part	$X > 1$
MePD	Medial amygdaloid nucleus, posterodorsal part	$0.01 < X < 0.49$
MePV	Medial amygdaloid nucleus, posteroventral part	$0.01 < X < 0.49$
PLCo	Posterolateral cortical amygdaloid area	$0.01 < X < 0.49$
PMCo	Posteromedial cortical amygdaloid area	$0.01 < X < 0.49$
BASAL GANGLIA		
MS	Medial septal nucleus	$0.01 < X < 0.49$
CORTEX		
AIP	Agranular insular cortex, posterior part	$0.01 < X < 0.49$
Au1	Primary auditory cortex	$0.01 < X < 0.49$
AuD	Secondary auditory cortex, dorsal area	$0.01 < X < 0.49$
AuV	Secondary auditory cortex, ventral area	$0.01 < X < 0.49$
Cg1	Cingulate cortex, area 1	$0.49 < X < 0.99$
Cg2	Cingulate cortex, area 2	$0.49 < X < 0.99$
CxA	Cortex-amygdala transition zone	$0.49 < X < 0.99$
DEn	Dorsal endopiriform claustrum	$0.01 < X < 0.49$
DI	Dysgranular insular cortex	$0.01 < X < 0.49$
DIEnt	Dorsal intermediate entorhinal cortex	$0.01 < X < 0.49$
DLEnt	Dorsolateral entorhinal cortex	$0.01 < X < 0.49$
DP	Dorsal peduncular cortex	$0.49 < X < 0.99$
Ect	Ectorhinal cortex	$0.01 < X < 0.49$
LO	Lat orbital cortex	$0.49 < X < 0.99$
MO	Medial orbital cortex	$0.49 < X < 0.99$
MI	Primary motor cortex	$0.01 < X < 0.49$
M2	Secondary motor cortex	$0.01 < X < 0.49$
PRh	Perirhinal cortex	$0.01 < X < 0.49$
PRh	Perirhinal cortex	$0.01 < X < 0.49$
S1BF	Primary somatosensory cortex, barrel field	$0.01 < X < 0.49$
S1DZ	Primary somatosensory cortex, dysgranular zone	$0.01 < X < 0.49$
S1FL	Primary somatosensory cortex, forelimb region	$0.01 < X < 0.49$
S1HL	Primary somatosensory cortex, hindlimb region	$0.01 < X < 0.49$
S1ULp	Primary somatosensory cortex, upper lip region	$0.01 < X < 0.49$
S2	Secondary somatosensory cortex	$0.01 < X < 0.49$
TeA	Temporal association cortex	$0.01 < X < 0.49$
V2L	Secondary visual cortex, lateral area	$0.01 < X < 0.49$
VEn	Ventral endopiriform claustrum	$0.49 < X < 0.99$
VO	Ventral orbital cortex	$0.49 < X < 0.99$
HYPOCAMPE		
CA1	Field ca1 of the hippocampus	$0.01 < X < 0.49$
CA2	Field ca2 of the hippocampus	$0.01 < X < 0.49$
CA3	Field ca3 of the hippocampus	$X = 0$
DG	Dentate gyrus	$X = 0$
HYPOTHALAMUS		
AHA	Anterior hypothalamic area, posterior part	$X > 1$
Arc	Arcuate hypothalamic nucleus	$X > 1$
DA	Dorsal hypothalamic area	$X > 1$
DM	Dorsomedial hypothalamic nucleus	$X > 1$
LA	Lateroanterior hypothalamic nucleus	$0.49 < X < 0.99$
LH	Lateral hypothalamic area	$X > 1$
MPA	Medial preoptic area	$X > 1$
PaAP	Paraventricular hypothalamic nucleus, anterior parvic	$X > 1$
PaLM	Paraventricular hypothalamic nucleus, lateral magnoce	$X > 1$
PaV	Paraventricular hypothalamic nucleus, ventral part	$X > 1$
Pe	Periventricular hypothalamic nucleus	$0.01 < X < 0.49$
PH	Posterior hypothalamic nucleus	$0.01 < X < 0.49$
PMV	Premammillary nucleus, ventral part	$X > 1$
Te	Terete hypothalamic nucleus	$0.49 < X < 0.99$
VMH	Ventromedial hypothalamic nucleus	$X > 1$
SCH	Supra chiasmatic nucleus	$X = 0$
MIDBRAIN/HINDBRAIN		
APTD	Anterior pretectal nucleus, dorsal part	$0.49 < X < 0.99$
InC	Interstitial nucleus of Cajal	$X > 1$
IP	Interpeduncular nucleus	$X > 1$
IF	Interfascicular nuclei	$X > 1$
SN	Subs. Nigra	$0.49 < X < 0.99$
OLFACTORY SYSTEM		
AOB	Accessory olfactory bulb	$0.01 < X < 0.49$
AON	Anterior olfactory nuclei	$0.49 < X < 0.99$
TT	Dorsal tenia tecta	$0.49 < X < 0.99$
CoPyr	Pyriform cortex	$0.49 < X < 0.99$
MOB	Main olfactory bulb	$0.01 < X < 0.49$
SEPTUM		
Ts	Triangular septum nuclei	$0.49 < X < 0.99$
STRIATUM		
AA	Anterior amygdaloid area	$0.49 < X < 0.99$
ACo	Anterior cortical amygdaloid area	$0.49 < X < 0.99$
CPu	Caudate putamen (striatum)	$0.01 < X < 0.49$
ICjM	Island of Calleja, major island	$0.49 < X < 0.99$
LSD	Lateral septal nucleus, dorsal part	$0.49 < X < 0.99$
LSI	Lateral septal nucleus, intermediate part	$0.49 < X < 0.99$
TECTUM		
DpG	Deep gray layer of the superior colliculus	
DpWh	Deep white layer of the superior colliculus	
THALAMUS		
AD	Anterodorsal thalamic nucleus	$X = 0$
APTD	Anterior Pretectal nucleus, Dorsal	$X = 0$
CM	Central medial thalamic nucleus	$X > 1$
DLG	Dorsal lateral geniculate nuclei	$X = 0$
Gus	Gustatory thalamus nuclei	$0.01 < X < 0.49$
IGL	Intra geniculate leaf	$X > 1$
LDDM	Laterodorsal thalamic nucleus, dorsomedial part	$0.01 < X < 0.49$
LDVL	Laterodorsal thalamic nucleus, ventrolateral part	$0.01 < X < 0.49$

(Continued)

(Continued)

Table 1 | Continued

LHbL	Lateral habenular nucleus, lateral part	$X = 0$
LHbM	Lateral habenular nucleus, medial part	$X = 0$
MD	Mediodorsal thalamic nucleus	$X > 1$
MDM	Mediodorsal thalamic nucleus, medial part	$0.01 < X < 0.49$
OPT	Olivary pretectal nucleus	$X = 0$
PAG	Thalamus gray	$X > 1$
PC	Paracentral thalamic nucleus	$X > 1$
PF	Parafacicular thalamus nuclei	$X > 1$
Po	Post thalamus nuclei	$0.01 < X < 0.49$
PT	Paratenial thalamic nucleus	$X > 1$
PV	Paraventricular thalamic nucleus	$X > 1$
PVA	Paraventricular thalamic nucleus, anterior part	$X > 1$
PVP	Paraventricular thalamic nucleus, posterior part	$X > 1$
Re	Reuniens thalamic nucleus	$X > 1$
sm	Stria medullaris	$X > 1$
VLGMC	Vent lat genic magn	$0.49 < X < 0.99$
VLGPC	Vent lat genic magn	$0.49 < X < 0.99$
VL	Ventro lateral thalamus	$X = 0$
VPL	Ventro-postero-lateral thalamus	$X = 0$
VPM	Ventro postero medial thalamus	$X = 0$
SCO	Sub commissural organ	$0.49 < X < 0.99$
SI	Substancia inominata	$0.49 < X < 0.99$
cp	Cereb pedunc basal pt	$X > 1$

(TS) area of the **septum** appeared to be stained consistently (**Figure 2F**).

The orexin A fibers were most abundant in **the hypothalamus** (**Figure 3**). The whole paraventricular area appeared to be very rich in orexin A fibers. In the anterior part of the hypothalamus (**Figure 3A**) the following parts were densely stained: the latero anterior hypothalamic nucleus (AHA); the medial preoptic area (MPA); the paraventricular anterior parvicellular part (PaAP) of the hypothalamic nucleus and the anterior LH. In contrast, no labeling was observed in both suprachiasmatic (SCh; **Figure 3A**) and supraoptic nuclei (not shown). In the LH, there is the orexin A neuron cell body population (**Figure 3B**). The dorso medial hypothalamus (DM), the ventral medial hypothalamus nucleus (VMH), and the arcuate nucleus (Arc) were densely stained. Caudally, the LH, the VMH, and the arcuate nucleus were stained (**Figure 3C**). **Figures 3D,E** present magnifications of the orexin A neuronal cell bodies and orexin A fibers respectively.

In the **OB**, there were fewer orexin A fibers than in the hypothalamic or thalamic areas; nonetheless they appeared to be present (**Figure 4**). According to the literature, the mitral layer in rats contains no orexin A fibers (Peyron et al., 1998). By contrast, orexin A fibers were seen in all the different layers of the main olfactory bulb (MOB), including the glomerular and the mitral cell layers (**Figure 4A**). Unlike the MOB, the accessory olfactory bulb (AOB) seemed to be devoid of orexin A fibers except in the granular cell layer (**Figure 4B**).

In the **olfactory cortex**, the density of orexin A appeared to lie between the MOB and the hypothalamus (**Figure 5**). Relatively dense staining was observed in the anterior olfactory nucleus (AOM and AOP), in the ventral and dorsal tenia tecta (VTT and DTT; **Figure 5B**). The same occurs in the piriform (Pir) and the entorhinal cortices (**Figure 5A**). We also investigated the amygdala, which is not olfactory *per se*, but is strongly connected to the olfactory system (**Figure 5A**). In areas of the amygdala, the staining was very dense as for instance in the medial amygdaloid nucleus (Me).

DEVELOPMENTAL EXPRESSION OF OREXIN

We also analyzed orexin A immunolocalization at different developmental stages, ranging from E11 to P11. We found the first evidence of the clear expression of orexin A at P11 (**Figures 6A,B**). At this stage, cell bodies in the LH appeared clearly stained even though just a few fibers were manifest. Orexin A and B are produced from a common polypeptide precursor, prepro-orexin *(Ppox)* by proteolytic processing (de Lecea et al., 1998; Sakurai et al., 1998). In order to confirm immunocytochemical data, we performed a real-time PCR analysis using *Ppox* primers (**Figure 7**). We showed that the level of expression of *Ppox* is barely detectable at E17 (RQ = 1.19) and very low at P3 (RQ = 4.17). In contrast, a strong increase in the level of expression was observed at P11 (RQ = 344.4) and in the adult stage (RQ = 1944.11). *Ppox* mRNA was undetectable in the liver at any developmental stage and in cerebellum of P11 and adult (data not shown).

DISCUSSION

Our data showed orexin A immunostaining in mice when compared with that described in rats. Orexin was found in nearly all brain areas except in the caudate putamen and cerebellum, with a strong expression in thalamus and hypothalamus. Moreover, while in the MOB was detected a sparse orexin A labeling throughout the different layers, almost no presence was detected in the AOB. The developmental expression of orexin A supports the hypothesis that orexin expression only appears post-natally.

ADULT OREXIN PATTERNS

Even though convergent data revealed a link between olfactory perception and satiety (Pager et al., 1972; Pager, 1978; Yeomans, 2006), the neuroanatomical basis for this relationship and the exact connectome between olfaction centers and the hypothalamus is poorly known. **Figure 1** summarizes the neuroanatomical connection between olfactory centers and the hypothalamus. From the peripheral olfactory system to the hypothalamus, two direct connections are described that do not synapse in the OB (**Figure 1A**). The first, the extra bulbar olfactory pathway (EBOP), is mainly known in lower vertebrates (fish, amphibians; Eisthen and Polese, 2006) and is composed of sensory neurons located in the OE, which project onto the preoptic area (POA) of the hypothalamus. The second, the NT, is a complex structure identified in many vertebrates including mammals and humans (Johnston, 1914; Fuller and Burger, 1990; Wirsig-Wiechmann, 1993, 1997). It is composed of ganglion(s) in which the neuronal cell bodies are located (Eisthen and Polese, 2006; Mousley et al., 2006; Kawai et al., 2009) that send branches towards both the OE and anterior POA of the hypothalamus. Due to its complex structure, the NT is not very well known. This is regrettable because the NT is certainly one of the systems most likely to be involved in the neuromodulation of

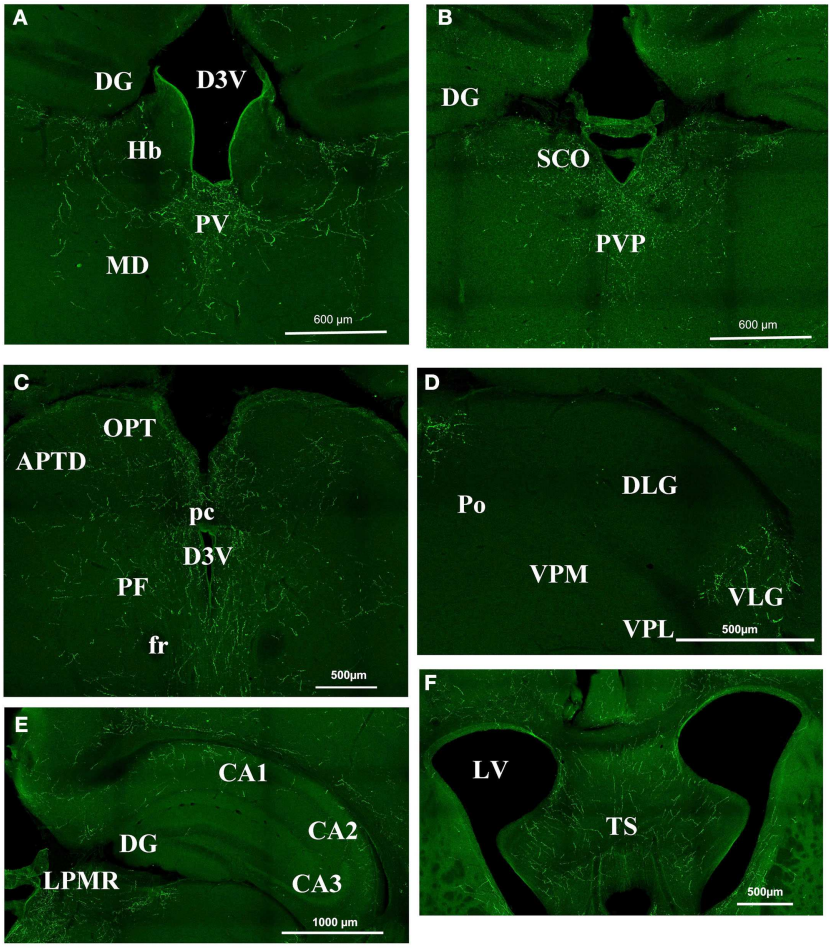

FIGURE 2 | Orexin staining in the thalamus, hippocampus, and septum. **(A)** Periventricular area Bregma −1.82. Strong staining is visible at the level of the PV, while there is no staining in the DG, the Hb, and the MD. **(B)** Periventricular area at Bregma −2.30. Note the strong staining in the PVP and SCO and still the absence of staining in the DG. **(C)** Periventricular area at Bregma −2.80. There is strong staining around the third ventricle, but staining is faint in the OPT and the APTD. **(D)** Geniculate nucleus. Orexin is present in the VLG but absentin the DLG, the Po, the VPM, and VPL. **(E)** Hippocampal structures at Bregma −2.3. Note the staining in CA1 CA2 but not in CA3. **(F)** Strong staining in the TS. APTD, anterior pretectal nucleus dors.; D3V, dorsal third ventricle; DG, dentate gyrus; DLG, dorsal lateral geniculate; fr, fasciculus retroflexus; Hb, habenular nucleus; LPMR, lat. post. thal. nu. LV, lateral ventricle; MD, medio dorsal thalamus nucleus; OPT, olivary pretectal nucleus; pc, post commissure; PF, para fascicular thalamus nucleus; Po, post. thal. nu.; PV, paraventricular thalamic nucleus; PVP, paraventricular thalamic nucleus post; SCO, sub commissural organ; TS, triangular septal nucleus; VLG, ventral lateral geniculate; VPL, ventro postero lateral thal; VPM, ventro postero med. thal.

the olfactory system, as it contains neuromodulatory peptides such as LHRH/GnRH and NPY neurons (Mousley et al., 2006; Kawai et al., 2009). However, both the EBOP and NT project to the POA, which is involved in the regulation of reproductive behavior rather than in food intake behavior, even though these two behaviors are inter-connected indirectly.

Besides, the system involving the NT, it has been possible to trace projections onto the LHRH/GnRH neurons localized in the POA, using Cre-loxP transgenic mice and/or pseudorabies virus infections (Boehm et al., 2005; Yoon et al., 2005). In **Figure 1A**, we present the projections from the olfactory and hypothalamic regions to the POA. Concerning the olfactory system, most olfactory cortex areas also appear to be connected to the OB and the OE. As for the hypothalamus connections, most of the hypothalamic nuclei appear to be connected to LHRH/GnRH neurons, among which are VMH, DMH, PVN, LH, and Arc. Therefore, LHRH/GnRH neurons, located in the POA, integrate many afferent signals; amongst which olfactory and hypothalamic inputs to regulate puberty onset, gametogenesis, estrus cycling, and sexual behavior (Gore, 2002) can be found. These connections appear to be bidirectional, since LHRH/GnRH appears to innervate the anterior piriform olfactory cortex (Boehm et al., 2005), indicating the possibility that LHRH/GnRH neurons could in turn modulate both olfactory/pheromonal processing. This has to be considered keeping in mind that both LHRH/GnRH and NPY in axolotl modulate and/or balance both sensitivity to food odorants and pheromones during reproduction periods (Mousley et al., 2006; Kawai et al., 2009).

In the context of olfactory system-hypothalamus connections (Price et al., 1991), the orexin network also has to be considered.

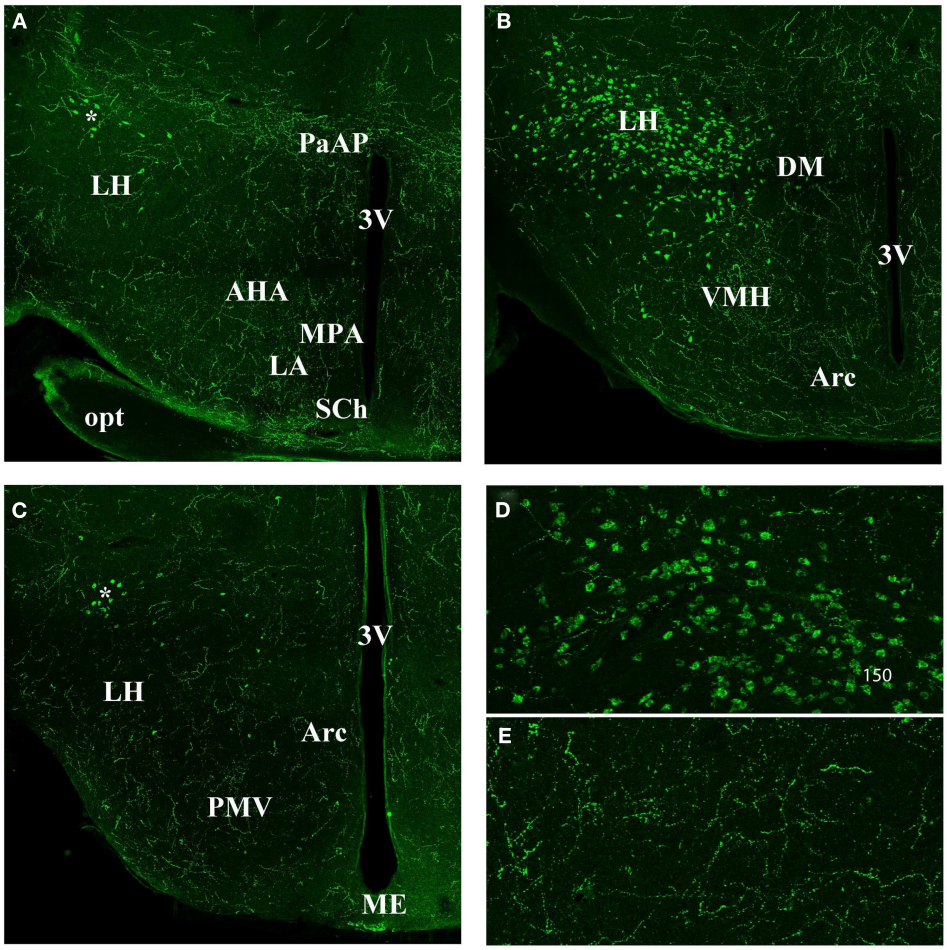

FIGURE 3 | Orexin staining in hypothalamic area (A) anterior part. Note the strong staining in the PaAP, few orexin cell bodies (*) in the anterior LH, and general high staining in the LH, AHA, MPA, LA. Note the absence of staining in the SCh. **(B)** Orexin staining in the hypothalamus at the level of the orexin neuron population. Note the staining in the DM, VMH, and Arc nucleus. **(C)** Hypothalamus at the Posterior LH level. Note the few orexin positive neurons (*). Note general staining in the whole hypothalamus including LH, PMV, Arc, and Me. **(D)** Magnification of the orexin neuron cell bodies. **(E)** Magnification of orexin fibers in the hypothalamus. 3V, third ventricle; AHA, anterior hypothal. area; Arc, arcuate nucleus; DM, dorso medi hypothal. nu.; LA, lateroant. hypothal. nu.; LH, lateral hypothalamus; MPA, med. preoptic area nu.; ME, med. amyg. nu.; opt, optical nerve. PaAP, pa. anterior parvicell. pt.; PMV, premammill. nu. ventral; SCh, suprachiasmatic nu.; VMH, ventral hypothalamic nu.

Orexins are neuropeptides involved in sleep/waking regulation and food intake behavior (Sakurai et al., 1998, 2010; Aimé et al., 2007; Prud'homme et al., 2009). In rats, orexin neuron cell bodies are located in the perifornical nucleus, and in the dorsal and lateral hypothalamic areas (LHA; Peyron et al., 1998; Nambu et al., 1999). Interestingly, it has been suggested that differentiations in each LHA are involved in the control of specific behavior, with the involvement of the LHA suprafornical region in the control of food intake behavior (Hahn and Swanson, 2010, 2012). High resolution studies of the orexin neuron population in the LH have been carried out (Swanson et al., 2005) showing the extreme complexity of this brain area. In the present study, we focus on the orexin projection fibers – especially in the OB- rather than on the specific segregation of orexin cell bodies within the hypothalamus.

On the one hand, in mice, it has been demonstrated that orexin A neurons receive input from olfactory cortex areas, such as the tenia tecta (**Figure 1B**; Sakurai et al., 2005). On the other hand, in rats, it has been demonstrated that orexin neurons send projections to the olfactory cortex and OB (**Figure 1B**; Peyron et al., 1998). The aim of this work was to validate in mice the orexin projection patterns as described in rats (Peyron et al., 1998) with a special focus on the olfactory system.

Our present data show that the main orexin patterns in mice share many features with those in rats (Peyron et al., 1998; Nambu et al., 1999). The comparison of orexin A vs. orexin B staining attests the specificity of orexin A staining (Appendix). Extensive projections were present in nearly all brain areas except the cerebellum, and a high concentration of orexin projections was found in the paraventricular area of the hypothalamus and the thalamus. Amongst the differences to be noted is the absence of staining in the caudate putamen. Otherwise, there was only a small difference between rats and mice in terms of the relative level of the presence of orexin A fibers.

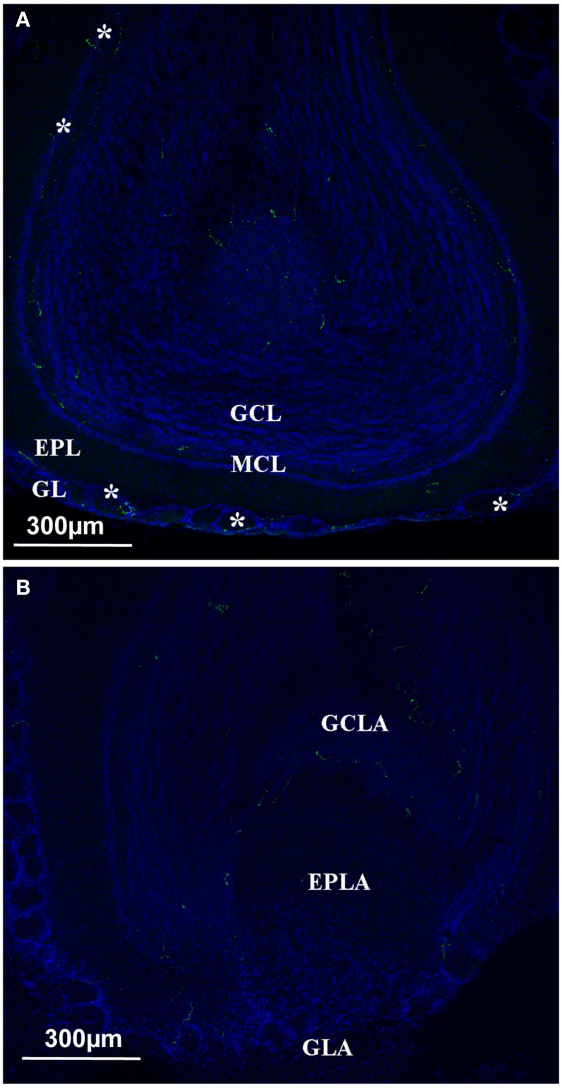

FIGURE 4 | Orexin staining at the level of the olfactory bulb. (A) Main olfactory bulb; the orexin profile (green and white star) could be observed in all the different layers, including the Mitral cell layer arrow). **(B)** Orexin staining at the level of the Accessory Olfactory bulb. No staining at the level of the AOB except the GCLA. EPL, external plexiform layer; EPLA, external plexiform layer of the accessory olfactory bulb; GL, glomerular layer; GCL, granular cell layer; GCLA, granular cell layer of the accessory olfactory bulb; GLA, glomerular layer of the accessory olfactory bulb; MCL, mitral cell layer.

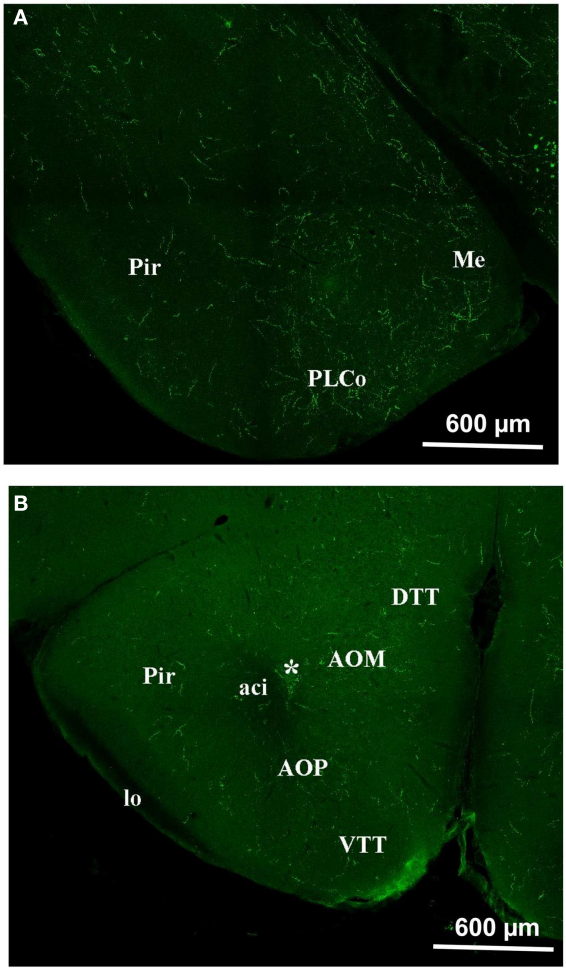

FIGURE 5 | Orexin staining in the olfactory cortex and the Amygdala. (A) Piriform cortex and amygdala. Note the intense staining in the amygdala and also, though to a lesser extent, in the piriform cortex. **(B)** Olfactory cortex. Note the staining at the level of the DTT, VTT, AOM, AOP, Pir. *E/OV, Ependy/olfactory ventricle; aci, anterior commissure intrabulbar; AOM, anterior olfactory nucleus anterior; AOP, anterior olfactory nucleus posterior; DTT, dorsal tenia tecta; lo: lateral olfactory tract; Me, med amygdala; Pir, piriform cortex; PLCo, postlat cx amygdala nu.; VTT, ventral tenia tecta.

We then investigated in more detail the orexin projections at the level of the OB and olfactory cortex in mice. At the OB level, the density of orexin fibers was noticeably low. Nevertheless, none of the different layers were devoid of orexin fibers, and clear fibers could be seen in the mitral cell layer. At the level of the OB, the pattern of distribution appeared to be different in mice and rats, since in rats few orexin fibers were located in the glomerular and internal granular layers and none in the mitral cell layer (Peyron et al., 1998). To our knowledge, the AOB has not been investigated in rats. In mice, we found that the AOB was nearly devoid of orexin projections, except for the granular level of the AOB.

Our results show that the orexin A pattern is similar to those previously described in rats. Orexin fibers on the OB could have two origins. The first origin could be that fibers come from only one cell body population- those that only we and other researchers found to be located in the LH. The second origin could be that fibers, at least in the OB, originate from the olfactory mucosa, since some olfactory receptor neurons are orexin positive (Caillol et al., 2003). However, the second hypothesis seems to be ruled out since the olfactory neurons only project in the glomerular layer, and that we find orexin fibers in all the different layers of the OB. Thus, the projection of LH orexin neurons to the OB seems to be consensual. However, we cannot claim that synaptic connections of these orexin projections occur at the OB level. In order to establish the precise circuitry between LH and OB, the whole circuitry has to be investigated in detail using a trans-synaptic tracer

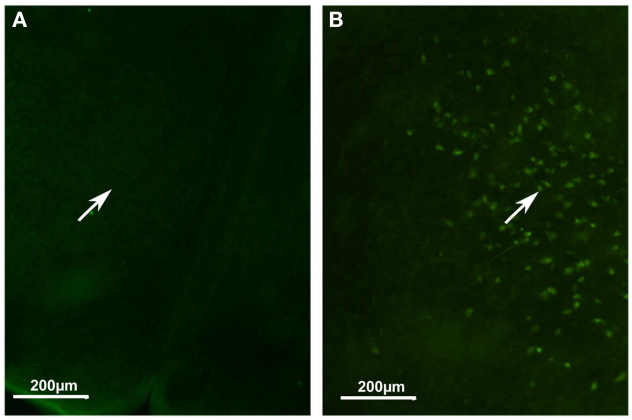

FIGURE 6 | Developmental expression of orexin A in mice. (A) Hypothalamic area at P2. **(B)** Hypothalamic area at P11. Note orexin cell bodies only in **(B)** (white arrow).

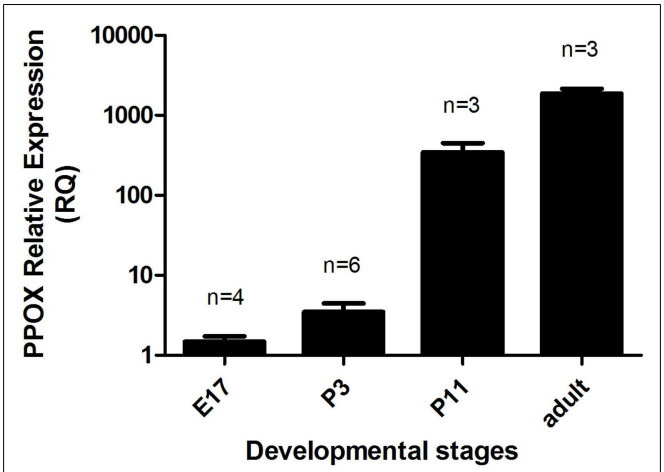

FIGURE 7 | Relative gene expression of Ppox in the brains of E17 and P3 mice, and in the hypothalamus of P11 and adult males. Error bars represent the standard error. The number of samples per group is indicated above each column. The relative quantity of Ppox in each sample was normalized to the quantity of Tbp.

strategy to demonstrate that LH orexin neurons constitute a true neuronal circuit between the OB and the LH.

DEVELOPMENTAL OREXIN PATTERNS

Considering the developmental expression pattern, orexin has been reported in rats as early as E19 (Van der Pol et al., 2001; Steininger et al., 2004). However, this is highly controversial since other authors have not reported orexinergic neurons before post-natal day 15 (Yamamoto et al., 2000), or at best during the first post-natal week (Stoyanova et al., 2010). Our immunocytochemical results tend to support the late expression of orexin neurons, since we found in mice no evidence of orexin expression at P2, while at P11 instead we showed the presence of orexin neuronal cell bodies. Using qPCR, we observed that significant variations in *Ppox* mRNA reflect the synthesis of orexin peptides. Indeed, our qPCR results validate our immunohistological results, since at P2–3 the range of orexin expression is around 500 times lower than that in adults. This supports the idea that the beginning of orexin expression should be between P2–3 and P11. However, the low level of orexin fibers suggests that the full development of orexin neurons is not complete at P11 in mice.

CONCLUSION

In this study we demonstrate that most of the characteristics of orexin in mice are similar to those reported in rats. Since it has been demonstrated in rats that orexin could modulate olfactory perception depending on the energy balance of the body, this work strongly supports the idea that this is also true in mice. However, trans-synaptic tracing experiments need to be done in order to clearly demonstrate connectivity between the two systems.

ACKNOWLEDGMENTS

We would like to thanks Prof. P. Bastable and N. Winn for English editing of this paper. This work was supported by Research grant BFU2010-15564 from the Spanish Ministry of Economy and Competitiveness (MINECO) and by INRA (National Institute for Agronomical Research) and the Burgundy Regional Council (Conseil Régional de Bourgogne).

REFERENCES

Aimé, P., Duchamp-Viret, P., Chaput, M. A., Savigner, A., Mahfouz, M., and Julliard, A. K. (2007). Hunger increases and satiation decreases rat olfactory detection performances for a neutral odor. *Behav. Brain Res.* 179, 258–264.

Apelbaum, A., Perrut, A., and Chaput, M. (2005). Orexin A effects on the olfactory bulb spontaneous activity and odor responsiveness in freely breathing rats. *Regul. Pept.* 129, 49–61.

Boehm, U., Zou, Z., and Buck, L. B. (2005). Feedback loops link odor and pheromone signaling with reproduction. *Cell* 123, 683–695.

Cabanac, M., and Duclaux, R. (1973). Olfactory-gustatory alliesthesia and food intake in humans. *J. Physiol.* 66, 113–135.

Caillol, M., Aïoun, J., Baly, C., Persuy, M. A., and Salesse, R. (2003). Localization of orexins and their receptors in the rat olfactory system: possible modulation of olfactory perception by a neuropeptide synthetized centrally or locally. *Brain Res.* 960, 48–61.

de Lecea, L., Kilduff, T. S., Peyron, C., Gao, X., Foye, P. E., Danielson, P. E., et al. (1998). The hypocretins: hypothalamus-specific peptides with neuroexcitatory activity. *Proc. Natl. Acad. Sci. U.S.A.* 6, 322–327.

Doucette, W., Milder, J., and Restrepo, D. (2007). Adrenergic modulation of olfactory bulb circuitry affects odor discrimination. *Learn. Mem.* 14, 539–547.

Doucette, W., and Restrepo, D. (2008). Profound context-dependent plasticity of mitral cell responses in olfactory bulb. *PLoS Biol.* 95, e258. doi:10.1371/journal.pbio.0060258

Duclaux, R., Feisthauer, J., and Cabanac, M. (1973). Effects of a meal on the pleasantness of food and nonfood odors in man. *Physiol. Behav.* 10, 1029–1033.

Eisthen, H. L., and Polese, G. (2006). "Evolution of vertebrate olfactory subsystems," in *Evolution of Nervous Systems, Vol 2: Non-mammalian Vertebrates,* ed. J. H. Kaas (Oxford: Academic Press), 355–406.

Elias, C. F., Saper, C. B., Maratos-Flier, E., Tritos, N. A., Lee, C., Kelly, J., et al. (1998). Chemically defined projections linking the mediobasal hypothalamus and the lateral hypothalamic area. *J. Comp. Neurol.* 402, 442–459.

Fadool, D. A., Tucker, K., and Pedarzani, P. (2011). Mitral cells of the olfactory bulb perform metabolic sensing and are disrupted by obesity at the level of the Kv1.3 ion channel. *PLoS ONE* 6, e24921. doi:10.1371/journal.pone.0024921

Fletcher, M. L., and Chen, W. R. (2010). Neural correlates of olfactory learning: critical role of centrifugal neuromodulation. *Learn. Mem.* 17, 561–570.

Friedman, J. M. (2002). The function of leptin in nutrition, weight and physiology. *Nutr. Rev.* 60, 85–87.

Fuller, G. N., and Burger, P. C. (1990). Nervus terminalis (cranial nerve zero) in the adult human. *Clin. Neuropathol.* 9, 279–283.

Garcia-Llanes, F. J., Crespo, C., Blasco-Ibanez, J. M., Marques-Mari, A. I., and Martinez-Guijarro, F. J. (2003). VIP-containing deep short-axon cells of the olfactory bulb innervate interneurons different from granule cells. *Eur. J. Neurosci.* 18, 1751–1763.

Gore, A. C. (2002). *GnRH: The Master Molecule of Reproduction.* Norwell, MA: Kluwer Academic Publisher.

Hahn, J. D., and Swanson, L. W. (2010). Distinct patterns of neuronal inputs and outputs of the juxtaparaventricular and suprafornical regions of the lateral hypothalamic area in the male rat. *Brain Res. Rev.* 64, 14–103.

Hahn, J. D., and Swanson, L. W. (2012). Connection of the lateral hypothalamic area juxtadorsomedial region in the male rat. *J. Comp. Neurol.* 520, 1831–1890.

Hass, N., Haub, H., Stevens, R., Breer, H., and Schwarzenbacher, K. (2008). Expression of adiponectin receptor 1 in olfactory mucosa of mice. *Cell Tissue Res.* 334, 187–197.

Horvath, T. L., and Gao, X. B. (2005). Input organization and plasticity of hypocretin neurons: possible clues to obesity's association with insomnia. *Cell Metab.* 1, 279–286.

Johnston, J. B. (1914). The nervus terminalis in man and mammals. *Anat. Rec.* 8, 185–198.

Julliard, A. K., Chaput, M. A., Apelbaum, A., Aimé, P., Mahfouz, M., and Duchamp-Viret, P. (2007). Changes in rat olfactory detection performance induced by orexin and leptin mimicking fasting and satiation. *Behav. Brain Res.* 183, 123–129.

Kawai, T., Oka, Y., and Eisthen, H. (2009). The role of the terminal nerve and GnRH in olfactory system neuromodulation. *Zool. Sci.* 26, 669–680.

Matsutani, S., Senba, E., and Tohyama, M. (1988). Neuropeptide- and neurotransmitter-related immunoreactivities in the developing rat olfactory bulb. *J. Comp. Neurol.* 272, 331–342.

Mousley, A., Polese, G., Marks, N., and Eisthen, L. (2006). Terminal nerve-derived neuropeptide Y modulates physiological responses in the olfactory epithelium of hungry axolotls. *J. Neurosci.* 26, 7707–7717.

Nambu, T., Sakurai, T., Mizukami, K., Hosoya, Y., Yanagisawa, M., and Goto, K. (1999). Distribution of orexin neurons in the adult rat brain. *Brain Res.* 827, 243–260.

Nixon, J. P., and Smale, L. (2007). A comparative analysis of the distribution of immunoreactive orexin A and B in the brains or nocturnal and diurnal rodents. *Behav. Brain Funct.* 3, 28.

Oka, Y. (1997). "The gonadotropin-releasing hormone (GnRH) neuronal system of fish brain as a model system for the study of peptidergic neuromodulation," in *GnRH Neurons: Genes to Behavior*, ed. I. S. Parthat and Y. Sakuma (Tokyo: Brain Shuppan Publishers), 245–276.

Pager, J. (1978). Ascending olfactory information and centrifugal influx contributing to a nutritional modulation of the rat mitral cell responses. *Brain Res.* 140, 251–269.

Pager, J., Giachetti, I., Holley, A., and Le Magnen, J. (1972). A selective control of olfactory bulb electrical activity in relation to food deprivation and satiety in rats. *Physiol. Behav.* 9, 573–579.

Palouzier-Paulignan, B., Lacroix, M. C., Aimé, P., Baly, C., Caillol, M., Congar, P., et al. (2012). Olfaction under metabolic influences. *Chem. Senses* 37, 769–797.

Peyron, C., Tighe, D. K., van deb Pol, A. N., de Lecea, L., Heller, H. C., Sutcliffe, J. G., et al. (1998). Neurons containing hypocretin (orexin) project to multiple neuronal system. *J. Neurosci.* 18, 9996–10015.

Pinto, S., Roseberry, A. G., Liu, H., Diano, S., Shanabrough, M., Cai, X., et al. (2004). Rapid rewiring of rcuate nucleus feeding circuits by leptin. *Science* 304, 110–115.

Price, J. L., Slotnick, B. M., and Revial, M. F. (1991). Olfactory projections to the hypothalamus. *J. Comp. Neurol.* 306, 447–461.

Prud'homme, M. J., Lacroix, M. C., Badonnel, K., Gougis, S., Baly, C., Salesse, R., et al. (2009). Nutritional status modulates behavioural and olfactory bulb Fos responses to isoamyl acetate or food odour in rats: role of orexin and leptin. *Neuroscience* 162, 1287–1298.

Royet, J. P., Gervais, R., and Araneda, S. (1983). Effect of local 6-OHDA and 5,6-DHT injections into the rat olfactory bulb on neophobia and learned aversion to a novel food. *Behav Brain Res.* 10, 297–309.

Sakurai, T., Amemiya, A., Ishii, M., Matsuzaki, I., Chemelli, R. M., Tanaka, H., et al. (1998). Orexins and orexin receptors: a family of hypothalamic neuropeptides and G protein-coupled receptors that regulate feeding behavior. *Cell* 92, 573–585.

Sakurai, T., and Mieda, M. (2011). Connectomics of orexin-producing neurons: interface of systems of emotion, energy homeostasis and arousal. *Trends Pharmacol. Sci.* 32, 451–462.

Sakurai, T., Mieda, M., and Tsujino, N. (2010). The orexin system: role in sleep/wake regulation. *Ann. N. Y. Acad. Sci.* 149–169.

Sakurai, T., Nagata, R., Yamanaka, A., Kawamura, H., Tsujino, N., Muraki, Y., et al. (2005). Input of orexin/hypocretin neurons revealed by a genetically encoded tracer in mice. *Neuron* 46, 297–308. [Erratum in: *Neuron* 2005, 46, 837].

Savigner, A., Duchamp-Viret, P., Grosmaitre, X., Chaput, M., Garcia, S., Ma, M., et al. (2009). Modulation of spontaneous and odorant-evoked activity of rat olfactory sensory neurons by two anorectic peptides, insulin and leptin. *J. Neurophysiol.* 101, 2898–2906.

Steininger, T. L., Kilduff, T. S., Behan, M., Benca, R. M., and Landry, C. F. (2004). Comparison of hypocretin/orexin and melanin-concentrating hormone neurons and axonal projections in the embryonic and postnatal rat brain. *J. Chem. Neuroanat.* 27, 165–181.

Stoyanova, I. L., Rutten, W. L. C., and le Feber, J. (2010). Orexin-A and orexin-B during the postnatal development of the rat brains. *Cell. Mol. Neurobiol.* 30, 81–89.

Swanson, L. W., Sanchez-Watt, G., and Watt, A. G. (2005). Comparison of melanin-concentrating hormone and hypocretin/orexin mRNA expression patterns in a new parceling scheme of the lateral hypothalamic zone. *Neurosci. Lett.* 387, 80–84.

Tanganelli, S., Fuxe, K., Antonelli, T., O'Connor, W. T., and Ferraro, L. (2001). Cholecystokinin/dopamine/GABA interactions in the nucleus accumbens: biochemical and functional correlates. *Peptides* 22, 1229–1234.

Van der Pol, A. N., Patrylo, P. R., Ghosh, P. K., and Gao, X. B. (2001). Lateral hypothalamus: early developmental expression and response to hypocretin (orexin). *J. Comp. Neurol.* 433, 349–363.

Wirsig-Wiechmann, C. R. (1993). Nervus terminalis lesions: I. No Effect on pheromonally induced testosterone surges in the male Hamster. *Physiol. Behav.* 53, 251–255.

Wirsig-Wiechmann, C. R. (1997). Nervus terminalis lesions: II. Enhancement of lordosis induced by tactile stimulation in the hamster. *Physiol. Behav.* 61, 867–871.

Yamamoto, Y., Ueta, Y., Hara, Y., Serino, R., Nomura, M., Shibuya, I., et al. (2000). Postnatal development of orexin/hypocretin in rats. *Brain Res. Mol. Brain Res.* 78, 108–119.

Yeomans, M. R. (2006). Olfactory influences on appetite and satiety in humans. *Physiol. Behav.* 89, 10–14.

Yoon, H., Enquist, L. W., and Dulac, C. (2005). Olfactory inputs to hypothalamic neurons controlling reproduction and fertility. *Cell* 123, 669–682.

Yoshida, K., McCornack, S., Espana, R. A., Crocker, A., and Scammel, T. E. (2006). Afferent to the orexin neurons of the rat brain. *J. Comp. Neurol.* 494, 845–861.

Conflict of Interest Statement: The authors declare that the research was conducted in the absence of any commercial or financial relationships that could be construed as a potential conflict of interest.

Received: 17 May 2012; accepted: 06 October 2012; published online: 08 November 2012.

Citation: Gascuel J, Lemoine A, Rigault C, Datiche F, Benani A, Penicaud L and Lopez-Mascaraque L (2012) Hypothalamus-olfactory system crosstalk: orexin A immunostaining in mice. Front. Neuroanat. ***6****:44. doi: 10.3389/fnana.2012.00044*

APPENDIX

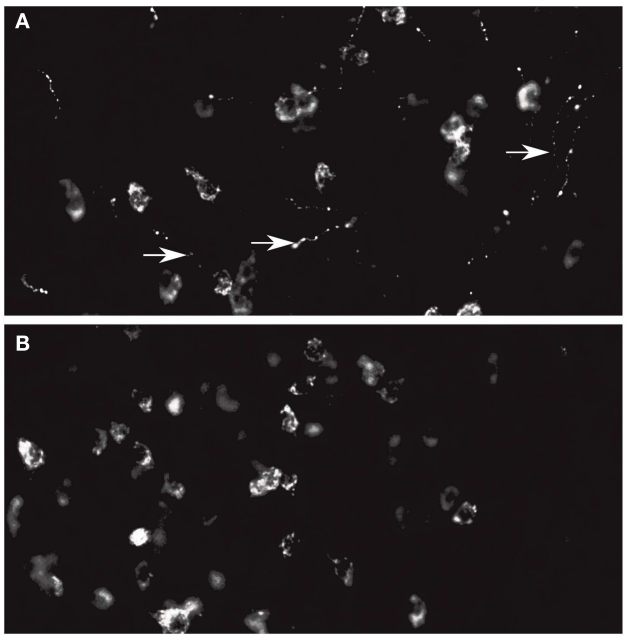

FIGURE A1 | (A) Orexin A staining in the LH. Note the staining at the level of the cell bodies and fibers. **(B)** Orexin B staining in the LH. Note that the fibers are not stained. In this experiments only primary antibody is different.

frontiers in
NEUROANATOMY

ORIGINAL RESEARCH ARTICLE
published: 21 August 2012
doi: 10.3389/fnana.2012.00033

Differential efferent projections of the anterior, posteroventral, and posterodorsal subdivisions of the medial amygdala in mice

Cecília Pardo-Bellver[1‡], Bernardita Cádiz-Moretti[1‡], Amparo Novejarque[2†], Fernando Martínez-García[2] and Enrique Lanuza[1]*

[1] *Facultat de Ciències Biològiques, Laboratory of Functional and Comparative Neuroanatomy, Departament de Biologia Cel·lular, Universitat de València, València, Spain*

[2] *Facultat de Ciències Biològiques, Laboratory of Functional and Comparative Neuroanatomy, Departament de Biologia Funcional i Antropologia Física, Universitat de València, València, Spain*

Edited by:
Micheal Baum, Boston University, USA

Reviewed by:
Hong-Wei Dong, UCLA School of Medicine, USA
Aras Petrulis, Georgia State University, USA
Brett DiBenedictis, Boston University, USA

***Correspondence:**
Enrique Lanuza, Facultat de Ciències Biològiques, Departament de Biologia Cel·lular, Universitat de València, Carrer Dr. Moliner 50, ES-46100 Burjassot, Valencia, Spain.
e-mail: enrique.lanuza@uv.es

†Present address:
Amparo Novejarque, Faculty of Medicine, Department of Surgery and Cancer, Imperial College London, Chelsea and Westminster Hospital, London, UK.

‡Cecília Pardo-Belluer and Bernardia Cárdiz-Moretti are co-first authors of this work.

The medial amygdaloid nucleus (Me) is a key structure in the control of sociosexual behavior in mice. It receives direct projections from the main and accessory olfactory bulbs (AOB), as well as an important hormonal input. To better understand its behavioral role, in this work we investigate the structures receiving information from the Me, by analysing the efferent projections from its anterior (MeA), posterodorsal (MePD) and posteroventral (MePV) subdivisions, using anterograde neuronal tracing with biotinylated and tetrametylrhodamine-conjugated dextranamines. The Me is strongly interconnected with the rest of the chemosensory amygdala, but shows only moderate projections to the central nucleus and light projections to the associative nuclei of the basolateral amygdaloid complex. In addition, the MeA originates a strong feedback projection to the deep mitral cell layer of the AOB, whereas the MePV projects to its granule cell layer. The Me (especially the MeA) has also moderate projections to different olfactory structures, including the piriform cortex (Pir). The densest outputs of the Me target the bed nucleus of the stria terminalis (BST) and the hypothalamus. The MeA and MePV project to key structures of the circuit involved in the defensive response against predators (medial posterointermediate BST, anterior hypothalamic area, dorsomedial aspect of the ventromedial hypothalamic nucleus), although less dense projections also innervate reproductive-related nuclei. In contrast, the MePD projects mainly to structures that control reproductive behaviors [medial posteromedial BST, medial preoptic nucleus, and ventrolateral aspect of the ventromedial hypothalamic nucleus], although less dense projections to defensive-related nuclei also exist. These results confirm and extend previous results in other rodents and suggest that the medial amygdala is anatomically and functionally compartmentalized.

Keywords: vomeronasal amygdala, olfactory amygdala, ventromedial hypothalamus, sexual behavior, defensive behavior, chemical signals

Abbreviations: 3V, 3rd ventricle; AAD, anterior amygdaloid area, dorsal part; AAV, anterior amygdaloid area, ventral part; ac, anterior commissure; AcbC, accumbens nucleus, core; AcbSh, accumbens nucleus, shell; ACo, anterior cortical amygdaloid nucleus; AHA, anterior hypothalamic area, anterior part; AHi, amygdalohippocampal area; AHP, anterior hypothalamic area, posterior part; AI, agranular insular cortex; AOB, accessory olfactory bulb; AOM, anterior olfactory nucleus, medial part; AON, anterior olfactory nucleus; AOP, anterior olfactory nucleus, posterior part; APir, amygdalopiriform transition area; Arc, arcuate hypothalamic nucleus; Astr, amygdalostriatal transition area; AVPe, anteroventral periventricular nucleus; BAOT, bed nucleus of the accessory olfactory; BLA, basolateral amygdaloid nucleus, anterior part; BLP, basolateral amygdaloid nucleus, posterior part; BLV, basolateral amygdaloid nucleus, ventral part; BMA, basomedial amygdaloid nucleus, anterior part; BMP, basomedial amygdaloid nucleus, posterior part; BST, bed nucleus of the *stria terminalis*; BSTIA, BST, intraamygdaloid division; BSTLD, BST, lateral division, dorsal part; BSTLI, BST, lateral division, intermediate part; BSTLP, BST, lateral division, posterior part; BSTLV, BST, lateral division, ventral part; BSTMA, BST, medial division, anterior part; BSTMPI, BST, medial division, posterointermediate part; BSTMPL, BST, medial division, posterolateral part; BSTMPM, BST, medial division, posteromedial part; BSTMV, BST, medial division, ventral part; CA1, field CA1 of hippocampus; cc, corpus callosum; CeC, central amygdaloid nucleus, capsular part; CeL, central amygdaloid nucleus, lateral division; CeM, central amygdaloid nucleus, medial division; Cl, claustrum; cp, cerebral peduncle; CPu, caudate putamen; CxA, cortex-amygdala transition zone; DEn, dorsal endopiriform nucleus; DM, dorsomedial hypothalamic nucleus; DTT, dorsal *tenia tecta*; ec, external capsule; Ent, entorhinal cortex; f, fornix; fmi, forceps minor of the corpus callosum; GlA, glomerular layer of the AOB; GrA, granule cell layer of the AOB; GrO, granular cell layer of the olfactory bulb; HDB, nucleus of the horizontal limb of the diagonal band; I, intercalated nuclei of the amygdala; ic, internal capsule; ICj, islands of Calleja; ICjM, major island of Calleja; IL, infralimbic cortex; IPAC, interstitial nucleus of the posterior limb of the anterior commissure; LA, lateroanterior hypothalamic nucleus; La, lateral amygdaloid nucleus; LH, lateral hypothalamic area; LHb, lateral habenular nucleus; lo, lateral olfactory tract; LOT, nucleus of the lateral olfactory tract; LPO, lateral preoptic area; LSD, lateral septal nucleus, dorsal part; LSI, lateral septal nucleus, intermediate part; LSV, lateral septal nucleus, ventral part; LV, lateral ventricle; MD, mediodorsal thalamic nucleus; Me, medial amygdaloid nucleus; MeA, medial amygdaloid nucleus, anterior part; MePD, medial amygdaloid nucleus, posterodorsal part; MePV, medial amygdaloid nucleus, posteroventral part; MGP, medial globus pallidus; MiA, mitral cell layer of the AOB; ML, medial mammillary nucleus, lateral part; MM, medial mammillary nucleus, medial part; MPA, medial preoptic area;

INTRODUCTION

The main and accessory olfactory systems provide key sensory inputs to the network of neural structures controlling sociosexual behaviors in rodents (Swann et al., 2009). This network is composed of a number of interconnected nuclei rich in neurons expressing receptors for sexual steroids, including the medial amygdaloid nucleus (Me), the posterior bed nucleus of the stria terminalis (BST), the lateral ventral septum, and the medial preoptic area (MPA) (Newman, 1999). Among these structures, only the Me receives convergent projections from the main and accessory olfactory bulbs (AOB) (Scalia and Winans, 1975; Pro-Sistiaga et al., 2007; Kang et al., 2009, 2011). The efferent connections of the Me have been studied in detail in male rats (Canteras et al., 1995) and male hamsters (Gomez and Newman, 1992; Coolen and Wood, 1998; Maras and Petrulis, 2010a). These studies have revealed that the Me is a heterogeneous structure in which at least three subdivisions can be clearly recognized. The anterior division of the medial amygdaloid nucleus (MeA) is connected with structures implicated in defensive, agonistic as well as in reproductive behaviors. The posterodorsal subdivision (MePD) contains the highest density of androgen and estrogen receptors (Simerly et al., 1990; Cooke, 2006) and is connected mainly with structures implicated in reproductive behaviors (Canteras et al., 1995). And finally, the posteroventral subdivision (MePV) projects preferentially to structures suggested being involved in defensive behaviors (Canteras, 2002). These anatomical subdivisions also fit the expression pattern of genes of the Lhx family of transcription factors. Thus, the MeA expresses mainly Lhx5, the MePD Lhx6, and the MePV Lhx9 (Choi et al., 2005). Recent studies on the developmental origins of the Me cells (García-López et al., 2008; García-Moreno et al., 2010; Bupesh et al., 2011) have shown that the Lhx9-expressing cells of the MePV originate in the ventral pallium, and consequently are glutamatergic projection neurons (Choi et al., 2005). In contrast, the Lhx6 neurons of the MePD are GABAergic cells originated in the caudoventral medial ganglionic eminence (and therefore they are neurons of pallidal nature). Finally, the MeA contains a population of Lhx5-expressing neurons originated in the hypothalamic supraoptoparaventricular domain (Abellán et al., 2010) and also abundant nitrergic cells originated from the commissural preoptic area (Hirata et al., 2009; Bupesh et al., 2011).

The neuroanatomical and developmental data discussed above for the different subdivisions of the Me are consistent with a number of functional studies in several rodent species. In mice and hamsters, the MeA has been shown to be activated by sexual and non-sexual social odors, and also by chemicals derived from heterospecific individuals (Meredith and Westberry, 2004; Samuelsen and Meredith, 2009). The MeA seems to categorize the detected chemical stimuli and then relay sex-related information to the MePD (Petrulis, 2009; Maras and Petrulis, 2010b), which consequently is mainly activated by sexually related chemical signals (hamsters: Fernandez-Fewell and Meredith, 1994; Kollack-Walker and Newman, 1997; mice: Choi et al., 2005; rats: Bressler and Baum, 1996; gerbils: Heeb and Yahr, 1996). Accordingly, electrolytic lesions of the transition between the MeA and the MePD are most effective in abolishing the attraction of female mice for sex-derived chemical signals (DiBenedictis et al., 2012) and similar results have been obtained in male hamsters with lesions that functionally disconnect the MeA and the MePD (Maras and Petrulis, 2010c). On the other hand, the MePV display a strong response when mice are exposed to predator (cat) odors (Choi et al., 2005; Samuelsen and Meredith, 2009), a response that has been also reported in rats exposed to cat odors (Dielenberg et al., 2001).

Surprisingly, the efferent connections of the Me in mice have been only partially examined in a single study, which reports data in males mainly regarding the MePD (Usunoff et al., 2009). Given that mice are widely use in behavioral neuroscience studies, due to the availability of genetically modified animals that allow exploring the molecular basis of behavior, it is of interest to obtain direct anatomical data in this species. In addition, since there are relevant differences in different strains of mice regarding reproductive (Vale et al., 1973, 1974; Burns-Cusato et al., 2004; Dominguez-Salazar et al., 2004) and defensive (Belzung et al., 2001; Yang et al., 2004) behaviors, which are major functions of the Me, in the present study we compare the efferent projections of the medial amygdala of the C57BL/6J and CD1 strains of mice. Since our prior behavioral studies about sexual attraction toward male pheromones were performed in females (see Martínez-García et al., 2009), we decided to study the efferent projections of the Me in female mice. This allows comparing the pattern of efferent projections of the Me of females (our findings) with previous published results, which were mostly obtained in males.

MPO, medial preoptic nucleus; MS, medial septal nucleus; MTu, medial tuberal nucleus; opt, optic tract; Pa, paraventricular hypothalamic nucleus; PAG, periaqueductal gray; Pe, periventricular hypothalamic nucleus; PH, posterior hypothalamic area; Pir, piriform cortex; PLCo, posterolateral cortical amygdaloid nucleus; PMCo, posteromedial cortical amygdaloid nucleus; PMD, premammillary nucleus, dorsal part; PMV, premammillary nucleus, ventral part; Po, posterior thalamic nuclear group; PrL, prelimbic cortex; PSTh, parasubthalamic nucleus; PT, paratenial thalamic nucleus; PV, paraventricular thalamic nucleus; Re, reuniens thalamic nucleus; Rt, reticular thalamic nucleus; SCh, suprachiasmatic nucleus; SFi, septofimbrial nucleus; SHi, septohippocampal nucleus; SHy, septohypothalamic nucleus; SI, *substantia innominata*; SM, nucleus of the *stria medullaris*; sm, *stria medullaris*; SN, *substantia nigra*; sox, supraoptic decussation; st, *stria terminalis*; STh, subthalamic nucleus; SuM, supramammillary nucleus; TC, tuber cinereum area; Tu, olfactory tubercle; VDB, nucleus of the vertical limb of the diagonal band; VEn, ventral endopiriform nucleus; VMH, ventromedial hypothalamic nucleus; VMHC, ventromedial hypothalamic nucleus, central part; VMHDM, ventromedial hypothalamic nucleus, dorsomedial part; VMHVL, ventromedial hypothalamic nucleus, ventrolateral part; VP, ventral pallidum; VTA, ventral tegmental area; VTT, ventral *tenia tecta*; ZI, *zona incerta*.

MATERIALS AND METHODS

ANIMALS

For these studies, we used 17 adult (more than two months of age) female mice *Mus musculus*, from the C57BL/J6 ($n = 10$) and the CD1 ($n = 7$) strains (Charles River, L'Arbresle Cedex, France) with body weights between 18.1–25.1 g and 37.5–45.1 g respectively. Animals were housed in cages with water and food available *ad libitum*, either in natural conditions or in a 12 h light: dark cycle, at 21–22°C. We treat them according to the EEC guidelines for European Communities Council Directives of 24th November 1986 (86/609/EEC), and experimental procedures were approved

by the Committee of Ethics on Animal Experimentation of the University of Valencia.

SURGERY AND TRACER INJECTIONS

To study the projections arising from the different divisions of the Me (anterior, posteroventral, and posterodorsal), we performed iontophoretic injections of two different dextranamine conjugates as anterograde tracers. Biotin-conjugated dextranamine (BDA, 10,000 MW, lysine fixable, Invitrogen, Carlsbad, CA, USA) was used diluted at 5% in phosphate buffer (PB) 0.01 M, pH 8.0, and tetrametylrhodamine-conjugated dextranamine (RDA, fluoro-ruby, 10,000 MW, lysine fixable, Molecular Probes, Eugene, OR, USA) was used diluted at 10% in PB 0.01 M, pH 7.6. We delivered the tracers from glass micropipettes (10–50 μm diameter tips) by means of positive current pulses (7on/7off s, 3–5 μA, 10–15 min) using a current generator (Midgard Precision Courrent Source, Stoelting). Two to five minutes after the termination of each injection, the pipette was withdrawn while passing retention current (−0.8 μA).

For surgery, animals were anaesthetized either with intraperitoneal injections of a 3:2 ketamine (75 mg/kg, Merial laboratorios, Barcelona, Spain) and medotomedine (1 mg/kg, Pfizer, Alcobendas, Madrid, Spain) solution, complemented with atropine (Sigma, St. Louis, MO, USA; 0.04 mg/kg, IP) to reduce cardio-respiratory depression ($n = 6$) or by inhalation of isofluorane (1.5%) delivered in oxygen (0.9 L/min) (MSS Isoflurane Vaporizer, Medical Supplies and Services Int'l Ltd, UK) using a mouse anaesthetic mask ($n = 11$). We also injected them butorfanol (Fort Dodge Veterinaria, Girona, Spain; 5 mg/kg, subcutaneous) as analgesic. During surgery, animals were on top of a thermic blanket to maintain their body temperature and eye-drops (Siccafluid, Thea S.A Laboratories, Spain) were applied to prevent eye ulceration. After fixing the mouse head in the stereotaxic apparatus (David Kopf, 963-A, Tujunga CA, USA) we drilled a small hole above the medial amygdala. Following tracer injection, we closed the wound with Histoacryl (1050052, Braun, Tuttlinger, Germany). After surgery, animals anaesthetized with the ketamine-medotomedine solution received then injections of atipamezol (Pfizer, Alcobendas, Madrid, Spain; 1 ml/kg, intramuscular) to revert the medotomedine effects.

In the first nine tracer injections (performed in C57 mice) we observed that labeled fibers in the contralateral hemibrain were absent or negligible (see "Results"), so we decided to perform one injection per hemisphere in the rest of the mice, to minimize the number of animals. Following Paxinos and Franklin (2004) in C57mice we used the following coordinates relative to bregma. For MeA: AP −1.1 mm, L −2.0 mm, and D −5.25 mm. For MePD: AP −1.7 mm, L −2.2 mm, and D −5.2 mm. For MePV: AP −1.94 mm, L −2.1 mm, and D −5.3 mm. Coordenates were adapted to CD1 mice as follows: MeA: AP −1.7 to −1.4 mm, L ±2.1 mm, and D −5.10 to −5.3 mm; MePD: AP −1.9 mm, L ±2.1 mm, and D −5.1 mm; MePV: AP −1.9 mm, L ±2.1 mm, and D −5.1 to –5.48 mm.

HISTOLOGY

Six to eight days after the injections, animals were deeply anesthetized with an overdose of sodium pentobarbital (Sigma) (90 mg/kg) and perfused with saline solution (0.9%) followed by 4% paraformaldehyde diluted in PB (0.1 M, pH 7.6). Brains were removed from the skull, postfixed for 4 h in the same fixative and cryoprotected with 30% sucrose solution in PB at 4°C until they sank. Using a freezing microtome we obtained frontal sections (40 μm) through the brain that were collected in four matching series. In some animals, the olfactory bulbs were cut at 30 μm.

For the detection of BDA, we inactivated the endogenous peroxidase with 1% H_2O_2 [in 0.05 M Tris buffer saline (TBS) pH 7.6] for 15 min and then incubated the sections for 90 min in ABC complex (Vectastain ABC elite kit, Vector Labs, Burlingame, CA, USA) diluted 1:50 in TBS-Tx (Triton X-100 0.3% in TBS 0.05 M pH 7.6). After rinsing thoroughly with buffer, we developed the peroxidase activity with 0.025% diaminobenzidine in PB (0.1 M, pH 8.0), with 0.01% H_2O_2 and 0.1% nickel ammonium sulphate. For the RDA immunohistochemical detection, we inactivated the endogenous peroxidase as previously described. Then, sections were incubated overnight in a specific primary antibody against tetrametylrhodamine raised in rabbit (Molecular Probes, Cat. #A-6397) diluted 1:4000 in TBS-Tx, followed by a standard peroxidase-antiperoxidase (PAP) method (goat anti-rabbit IgG, 1:100, Nordic Immunological Laboratories, Tilburg, The Netherlands; rabbit PAP, 1:800, Nordic Immunological Labs). Peroxidase activity was revealed as described before, but nickel was not used.

The sections were mounted onto gelatinized slides, counterstained with Nissl staining, dehydrated with graded alcohols, cleared with xylene and coverslipped with Entellan (Merck, Darmstadt, Germany). We observed the sections using an Olympus CX41RF-5 microscopy and photographed them using a digital Olympus XC50 camera. We arranged the pictures with Adobe Photoshop 7.0 (AdobeSystems, MountainView, CA, USA) and design the line drawings and their labeling using Adobe Photoshop and Adobe Illustrator (Adobe Systems).

RESULTS

For the description of the distribution of anterograde labeling resulting from the different injections in the Me, we follow the nomenclature of the atlas of the mouse brain by Paxinos and Franklin (2004). To simplify the description of the intra-amygdaloid projections, the term "olfactory amygdala" is used, following Kevetter and Winans (1981a), for the amygdaloid structures that are direct targets of the main olfactory bulb and the term "vomeronasal amygdala" is used to refer to amygdaloid structures that are direct targets of the AOB (Kevetter and Winans, 1981b). The term "chemosensory amygdala" includes both the olfactory and the vomeronasal amygdala (Gutiérrez-Castellanos et al., 2010).

The projection densities in the different targets of the Me subnuclei (anterior, posterodorsal and posteroventral), are subjectively classified as (see **Table 1**): very dense, dense, moderate, sparse, and very sparse. We considered very dense the projection through the *stria teminalis*, and very sparse the areas where we could observe only 2–5 labeled fibers.

The injection sites obtained in the medial amygdala are described below. In addition, we obtained one injection located in the substantia innominata (SI) above the MeA, and another

Table 1 | Semiquantitative rating of the density of the anterograde labeling resulting after tracer injections in three subnuclei of the medial amygdaloid nucleus.

		MeA	MePD	MePD/PV	MePV
AMYGDALA					
	MeA	Injection	+++	++++	+++
Vomeronasal	MePD	+++	Injection	Injection	++++
	MePV	+++	+++	Injection	Injection
	PMCo	+++	++	++++	++++
	BAOT	+++	+++	(not found)	+++
	AAD/AAV	++	++	++	+/++
	AHi	+++	++	++	++
Olfactory	ACo	++	+++	+++	++
	CxA	+	+	++	+↓
	PLCo	+++	++	+++	+++
	LOT	+	+	+	+↓
Central	CeM	++	++	++	+
	CeL	+	+↓	+	+↓
	CeC	+++	+↓	+	–
	Astr	++	–	–	–
	BSTIA	+++	++	++	++
Basolateral complex	BLA	+↓	+↓	+↓	–
	BLP/BLV	+	+	+	+
	BMA	++	++	+++	++
	BMP	+	+	+	++
	La	+	+	+	+↓
OLFACTORY SYSTEM/CORTEX					
AOB (MiA/GrA/GlA)		+++/++/+	–	+/+++/–	+/+++/–
Olfactory system	GrO	+↓	–	–	–
	Pir	+	+	+	+
	DEn/VEn	+	+↓	+	+↓
	AON	+	–	+	+↓
	Tenia tecta	++	–	+	+
Cortex	AI	+	–	+↓	+↓
	PrL	+	–	–	–
	IL	+	–	–	–
	CI	+	–	–	–
Hippocampal formation	Ent	+	+↓	+↓	+↓
	Hippocampus	+	++	+	++
BST/SEPTUM/STRIATUM					
BSTL	BSTLD	++↑	–	+	+↓
	BSTLP	++	+↓	+	+↓
	BSTLV	++	+↓	+	+↓
BSTM	BSTMA	++	++	+++	+++
	BSTMPM	++	++++	++++	++++
	BSTMPI	++++	++	+++	++
	BSTMV	++	++	++	+
	BSTMPL	+++	+++	+++	++
Lateral septal complex	LSI	++↑	+	++	+
	LSV	++	+	++	++
	LSD	+	+↓	+	+
	SHy	++	++	++	+++
	SHi	+	+↓	+	+↓
Medial septum/ Diagonal Band	MS	+	–	+	+↓
	HDB	++↑	–	+	+
	VDB	++	–	+	+

(Continued)

Table 1 | Continued

		MeA	MePD	MePD/PV	MePV
Striato-pallidum	VP	+	+	+	–
	Acb	+	+	+	–
	Tu	++	–	+↓	+↓
	ICj	+	–	+↓	+↓
	SI	++	++	++	++
	IPAC	++	–	+↓	+↓
HYPOTHALAMUS					
Preoptic	MPA	++	++	++	+
	MPO	++	+++	++	++
	LPO	+	+	+	+↓
	AVPe	–	++	+	–
Anterior	AHA/AHP	++	++	++	+
	Pa	+	+	+	+↓
	Pe	+	+	+	+↓
	LA	+	+	+	+
	SCh	–	+	+	–
Tuberal	VMHDM	+++	+	+++	++
	VMHVL	++	+++	+++	++
	DM	+	+	+	+↓
	LH	+	+	+	+
	Arc	+	+	+	+
Mammilary	PMD	+	+↓	+	+
	PMV	++	+++	+++	+++
	MM/ML	+	+	+	+
	SuM	+	+	+	+
	PH	+	+	+	–
THALAMUS					
	SM	+++	+++	+++	++
	Re	+↑	+	+	+↓
	PV	+	+	+	+
	MD	+	–	–	–
	LHb	+	–	–	–
	PT	+	–	–	–
	ZI	+	–	–	–
	STh	+	+	+	+
	PSTh	+	+	+	–
BRAINSTEM AND MIDBRAIN					
	PAG	+	+	+	+
	VTA	+	+	+	+
	Rostral linear raphe nucleus	+↓	–	–	–
	Dorsal raphe nucleus	+↓	–		–
	SN	–	+	+	–

++++, Very dense; +++, Dense; ++, Moderate; +, Scarce; +↓, very sparse.

one restricted to the optic tract (opt) medial to the MeA (not shown). These injections are used as controls for the specificity of the anterograde labeling resulting from the medial amygdala injections (see below).

INJECTIONS IN MeA

Injections sites

In eight experiments the injection affected the MeA, in five of which the tracer is entirely confined to this subnucleus. Of the restricted injections (**Figures 1A,B**), two correspond to single injections in the C57BL/6J strain and are used to describe both ipsilateral and contralateral projections of the MeA (**Figure 1**, injections M0331 and M1120). The remaining three injections, which correspond to CD1 mice, are used to describe the ipsilateral projections. In injections M1143R and M1144L (**Figures 1A,B**) small tracer deposits appear along the micropipette track, located in the internal capsule (ic), medial globus pallidus (MGP), *SI*, and the opt, and therefore are used only to check the labeling found

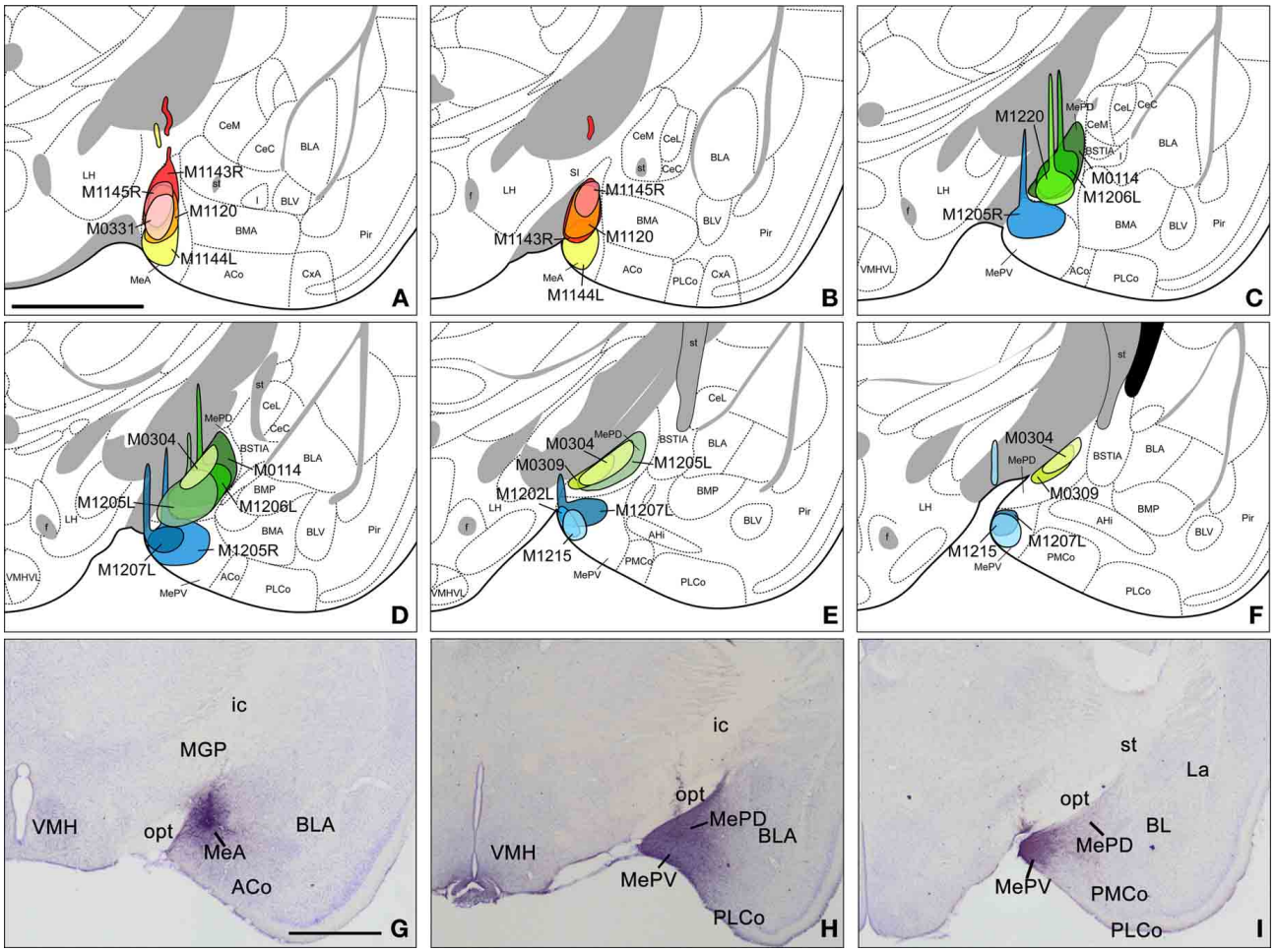

FIGURE 1 | Injection sites in the anterior, posterodorsal, and posteroventral subdivisions of the medial amygdaloid nucleus. **(A–F)** Schematic drawings representing the extent of the tracer injections in the anterior medial amygdaloid nucleus (MeA), the posterodorsal medial amygdaloid nucleus (MePD), and the posteroventral medial amygdaloid nucleus (MePV). MeA injections are represented in warm colors (**Figures 1A** and **B**), MePD in green and MePV in blue (**Figures 1C–F**). Colored areas represent single injections and are identified with the animal code. For those animals with two injections, each one is identified with either an R (right hemisphere) or an L (left hemisphere). **(G–I)** Photomicrographs of nissl-stained sections through the amygdala of the mouse showing representative injections sites. **(G)** Injection site in the MeA of a CD1 mouse. **(H)** Injection site in the MePD of a CD1 mouse. **(I)** Injection site in the MePV of a CD1 mouse. For abbreviations, see list. Scale bar in **A**, valid for **B**–**I** = 1 mm.

in restricted injections. In the three additional cases the injections extended caudally and affected also the posterior subdivisions of the Me.

Anterograde labeling resulting from injections in the MeA

The injections of neural tracers in the MeA give rise to anterograde labeling in a complex range of cerebral nuclei. Intra-amygdalar axons spread directly from MeA, while fiber labeling coursing outside the amygdala follows two main pathways: the *stria terminalis*, where labeled axons are located in the medial aspect, and the ventral amygdalofugal pathway (*ansa peduncularis*), where axons progress across the *SI*. The output of the MeA is mostly ipsilateral, with scarce fiber labeling present in contralateral nuclei, as described below. Since no differences were observed in the anterograde labeling resulting from experiments in the C57BL/J6 and CD1 strains [except in the olfactory tubercle (Tu) see below], the results obtained in both strains are described together.

Amygdala. Tracer injections in the MeA give rise to anterogradely labeled fibers that extend to other amygdalar regions (see **Table 1**). Fiber labeling appears throughout the rest of the Me, with dense terminal fields observed in both MePD and MePV subnuclei (**Figure 2J**). Dense fiber labeling is observed in the posteromedial (PMCo) and posterolateral (PLCo) cortical amygdaloid nuclei (**Figure 3A**), amygdalohippocampal area (AHi) (**Figures 2I–M**) and bed nucleus of the accessory olfactory tract (BAOT) (not shown, see **Table 1**). Other regions of the chemosensory amygdala display a moderate density of fiber labeling, such as the anterior cortical nucleus (ACo) and the anterior amygdaloid area, mainly in its ventral division (AAV) (**Figures 2G,H**). Finally, some other chemosensory structures of

the amygdala display only sparse anterograde labeling, such as the corticoamygdaloid transition area (CxA), or are mostly devoid of the labeled axons resulting from MeA injections, such as the nucleus of the lateral olfactory tract (LOT) (a small amount of fibers of passage are observed in layer 1 and a few labeled fibers are present in layer 3, **Figures 2H,I**). In the central nucleus anterogradely labeled fibers give rise to a moderate terminal field in the medial (CeM) and capsular (CeC) parts (somewhat denser

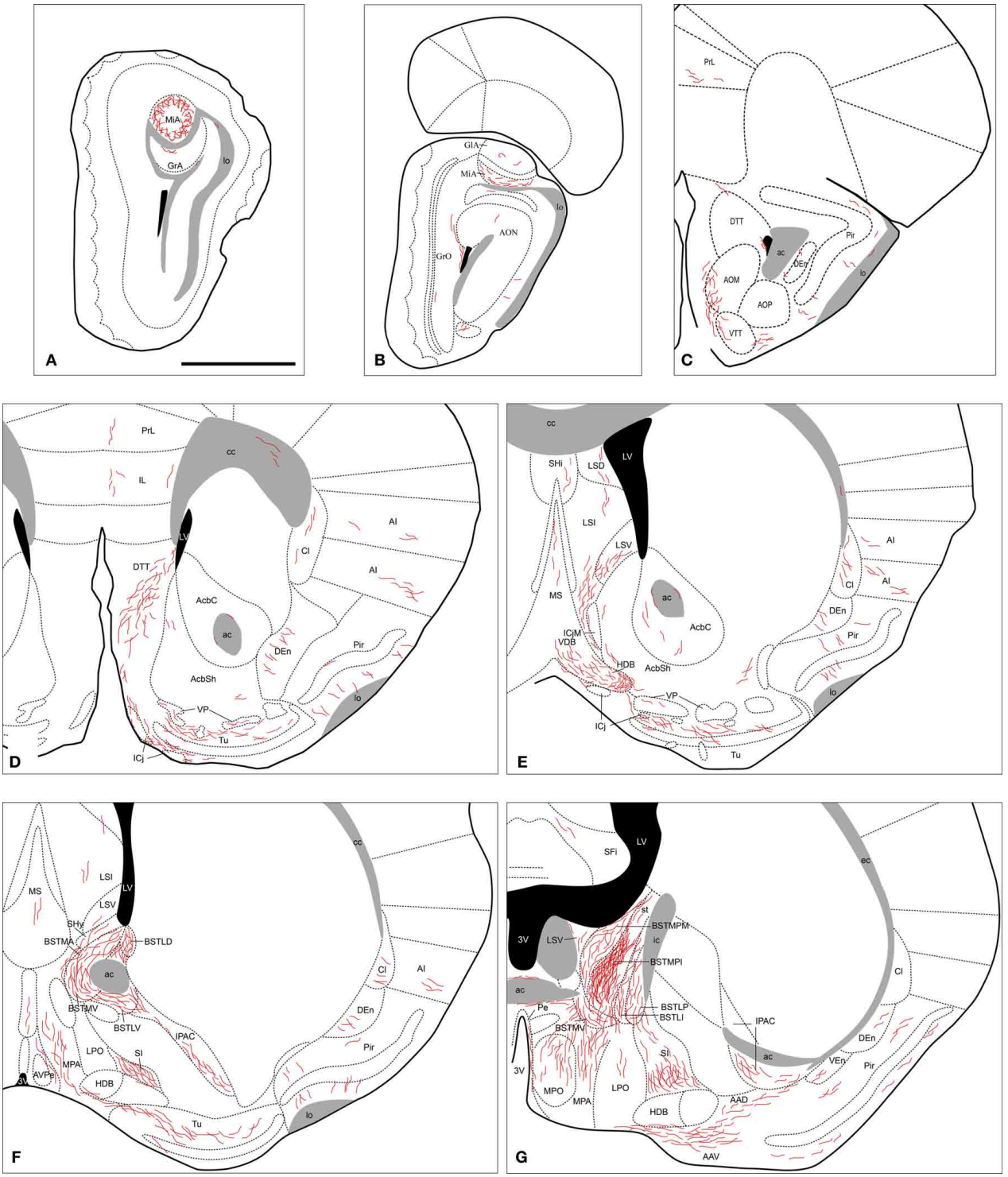

FIGURE 2 | Continued

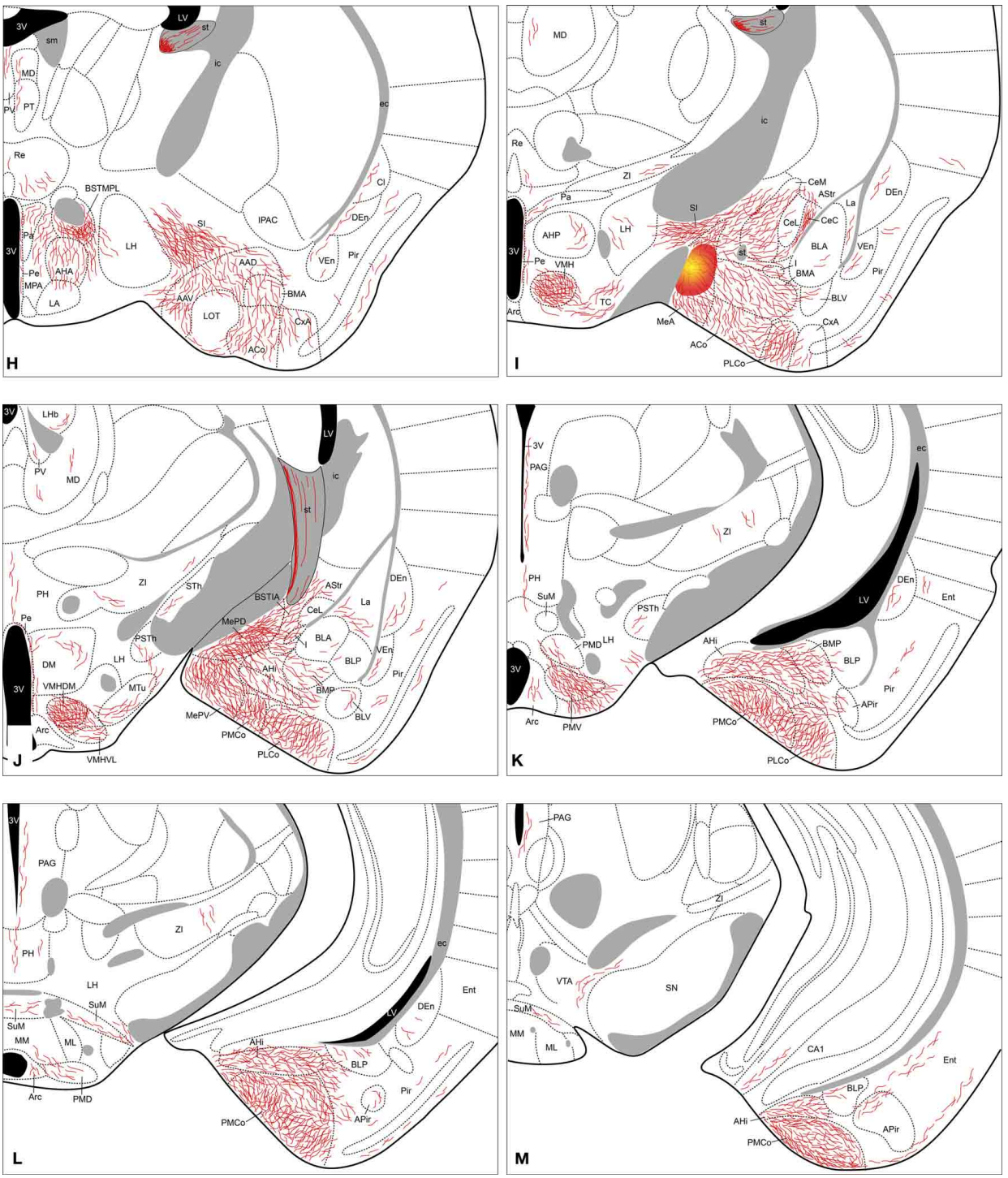

FIGURE 2 | Semi-schematic drawings of transverse sections through the mouse brain showing the distribution of anterogradely labeled fibers following a tracer injection in the MeA. The injection site is depicted in panel **(I)**. **A** is rostral, **M** is caudal. The semi-schematic drawings were made based on an injection in a C57BL/J6 mouse. For abbreviations, see list. Scale bar: 1 mm.

at the CeC), and also in the amygdalostriatal transition area, with sparse anterograde labeling observed in the lateral part (CeL) (**Figures 2I,J**). Dense anterograde labeling appears also in the intra-amygdaloid division of the bed nucleus of the *stria terminalis* (BSTIA) (**Figure 2J**) and a moderate density in the intercalated mass (I) located between the basolateral and basomedial nuclei (**Figures 2I,J**). Within the basolateral amygdaloid complex, a moderate density of fiber labeling is present in the

anterior basomedial amygdaloid nucleus (BMA) (**Figures 2H–K**), and only sparse anterograde labeling appears in the lateral (La) and basolateral nuclei (**Figures 2I–M**).

Olfactory bulbs and cerebral cortex. Fiber labeling arising from the MeA injection extends rostrally through the accessory olfactory tract to end in the AOB, where we observe dense anterograde labeling in the ventral aspect of the mitral cell layer, a moderate density of labeled fibers in the granular layer and a few fibers in the glomerular layer, apparently in the posterior AOB (**Figures 2A,B,** and **4A**). Some labeled axons apposed to the wall of the lateral ventricle run dorsally to the AOB, crossing the granular cell layer of the dorsomedial olfactory bulb (**Figure 2B**). Fiber labeling from the MeA is also present in the prefrontal cortex,

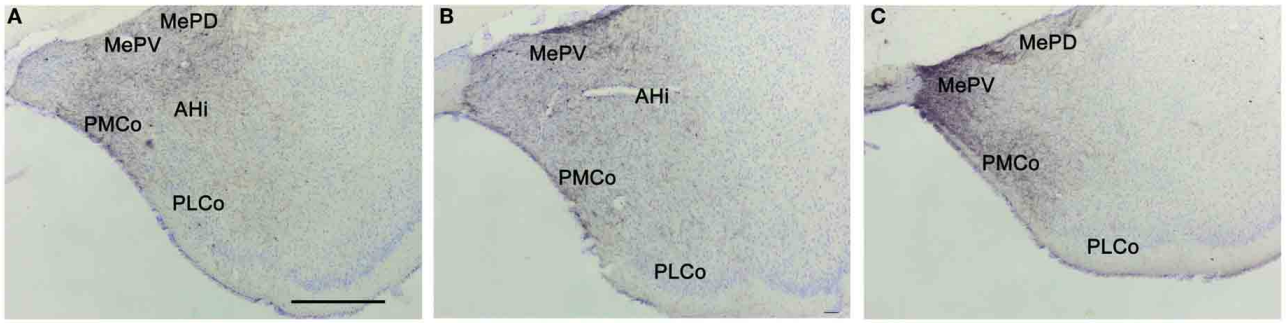

FIGURE 3 | Anterograde labeling in the amygdala after tracer injections in the different subdivisions of the medial amygdaloid nucleus. Photomicrographs of transverse sections through the amygdala of CD1 animals receiving tracer injections in the MeA **(A)**, MePD **(B),** and MePV **(C)**. **(A–C)** Note that in all cases dense anterograde labeling is observed in the vomeronasal amygdala. For abbreviations, see list. Scale bar in **A** (valid for **B** and **C**): 500 μm.

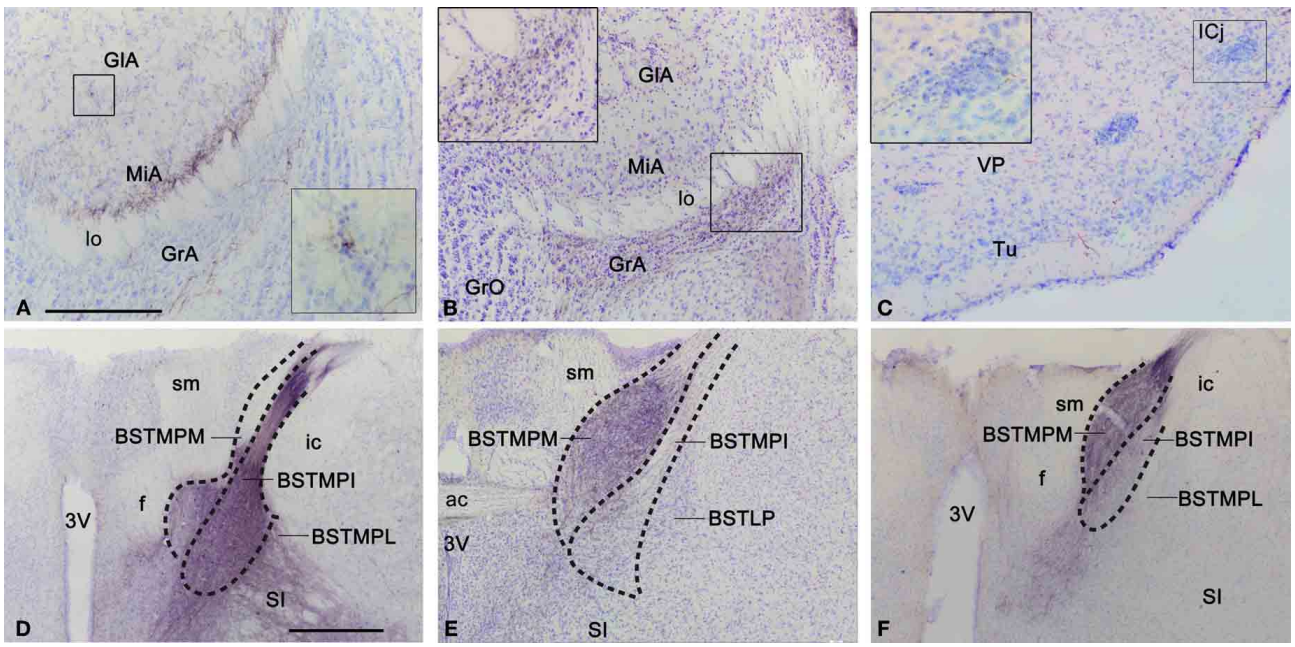

FIGURE 4 | Anterograde labeling in the accessory olfactory bulb, olfactory tubercle, and bed nucleus of the *stria terminalis* after tracer injections in the medial amygdaloid nucleus. (A) Nissl-stained transverse section through the accessory olfactory bulb of a CD1 animal with a tracer injection in the MeA, showing the centrifugal projections to the deep aspect of the mitral cell layer. The inset shows a high magnification view of a labeled fiber next to a glomerulus. **(B)** Nissl-stained transverse section through the accessory olfactory bulb of a CD1 animal with a tracer injection in the MePV, showing the centrifugal projections to the granule cell layer. The inset shows a high magnification view of these labeled fibers. **(C)** Photomicrograph of a transverse section through the ventromedial olfactory tubercle of a C57BL/J6 animal with a tracer injection in the MeA. Note that some of the labeled fibers apparently innervate the islands of Calleja. **(D–F)** Photomicrographs of Nissl-stained transverse sections through the bed nucleus of the *stria terminalis* of animals receiving tracer injections in the MeA **(D)**, MePD **(E),** and MePV **(F)**. Note that in **D** the densest labeling is in the medial posterointermediate division, whereas in **(E)** and **(F)** the densest labeling is in the medial posteromedial division. These photomicrographs correspond to a C57BL/J6 mouse injection **(D)** and CD1 mice injections **(E,F)**. For abbreviations, see list. Scale bar in **(A)** [valid for **(B)** and **(C)**: 250 μm. Scale bar in **D** [valid for **(E)** and **(F)**]: 500 μm.

where sparse anterograde labeling is observed in the prelimbic and infralimbic cortices (**Figures 2C,D**). A moderate amount of fibers is present in the dorsal as well as ventral *tenia tecta* and the piriform cortex (Pir) (with more labeled fibers present in layers 1 and 3) (**Figures 2C,D**). In addition, a sparse innervation is observed in other cortical regions such as the anterior olfactory nucleus (mainly in the medial and ventral areas), the endopiriform nucleus (**Figures 2C–L**), the agranular insular cortex and claustrum (**Figures 2F–H**). Finally, a few axons extend caudally into the entorhinal cortex (Ent) and field CA1 of the ventral hippocampus (**Figure 2M**).

Septum, striatum and bed nucleus of the stria terminalis. In the septum, at rostral levels there is moderate axonal labeling in the lateral septal complex, which appears denser in its intermediate (LSI) than in its ventral division (LSV), with sparse anterograde labeling appearing also in its dorsal division (LSD) (**Figures 2E,F**). Some anterogradely labeled axons are also observed in the medial septal nucleus (**Figures 2E,F**). In addition, moderately dense anterograde labeling is present at the septohypothalamic nucleus (SHy), and a few fibers appear in the septohippocampal nucleus (SHi) (**Figures 2E,F**). In the nucleus of the diagonal band there is a moderate density of anterograde labeling in the vertical and the horizontal limb, especially in the anterolateral part of the horizontal limb (**Figures 2E–G**), next to the boundary with the Tu. A number of fibers are also present next to the medial border of the major island of Calleja (**Figure 2E**).

Within the ventral striatum, a small number of fibers are observed in the nucleus accumbens (**Figures 2D,E**). There is a moderate labeling in the Tu, with axons mainly surrounding the islands of Calleja (**Figures 2D–F** and **4C**). Only a few fibers enter both the ventromedial and the major islands. This anterograde labeling in the Tu appears denser in the injections performed in the C57BL/6J than in the CD1 animals. In the ventral pallidum, sparse anterograde labeling is observed (**Figures 2D,E**). In addition, the SI displays a moderate amount of anterograde labeling and fibers of passage belonging to the ventral amygdalofugal pathway (**Figures 2F–I**). Numerous fibers are also found in the interstitial nucleus of the posterior limb of the anterior commissure (IPAC) (**Figures 2F–G**).

Fibers arriving to the BST mainly course through the *stria terminalis*, which shows a very dense fiber labeling (**Figures 2H–J**). The injections in the MeA resulted in dense anterograde labeling in the BST, both in its medial and lateral divisions (see **Table 1**). A moderately dense terminal field is observed in the lateral BST, especially in the laterodorsal BST (**Figures 2F,G**). Fiber labeling is also very dense in the posterointermediate medial BST (BSTMPI), dense innervation in the posterolateral medial BST (BSTMPL) and moderate in the anteromedial BST (BSTMA), ventromedial BST (BSTMV), and medial posteromedial BST (BSTMPM) (**Figures 2F–H** and **4D**).

Hypothalamus. Following injections in the MeA, abundant anterograde labeling appears in many hypothalamic nuclei (**Table 1**). At **preoptic** levels, there is a moderate amount of anterograde labeling in the medial preoptic nucleus (MPO) and MPA (**Figures 2F,G**). A few labeled fibers can also be found in the lateral preoptic area (LPO) (**Figure 2G**). At **anterior** levels, the anterior hypothalamic area has a moderate labeling (which is less dense in its posterior part) (**Figures 2H,I**). A low density of labeled fibers is also observed in the lateroanterior hypothalamic nucleus (LA), the paraventricular hypothalamic nucleus (Pa), mainly in its anterior part, and the periventricular hypothalamic nucleus (Pe) (**Figures 2F–J**). In the **tuberal** region, the ventromedial hypothalamic nucleus shows a heterogeneous fiber labeling. The central (VMHC) and dorsomedial (VMHDM) parts contain dense anterograde labeling, whereas the ventrolateral (VMHVL) part shown only moderate density of fiber labeling (**Figures 2I,J** and **5A**). In addition, a few axons can be observed in the dorsomedial nucleus (DM) and the arcuate nucleus (Arc) (**Figures 2J–L**). Finally, scarce fiber labeling can be found in the lateral hypothalamic area (LH) (**Figures 2H–K**). At **mammillary** levels, moderate anterograde labeling is seen in the ventral premammillary nucleus (PMV), with a few fibers present also in its dorsal part (PMD) (**Figures 2K,L** and **5D**). There is also sparse labeling in the supramammillary nucleus (SuM), medial mammillary nucleus (MM), and the posterior hypothalamic area (PH) (**Figures 2J–M**).

Thalamus. The injections in the MeA do not result in a wide distribution of anterograde labeling in the thalamus. Some axons progress through the *stria medullaris* and apparently reach the paraventricular thalamic nucleus (PV) and the lateral habenula (LHb) (**Figures 2H–J**). A dense terminal field is observed in the nucleus of the *stria medullaris* (not shown). There is sparse labeling in the nucleus reuniens (Re) (**Figures 2H,I**), mediodorsal nucleus (MD) and parataenial thalamic nucleus (PT) (**Figures 2H–J**). Finally, a few labeled axons appear also in the *zona incerta*, subthalamic nucleus (STh) and parasubthalamic nucleus (PSTh) (**Figures 2I–K**).

Brainstem and midbrain. Anterograde labeling is present in the periaqueductal gray (PAG) and the ventral tegmental area (VTA) (**Figures 2K–M** and **6**). Moreover, a few fibers can be seen in the dorsal raphe nucleus and the rostral linear raphe nucleus (not shown).

Contralateral labeling. Although injections in the MeA give rise mainly to ipsilateral labeling, a few axons cross the midline in the anterior commissure, the supraoptic decussation (sox) and the supramammilary decussation. In the contralateral hemisphere, scarce anterograde labeling appears generally in those structures that present a dense ipsilateral projection (with the exception of the contralateral amygdala, which appears devoid of labeling). Thus, a few fibers can be observed in the contralateral *tenia tecta*, Tu, diagonal band, lateral septum, BST, Re, and several parts of the hypothalamus, mainly in MPA, ventromedial hypothalamic nucleus, and PMV.

Anterograde labeling found in non-restricted injections. In the two cases (**Figure 1A**, injections M1143R and M1144L) where some tracer contamination appears in the ic, MGP, SI, and opt, we observe fibers running through the forceps minor of the corpus callosum (fmi), the external capsule (ec), the basal part of the cerebral peduncle (cp), and sox. As a consequence, very

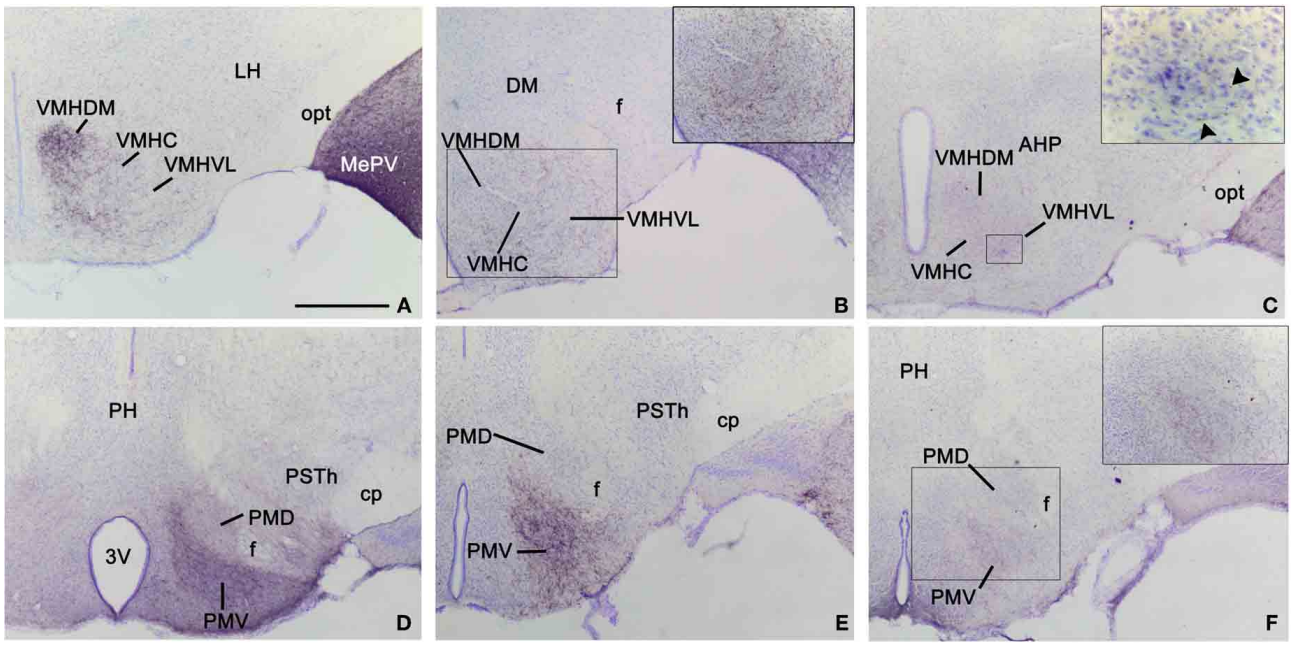

FIGURE 5 | Anterograde labeling in the hypothalamus following tracer injections in the medial amygdaloid nucleus. Photomicrographs of transverse sections through the hypothalamus of animals receiving tracer injections in the MeA **(A,D)**, MePD **(B,E)**, and MePV **(C,F)**. **(A–C)** Pattern of anterograde labeling in the ventromedial hypothalamic nucleus (VMH) in CD1 animals. Injections in MeA resulted in dense fiber labeling in the dorsomedial VMH **(A)**, whereas injection in MePD give rise to dense labeling in the ventrolateral VMH **(B)**. The MePV does not appear to innervate preferentially the dorsomedial or ventrolateral subdivision. **(D–F)** Pattern of anterograde labeling in the premammillary hypothalamus. All three subdivisions of the medial amygdaloid nucleus mainly project to the ventral premammillary nucleus, with the densest projections originated by the MeA **(D)** and the MePD **(E)**. Premammillary hypothalamus photomicrographs correspond to a C57BL/J6 mouse injection **(D)** and CD1 mice injections **(E,F)**. For abbreviations, see list. Scale bar in **A** (valid for **B–F**): 500 μm.

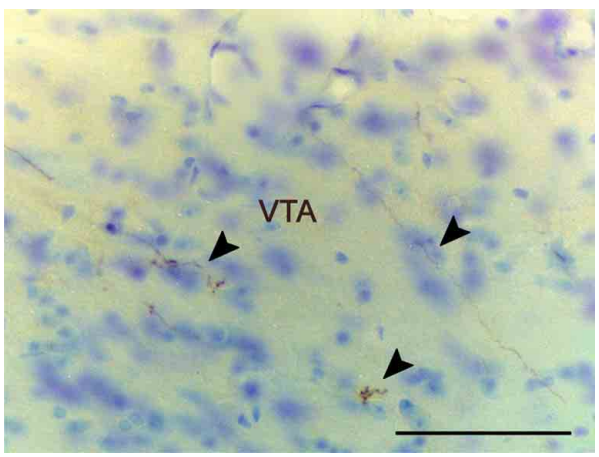

FIGURE 6 | Anterograde labeling in the ventral tegmental area following a tracer injections in the anterior medial amygdaloid nucleus. Arrowheads point to scattered labeled fibers. Experiment performed in a CD1 mice. Scale bar: 25 μm.

scarce labeling is present in substantia nigra (SN), parafascicular thalamic nucleus, and ventral posterior thalamic nuclei. We observe sparse to moderate fibers in the caudate-putamen (CPu), STh, supraoptic nucleus, and the lateral part of the LHb.

INJECTIONS IN MePD

Injections sites

The experiments performed resulted in eight injections affecting the MePD. Six of them are confined almost entirely to this nucleus (**Figures 1C–F**), while two of them affect both the MePD and MePV. Three of the restricted injections correspond to single tracer injections in the C57BL/6J strain and are used to describe the ipsilateral and contralateral projections of the MePD. The remaining restricted injections are done in CD1 mice that received also injections in the contralateral hemisphere, and therefore are used only to corroborate the ipsilateral labeling. In one of the CD1 injections the tracer extended beyond the boundary with the MePV (**Figure 1D**, injection M1205L). In another case the injection involved the MeA (**Figures 1C,D**, injection M1206L). In both cases, some of the nuclei or fiber tracts located along the micropipette track present small tracer deposits, including the primary somatosensory cortex, trunk region, the reticular thalamic nucleus (Rt), the ic, the MGP, and the opt (**Figures 1C,D**, injections M1205L and M1206L).

Anterograde labeling resulting from injections in the MePD

As shown for the MeA, the efferents of the posterodorsal region of the Me (MePD) reach a complex range of cerebral nuclei. Axons originated from the MePD follow the same major pathways described for the MeA. However, in this case the majority of the labeled fibers courses through the *stria terminalis*, with less

anterogradely labeled axons found in the ventral amygdalofugal pathway. The output of the MePD is mostly ipsilateral, although a few axons appear in contralateral nuclei (described below). As reported above, the anterograde labeling resulting from experiments in the C57BL/J6 and CD1 strains shows no difference.

Amygdala. From the MePD labeled axons extend to other amygdalar regions (**Table 1**). There is a very dense anterograde labeling in the rest of the Me (**Figures 7E–G**). In the cortical amygdaloid nuclei, dense anterograde labeling is present in ACo, and a moderate density of labeled fibers appears in

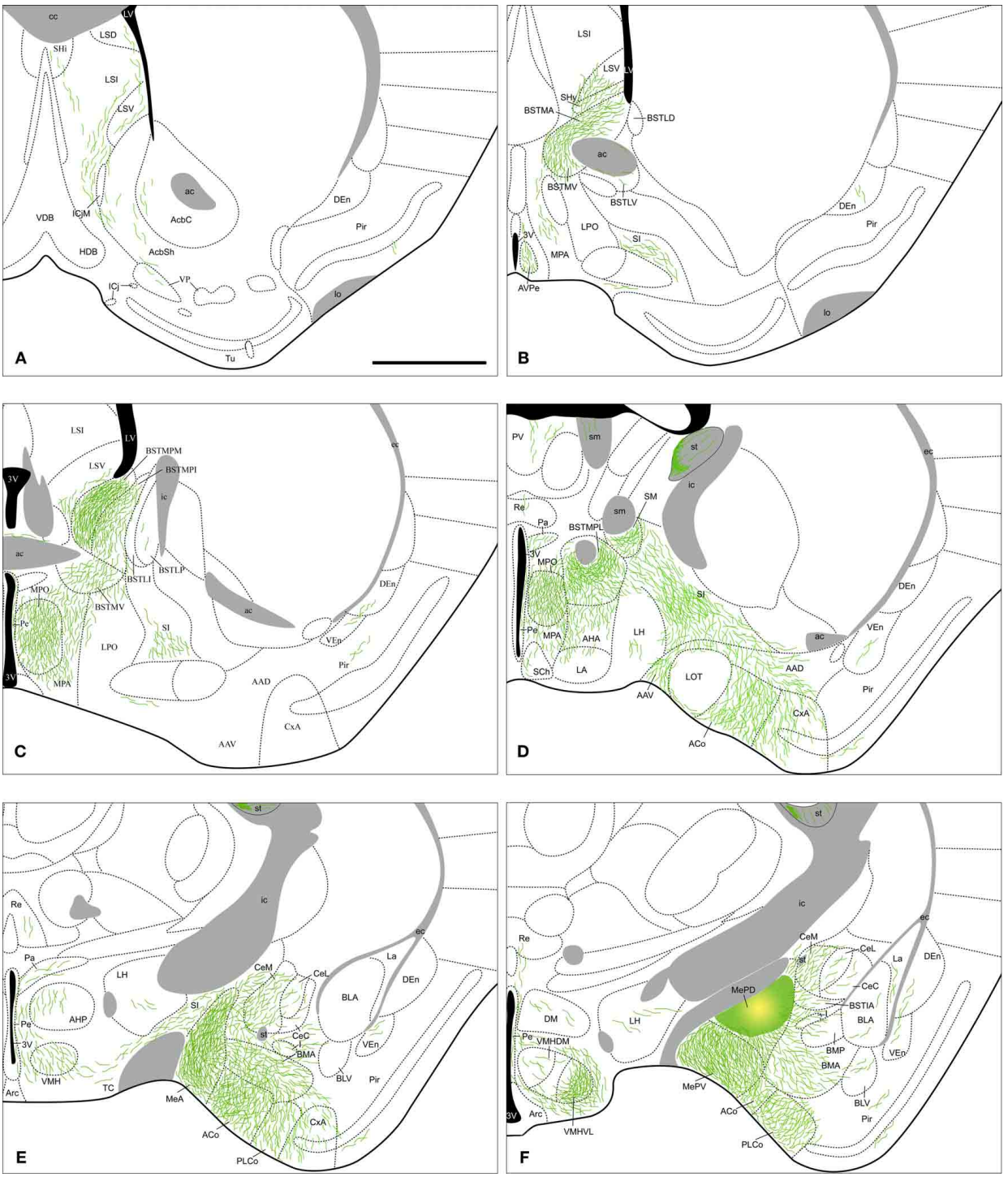

FIGURE 7 | Continued

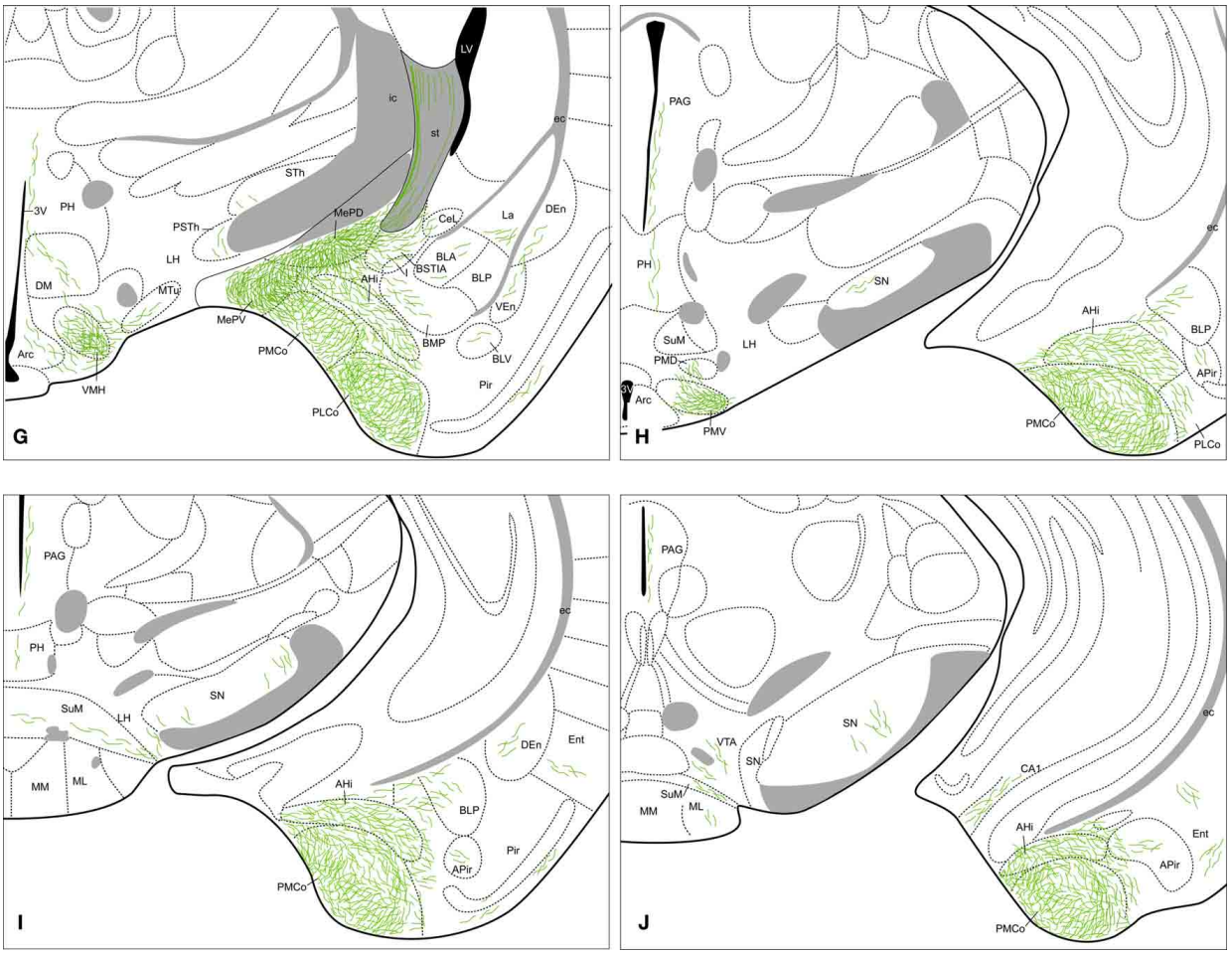

FIGURE 7 | Summary of the distribution of anterograde labeling following a tracer injection in the MePD, plotted onto semi-schematic drawings of transverse sections through the mouse brain. The injection site is depicted in panel **(F)**. **A** is rostral, **J** is caudal. The semi-schematic drawings were made based on an injection in a C57BL/J6 mouse. For abbreviations, see list. Scale bar: 1 mm.

the PLCo and PMCo (**Figures 7D–J** and **3B**). Within the rest of the chemosensory amygdala, the anterior amygdaloid area shows also a moderate density of anterograde labeling, whereas the cortex-amygdala transition zone displays only scarce labeled fibers (**Figures 7D,E**) and the LOT is mostly devoid of axonal labeling (although some labeled fibers can be observed in layer 1, **Figure 7D**). In agreement with its proposed association with the vomeronasal amygdala (Swanson and Petrovich, 1998), the AHi also contains a moderate density of labeled fibers (**Figures 7G–J**) and the BAOT shows dense labeling (**Table 1**). In the central nucleus, a heterogeneous innervation is found following the injections in the MePD. A moderate density of labeled fibers is observed in the CeM (and also in the BSTIA), whereas sparse fiber labeling appears in the CeL and CeC (and also in the I) (**Figures 7E–G**). Within the basolateral amygdaloid complex, the basomedial nucleus shows moderately dense axonal labeling in its anterior part (**Figures 7E,F**). The posterior part of the basomedial nucleus, as well as the basolateral and lateral nuclei, show sparse anterograde labeling (**Figures 7F–I**).

Olfactory bulbs and cerebral cortex. The anterograde labeling observed in olfactory and cortical structures following injections into the MePD is very scarce. Only a small terminal field appears in the CA1 field of the hippocampus (**Figure 7J**). Apart from that, sparse labeling is observed in the Pir (with more labeled fibers present in its posterior zone) and endopiriform nucleus (**Figures 7A–I**), and at caudal telencephalic levels in the Ent (**Figures 7I,J**).

Septum, striatum, and bed nucleus of the stria terminalis. In the septum, sparse anterograde labeling is present in the dorsal, intermediate, and ventral divisions of the lateral septal complex (**Figures 7A–C**), with no fiber labeling being observed in the medial septum/diagonal band complex. A moderate innervation is observed in the SHy and a few fibers are present in the SHi (**Figures 7A,B**). In the ventral striatum, sparse innervation is present in the medial core and shell of the nucleus accumbens (**Figure 7A**), but no labeling appears in the Tu or the associated islands of Calleja. Anterograde labeling is also very scarce in the ventral pallidum (**Figure 7A**). Finally, the SI has a moderate

labeling as well as fibers of passage coursing through the ventral amygdalofudal pathway (**Figures 7B–E**).

Regarding the BST, dense anterograde labeling appears in its medial division, especially in the BSTMPM, where it is very dense (**Figure 7C**, **Table 1**). In addition, dense anterograde labeling is observed in the BSTMPL and a moderate density of fiber labeling is present in the BSTMA, BSTMV, and BSTMPI (**Figures 7B–D** and **4E**). In contrast, the subnuclei composing the lateral division of the BST show very scarce labeling.

Hypothalamus. In the **preoptic** hypothalamus, dense fiber labeling is observed in the MPO (**Figures 7C,D**), while the anteroventral periventricular nucleus and the anterior MPA show a moderately dense labeling (a lower number of labeled fibers is observed in the caudal MPA) (**Figures 7B–D**). A few fibers can also be found in the LPO (**Figure 7C**). At **anterior** levels, the anterior hypothalamic area has a moderate labeling (especially in its rostral part) (**Figures 7D,E**). In the rest of the anterior hypothalamus, only a sparse innervation is observed in the LA, suprachiasmatic nucleus, Pa and Pe (**Figures 7D,E**). In the **tuberal** region, labeled axons resulting after the MePD injections give rise to a dense innervation in the shell of the ventromedial hypothalamic nucleus and in the VMHVL, whereas only a scarce density of labeled fibers is present in the VMHDM and VMHC (**Figures 7E–G** and **5B**). In addition, a few axons can be observed in the DM, Arc, and LH (**Figures 7D–G**). At **mammillary** levels, the PMV shows dense anterograde labeling, while the PMD shows sparse labeling (**Figures 7H** and **5E**). A few anterogradely labeled fibers are also present in the SuM, MM, and PH (**Figures 7G–J**).

Thalamus. The injections in the MePD results in scarce anterograde labeling in the thalamus. Only the axons coursing through the *stria medullaris* apparently give rise to dense anterograde labeling in the nucleus of the *stria medullaris* (**Figure 7D**). In addition, sparse fiber labeling is present in the Re, PV, STh, and the PSTh (**Figures 7D–G**).

Brainstem and midbrain. In animals with injections in the MePD, some labeled axons run caudally to reach the PAG and to a lesser extent also the VTA (**Figures 7H–J**). Sparse labeling is also observed in the *SN* (**Figures 7H–J**), mainly in its reticular part.

Contralateral labeling. The anterograde labeling resulting from the injections in the MePD is mostly ipsilateral, but a few labeled axons are observed to cross the midline in the anterior commissure and the sox. Contralateral labeling is present in the same nuclei that show dense ipsilateral fiber labeling. Thus, sparse anterograde labeling appears in the lateral septum, BST, and the hypothalamus, mainly in MPA, ventromedial hypothalamic nucleus, and PMV.

Anterograde labeling found in non-restricted injections. In the injections M1206L and M1205L, in which tracer contamination occurred in the somatosensory cortex (trunk region), Rt, ic, MGP, and opt, we observe sparse labeling in areas in which no fiber labeling appears following the restricted injections in the MePD. Labeled fibers run through the ec, optic chiasm and the sox, and anterograde labeling is present in the parietal insular cortex, CPu, the ventral posterior thalamic nuclei, posterior thalamic nuclear group (Po), *SN,* and several structures in the visual thalamus.

We observe sparse to moderate fiber labeling in the lateral part of LHb, which also contains labeled axons in the restricted MePD injections.

INJECTIONS IN MePV

Injections sites

We have obtained four injections confined almost entirely to the MePV, two in the C57BL/6J strain (**Figures 1E,F**, injections M1202L and M1215) and two in the CD1 strain (**Figures 1C–F**, injections M1205R and M1207L). In the injections M1205R and M1207L, small tracer deposits are present along the micropipette track, located at the primary somatosensory cortex (trunk region), the cp, the opt, the STh (**Figures 1C–F**), and caudally the SN, *pars reticulata*. In another case, small tracer deposit are present in the cp, STh, and the pyramidal cell layer of the hippocampus (**Figures 1E,F**, injection M1215). In addition, to describe the MePV projections we also study the two injections encompassing the MePD and MePV described above (see section "Injections sites") and an additional one that affected the caudal MePV and the medial aspect of the PMCo. In the case of the MePV the contralateral projections are described based on a C57BL/J6 injection (**Figures 1E,F**, M1215).

Anterograde labeling resulting from injections in the MePV

The labeled fibers resulting from the injections in the MePV course through the same pathways described above for the MeA and MePD injections, the *stria terminalis* and the ventral amygdalofudal pathway. In fact, a very dense group of axons leaving the injection site surrounds the MePD to reach the *stria terminalis* in their way out of the amygdala (**Figure 8I**). As reported with MePD efferents, no differences between strains appear in the anterograde labeling observed following tracer injections in the MePV. The output of the MePV is mostly ipsilateral, although a few axons appear in contralateral nuclei, as described below.

Amygdala. Following MePV injections, dense anterograde labeling is found in the other subnuclei of the Me (**Figures 8G–I**). In the rest of the vomeronasal amygdala, there is very dense anterograde labeling in the PMCo (**Figures 8I–L** and **3C**) and a dense labeling in the BAOT (not shown, see **Table 1**). In addition, the anterior amygdaloid area shows moderate labeling in its ventral part (**Figure 8F**). The AHi (which is strongly interconnected with the vomeronasal amygdala, Swanson and Petrovich, 1998) displays also moderately dense anterograde labeling (**Figures 8I–K**). In the olfactory amygdala, moderately dense axonal labeling is present in the ACo and the PLCo (**Figures 8F–J**), while the cortex-amygdala transition zone has only a very sparse anterograde labeling (**Figures 8F,G**). The LOT is mostly devoid of the MePV axons, but some fibers can be observed in layer 1 (**Figure 8F**). The central nucleus and associated intra-amygdaloid BST show scarce and heterogeneous anterograde labeling following the MePV injections, with light labeling in the CeM, only a few fibers in the

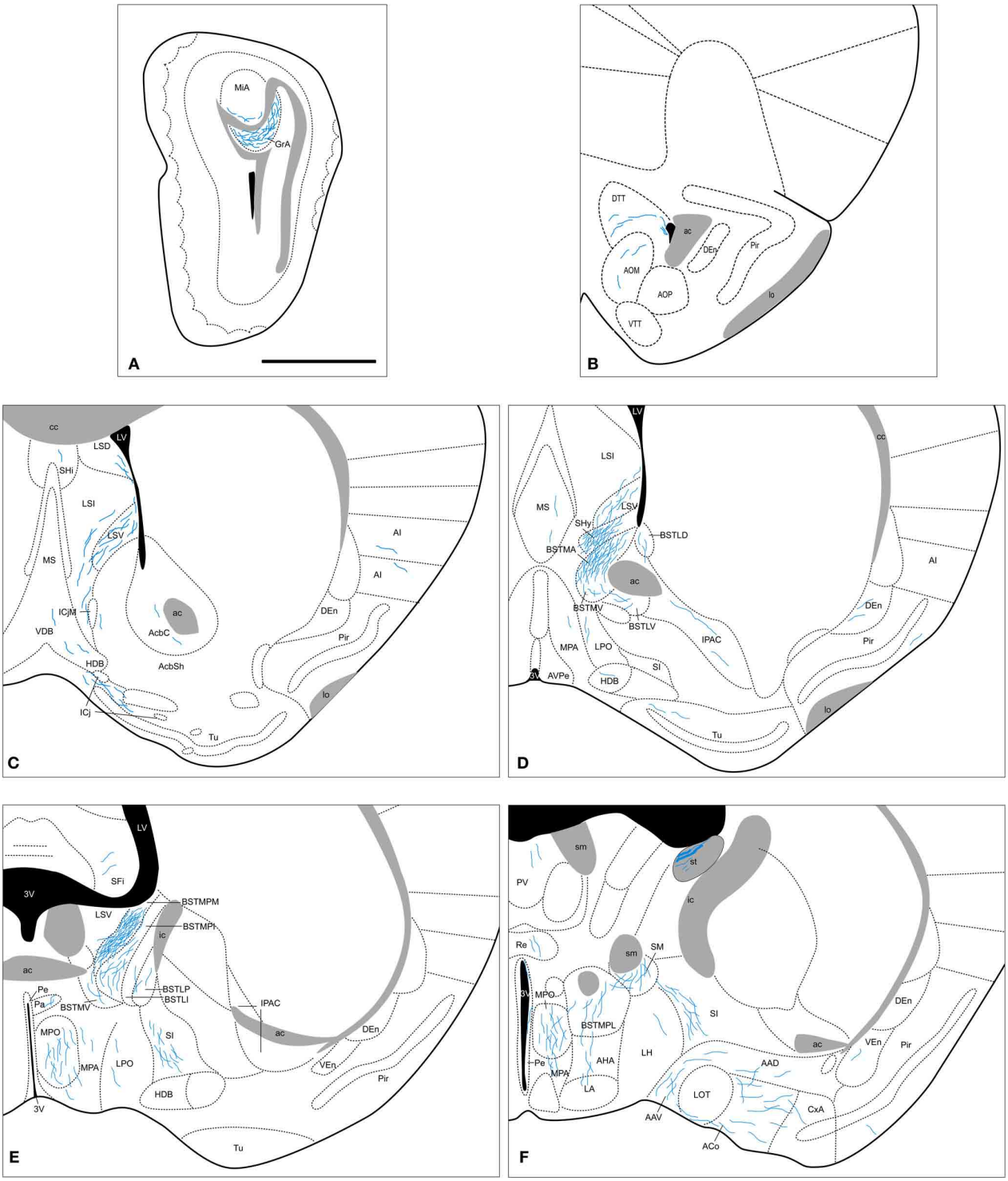

FIGURE 8 | Continued

CeL and no labeling in the CeC (**Figures 8G–I**). Scarce labeling is observed in the I and, in contrast, the BSTIA shows moderately dense labeling (**Figures 8G–I**). Finally, within the basolateral amygdaloid complex, only the basomedial nucleus has a moderate innervation both in its anterior and posterior parts (**Figures 8G–J**), whereas sparse anterograde labeling is observed in the ventral basolateral amygdaloid nucleus, and only a few fibers are present in the La (**Figures 8G–J**).

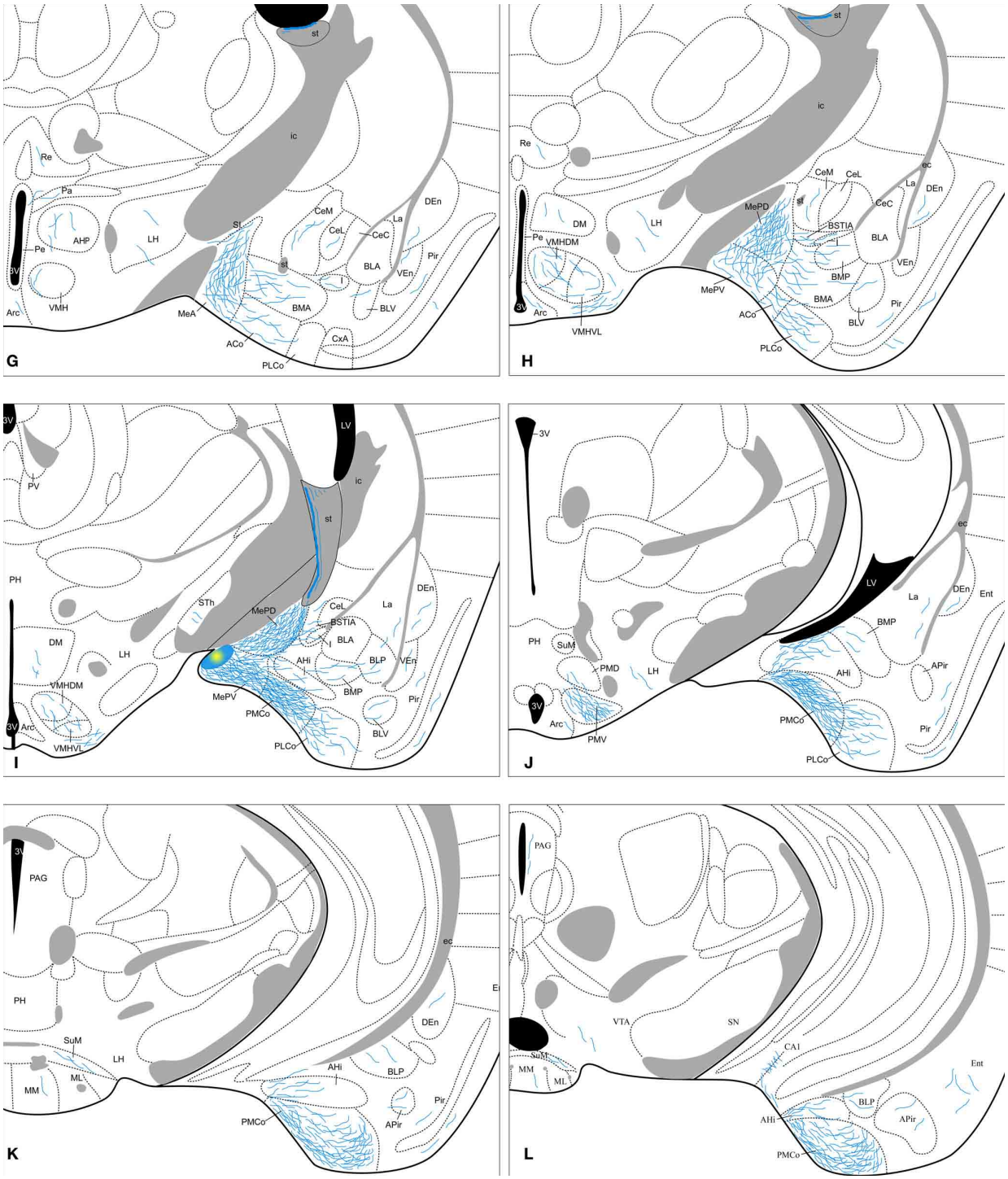

FIGURE 8 | Semi-schematic drawings of transverse sections through the mouse brain showing the distribution of anterogradely labeled fibers following tracer injections in the MePV. The injection site is depicted in panel **I**. **A** is rostral, **L** is caudal. The semi-schematic drawings were made based on two injections, one in a C57BL/J6 mouse and another in a CD1 mouse. For abbreviations, see list. Scale bar: 1 mm.

Olfactory bulbs and cerebral cortex. Axons from the MePV course rostrally to innervate the AOB, where dense anterograde labeling is present in the granular layer and sparse labeling in the deep mitral cell layer (**Figures 8A** and **4B**). In the olfactory system, sparse innervation is present in the Pir (with more labeled fibers present in its posterior zone) and dorsal *tenia tecta* (**Figures 8B–K**). In addition, very scarce labeling is present in the agranular insular cortex, endopiriform nucleus, and medial part

of the anterior olfactory nucleus (**Figures 8B–K**). Within the hippocampal formation, a few axons extend caudally into the Ent and a moderate amount of labeling appears in the CA1 field of the hippocampus (**Figure 8L**).

Septum, striatum, and bed nucleus of the stria terminalis. In the septal complex, at rostral levels the injections in the MePV result in anterograde labeling in the lateral septal nucleus (moderate in the LSV and scarce in the LSI and LSD divisions, **Figures 8C,D**). In addition, the SHy has a dense innervation (**Figure 8D**) while only a few axons are observed at the SHi (**Figure 8C**). Scarce labeling is found in the medial septum/diagonal band complex (**Figures 8C,D**).

In the ventral striatum, very scarce labeling is observed in the nucleus accumbens, Tu and islands of Calleja (**Figures 8C,D**). Also the SI has moderately dense labeling (**Figures 8E–G**) and very few fibers are present in the IPAC (**Figure 8D**).

From the injection site in the MePV labeled fibers run in the *stria terminalis* to reach the BST, where they give rise to a heterogeneous pattern of anterograde labeling. In the medial BST, labeling is very dense in the BSTMPM, dense in the BSTMA, intermediate in the BSTMPL and the BSTMPI, and relatively light and diffuse in the BSTMV (**Figures 8D–F** and **4F**). In contrast, all the subnuclei of the lateral BST show very scarce anterograde labeling (**Figures 8D,E**; see **Table 1**).

Hypothalamus. None of our injections in the MePV shows dense labeled terminal fields in the hypothalamus (**Table 1**). At **preoptic** levels, moderately dense labeling is observed in the MPO and sparse anterograde labeling appears in the MPA (**Figures 8D–F**), with very few fibers present in the LPO (**Figures 8D,E**). At **anterior** levels, the anterior hypothalamic area and LA show a low density of anterograde labeling (**Figures 8F,G**). In the **tuberal** region, there is a moderately dense labeling in the VMHVL and VMHDM (**Figures 8G–I** and **5C**). Of note, dense labeling is observed just ventrolateral to the VMHVL (**Figures 8H,I**). A few labeled axons can be also observed in the LH and Arc, and very few in the DM (**Figures 8F–J**). At **mammillary** levels, the premammillary nucleus shows a few labeled fibers in the PMD, but a dense labeled terminal field in the PMV (**Figures 8J** and **5F**). Also, a few fibers are observed in the SuM and MM (**Figures 8K,L**).

Thalamus. The injections in the MePV result in anterograde labeling in a few thalamic nuclei. Some axons give rise to sparse terminal labeling in the PV and, to a lesser extent, in the Re and STh (**Figures 8F–I**). Axons progressing through the *stria medullaris* apparently provide a moderately dense innervation to the nucleus of the *stria medullaris* (**Figure 8F**).

Brainstem and midbrain. Axons from the MePD course caudally and give rise to sparse anterograde labeling in the PAG and VTA (**Figure 8L**).

Contralateral labeling. The anterograde labeling resulting from the injections in the MePV is mostly ipsilateral, but a few labeled axons cross the midline in the anterior commissure and the sox. In the contralateral hemisphere, anterograde labeling appears generally in those structures that present a dense ipsilateral projection. Thus, sparse anterograde labeling appears in the ventral lateral septum, BST, and the hypothalamus, mainly in MPO, anterior hypothalamic area, ventromedial hypothalamic nucleus, and PMV.

INJECTIONS IN THE SUBSTANTIA INNOMINATA AND THE OPTIC TRACT

In the injection located in the SI, dorsal to the MeA, we observe fiber labeling in the telencephalon coursing through the fmi, with anterograde labeling present in the parietal insular cortex and CPu. In the diencephalon, axonal labeling appears in the lateral LHb, lateral geniculate complex, ventral posterior thalamic nuclei, Po, STh, and sox. Finally, in the brainstem labeled fibers are located in the SN, both in its parts *compacta* and *reticulata*.

We obtained one injection restricted to the opt medial to the MePV. As expected, this case resulted in anterograde labeling being present in the different structures composing the visual thalamus, the pretectum and the superior colliculus (not shown).

DISCUSSION

The results presented in this work confirm in female mice the heterogeneity of the efferent projections of the Me previously reported in other male rodents (Gomez and Newman, 1992; Canteras et al., 1995; Coolen and Wood, 1998). This cytoarchitectonic and hodological compartmentalization of the Me is consistent also with the heterogeneous developmental territories that give rise to neuronal populations of this nucleus (García-López et al., 2008; García-Moreno et al., 2010; Bupesh et al., 2011), as well as with the expression of the genes encoding different transcription factors of the Lhx family (Choi et al., 2005).

In the present work we have compared the pattern of efferent projections of the anterior, posteroventral, and posterodorsal subdivisions of the Me in two different strains of mice, namely C57BL/6J (an inbred strain very often used in the generation of genetically modified animals) and CD1 (an outbred strain commonly used in behavioral studies). The results show that there are no relevant differences in the organization of the efferent projections of the three subdivisions between the two strains. In fact, the results we have found in female subjects of both strains are very similar to those reported in male rats and hamsters, suggesting that the inter-strain and inter-species differences in reproductive (Vale et al., 1973, 1974; Burns-Cusato et al., 2004; Dominguez-Salazar et al., 2004) and defensive (Belzung et al., 2001; Yang et al., 2004) behaviors cannot be attributed to differences in the pattern of efferent projections originated by the Me. Instead they may be due to differences at molecular level (e.g., expression of neurotransmitters or their receptors in the relevant connections). In addition, in the present work we have used female mice as experimental subjects. As far as we know, all of the previous reports of the efferent projections of the Me used male subjects (rats: Canteras et al., 1995; hamsters: Gomez and Newman, 1992; Coolen and Wood, 1998; mice: Choi et al., 2005; Usunoff et al., 2009). As already stated, the efferent projections of the Me subdivisions found in female mice are very similar to the previous results in male mice, as well as in male rats and hamsters. Since the medial amygdala, and specifically its posterodorsal

subdivision, has been shown to be sexually dimorphic (Cooke et al., 1999), the present results suggest that the sexual dimorphism does not include the pattern of organization of its efferent projections (Simerly, 2002), at least as revealed by our qualitative study. Of course, quantitative analysis of particular pathways may uncover sexual differences in the magnitude of some of these efferent projections, or in their neurochemical features.

The efferent projections originated from all three subnuclei of the Me present a common component and a number of relevant differences. As described previously for the other amygdaloid efferents in the rat and mouse (Canteras et al., 1995; Petrovich et al., 1996; Novejarque et al., 2011) efferents from all three subnuclei of the Me course through the same tracts, namely the *stria terminalis* and the ventral amygdalofugal pathway (*ansa peduncularis*), which converge at rostral levels. Within the *stria terminalis*, the efferent projections from the Me course medially, as described also in male rats (Canteras et al., 1995) and male hamsters (Gomez and Newman, 1992). On the other hand, as reported in male rats (Canteras et al., 1995), the MeA contributes to the ventral amygdalofugal pathway more than the posterior Me. Experimental evidence in male hamsters suggests that the projection to the hypothalamus courses exclusively through the *stria terminalis* (Maragos et al., 1989). Consistent with this view, our results suggest that the ventral amygdalofugal pathway contains mainly fibers directed to the ventral striato-pallidum, some of which apparently continue rostrally to reach the AOB. In fact, the existence of a non-strial pathway from the vomeronasal amygdala to the AOB has been demonstrated in the mouse (Barber, 1982).

The projections of all three medial amygdaloid subnuclei are mainly ipsilateral, with only a few axons observed crossing the midline through the anterior commissure, the supraoptic commissure, and the supramammilary decussation. These contralateral axons lightly innervate the zones corresponding to the densest terminal fields observed in the ipsilateral hemisphere, as reported previously in male rats (Canteras et al., 1995).

The additional labeling that we obtained in the cases in which tracer leakage occurs along the pipette track does not interfere with the labeling found following restricted injections, since most of it terminates in different structures. The only target that probably receives a light projection from the Me and also an important one from the dorsally located *SI* is the LHb, as revealed by restricted injections in both MeA and SI (see "Results"). This is consistent with previous reports on the projections of the Me (Gomez and Newman, 1992; Canteras et al., 1995; Coolen and Wood, 1998) and of the SI (Grove, 1988). In addition, the SI also shows important projections to the VTA (Geisler and Zahm, 2005), and accordingly our injections in the Me and in the SI result in anterograde labeling in the VTA. Nevertheless, retrograde tracing after injections in the VTA confirm that at least the MeA and MePD do project to the VTA (Martinez-Hernandez et al., unpublished data).

INTRAMYGDALOID PROJECTIONS OF THE MEDIAL AMYGDALOID NUCLEUS

As described in previous works, our results confirm in the mouse that the different subnuclei of the Me show dense bidirectional interconnections. However, our material reveals that the projections of the MePD to the rest of the Me are more important than suggested by previous studies in male rats (Canteras et al., 1995). By analysing the effects of lesions of the Me in the male Syrian hamster, Maras and Petrulis (2010a,b,c) proposed a functional interpretation for these anatomical data, which is fully supported by our findings in female mice. The MeA would filter the chemosensory information received from the olfactory bulbs that would then be relayed to the posterior medial amygdala. The abundant cells expressing receptors for sexual steroids in the MePD of the hamster (Wood et al., 1992) and the mouse (Mitra et al., 2003) make it a nodal center for the hormonal control of the response to odors and pheromones in the context of reproductive behavior. On the other hand, the projections from the MePD to the rest of the Me, which according to our results are very important in the mouse, would allow an integration of odor/pheromone information with endocrine signals.

In addition, it has been shown in male hamsters that the MeA responds to heterospecific chemosensory stimuli, whereas the MePD seems to be inhibited by this type of stimuli (Meredith and Westberry, 2004). It has been suggested that the anatomical basis of this phenomenon include a projection from the MeA to the GABA-enriched intercalated cell mass, which in turn would inhibit the MePD cells (Meredith and Westberry, 2004). Our anatomical results indicate that the projection from the MeA to the intercalated cell mass located next to the MePD is present in female mice, and therefore a similar mechanism may operate so that the reproductive-related circuit is inhibited by heterospecific odors. However, a recent study in rats show that the exposure to a live cat induce c-fos expression in all subdivisions of the medial amygdala (Martinez et al., 2011), thus suggesting that, at least in this situation, heterospecific-induced inhibition of the MePD does not take place.

The Me gives rise to important intramygdaloid projections, especially directed to the chemosensory amygdala (Gutiérrez-Castellanos et al., 2010). Among the projections to the olfactory amygdala (Kevetter and Winans, 1981a; Cadiz-Moretti et al., in press; see **Figure 8**), all three subdivisions project to the anterior cortical and posterolateral cortical nuclei, as it has been reported previously in different male rodents (hamsters, Coolen and Wood, 1998; rat, Canteras et al., 1995; mice, Usunoff et al., 2009). Our results reveal also a previously unnoticed sparse projection of the Me to the the cortico-amygdaloid transition area and the LOT (only mentioned by Gomez and Newman, 1992).

Among the projections innervating the vomeronasal amygdala (Kevetter and Winans, 1981b; see **Figure 8**), projections from the three subnuclei terminate in the posteromedial cortical nucleus and in the anterior amygdaloid area (which also receives direct projections from the AOB, Cadiz-Moretti et al., in press). In addition, the amygdalo-hippocampal transition area (which is not strictly chemosensory amygdala but it is strongly related to vomeronasal structures, see Swanson and Petrovich, 1998; Martínez-García et al., 2012), is also interconnected with the Me, especially with the posterodorsal and posteroventral divisions (present results, Canteras et al., 1992, 1995).

In summary, the Me not only receives direct projections from the main and AOBs (Scalia and Winans, 1975; Pro-Sistiaga et al., 2007; Kang et al., 2009, 2011; Cadiz-Moretti et al., in press), but also shows strong connections with both the olfactory and the vomeronasal components of the amygdala. In male rats and hamsters these intra-amygdaloid connections are reciprocal (Coolen and Wood, 1998; Pitkänen, 2000; Majak and Pitkänen, 2003), suggesting that the Me plays a relevant role in processing together the olfactory and vomeronasal chemical signals from conspecifics and heterospecifics (Baum and Kelliher, 2009; Keller et al., 2009; Martínez-García et al., 2009).

In contrast to the dense projection to the chemosensory cortical nuclei of the amygdala, the Me gives rise to relatively minor projections to the nuclei that compose the basolateral amygdaloid complex. Only the anterior basomedial nucleus apparently receives a moderate projection from all three medial amygdaloid subnuclei, although a minor projection to the lateral (ventral subnuclei) and basolateral nuclei also exists. These results are in agreement with the previous reports in several male rodents (Canteras et al., 1995; Coolen and Wood, 1998; Usunoff et al., 2009). Since the lateral and basolateral nuclei play a critical role in fear learning (Nader et al., 2001), the Me might play a secondary role in olfactory fear conditioning, an issue that remains to be clarified (Otto et al., 2000; Walker et al., 2005). Of note, when cat odor is used as unconditioned stimulus, the contextual fear acquired is dependent of both the basolateral and the medial amygdaloid nuclei (Li et al., 2004). In addition, the projection to the basolateral nucleus might also be involved in attaching incentive value to olfactory stimuli. In fact, the basolateral nucleus densely innervates the ventral striatum (Novejarque et al., 2011), a projection that is known to play a critical role in many motivated behaviors (Shiflett and Balleine, 2010; Stuber et al., 2011).

Finally, parts of the central nucleus of the amygdala receive substantial projections from the Me. In particular, the medial subdivision of the central nucleus receives moderate projections from all three Me subnuclei, and only the MeA gives rise to substantial projections to the capsular subdivision of the central nucleus. These results agree with previous reports in male mice (Usunoff et al., 2009) and hamsters (Gomez and Newman, 1992; Coolen and Wood, 1998), although in hamsters the capsular subdivision was not considered. The results reported in male rats are slightly different, since the MeA, MePD and MePV were found to moderately project to the capsular subdivision of the central nucleus and only the MeA gives rise to a moderate projection to the CeM (Canteras et al., 1995). The central nucleus of the amygdala is known to project to hypothalamic and brainstem targets that directly mediate fear and anxiety responses (Davis, 2000). These descending projections originate mainly from the medial division of the central nucleus (Rosen et al., 1991), and therefore the projections from the medial amygdala to the CeM are a direct link with a key structure mediating fear responses. However, lesions of the Me significantly reduce the unconditioned freezing induced by cat-derived odors, whereas lesions of the central nucleus have no effect (Li et al., 2004). Therefore, the functional significance of the projections from the Me to the CeM remains to be clarified.

PROJECTIONS OF THE MEDIAL AMYGDALOID NUCLEUS TO THE BED NUCLEUS OF THE STRIA TERMINALIS, HIPPOCAMPUS, SEPTUM, AND VENTRAL STRIATUM

The BST is a major recipient of efferent projections of the Me. Our results indicate that the different BST subdivisions display differential inputs from the subnuclei of the Me. Thus, the MeA gives rise to moderate projections to the lateral subdivisions of the BST (especially to the laterodorsal subnuclei of the BST). In contrast, the MePD and MePV originate only scarce projections to the lateral BST. This specific projection from the MeA to the lateral BST has not been reported in previous works (Gomez and Newman, 1992; Canteras et al., 1995), although a minor projection to lateral aspects of the anterior BST was illustrated by Coolen and Wood (1998). However, differences in the parcellation scheme of the BST may partially explain this discrepancy: in the rat projections from the MeA have been described to the anterolateral, subcommissural, and rhomboid subnuclei of the BST (Dong et al., 2001), which are included in the lateroventral BST and lateral posterior BST in our study (following the atlas of Paxinos and Franklin, 2004). In fact, a moderate input from the MeA to the lateroventral BST has been confirmed by means of retrograde tracing studies in the rat (Shin et al., 2008). In general, the lateral divisions of the BST are strongly interrelated with the central nucleus and are believed to be involved in eliciting fear and defensive or stress-related responses (Gray et al., 1993; Choi et al., 2007). A recent study in mice has revealed that the vomeronasal organ has many more receptors for predator-derived stimuli than it was previously believed (Isogai et al., 2011), and therefore it is not surprising that the Me has direct projections to the relevant areas of the BST. In this sense, the fact that mainly the MeA and, to a lesser extent, the MePV project to the lateral BST is consistent with the data showing that these subnuclei respond to predator-derived chemicals (Samuelsen and Meredith, 2009).

In contrast to the moderate and restricted projection to the lateral BST from the MeA, the medial subnuclei of the BST are densely innervated by all three medial amygdaloid subdivisions. The density of the main projections is different according to the subnucleus of origin: the MeA innervates most densely the medial posterointermediate BST subdivision, whereas the MePD innervates preferentially the medial posteromedial subdivision, and the MePV gives rise to the densest projection to the medial anterior BST. A similar pattern of projections has been shown previously for the MeA and MePD in several male rodents (hamsters: Gomez and Newman, 1992; Coolen and Wood, 1998; rats: Canteras et al., 1995; Dong et al., 2001; mice: Usunoff et al., 2009). It should be noted, however, that the efferents of the MePV have only been studied previously in male rats (Canteras et al., 1995; Dong et al., 2001). In our results the main projection from the MePV terminates in the medial anterior BST, whereas in male rats the main efferent from the MePV innervates the posterointermediate BST (interfascicular and transverse subnuclei of the posterior division, in their nomenclature, see Dong et al., 2001). Two alternative explanations to this discrepancy are possible, interspecies differences between rats and mice or sex differences between males and females. Further research on the MePV efferents will be necessary to solve this question.

The pattern of projections to the medial divisions of the BST is consistent with the proposed functional roles of the different subnuclei of the Me. The MeA seems to filter and categorize the received chemosensory information, which would be relayed: (1) to the neural circuit for socio-sexual behavior (pheromones) through projections to the MePD and posteromedial BST; and (2) to the neural circuit for defensive behavior (e.g., predator-derived chemosignals) through projections to the MePV and posterointermediate BST (Samuelsen and Meredith, 2009). In fact, the MePD projects massively to the posteromedial BST, and both nuclei are sexually dimorphic and enriched in steroid-sensitive cells involved in the control of sexual behavior (Mitra et al., 2003; Swann et al., 2009). In contrast, the MePV has been said to project mainly to structures involved in defensive behavior (Canteras, 2002; Choi et al., 2005). However, our results indicate that the MePV innervates the posteromedial BST and the anteromedial BST. The latter, in turn, gives rise to important projections to the hypothalamic neurosecretory system (Dong and Swanson, 2006), including the vasopressinergic and oxytocinergic neurons of the paraventricular nucleus. Since these neuropeptides in the Me have been shown to play a role in diverse social behaviors (Arakawa et al., 2010; Gabor et al., 2012), these data suggest that the MePV may be involved not only in defensive responses to predators, but also in the control of other non-sexual behaviors, such as agonistic encounters with same sex conspecifics or aversion to illness-derived social odors (Arakawa et al., 2010).

The three subdivisions of the Me give rise to moderate projections to the lateral septum, which target mainly its ventral and intermediate divisions. Noteworthy, the ventral division is enriched in vasopressin innervation, and this projection is sexually dimorphic (Wang et al., 1993) with more density of vasopressinergic terminals in males. This pathway may convey sociosexual (and maybe also predator-derived) chemosensory information to the lateral septum so that it can be integrated with the special and contextual information relayed by the hippocampal formation. The convergence of sociosexual and contextual information would allow the animal to elicit appropriate reproductive/defensive/aggressive behaviors as a function of its contextual situation (Lanuza and Martínez-García, 2009). In this regard, we have observed a minor projection to the ventralmost tip of the ventral hippocampus, which is common to all three subdivisions of the Me. Although this projection is certainly a very small one, it provides a direct route for the chemosensory stimuli processed in the Me to influence the contextual information processed in the ventral hippocampus (**Figure 9**). In rats, this same area of the ventral hippocampus has also been shown to receive substantial projections from the posteromedial cortical nucleus of the amygdala (Kemppainen et al., 2002) and to project back to AOB (de la Rosa-Prieto et al., 2009). Therefore, it is clearly a distinct subdivision of the ventral hippocampus that may be involved in integrating information about chemical signals with spatial or contextual cues.

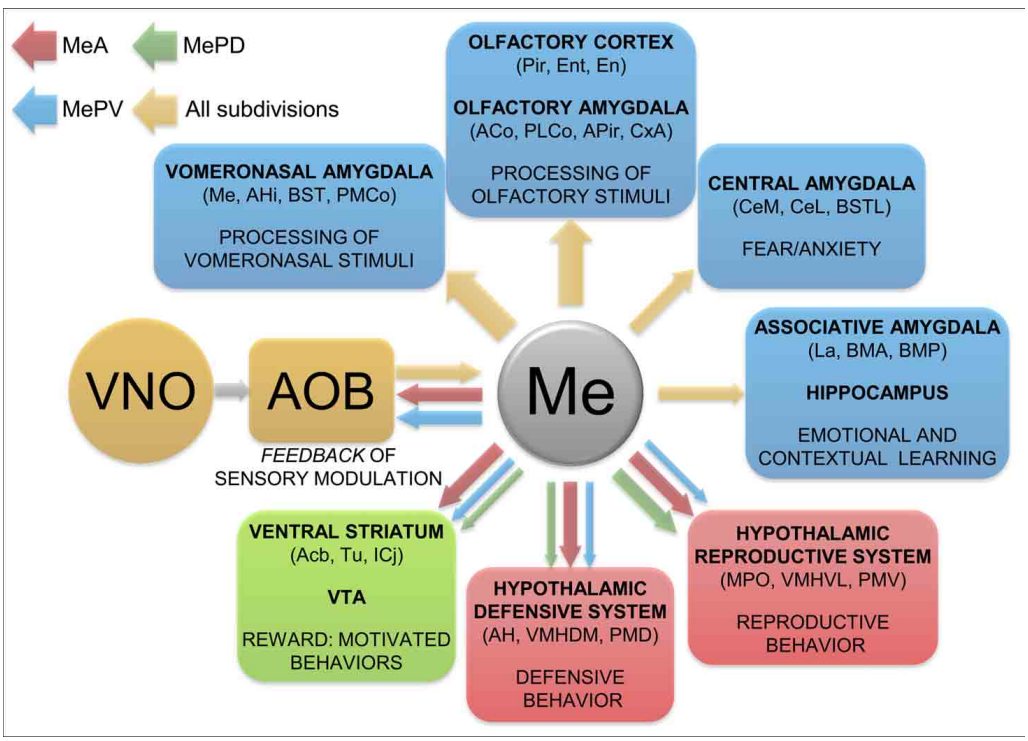

FIGURE 9 | Summary and functional interpretation of the efferent projections arisen from the medial amygdaloid nucleus. Schematic representation of the main efferent projections of the medial amygdaloid nucleus, organized by functional systems. The differential projections of the different subdivisions are represented in red (MeA), green (MePD) and blue (MePV) colors. The thickness of the arrows roughly represents the density of the projections.

According to our results, the Me displays scarce projections to some areas within the ventral striatum, mainly the ventromedial accumbens shell and adjacent Tu, which, as reported previously in male rats (Canteras et al., 1995) and hamsters (Gomez and Newman, 1992; Coolen and Wood, 1998), mainly arise from the MeA. The MePD and MePV contribute only with a few axons to this projection, although Usunoff et al. (2009) recently reported a significant projection from the MePD to the accumbens core, Tu and some islands of Calleja which we have not observed. The innervation in the medial Tu from the MeA reaches the vicinity of the ventromedial islands of Calleja. This area has also been reported to receive a direct input from the posteromedial cortical amygdala (Ubeda-Bañon et al., 2008; Novejarque et al., 2011), the other major target of the vomeronasal information. Therefore, this area of the ventral striato-pallidum may be specialized in processing the biological significance of pheromonal signals (**Figure 9**). In fact, the Tu is strongly related to the reward system of the brain (Ikemoto, 2007) and it may play a role in social odor processing (Wesson and Wilson, 2011).

DIFFERENTIAL CENTRIFUGAL PROJECTIONS TO THE AOB FROM THE MEDIAL AMYGDALOID SUBNUCLEI (FIGURE 9)

Our results confirm and extend previous works showing that the Me gives rise to important feedback projections to the AOB (Barber, 1982; Gomez and Newman, 1992; Canteras et al., 1995; Coolen and Wood, 1998; Fan and Luo, 2009). However, a number of differences between the present results and previous works should be highlighted. On the one hand, we have found that the projection from the MeA innervates mainly the ventral aspect of the mitral cell layer, in agreement with the description in mice (Barber, 1982), male rats (Canteras et al., 1995) and male hamsters (Gomez and Newman, 1992; Coolen and Wood, 1998). In the context of the cytoarchitecture of the AOB, this portion of the ill-organised mitral cell layer might represent the internal plexiform layer (Larriva-Sahd, 2008). However, a recent report in C57BL/6 male mice did not found this projection (Fan and Luo, 2009), maybe because the injections of retrograde tracers in the mitral cell layer of the AOB were too small. However, sex differences cannot be currently discarded. In addition, we also found that tracer injections in the MeA result in a few fibers in the glomerular layer of the posterior AOB, a light projection that may have important functional significance as it might modulate the input to particular glomeruli.

Regarding the feedback projection from the MePV to the granular layer of the AOB, it was not found in previous works in male rats (Canteras et al., 1995) or male hamsters (Gomez and Newman, 1992; Coolen and Wood, 1998), in the latter case probably because the injections in the posterior Me were located in a dorsal position. In contrast, this projection has been reported in male mice (Fan and Luo, 2009), and characterized as glutamatergic. Since the MePV contains a subpopulation of glutamatergic cells originated by the ventral pallium (Bupesh et al., 2011), it is likely that at least some of them give rise to the excitatory feedback projection to the granular layer of the AOB.

PROJECTIONS OF THE MEDIAL AMYGDALOID NUCLEUS TO THE OLFACTORY SYSTEM

In addition to the projections targeting olfactory or vomeronasal amygdaloid nuclei already discussed, direct projections of the Me, originated mainly from the MeA, innervate a variety of structures of the olfactory system (including the piriform and entorhinal cortices, endopiriform nucleus, anterior olfactory nucleus and *tenia tecta*) (**Figure 9**). Only the MeA gives rise to significant projections to the anterior Pir, particularly around the lo, where they may converge with a light innervation directly originated by the mitral cells of the AOB (Cadiz-Moretti et al., in press). Therefore, as suggested previously (see Martínez-García et al., 2012), the Pir should not be viewed as a primary olfactory cortex, but as an associative chemosensory cortex.

PROJECTIONS OF THE MEDIAL AMYGDALOID NUCLEUS TO THE HYPOTHALAMUS

The hypothalamus is, together with the BST, the main target of the efferent projections of the Me. This fact has frequently led to the interpretation that the Me relays the information about pheromones, detected by the vomeronasal organ, to the hypothalamic circuits involved in the control of social and reproductive behavior (Tirindelli et al., 1998; Luo and Katz, 2004). However, as we have already discussed, the Me has a more complex role and, accordingly, its projections to the hypothalamus show a complex pattern (Choi et al., 2005). In general, the MeA and MePV project to hypothalamic structures involved both in reproductive and defensive behaviors, whereas the MePD shows a much more delimitated pattern of projections, innervating mainly hypothalamic structures known to be involved in reproductive behaviors (Petrovich et al., 2001; Choi et al., 2005). Our results are consistent with this pattern of organization (**Figure 8**), with some exceptions that are discussed below.

As described in male rats (Canteras et al., 1995; Petrovich et al., 2001) and hamsters (Gomez and Newman, 1992; Coolen and Wood, 1998), the hypothalamic targets of the MeA include not only the structures of the behavioral column controlling reproductive responses (Swanson, 2000), such as the MPO, ventrolateral VMH, and PMV, but also the structures of the behavioral column controlling defensive responses (Swanson, 2000; Canteras, 2002), such as the anterior hypothalamic area, dorsomedial VMH and (lightly innervated) the dorsal premmamillary nucleus. In contrast, the main hypothalamic targets of the MePD are the nuclei involved in reproductive behavior (MPO, anteroventral periventricular nucleus, ventrolateral VMH, and ventral premmamillary nucleus, Canteras et al., 1995; Petrovich et al., 2001). Regarding the hypothalamic projections of the MePV, our injections in this subdivision have resulted in relatively scarce anterograde labeling of hypothalamic structures. This may be due either to interspecific differences or to the presence of sexual dimorphism in these particular efferent projections. In any case, the major discrepancy of our results with those in male rats (Canteras et al., 1995; Petrovich et al., 2001) is the scarcity of projections to the hypothalamus of the MePV and, in particular, to the anterior hypothalamic area, which is part of the neural circuitry for defensive behaviors. In addition, we have found a very light projection to the dorsal premammillary nucleus, originated mainly in the

MeA, but also in the MePD and MePV. A minor projection from the MeA and MePV to the dorsal premammillary nucleus has also been described in male rats using retrograde tracing (Comoli et al., 2000).

Another interesting result of our experiments is the presence of a relatively dense field of anterograde labeling in the PMV after tracer injections in the MePV. Although this confirms previous observations in the rat by Canteras et al. (1995), it does not fit a simple role of the MePV in anti-predatory defensive reactions, but suggests instead a possible modulation of socio-sexual behaviors mediated by this subnucleus. Since cells in the MePV are preferentially activated by predator-related chemosignals (Choi et al., 2005) this pathway might contribute to inhibiting sexual behavior in threatening contexts, an issue that clearly requires further study.

PROJECTIONS TO THE THALAMUS AND THE BRAINSTEM ORIGINATED BY THE MEDIAL AMYGDALOID NUCLEUS

The only thalamic nucleus that receives a dense input from the Me (all three subdivisions) is the nucleus of the *stria medullaris*, as described previously by Usunoff et al. (2009) in male mice. In addition, a light projection common to the three medial amygdaloid subdivisions innervate the paraventricular and reuniens nuclei of the midline thalamus. The Re projects (among other targets) to the piriform and entorhinal cortices (Vertes et al., 2006). Therefore, this thalamic relay provides an additional indirect pathway for vomeronasal information to influence olfactory inputs to the hippocampal formation. On the other hand, the paraventricular nucleus projects back to the Me, as well as to other amygdaloid structures and to the nucleus accumbens, Tu and bed nucleus of stria terminalis (Vertes and Hoover, 2008). These connections suggest that the paraventricular nucleus is likely involved in the set of emotional behaviors controlled by the amygdala/BST and the ventral striatum.

The Me provides only a light input to the brainstem, targeting the VTA and the PAG. The input to the VTA may be related to the reinforcing value that sexual pheromones have been shown to possess (Martínez-Ricós et al., 2007, 2008), although lesions of the dopaminergic cells of the VTA do not affect the attraction elicited by these sexual stimuli (Martínez-Hernández et al., 2006). In contrast, the projections of the PAG may be related to the elicitation of defensive behaviors by predator odors or chemical signals from dominant conspecifics (Motta et al., 2009). However, the few axons observed are not located in any of the longitudinal columnar regions of the periaqueductal grey described to be involved in different emotional behaviors (Bandler and Shipley, 1994), but oriented dorsoventrally next to the ventricle.

CONCLUSIONS AND FUNCTIONAL REMARKS

The efferent projections of the three subdivisions of the Me revealed by our results show the following main characteristics (**Figure 9**):

1. The pattern of efferent projections of the medial amygdaloid subnuclei found in female mice is very similar to that reported in male rats and male hamsters. However, there are two relevant exceptions regarding the main projections originated from the MePV. First, in the present report in female mice we have found a very dense projection to the BSTMPM and a moderate projection to the BSTMPI, while the opposite pattern was found in male rats (Canteras et al., 1995). Second, in female mice the MePV gives rise to relatively light projections to the hypothalamus, whereas dense projections were reported in male rats (Canteras et al., 1995). Further research will be necessary to check whether these discrepancies are due to interspecific differences or to the presence of a certain degree of sexual dimorphism in these projections.
2. The Me (especially its anterior part) is strongly interconnected with the other structures receiving vomeronasal information from the AOB. This connectivity suggests that the information detected by the vomeronasal system is subjected to a complex intrinsic processing before being relayed to other structures. The necessity of complex processing of vomeronasal stimuli prior to its relay may be related not only to the complexity of the vomeronasal stimuli involving both volatile and involatile components (Zufall and Leinders-Zufall, 2007), but also to the fact that these vomeronasal stimuli are not merely related to reproductive behavior, as originally thought (Powers and Winans, 1975). For instance, it is known that the vomeronasal organ detects also aggression-eliciting chemical signals from same-sex conspecifics (Clancy et al., 1984; Chamero et al., 2007), molecules derived from a wide range of predators which induce defensive behaviors (Papes et al., 2010; Isogai et al., 2011), illness-related molecules (Rivière et al., 2009) which are likely to induce an avoidance response (Arakawa et al., 2010), and sulphated steroids present in the urine of conspecifics, which are likely to signal their physiological status (Nodari et al., 2008). Obviously, different neural circuits should be activated in response to each one of these vomeronasal stimuli.
3. The Me (especially its anterior part) has strong interconnections also with different structures of the main olfactory system, including the olfactory amygdala and the Pir. Therefore, there are anatomical pathways allowing for ample integration of olfactory and vomeronasal information in structures usually considered strictly as part of the olfactory system (Gutiérrez-Castellanos et al., 2010). This strongly supports new views on the complementary role of the olfactory and vomeronasal systems (Baum and Kelliher, 2009; Martínez-García et al., 2009).
4. The Me shows light projections to the basolateral amygdaloid complex and moderate projections to the central amygdala. These anatomical data suggest a minor role of the Me in fear learning (at least in the fear conditioning paradigm). In contrast, the Me has been showed to be involved in both unconditioned (Li et al., 2004) and learned (Takahashi et al., 2007) fear responses to predator odors.
5. The anterior and posteroventral subdivisions of the Me project to key structures of the circuit involved in the defensive response against predators. This circuit includes the posterointermediate part of the medial BST, the anterior hypothalamic area, the dorsomedial part of the VMH, and the dorsal premmamillary nucleus (Canteras, 2002). However, as suggested above, parts of this circuit may also be involved in agonistic behaviors, such as aggressive responses against same-sex

conspecifics (Motta et al., 2009), or avoidance of parasitized conspecifics (Arakawa et al., 2010). Further research is needed to clarify whether there are subsystems within this global defensive system for these different behavioral responses. In this context, the projections of the MePV to nuclei related to reproductive behaviors (e.g., the ventral premammillary hypothalamus) can be interpreted as a pathway for inhibition of reproduction in the presence of predators or parasitized conspecifics.

6. The posterodorsal medial amygdaloid subnucleus mainly projects to the neural circuit for reproductive behaviors (Swanson, 2000), which includes the posteromedial part of the medial BST, the MPO, the ventrolateral part of the VMH, and the ventral premmamillary nucleus. Although there are numerous experimental evidences in support to this view (see Swann et al., 2009, for a review), we want to point out that parts of this circuit may be involved in non-sexual aspects of reproductive behavior, such as maternal aggression (Hasen and Gammie, 2006). In fact, a recent study has revealed the presence within the ventrolateral part of the VMH of male mice of mainly distinct neuronal subpopulations involved in fighting against male intruders and in mating (Lin et al., 2011). Therefore, the systems mediating reproductive and aggressive responses are not fully segregated.
7. It is interesting to note that the Me (especially the MeA) gives rise to light projections to the major structures of the brain system of reward, namely the VTA, the medial shell of the nucleus accumbens, and the Tu (including the islands of Calleja). Indirect projections to the ventral striatum also exist through the basolateral amygdala. Previous work has shown that male pheromones are attractive to female mice and can be used as appetitive unconditioned stimuli to induce learning (Moncho-Bogani et al., 2002; Agustín-Pavón et al., 2007; Martínez-Ricós et al., 2007; Ramm et al., 2008; Roberts et al., 2010). The projections from the Me to the reward system may be involved in processing the hedonic value of sexual pheromones. This hypothesis is consistent with data in hamsters showing that lesions of the Me abolish the female attraction toward male-derived chemical signals (Petrulis and Johnston, 1999). A recent report in mice has also shown that lesions of the medial amygdala blocked the preference of females for male urine, although in this case only lesions that included the posterior medial amygdala were effective (DiBenedictis et al., 2012), whereas lesions restricted to the anterior subdivision had no effect, suggesting that the connections originated by the posterior subdivisions are sufficient to mediate the female preference for male-derived chemicals. Of note, the basolateral amygdala is known to play a relevant role in reward learning (Baxter and Murray, 2002), but the extent to which the Me (and other structures of the chemosensory amygdala) participate in the rewarding aspects of pheromones (or chemical signals with hedonic value) is unknown.

ACKNOWLEDGMENTS

Funded by the Spanish Ministry of Science-FEDER (BFU2010-16656). Cecília Pardo-Bellver is a predoctoral fellow of the "Atracció de Talent" program of the University of València, and Bernardita Cádiz-Moretti is a predoctoral fellow of the "Becas Chile" program of the Government of Chile.

REFERENCES

Abellán, A., Vernier, B., Rétaux, S., and Medina, L. (2010). Similarities and differences in the forebrain expression of Lhx1 and Lhx5 between chicken and mouse: insights for understanding telencephalic development and evolution. *J. Comp. Neurol.* 518, 3512–3528.

Agustín-Pavón, C., Martínez-Ricós, J., Martínez-García, F., and Lanuza, E. (2007). Effects of dopaminergic drugs on innate pheromone-mediated reward in female mice: a new case of dopamine-independent "liking". *Behav. Neurosci.* 121, 920–932.

Arakawa, H., Arakawa, K., and Deak, T. (2010). Oxytocin and vasopressin in the medial amygdala differentially modulate approach and avoidance behavior toward illness-related social odor. *Neuroscience* 171, 1141–1151.

Bandler, R., and Shipley, M. T. (1994). Columnar organization of the midbrain periaqueductal gray: modules for emotional expression. *Trends Neurosci.* 17, 379–389.

Barber, P. C. (1982). Adjacent laminar terminations of two centrifugal afferent pathways to the accessory olfactory bulb in the mouse. *Brain Res.* 245, 215–221.

Baum, M. J., and Kelliher, K. R. (2009). Complementary roles of the main and accessory olfactory systems in mammalian mate recognition. *Annu. Rev. Physiol.* 71, 141–160.

Baxter, M. G., and Murray, E. A. (2002). The amygdala and reward. *Nat. Rev. Neurosci.* 3, 563–573.

Belzung, C., El Hage, W., Moindrot, N., and Griebel, G. (2001). Behavioral and neurochemical changes following predatory stress in mice. *Neuropharmacology* 41, 400–408.

Bressler, S. C., and Baum, M. J. (1996). Sex comparison of neuronal Fos immunoreactivity in the rat vomeronasal projection circuit after chemosensory stimulation. *Neuroscience* 71, 1063–1072.

Bupesh, M., Legaz, I., Abellán, A., and Medina, L. (2011). Multiple telencephalic and extratelencephalic embryonic domains contribute neurons to the medial extended amygdala. *J. Comp. Neurol.* 519, 1505–1525.

Burns-Cusato, M., Scordalakes, E. M., and Rissman, E. F. (2004). Of mice and missing data: what we know (and need to learn) about male sexual behavior. *Physiol. Behav.* 83, 217–232.

Cadiz-Moretti, B. J., Martínez-García, F., and Lanuza, E. (in press). "Neural substrate to associate odorants and pheromones: convergence of projections from the main and accessory olfactory bulbs in mice," in *Chemical Signals in Vertebrates 12*, eds M. East and M. Dehnhard (Berlin, Springer).

Canteras, N. S. (2002). The medial hypothalamic defensive system: hodological organization and functional implications. *Pharmacol. Biochem. Behav.* 71, 481–491.

Canteras, N. S., Simerly, R. B., and Swanson, L. W. (1992). Connections of the posterior nucleus of the amygdala. *J. Comp. Neurol.* 324, 143–179.

Canteras, N. S., Simerly, R. B., and Swanson, L. W. (1995). Organization of projections from the medial nucleus of the amygdala: a PHAL study in the rat. *J. Comp. Neurol.* 360, 213–245.

Chamero, P., Marton, T. F., Logan, D. W., Flanagan, K., Cruz, J. R., Saghatelian, A., Cravatt, B. F., and Stowers, L. (2007). Identification of protein pheromones that promote aggressivebehaviour. *Nature* 450, 899–902.

Choi, D. C., Furay, A. R., Evanson, N. K., Ostrander, M. M., Ulrich-Lai, Y. M., and Herman, J. P. (2007). Bed nucleus of the stria terminalis subregions differentially regulate hypothalamic-pituitary-adrenal axis activity: implications for the integration of limbic inputs. *J. Neurosci.* 27, 2025–2034.

Choi, G. B., Dong, H. W., Murphy, A. J., Valenzuela, D. M., Yancopoulos, G. D., Swanson, L. W., and Anderson, D. J. (2005). Lhx6 delineates a pathway mediating innate reproductive behaviors from the amygdala to the hypothalamus. *Neuron* 46, 647–660.

Clancy, A. N., Coquelin, A., Macrides, F., Gorski, R. A., and Noble, E. P. (1984). Sexual behavior and aggression in male mice: involvement of the vomeronasal system. *J. Neurosci.* 4, 2222–2229.

Comoli, E., Ribeiro-Barbosa, E. R., and Canteras, N. S. (2000). Afferent connections of the dorsal

premammillary nucleus. *J. Comp. Neurol.* 423, 83–98.

Cooke, B. M. (2006). Steroid-dependent plasticity in the medial amygdala. *Neuroscience* 138, 997–1005.

Cooke, B. M., Tabibnia, G., and Breedlove, S. M. (1999). A brain sexual dimorphism controlled by adult circulating androgens. *Proc. Natl. Acad. Sci. U.S.A.* 96, 7538–7540.

Coolen, L. M., and Wood, R. I. (1998). Bidirectional connections of the medial amygdaloid nucleus in the Syrian hamster brain: simultaneous anterograde and retrograde tract tracing. *J. Comp. Neurol.* 399, 189–209.

Davis, M. (2000). "The role of the amygdale in conditioned and unconditioned fear and anxiety," in *The Amygdala. A Functional Analysis,* 2nd Edn. ed J. P. Aggleton (Oxford, UK: Oxford University Press), 213–287.

de la Rosa-Prieto, C., Ubeda-Banon, I., Mohedano-Moriano, A., Pro-Sistiaga, P., Saiz-Sanchez, D., Insausti, R., and Martinez-Marcos, A. (2009). Subicular and CA1 hippocampal projections to the accessory olfactory bulb. *Hippocampus* 19, 124–129.

DiBenedictis, B. T., Ingraham, K. L., Baum, M. J., and Cherry, J. A. (2012). Disruption of urinary odor preference and lordosis behavior in female mice given lesions of the medial amygdala. *Physiol. Behav.* 105, 554–559.

Dielenberg, R. A., Hunt, G. E., and McGregor, I. S. (2001). "When a rat smells a cat": the distribution of Fos immunoreactivity in rat brain following exposure to a predatory odor. *Neuroscience* 104, 1085–1097.

Dominguez-Salazar, E., Bateman, H. L., and Rissman, E. F. (2004). Background matters: the effects of estrogen receptor alpha gene disruption on male sexual behavior are modified by background strain. *Horm. Behav.* 46, 482–490.

Dong, H. W., Petrovich, G. D., and Swanson, L. W. (2001). Topography of projections from amygdala to bed nuclei of the stria terminalis. *Brain Res. Rev*. 38, 192–246.

Dong, H. W., and Swanson, L. W. (2006). Projections from bed nuclei of the stria terminalis, anteromedial area: cerebral hemisphere integration of neuroendocrine, autonomic, and behavioral aspects of energy balance. *J. Comp. Neurol.* 494, 142–178.

Fan, S., and Luo, M. (2009). The organization of feedback projections in a pathway important for processing pheromonal signals. *Neuroscience* 161, 489–500.

Fernandez-Fewell, G. D., and Meredith, M. (1994). c-fos expression in vomeronasal pathways of mated or pheromone-stimulated male golden hamsters: contributions from vomeronasal sensory input and expression related to mating performance. *J. Neurosci.* 14, 3643–3654.

Gabor, C. S., Phan, A., Clipperton-Allen, A. E., Kavaliers, M., and Choleris, E. (2012). Interplay of oxytocin, vasopressin, and sex hormones in the regulation of social recognition. *Behav. Neurosci.* 126, 97–109.

García-López, M., Abellán, A., Legaz, I., Rubenstein, J. L., Puelles, L., and Medina, L. (2008). Histogenetic compartments of the mouse centromedial and extended amygdala based on gene expression patterns during development. *J. Comp. Neurol.* 506, 46–74.

García-Moreno, F., Pedraza, M., Di Giovannantonio, L. G., Di Salvio, M., López-Mascaraque, L., Simeone, A., and De Carlos, J. A. (2010). A neuronal migratory pathway crossing from diencephalon to telencephalon populates amygdala nuclei. *Nat. Neurosci.* 13, 680–689.

Geisler, S., and Zahm, D. S. (2005). Afferents of the ventral tegmental area in the rat-anatomical substratum for integrative functions. *J. Comp. Neurol.* 490, 270–294.

Gomez, D. M., and Newman, S. W. (1992). Differential projections of the anterior and posterior regions of the medial amygdaloid nucleus in the Syrian hamster. *J. Comp. Neurol.* 317, 195–218.

Gray, T. S., Piechowski, R. A., Yracheta, J. M., Rittenhouse, P. A., Bethea, C. L., and Van de Kar, L. D. (1993). Ibotenic acid lesions in the bed nucleus of the stria terminalis attenuate conditioned stress-induced increases in prolactin, ACTH and corticosterone. *Neuroendocrinology* 57, 517–524.

Grove, E. A. (1988). Efferent connections of the substantia innominata in the rat. *J. Comp. Neurol.* 277, 347–364.

Gutiérrez-Castellanos, N., Martínez-Marcos, A., Martínez-García, F., and Lanuza, E. (2010). Chemosensory function of the amygdala. *Vitam. Horm*. 83, 165–196.

Hasen, N. S., and Gammie, S. C. (2006). Maternal aggression: new insights from Egr-1. *Brain Res.* 1108, 147–156.

Heeb, M. M., and Yahr, P. (1996). c-Fos immunoreactivity in the sexually dimorphic area of the hypothalamus and related brain regions of male gerbils after exposure to sex-related stimuli or performance of specific sexual behaviors. *Neuroscience* 72, 1049–1071.

Hirata, T., Li, P., Lanuza, G. M., Cocas, L. A., Huntsman, M. M., and Corbin, J. G. (2009). Identification of distinct telencephalic progenitor pools for neuronal diversity in the amygdala. *Nat. Neurosci.* 12, 141–149.

Ikemoto, S. (2007). Dopamine reward circuitry: two projection systems from theventral midbrain to the nucleus accumbens-olfactory tubercle complex. *Brain Res. Rev.* 56, 27–78.

Isogai, Y., Si, S., Pont-Lezica, L., Tan, T., Kapoor, V., Murthy, V. N., and Dulac, C. (2011). Molecular organization of vomeronasal chemoreception. *Nature* 478, 241–245.

Kang, N., Baum, M. J., and Cherry, J. A. (2009). A direct main olfactory bulb projection to the 'vomeronasal' amygdala in female mice selectively responds to volatile pheromones from males. *Eur. J. Neurosci.* 29, 624–634.

Kang, N., Baum, M. J., and Cherry, J. A. (2011). Different profiles of main and accessory olfactory bulb mitral/tufted cell projections revealed in mice using an anterograde tracer and a whole-mount, flattened cortex preparation. *Chem. Senses* 36, 251–260.

Keller, M., Baum, M. J., Brock, O., Brennan, P. A., and Bakker, J. (2009). The main and the accessory olfactory systems interact in the control of mate recognition and sexual behavior. *Behav. Brain Res.* 200, 268–276.

Kemppainen, S., Jolkkonen, E., and Pitkänen, A. (2002). Projections from the posterior cortical nucleus of the amygdala to the hippocampal formation and parahippocampal region in rat. *Hippocampus* 12, 735–755.

Kevetter, G. A., and Winans, S. S. (1981a). Connections of the corticomedial amygdala in the golden hamster. II. Efferents of the "olfactory amygdala". *J. Comp. Neurol.* 197, 99–111.

Kevetter, G. A., and Winans, S. S. (1981b). Connections of the corticomedial amygdala in the golden hamster. I. Efferents of the "vomeronasal amygdala". *J. Comp. Neurol.* 197, 81–98.

Kollack-Walker, S., and Newman, S. W. (1997). Mating-induced expression of c-fos in the male Syrian hamster brain: role of experience, pheromones, and ejaculations. *J. Neurobiol.* 32, 481–501.

Lanuza, E., and Martínez-García, F. (2009). "Evolution of septal nuclei," in *Encyclopedia of Neurocience,* eds M. D. Binder, N. Hirokawa, and U. Windhorst (Berlin, Springer), 1270–1278.

Larriva-Sahd, J. (2008). The accessory olfactory bulb in the adult rat: a cytological study of its cell types, neuropil, neuronal modules, and interactions with the main olfactory system. *J. Comp. Neurol.* 510, 309–350.

Li, C. I., Maglinao, T. L., and Takahashi, L. K. (2004). Medial amygdala modulation of predator odor-induced unconditioned fear in the rat. *Behav. Neurosci.* 118, 324–332.

Lin, D., Boyle, M. P., Dollar, P., Lee, H., Lein, E. S., Perona, P., and Anderson, D. J. (2011). Functional identification of an aggression locus in the mouse hypothalamus. *Nature* 470, 221–226.

Luo, M., and Katz, L. C. (2004). Encoding pheromonal signals in the mammalian vomeronasal system. *Curr. Opin. Neurobiol.* 14, 428–434.

Majak, K., and Pitkänen, A. (2003). Projections from the periamygdaloid cortex to the amygdaloid complex, the hippocampal formation, and the parahippocampal region: a PHA-L study in the rat. *Hippocampus* 13, 922–942.

Maragos, W. F., Newman, S. W., Lehman, M. N., and Powers, J. B. (1989). Neurons of origin and fiber trajectory of amygdalofugal projections to the medial preoptic area in Syrian hamsters. *J. Comp. Neurol.* 280, 59–71.

Maras, P. M., and Petrulis, A. (2010a). Anatomical connections between the anterior and posterodorsal sub-regions of the medial amygdala: integration of odor and hormone signals. *Neuroscience* 170, 610–622.

Maras, P. M., and Petrulis, A. (2010b). The anterior medial amygdala transmits sexual odor information to the posterior medial amygdala and related forebrain nuclei. *Eur. J. Neurosci.* 32, 469–482.

Maras, P. M., and Petrulis, A. (2010c). Lesions that functionally disconnect the anterior and posterodorsal sub-regions of the medial amygdala eliminate opposite sex odor preference in male Syrian hamsters (*Mesocricetus auratus*). *Neuroscience* 165, 1052–1062.

Martínez-García, F., Martínez-Ricós, J., Agustín-Pavón, C., Martínez-Hernández, J., Novejarque, A., and Lanuza, E. (2009). Refining the dual olfactory hypothesis: pheromone reward and odour experience. *Behav. Brain Res.* 200, 277–286.

Martínez-García, F., Novejarque, A., Gutiérrez-Castellanos, N., and Lanuza, E. (2012). "Chapter 6 - Piriform Cortex and Amygdala," in *The Mouse Nervous System*, eds C. Watson, G. Paxinos, and L. Puelles (San Diego, CA: Academic Press), 140–172.

Martínez-Hernández, J., Lanuza, E., and Martínez-García, F. (2006). Selective dopaminergic lesions of the ventral tegmental area impair preference for sucrose but not for male sexual pheromones in female mice. *Eur. J. Neurosci.* 24, 885–893.

Martinez, R. C., Carvalho-Netto, E. F., Ribeiro-Barbosa, E. R., Baldo, M. V., and Canteras, N. S. (2011). Amygdalar roles during exposure to a live predator and to a predator-associated context. *Neuroscience* 172, 314–328.

Martínez-Ricós, J., Agustín-Pavón, C., Lanuza, E., and Martínez-García, F. (2007). Intraspecific communication through chemical signals in female mice: reinforcing properties of involatile male sexual pheromones. *Chem. Senses* 32, 139–148.

Martínez-Ricós, J., Agustín-Pavón, C., Lanuza, E., and Martínez-García, F. (2008). Role of the vomeronasal system in intersexual attraction in female mice. *Neuroscience* 153, 383–395.

Meredith, M., and Westberry, J. M. (2004). Distinctive responses in the medial amygdala to same-species and different-species pheromones. *J. Neurosci.* 24, 5719–5725.

Mitra, S. W., Hoskin, E., Yudkovitz, J., Pear, L., Wilkinson, H. A., Hayashi, S., Pfaff, D. W., Ogawa, S., Rohrer, S. P., Schaeffer, J. M., McEwen, B. S., and Alves, S. E. (2003). Immunolocalization of estrogen receptor beta in the mouse brain: comparison with estrogen receptor alpha. *Endocrinology* 144, 2055–2067.

Moncho-Bogani, J., Lanuza, E., Hernández, A., Novejarque, A., and Martínez-García, F. (2002). Attractive properties of sexual pheromones in mice: innate or learned? *Physiol. Behav.* 77, 167–176.

Motta, S. C., Goto, M., Gouveia, F. V., Baldo, M. V., Canteras, N. S., and Swanson, L. W. (2009). Dissecting the brain's fear system reveals the hypothalamus is critical for responding in subordinate conspecific intruders. *Proc. Natl. Acad. Sci. U.S.A.* 106, 4870–4875.

Nader, K., Majidishad, P., Amorapanth, P., and LeDoux, J. E. (2001). Damage to the lateral and central, but not other, amygdaloid nuclei prevents the acquisition of auditory fear conditioning. *Learn. Mem.* 8, 156–163.

Newman, S. W. (1999). The medial extended amygdala in male reproductive behavior. A node in the mammalian social behavior network. *Ann. N.Y. Acad. Sci.* 29, 242–257.

Nodari, F., Hsu, F. F., Fu, X., Holekamp, T. F., Kao, L. F., Turk, J., and Holy, T. E. (2008). Sulfated steroids as natural ligands of mouse pheromone-sensing neurons. *J. Neurosci.* 28, 6407–6418.

Novejarque, A., Gutiérrez-Castellanos, N., Lanuza, E., and Martínez-García, F. (2011). Amygdaloid projections to the ventral striatum in mice: direct and indirect chemosensory inputs to the brain reward system. *Front. Neuroanat.* 5:54. doi: 10.3389/fnana.2011.00054

Otto, T., Cousens, G., and Herzog, C. (2000). Behavioral and neuropsychological foundations of olfactory fear conditioning. *Behav. Brain Res.* 110, 119–128.

Papes, F., Logan, D. W., and Stowers, L. (2010). The vomeronasal organ mediates interspecies defensive behaviors through detection of protein pheromone homologs. *Cell* 141, 692–703.

Paxinos, G., and Franklin, K. B. J. (2004). *The Mouse Brain in Stereotaxic Coordinates,* 3rd Edn. San Diego, CA: Academic Press.

Petrovich, G. D., Canteras, N. S., and Swanson, L. W. (2001). Combinatorial amygdalar inputs to hippocampal domains and hypothalamic behavior systems. *Brain Res. Brain Res. Rev.* 38, 247–289.

Petrovich, G. D., Risold, P. Y., and Swanson, L. W. (1996). Organization of projections from the basomedial nucleus of the amygdala: a PHAL study in the rat. *J. Comp. Neurol.* 374, 387–420.

Petrulis, A. (2009). Neural mechanisms of individual and sexual recognition in Syrian hamsters (*Mesocricetus auratus*). *Behav. Brain Res.* 200, 260–267.

Petrulis, A., and Johnston, R. E. (1999). Lesions centered on the medial amygdala impair scent-marking and sex-odor recognition but spare discrimination of individual odors in female golden hamsters. *Behav. Neurosci.* 113, 345–357.

Pitkänen, A. (2000). "Connectivity of the rat amygdaloid complex," in *The Amygdala. A Function Alanalysis,* 2nd Edn. ed J. P. Aggleton (Oxford, UK: Oxford University Press), 31–115.

Powers, J. B., and Winans, S. S. (1975). Vomeronasal organ: critical role in mediating sexualbehavior of the male hamster. *Science* 187, 961–963.

Pro-Sistiaga, P., Mohedano-Moriano, A., Ubeda-Bañon, I., Del Mar Arroyo-Jimenez, M., Marcos, P., Artacho-Pérula, E., Crespo, C., Insausti, R., and Martinez-Marcos, A. (2007). Convergence of olfactory and vomeronasal projections in the rat basal telencephalon. *J. Comp. Neurol.* 504, 346–362.

Ramm, S. A., Cheetham, S. A., and Hurst, J. L. (2008). Encoding choosiness: female attraction requires prior physical contact with individual male scents in mice. *Proc. Biol. Sci.* 275, 1727–1735.

Rivière, S., Challet, L., Fluegge, D., Spehr, M., and Rodriguez, I. (2009). Formyl peptidereceptor-like proteins are a novel family of vomeronasal chemosensors. *Nature* 459, 574–577.

Roberts, S. A., Simpson, D. M., Armstrong, S. D., Davidson, A. J., Robertson, D. H., McLean, L., Beynon, R. J., and Hurst, J. L. (2010). Darcin: a male pheromone that stimulates female memory and sexual attraction to an individual male's odour. *BMC Biol.* 8, 75.

Rosen, J. B., Hitchcock, J. M., Sananes, C. B., Miserendino, M. J., and Davis, M. (1991). A direct projection from the central nucleus of the amygdala to the acoustic startle pathway: anterograde and retrograde tracing studies. *Behav. Neurosci.* 105, 817–825.

Samuelsen, C. L., and Meredith, M. (2009). Categorization of biologically relevant chemicalsignals in the medial amygdala. *Brain Res.* 1263, 33–42.

Scalia, F., and Winans, S. S. (1975). The differential projections of the olfactory bulb and accessory olfactory bulb in mammals. *J. Comp. Neurol.* 161, 31–55.

Shiflett, M. W., and Balleine, B. W. (2010). At the limbic-motor interface: disconnection of basolateral amygdala fromnucleus accumbens core and shell reveals dissociable components of incentive motivation. *Eur. J. Neurosci.* 32, 1735–1743.

Shin, J. W., Geerling, J. C., and Loewy, A. D. (2008). Inputs to the ventrolateral bed nucleus of the stria terminalis. *J. Comp. Neurol.* 511, 628–657.

Simerly, R. B. (2002). Wired for reproduction: organization and development of sexually dimorphic circuits in the mammalian forebrain. *Annu. Rev. Neurosci.* 25, 507–536.

Simerly, R. B., Chang, C., Muramatsu, M., and Swanson, L. W. (1990). Distribution of androgen and estrogen receptor mRNA-containing cells in the rat brain: an *in situ* hybridization study. *J. Comp. Neurol.* 294, 76–95.

Stuber, G. D., Sparta, D. R., Stamatakis, A. M., van Leeuwen, W. A., Hardjoprajitno, J. E., Cho, S., Tye, K. M., Kempadoo, K. A., Zhang, F., Deisseroth, K., and Bonci, A. (2011). Excitatory transmission from the amygdala to nucleus accumbens facilitates reward seeking. *Nature* 475, 377–380.

Swann, J., Fabre-Nys, C., and Barton, R. (2009). "Hormonal and pheromonal modulation of the extended amygdala: implications for social behaviour," in *Hormones, Brain and Behavior,* 2nd Edn. eds D. W. Pfaff, A. P. Arnold, S. E. Fahrbach, A. M. Etgen, and R. T. Rubin (New York, NY: Academic Press, Elsevier), 441–472.

Swanson, L. W. (2000). Cerebral hemisphere regulation of motivated behavior. *Brain Res.* 886, 113–164.

Swanson, L. W., and Petrovich, G. D. (1998). What is the amygdala? *Trends Neurosci.* 21, 323–331.

Takahashi, L. K., Hubbard, D. T., Lee, I., Dar, Y., and Sipes, S. M. (2007). Predator odor-induced conditioned fear involves the basolateral and medial amygdala. *Behav. Neurosci.* 121, 100–110.

Tirindelli, R., Mucignat-Caretta, C., and Ryba, N. J.(1998). Molecular aspects of pheromonal communication via the vomeronasal organ of mammals. *Trends Neurosci.* 21, 482–486.

Ubeda-Bañon, I., Novejarque, A., Mohedano-Moriano, A., Pro-Sistiaga, P., Insausti, R., Martínez-García, F., Lanuza, E., and Martinez-Marcos, A. (2008). Vomeronasal inputs to the rodent ventral striatum. *Brain Res. Bull.* 75, 467–473.

Usunoff, K. G., Schmitt, O., Itzev, D. E., Haas, S. J., Lazarov, N. E., Rolfs, A., and Wree, A. (2009). Efferent projections of the anterior and posterodorsal regions of the medial nucleus of the amygdala in the mouse. *Cells Tissues Organs* 190, 256–285.

Vale, J. R., Ray, D., and Vale, C. A. (1973). The interaction of genotype and exogenous neonatal androgen and estrogen: sex behavior in female mice. *Dev. Psychobiol.* 6, 319–327.

Vale, J. R., Ray, D., and Vale, C. A. (1974). Neonatal androgen treatment and sexual behavior in males of three inbred strains of mice. *Dev. Psychobiol.* 7, 483–488.

Vertes, R. P., and Hoover, W. B. (2008). Projections of the paraventricular and paratenial nuclei of the dorsal midline thalamus in the rat. *J. Comp. Neurol.* 508, 212–237.

Vertes, R. P., Hoover, W. B., Do Valle, A. C., Sherman, A., and Rodriguez, J. J. (2006). Efferent projections of reuniens and rhomboid nuclei of the thalamus in the rat. *J. Comp. Neurol.* 499, 768–796.

Walker, D. L., Paschall, G. Y., and Davis, M. (2005). Glutamate receptor antagonist infusions into the basolateral and medial amygdala reveal differential contributions to olfactory vs. context fear conditioning and expression. *Learn. Mem.* 12, 120–129.

Wang, Z., Bullock, N. A., and De Vries, G. J. (1993). Sexual differentiation of vasopressin projections of the bed nucleus of the stria terminals and medial amygdaloid nucleus in rats. *Endocrinology* 132, 2299–2306.

Wesson, D. W., and Wilson, D. A. (2011). Sniffing out the contributions of the olfactory tubercle to the sense of smell: hedonics, sensory integration, and more? *Neurosci. Biobehav. Rev.* 35, 655–668.

Wood, R. I., Brabec, R. K., Swann, J. M., and Newman, S. W. (1992). Androgen andestrogen concentrating neurons in chemosensory pathways of themale Syrian hamster brain. *Brain Res.* 596, 89–98.

Yang, M., Augustsson, H., Markham, C. M., Hubbard, D. T., Webster, D., Wall, P. M., Blanchard, R. J., and Blanchard, D. C. (2004). The rat exposure test: a model of mouse defensive behaviors. *Physiol. Behav.* 81, 465–473.

Zufall, F., and Leinders-Zufall, T. (2007). Mammalian pheromone sensing. *Curr. Opin. Neurobiol.* 17, 483–489.

Conflict of Interest Statement: The authors declare that the research was conducted in the absence of any commercial or financial relationships that could be construed as a potential conflict of interest.

Received: 18 May 2012; accepted: 27 July 2012; published online: 21 August 2012.
Citation: Pardo-Bellver C, Cádiz-Moretti B, Novejarque A, Martínez-García F and Lanuza E (2012) Differential efferent projections of the anterior, posteroventral, and posterodorsal subdivisions of the medial amygdala in mice. Front. Neuroanat. ***6****:33. doi: 10.3389/fnana.2012.00033*

frontiers in
NEUROANATOMY

ORIGINAL RESEARCH ARTICLE
published: 30 August 2012
doi: 10.3389/fnana.2012.00035

A further analysis of olfactory cortex development

María Pedraza and Juan A. De Carlos*

Lab of Telencephalic Development (A-21), Department of Molecular, Cellular and Developmental Neuroscience, Instituto Cajal (Consejo Superior de Investigaciones Científicas), Madrid, Spain

Edited by:
Jorge A. Larriva-Sahd, Universidad Nacional Autónoma de México, Mexico

Reviewed by:
Antonio Pereira, Federal University of Rio Grande do Norte, Brazil
Patricia Gaspar, INSERM, France
Veronica Martinez-Cerdeno, University of California at Davis, USA

***Correspondence:**
Juan A. De Carlos, Lab of Telencephalic Development (A-21), Department of Molecular, Cellular and Developmental Neuroscience, Instituto Cajal (Consejo Superior de Investigaciones Científicas), Avenida del Doctor Arce, 37, Madrid, Spain.
e-mail: decarlos@cajal.csic.es

The olfactory cortex (OC) is a complex yet evolutionarily well-conserved brain region, made up of heterogeneous cell populations that originate in different areas of the developing telencephalon. Indeed, these cells are among the first cortical neurons to differentiate. To date, the development of the OC has been analyzed using birthdating techniques along with molecular markers and *in vivo* or *in vitro* tracking methods. In the present study, we sought to determine the origin and adult fate of these cell populations using ultrasound-guided *in utero* injections and electroporation of different genomic plasmids into the lateral walls of the ventricles. Our results provide direct evidence that in the mouse OC, cell fate is determined by the moment and place of origin of each specific cell populations. Moreover, by combining these approaches with the analysis of specific cell markers, we show that the presence of pallial and subpallial markers in these areas is independent of cell origin.

Keywords: mouse, olfactory system, pallium, subpallium, Tbr1

INTRODUCTION

The cell populations that give rise to different structures during the embryonic development of the nervous system originate in multiple and distinct germinative regions, frequently far from the site at which they ultimately settle. These cells migrate along well-established routes to occupy their final position and differentiate into adult neurons. Accordingly, neuroblast displacement is a source of cellular variability in any given structure. Neuroblasts migrate using radial and/or tangential migratory pathways. While radial movement involves the use of the radial glia as a scaffold (Rakic, 1972), tangential migration occurs independent of glial cells and follows an orthogonal route, parallel to the pial surface. This latter form of migration allows migratory cells to colonize locations at a significant distance from their origin (De Carlos et al., 1996; García-Moreno et al., 2010).

It has been proposed that each encephalic structure is comprised of multiple cell populations that are generated at diverse locations during a specific embryonic time-window, each expressing distinctive cell markers (García-Moreno et al., 2008). However, extreme caution is required when attributing a specific marker to a given cell population, which may display non-uniform expression during its spatio-temporal development. Several specific markers for distinct areas of the nervous system have been described. For example, the telencephalon is anatomically divided into the pallium and subpallium, due to the influence of dorsal (Lee and Jessell, 1999; Liem et al., 2000) and ventral (Echelard et al., 1993; Fan and Tessier-Lavigne, 1994; Martí et al., 1995) cues during development. These zones give rise to cell populations that express specific markers, such as the T-box brain 1 (Tbr1), proposed to be a typical marker of pallium-derived cells (Puelles et al., 2000). However, Tbr1 expression in pallial cells has also been described, regardless of their site of origin (Bulfone et al., 1995).

The olfactory cortex (OC) is composed of a variety of structures located in the most ventrolateral region of the mammalian telencephalon, namely the anterior olfactory nucleus, olfactory tubercle (OT), piriform cortex (PC), olfactory amygdaloid nuclei, and enthorrinal cortex (EC). Efferent projections from the olfactory bulb converge to form the lateral olfactory tract (lot), which runs through the outer portion of the PC. In rodents, the OC is one of the first structures to form in the telencephalon, even before the neocortex (García-Moreno et al., 2008). Several proliferative areas have been described from which cells migrate toward the OC, specifically colonizing the PC and OT. These include the lateral ganglionic eminence (LGE), dorsal telencephalon, rostromedial telencephalic wall, and the septoeminential sulcus. Each area gives rise to a cell population expressing specific markers in the embryo, including Tbr1, calretinin (CR), calbindin (CB), and reelin (Reln). However, the differentiation of these cells, which are derived from distinct germinative areas, and their expression during the development of the OC remain poorly understood. To better understand how this structure matures and how the distinct cell populations that contribute to this tissue are established, we have studied the expression of specific markers (Tbr1, CR, CB, and Reln) during the development of the OC.

MATERIALS AND METHODS

ANIMALS

C57BL6 mice were raised at the animal facility of the Cajal Institute, in compliance with the current Spanish legislation (R.D. 1201/2005 and L.32/2007) and European Union

Council Guidelines (2003/65/CE) concerning the care and use of experimental animals. The day of detection of the vaginal plug was considered embryonic day 0 (E0). Embryos were anesthetized by hypothermia, while pregnant mice ($n = 10$) were anesthetized by intraperitoneal injection with Equithesin (3 mL/kg body weight). Thirty embryos were used for immunohistochemistry studies and an additional 20 were electroporated *in utero*. The distribution of the animals used and their survival time is shown in the table below.

	Pregnant mice	E11	E12	E14	E18	P15	
Immunohistochemistry	7		8	8	8	6	
In utero experiments	3	20	Survival until P15				75%

ULTRASOUND-GUIDED *in utero* PLASMID INJECTIONS AND ELECTROPORATION

The plasmids used were pPB-Ubc-EGFP and mPBase (transposase), kindly provided by Prof. A. Bradley [Cambridge, UK; plasmid described in Yusa et al. (2009)]. The GFP-plasmid contains specific regions recognized by the transposase that facilitates its integration into the genome. Using an ultrasound guided injection system (VeVo 770®:VisualSonics Inc. Toronto, Canada), embryos were injected to specifically label newly generated cells (pallium or subpallium). Briefly, E10–E12 pregnant mice were anesthetized with isoflurane (Isova vet, ref. 240055: Centauro, Barcelona, Spain), their uterine horns were exposed through the abdominal wall and they were covered with pre-warmed ultrasound gel (Parker Laboratories Inc., NJ, USA). A volume of 1–2 μl of the recombinant plasmid solution was injected in the lateral ventricle of each embryo and they were electroporated with 5 pulses (50 ms) using a BTX Electroporator ECM 830 (BTX: MA, USA). Electroporation was achieved by discharging a 500 μF capacitor charged to 25 V with a sequencing power supply via a pair of round platinum plates (5 mm diameter). The uterine horns were then set back into the abdominal cavity, which was filled with warm physiological saline, and the abdominal muscle and skin were closed with silk sutures. After surgery, pregnant mice received a subcutaneous injection of the antibiotic enrofloxacine (Baytril, 5 mg/Kg: Bayer, Leverkusen, Germany) and an intraperitoneal injection of the anti-inflammatory/analgesic ketorolac (Droal, 300 μg/Kg VITA Laboratories, Barcelona, Spain). The injected embryos were transcardially perfused at postnatal stages, with 4% paraformaldehyde (PF) in 0.1 M phosphate buffer (PB, pH 7.2), and their brains were removed, embedded in agar, and coronal sectioned at 50 μm with a vibratome.

IMMUNOHISTOCHEMISTRY

Single and dual immunohistochemistry was performed as described previously (García-Moreno et al., 2008), using the following primary antibodies: mouse-anti-Reelin (1:1000; MAB5364, Clone G10, Chemicon; Temecula, CA); rabbit-anti-Calbindin-D28K (1:10,000; CB38, Swant, Bellinzona, Switzerland); rabbit-anti-Calretinin antiserum (1:2000; 7699/4, CR, Swant); rabbit-anti-Tbr1 (1:1000; AB9616, Chemicon); rat-anti-GFP (1:20,000; 4404-84, Nacalai Tesque, Kyoto, Japan).

The following secondary antibodies were used: Alexa 568 goat-anti-rabbit IgG (1:2000; A11011, Molecular Probes); Alexa 568 anti-mouse IgG (1:2000; A11004, Molecular Probes); Alexa 488 anti-rat (1:2000; A11034, Molecular Probes).

For all antibodies a series of control sections was processed without the primary antibody in which no specific staining was detected. Sections were mounted on gelatinized slides and counterstained with 0.002% bisbenzimide in PBS (Hoechst 33258: Sigma, St. Louis, MO).

EQUIPMENT AND SETTINGS

Injected embryos were examined under a fluorescence-dissecting microscope (Leica MZFL-III) and after mounting with a mixture of glycerol-phosphate buffer (PB, 1:1), fluorescent sections were analyzed under a fluorescent microscope (Nikon, Eclipse E600) equipped with a digital camera (Nikon DMX 1200F) and the appropriate filter cubes: rhodamine (569–610 nm) and fluorescein (450–490 nm), to visualize Alexa 568 and GFP/Alexa 488, respectively. Bisbenzimide labeling was analyzed with ultraviolet illumination.

RESULTS

TEMPORAL EXPRESSION PATTERNS IN THE OLFACTORY CORTEX

To analyze the spatio-temporal expression of different proteins during the development of the OC, we performed immunohistochemistry for the following markers at E12, E14, E18, and in adulthood: Tbr1, CR, CB, and Reln.

Tbr1 expression during olfactory cortex development

At the earliest selected embryonic stage, E12, significant Tbr1 expression was observed in the rostral and caudal areas of the PC (**Figures 1A,B**), and in the mantle zone of the LGE, but not in the OT. At E14, Tbr1 expression was clearly detected in both the cortical neuroepithelium and the PC (**Figures 2A,B**), and Tbr1 was consistently expressed from the rostral to caudal portions of the PC. At E18, Tbr1 expression was restricted to the PC and endopiriform nucleus (End; **Figures 3A,B**), and finally, Tbr1 expression was restricted to layers II and III in the mature PC (**Figures 4A,B**).

CR expression during olfactory cortex development

The expression pattern of CR observed at E12 was similar to that of Tbr1, albeit more restricted to the PC (**Figures 1C,D**), with no labeling observed in the OT. CR expression persisted in the PC at E14 (**Figures 2C,D**) and this protein was also detected in the lot (**Figure 2D**). CR expression in the lot was maintained at E18 (**Figures 3C,D**) and in adult mice (**Figure 4C**), as well as in layer II of the PC (**Figures 4C,D**).

CB expression during olfactory cortex development

In contrast to Tbr1 and CR, at E12 (**Figures 1E,F**) and E14 (**Figures 2E,F**) CB expression was restricted to the OT, with no labeling detected in the PC. Similarly, unlike Tbr1 and CR, CB expression was limited to the End at E18 (**Figure 3E**) and in adulthood, CB expression was limited to layer III of the PC (**Figures 4E,F**).

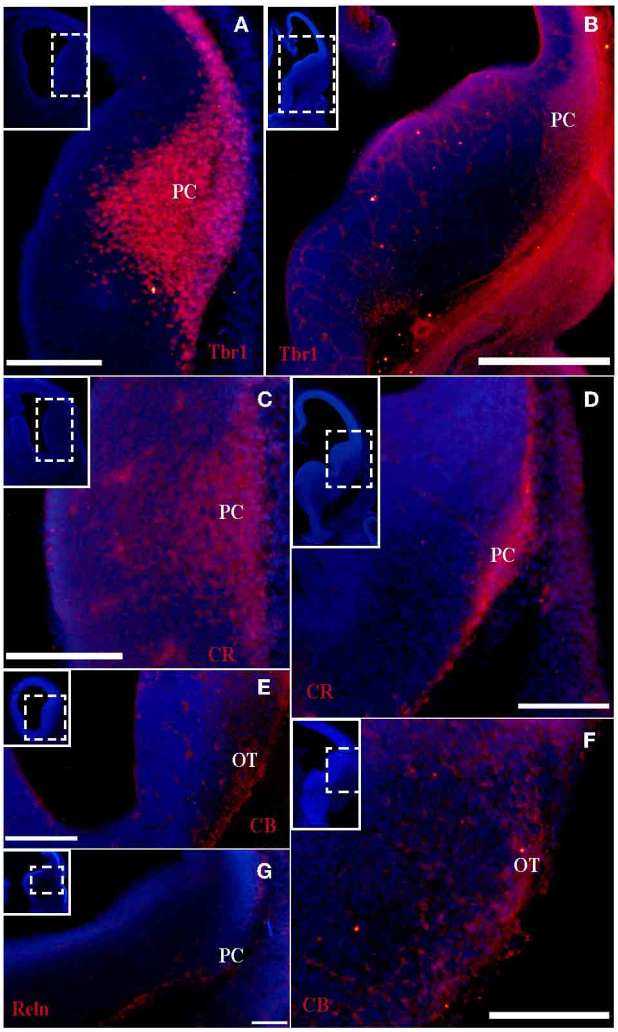

FIGURE 1 | Tbr1, CR, CB, and Reln (red) expression in the olfactory cortex at E12. (A–D) Tbr1 and CR expression in the rostral and caudal regions of the piriform cortex. **(E,F)** CB is expressed in the OT but not the PC. **(G)** Reln expression is restricted to the outermost portion of the PC. Coronal sections; midline is to the left and dorsal is up. Blue corresponds to the bisbenzimide counterstaining. Scale bars: **A–F**, 500 μm; **G**, 100 μm.

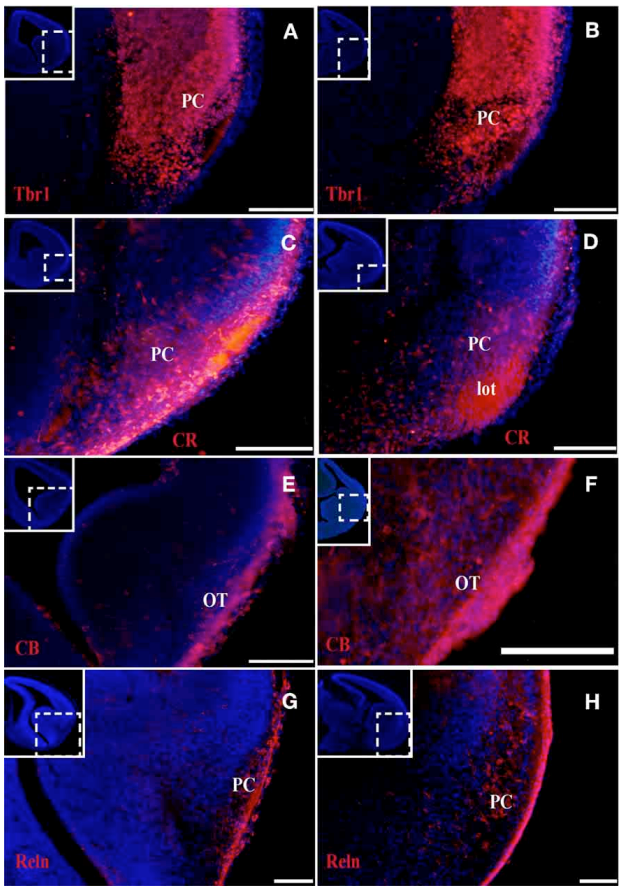

FIGURE 2 | Tbr1, CR, CB, and Reln (red) expression in the olfactory cortex at E14. (A–D) Tbr1 and CR expression in the rostral and the caudal regions of the piriform cortex. CR expression in the lot **(D)**. **(E,F)** CB is expressed in the OT but not the PC. **(G,H)** Reln expression is restricted to the outermost portion of the PC. Coronal sections; midline is to the left and dorsal is up. Blue corresponds to the bisbenzimide counterstaining. Scale bars: **A–F**, 500 μm; **G** and **H**, 100 μm.

Reln expression during olfactory cortex development

Reln expression at E12 was limited to the most superficial portion of PC (**Figure 1G**). At E14, this pattern had changed and Reln occupied the inner portion of the PC (**Figures 2G,H**). A global increase in Reln expression was observed at later stages.

MARKERS ASSOCIATED WITH SITES OF CELL ORIGIN

Because cell tracers did not allow all pallial/subpallial-derived cells to be identified, we tracked cells originating in the pallial or subpallial areas and characterized them at the molecular level upon reaching their destiny.

In order to mark the injection site (site of cell origin) throughout our lengthy experiments, we electroporated a GFP-expressing plasmid that becomes integrated into the genome of the cells. If integration is not achieved, the tagged plasmid is diluted over successive cell divisions and ultimately disappears, providing a means of identifying the precise area where electroporation occurred (site of origin of the labeled cells).

At P15, GFP cells transfected in the pallium at E11 were detected in the OC (**Figures 5A–C**). Despite being generated in pallium (with no contamination from subpallial areas; **Figure 5A**), we observed few GFP cells co-expressing Tbr1, which has been proposed as a marker of pallial-generated cells (**Figures 5A,B**), and we detected no pallial-generated cells expressing CR (**Figure 5C**). Unexpectedly, after electroporation of cells generated in the subpallium (**Figure 5D**), most GFP cells co-expressed Tbr1 (**Figure 5E**) but not CR (**Figure 5F**) in the OC.

DISCUSSION

RESTRICTION AND SPECIFICITY OF MARKERS IN DIFFERENT AREAS DURING THE DEVELOPMENT OF THE OLFACTORY CORTEX

Marker expression in distinct telencephalic cell populations varies during embryonic development and adulthood. This reflects

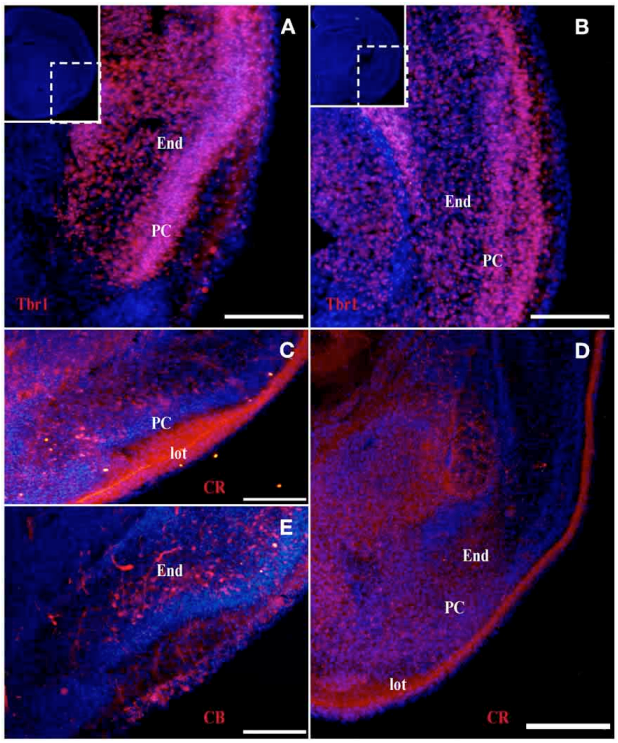

FIGURE 3 | Tbr1, CR, and CB (red) expression in the olfactory cortex at E18. (A–D) Tbr1 and CR expression in the rostral and the caudal regions of the piriform cortex. Both Tbr1 and CR are expressed in the End **(A,B,D)**, whereas only CR is expressed in the lot **(C)**. **(E)** CB is only expressed in the End. Coronal sections; midline is to the left and dorsal is up. Blue corresponds to the bisbenzimide counterstaining. Scale bars: 500 μm.

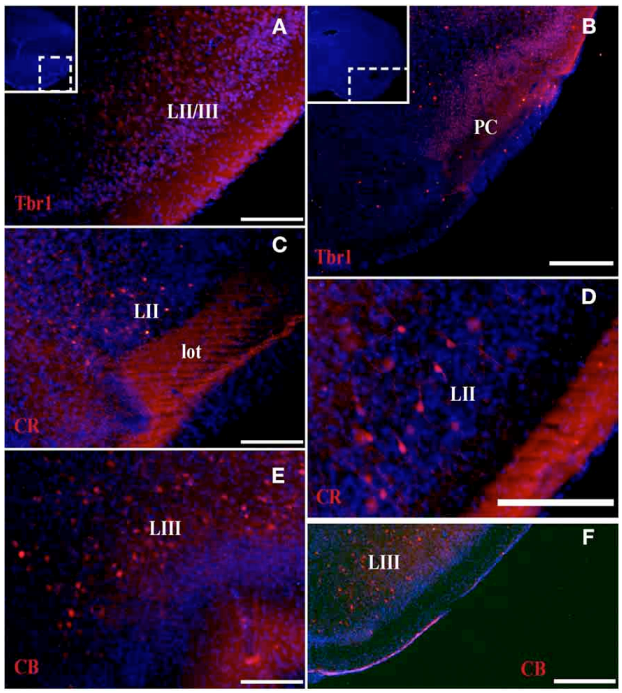

FIGURE 4 | Tbr1, CR, and CB (red) expression in the olfactory cortex in adult mice. (A,B) Tbr1 expression in layers II and III of the PC. **(C,D)** CR is expressed in layer II of the PC and in the lot. **(E,F)** CB expression is restricted to the layer III in the piriform cortex. Coronal sections; midline is to the left and dorsal is up. Blue corresponds to the bisbenzimide counterstaining. Scale bars: 500 μm.

either the cellular contribution of different germinative areas, the rearrangement of distinct cell populations, and the silencing or new expression of specific markers.

The formation of the OC begins early in development and continues throughout the embryonic stages. This region is comprised of several structures that are formed by many cell populations that originate in diverse areas of the telencephalon (García-Moreno et al., 2008), resulting in significant phenotypic variability. Accordingly, the different markers analyzed are not expressed constantly throughout development. We previously demonstrated that at early developmental stages, Tbr1, Reln, and CR serve as specific markers of the presumptive PC, while CB is expressed in the presumptive OT (García-Moreno et al., 2008). In the present study, we performed a temporal analysis of these markers from early murine developmental stages through adulthood.

Tbr1 expression was relatively constant throughout development, and was initially expressed in the presumptive PC before it was subsequently limited to layers II and III in adulthood. CR expression was constant in the PC throughout development, but was restricted to layer II and the lot in the adult OC. By contrast, CB labeling was absent in the embryonic OC, but was expressed in layer III of the PC in adult mice. Reln expression was profusely observed in early embryonic stages and becomes diffuse in late stages.

In summary, because Tbr1 and CR expression remain constant throughout the development of the OC, they represent valid and useful markers of specific structures within the OC. The same cannot be said of CB and Reln, due to their fluctuating expression during the development of the OC.

Tbr1 AS A USEFUL STRUCTURAL MARKER BUT IS NOT A RELIABLE MARKER OF PALLIAL-DERIVED CELLS

The origins of diverse brain structures remains a contentious issue, in part because most studies are based on the use of specific markers, the expression of which may fluctuate during development. We propose that these currently used tracking methods are inadequate and as such, we have tracked the development of two specific cell populations derived from the pallium and subpallium. Although electroporation labels a larger area than that labeled using tracers (such as CFDA) or retroviruses, this experimental approach allows the origin of the labeled cells to be identified (taking into account that we labeled either pallial or subpallial origins, but not both), which is not possible using the other methods cited above. Thus, this technique allowed us to analyze the migration of some cell populations from their site of generation to the OC.

While Tbr1 has been proposed as a specific marker of pallium-derived cells (Puelles et al., 2000), our findings demonstrate that the OC contains many cells of pallial origin that do not express

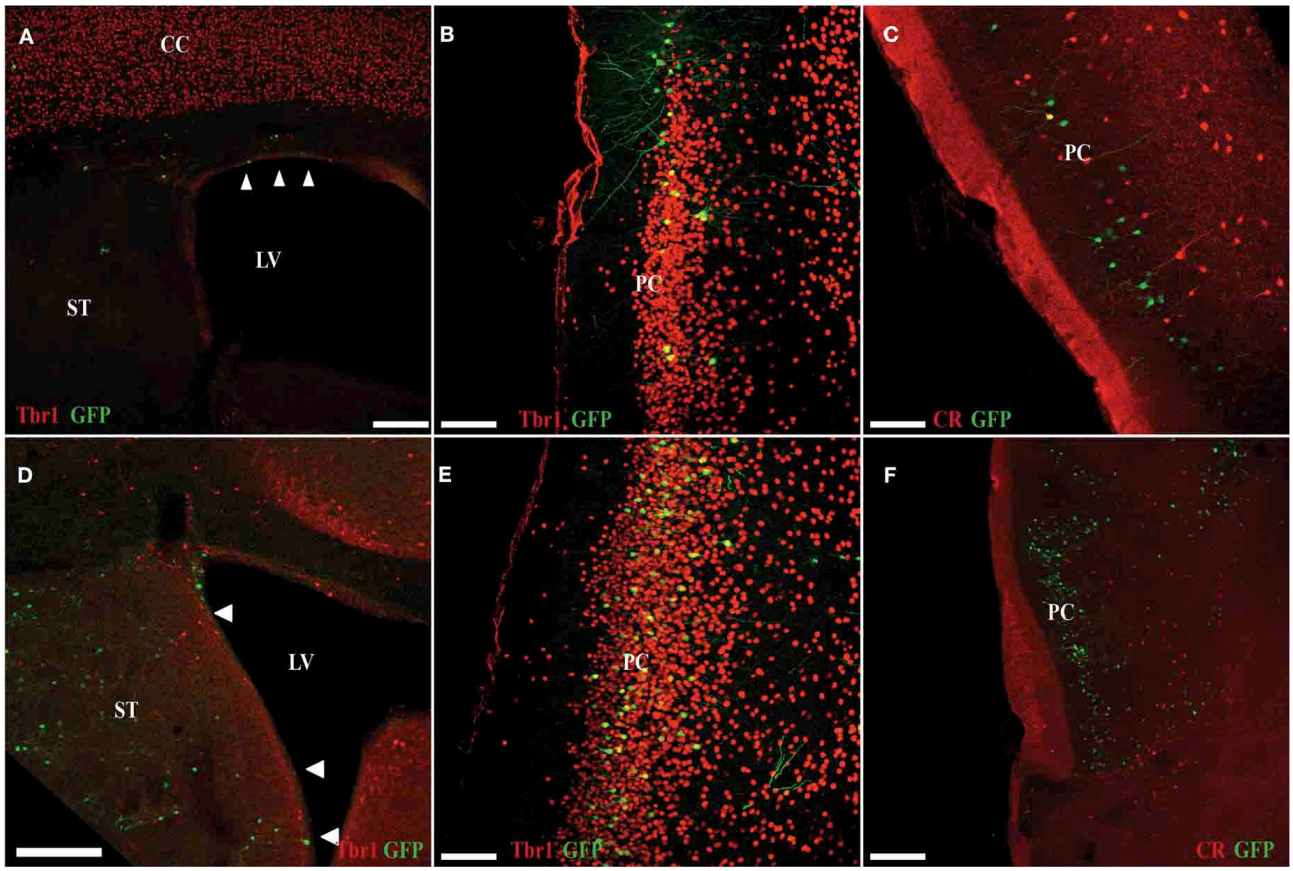

FIGURE 5 | Electroporation of a GFP plasmid into pallial (A–C) and subpallial (D–F) areas of E11 mice (sacrificed at P5). (A–C) Many of GFP cells that originate in the ventricular zone of the pallium (green) do not co-express Tbr1 (red; **A,B**). **(C)** Pallial-derived GFP cells do not express CR (red). **(D–F)** Many of the GFP-cells that originate in the ventricular zone of the subpallium (green) co-express Tbr1 (red; **D,E**). **(F)** Subpallial-derived cells do not express CR (red). Coronal sections; midline is to the right and dorsal is up. Scale bars: **A,D**, 200 μm; **B,C,E,F**, 100 μm.

this marker. Moreover, we found that many cells originating in subpallium express this marker in the OC. Taken together, these results underscore the importance of using cellular tracking methods to determine the origin of different cell populations, instead of relying solely on the expression patterns of specific cell markers.

ACKNOWLEDGMENTS

Work supported by grant BFU2010-21377 from the Spanish Ministerio de Ciencia e Innovación. We thank Sandra Rodríguez and Raul Nuñez for technical assistance and Mark Sefton for editorial assistance. This paper is dedicated to José Pedraza.

REFERENCES

Bulfone, A., Smiga, S. M., Shimamura, K., Peterson, A., Puelles, L., and Rubenstein, J. L. (1995). T-brain-1, a homolog of Brachyury whose expression defines molecularly distinct domains within the cerebral cortex. *Neuron* 15, 63–78.

De Carlos, J. A., López-Mascaraque, L., and Valverde, F. (1996). Dynamics of cell migration from the lateral ganglionic eminence in the rat. *J. Neurosci.* 16, 6146–6156.

Echelard, Y., Epstein, D. J., St-Jacques, B., Shen, L., Mohler, J., McMahon, J. A., and McMahon, A. P. (1993). Sonic hedgehog, a member of a family of putative signaling molecules, is implicated in the regulation of CNS polarity. *Cell* 75, 1417–1430.

Fan, C. M., and Tessier-Lavigne, M. (1994). Patterning of mammalian somites by surface ectoderm and notochord: evidence for sclerotome induction by a hedgehog homolog. *Cell* 79, 1175–1186.

García-Moreno, F., López-Mascaraque, L., and De Carlos, J. A. (2008). Early telencephalic migration topographically converging in the olfactory cortex. *Cereb. Cortex* 18, 1239–1252.

García-Moreno, F., Pedraza, M., Di Giovannantonio, L. G., Di Salvio, M., López-Mascaraque, L., Simeone, A., and De Carlos, J. A. (2010). A neuronal migratory pathway crossing from diencephalon to telencephalon populates amygdala nuclei. *Nat. Neurosci.* 13, 680–689.

Lee, K. J., and Jessell, T. M. (1999). The specification of dorsal cell fates in the vertebrate central nervous system. *Annu. Rev. Neurosci.* 22, 261–294.

Liem, K. F. Jr., Jessell, T. M., and Briscoe, J. (2000). Regulation of the neural patterning activity of sonic hedgehog by secreted BMP inhibitors expressed by notochord and somites. *Development* 127, 4855–4866.

Martí, E., Bumcrot, D. A., Takada, R., and McMahon, A. P. (1995). Requirement of 19K form of Sonic hedgehog for induction of distinct ventral cell types in CNS explants. *Nature* 375, 322–325.

Puelles, L., Kuwana, E., Puelles, E., Bulfone, A., Shimamura, K., Keleher, J., Smiga, S., and Rubenstein, J. L. (2000). Pallial and subpallial derivatives in the embryonic chick and mouse

telencephalon, traced by the expression of the genes Dlx-2, Emx-1, Nkx-2.1, Pax-6, and Tbr-1. *J. Comp. Neurol.* 424, 409–438.

Rakic, P. (1972). Mode of cell migration to the superficial layers of fetal monkey neocortex. *J. Comp. Neurol.* 145, 61–84.

Yusa, K., Rad, R., Takeda, J., and Bradley, A. (2009). Generation of transgene-free induced pluripotent mouse stem cells by the piggyBac transposon. *Nat. Methods* 6, 363–369.

Conflict of Interest Statement: The authors declare that the research was conducted in the absence of any commercial or financial relationships that could be construed as a potential conflict of interest.

Received: 21 May 2012; accepted: 14 August 2012; published online: 30 August 2012.

Citation: Pedraza M and De Carlos JA (2012) A further analysis of olfactory cortex development. Front. Neuroanat. ***6****:35. doi: 10.3389/fnana.2012.00035*

frontiers in
NEUROANATOMY

ORIGINAL RESEARCH ARTICLE
published: 27 June 2012
doi: 10.3389/fnana.2012.00023

Cytological organization of the alpha component of the anterior olfactory nucleus and olfactory limbus

Jorge Larriva-Sahd*

Instituto de Neurobiología, Universidad Nacional Autónoma de México, Querétaro, México

Edited by:
Micheal Baum, Boston University, USA

Reviewed by:
Alino Martinez-Marcos, Universidad de Castilla, Spain
Daniel W. Wesson, Case Western Reserve University, USA

****Correspondence:***
Jorge Larriva-Sahd, Instituto de Neurobiología, Universidad Nacional Autónoma de México, Boulevard Juriquilla 3002,Querétaro, CP 76230, México.
e-mail: jlsneuro@unam.mx

This study describes the microscopic organization of a wedge-shaped area at the intersection of the main (MOB) and accessory olfactory bulbs (AOBs), or olfactory limbus (OL), and an additional component of the anterior olfactory nucleus or alpha AON that lies underneath of the AOB. The OL consists of a modified bulbar cortex bounded anteriorly by the MOB and posteriorly by the AOB. In Nissl-stained specimens the OL differs from the MOB by a progressive, antero-posterior decrease in thickness or absence of the external plexiform, mitral/tufted cell, and granule cell layers. On cytoarchitectual grounds the OL is divided from rostral to caudal into three distinct components: a stripe of glomerular-free cortex or preolfactory area (PA), a second or necklace glomerular area, and a wedge-shaped or interstitial area (INA) crowned by the so-called modified glomeruli that appear to belong to the anterior AOB. The strategic location and interactions with the main and AOBs, together with the previously noted functional and connectional evidence, suggest that the OL may be related to both sensory modalities. The alpha component of the anterior olfactory nucleus, a slender cellular cluster (i.e., 650 × 150 μm) paralleling the base of the AOB, contains two neuron types: a pyramidal-like neuron and an interneuron. Dendrites of pyramidal-like cells (P-L) organize into a single bundle that ascends avoiding the AOB to resolve in a trigone bounded by the edge of the OL, the AOB and the dorsal part of the anterior olfactory nucleus. Utrastructurally, the neuropil of the alpha component contains three types of synaptic terminals; one of them immunoreactive to the enzyme glutamate decarboxylase, isoform 67.

Keywords: olfactory limbus, interstitial neurons, anterior olfactory nucleus, cytology

INTRODUCTION

While the cytological organization of the rodent main and accessory olfactory bulbs (AOB) has been depicted and most of its constituent neurons are known, growing evidence suggests that the structural and functional differentiation of the bulbar cortex is not homogeneous. In fact, both the main (MOB) and AOBs possess distinct neurons embedded in a neuropil that yields the characteristic laminated appearance when studied with both silver and aniline stains (Macrides and Davis, 1983). Neurons in the MOB are distributed into two structural domains: a stratified cortex and a medulla or core. Periglomerular or juxtaglomerular superficial short axon neurons, external tufted, satellite, and von Gehughten cells are primarily found in the external granule and external plexiform (EPL) layers. A distinct row of mitral cells underscores the EPL. Below the mitral cell layer, there is a cell-poor stratum or internal plexiform area bounding the deeper granule cell layer that arbors the homonymous cells and scattered local circuit neurons, namely, Blanes, Cajal, and Golgi neurons (Valverde, 1965, see Kosaka and Kosaka, 2011). Neurons having structural and immunohistochemical features of interneurons may send collaterals to supragranular layers in the main and accessory (Larriva-Sahd, 2008) olfactory bulbs, or even send projecting fibers beyond the confines of the MOB (Kosaka and Kosaka, 2007; Eyre et al., 2008).

The bulbar medulla, pierced by a rostral extension of the lateral ventricle that in laboratory rodents obliterates after birth, contains clustered epithelial ependymal cells, and cell progentiors in various stages of differentiation (Doetsch et al., 1997) to granule and periglomerular cells (Lledo et al., 2008). An additional set of neurons, has been recently described in association with to the rostral migratory stream, the so-called "medullary neurons" (Paredes and Larriva-Sahd, 2010).

Although most neuron types found in the AOB mimic those encountered in the MOB, striking regional differences in their overall organization have been detected (see Larriva-Sahd, 2008). Indeed, structural and physiological evidence suggests that the transition between the MOB and AOB is not sharp. A distinct set of glomeruli outlining those in the posterior aspect of the MOB, and the foremost of the AOB, have been described. These glomeruli that have been referred to as the glomerular necklace (NG) (Shinoda et al., 1989), exhibit striking physiological (see Stowers and Logan, 2010) and, connectional (Ring et al., 1997;

Abbreviations: aAON, anterior olfactory nucleus, alpha component; AOB, Accessory olfactory bulb; EPL, external plexiform layer; GAD67, enzyme glutamic acid decarboxylase, isoform 67; GAD-i, immunoreactivity to the enzyme glutamic acid decarboxylase, isoform 67; INA, interstitial area of the olfactory limbus; INBi, Interstitial neuron bulbi, interneuron; INBp, Interstitial neuron bulbi, projecting cell; LOT, lateral olfactory tract; MOB, Main olfactory bulb; NG, necklace glomerulus; NGA, Olfactory limbus, area of the necklace glomeruli; OL, olfactory limbus; PA, Preolfactory area of the olfactory limbus; P-L, pyramidal-like cell.

Fuss et al., 2005) differences, from those in the rest of the bulbar cortex. Unlike olfactory glomeruli that are known to be responsive for volatile substances interacting with nasal olfactory receptors, modified glomeruli are selectively activated by a nipple-associated pheromone (Greer et al., 1982). Further, connectional evidence has defined that those glomeruli adjacent to the AOB represent a unique subset of the NG (Fuss et al., 2005) as they receive axons from the ganglion discovered by Grueneberg (1973) in the nasal vestibule. Interestingly, expression of mRNA's encoding neuromodulators (i.e., CCK and VIP) and hypothalamic releasing hormones (TRH and CRH) (Senba et al., 1990), is higher in both glomeruli and neuropil at the MOB-AOB boundary with respect to both the MOB and AOB themselves. Lastly, are the so-called interstitial neurons of the bulbi (INBs) that represent another marked structural specialization in the oral interaction of the AOB with the MOB. In fact, INBs seem to be a unique neuron group whose pyramidal-like and short axon neurons stand out from the native neurons populating the adjacent MOB and AOB (Larriva-Sahd, 2008).

A third small neuron group lies between the base of the AOB and the bulbar core white matter. Santiago Ramón y Cajal (1904) discovered this cluster in aniline-stained sections defining that it was composed by large, polygonal neurons, hence, different from those observed in the rest of the bulbar cortex. Likewise, in the 1960s Lohman (1963), studying the AON in Nissl-stained sections incorporated this nucleus to the "pars rostralis of the anterior olfactory nucleus." Similarly, Macrides and Davis (1983) endorsed this neuron group to the AON including it to the "dorsal sector of pars externa of the AON." Then, Valverde et al. (1989) outlined the first Golgi description of the "cell group alpha of the nucleus olfactorius anterior" (aAON). Lastly, DeCarlos et al. (1989) studying the connectivity of the AON in the same species, found that the "α group" projects to the contralateral MOB.

As part of a series of ongoing studies aimed at depicting the neuronal organization of the rodent rhinencephalon (Larriva-Sahd, 2008, 2010; Paredes and Larriva-Sahd, 2010), the present study was conducted to describe the cytological organization of the aAON and a complex region between the anterior aspect of the AOB and the caudal limit of the MOB. The study was primarily conducted in specimens from adult rats, although mouse and guinea—pig specimens from our collection were examined to define interspecies homology. The study combines silver, aniline, immunohistochemistry, and electron microscopic techniques.

MATERIALS AND METHODS

ANIMALS

Male Sprague-Dawley rats killed at 10 weeks of age were used. The animals were kept at constant temperature (24°C) and photoperiods (14 h light—10 h dark), with free access to food and water. All experimental manipulations and sacrifices were made according to the ethical policies of animal care and handling of our institute.

SILVER IMPREGNATIONS

Rapid golgi

Due to the capriciousness of impregnation obtained with the rapid-Golgi technique, 330 adult rat brains were used from our archive (Larriva-Sahd, 2008, 2010). Additionally, one-hundred brains from age-matched adult CD3 mice ($n = 90$) (Paredes and Larriva-Sahd, 2010) and guinea pigs ($n = 10$) were included. Each animal was sacrificed by decapitation under deep anesthesia with pentobarbital (30 mg/kg), and the brain was removed. Tissue blocks consisted of 3 to 4-mm-thick brain samples trimmed in sagittal, coronal, or horizontal planes. Each tissue block was left for 15–20 days in an aqueous solution containing 3% potassium dichromate and 0.25% osmium tetroxide and transferred to a 0.75% silver nitrate solution for the following 20 days. Then, each tissue block was held within an external shell of paraffin, and 150 μm-thick sections were cut on a sliding microtome. The sections were then left for 10 min in 70% ethyl alcohol, dehydrated in graded solutions of propyl alcohol-water, cleared in terpineol-xylene, mounted, and coverslipped with Entellan.

Golgi-Cox-Nissl

Additional adult rat brains ($n = 20$) were obtained (vide supra) and stored for 15–20 weeks in a solution containing: 1% potassium dichromate, 0.8% potassium chromate, and 1% mercuric chloride dissolved in deionized water. Each brain was cut sagittally or coronally into 140 μm sections in a sliding microtome. Next, the sections were mounted on slides and immersed in a solution of T-Max (Kodak) in deionized water (1:65) for 30 min, following a 15-min fixation in rapid-fixer (Kodak) diluted 1:30 into water. Then, the slides were left for 15 min in deionized water and counterstained with the Nissl technique. Finally, sections were dehydrated in graded solutions of ethanol-water, cleared in terpineol-xylene, and coverslipped with resin.

Nissl staining

The cytoarchitecture of the olfactory bulb was studied in transverse and sagittal sections from the brains of five adult Wistar albino rats that were successively weighed, deeply anesthetized with pentobarbital (300 mg/2.5 kg), and perfused through the heart with 4% paraformaldehyde dissolved in phosphate buffer (PB, 0.15 M, pH 7.4). The brains were transferred to fresh fixative and left overnight at 4°C. Then, each brain was cryoprotected with 40% sucrose dissolved in distilled water and cut at 40 μm intervals. Then, the tissue samples were immersed for 20 min in a solution containing 0.1 gm of cresyl-violet, 0.3 ml glacial acetic acid dissolved in 100 ml of distilled water. Following staining sections were dehydrated in graded etyl-alcohols, cleared in xylene and coverslipped with Entellan.

Electron microscopy

To determine the ultrastructural characteristics of the aAOB neurons and surrounding neuropil, the brains of six adult rats were processed as detailed elsewhere (Larriva-Sahd, 2004, 2006). In short, deeply anesthetized rats (vide supra) were perfused through the left ventricle with 250 ml of 4% paraformaldehyde-2.5% glutaraldehyde in 0.15 M PB, pH 7.3. Following dissection, the brain was immersed in additional fixative and stored overnight at 4°C. After 24 h, half to one millimeter sagittal slices through the olfactory bulb and its peduncle were obtained. Areas of interest were sampled under a dissecting microscope and post-fixed for one h in 1% osmium tetroxide dissolved in the same buffer as the aldehydes, dehydrated, and flat embedded in epoxy

resins. Half to one-micrometer-thin sections were obtained from the tissue blocks with a Leica ultramicrotome equipped with glass knives. The sections were stained with toluidine blue and coverslipped. From the surface of these trimmed blocks, ultrathin sections ranging from 80 to 90 nm were obtained with a diamond knife and mounted on 200-mesh copper grids. The sections were sequentially stained with aqueous solutions of uranium acetate and lead citrate and then studied in a JEOL 1010 electron microscope.

Immunocytochemistry

Three supplementary aldehyde-fixed rat brains were utilized for pre-embedding immunocytochemistry. Eighty-micron-thick sections were obtained with a vibratome, at room temperature. Sagittal sections containing the areas of interest were processed. Sections were collected in 0.1 M PB, pH 7.2, and preincubated for 60 min in a 0.1 M solution containing 0.1 M PB, 0.8% bovine serum albumin, 0.9% sodium chloride, 0.5% normal goat serum (NGS), and 2 mM sodium azide. Then, sections were incubated overnight (i.e., 10 h) with the rabbit polyclonal antiserum directed against GAD 67 (Chemicon, International). The primary antibody was diluted 1:3000 or 1:2500 in 0.1 M Tris-PB (TBP) with 3% NGS. After rinsing in PB (three times for 10 min each), the sections were incubated for 1 h in the biotinylated secondary antibody that consisted of goat anti-rabbit IgG (Vector Laboratories, Burlingame, CA, USA) diluted to 1:500 in 0.1 M PB with 3% NGS. Sections were then incubated with the avidin-biotin-peroxidase conjugate (1:100 in 0.1 M TPB; Vector Laboratories) for 40 min, and rinsed sequentially in TPB and 0.05 M Tris-HCl buffer, pH 7.6. For visualization of immunoreactive sites, sections were treated with 0.05% 3,3′-diaminobenzidine and 0.01% hydrogen peroxide for 5 min. Lastly, sections were rinsed, and postfixed in osmium tetroxide and further processed for electron microscopic observations.

DATA ANALYSIS

Light microscopy

A total of 30 drawings from complete neurons were used to assess the structure and proportions of each cell type. Measurements from the two neuron types found at the "alpha anterior olfactory nucleus or cell group α" (aAON) according to Valverde et al. (1989) were obtained from digital reproductions of drawings with a personal computer aided by Kontron 400 software (Carl Zeiss). Size of the neuron somata was determined in toloudine—blue stained specimens that had been sectioned at one micrometer and included the aAON and the dorsal component of the anterior olfactory nucleus. A total of 100 neurons were photographed per animal ($n = 5$) and the somatic areas measured with the Kontron software. Areas were pooled per site and compared with the Students *t*-test.

Illustrations obtained by scanning representative drawings were framed, sized, and labeled with photoediting software (Adobe Photoshop 7). Photomontages from specimens were made from series of 4–25 images obtained at different focal depths with a digital camera (AxioCam MRc, Zeiss; Carl Zeiss, Germany). Then, areas in sharp focus were "cut" and merged down with the software. No modifications other than in color, contrast, size, and labeling were made of the original images.

Electron microscopy

To define the numerical densities of synapses, synaptic boutons, and axo-axonic (i.e., synapto-synaptic) terminals, specimens from five adult male rats were utilized. Numerical density of synaptic boutons included those showing pre-, and postsynaptic specializations and a florid granular content, allowing unambiguous identification (vide infra); terminals that were partially sectioned, or lacked an identifiable postsynaptic target were neglected.

RESULTS

Given the fact that the transition between the AOB with the MOB is not sharp (Larriva-Sahd, 2008), and since this territory has not previously been described, it is necessary to provide a general description of this frontier before dealing with the native cellular elements. Hence, the term olfactory limbus (OL) will be used to refer to it throughout this study. The use of this term is further justified by the fact that in adult rodents the cytological characteristics of the OL differ from those of the MOB and AOB as presented next.

INTERACTION BETWEEN THE MAIN AND ACCESSORY OLFACTORY BULBS: THE OLFACTORY LIMBUS

Olfactory limbus

Naked eye or low magnification inspection of the dorsal surface of the rat olfactory bulb reveals an almond-shaped elevation that follows the anterior pole of the frontal lobe, lying dorsally **(Figures 1**,**2A**,**3E**,**4)**. This eminence between the MOB and AOB encompasses a heterotypical bulbar cortex or OL. The most obvious characteristic of the OL is the variable extent of modification from the laminar pattern observed throughout the olfactory bulb. Laterally and medially (i.e., distal) to the AOB, the OL is continuous with the caudal end of the MOB

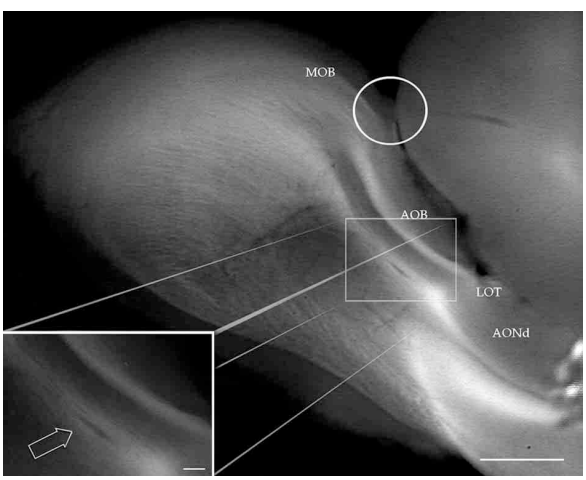

FIGURE 1 | Digital photograph from the dissecting microscope showing the rat olfactory bulb after a sagittal cut. At the junction of the main (MOB) and accessory (AOB) olfactory bulbs, the olfactory limbus (encircled) protrudes dorsally. LOT, lateral olfactory tract. AONd, dorsal component of the anterior olfactory nucleus. Inset: high magnification view of the alpha anterior olfactory nucleus (arrow) lying in the bulbar white matter, underneath the AOB. Scale bars: 0.4 mm in A, 150 μm in insert.

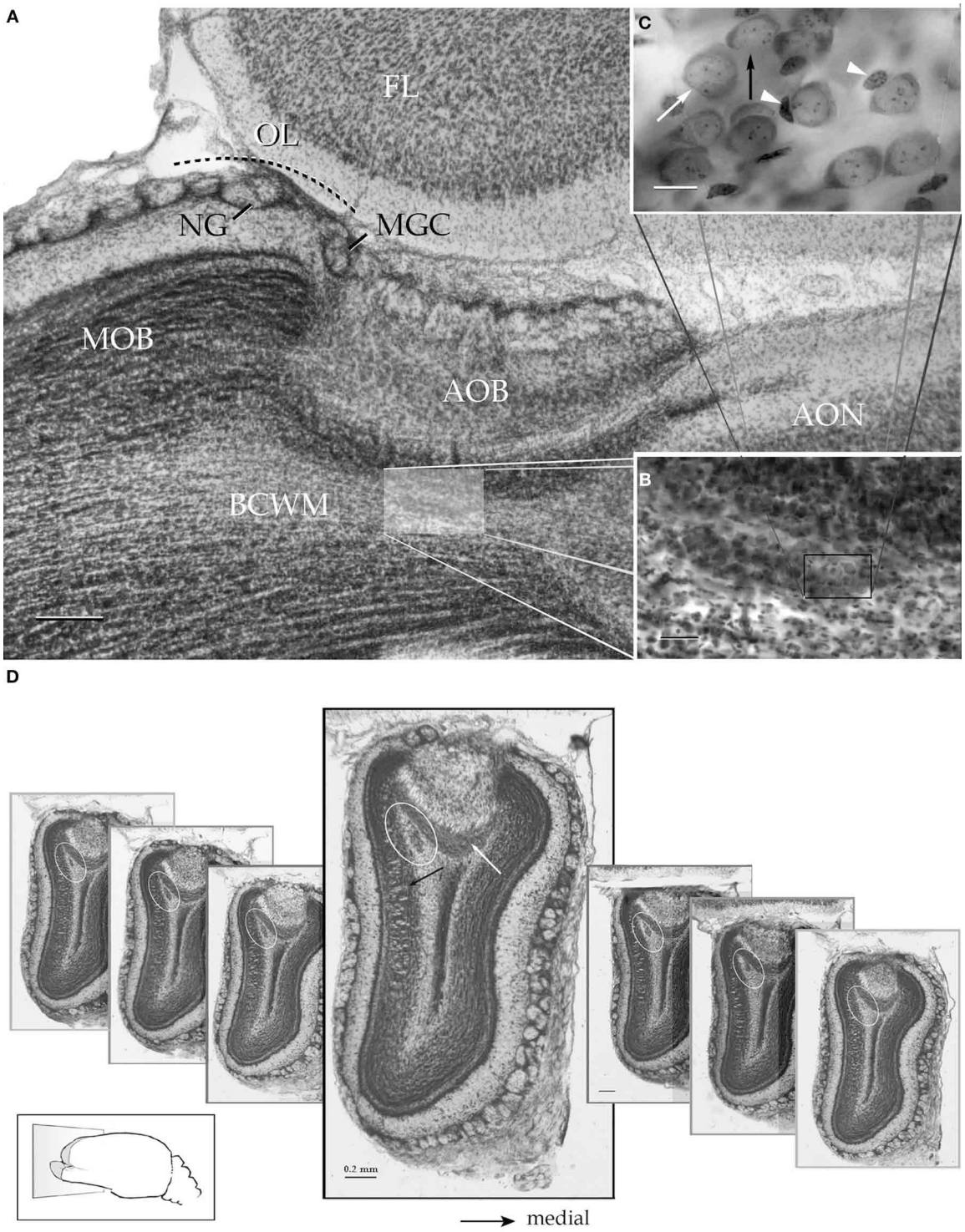

FIGURE 2 | Survey pictures of the olfactory bulb and the alpha component of the anterior olfactory nucleus as seen after thionine staining. (A) Sagittal section. The alpha component of the anterior olfactory nucleus (shaded) is embedded in the bulbar core white matter (BCWM), coursing horizontally, beneath the accessory olfactory bulb (AOB). FL, frontal lobe. **(B)** The spindle-shape alpha nucleus surrounded by the deep bulbar white matter is composed of dense packaged neurons. **(C)** High magnification micrograph from the alpha nucleus that is composed of polygonal (white arrow) and oblong, somewhat smaller, neurons (black arrow). The former neurons may exhibit an associated satellite cell (arrowheads). **(D)** Serial transverse sections from caudal (right) to rostral (left) showing the alpha component (encircled) in its rostrocaudal extent; note that the nucleus lies in a triangular area bounded by the granule cell (black arrow) and internal cellular (white arrow) layers of the main and accessory olfactory bulbs, respectively. Scale bars = 200 μm in **A** and **D**, 50 in **B**, and 10 in **C**. Nissl technique, adult rat brain.

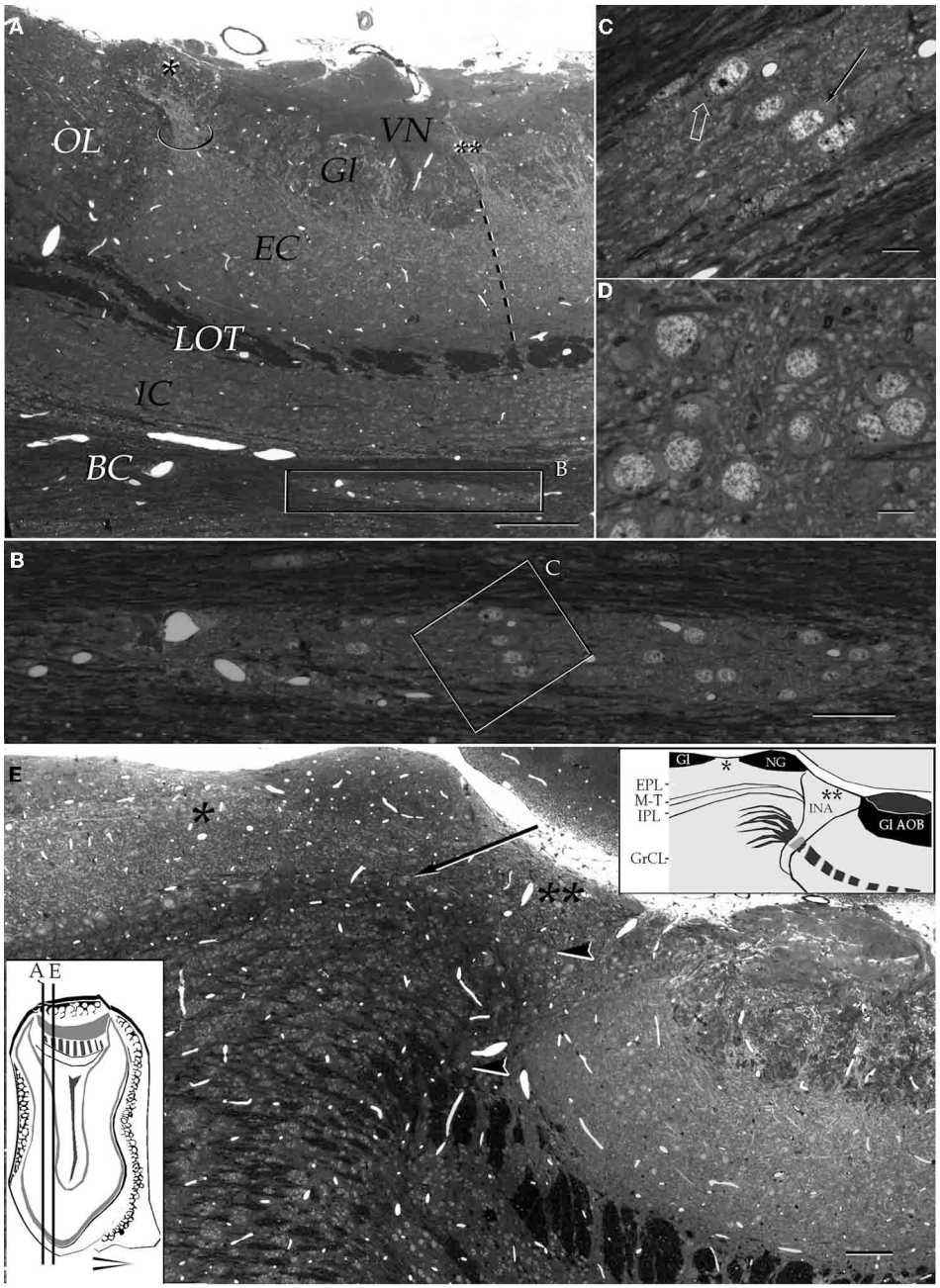

FIGURE 3 | Light micrographs from plastic-embedded longitudinal sections through the olfactory bulb. (A) Section at the caudal intersection of the main olfactory bulb with the accessory olfactory bulb (right side). Note the dendritic bundle (circle) arising from the external cellular layer (EC) and resolving at the base of a modified glomerulus (asterisk), adjacent to the olfactory limbus (OL). Beneath, embedded in the bulbar core white matter (BC), lies the alpha component of the anterior olfactory nucleus (boxed). VN, vomeronasal nerve layer; GI, glomerular layer; LOT, lateral olfactory tract; IC, internal cellular layer. At the glomerular-free area of the accessory olfactory bulb the linea alba (dashed) separates the external cellular layer in a rostral (left) and caudal halves. **(B)** Higher magnification of the alpha component of the anterior olfactory nucleus. **(C)** Neuron somata from the alpha component of the anterior olfactory nucleus (boxed in **B**). A neuronal cluster made up of medium-sized neurons (solid arrow) and a large neuron whose cytoplasm contains Nissl substance (hollow arrow). **(D)** Neuron somata in the dorsal part of the anterior olfactory nucleus at the same magnification as the micrograph shown in **C**; note the difference in size and distribution of neurons in comparison to those from the alpha component shown in **C**. **(E)** Micrograph depicting the olfactory limbus between the main (left) and accessory olfactory bulbs. At the upper left is the caudal end of the main olfactory bulb, followed by the glomerular-free preolfactory (asterisk) area. The latter faces a second area or the necklace glomeruli whose external plexiform (EPL) and mitral/tufted cell (M-T) layers become indistinct and hypocellular (arrow), respectively. Following caudally is a wedge-shaped or interstitial area (double asterisk) (INA) that lacks laminar organization, having clusters of cells of assorted size (arrow-heads). GI-AOB, glomerular layer of the accessory olfactory bulb; IPL, internal plexiform layer; GrCL, granule cell layer. Scale bars: 100 μm in **A**, 40 in **B** and **E**, and 10 in **C** and **D**. One-micrometer-thick sections, adult rat brain, toluidine blue staining.

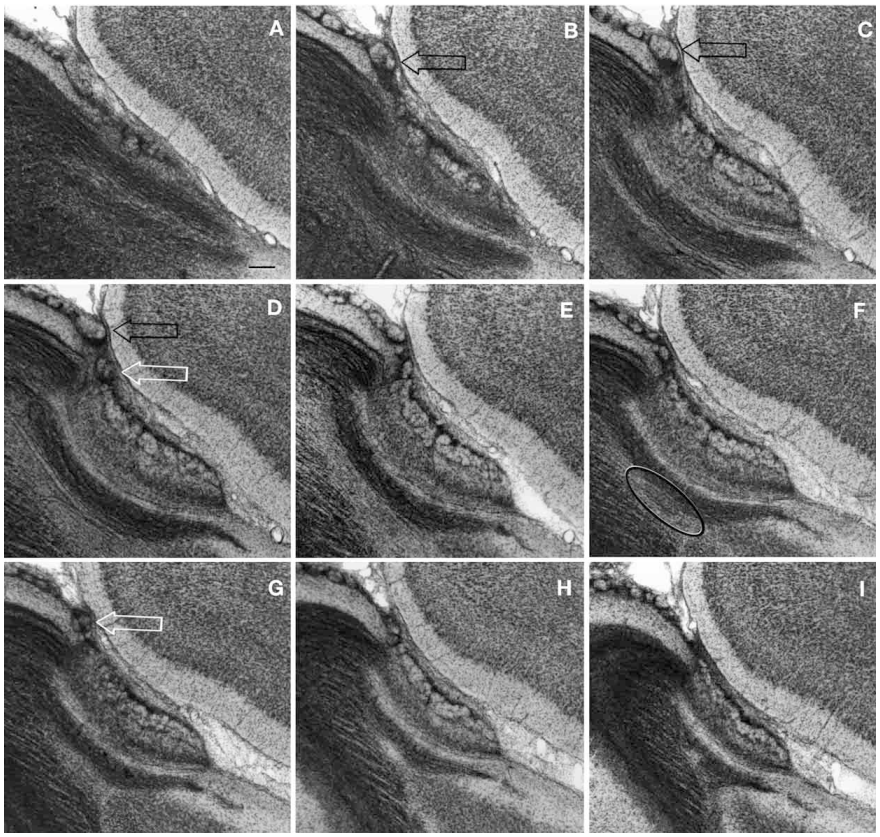

FIGURE 4 | Successive Nissl-stained sections from lateral (A) to medial (I) through the olfactory limbus. Note that glomeruli from the modified glomerular complex lie on the anterior part of the accessory olfactory bulb (white arrows) and those from the necklace (black arrows) crown the homonymous area of the olfactory limbus. Circle = alpha component of the anterior olfactory nucleus. Scale bar = 100 μm. Adult rat brain.

that resolves in the cisura circularis (Lohman and Mentink, 1969).

Parceling of the olfactory limbus

According to the internal structure of the OL it can be divided into three areas. The foremost or preolfactory area (PA) consists of a modified main olfactory cortex having the following dissimilarities (**Figure 3E**): it lacks glomeruli, is thinner than the adjacent MOB cortex, and its row of mitral cells that, in the MOB underscores the mitral-tufted cell layer, contains fewer and smaller mitral cells. Concurrently, the PA exhibits a rudimentary external plexiform layer (EPL) that is more slender than that in the adjacent MOB. Lastly, the internal plexiform and granule cell layers are thinner than their MOB counterparts. Following caudally, is the second area of the necklace glomeruli (NGA), it is the most prominent due to one or two solitary glomeruli that bulge-up to the pial surface. In addition to location, necklace glomeruli (NG) stand out from those in the MOB and AOB, in that they are bigger and hypercellular (**Figures 4B–F**). Still another, important difference of NGs in the OL from those located elsewhere is that they are united by cellular bridges that contain a fibrous core (**Figure 5B**) (see Shinoda et al., 1989). Underneath the NG, the region equivalent to the EPL reaches its minimum in terms of both thickness and cellularity and, like in the PA, it is discontinuous having fewer and smaller, mitral-and tufted-cells (**Figures 3F**,**6**). A third, or interstitial area (INA), consists of a relatively hypocellular, wedge-shaped area between the anterior aspect of the AOB and the caudal part of the NGA. Superficially the INA is somewhat lower than the adjacent NGA as it lacks glomeruli or, more commonly, exhibits two or three modified glomeruli similar to those seen in the new-born rodent and referred to as the modified glomerular complex (MGC) (Teicher et al., 1980). Sagittal sections through the oral part of the AOB reveal that these MGC arise from principal cell dendrites in the AOB. In fact these distal dendrites bend rostrally to overlie the posterior INA (**Figures 2A**,**3A**,**4D**). The deep part of the INA is triangular in shape with the apex proceeding ventrally to resolve in the deep bulbar white matter (**Figures 3E**,**4**,**5B**). While the posterior aspect of the INA faces the AOB, its lower third is pierced by the convergent fibers of the lateral olfactory tract (LOT) on their way to the AOB (see Figures 25,26A in Larriva-Sahd, 2008). The INA stands out from the former two areas, and from the entire olfactory bulb in that is devoid of a laminar organization (**Figures 2**,**3**,**4**,**5**). Concurrently, several peculiarities differentiate the IN from the surrounding structures. The first is that neurons therein (vide infra) form small cellular clusters. Second, it lacks a granule cell layer. Furthermore, the LOT that in the

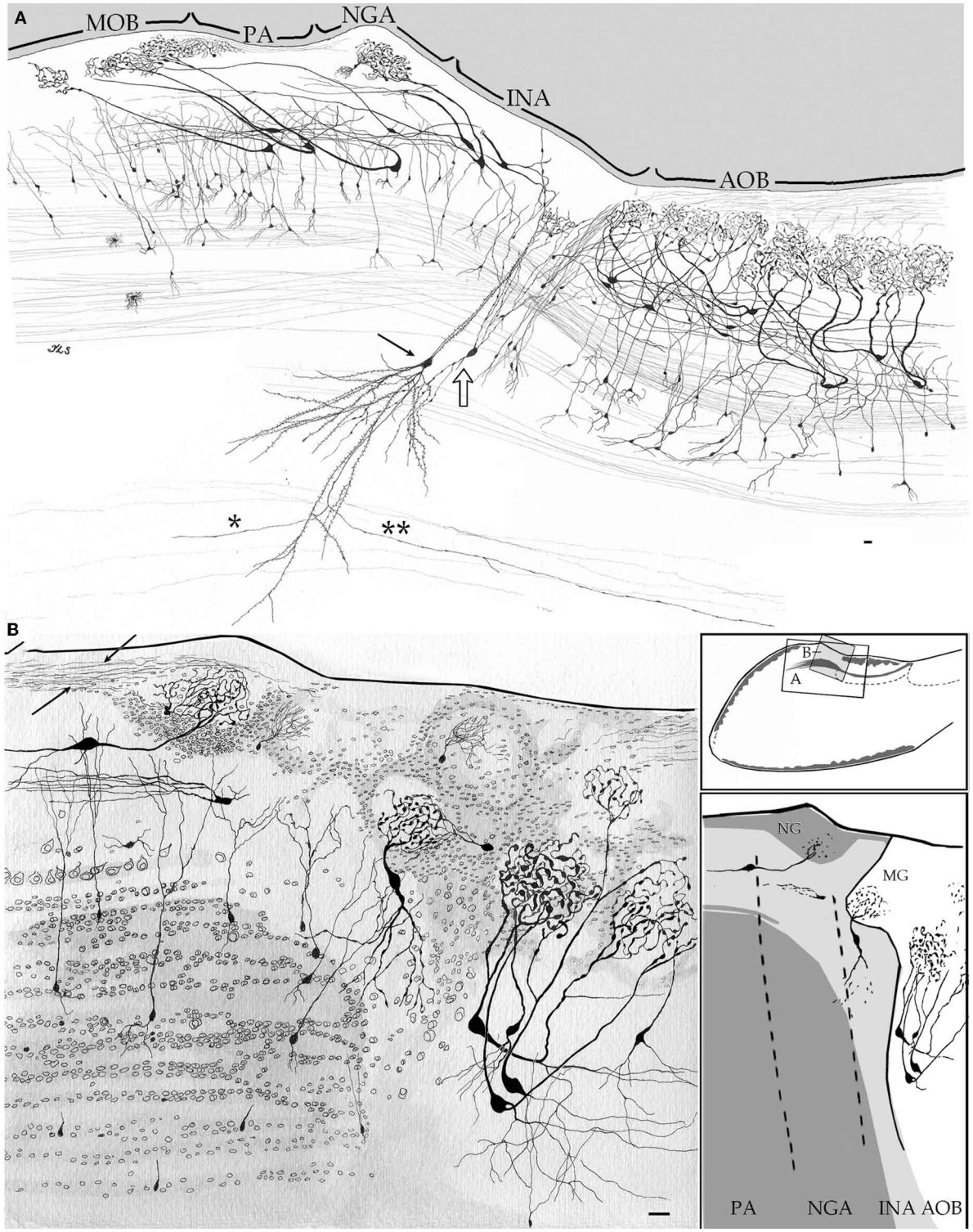

FIGURE 5 | Camera lucida drawings from sagittal sections through the olfactory limbus and adjacent structures. (A) The drawing accounts for the cellular contents and parceling in the olfactory limbus. Note that glomeruli in the main olfactory bulb (MOB) receive dendrites from mitral cells whose somata lie in the preofactory (PA) and necklace (NGA) areas of the olfactory limbus. A projecting interstitial neuron of the bulbi (arrow) lying deep in the homonymous area (INA) sends a descending axon that forks into rostrally (asterisk) and a caudally (double asterisk) directed branches. Interstitial neuron of the bulbi, interneuron (hollow arrow). **(B)** Drawing showing the neuronal distribution as seen in a specimen after a two-step strain, Golgi-Cox-Nissl. Arrows, fibrils arising from a necklace glomerulus; PA, NGA, INA, preolfactory, necklace glomeruli, and interstitial areas. Scale bars = 30 μm. Adult rat brain, rapid-Golgi (A), and Golgi-Cox-Nissl (B) techniques.

MOB and AOB forms a well-defined layer, in the deep INA acquires a reticular appearance due to scattered myelinated fibers and small bundles that, as a rule, diverge in various directions (**Figures 3E**,**5A**).

CYTOLOGY OF THE OLFACTORY LIMBUS

Although the neuron phenotypes identified thus far in the OL are, in most respects, comparable to those observed in the MOB, they exhibit a different organizational strategy. In fact, the laminated appearance of the MOB and AOB observed in aniline-stained specimens (**Figures 2**,**3**,**4**), that results from the layered coalescence of somata, is modified in the PA and NGA areas, and lost in the INA. This laminar disruption and the ensuing assorted distribution of neurons have little repercussion in the basic somato-dendritic features of the neurons. In fact, virtually all neuron-types observed throughout the olfactory cortex correspond to those seen in the OL although it must be stressed that here they exhibit curved, bent, or even twisted processes. This regional cellular pleiomorphism is better evidenced in specimens processed with a combination of silver and aniline techniques (**Figures 5B**,**6**).

The first and perhaps most obvious, OL specialization is that a set of mitral cell somata lie posteriorly with respect to their tributary glomeruli (**Figure 5A**). Consequently, apical dendrites arising from mitral cells in the OL run diagonal, nearly horizontally, to reach glomeruli that are located more rostrally. Clearly, the caudal displacement of the mitral cell somata with respect to their tributary glomeruli lying rostrally, differs from the vertical ascent normally observed for glomerular dendrites of mitral cells in the MOB (Figures 4A,B in Larriva-Sahd, 2008). That conclusion that tilted apical dendrites are a distinctive feature of mitral cells in the OL is afforded by the absence of them in the caudal aspect of the MOB, beyond the OL domain (**Figure 7**). In short, the "glomerular shift" observed in the OL yields to mital cell somata and their associated interneurons and granule cells are located caudally with respect to their tributary glomeruli (**Figure 5A**). Although dendritic polarization displayed by some mitral cells does not seem to apply to the tufted (**Figure 6**), short-axon (**Figure 8**) or granule cells, more subtle variations in dendritic bending or even twisting can also be observed throughout the OL (**Figures 5A,B**,**6**).

In the deep area of the INA, just anterior to the internal cellular and LOT layers of the AOB, there is a streak of medium to large-sized neurons. These neurons whose somata were described in Nissl-stained specimens from hamster (Lohman, 1963; Lohman and Mentink, 1969), correspond to those collectively termed interstitial neurons of the bulbi (INBs) (Larriva-Sahd, 2008) (**Figures 3E**,**5A**,**8C**). On cytological grounds INBs actually include two cell types, namely, pyramidal-like or projecting (INBp) and interneurons or intrinsic neurons (INBi). Like elsewhere in the neo-and olfactory cortices, pyramidal-like INB's represent the out-put cell. Most INBp dendrites exhibit a moderate to high number of spines and, as implicit, mimic the structure of their neo-cortical homologs. A striking feature of the INBp axon is that, having descended to the deep bulbar white matter, it divides into an anterior and a posterior (i.e., descending) fibril (**Figures 5A**,**6C**), in the same fashion as that described by Valverde (1965) in the new-born rodent anterior olfactory nucleus. A typical INBi has a bottle-shaped soma with varicose, bold dendrites. The axon of an INBi arises from a proximal dendrite (**Figures 8E,F**) or, less frequently, from the soma itself (**Figure 8C**) (see Larriva-Sahd, 2008). Soon afterwards, the INBi parent axon divides dichotomously at relatively short intervals (i.e., $<30\,\mu m$) thereby originating a dense axonal framework that distributes in the neuropil of the INA and in the adjacent granule and internal cellular layers. Although an INBi shares striking

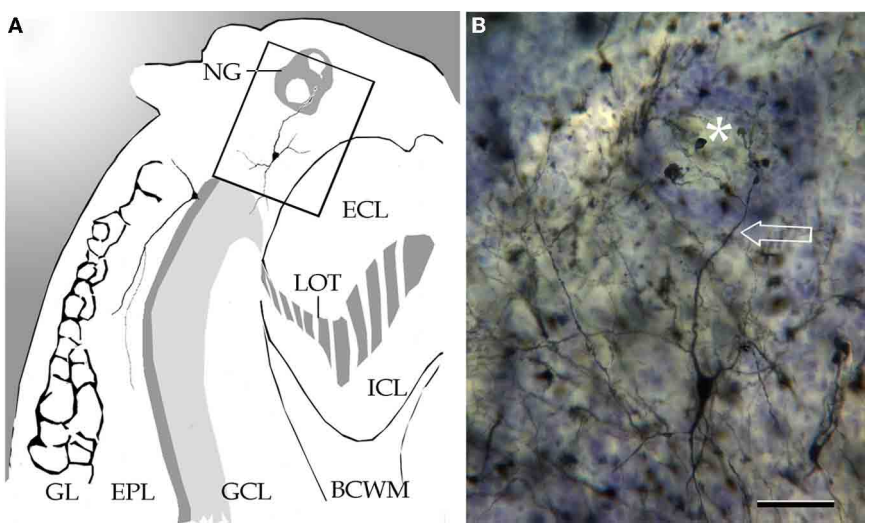

FIGURE 6 | Coronal section through the left olfactory bulb. **(A)** Diagramatic drawing showing a necklace glomerulus (NG). BCWM, bulbar core white matter; ECL, external cellular layer; EPL, external plexiform layer; GCL, granule cell layer; GI, glomerular layer; ICL, internal cellular layer; LOT, lateral olfactory tract. **(B)** A tufted cell sending a glomerular dendrite (arrow) to a necklace glomerulus (asterisk). Adult rat brain, Cox-Nissl technique. Scale bar = $50\,\mu m$.

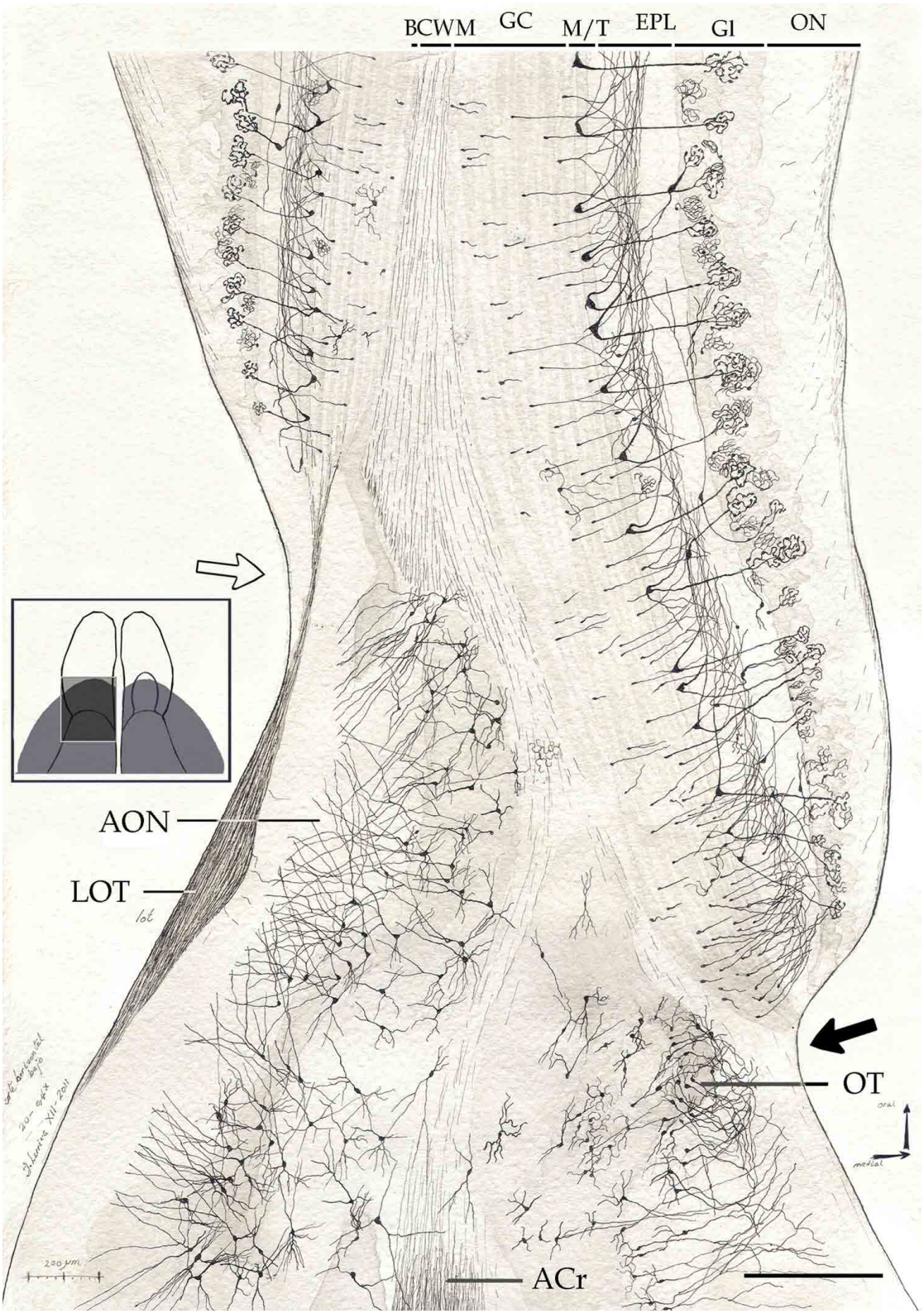

FIGURE 7 | Survey camera lucida drawing from the olfactory peduncle in a horizontal section. Note the mode of resolution of the main olfactory cortex at the medial (black arrow) and lateral (hollow arrow) aspects of the fissura circularis. ACr, anterior commissure, pars rostralis; BCWM, bulbar core white matter; EPL, external plexiform layer; GC, granule cell layer; GI, glomerular layer; LOT, lateral olfactory tract; M/T, mitral-tufted cell layer; ON, olfactory nerve layer; OT, olfactory tubercle. Cox-Nissl technique, adult rat brain. Scale bar = 200 μm.

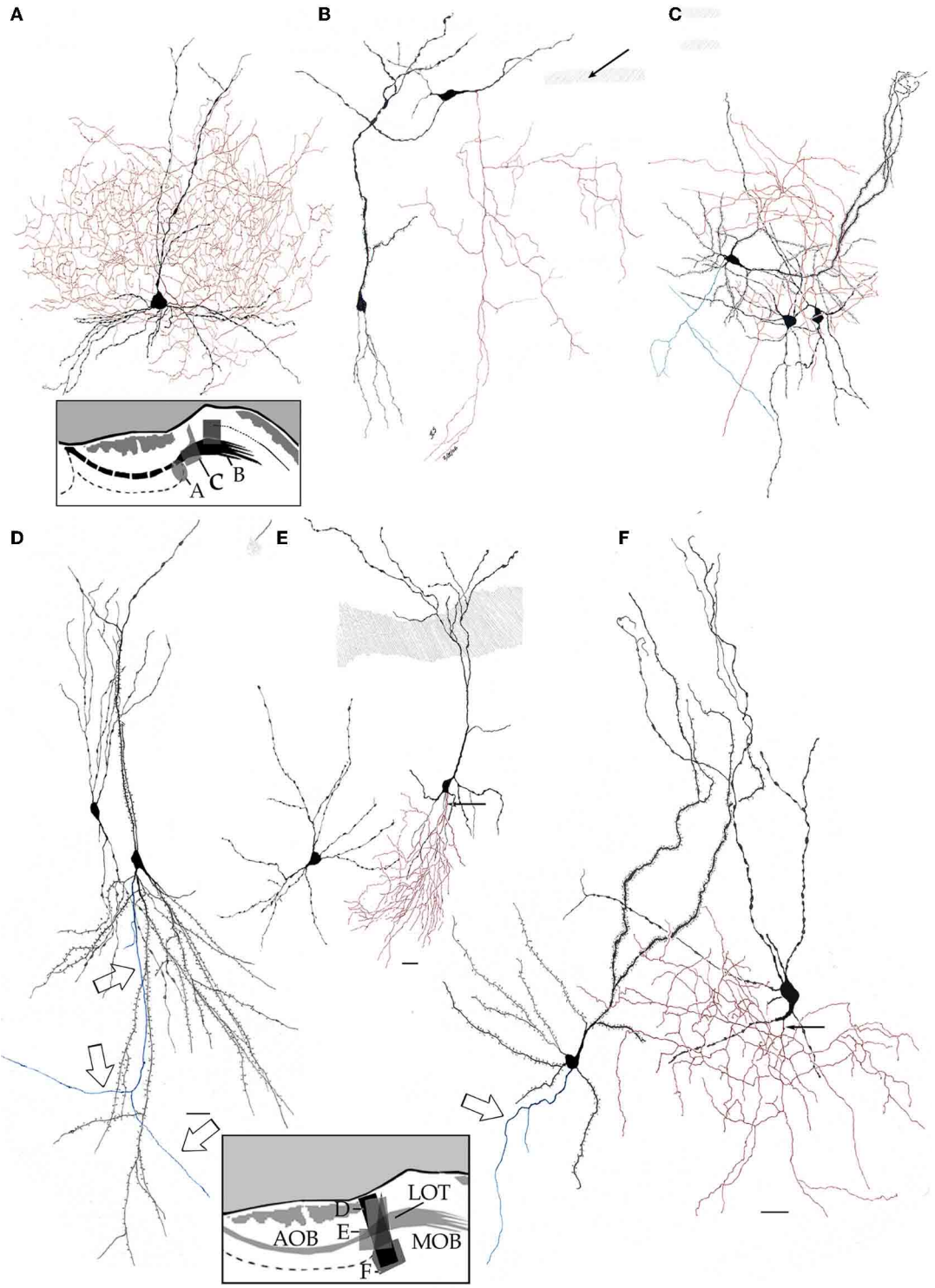

FIGURE 8 | High magnification drawings from bulbar neurons with projecting (blue) and local (red) axons. Somata and dendrites from the latter are nearly identical in shape, thickness, and varicosities. **(A)** Main accessory cell of the accessory olfactory bulb with a profuse axonal (red) field. **(B)** Deep short axon cell whose descending axon (red) distributes in the granule cell layer of the main olfactory bulb. **(C)** Two interstitial bulbar interneurons with ascending axon and a projecting cell whose axon (green) divides into two descending collaterals. **(D)** Examples of interstitial neurons. The projecting cell (right) emits a descending axon (arrows). **(E)** A projecting cell whose parent axon provides a huge number of collaterals to the adjacent neuropil. **(F)** Pyramidal-like and a short-axon neurons in the alpha component of the anterior olfactory nucleus. Adult rat brain rapid-Golgi method. Scale bar = 15 μm.

somato-dendritic similarities with certain MOB (Macrides and Davis, 1983; Kosaka and Kosaka, 2011) AOB (Larriva-Sahd, 2008) and medullary bulbar area (Paredes and Larriva-Sahd, 2010) interneurons, its axon is primarily distributed in the adjacent INA neuropil.

Regional differences of the olfactory limbus

The lack of a lattice-like, linear array displayed by most biological objects applies to the structure of the OL in that it varies from one histological section to the next. Although the tripartite division of the OL recommended here persists throughout the medial-lateral extent of the main-AOB interface, subtle differences are evidenced in successive sections through the OL (**Figure 4**). First is the presence of one or two small glomeruli that lie anterior aspect of the AOB. These glomeruli that ride on INA, appear to be part of the "modified glomerular complex" observed by Greer et al. (1982) in the newborn rat, and are most evident in sections through the medial half of the AOB. Serial sections depict that these are, in fact, smaller and inconstant throughout the rostral AOB. The same applies to the large NG found in the homonymous area, that is frequently seen in sections through the medial AOB half (**Figures 4B–D**), and is less evident or even absent in more lateral sections (**Figures 4F–I**). The medial and lateral aspects of the AOB are bounded by the MOB anteriorly and by the dorsal AON, caudally. Hence, the confluence of the three distinct cortices at either side of the AOB gives rise to a medial and a lateral olfactory "triad." Due to the caudal expansion of the MOB, the medial triad is located caudally with respect to the lateral one. Further, the lateral olfactory triad is asymmetrical in that it accepts the distal processes of pyramidal-like cells (P-L), whose somata lie at the base of the AOB (see below) (**Figure 9**). Lastly, one can appreciate in successive longitudinal sections through the olfactory bulb that two elements of the OL, the PO and NGA, persist throughout the entire caudal ribbon of the MOB cortex with a progressive decrease in thickness along the fissura circularis (**Figure 7**) that defines the caudal end of the MOB.

Summarizing, the OL, a broad area of interaction between the MOB and AOB is characterized by a partial or complete modification of the laminar plan of organization observed throughout the bulbar cortex. Despite the disruption of the strata the OL is composed of three distinct components having, in turn, predictable histological and cytological organization.

ALPHA GROUP OF THE ANTERIOR OLFACTORY NUCLEUS

General organization

Unstained (**Figure 1**) or aniline-stained (**Figures 2**,**3A**,**B**,**C**,**4F**) sections through the olfactory bulb show a distinct, fusiform collection of neurons that parallels the middle third of the AOB. The nucleus consists of a compact neuronal cluster measuring 100 × 150 × 650 microns in the horizontal, vertical, and anteroposterior

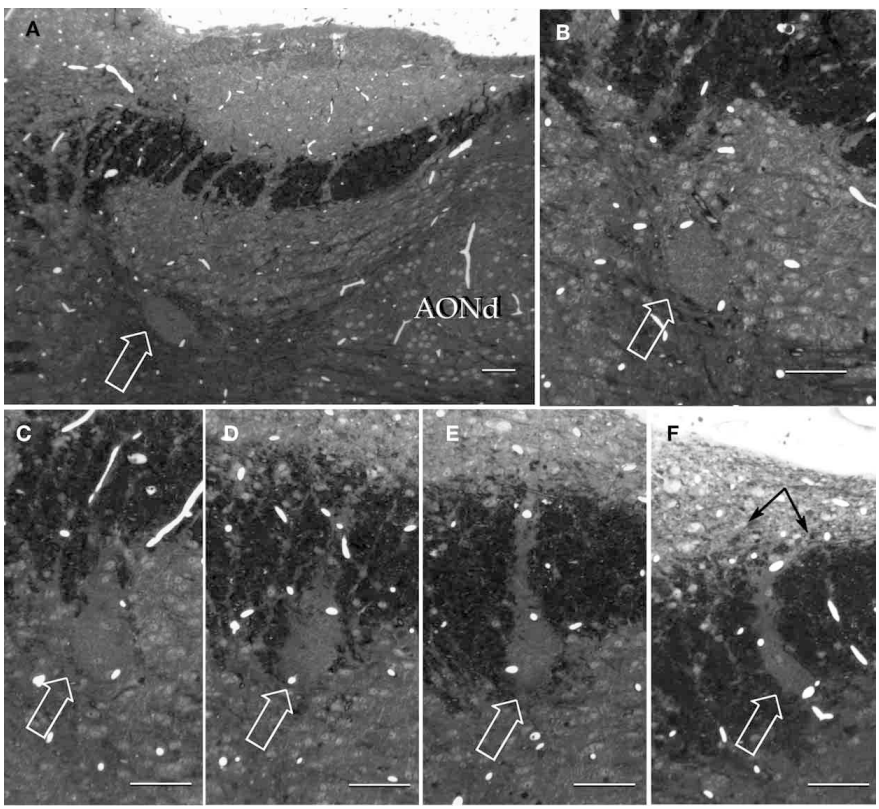

FIGURE 9 | Semi-serial, sagittal sections through the accessory olfactory bulb Note the progressive ascent of the dendritic bundle (hollow arrows) from medial (A) to lateral (F), to resolve under (black arrows) the pial covering in F. Adult rat brain, epon embedding, one-micron thin section, toluidine-blue staining. Scale bars = 50 μm.

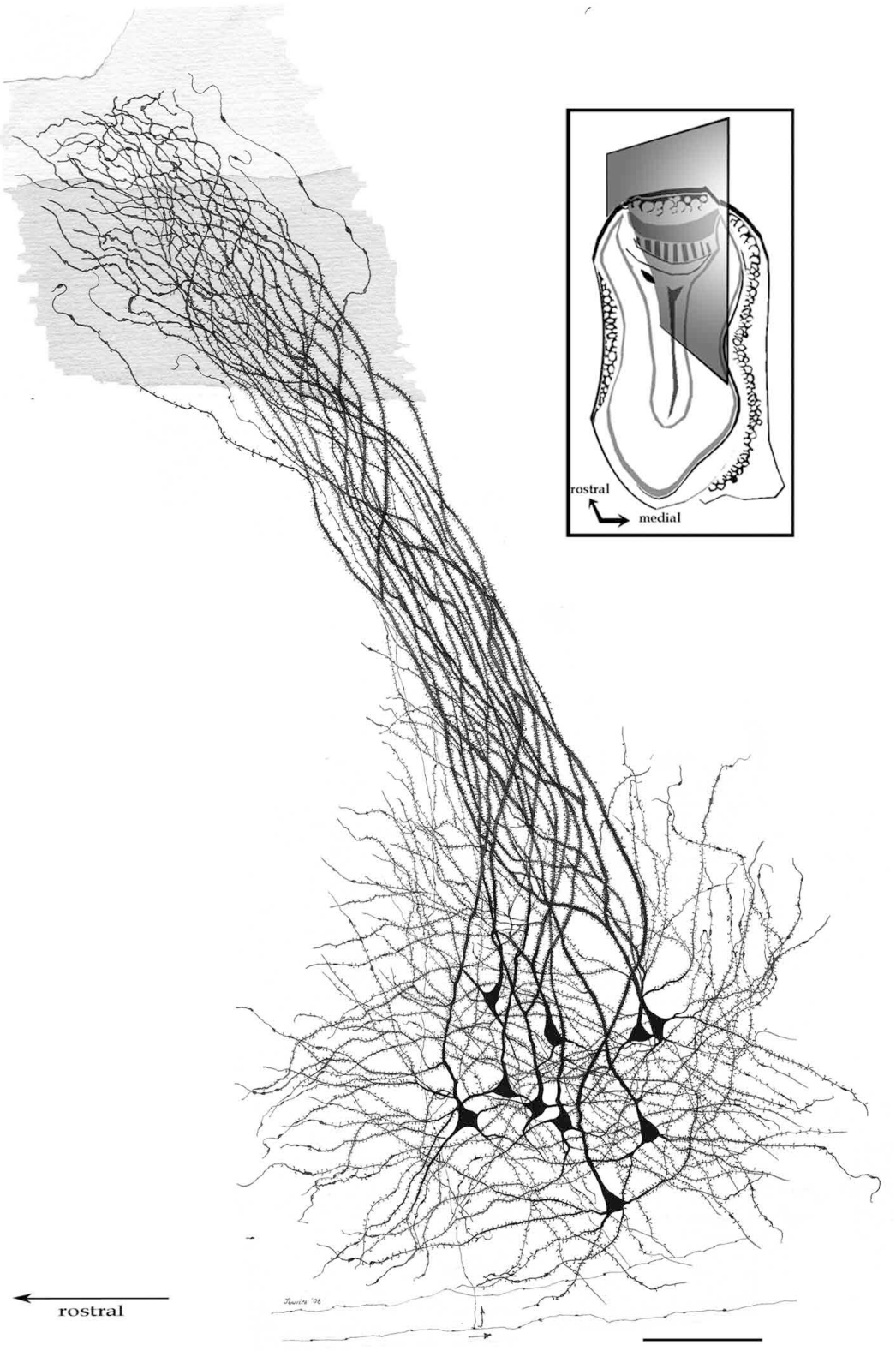

FIGURE 10 | Pyramidal-like cells in the alpha component of the anterior olfactory nucleus. The spiral path followed by apical, spiny, dendrites in their ascent can be seen. Note that distal, aspiny, dendrites impinge on the lateral olfactory tract (shaded). Fibers at the bottom belong to the deep bulbar white matter; one of them sends along collateral (arrow) that penetrates the nuclear neuropil. Adult rat brain, sagittal section, rapid-Golgi technique. Scale bar = 100 μm.

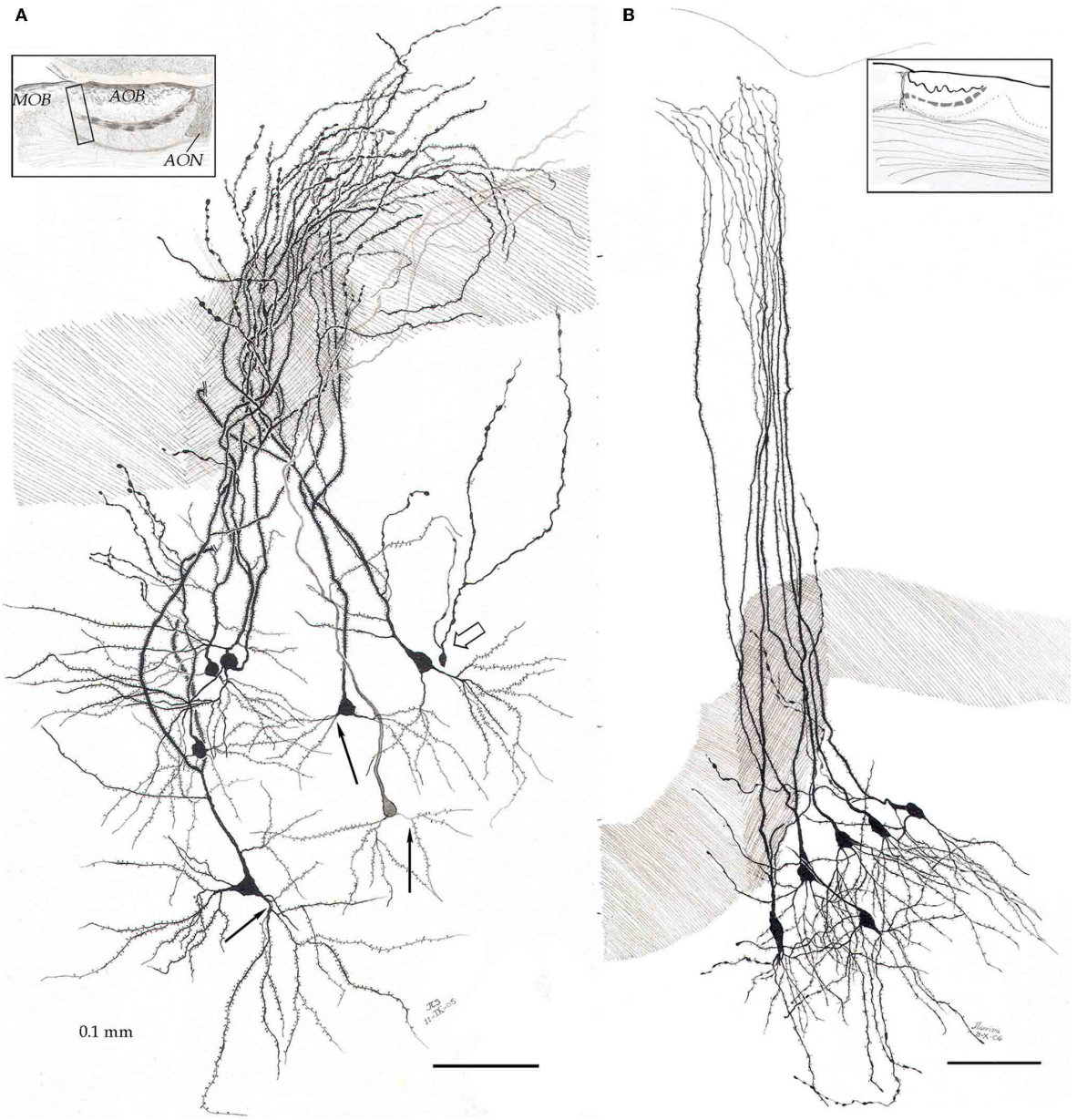

FIGURE 11 | Pyramidal-like cells in the alpha component of the anterior olfactory nucleus. (A) In the mouse, apical dendrites curve along the lateral aspect of the accessory olfactory bulb to pierce the lateral olfactory tract (dashed), resolving in the lateral olfactory triad (see text). Note that basilar dendrites arising from pyramidal-like neurons, divide in a tripartite manner (black arrows). Hollow arrow = granule cell. **(B)** In the guinea pig, pyramidal-like cells send vertical, nearly straight shafts that proceed through the lateral olfactory tract (dashed) and terminate under the piamatter. AOB, accessory olfactory bulb; AON, anterior olfactory nucleus, MOB, main olfactory bulb. Adult rat brain, rapid-Golgi technique, sagittal sections. Scale bars = 100 μm.

axes, respectively. In about two out of 10 specimens, the aAON shifts its position underscoring the rostral third of the AOB (**Figures 3A**,**B**,**C**). Regardless of its location the bulbar core white matter encases the nucleus. High magnification inspection of the aAON reveals that it is composed of a double population of neurons (2C and 3C). A first or pyramidal-like neuron (P-L), whose soma is triangular, measures 20–27 μm in its longest axis. The nucleus of a P-L is rounded and contains a distinct nucleolus surrounded by a basophilic cytoplasm due to patches of Nissl substance. A small satellite cell is commonly associated with P-Ls. A second, smaller neuron consists of a round to pear-shap cell measuring 13–16 μm in its widest axis. The nucleus is also rounded or oval containing coarse granular chromatin and two or three small indistinct nucleololi. Cytoplasmic basophilia is concentrated at the two cellular poles. Mophometry discloses that the aAON somata bear significantly different, albeit larger

(i.e., 156 μm^2), somatic areas than those from the dAON (i.e., 124 μm^2) (see Brunjes et al., 2011).

Principal cell

By-and-large, pyramidal-like neurons (P-L) are the most common neuron-type in the aAON. Although P-Ls lie in the nuclear domain, their ascending dendrites that proceed dorsally, build-up a well-defined bundle. These ascending dendrites that follow an helicoidal path, pierce the lateral part of the INA to terminate underneath the pial covering (**Figures 9**,**10**). The overall direction of the resulting bundle is not straight, especially in the adult rat (**Figure 10**) and mouse (**Figure 11A**). In these species, as soon as the apical dendrite leaves the nuclear domain, it arches antero-laterally, avoiding the MOB and AOB to resolve in the lateral olfactory triad. Because of this heterodox trajectory, diagonal (**Figure 10**) or serial (**Figure 9**) sections are required to visualize the full dendritic arbor of a pyramidal cell. Alternatively, pyramidal cells from guinea-pig specimens, whose principal cell exhibits straight apical dendrites, may suit that purpose (**Figure 11B**). The tridimensional distribution of P-L processes with respect to the adjacent structures is diagrammatically depicted in **Figure 12**. Occasional (i.e., about 2 from 10) pyramidal cells possess one or two supernumerary, thick dendrites that arise from the base of the main apical branch, running diagonally. As soon as ascending dendrites pierce the LOT they divide once or twice to form distal terminal tributaries. A distinctive feature of these distal branches is the presence of bold, rounded, varicosities united by thin cytoplasmic shafts. Like typical isocortical pyramids (Feldman, 1984), most P-L's dendrites are densely covered by numerous spines (**Figures 13**,**14D**), although terminal branches are virtually devoid of them (**Figures 10**,**11**). A peculiar feature of basilar dendrites of a P-L is that they divide originating three daughter dendrites (**Figure 11A**). This tripartite branching assumed by basilar dendrites distinguishes a P-L from other neo-cortical pyramids (Lorente de Nó, 1949). The axon of a P-L behaves in the same manner as most pyramidal cells observed in the INBp (**Figure 11A**) and olfactory peduncle (i.e., anterior olfactory nucleus) (see Valverde, 1965), since it descends to the bulbar core white matter leaving 2–8 recurrent collaterals that distribute in the overlying internal cellular layer of the AOB (**Figure 13**). Distally, the stem axon divides, originating two fibrils that proceed further caudally and rostrally, respectively (14B).

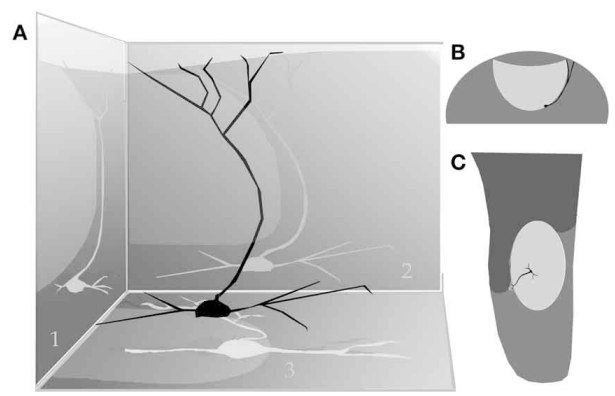

FIGURE 12 | (A) Diagram showing the path of the pyramidal cell (black) apical dendrite with respect to the anterior (1), lateral (2), and basal (3) aspect of the accessory olfactory bulb (shaded, egg-shaped). **(B)** Dendritic trajectory of a pyramidal-like cell with respect to the accessory olfactory bulb (lighter) in a coronal view (lateral, right side). **(C)** Dorsal view.

Interneurons

One out of 10 neurons observed in the aAON consists in an interneuron (INBi) (Larriva-Sahd, 2008). INBis appear to correspond to the pear-shaped somata observed in aniline-stained specimens (**Figure 2C**). The smato-dendritic features of INBi (**Figure 13**) mimic, in several respects, those observed in other aspiny short-axon neurons in the bulbar cortex (**Figures 8A,B**) (see **Figure 10**, Larriva-Sahd, 2008), and medulla (Paredes and Larriva-Sahd, 2010) in that the soma is smooth, originating two or three primary dendrites that soon afterwards (i.e., $<30\,\mu m$) give rise to secondary and tertiary dendrites, usually the most distal branches. Dendrites are, as a rule, varicose and virtually devoid of spines (**Figures 13**,**14C,D**). What seems to be unique of aAOB intrinsic neurons from other bulbar interneurons is that their axon distributes primarily in the aAON neuropil, creating a dense axonal framework in the nucleus proper. As a matter of fact, the interneuron axon is an important source of intrinsic fibrils that structure the aAON neuropil (**Figures 13A**,**14C**), although is not uncommon for axon fibrils to invade the adjacent external cellular layer of the AOB (**Figure 13A**). At high magnification one can observe that the axon displays numerous en passage and terminal boutons (**Figure 14C**) unlike terminal fibrils from other sources (**Figures 13B**,**14A,B,E**). Additional fibrils in the aAON neuropil include collaterals from the P-L axon (**Figures 13**,**14B**) and from the deep bulbar white matter (**Figure 14E**). In precis, the aAON neuropil is composed of terminal axonal fields arising from the P-L, interneurons and from the surrounding white matter.

Immunocytochemistry

Light microscopic observation of specimens incubated with antibodies to GAD67, reveals that the aAON is composed of immunoreactive (GAD67-I) cells (**Figure 14F**), and numerous GAD67-I punctae (14G). GAD67-I neurons display diffuse, brownish reaction products throughout the cytoplasm acquiring a ring-shape due to a pale nuclear area.

ELECTRON MICROSCOPY AND IMMUNOCYTOCHEMISTRY

Neurons

Survey electron micrographs of the aAON (**Figure 15**) reveal that it is composed of cellular clusters of two or three neurons surrounded by a relatively homogeneous neuropil with a paucity of thin myelinated fibers. Neurons are rounded or spindle-shaped with a central nucleus of smooth profile. A signal feature of aAON neurons is that their somata appose each other directly, without an intervening neuropil or glia. Occasional satellite cells (**Figures 2C**,**16B**) or astrocytes (**Figure 16C**) lie adjacent to the neuronal clusters. The neuronal nucleus is generally smooth and it contains abundant euchromatin with small, scattered chromatin aggregates that are embedded in a low-density karyoplasm. A distinct solitary nucleolus may be seen

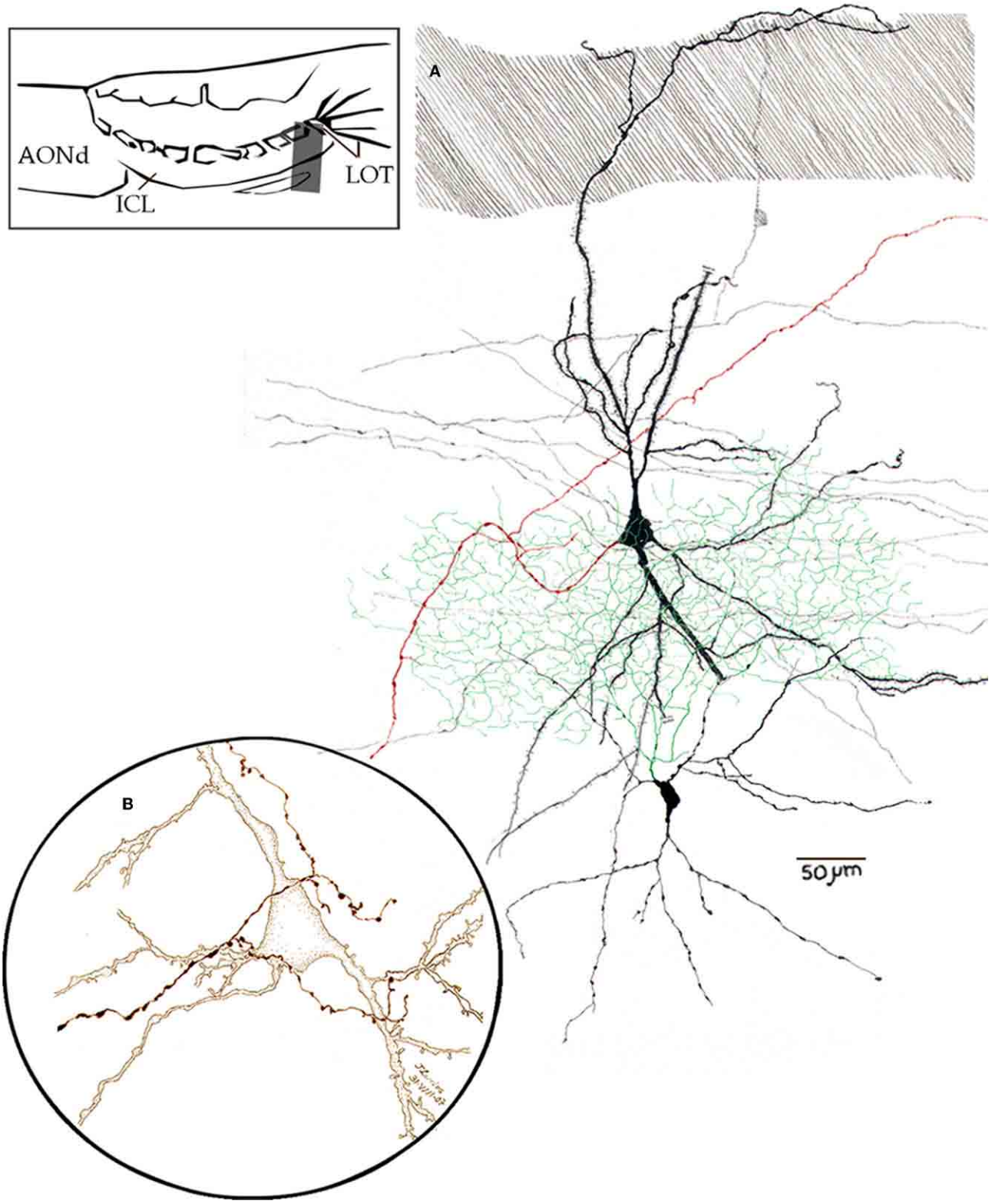

FIGURE 13 | Camara lúcida drawings from neurons in the alpha component of the anterior olfactory nucleus. **(A)** An interneuron whose axon (green) divides massively in the nuclear neuropil; the pyramidal-like cell gives rise to a forked axon (red), and the parent fiber proceeds caudo-ventrally. **(B)** High magnification of a pyramidal-like cell and a terminal fibril that arose from the bulbar core white matter. Adult mouse, rapid-Golgi technique.

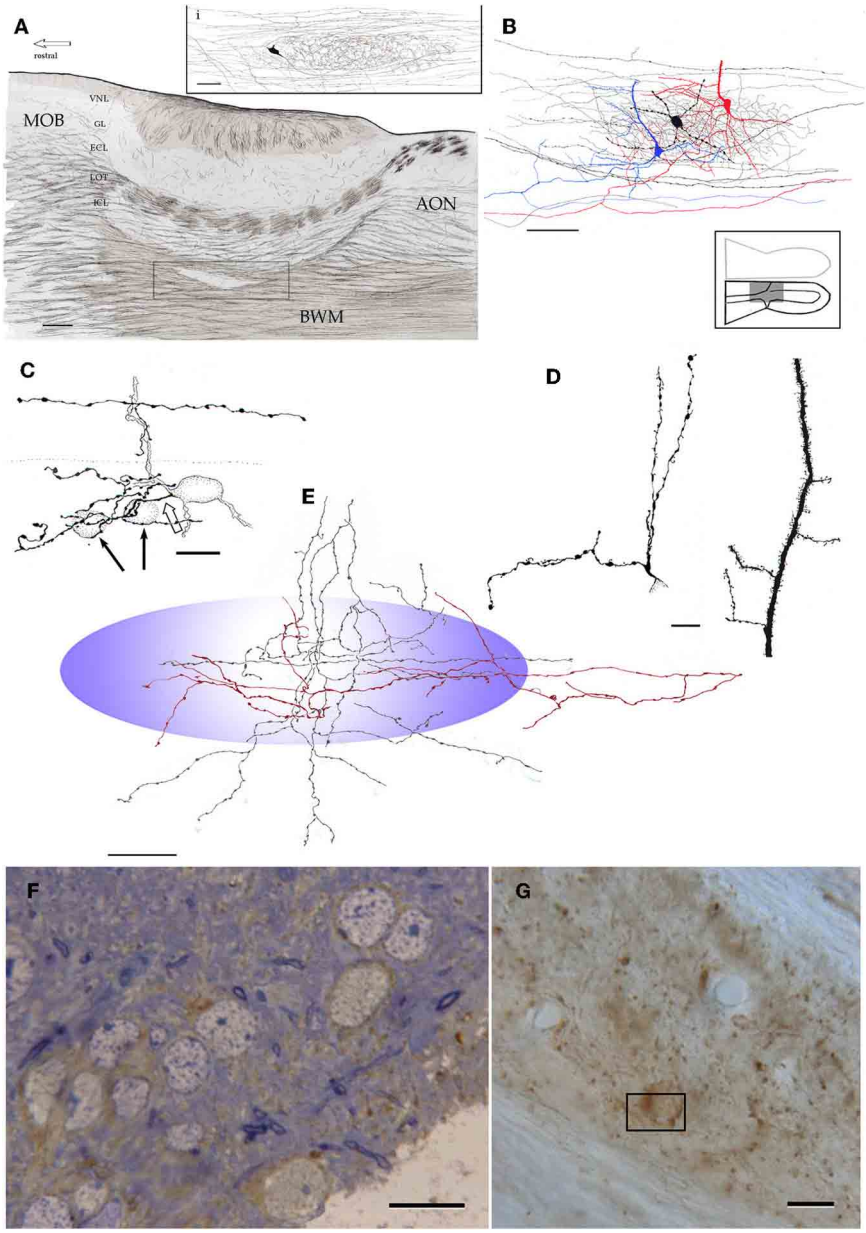

FIGURE 14 | Microscopic organization of the alpha component of the anterior olfactory nucleus. (A) Fiber systems associated with the olfactory bulbar cortex and alpha component of the anterior olfactory nucleus (framed). The inset shows the distribution of a single axon and its terminal field in the nuclear neuropil. **(B)** Contribution of the pyramidal-like cell (blue and red) and interneuron (black) axons to the nuclear neuropil. **(C)** High magnification view of the soma and proximal dendrites of an interneuron in the alpha component; an axon collateral arising from a fiber in the deep bulbar white matter at the top. **(D)** Proximal dendrites of a short-axon (left) and pyramidal-like neurons. **(E)** Contribution of axons and their collaterals to the neuropil of the alpha component (blue). Proximal dendrites from an interneuron (left) and a pyramidal-like cell. Note that the latter is covered by numerous dendritic spines. **(F)** Immunohistochemistry for glutamic acid decarboxylase, isoform 67 (GAD67) in the alpha component in a one-micron thin section counterstained with toluidine-blue. **(G)** Unstained, plastic-embedded section showing the pattern of GAD67 immunoreactivity in the alpha component. Note the lack of labeling in the white matter (upper right and lower left). Scale bars = 100 μm in **A**, 20 in inset and **E**, 40 in **B**, 15 in **C**, **D**, **F** and **G**.

occurring centrally or adjacent to the nuclear envelope. The cytoplasm exhibits focal areas of rough endoplasmic reticulum (RER) adopting the form of isolated, scattered cisternae. Adjacent to the RER there are two or three Golgi areas associated with membrane—bounded structures with high electron—dense matrices (**Figure 16A**) and multivesicular bodies. The cell profile is smooth although occasional indentations due to synaptic terminals can be seen. In appropriate sectioning planes one or two proximal dendrites from the somatic cytoplasm can be seen.

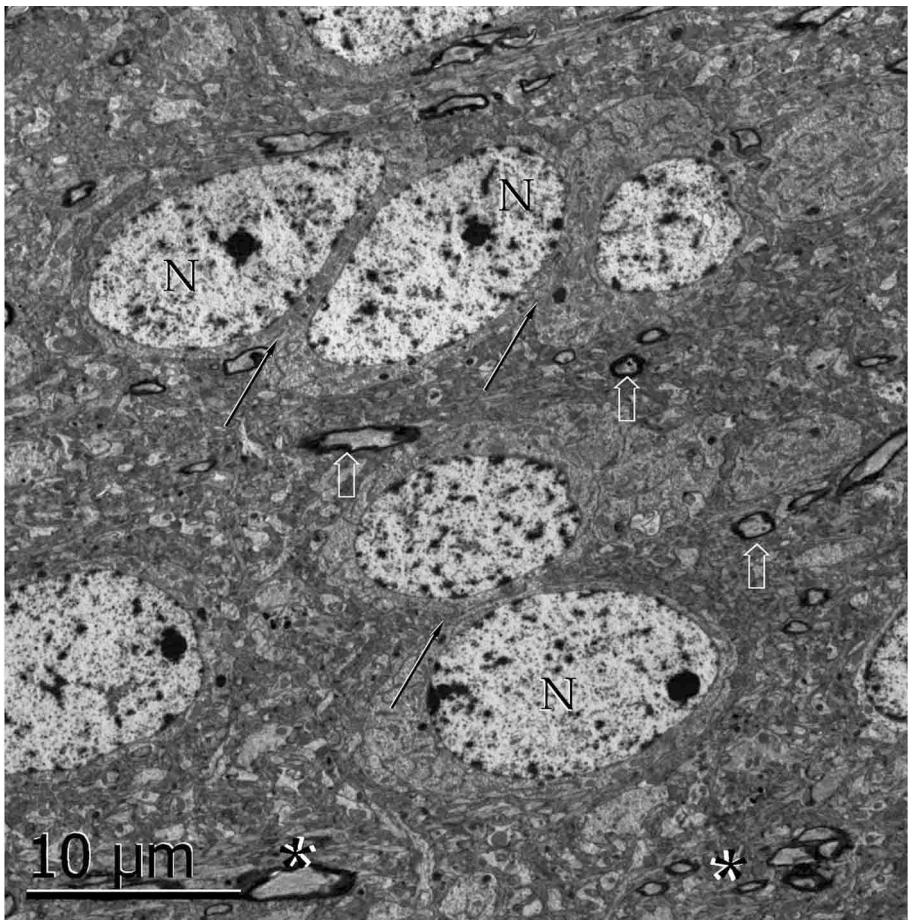

FIGURE 15 | Survey electron micrograph of neurons in the alpha component of the anterior olfactory nucleus. Note the apposition of somata (arrows). N, cell nucleus; arrows, myelinated axons. Uranium-lead contrast, adult rat brain.

Neuropil

The aAON neuropil proper is relatively homogeneous throughout the nucleus. In addition to isolated myelinated fibers (**Figure 15**), the neuropil exhibits the following specializations. Asymetrical axo-spinous contacts account for most (i.e., 92%) of the contacts of the aAON neuropil, followed by axo-shaft (5%) and occasional axo-somatic (<3%) contacts (17A and B). Somatic terminals include asymmetrical and reciprocal (**Figure 17C**) synapses, in order of frequency. The latter are indistinguishable from those in the rodent MOB, described earlier between mitral cells somata or their dendrites (Hirata, 1964, see Toida et al., 1996).

Immunocytochemistry

Scattered somata and synapses exhibit immunoreactivity to the glutamic acid decarboxylase 67 isoform (GAD-I) (**Figure 18A**). A set of neurons contain a coarse electron-dense material free in the cytoplasm or associated to the Golgi apparatus; this material is similar in appearance to that corresponding to immunoreactive sites (**Figure 18B**) (Toida et al., 1996; Barbaresi, 2005). GAD-I was also found in synaptic boutons, most commonly in axo-shaft and axo-somatic terminals (**Figure 18D**); in either case the post-synaptic element was devoid of GAD-I material. Furthermore, no GAD-I was found in axo-spinous terminals (**Figure 18C**). The frequent association of the GAD-I material precluded identification of the active zones associated with the synaptic apparatus and, therefore, their distribution at either side of the synaptic cleft.

DISCUSSION

Correlates for the functional involvement of the OL, should be based on the various earlier observations in this poorly understood area. Perhaps the first observation suggesting glomerular differentiation throughout the bulbar cortex was made in the new born rat and showed that glomerular glucose uptake at the MOB-AOB junction was enhanced following exposure to a nipple-derived pheromone. The term "modified glomerular complex" (MG) was coined to refer to these specialized glomeruli (Teicher et al., 1980; Greer et al., 1982). Further support for a bulbar parceling was supplied by the identification of a group of glomeruli that crown the caudal end of the MOB. Because these 8–9 glomeruli are mutually linked among them by fibrillar bridges, the term "necklace glomeruli" (NG) was introduced by Shinoda et al. (1989). On the basis of their connectional and immunohistochemical characteristics, the same authors regarded

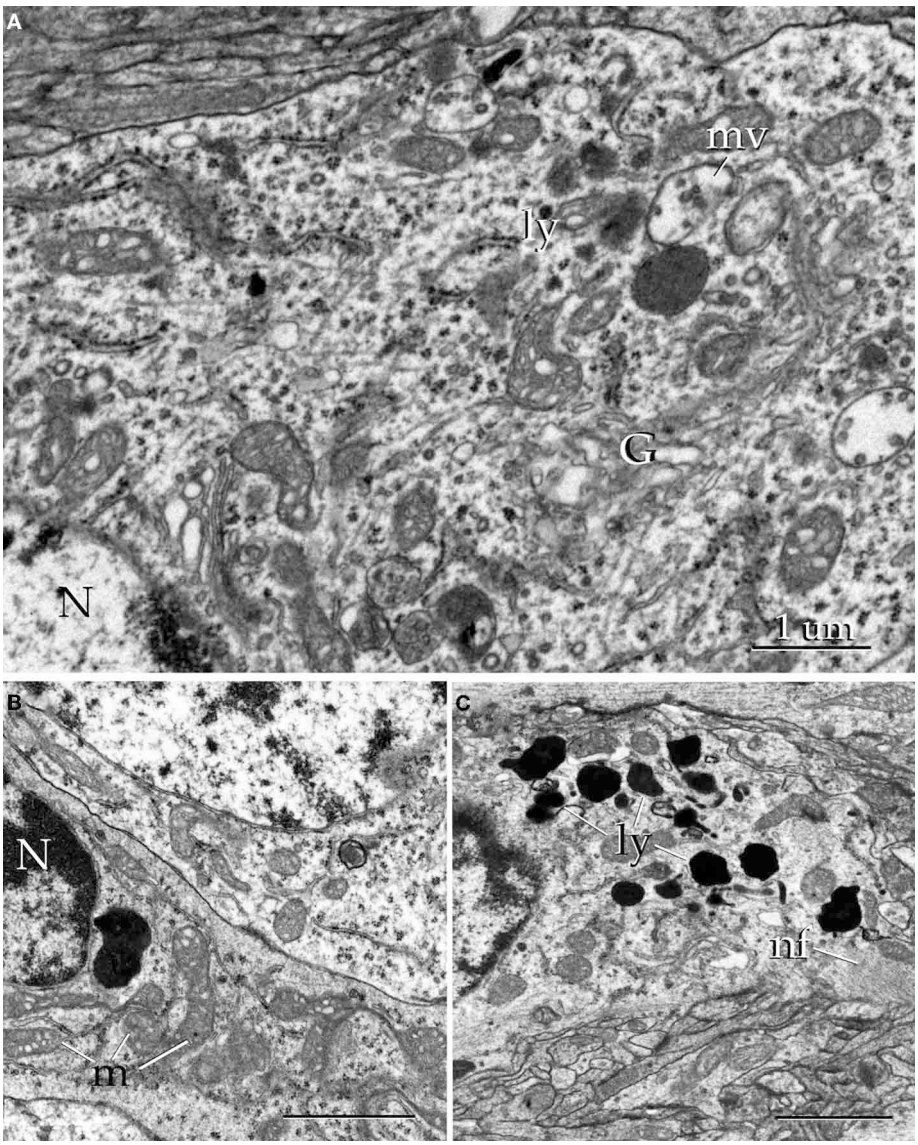

FIGURE 16 | Electron micrographs of the alpha component of the anterior olfactory nucleus. (A) Juxtanuclear cytoplasm of a neuron containing Golgi apparatus (G), electron-dense bodies (ly), and multivesicular bodies (mv). N, cell nucleus. **(B)** Nucleus (N) and cytoplasmic contents from a satellite cell. m, mitochondria. **(C)** Cytoplasm from an astrocyte containing numerous electron-dense structures (ly) and filament bundles (nf). Uranium-lead contrast, adult rat brain. Scale bars = 0.5 μm in **B** and **C**.

one of the MG as an integral part of the NG system. Present observations support the idea that one or two glomeruli from the former MG belong to the oral part of the AOB. In fact, inspection of the foremost part of the AOB show that glomerular dendrites of overlaying glomeruli arise primarily from large principal cells therein (**Figures 3A**,**5B**). This observation provides structural evidence for the AOB involvement in the pheromonal activation observed in the MG (Teicher et al., 1980; Greer et al., 1982). Actually exposition to the male rat to female urine (Pereno et al., 2011) increases Fos expression in the rostral half of the AOB with respect to the caudal, reaching the peak in the foremost AOB (Honda et al., 2008). As a matter of fact, illustrations shown in the latter studies (Honda et al., 2008; Pereno et al., 2011) suggest that cells in the OL area described here are also activated by pheromone exposure of the male rat. Further, stimulation by odorants or pheromones brings about successive activation of the MOB and AOB, reaching the peak in bold signal along the rosatral part of the AOB (Xu et al., 2005). Still another set of observations that distinguishes the OL from the rest of the bulbar cortex is its reception of axons arising in Grueneberg ganglion, a putative chemoreceptor located at the nasal vestibule (Grueneberg, 1973). In fact, Grueneberg ganglion projects to those glomeruli "in close apposition to the AOB" (Fuss et al., 2005), strengthen the notion that neurons there in are associated with chemosignal recognition and decoding (see Stowers and Logan, 2010).

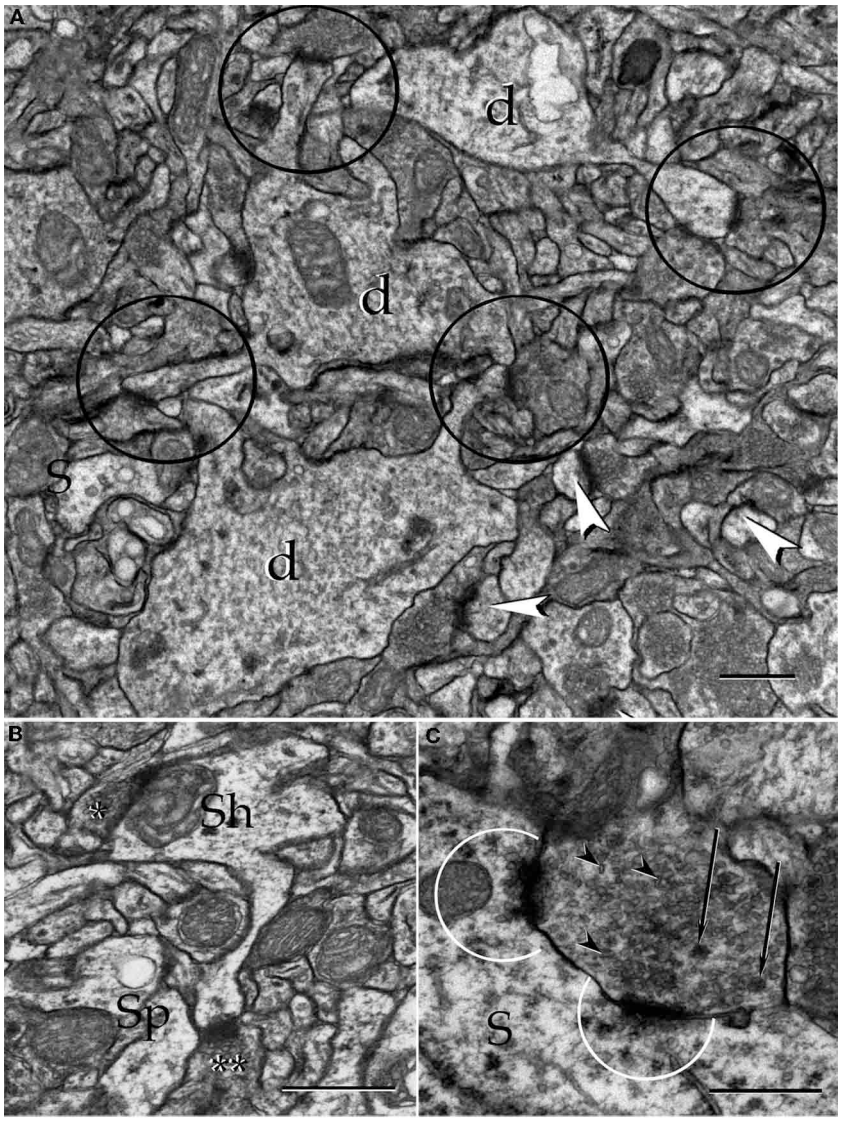

FIGURE 17 | Electron micrographs from the neuropil of the alpha component of the anterior olfactory nucleus. (A) Proximal dendrites (d) and axo-spinous, asymmetircal synapses, prevail in the neuropil. **(B)** An axo-shaft (Sh) and axo-spinous synapses. Asterisks, synaptic boutons. **(C)** A reciprocal synapse containing agranular (arrow-heads), and dense-core (arrows) vesicles establishes contact with the soma (S). Note the presence of numerous agranular vesicles in that part of the cytoplasm adjacent to the active zones (encircled). Uranium-lead contrast, adult rat brain. Scale bars = 1 μm in **A**, 0.5 μm in **B** and **C**.

An even more difficult task is to foresee the possible functional implication of our INBs described earlier (Larriva-Sahd, 2008) and ascribed here to the INA of the OL. To start with there is the association of the INB dendrites with fibers traveling in the LOT, a fiber system that conducts the efferent fibers arising from mitral/tufted and large principal cells, the only known output from the MOB and AOB, respectively. This association led me to speculate that the IFNs, which appear to be the foremost signature of cortical-like organization (i.e., afferent fibers, local circuit plus pyramidal cells), may represent a cellular substrate for relaying nerve impulses from both the MOB and AOB. Although this hypothesis requires further physiological evidence our current work, indicating that neurons in the INA-OL respond to electrical stimuli applied separately to either the main or AOBs, enhances the validity of our recent proposal. Whichever functional involvement for the OL emerges from future research, our anatomical frame provides a structural base line to define the physiological role of the distinct areas and cell-types depicted here.

THE ALPHA ANTERIOR OLFACTORY NUCLEUS: AN ORPHAN CELL GROUP?

The aAON was first described by Ramón y Cajal who stated that, although neurons therein were resistant to silver impregnations, the cluster of neurons was composed of large, polygonal cells as revealed by aniline-stained specimens. Only a laconic statement about them was made: "neurons with large nuclei, surrounded

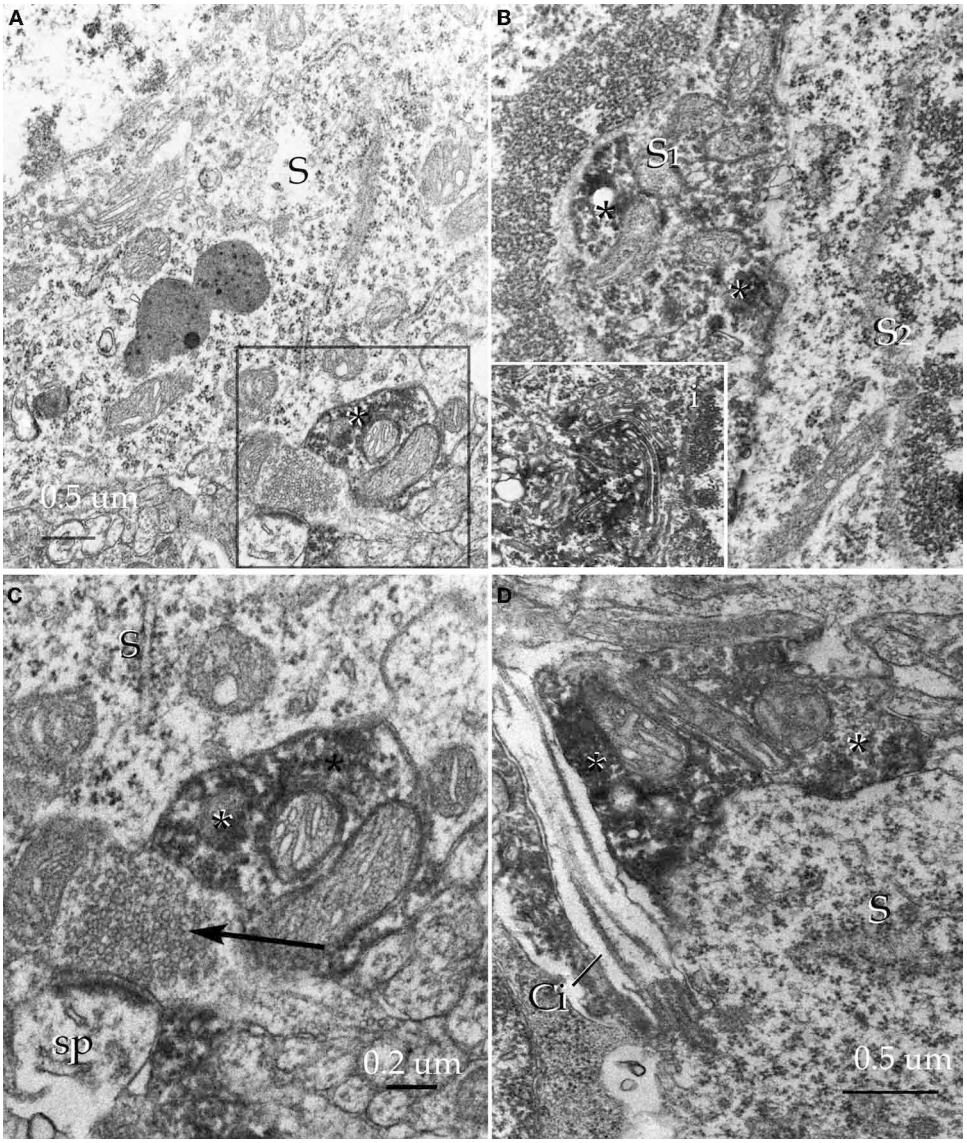

FIGURE 18 | Pre-embedding immunocytochemistry for glutamic acid decarboxylase, isoform 67 in the alpha component of the anterior olfactory nucleus. (A) Adjacent to an unlabeled soma (S) an immunoreactive synaptic terminal (asterisk) can be seen. **(B)** Somata of an unlabeled (S2) and an immunoreactive (S1) neuron. Note the high electron density of the amorphous material (asterisks) corresponding to immunoreactivity. i. High magnification view of the immunoreactive material assoaciated with the cisternae of the Golgi apparatus. **(C)** A labeled juxta-somatic synapse (asterisk) adjacent to an axo-spinous terminal that is devoid of immunoreactivity. S, soma. **(D)** A putative axo-somatic bouton positive for GAD67 (asterisks); note the emergency of a cilium at the periphery of the soma (S). Uranium-lead contrast, adult rat brain.

by a cytoplasm with fine granular chromatin resembling local association neurons, but having been unable to impregnate them with silver chromate, we ignore their structural characteristics and their connectivity as well" (Ramón y Cajal, 1904), closing by stating that this "foco de neuronas grandes" might correspond to short-axon neurons ("corpúsculos de Golgi") displaced from the granule cell layer of the AOB." In subsequent studies the same cell group was ascribed to an anterior component of the AON and, more recently, Valverde et al. (1989) termed it the alpha component of the AON. Actually the latter authors working in hedgehog specimens reported, for the first time, that the aAON was composed of pyramidal cells wedged between the M and AOB; no short-axon neurons were noted. Our study confirms this observation and extends it to the adult rat, mouse and guinea pig, thereby adding further cytological characteristics about the pyramidal-like neurons in these species. Furthermore, a set of aAON neurons corresponds to typical short-axon cells (vide infra), suggesting that the internal circuitry may involve the same fundamental elements as the cortical units, described by Lorente de Nó (1949), namely, afferent fibers, short-axon, and projecting neurons. Our electron microscopic observations disclosed further information regarding the synaptic organization of the nuclear

neuropil at the subcellular level as well as the mode of termination of putative inhibitory terminals showing GAD immunoreactivity (see Barbaresi, 2005). All together, these observations are relevant for the eventual understanding of both the internal nuclear circuitry and its physiological involvement. Lastly, the morphometric analysis of neuron-somata measurements indicates a difference between the dAON and aAON (see Brunjes et al., 2011) that, coupled with the difference of their overall appearance in both rapid-Golgi and aniline-stained specimens might underlie dissimilar physiological involvement.

FUNCTIONAL CORRELATES FOR THE aAON

In physiological terms, virtually nothing it is known about the aAON; however, some straightforward correlates, consisting with the structure and interactions of this nucleus can be made. In fact, afferent fiber systems that send terminal axonal fields or axon collaterals to aAON neurons derive from the deep bulbar white matter and from the LOT itself. Because the bulbar core white matter conducts fibers arising from the AON at either side of the brain (Valverde, 1965; DeCarlos et al., 1989; Yan et al., 2008), and because the LOT conducts fiber systems arising from the MOB and AOB, a mandatory working hypothesis is that the aAOB decodes olfactory information, perhaps that related to both the main and accessory olfactory systems. The growing concept that olfactory glomeruli in the MOB project centrally, ipsi-, and contra-laterally in a highly ordered fashion (Yan et al., 2008; Stowers and Logan, 2010; see Baum, in this volume), opens the attractive possibility of defining the glomerular and central interactions of the aAOB (see DeCarlos et al., 1989), which would be a fundamental step towards defining the functional role of the aAON.

NOVEL DOMAINS, NOVEL NEURONS?

It has long been assumed that the heterogeneous class of interneurons lying in the deep olfactory bulb (i.e., granule cell and internal cellular layers of the MOB and AOB, respectively) belongs to the "deep short-axon neurons" (López-Mascaraque et al., 1986, see Kosaka and Kosaka, 2011). Having added some candidates to this broad category it seems reasonable to outline our normative foundation to classify them into specific cell types (Larriva-Sahd, 2008, 2010; Paredes and Larriva-Sahd, 2010). Most neurons of the central nervous system are profusely interconnected by numerous pathways. This richness of connections is due not only to the high number of neurons and pathways but also to the branching of the axons and their collaterals and to the overlap between the fields of distribution of the branches from different axons (Lorente de Nó, 1938). Unlike most mammalian non-neural epithelial cells that exhibit a relative simple cellular interaction with their homologs, neurons, although alike, may usually be surrounded by discreet yet remarkably different driving influence, the influence indulge by axonal inputs. Thus, defining the distribution of the neuron's dendritic and axonal fields is a crucial step, for the ultimate understanding of the functional role of a neuron (Miles et al., 1996; DeFelipe, 2002). Therefore, it is fair to assume that two neurons with a nearly identical structural and immunohistochemical properties but associated with dissimilar bulbar areas and hence, with different fiber and cellular domains, should assume different functional roles. The top panels of **Figure 6** reproduce three interneurons that, on the sole basis of their somato-dendritic structure, might initially be classed in the same group (i.e., deep, short axon neurons). Indeed, all of them possess a spindle-or pear-shaped soma and give rise to various dendrites with few, or devoid of spines. However, if further dendritic and axonal criteria (i.e., topography, shape and dimensions) are added to the somato-dendritic picture, the former grouping would be too general or even simplistic. With these supporting arguments, we decided to classifying these neurons as separate entities. In précis, although the short axon-interstitial neurons of the bulbi, the main-accessory cell (see Pressler and Strowbridge, 2006; Larriva-Sahd, 2008), and the medullary interneuron (Paredes and Larriva-Sahd, 2010), and the interneuron described here in the aAOB, share somato-dendritic features between them, their association with distinct fiber systems and putative synaptic targets justify to classify them as separate entities.

ACKNOWLEDGMENTS

This work is dedicated to the memory of Professor Edward (Ted) G. Jones. supported by a grant from PAPIT: IN206511. The author thanks Gema Martínez Cabrera for her careful technical help and Dr. Dorothy Pless for her effective revision of the manuscript.

REFERENCES

Barbaresi, P. (2005). GABA-immunoreactive neurons and terminals in the cat periaqueductal gray matter: a light and electron microscopic study. *J. Neurocytol.* 34, 371–487.

Brunjes, P. C., Kay, R. B., and Arrivillaga, J. P. (2011). The mouse olfactory peduncle. *J. Comp. Neurol.* 519, 2870–2886.

DeCarlos, J. A., López-Mascaraque, L., and Valverde, F. (1989). Connections of the olfactory bulb and nucleus olfactorius anterior in the hedgehog (*Erinaceus europaeus*). *J. Comp. Neurol.* 279, 601–618.

DeFelipe, J. (2002). Cortical interneurons: from Cajal to (2001). *Prog. Brain Res.* 136, 215–238.

Doetsch, F., García-Verdugo, J. M., and Álvarez-Buylla, A. (1997). Cellular composition and three-dimensional organization of the subventricular germinal zone in the adult mammal brain. *J. Neurosci.* 17, 5046–5061.

Eyre, M. D., Antal, M., and Nusser, Z. (2008). Distinct deep short-axon cell subtypes of the main olfactory bulb provide novel intrabulbar and extrabulbar GABAergic connections. *J. Neurosci.* 28, 8217–8229.

Feldman, M. (1984). "Morphology of the neocortical pyramidal neuron," in *Cerebral Cortex*, Vol. 1, eds A. Peters and E. G. Jones (New York, NY: Plenum Press), 123–200.

Fuss, S. H., Omura, M., and Mombaerts, P. (2005). The Grueneberg ganglion of the mouse projects axons to glomeruli in the olfactory bulb. *Eur. J. Neurosci.* 22, 2649–2654.

Greer, C. A., Stewart, W. B., Teicher, M. H., and Shepherd, G. M. (1982). Functional development of the olfactory bulb and a unique glomerular complex in the neonatal rat. *J. Neurosci.* 2, 1744–1759.

Grueneberg, H. (1973). A ganglion probably belonging to the N. Terminalis system in the nasal mucosa of the mouse. *Z. Anat. Entwicklungsgesch.* 140, 39–52.

Hirata, Y. (1964). Some observations on the fine structure of the synapses in the olfactory bulb of the mouse, with particular reference to the atypical synaptic configuration. *Arch. Histol. Jpn.* 24, 293–302.

Honda, N., Sakamoto, H., Inamura, K., and Kashiwayanagi, M. (2008). Changes in Fos expression in the accessory olfactory bulb of sexually experienced male rats after exposure to female urinary pheromones. *Eur. J. Neurosci.* 27, 1980–1988.

Kosaka, T., and Kosaka, K. (2011). "Interneurons" in the olfactory bulb revisited. *Neurosci. Res.* 69, 93–99.

Kosaka, T., and Kosaka, K. (2007). Heterogeneity of nitric oxide syntetase-containing neurons in the mouse olfactory bulb. *Neurosci. Res.* 57, 165–178.

Larriva-Sahd, J. (2004). Juxtacapsular nucleus of the stria terminalis of the adult rat: extrinsic inputs, cell types, and neuronal modules: a combined Golgi and electron microscopic study. *J. Comp. Neurol.* 475, 220–237.

Larriva-Sahd, J. (2006). A histological and cytological study of the bed nuclei of the stria terminalis of the adult rat. II. Oval nucleus: extrinsic inputs, cell types, and neuronal modules. *J. Comp. Neurol.* 497, 772–807.

Larriva-Sahd, J. (2010). Chandelier and interfascicular neurons in the adult mouse piriform cortex. *Front. Neuroanatomy* 4:148. doi: 10.3389/fnana.2010.00148

Larriva-Sahd, J. (2008). The accessory olfactory bulb in the adult rat: a cytological study of its cell types, neuropil, neuronal modules, and interactions with the main olfactory system. *J. Comp. Neurol.* 510, 309–350.

Lledo, P. M., Merkle, F. T., and Alvarez-Buylla, A. (2008). Origin and function of olfactory bulb interneuron diversity. *Cell* 31, 392–400.

Lohman, A. H. M., and Mentink, G. M. (1969). The lateral olfactory tract and the anterior commissure, and the cells of the olfactory bulb. *Brain Res.* 12, 396–413.

Lohman, A. H. M. (1963). The anterior olfactory lobe of the guinea pig. *Acta. Anat.* 45, 9–109.

Lorente de Nó, R. (1938). Analysis of the activity of the chains of internuncial neurons. *J. Neurophysiol.* 1, 207–244.

Lorente de Nó, R. (1949). "Cerebral cortex: architecture, intracortical connections, motor projections," in *Physiology of the Nervous System*, ed J. F. Fulton (New York, NY: Oxford University Press), 288–312.

López-Mascaraque, L., De Carlos, J. A., and Valverde, F. (1986). Structure of the olfactory bulb of the hedgehog (*Erniaceus europaeus*): description of cell types in the granule layer. *J. Comp. Neurol.* 253, 135–152.

Macrides, F., and Davis, B. J. (1983). "The olfactory bulb," in *Chemical Neuroanatomy*, ed P. C. Emson (New York, NY: Raven Press), 391–426.

Martel, K. L., and Baum, M. (2009). A centrifugal pathway to the mouse accessory olfactory bulb from the medial amygdale conveys gender-specific volatile pheromonal signals. *Eur. J. Neurosci.* 29, 368–376.

Miles, R., Toth, K., Gulyas, A. I., Hajos, N., and Freund, T. F. (1996). Differences between somatic and dendritic inhibition in the hippocampus. *Neuron* 16, 815–823.

Paredes, G., and Larriva-Sahd, J. (2010). Medullary neurons in the core white matter of the olfactory bulb: a new cell type. *Cell Tissue Res.* 339, 281–295.

Pereno, G. L., Balaszczuk, V., and Beltramino, C. A. (2011). Detection of conspecific pheromones elicit fos expression in GABA and calcium-binding cells of the rat vomeronasal system-medial extended amygdala. *J. Physiol. Biochem.* 67, 71–85.

Pressler, R. T., and Strowbridge, B. W. (2006). Blanes cell mediate persistent feedforward inhibition onto granule cells in the olfactory bulb. *Neuron* 49, 889–904.

Ramón y Cajal, S. (1904). "Corteza Olfativa," in *Textura del Sistema Nervioso Central del Hombre y los Vertebrados* Vol. 2, Imprenta y Librería Nicolás Moya, España.

Ring, G., Mezza, R. C., and Schwob, L. E. (1997). Immunohistochemical identification of discrete subsets of rat olfactory neurons and the glomeruli that they innervate. *J. Comp. Neurol.* 388, 415–434.

Senba, E., Simmons, D. M., and Swanson, L. W. (1990). Localization of neuropeptide precursor-synthesizing neurons in the rat olfactory bulb: a hybridization histochemical study. *Neuroscience* 38, 629–641.

Shinoda, K. Y., Shiotani, Y., and Osawa, Y. (1989). "Necklace olfactory glomeruli" form unique components of the rat primary olfactory system. *J. Comp. Neurol.* 284, 362–373.

Stowers, L., and Logan, D. W. (2010). Olfactory mechanisms of sterotyped behavior: on the scent of specialized circuits. *Curr. Opin. Neurobiol.* 20, 274–280.

Teicher, M. H., Stewart, W. B., Kauer, J. S., and Shepherd, G. (1980). Suckling pheromone stimulation of a modified glomerular region in the developing rat olfactory bulb revealed by the 2-deoxyglucose method. *Brain Res.* 194, 530–535.

Toida, K., Kosaka, K., Heizmann, C. W., and Kosaka, T. (1996). Electron microscopic serial-secrioning/reconstruction study of parvalbumin-containing neurons in the external plexiform layer of the rat olfactory bulb. *Neuroscience* 72, 449–466.

Valverde, F., López-Mascaraque, L., and De Carlos, J. A. (1989). Structure of the nucleus olfactorius anterior of the hedgehog (*Erinaceus europaeus*). *J. Comp. Neurol.* 279, 581–600.

Valverde, F. (1965). *Studies of the Pyriform Lobe.* Cambridge, MA: Harvard University Press.

Xu, F., Schafer, M., Kida, I., Schafer, J., Liu, N., Rothman, D. L., Hyder, F., Restrepo, D., and Shepherd, G. M. (2005). Simultaneous activation of mouse main and accessory olfactory bulbs by odors and pheromones. *J. Comp. Neurol.* 489, 491–500.

Yan, Z., Tan, J., Qin, C., Lu, Y., Ding, C., and Luo, M. (2008). Precise circuitry links bilaterally symmetric olfactory maps. *Neuron* 58, 613–624.

Conflict of Interest Statement: The author declares that the research was conducted in the absence of any commercial or financial relationships that could be construed as a potential conflict of interest.

Received: 21 May 2012; paper pending published: 01 June 2012; accepted: 06 June 2012; published online: 27 June 2012.

Citation: Larriva-Sahd J (2012) Cytological organization of the alpha component of the anterior olfactory nucleus and olfactory limbus. Front. Neuroanat. ***6****:23. doi: 10.3389/fnana.2012.00023*

frontiers in
NEUROANATOMY

REVIEW ARTICLE
published: 24 December 2012
doi: 10.3389/fnana.2012.00050

Mutual influences between the main olfactory and vomeronasal systems in development and evolution

Rodrigo Suárez [1,2†]***, Diego García-González*** [3†] ***and Fernando de Castro*** [3*]

[1] *Queensland Brain Institute, The University of Queensland, St Lucia, Brisbane, QLD, Australia*
[2] *Departamento de Biología, Facultad de Ciencias, Universidad de Chile, Santiago, Chile*
[3] *Grupo de Neurobiología del Desarrollo-GNDe, Hospital Nacional de Parapléjicos-SESCAM, Toledo, Spain*

Edited by:
Jorge A. Larriva-Sahd, Universidad Nacional Autónoma de México, Mexico

Reviewed by:
Alino Martinez-Marcos, Universidad de Castilla, Spain
Jorge A. Larriva-Sahd, Universidad Nacional Autónoma de México, Mexico

****Correspondence:***
Fernando de Castro, Grupo de Neurobiología del Desarrollo-GNDe, Hospital Nacional de Parapléjicos, Finca "La Peraleda" s/n, E-45071 Toledo, Spain.
e-mail: fdec@sescam.jccm.es

† These authors equally contributed to this work.

The sense of smell plays a crucial role in the sensory world of animals. Two chemosensory systems have been traditionally thought to play-independent roles in mammalian olfaction. According to this, the main olfactory system (MOS) specializes in the detection of environmental odorants, while the vomeronasal system (VNS) senses pheromones and semiochemicals produced by individuals of the same or different species. Although both systems differ in their anatomy and function, recent evidence suggests they act synergistically in the perception of scents. These interactions include similar responses to some ligands, overlap of telencephalic connections and mutual influences in the regulation of olfactory-guided behavior. In the present work, we propose the idea that the relationships between systems observed at the organismic level result from a constant interaction during development and reflects a common history of ecological adaptations in evolution. We review the literature to illustrate examples of developmental and evolutionary processes that evidence these interactions and propose that future research integrating both systems may shed new light on the mechanisms of olfaction.

Keywords: odorant, pheromone, neuroethology, neurogenesis, axon guidance, cell migration, cerebral cortex

THE HYPOTHESIS OF DUAL OLFACTION

The ability to sense the chemical landscape has played an important role in animal evolution. The sensory systems involved in vertebrate chemoreception have specialized and diversified following a close relationship with the ecological conditions that animals face throughout both ontogeny and phylogeny. These two systems have been traditionally regarded as functional and anatomically independent, involving parallel processing of distinct sets of molecules, related to different behavioral contexts and involving distinct telencephalic connections [for specific review, see Ache and Young (2005)]. Consequently, this long held view has suggested that the processing of environmental odors occurs exclusively by the main olfactory system (MOS) and pheromones by the vomeronasal system (VNS). Therefore, the notion of "dual olfaction" refers to these seemingly independent paths of processing distinct stimuli resulting in distinct types of behaviors (Winans and Scalia, 1970; Scalia and Winans, 1975). However, in spite of anatomical and functional differences, recent findings strongly suggest that the MOS and VNS play synergistic roles in the regulation of a range of olfactory-guided behaviors, from foraging and defensive contexts to reproductive and social interactions, and show overlap in some of their central projections [for specific reviews, see Buck (2000); Dulac and Torello (2003); Ache and Young (2005); Baum (2012)].

We will discuss here the hypothesis that the synergistic actions of the MOS and VNS in vertebrates are not limited to olfactory perception and regulation of behavior, but they are also intimately related (1) during ontogeny, by sharing molecular and cellular processes, and (2) during phylogeny, by showing similar adaptations to changing ecological scenarios.

GENERAL STRUCTURE OF THE MAMMALIAN OLFACTORY SYSTEMS

In the MOS, a group of olfactory sensory neurons (OSN) located at the roof of the nasal cavity [mainly at the olfactory epithelium (OE), plus two additional regions known as the Grüneberg ganglion and the septal organ] project to glomerular neuropil at the olfactory bulb [OB; **Figure 1A**; for a specific review, see Fleischer and Breer (2010)]. The OE consists of multiple laminar folds of neuroepithelium, where volatile molecules come into contact with the mucosa during either passive respiration or active sniffing. Each OSN extends multiple cilia into the mucous lining of the neuroepithelium, where only one olfactory receptor gene is expressed. Their activation triggers a cAMP cascade and the activation of cyclic nucleotide-gated and calcium-activated chloride channels [for a review, see Mombaerts (2004)]. There are millions of OSNs [1] in the OE, each of them expresses just one of ∼1000 olfactory receptor genes (it is the largest gene family within mammalian genomes; Buck and Axel, 1991), and those OSNs expressing the same receptor (∼5000–10000 neurons) converge their axons to a single glomeruli at each half of the OB (Ressler et al., 1994; Vassar et al., 1994; Strotmann, 2001; Strotmann et al., 2004; Mombaerts, 2006; de Castro, 2009; Martínez-Marcos, 2009). Thus, each of the ∼2000 glomeruli of

[1] The estimated number of OSNs is 5–10 million in rodents and humans and up to 50 million in rabbits.

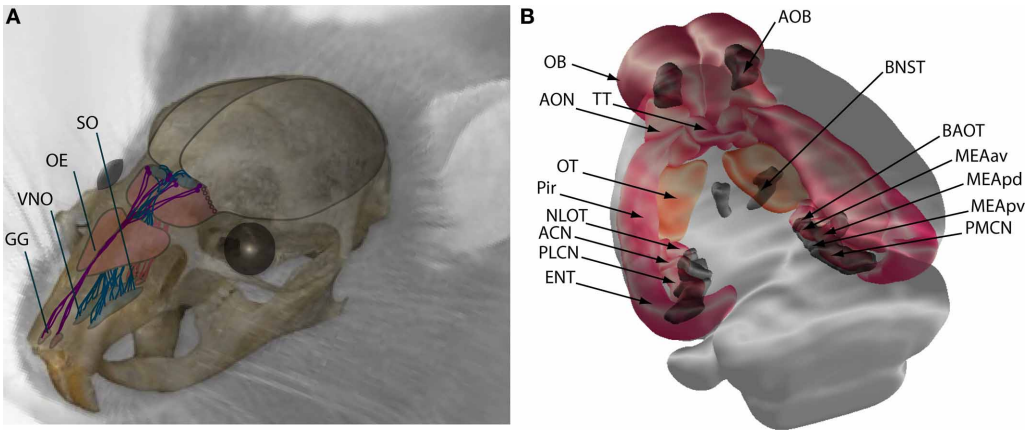

FIGURE 1 | Schematic representation of the main olfactory (MOS) and vomeronasal systems (VNS) in mice. (A) Sensory neurons of the MOS are located in the nasal cavity at the olfactory epithelium (OE), Grüneberg ganglion (GG), and septal organ (SO), from where they send projections to the OB. Neurons of the VNS are located in the vomeronasal organ (VNO) and send axonal projections to the accessory olfactory bulb (AOB). **(B)** Central projections of the OB (pink and orange) terminate at the anterior olfactory nucleus (AON), tenia tecta (TT), olfactory tubercle (OT), piriform cortex (Pir), nucleus of the lateral olfactory tract (NLOT), anterior cortical nucleus (ACN) and posterolateral cortical nucleus (PLCN) of the amygdala, and entorhinal cortex (ENT). Central projections of the VNS are shown in dark gray, the accessory olfactory bulb (AOB) projects to the bed nucleus of the stria terminalis (BNST), the bed nucleus of the accessory olfactory tract (BAOT), the medial amygdala anteroventral (MEAav), posterodorsal (MEApd), posteroventral (MEApv), and posteromedial cortical nucleus (PMCN).

the OB represents convergent projections of OSNs expressing the same receptor and is innervated by the apical dendrite of a single mitral/tufted cell (Mombaerts, 2006). This organization has been regarded as a "labeled line" of olfactory processing (Luo and Katz, 2004), as each mitral cell represents the activation of a single type of olfactory receptor and, after horizontal processing by periglomerular and granular interneurons, project to the telencephalic structures collectively known as olfactory cortex (OC; see below).

Conversely, the vomeronasal organ (VNO) is a close-ended tubular structure, located bilaterally at the base of the nasal septum, which opens to the mouth and/or nostrils, allowing influx of fluids containing pheromones by a vascular pumping mechanism performed by exploring animals (Meredith et al., 1980). Vomeronasal sensory neurons (VSNs) expose microvilli to the lumen of the VNO where they express a different subset of G-protein coupled receptors, either V1R or V2R, associated to either $G\alpha_{i2}$ or $G\alpha_o$ proteins, and project to rostral or caudal regions of the accessory olfactory bulb (AOB), respectively (Dulac and Axel, 1995; Berghard and Buck, 1996; Herrada and Dulac, 1997; Matsunami and Buck, 1997; Ryba and Tirindelli, 1997; Buck, 2000; Dulac and Wagner, 2006). Sensory transduction involves the activation of the IP3/DAG cascade and TRPC2 channels (Zufall et al., 2005). VRNs of apical or basal subdomains of the VNO express one receptor protein out of ∼200 V1R or 80 V2R genes, respectively. However, in the AOB, each VSN projects to 6–30 glomeruli and each mitral cell innervates 3–9 glomeruli from neurons expressing the same or genetically related receptors (Belluscio et al., 1999; Rodríguez et al., 1999; Del Punta et al., 2002; Wagner et al., 2006; Larriva-Sahd, 2008). Therefore, it seems that sensory coding follows different rules between both chemosensory systems, with the VNS showing a high degree of synaptic integration from distinct receptors, possibly relating with a highly synthetic role in discerning qualitative aspects of pheromones (Holy et al., 2000; Luo et al., 2003; Ben-Shaul et al., 2010; Isogai et al., 2011).

The projections of the OB and AOB are remarkably different. The OB projects to the anterior olfactory nucleus, taenia tecta, olfactory tubercle, piriform cortex, anterior and posterolateral amygdaloid nuclei, and the lateral part of the entorhinal cortex. All of these projections form the medial and lateral olfactory tract (LOT), which also contains the equivalent efferents from the AOB (**Figure 1B**; Devor, 1976; Shipley and Adamek, 1984; Greer, 1991; Butler and Hodos, 2005; de Castro, 2009; Martínez-Marcos, 2009).

Recent studies have confirmed the existence of different projection patterns of OB efferents. Axons from mitral cells project widely to the OC, including the entire piriform cortex, while axons from tufted cells project to the more rostral structures, including the anterior portion of the piriform cortex (Haberly and Price, 1977; Nagayama et al., 2010; Fukunaga et al., 2012). These differences are related to different activation of mitral and tufted cells in response to OSN inputs and, consequently, diversify OB activity and processing signals on their way to the OC, ameliorating odorant discrimination (Fukunaga et al., 2012). The tertiary efferents from the OC structures can be summarized as follows: the piriform cortex projects to the endopiriform nucleus (connected, in turn, with the medial or vomeronasal amygdala, see below), the entorhinal cortex projects mainly to the hippocampus (forming the perforant path), and the olfactory amygdala project to the vomeronasal amygdaloid nuclei (Kang et al., 2009; Martínez-Marcos, 2009). In contrast, the AOB projects to medial striatal and subcortical amygdaloid nuclei, named the vomeronasal amygdala (**Figure 1B**; Winans and Scalia, 1970; Scalia and Winans, 1975; Devor, 1976; Shipley and Adamek, 1984; Price, 1986; Martínez-Marcos, 2009;

Kang et al., 2011). The VNS seems to preserve some segregation between the areas of the AOB receiving input from VSNs expressing different vomeronasal receptors and their telencephalic projections (Mohedano-Moriano et al., 2007; Martínez-Marcos, 2009). The nuclei in receipt of AOB projections send tertiary projections exclusively to other structures of the VNS (including the AOB) and hypothalamic nuclei, with scarce fibers from the posteromedial amygdala making synapses on the hippocampal formation. Interestingly, there is a high degree of integration of centrifugal projections from nuclei in receipt of both OB and AOB projections (Mohedano-Moriano et al., 2007, 2008, 2012; Martínez-Marcos, 2009).

Despite the evidence supporting behavioral and anatomical differences between the MOS and the VNS, recent studies have shown an important overlap in the responses of each system to a range of ligands (odorants and pheromones), in the expression of receptors and other signaling components, in their telencephalic projections, and in their physiological and behavioral responses, prompting a review of the hypothesis of "dual olfaction" as it was originally raised [for specific reviews, see Brennan and Zufall (2006); Baum and Kelliher (2009)].

ONTOGENETIC PERSPECTIVES: THE DEVELOPMENT OF THE MAIN OLFACTORY AND VOMERONASAL SYSTEMS

Early in embryogenesis, the olfactory placode differentiates from the lateral surface ectoderm of the vertebrate head and gives rise to the sensory neurons reviewed in this work (OSNs and VSNs), as well as to gonadotropin-releasing hormone (GnRH) neurons (Schwanzel-Fukuda and Pfaff, 1989; Wray et al., 1989; Forni et al., 2011). All other olfactory and vomeronasal structures are telencephalic derivatives. A summary of the major events in development of these structures (i.e., neurogenesis-proliferation, cell migration and differentiation, axonal guidance and synaptogenesis) is illustrated in **Figure 2**, using the mouse time scale [for specific reviews, see López-Mascaraque and de Castro (2002, 2004); de Castro (2009)].

FATE DETERMINATION OF OLFACTORY AND VOMERONASAL SENSORY NEURONS

As discussed above, the olfactory placode gives rise to three major neuron classes: OSNs, VSNs, and GnRH neurons. Despite growing evidence for the functional importance of these cell types, many aspects of their biology, such as the regulation of their cell fate and the molecular interactions at the OE as a neurogenic niche, remain poorly understood. These processes have become a subject of increasing interest as they may help unravel important questions regarding CNS regeneration, such as the production and functional integration of newborn neurons throughout ontogeny [for a specific review, see Schwob (2002)]. The functional identity of OSNs and their pattern of projections to the OB depend on the selective expression of a single olfactory receptor (Lomvardas et al., 2006). However, the overall identity of OSN precursors in subregions of the OE is affected by the graded expression of a set of molecules that act in a dose-dependent manner (Tucker et al., 2010). Although this graded pattern of expression reflects major differences between precursor cells in the lateral and medial portions of the OE, the existence of transition zones in the OE supports a combinatorial effect of factors modulating OSN fate choice (Tucker et al., 2010).

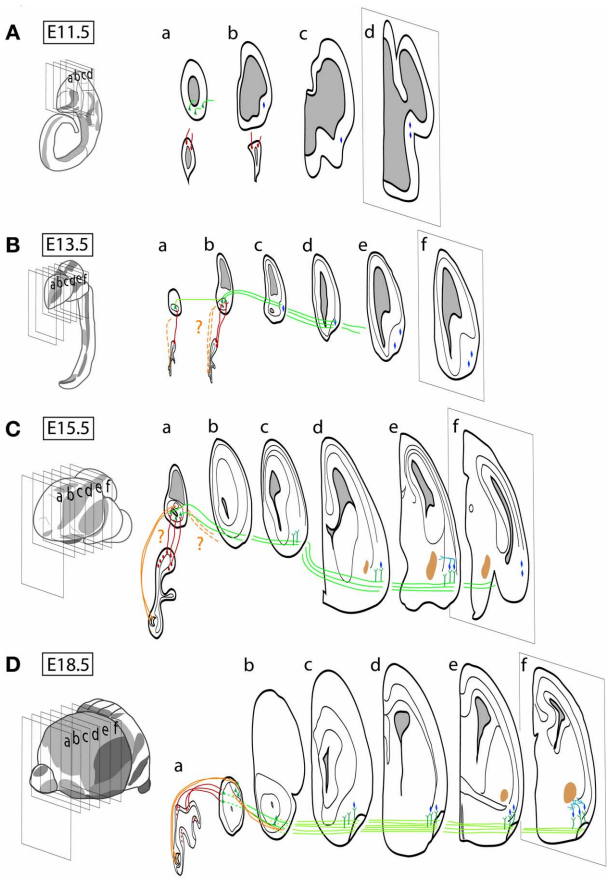

FIGURE 2 | Schematic representation of the spatio-temporal neurogenic pattern and its connections within the olfactory systems during embryonic development in the mouse. (A) At approximately embryonic day 9.5 (E9.5), the olfactory placode starts to form with the first signs of neurogenesis in the presumptive OE, while the first neurons are generated by E11 at the OB and by E10 at the OC. **(B)** The first axons emerging from the olfactory placode are identified before E10.5, and they form clear olfactory and vomeronasal nerves between E11 and E12, which form synapses in the OB and AOB around E13.5 (dotted lines suggest the first axons from the VNO arriving into the AOB). **(A)** First LOT axons (AOB) are observed between E11.5 and E12 and **(B)** LOT covers the OC surface by E13.5. **(C)** Axon collaterals emerge from the LOT in gross amount E15.5, colonizing the OC structures. **(D)** OSN axons, diffusely innervating the OB at E13.5, reorganize topographically innervating protoglomeruli by E17.5 in a process which extends until postnatal stages (not illustrated). The maturation of synapses between OSN and OB neurons occurs by E17–E18, while AOB synapses mature by the end of the first postnatal week (not illustrated). The definitive OB and AOB layering depends on the arrival of the prospective interneurons generated in their neurogenic niche at the forebrain SVZ (see text for details).

During early development of the olfactory pits, the expression of several molecules, such as the zinc-finger transcription factors Fezf1 and Fezf2, begins to differ between the presumptive vomeronasal and main olfactory regions. As early as E10.5, Fezf1 is expressed in both the OE and VNO, while Fezf2 expression is restricted to the VNO. By birth, Fezf1 becomes almost

exclusively present in the OE, while Fezf2 retains its expression in the VNO (**Figure 3**; Eckler et al., 2011). Another zinc-finger transcription factor, BCl11b/Ctip2, plays an important role in the fate determination of VSNs into one of the two vomeronasal subtypes (Enomoto et al., 2011).

The development of OSNs and VSNs depends on complex interactions among proliferative and pro-differentiation transcription factors, sharing similar differentiation processes ruled by the neurogenic bHLH transcription factors Mash1, Ngn1, and NeuroD, which are sequentially expressed by neuronal progenitors, precursors, and differentiating neurons, respectively (**Figure 3**; Guillemot et al., 1993; Cau et al., 1997, 2002; Murray et al., 2003; Beites et al., 2005; Tucker et al., 2010; Enomoto et al., 2011; Packard et al., 2011; Suárez, 2011). These shared mechanisms may indicate that the genetic machinery involved in the maturation of functional chemosensory neurons has been conserved throughout evolution of both sensory systems. The frontal-nasal mesenchyme secretes essential inductive signals for the early development of the olfactory placode: the strong morphogen FGF-8 instructs the olfactory primordium to express high levels of *Meis1* (mainly at the lateral OE), as well as *Sox-2* and *Ascl1* genes (mainly at the medial OE). Altogether, these transcription factors regulate the differentiation from multipotent precursors to the three types of postmitotic neurons (**Figure 3**). Consequently, Meis1-expressing OE precursors have been recently implicated as the initial source of OSNs, VSNs, and GnRH neurons (Tucker et al., 2010).

ZONAL SEGREGATION AND AXONAL PATHFINDING TO OB AND AOB GLOMERULI

Although the identification of olfactory receptors in the growth cones of the OSNs gave rise to speculations about their potential role in axon guidance, the relative contribution of these molecules versus the role of early sensory activity on olfactory targeting remains far for conclusive (Feinstein and Mombaerts, 2004; Priest and Puche, 2004; Mombaerts, 2006; Hovis et al., 2012). Most of these guidance processes relies on the orchestration of secreted chemoattractants orienting olfactory axons on their mesodermic way to the OB (such as HGF, retinoic acid, Wnt5a, with the collaboration of the adhesion molecule PSA-NCAM) as well as the intra bulbar gradients of both chemoattractants (IGF-1, Sema 3F) and chemorepellents (Sema 3A, Slit-1 and -2), which determine the pattern of OB glomeruli innervation (**Figure 4Aa1**; López-Mascaraque and de Castro, 2002; St John et al., 2002; Schwarting and Henion, 2008; de Castro, 2009; Imai, 2012).

On the contrary, relatively little is known about AOB glomerulus innervation. Depending on their basal-apical location, VSN axons express or not a battery of receptors (neuropilin-2, robo-1, ephA6) that affect their responses to the preliminary Sema 3F-due fasciculation and, once at the target, the production of Slit-1 (anterior part) or Slit-3/ephA6 (posterior part) within the AOB (**Figures 4Aa2–a3**).

Altogether, the available data reflect shared mechanisms between both systems in the organization of the first synaptic relay (secreted semaphorins and slits), as well as mechanisms that seem exclusive of the MOS (secreted morphogens—retinoic

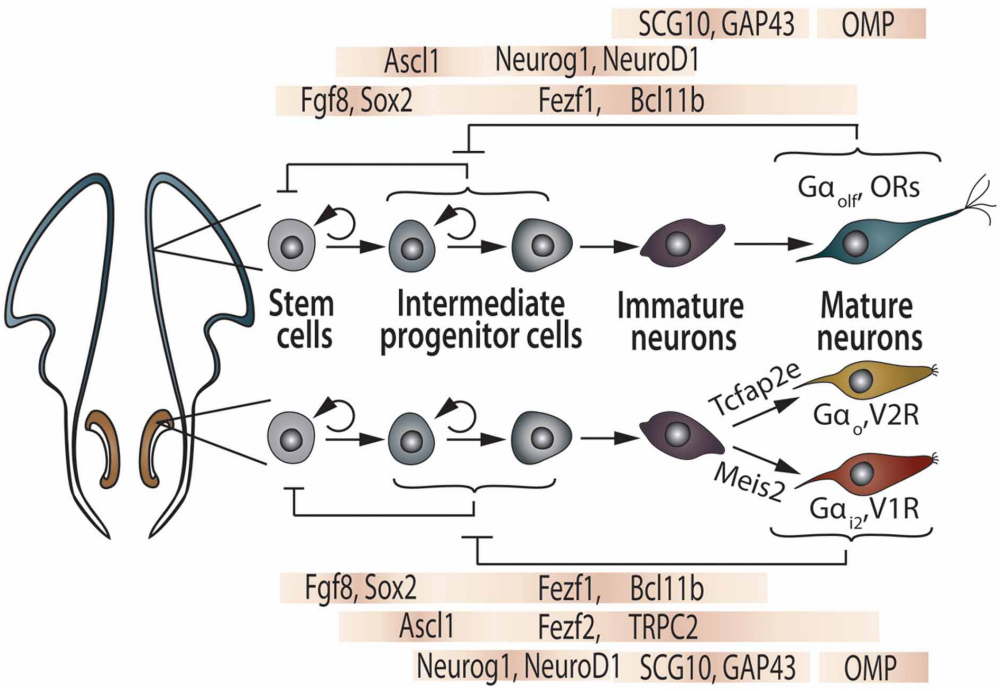

FIGURE 3 | Transcription factors controlling generation and maturation of OSN and VSN. The OSN (top) and VSN (bottom) lineages are illustrated in parallel. Inhibitory feedback mechanisms are proposed to be acting on intermediate progenitor cells by mature neurons as well as regulation of stem cell pool by intermediate progenitors. See text and references therein for further explanations.

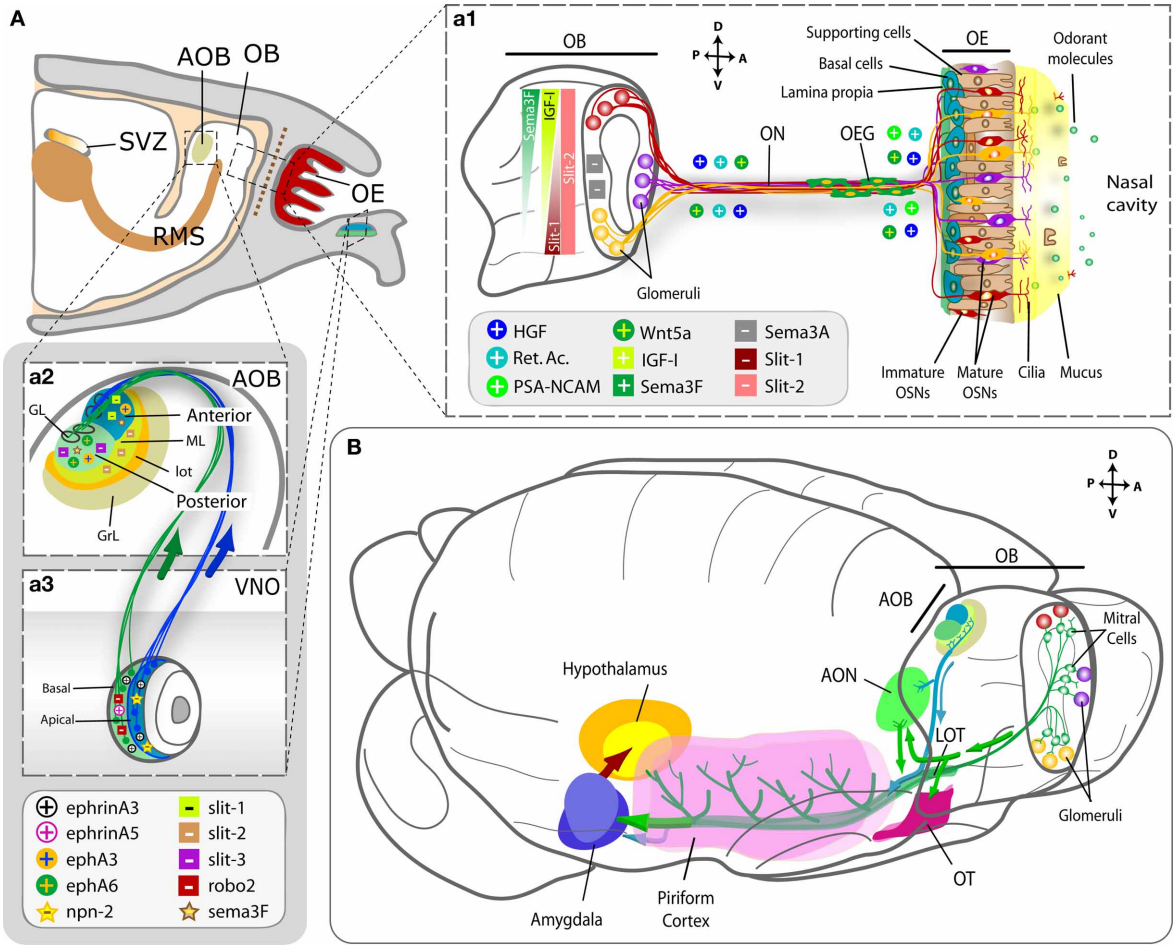

FIGURE 4 | Molecules involved in the formation of the olfactory and vomeronasal nerves and the LOT. (A) Sagittal section of the rodent forebrain representing the olfactory structures. Panel **(a1)** represents the wiring between the OE and the OB, where each OSN expresses a single olfactory receptor gene and the axons from all cells expressing that particular receptor converge onto one or a few glomeruli (GL) in the OB. Molecules secreted from the OB form the olfactory nerve are represented as "+" when they attract/promote axon growth and as "−" when they repel/inhibit it. Spatial IGF-1, Sema 3A, Sema 3F, and Slit-1 gradients are crucial to address axons to their zonal targets within the OB. Panels **(a2** and **a3)** show in detail the VNO and the AOB structures and their connections, with layer-specific representation of the cues involved in the process. **(B)** Schematics showing the spatial relationship of the centripetal projections from the OB (in green) and AOB (in blue) to their recipient structures in the cortex. Abbreviations: AOB, accessory olfactory bulb; AON, anterior olfactory nucleus; GL, glomerular layer; GrL, granule layer; LOT, lateral olfactory tract; ML, mitral cell layer; OB, olfactory bulb; OE, olfactory epithelium; OEG, olfactory ensheathing glia; ON, olfactory nerve; OSN, olfactory sensory neuron; RMS, rostral migratory stream; SVZ, subventricular zone; OT, olfactory tubercle; VNO, vomeronasal organ.

acid, Wnt, IGF-1, HGF-, the adhesion cue PSA-NCAM) or of the VNS (ephrins).

NEUROGENESIS AND CELL MIGRATION IN THE OLFACTORY FOREBRAIN

One of the most striking characteristics of the olfactory system is that active physiological neurogenesis occurs throughout ontogeny. While in the OE new OSNs are generated to replace those dying, in the subventricular zone (SVZ) of the forebrain new interneuron precursors are generated which migrate and integrate in both the OB and AOB [**Figure 5**; for a specific review see Lledó et al. (2008)]. Both neurogenic processes start early in development (by E10.5 in a mouse-based chronology; **Figures 2**, **5**) and the latter shows peaks just before (E17) and after birth (P2–P7), giving rise to its mature aspect a short time after that. By P15, the astrocytic channels allowing the migration of chains of newly generated neuroblasts are present (Petreanu and Álvarez-Buylla, 2002). Slit-2 forces neuroblasts to leave the SVZ neurogenic niche and (with the actions of motogenic and attractive anosmin-1, FGF-2, and HGF) migrate to form the rostral migratory stream (RMS), before reaching its mature aspect with astrocytic channels (Hu, 1999; Wu et al., 1999; Garzotto et al., 2008; García-González et al., 2010; Murcia-Belmonte et al., 2010). These active neurogenic processes make the OB an interesting model for the study of physiological plasticity in the adult brain. While fast-growing axons from newly generated OSNs project toward their respective OB glomeruli, a comparatively smaller contingent of newly generated interneurons (periglomerular and

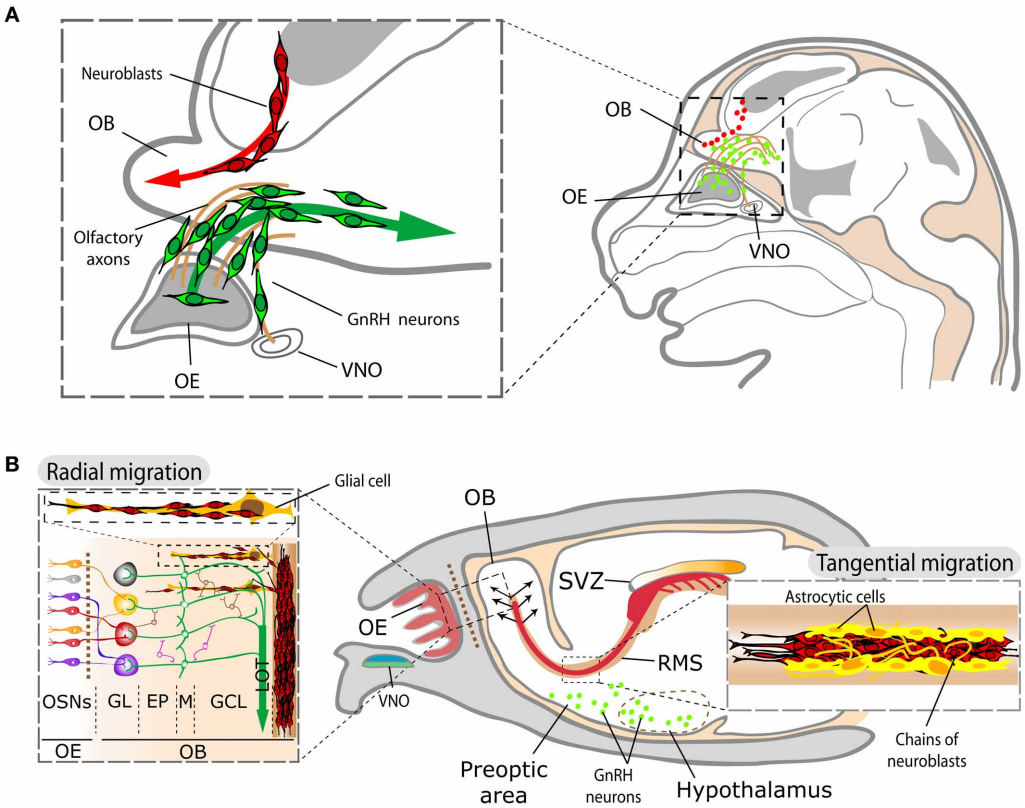

FIGURE 5 | Schematic representation of SVZ and GnRH neuroblast migration within the olfactory system. (A) During development, neuroblasts originated in the lateral ganglionic eminences migrate toward the OB (red cells). GnRH-1 neuroblasts (green cells) generated in the OE follow the olfactory and vomeronasal axons on their way to the hypothalamus. **(B)** In the adult, the contingent of migrating SVZ neuroblasts (in red) forms the RMS toward the OB, whereas GnRH neurons (in green) are located in several areas comprising the preoptic area and the hypothalamus. The inset on the right illustrates the aspect of mature RMS, with the chains of migrating neuroblasts (in red) advancing among astrocytic channels (in yellow). Once they reach the OB, SVZ neuroblasts migrate radially to their final targets within the OB (left panel). Abbreviations: EP, external plexiform layer; GL, glomerular layer; GCL, granule layer; LOT, lateral olfactory tract; M, mitral cells; OB, olfactory bulb; OE, olfactory epithelium; OSN, olfactory sensory neuron; RMS, rostral migratory stream; SVZ, subventricular zone; VNO, vomeronasal organ.

granule cells) differentiate and develop synaptic connections to integrate in functional micro-circuits, modulating firing properties of projection neurons (Belluzzi et al., 2003). Interestingly, the rate of arrival and maturation of new OB afferents from the OE is almost identical during postnatal development and in maturity, while the maturation of newly generated interneurons is remarkably slower in adults than in young animals (Carleton et al., 2003; Lemasson et al., 2005; Grubb et al., 2008; Lledó et al., 2008). The nature of the different dynamics of integration of new functional units from both neurogenic niches remains a challenge for researchers. However, the constant exposure of OSNs to the environment may imply high death rates, requiring a continuous renewal to assure reliable connections to the OB, while interneuron generation and replacement in the OB may relate to distinct olfactory memory capabilities/requirements throughout life and would be necessary to balance death of OB interneurons (Grubb et al., 2008; Mouret et al., 2009). This kind of olfactory *perpetuum mobile* converging in the OB perhaps makes it the CNS structure with the highest and most complex degree of synaptic plasticity, a particularity that would be taken as a reflection of what has been suggested for the developing OB (López-Mascaraque and de Castro, 2002, 2004).

GnRH NEURONS: OLFACTORY INTERACTIONS AND NEUROENDOCRINE CONTROL OF BEHAVIOR

Three different GnRH forms have been detected in vertebrates, each encoded by a different gene: GnRH-1 (the hypothalamic form, present in chromosome 8 in humans), GnRH-2 (the midbrain form in many mammals but not in mice or rats), and GnRH-3 (the nervous terminalis–telencephalic, primarily in teleosts), and only the first one appears to be associated to olfactory sensory pathways or KS pathogeny (Whitlock, 2005; Wray, 2010).

GnRH-1 neuroblasts display a second migratory process: once generated in the nasal pit, they follow olfactory and vomeronasal axons and enter the forebrain on the way to their final physiological location in the preoptic area and hypothalamus (**Figure 4**; Schwanzel-Fukuda and Pfaff, 1989; Wray et al., 1989). FGF8 is involved in the induction and differentiation of the mouse nasal placode and the loss of this morphogen results in the absence

of VSN and GnRH-1 neurons (Kawauchi et al., 2005; Chung and Tsai, 2010). In agreement with this, out of all the different receptors involved in migration, FGFR1 is expressed by both SVZ and GnRH-1 neuroblasts to respond to FGF2- and/or anosmin-1 to reach the OB and the hypothalamus, respectively, during development (Cariboni et al., 2004; Gill et al., 2004; García-González et al., 2010). This capital role of FGFR1-signaling is also maintained in the SVZ neurogenic niche during adulthood (**Figure 4**). Indeed, the lack of migration of GnRH-1 neurons forms the basis of the hypogonadotropic hypogonadism observed in Kallmann syndrome, a genetic disorder from either FGFR1 and/or anosmin-1 gene disruption, which also results in anosmia (Dodé et al., 2003; Dodé and Hardelin, 2009).

The neuroendocrine GnRH-1 system is essential for vertebrate reproduction. In mammals, the number of GnRH-1-secreting neurons is low (∼800 in the mouse), scattered from the OB to the hypothalamus, where the majority of them sends their axons to the medial eminence of the pituitary gland (Schwanzel-Fukuda and Pfaff, 1989; Wray et al., 1989). There, the pulsatile release of GnRH-1 to the portal capillary system controls secretion of gonadotropins from cells in the anterior pituitary and, consequently, the gonadal function (Gore, 2002; Foster et al., 2006).

As discussed in detail in the following section, mating behavior is dependent on chemosensory inputs from the MOS and VNS, whose central pathways contain fibers and cell bodies of GnRH-1 neurons. For instance, GnRH-1 can excite or inhibit neurons at the medial preoptic area (Pan et al., 1988), facilitate or suppress chemosensory responses in the amygdala (Westberry and Meredith, 2003); and stimulation of GnRH-1 receptors can cause short-term facilitation of sexual behavior (Dorsa and Smith, 1980; Sakuma and Pfaff, 1983). More recently, two independent tracer studies have shown that GnRH-1 neurons integrate to both MOS and VNS structures, primarily in the piriform cortex and the olfactory and vomeronasal amygdala (Boehm et al., 2005; Yoon et al., 2005). Consistent with this, some of these neurons in the vomeronasal (medial) amygdala are activated when female mice are exposed to the pheromone alpha-farnesene (produced by males in urine), inducing oestrus (Novotny, 2003; Boehm et al., 2005). Some neurons in the anterior cortical nucleus of the olfactory amygdala, mainly innervated by OB projection neurons (Dulac and Wagner, 2006) are activated by this pheromone, which suggests the involvement of the MOS in the response to pheromones, and raises the possibility that signals representing the same chemical, but originated separately in the OE and the VNO, may converge onto the same cortical neurons (Boehm et al., 2005). The presence of feedback loops between the hypothalamus and both the MOS and the VNS suggest that the neuroendocrine status of the animal may also modulate perception of these substances. Despite the relatively low number of GnRH-1 neurons, they have been reported to receive synaptic input from at least 10000 neurons in 26 different areas of the brain (including both MOS and VNS, but also regions involved in sexual behavior, arousal, reward, etc.) and send synaptic contacts to up to 50,000 neurons in 53 different brain areas involved in odor and pheromone processing, hunger, sexual behavior, defensive behavior, motility, etc. (Boehm et al., 2005). Altogether, these findings may suggest a mechanism in which GnRH-1 neurons integrate diverse information regarding the internal state of the animal and its external environment, modulating reproductive physiology and diverse functions to maximize reproductive success (Boehm et al., 2005).

EARLY EXPOSURE TO SCENTS IN THE DEVELOPMENT OF CHEMOSENSORY SYSTEMS

At birth, pups are exposed to a new and rich olfactory world that signal the position of their siblings, their mother, and the milk she provides. This chemical landscape is particularly relevant for altricial species, such as mice and rats, which are born with poorly developed visual and auditory senses and rely heavily on olfactory cues. Olfactory lesions in newborn pups lead to starvation by deficient nipple search and suckling behaviors, as at least more than half intact functional OMP^+-OSNs are required to display these behaviors (Kawagishi et al., 2009). Suckling pups whose mothers are scented with artificial odorants develop a long-lasting preference for those scents (Hudson et al., 2002; Sevelinges et al., 2009), suggesting that olfactory imprinting is important for the development of adult olfactory preferences (Moriceau and Sullivan, 2005). Interestingly, the formation of early olfactory memories is associated with different emotional values with increasing relevance of the environmental context during the transition from full mother-dependence to weaning (Moriceau and Sullivan, 2006).

Early olfactory experience, possibly even before birth, may produce long-lasting effects in both the MOS and VNS (Garrosa et al., 1998; Hovis et al., 2012). Indeed, urine-derived pheromones applied to immature VSN *in vitro* induce proliferation and survival of progenitors, with the concurrent phosphorylation of *Erk*, *Ark*, and *Creb* genes (Xia et al., 2010). Similarly, exposure of young pups to mice urine of a different strain abolishes the development of adult preference to their own strain and promotes epigenetic alterations in vomeronasal receptor genes and other proteins involved in chemosignaling. This suggests that the early semiochemical landscape plays an instructive role in shaping the receptive profile of maturing VSNs (Broad and Keverne, 2012). Similarly, early postnatal chemoreception affects the formation of specific connections between OSN and OB glomeruli, olfactory learning capabilities, and olfactory receptor turnover (Zou et al., 2004; Kerr and Belluscio, 2006; Sawada et al., 2011). Moreover, OSN maturation coincides with the development of sensory selectivity during the first 2–3 weeks of age, and electrical activity at the OB is required for OSN plasticity and maintenance (Lee et al., 2011).

MUTUAL INTERACTIONS IN THE REGULATION OF SEXUAL BEHAVIOR

As previously discussed, the existence of a functional independence between the olfactory and VNSs has been assumed for many years. However, it has recently been contradicted by new data providing evidence that the MOS is directly involved in pheromone-evoked behavior and endocrine responses, while the VNS regulates sex-specificity of the behavioral responses (Dulac and Kimchi, 2007). Whereas total bulbectomy abolishes both mating and aggressive behaviors, VNO surgical removal or chemical-induced OE ablation alone provokes more specific

effects, suggesting the direct involvement of both the MOS and the VNS in the mediation of the neuroendocrine response to predator odors (Masini et al., 2010). More recently, selective genetic inactivation of OE has shown to be a useful tool to address this question. The genetic ablation of a cyclic nucleotide-gated channel (only expressed in most OSNs but not in VSNs) or type III adenylyl-cyclase activity (which blocks OSN signaling) in male mice leads to impaired sexual behavior and diminished aggressive responses toward intruders (Wong et al., 2000; Mandiyan et al., 2005; Yoon et al., 2005; Wang et al., 2006). Furthermore, in a different set of experiments, OB mitral cells in female mice were activated by a pheromone compound of male mouse urine (MTMT), suggesting the direct role of the MOS in pheromone detection (Lin et al., 2005). In summary, these results provide direct evidence that the MOS is required for the detection of some pheromones involved in sexual and aggressive behaviors.

Together with this, genetic ablation of the TRPC2 channel, essential for VNO-mediated pheromone signaling, causes several behavioral abnormalities in mice, consisting of indiscriminate courtship and mounting of males toward both males and females, and to the absence of aggression to male intruders (Leypold et al., 2002; Stowers et al., 2002). However, these male mice are able to display a normal mating behavior with females. These data demonstrate that VNS activity is not obligatory for launching mating behavior although it is necessary for sex discrimination and aggression between males.

EVOLUTIONARY PERSPECTIVES: PHYLOGENETIC INTERACTIONS UNDER CHANGING ECOLOGICAL CONSTRAINTS

We have discussed that both chemosensory systems arise from similar pools of immature cells in spatially segregated regions of the developing nasal cavity, and that early developmental interactions regulate their differentiation into anatomically and functionally defined sensory systems with a partial overlap in their responses to ligands and central projections. In this section, we propose that the structure and function of these systems, as we observe today in extant mammals, are the result of mutual interactions under changing ecological scenarios, which can be traced back to their origins in the evolution of vertebrates.

EVOLUTION OF VERTEBRATE OLFACTION: UNDERWATER SMELLING

Genomic analyses have shown the presence of intact olfactory receptor genes in amphioxus, suggesting that vertebrate-like olfaction was already present in early chordates, more than 500 million years ago (Churcher and Taylor, 2009; Grus and Zhang, 2009; Niimura, 2009), possibly having evolved from a group of genes present in the ancestors of protostomates and deuterostomates (Churcher and Taylor, 2011). Cyclostomes, such as hagfishes and lampreys, are the earliest extant chordates to show a distinctive olfactory system (Eisthen and Polese, 2007). Adult lampreys rely on olfaction for finding prey and sexual partners (Van Denbossche et al., 1997; Sorensen et al., 2005; Osório and Rétaux, 2008). However, it is not clear whether distinct neuronal structures are involved in distinct behaviors. The OSNs of lampreys project to a well-defined OB (Thornhill, 1967; Laframboise et al., 2007), and a subgroup of them, located at a structure termed accessory olfactory organ, terminate in medial domains of the OB (Ren et al., 2009). Interestingly, the lamprey genome has intact V1R and TRPC2 genes (Grus and Zhang, 2009), suggesting the evolution of alternative olfactory subsystems in early chordates (**Figure 6A**).

Both main olfactory and vomeronasal components are expressed in the OE of the teleost fishes in a structure known as olfactory rosette, through which water flows from the anterior and posterior nostrils. Distinct chemosensory neurons have been found to express ORs (Ngai et al., 1993a,b), V2Rs (Cao et al., 1998; Naito et al., 1998; Asano-Miyoshi et al., 2000; Pfister and Rodriguez, 2005), and V1Rs (Pfister and Rodriguez, 2005). Although fish do not present a compartimentalized VNO as in tetrapods, both ORs- and V1R-expressing neurons are spatially segregated in the OE (Hansen et al., 2004). Moreover, their projections to the OB terminate in non-overlapping glomerular domains (Sato et al., 2005), from where projecting neurons contacting each OE cell type project to the telencephalon in segregated bundles (Hamdani and Døving, 2007).

SCENTS CARRIED BY THE WIND: THE EVOLUTION OF TETRAPOD OLFACTION

Air breathing is thought to have evolved in early bony fish (Sarcopterygii) with the ability of gulping air into primitive lungs,

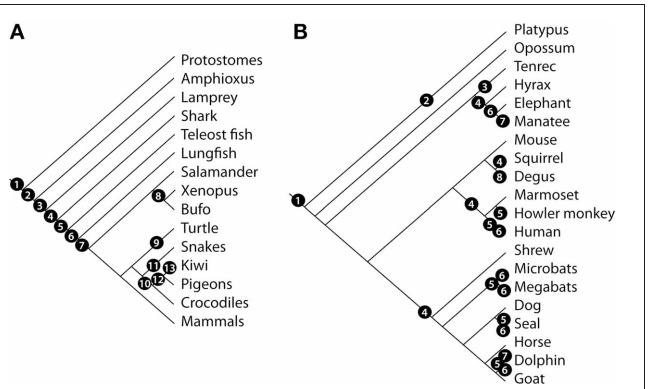

FIGURE 6 | Evolution of the vertebrate MOS and VNS. Cladogram showing the phylogenetic relationships of vertebrate species and relevant events related to the evolution of the MOS and VNS **(A)** according to the following numbers: 1, presence of a primitive olfactory system; 2, evolution of the classical vertebrate olfactory receptor (OR) genes; 3, evolution of the olfactory projections and origin of V1R and TRPC2 genes; 4, origin of V2R genes; 5, expression of ORs, V2R, and V1R in the OE; 6, origin of a distinctive VNS (VNO-AOB-MeA projection); 7, segregation of vomeronasal pathways; shift in receptor ratios associated to land colonization; 8, differential expression of G-proteins in aquatic vs. terrestrial species; 9, reduction of OR gene repertoire in aquatic species; 10, loss of the VNS in Archosauria; 11, expansion of vomeronasal structures in lepidosaurs; 12, evolution of bird-specific OR genes; 13, expansion of OR gene repertoire in terrestrial/nocturnal birds. **(B)** Evolution of the mammalian MOS and VNS. Cladogram showing the phylogenetic relationships of mammalian species and relevant events related to the evolution of the MOS and VNS. 1, Two-pathway segregated VNS, AOB dorsal to the OB; 2, amplification of V1R genes; 3, non-exclusive segregation of AOB glomeruli expressing $G\alpha_{i2}$ and $G\alpha_o$ proteins; 4, loss of the V2R—$G\alpha_o$ pathway; 5, pseudogenization of OR genes; 6, loss of the vomeronasal system; 7, loss of the OBs; 8, lateral AOB innervation and cell indentation between AOB subdomains.

possibly as an adaptation to drops in atmospheric oxygen during the Middle and Late Devonian (Packard, 1974; Clack, 2007). Later increases in atmospheric levels of oxygen, concurrent with the colonization of land by plants, insects, and the evolution of shallow and fresh water habitats, may have further fostered aerial respiration in primitive lungfish and the diversification of tetrapods (Graham et al., 1995; Holland, 2006). Airborne substances may have acquired behavioral relevance after the fusion of the posterior nostrils into the mouth, forming the tetrapod-characteristic choana, allowing the flux of air into the olfactory cavity (Zhu and Ahlberg, 2004). This acquired ability may have further fostered the specialization of both the main olfactory and VNSs to distinct ecological contexts. In fact, lungfish (*Protopterus sp*.) possess the most ancient form of distinctive segregation between olfactory and vomeronasal pathways from the nose to the brain (González et al., 2010; Nakamuta et al., 2012; Northcutt and Rink, 2012). In accordance with this notion, Eisthen (1997) proposed that the evolution of the VNS was not associated to the evolution of terrestrial habits, as fully aquatic salamanders have a functional VNS. We advance this idea by proposing that the origin of vomeronasal components occurred in aquatic vertebrates before the split of lungfish and amphibians, and that the ability to take air into the nostrils may have allowed bimodal olfactory functions and promoted further specializations in both systems.

Amphibians display a rich diversity of behaviors involving the concerted action of the MOS and VNS (Eisthen, 1992, 1997; Park et al., 2004; Eisthen and Polese, 2007; Houck, 2009; Woodley, 2010). Evidence for a shift from fully aquatic to partially aerial olfaction came from the studies of Freitag et al. (1995), who described in *Xenopus laevis* three separate chemoreceptive chambers: the VNO, and the lateral (LD) and medial diverticulum (MD) of the OE. Both MOE diverticula are separated by a valve-like structure that allows the entrance of water to the LD or air to the MD for underwater and aerial olfaction, respectively. These OE subdomains show expression of ORs associated to waterborne (class I ORs) and airborne (class II ORs) chemoreception, respectively. Furthermore, while fully aquatic teleost fish have mostly class I ORs, coelacanths (Sarcopterygii) and amphibians have both OR classes (Freitag et al., 1998; Mezler et al., 2001; Niimura and Nei, 2005).

Thus far, the macroevolutionary transition from aquatic to aerial respiration in tetrapods involved a change in the repertoire of chemosensory elements, influencing the specialization of both olfactory and vomeronasal sensory systems. Evidence for this comes from genomic studies reporting a shift in the expression of ORs and VRs, with different affinities for waterborne and airborne molecules, during the evolution of terrestrial habits in vertebrates (Shi and Zhang, 2007).

The evolution of the amniotic sac further prompted the colonization of land by vertebrates, resulting in an increased independence to water resources for laying eggs. This allowed the diversification of chemosensory systems associated to life on land. Interestingly, species that returned to aquatic habits tend to lose olfactory functions. This has been reported in aquatic turtles, which show a reduction in functional OR genes as compared with terrestrial species (Vieyra, 2011). Similarly, sea snakes have less OR functional genes than terrestrial snakes; this genetic deterioration is more pronounced in viviparous than oviparous sea snakes, as laying eggs on land might rely more on a keen sense of smell than underwater delivery of alive newborns (Kishida and Hikida, 2010).

The interactions between the MOS and VNS are particularly evident in olfactory behaviors of diapsid reptiles. For example, the VNS of squamates (snakes and lizards) not only participates in intraspecific socio-sexual interactions, but also plays a fundamental role in finding prey (Cooper, 1996). Actively foraging snakes and lizards can follow the odorous trail of prey by performing tongue flicks, which deliver semiochemicals to the VNO through bilateral openings in the palate (Halpern and Kubie, 1980). In garter snakes (*Thamnophis sirtalis*), tongue-flicking behavior is often preceded by activation of the MOS, reflecting integration of both chemosensory modalities in predatory contexts (Halpern et al., 1997; Zuri and Halpern, 2003). The AOB projects to the vomeronasal amygdala, whose size reaches up to one third of total brain volume in some species, while the OB projects to the rostromedial pallium, septum medialis, and lateral cortex (Halpern and Martinez-Marcos, 2003; Ubeda-Bañon et al., 2011).

Birds and their closest living relatives, crocodiles, lack a VNS. It has been postulated that the loss of vomeronasal structures dates back to the common ancestor of archosaurs (Senter, 2002). The complete lack of vomeronasal receptors in the chick genome (Shi and Zhang, 2007), further suggest an ancient loss of vomeronasal function. On the other hand, the relative size of the OBs in fossil and extant species suggests that olfaction has played an important role in the evolution of non-avian theropod dinosaurs and birds (Zelenitsky et al., 2011). Although the proportion of intact OR genes in birds is lower than in lizards, a recent expansion of a bird-specific OR gene family (Steiger et al., 2008), in addition to higher rates of OR diversification in nocturnal terrestrial birds (Steiger et al., 2009), suggest that olfaction in birds is more important than commonly thought (**Figure 6A**). In fact, olfaction in birds participates in recognition of gender (Balthazart and Taziaux, 2009) and individual identity of conspecifics (Coffin et al., 2011), as well as in foraging (Mardon et al., 2010) and navigation behavior (Gagliardo et al., 2011).

OLFACTION IN MAMMALS: SENSORY CONVERGENCES TO SIMILAR ECOTYPES

Fossil skull endocasts of basal mammaliforms from the Early Jurassic of China suggest that the evolution of the mammalian brain underwent a sequence of olfactory adaptations (Rowe et al., 2011). Similarly, olfaction has been proposed to have played an important role in the evolution of the isocortex of early mammals (Aboitiz et al., 2003).

The constant interactions between the MOS and the AOS during mammalian evolution are revealed by sharing similar patterns of diversification, between systems and between species, under similar ecological conditions. For example, the evolution of trichromatic vision in apes, and the perceptual changes associated to it, has been related to the sequential deterioration of vomeronasal components (Liman and Innan, 2003; Zhang and Webb, 2003). In some bats, the evolution of alternative

communication systems or foraging strategies may explain the convergent deterioration of the vomeronasal genes (Zhao et al., 2011) Similarly, the OR gene repertoire has shown high levels of deterioration in New World and Old World primate species that convergently evolved trichromacy (Gilad et al., 2004). The independent acquisition of aquatic habits in several mammalian lineages has resulted in deteriorarion of OR genes (Kishida et al., 2007; Hayden et al., 2010) and VNS components in cetaceans, manatees, and some pinnipeds (Meisami and Bhatnagar, 1998). Accordingly, genomic analyses of receptor genes in mammals have shown that ecological adaptations affect the pattern of expression of components from both MOS and VNS. For example, OR gene repertoires cluster species acording to similar ecotypes (aquatic, semi-aquatic, terrestrial, flying) rather than by phylogenetic relatedness (Hayden et al., 2010). For instance, the amount of functional V1R genes is higher in nocturnal and nest-living species than in diurnal and open-living species, respectively (Wang et al., 2010; Young et al., 2010). In carnivores, ungulates and primates, the V2R gene family has degenerated (Young and Trask, 2007), possibly associated to independent origins of visually conspicuous sexual dimorphisms, as recently proposed as a possible explanation for the independent loss of the posterior AOB in squirrels and hyraxes (Suárez et al., 2011a; **Figure 6B**).

Interestingly, although in most mammals studied so far the vomeronasal nerve follows the medial line on its way to the AOB, in caviomorph rodents it follows a lateral course, regardless of the ecotype of species (Suárez and Mpodozis, 2009; Suárez et al., 2011b), reflecting that not all olfactory traits show correlation with life history but rather some traits can be shared within a phylogenetic group.

In summary, the similar directions of change observed in both MOS and VNS under different ecological adaptations reveal their constant mutual interactions throughout phylogeny. These interactions, together with their close relationship with the ecological contexts of species, may allow us to make predictions relating life history to olfaction (and vice versa) in less studied species and may provide valuable tools for conservation efforts.

CONCLUDING REMARKS

The recent findings of shared mechanisms between the MOS and VNS have challenged the notion of olfaction as a dichotomous process and instead suggest that many sensory and behavioral processes require the interaction between them. We have presented and discussed evidence supporting the hypothesis that these interactions are not only present during olfactory perception and generation of behavior at particular moments of the life of an individual, but rather they are constantly affecting the course of development and evolution.

This strong interaction is reflected in the molecular and cellular mechanisms controlling early development of both olfactory systems, to shared sensory activity and behavioral responses at postnatal stages and similar patterns of adaptation to environmental changes during evolution. The convergent patterns of ecological adaptations of both systems in species that acquire similar ecological niches may become instrumental for conservation efforts of endangered or poorly studied species through the effective prediction of lifestyle aspects based on olfactory structures and vice versa.

Furthermore, the study of the interactions between the MOS and VNS may open new routes of discovery of brain function. For example, the continuous production and integration of new neurons, both at the periphery (OE and VNO) and central structures (OB and AOB), may shed new light on the understanding of normal and pathological brain function, with possible applications in the design of therapeutic strategies for neural regeneration.

ACKNOWLEDGMENTS

This work was supported by the Ministerio de Economía y Competitividad [SAF2009-07842] and Fundación Eugenio Rodríguez-Pascual (Spain) to Fernando de Castro. Diego García-González and Fernando de Castro are hired by SESCAM. Laura Fenlon provided valuable comments on the manuscript. Rodrigo Suárez received a short-term fellowship from IBRO in 2011 to visit our lab in Spain: we gestated the idea of the present work at that time.

REFERENCES

Aboitiz, F., Morales, D., and Montiel, J. (2003). The evolutionary origin of the mammalian isocortex: towards an integrated developmental and functional approach. *Behav. Brain Sci.* 26, 535–552.

Ache, B. W., and Young, J. M. (2005). Olfaction: diverse species, conserved principles. *Neuron* 48, 417–430.

Asano-Miyoshi, M., Suda, T., Yasuoka, A., Osima, S.-I., Yamashita, S., and Abe, K. (2000). Random expression of main and vomeronasal olfactory receptor genes in immature and mature olfactory epithelia of fugu rubripes. *J. Biochem.* 127, 915–924.

Balthazart, J., and Taziaux, M. L. (2009). The underestimated role of olfaction in avian reproduction? *Behav. Res.* 200, 248–259.

Baum, M. J. (2012). Contribution of pheromones processed by the main olfactory system to mate recognition in female mammals. *Front. Neuroanat.* 6:20. doi: 10.3389/fnana.2012.00020

Baum, M. J., and Kelliher, K. R. (2009). Complementary roles of the main and accessory olfactory systems in mammalian mate recognition. *Annu. Rev. Physiol.* 71, 141–160.

Beites, C. L., Kawauchi, S., Crocker, C. E., and Calof, A. L. (2005). Identification and molecular regulation of neural stem cells in the olfactory epithelium. *Exp. Cell Res.* 306, 309–316.

Belluscio, L., Koentges, G., Axel, R., and Dulac, C. (1999). A map of pheromone receptor activation in the mammalian brain. *Cell* 97, 209–220.

Belluzzi, O., Benedusi, M., Ackman, J., and LoTurco, J. J. (2003). Electrophysiological differentiation of new neurons in the olfactory bulb. *J. Neurosci.* 23, 10411–10418.

Ben-Shaul, Y., Katz, L. C., Mooney, R., and Dulac, C. (2010). *In vivo* vomeronasal stimulation reveals sensory encoding of conspecific and allospecific cues by the mouse accessory olfactory bulb. *Proc. Natl. Acad. Sci. U.S.A.* 107, 5172–5177.

Berghard, A., and Buck, L. B. (1996). Sensory transduction in vomeronasal neurons: evidence for Gao, Gai2, and adenylyl cyclase II as a major components of a pheromone signaling cascade. *J. Neurosci.* 16, 909–918.

Boehm, U., Zou, Z., and Buck, L. B. (2005). Feedback loops link odor and pheromone signaling with reproduction. *Cell* 18, 683–695.

Brennan, P. A., and Zufall, F. (2006). Pheromonal communication in vertebrates. *Nature* 444, 308–315.

Broad, K., and Keverne, E. (2012). The post-natal chemosensory environment induces epigenetic changes in vomeronasal receptor gene expression and a bias in olfactory preference. *Behav. Genet.* 42, 461–471.

Buck, L., and Axel, R. (1991). A novel multigene family may encode odorant receptors: a molecular basis for odor recognition. *Cell* 65, 175–187.

Buck, L. B. (2000). The molecular architecture of odor and pheromone sensing in mammals. *Cell* 100, 611–618.

Butler, A. B., and Hodos, W. (2005). *Comparative Vertebrate Neuroanatomy: Evolution and*

Adaptation. Hoboken, NJ: John Wiley and Sons, Inc.

Cao, Y., Oh, B. C., and Stryer, L. (1998). Cloning and localization of two multigene receptor families in goldfish olfactory epithelium. *Proc. Natl. Acad. Sci. U.S.A.* 95, 11987–11992.

Cariboni, A., Pimpinelli, F., Colamarino, S., Zaninetti, R., Piccolella, M., Rumio, C., et al. (2004). The product of X-linked Kallmann's syndrome gene KAL1 affects the migratory activity of gonadotropin-releasing hormone GnRH producing neurons. *Hum. Mol. Genet.* 13, 2781–2791.

Carleton, A., Petreanu, L. T., Lansford, R., Álvarez-Buylla, A., and Lledó, P. M. (2003). Becoming a new neuron in the adult olfactory bulb. *Nat. Neurosci.* 6, 507–518.

Cau, E., Casarosa, S., and Guillemot, F. (2002). Mash1 and Ngn1 control distinct steps of determination and differentiation in the olfactory sensory neuron lineage. *Development* 129, 1871–1880.

Cau, E., Gradwohl, G., Fode, C., and Guillemot, F. (1997). Mash1 activates a cascade of bHLH regulators in olfactory neuron progenitors. *Development* 124, 1611–1621.

Chung, W. C., and Tsai, P. S. (2010). Role of fibroblast growth factor signaling in gonadotropin-releasing hormone neuronal system development. *Front. Horm. Res.* 39, 37–50.

Churcher, A., and Taylor, J. (2009). Amphioxus (*Branchiostoma floridae*) has orthologs of vertebrate odorant receptors. *BMC Evol. Biol.* 9:242. doi: 10.1186/1471-2148-9-242

Churcher, A. M., and Taylor, J. S. (2011). The antiquity of chordate odorant receptors is revealed by the discovery of orthologs in the cnidarian *Nematostella vectensis*. *Genome Biol. Evol.* 3, 36–43.

Clack, J. A. (2007). Devonian climate change, breathing, and the origin of the tetrapod stem group. *Integr. Comp. Biol.* 47, 510–523.

Coffin, H. R., Watters, J. V., and Mateo, J. M. (2011). Odor-based recognition of familiar and related conspecifics: a first test conducted on captive humboldt penguins (*Spheniscus humboldti*). *PLoS ONE* 6:e25002. doi: 10.1371/journal.pone.0025002

Cooper, W. E. (1996). Preliminary reconstructions of nasal chemosensory evolution in Squamata. *Amphib. Reptil.* 17, 395–415.

de Castro, F. (2009). Wiring olfaction: the cellular and molecular mechanisms that guide the development of synaptic connections from the nose to the cortex. *Front. Neurosci.* 3:52. doi: 10.3389/neuro.22.004.2009

Del Punta, K., Puche, A., Adams, N. C., Rodriguez, I., and Mombaerts, P. (2002). A divergent pattern of sensory axonal projections is rendered convergent by second-order neurons in the accessory olfactory bulb. *Neuron* 35, 1057–1066.

Devor, M. (1976). Fiber trajectories of olfactory bulb efferents in the hamster. *J. Comp. Neurol.* 166, 31–47.

Dodé, C., and Hardelin, J. P. (2009). Kallmann syndrome. *Eur. J. Hum. Genet.* 17, 139–146.

Dodé, C., Levilliers, J., Dupont, J. M., De Paepe, A., Le Du, N., Soussi-Yanicostas, N., et al. (2003). Loss-of-function mutations in FGFR1 cause autosomal dominant Kallmann syndrome. *Nat. Genet.* 33, 463–465.

Dorsa, D. M., and Smith, E. R. (1980). Facilitation of mounting behavior in male rats by intracranial injections of luteinizing hormone-releasing hormone. *Regul. Pept.* 1, 147–155.

Dulac, C., and Axel, R. (1995). A novel family of genes encoding putative pheromone receptors in mammals. *Cell* 83, 195–206.

Dulac, C., and Kimchi, T. (2007). Neural mechanisms underlying sex-specific behaviors in vertebrates. *Curr. Opin. Neurobiol.* 6, 675–683.

Dulac, C., and Torello, A. T. (2003). Molecular detection of pheromone signals in mammals: from genes to behaviour. *Nat. Rev. Neurosci.* 4, 551–562.

Dulac, C., and Wagner, S. (2006). Genetic analysis of brain circuits underlying pheromone signaling. *Ann. Rev. Genet.* 40, 449–467.

Eckler, M. J., McKenna, W. L., Taghvaei, S., McConnell, S. K., and Chen, B. (2011). Fezf1 and Fezf2 are required for olfactory development and sensory neuron identity. *J. Comp. Neurol.* 519, 1829–1846.

Eisthen, H. (1992). Phylogeny of the vomeronasal system and of receptor cell types in the olfactory and vomeronasal epithelia of vertebrates. *Microsc. Res. Tech.* 23, 1–21.

Eisthen, H., and Polese, G. (2007). "Evolution of vertebrate olfactory subsystems," in *Evolution of Nervous Systems: A Comprehensive Reference,* ed J. H. Kaas (East Lansing, MI: Academic Press), 1–52.

Eisthen, H. L. (1997). Evolution of vertebrate olfactory systems. *Brain Behav. Evol.* 50, 222–233.

Enomoto, T., Ohmoto, M., Iwata, T., Uno, A., Saitou, M., Yamaguchi, T., et al. (2011). Bcl11b/Ctip2 controls the differentiation of vomeronasal sensory neurons in mice. *J. Neurosci.* 31, 10159–10173.

Feinstein, P., and Mombaerts, P. (2004). A contextual model for axonal sorting into glomeruli in the mouse olfactory system. *Cell* 117, 817–831.

Fleischer, J., and Breer, H. (2010). The Grueneberg ganglion: a novel sensory system in the nose. *Histol. Histopathol.* 25, 909–915.

Forni, P. E., Taylor-Burds, C., Melvin, V. S., Williams, T., and Wray, S. (2011). Neural crest and ectodermal cells intermix in the nasal placode to give rise to GnRH-1 neurons, sensory neurons, and olfactory ensheathing cells. *J. Neurosci.* 4, 6915–6927.

Foster, D. L., Jackson, L. M., and Padmanabhan, V. (2006). Programming of GnRH feedback controls timing puberty and adult reproductive activity. *Mol. Cell. Endocrinol.* 25, 254–255.

Freitag, J., Krieger, J., Strotmann, J., and Breer, H. (1995). Two classes of olfactory receptors in xenopus laevis. *Neuron* 15, 1383–1392.

Freitag, J., Ludwig, G., Andreini, I., Rössler, P., and Breer, H. (1998). Olfactory receptors in aquatic and terrestrial vertebrates. *J. Comp. Physiol. A* 183, 635–650.

Fukunaga, I., Berning, M., Kollo, M., Schmaltz, A., and Schaefer, A. T. (2012). Two distinct channels of olfactory bulb output. *Neuron* 26, 320–329.

Gagliardo, A., Ioalé, P., Filannino, C., and Wikelski, M. (2011). Homing pigeons only navigate in air with intact environmental odours: a test of the olfactory activation hypothesis with GPS data loggers. *PLoS ONE* 6:e22385. doi: 10.1371/journal.pone.0022385

García-González, D., Clemente, D., Coelho, M., Esteban, P. F., Soussi-Yanicostas, N., and de Castro, F. (2010). Dynamic roles of FGF-2 and Anosmin-1 in the migration of neuronal precursors from the subventricular zone during pre- and postnatal development. *Exp. Neurol.* 222, 285–295.

Garrosa, M., Gayoso, M. J., and Esteban, F. J. (1998). Prenatal development of the mammalian vomeronasal organ. *Microsc. Res. Tech.* 41, 456–470.

Garzotto, D., Giacobini, P., Crepaldi, T., Fasolo, A., and De Marchis, S. (2008). Hepatocyte growth factor regulates migration of olfactory interneuron precursors in the rostral migratory stream through Met-Grb2 coupling. *J. Neurosci.* 28, 5901–5909.

Gilad, Y., Wiebe, V., Przeworski, M., Lancet, D., and Pääbo, S. (2004). Loss of olfactory receptor genes coincides with the acquisition of full trichromatic vision in primates. *PLoS Biol.* 2:e5. doi: 10.1371/journal.pbio.0020005

Gill, J. C., Moenter, S. M., and Tsai, P. S. (2004). Developmental regulation of gonadotropin-releasing hormone neurons by fibroblast growth factor signaling. *Endocrinology* 145, 3830–3839.

González, A., Morona, R., López, J. M., Moreno, N., and Northcutt, G. R. (2010). Lungfishes, like tetrapods, possess a vomeronasal system. *Front. Neuroanat.* 4:130. doi: 10.3389/fnana.2010.00130

Gore, A. C. (2002). Gonadotropin-releasing hormone (GnRH) neurons: gene expression and neuroanatomical studies. *Prog. Brain Res.* 141, 193–208.

Graham, J. B., Aguilar, N. M., Dudley, R., and Gans, C. (1995). Implications of the late Palaeozoic oxygen pulse for physiology and evolution. *Nature* 375, 117–120.

Greer, C. A. (1991). "Structural organization of the olfactory system," in *Smell and Taste in Health and Disease,* eds T. V. Getchell, R. L. Doty, L. M. Bartoshuk, and J. B. Snow Jr. (New York, NY: Raven), 65–81.

Grubb, M. S., Nissant, A., Murray, K., and Lledó, P. M. (2008). Functional maturation of the fi rst synapse in olfaction: development and adult neurogenesis. *J. Neurosci.* 28, 2919–2932.

Grus, W. E., and Zhang, J. (2009). Origin of the genetic components of the vomeronasal system in the common ancestor of all extant vertebrates. *Mol. Biol. Evol.* 26, 407–419.

Guillemot, F., Lo, L. C., Johnson, J. E., Auerbach, A., Anderson, D. J., and Joyner, A. L. (1993). Mammalian achaete-scute homolog 1 is required for the early development of olfactory and autonomic neurons. *Cell* 75, 463–476.

Haberly, L. B., and Price, J. L. (1977). The axonal projection patterns of the mitral and tufted cells of the olfactory bulb in the rat. *Brain Res.* 129, 152–157.

Halpern, M., Halpern, J., Erichsen, E., and Borghjid, S. (1997). The role of nasal chemical senses in garter snake response to airborne odor cues from prey. *J. Comp. Psychol.* 111, 251–260.

Halpern, M., and Kubie, J. L. (1980). Chemical access to the vomeronasal organs of garter snakes. *Physiol. Behav.* 24, 367–371.

Halpern, M., and Martinez-Marcos, A. (2003). Structure and function of

the vomeronasal system: an update. *Prog. Neurobiol.* 70, 245–318.

Hamdani, E. H., and Døving, K. B. (2007). The functional organization of the fish olfactory system. *Prog. Neurobiol.* 82, 80–86.

Hansen, A., Anderson, K. T., and Finger, T. E. (2004). Differential distribution of olfactory receptor neurons in goldfish: structural and molecular correlates. *J. Comp. Neurol.* 477, 347–359.

Hayden, S., Bekaert, M. L., Crider, T. A., Mariani, S., Murphy, W. J., and Teeling, E. C. (2010). Ecological adaptation determines functional mammalian olfactory subgenomes. *Genome Res.* 20, 1–9.

Herrada, G., and Dulac, C. (1997). A novel family of putative pheromone receptors in mammals with a topographically organized and sexually dimorphic distribution. *Cell* 90, 763–773.

Holland, H. D. (2006). The oxygenation of the atmosphere and oceans. *Philos. Trans. R. Soc. Lond. B Biol. Sci.* 361, 903–915.

Holy, T. E., Dulac, C., and Meister, M. (2000). Responses of vomeronasal neurons to natural stimuli. *Science* 289, 1569–1572.

Houck, L. D. (2009). Pheromone communication in amphibians and reptiles. *Annu. Rev. Physiol.* 71, 161–176.

Hovis, K. R., Ramnath, R., Dahlen, J. E., Romanova, A. L., LaRocca, G., Bier, M. E., et al. (2012). Activity regulates functional connectivity from the vomeronasal organ to the accessory olfactory bulb. *J. Neurosci.* 6, 7907–7916.

Hu, H. (1999). Chemorepulsion of neuronal migration by Slit2 in the developing mammalian forebrain. *Neuron* 23, 703–711.

Hudson, R., Labra-Cardero, D., and Mendoza-Soylovna, A. (2002). Sucking, not milk, is important for the rapid learning of nipple-search odors in newborn rabbits. *Dev. Psychobiol.* 41, 226–235.

Imai, T. (2012). Positional information in neural map development: lessons from the olfactory system. *Dev. Growth Differ.* 54, 358–365.

Isogai, Y., Si, S., Pont-Lezica, L., Tan, T., Kapoor, V., Murthy, V. N., et al. (2011). Molecular organization of vomeronasal chemoreception. *Nature* 478, 241–245.

Kang, N., Baum, M. J., and Cherry, J. A. (2009). A direct main olfactory bulb projection to the 'vomeronasal' amygdala in female mice selectively responds to volatile pheromones from males. *Eur. J. Neurosci.* 29, 624–634.

Kang, N., Baum, M. J., and Cherry, J. A. (2011). Different profiles of main and accessory olfactory bulb mitral/tufted cell projections revealed in mice using an anterograde tracer and a whole-mount, flattened cortex preparation. *Chem. Senses* 36, 251–260.

Kawagishi, K., Yokouchi, K., Fukushima, N., Sakamoto, M., Sumitomo, N., and Moriizumi, T. (2009). Determination of functionally essential neuronal population of the olfactory epithelium for nipple search and subsequent suckling behavior in newborn rats. *Brain Res.* 76, 50–57.

Kawauchi, S., Shou, J., Santos, R., Hebert, J. M., McConnell, S. K., Mason, I., et al. (2005). Fgf8 expression defines a morphogenetic center required for olfactory neurogenesis and nasal cavity development in the mouse. *Development* 132, 5211–5223.

Kerr, M. A., and Belluscio, L. (2006). Olfactory experience accelerates glomerular refinement in the mammalian olfactory bulb. *Nat. Neurosci.* 9, 484–486.

Kishida, T., and Hikida, T. (2010). Degeneration patterns of the olfactory receptor genes in sea snakes. *J. Evol. Biol.* 23, 302–310.

Kishida, T., Kubota, S., Shirayama, Y., and Fukami, H. (2007). The olfactory receptor gene repertoires in secondary-adapted marine vertebrates: evidence for reduction of the functional proportions in cetaceans. *Biol. Lett.* 3, 428–430.

Laframboise, A. J., Ren, X., Chang, S., Dubuc, R., and Zielinski, B. S. (2007). Olfactory sensory neurons in the sea lamprey display polymorphisms. *Neurosci. Lett.* 414, 277–281.

Larriva-Sahd, J. (2008). The accessory olfactory bulb in the adult rat: a cytological study of its cell types, neuropil, neuronal modules, and interactions with the main olfactory system. *J. Comp. Neurol.* 510, 309–350.

Lee, A. C., He, J., and Ma, M. (2011). Olfactory marker protein is critical for functional maturation of olfactory sensory neurons and development of mother preference. *J. Neurosci.* 31, 2974–2982.

Lemasson, M., Saghatelyan, A., Olivo-Marín, J. C., and Lledó, P. M. (2005). Neonatal and adult neurogenesis provide two distinct populations of newborn neurons to the mouse olfactory bulb. *J. Neurosci.* 25, 6816–6825.

Leypold, B. G., Yu, C. R., Leinders-Zufall, T., Kim, M. M., Zufall, F., and Axel, R. (2002). Altered sexual and social behaviors in trp2 mutant mice. *Proc. Natl. Acad. Sci. U.S.A.* 99, 6376–6381.

Liman, E. R., and Innan, H. (2003). Relaxed selective pressure on an essential component of pheromone transduction in primate evolution. *Proc. Natl. Acad. Sci. U.S.A.* 100, 3328–3332.

Lin, D. Y., Zhang, S. Z., Block, E., and Katz, L. C. (2005). Encoding social signals in the mouse main olfactory bulb. *Nature* 24, 470–477.

Lledó, P. M., Merkle, F. T., and Álvarez-Buylla, A. (2008). Origin and function of olfactory bulb interneuron diversity. *Trends Neurosci.* 31, 392–400.

Lomvardas, S., Barnea, G., Pisapia, D. J., Mendelsohn, M., Kirkland, J., and Axel, R. (2006). Interchromosomal interactions and olfactory receptor choice. *Cell* 126, 403–413.

López-Mascaraque, L., and de Castro, F. (2002). The olfactory bulb as an independent developmental domain. *Cell Death Differ.* 9, 1279–1286.

López-Mascaraque, L., and de Castro, F. (2004). Protocortex versus protomap: a perspective from the olfactory bulb. *Rev. Neurol.* 9, 146–155.

Luo, M. M., Fee, M. S., and Katz, L. C. (2003). Encoding pheromonal signals in the accessory olfactory bulb of behaving mice. *Science* 299, 1196–1201.

Luo, M. M., and Katz, L. C. (2004). Encoding pheromonal signals in the mammalian vomeronasal system. *Curr. Opin. Neurobiol.* 14, 428–434.

Mandiyan, V. S., Coats, J. K., and Shah, N. M. (2005). Deficits in sexual and aggressive behaviors in Cnga2 mutant mice. *Nat. Neurosci.* 8, 1660–1662.

Mardon, J., Nesterova, A. P., Traugott, J., Saunders, S. M., and Bonadonna, F. (2010). Insight of scent: experimental evidence of olfactory capabilities in the wandering albatross (*Diomedea exulans*). *J. Exp. Biol.* 15, 558–563.

Martínez-Marcos, A. (2009). On the organization of olfactory and vomeronasal cortices. *Prog. Neurobiol.* 87, 21–30.

Masini, C. V., Garcia, R. J., Sasse, S. K., Nyhuis, T. J., Day, H. E., and Campeau, S. (2010). Accessory and main olfactory systems influences on predator odor-induced behavioral and endocrine stress responses in rats. *Behav. Brain Res.* 11, 70–77.

Matsunami, H., and Buck, L. B. (1997). A multigene family encoding a diverse array of putative pheromone receptors in mammals. *Cell* 90, 775–784.

Meisami, E., and Bhatnagar, K. P. (1998). Structure and diversity in mammalian accessory olfactory bulb. *Microsc. Res. Tech.* 43, 476–499.

Meredith, M., Marques, D., O'Connell, R., and Stern, F. (1980). Vomeronasal pump: significance for male hamster sexual behavior. *Science* 207, 1224–1226.

Mezler, M., Fleischer, J., and Breer, H. (2001). Characteristic features and ligand specificity of the two olfactory receptor classes from *Xenopus laevis*. *J. Exp. Biol.* 204, 2987–2997.

Mohedano-Moriano, A., De La Rosa-Prieto, C., Sáiz-Sánchez, D., Úbeda-Bañón, I., Pro-Sistiaga, P., De Moya-Pinilla, M., et al. (2012). Centrifugal telencephalic afferent connections to the main and accessory olfactory bulbs. *Front. Neuroanat.* 6:19. doi: 10.3389/fnana.2012.00019

Mohedano-Moriano, A., Pro-Sistiaga, P., Úbeda-Banon, I., Crespo, C., Insausti, R., and Martínez-Marcos, A. (2007). Segregated pathways to the vomeronasal amygdala: differential projections from the anterior and posterior divisions of the accessory olfactory bulb. *Eur. J. Neurosci.* 25, 2065–2080.

Mohedano-Moriano, A., Pro-Sistiaga, P., Ubeda-Bañón, I., de la Rosa-Prieto, C., Saiz-Sanchez, D., and Martinez-Marcos, A. (2008). V1R and V2R segregated vomeronasal pathways to the hypothalamus. *Neuroreport* 19, 1623–1626.

Mombaerts, P. (2004). Genes and ligands for odorant, vomeronasal and taste receptors. *Nat. Rev. Neurosci.* 5, 263–278.

Mombaerts, P. (2006). Axonal wiring in the mouse olfactory system. *Annu. Rev. Cell Dev. Biol.* 22, 713–737.

Moriceau, S., and Sullivan, R. M. (2005). Neurobiology of infant attachment. *Dev. Psychobiol.* 47, 230–242.

Moriceau, S., and Sullivan, R. M. (2006). Maternal presence serves as a switch between learning fear and attraction in infancy. *Nat. Neurosci.* 9, 1004–1006.

Mouret, A., Lepousez, G., Gras, J., Gabellec, M. M., and Lledó, P. M. (2009). Turnover of newborn olfactory bulb neurons optimizes olfaction. *J. Neurosci.* 29, 12302–12314.

Murcia-Belmonte, V., Esteban, P. F., García-González, D., and De Castro, F. (2010). Biochemical dissection of Anosmin-1 interaction with FGFR1 and components of the extracellular matrix. *J. Neurochem.* 115, 1256–1265.

Murray, R. C., Navi, D., Fesenko, J., Lander, A. D., and Calof, A. L. (2003). Widespread defects in the primary olfactory pathway caused by loss of Mash1 function. *J. Neurosci.* 23, 1769–1780.

Nagayama, S., Enerva, A., Fletcher, M. L., Masurkar, A. V., Igarashi, K. M., Mori, K., et al. (2010). Differential axonal projection of mitral and tufted cells in the mouse main olfactory system. *Front. Neural Circuits* 4:120. doi: 10.3389/fncir.2010.00120

Naito, T., Saito, Y., Yamamoto, J., Nozaki, Y., Tomura, K., Hazama, M., et al. (1998). Putative pheromone receptors related to the Ca2+-sensing receptor in Fugu. *Proc. Natl. Acad. Sci. U.S.A.* 95, 5178–5181.

Nakamuta, S., Nakamuta, N., Taniguchi, K., and Taniguchi, K. (2012). Histological and ultrastructural characteristics of the primordial vomeronasal organ in lungfish. *Anat. Rec. (Hoboken)* 295, 481–491.

Ngai, J., Chess, A., Dowling, M. M., Necles, N., Macagno, E. R., and Axel, R. (1993a). Coding of olfactory information: topography of odorant receptor expression in the catfish olfactory epithelium. *Cell* 72, 667–680.

Ngai, J., Dowling, M. M., Buck, L., Axel, R., and Chess, A. (1993b). The family of genes encoding odorant receptors in the channel catfish. *Cell* 72, 657–666.

Niimura, Y. (2009). On the origin and evolution of vertebrate olfactory receptor genes: comparative genome analysis among 23 chordate species. *Gen. Biol. Evol.* 1, 34–44.

Niimura, Y., and Nei, M. (2005). Evolutionary dynamics of olfactory receptor genes in fishes and tetrapods. *Proc. Natl. Acad. Sci. U.S.A.* 102, 6039–6044.

Northcutt, R. G., and Rink, E. (2012). Olfactory projections in the lepidosirenid lungfishes. *Brain Behav. Evol.* 79, 4–25.

Novotny, M. V. (2003). Pheromones, binding proteins and receptor responses in rodents. *Biochem. Soc. Trans.* 31, 117–122.

Osório, J., and Rétaux, S. (2008). The lamprey in evolutionary studies. *Dev. Gen. Evol.* 218, 221–235.

Packard, A., Giel-Moloney, M., Leiter, A., and Schwob, J. E. (2011), Progenitor cell capacity of NeuroD1-expressing globose basal cells in the mouse olfactory epithelium. *J. Comp. Neurol.* 519, 3580–3596.

Packard, G. C. (1974). The evolution of air-breathing in Paleozoic gnathostome fishes. *Evolution* 28, 320–325.

Pan, J. T., Kow, L. M., and Pfaff, D. W. (1988). Modulatory actions of luteinizing hormone-releasing hormone on electrical activity of preoptic neurons in brain slices. *Neuroscience* 27, 623–628.

Park, D., McGuire, J. M., Majchrzak, A. L., Ziobro, J. M., and Eisthen, H. L. (2004). Discrimination of conspecific sex and reproductive condition using chemical cues in axolotls (*Ambystoma mexicanum*). *J. Comp. Physiol. A. Neuroethol. Sens. Neural Behav. Physiol.* 190,i 415–427.

Petreanu, L., and Álvarez-Buylla, A. (2002). Maturation and death of adultborn olfactory bulb granule neurons: role of olfaction. *J. Neurosci.* 22, 6106–6113.

Pfister, P., and Rodriguez, I. (2005). Olfactory expression of a single and highly variable V1r pheromone receptor-like gene in fish species. *Proc. Natl. Acad. Sci. U.S.A.* 102, 5489–5494.

Price, J. L. (1986). Subcortical projections from the amygdaloid complex. *Adv. Exp. Med. Biol.* 203, 19–33.

Priest, C. A., and Puche, A. C. (2004). GABAB receptor expression and function in olfactory receptor neuron axon growth. *J. Neurobiol.* 60, 154–165.

Ren, X., Chang, S., Laframboise, A., Green, W., Dubuc, R., and Zielinski, B. (2009). Projections from the accessory olfactory organ into the medial region of the olfactory bulb in the sea lamprey (*Petromyzon marinus*): a novel vertebrate sensory structure? *J. Comp. Neurol.* 516, 105–116.

Ressler, K. J., Sullivan, S. L., and Buck, L. B. (1994). Information coding in the olfactory system: evidence for a stereotyped and highly organized epitope map in the olfactory bulb. *Cell* 79, 1245–1255.

Rodríguez, I., Feinstein, P., and Mombaerts, P. (1999). Variable patterns of axonal projections of sensory neurons in the mouse vomeronasal system. *Cell* 97, 199–208.

Rowe, T. B., Macrini, T. E., and Luo, Z.-X. (2011). Fossil evidence on origin of the mammalian brain. *Science* 332, 955–957.

Ryba, N. J. P., and Tirindelli, R. (1997). A new multigene family of putative pheromone receptors. *Neuron* 19, 371–379.

Sakuma, Y., and Pfaff, D. W. (1983). Modulation of the lordosis reflex of female rats by LHRH, its antiserum and analogs in the mesencephalic central gray. *Neuroendocrinology* 36, 218–224.

Sato, Y., Miyasaka, N., and Yoshihara, Y. (2005). Mutually exclusive glomerular innervation by two distinct types of olfactory sensory neurons revealed in transgenic zebrafish. *J. Neurosci.* 25, 4889–4897.

Sawada, M., Kaneko, N., Inada, H., Wake, H., Kato, Y., Yanagawa, Y., et al. (2011). Sensory input regulates spatial and subtype-specific patterns of neuronal turnover in the adult olfactory bulb. *J. Neurosci.* 31, 11587–11596.

Scalia, F., and Winans, S. S. (1975). The differential projections of the olfactory bulb and accessory olfactory bulbin mammals. *J. Comp. Neurol.* 161, 31–55.

Schwanzel-Fukuda, M., and Pfaff, D. W. (1989). Origin of luteinizing hormone-releasing hormone neurons. *Nature* 338, 161–164.

Schwarting, G. A., and Henion, T. R. (2008). Olfactory axon guidance: the modified rules. *J. Neurosci. Res.* 86, 11–17.

Schwob, J. E. (2002). Neural regeneration and the peripheral olfactory system. *Anat. Rec.* 269, 33–49.

Senter, P. (2002). Lack of a pheromonal sense in phytosaurs and other archosaurs, and its implications for reproductive communication. *Paleobiology* 28, 544–550.

Sevelinges, Y., Lévy, F., Mouly, A.-M., and Ferreira, G. (2009). Rearing with artificially scented mothers attenuates conditioned odor aversion in adulthood but not its amygdala dependency. *Behav. Brain Res.* 198, 313–320.

Shi, P., and Zhang, J. (2007). Comparative genomic analysis identifies an evolutionary shift of vomeronasal receptor gene repertoires in the vertebrate transition from water to land. *Genome Res.* 17, 166–174.

Shipley, M. T., and Adamek, G. D. (1984). The connections of the mouse olfactory bulb: a study using orthograde and retrograde transport of wheat germ agglutinin conjugated to horseradish peroxidase. *Brain Res. Bull.* 12, 669–688.

Sorensen, P. W., Fine, J. M., Dvornikovs, V., Jeffrey, C. S., Shao, F., Wang, J., et al. (2005). Mixture of new sulfated steroids functions as a migratory pheromone in the sea lamprey. *Nat. Chem. Biol.* 1, 324–328.

Steiger, S., Kuryshev, V., Stensmyr, M., Kempenaers, B., and Mueller, J. (2009). A comparison of reptilian and avian olfactory receptor gene repertoires: species-specific expansion of group gamma genes in birds. *BMC Genomics* 10:446. doi: 10.1186/1471-2164-10-446

Steiger, S. S., Fidler, A. E., Valcu, M., and Kempenaers, B. (2008). Avian olfactory receptor gene repertoires: evidence for a well-developed sense of smell in birds? *Proc. Biol. Sci.* 275, 2309–2317.

St John, J. A., Clarris, H. J., and Key, B. (2002). Multiple axon guidance cues establish the olfactory topographic map: how do these cues interact? *Int. J. Dev. Biol.* 46, 639–647.

Stowers, L., Holy, T. E., Meister, M., Dulac, C., and Koentges, G. (2002). Loss of sex discrimination and male-male aggression in mice deficient for TRP2. *Science* 295, 1493–1500.

Strotmann, J. (2001). Targeting of olfactory neurons. *Cell Mol. Life Sci.* 58, 531–537.

Strotmann, J., Levai, O., Fleischer, J., Schwarzenbacher, K., and Breer, H. (2004). Olfactory receptor proteins in axonal processes of chemosensory neurons. *J. Neurosci.* 24, 7754–7761.

Suárez, R. (2011). Molecular switches in the development and fate specification of vomeronasal neurons. *J. Neurosci.* 31, 17761–17763.

Suárez, R., Fernández-Aburto, P., Manger, P. R., and Mpodozis, J. (2011a). Deterioration of the gao vomeronasal pathway in sexually dimorphic mammals. *PLoS ONE* 6:e26436. doi: 10.1371/journal.pone.0026436

Suárez, R., Santibáñez, R., Parra, D., Coppi, A. A., Abrahão, L. M. B., Sasahara, T. H. C., et al. (2011b). Shared and differential traits in the accessory olfactory bulb of caviomorph rodents with particular reference to the semiaquatic capybara. *J. Anat.* 218, 558–565.

Suárez, R., and Mpodozis, J. (2009). Heterogeneities of size and sexual dimorphism between the subdomains of the lateral-innervated accessory olfactory bulb (AOB) of Octodon degus (*Rodentia: Hystricognathi*). *Behav. Brain Res.* 198, 306–312.

Thornhill, R. A. (1967). The ultrastructure of the olfactory epithelium of the lamprey lampetra fluviatilis. *J. Cell Sci.* 2, 591–602.

Tucker, E. S., Lehtinen, M. K., Maynard, T., Zirlinger, M., Dulac, C., Rawson, N., et al. (2010). Proliferative and transcriptional identity of distinct classes of neural precursors in the mammalian olfactory epithelium. *Development* 137, 2471–2481.

Ubeda-Bañon, I., Pro-Sistiaga, P., Mohedano-Moriano, A., Saiz-Sanchez, D., De La Rosa-Prieto, C., Gutiérrez-Castellanos, N., et al. (2011). Cladistic analysis of olfactory and vomeronasal systems. *Front. Neuroanat.* 5:3. doi: 10.3389/fnana.2011.00003

Van Denbossche, J., Youson, J. H., Pohlman, D., Wong, E., and Zielinski, B. S. (1997). Metamorphosis of the olfactory organ of the sea lamprey (*Petromyzon marinus* L.): morphological changes and morphometric analysis. *J. Morphol.* 231, 41–52.

Vassar, R., Chao, S. K., Sitcheran, R., Nunez, J. M., Vosshall, L. B., and Axel, R. (1994). Topographic organization of sensory projections to the olfactory bulb. *Cell* 79, 981–991.

Vieyra, M. L. (2011). Olfactory receptor genes in terrestrial, freshwater, and sea turtles: evidence for a reduction in the number of functional genes in aquatic species. *Chel. Conserv. Biol.* 10, 181–187.

Wagner, S., Gresser, A. L., Torello, A. T., and Dulac, C. (2006). A multireceptor genetic approach uncovers an ordered integration of VNO sensory inputs in the accessory olfactory bulb. *Neuron* 50, 697–709.

Wang, G., Shi, P., Zhu, Z., and Zhang, Y.-P. (2010). More functional V1R genes occur in nest-living and nocturnal terricolous mammals. *Genome Biol. Evol.* 2, 277–283.

Wang, Z., Balet Sindreu, C., Li, V., Nudelman, A., Chan, G. C., and Storm, D. R. (2006). Pheromone detection in male mice depends on signaling through the type 3 adenylyl ciclase in the main olfactory epithelium. *J. Neurosci.* 12, 7375–7379.

Westberry, J. M., and Meredith, M. (2003). The influence of chemosensory input and gonadotropin releasing hormone on mating behavior circuits in male hamsters. *Brain Res.* 6, 1–16.

Whitlock, K. E. (2005). Origin and development of GnRH neurons. *Trends Endocrinol. Metab.* 16, 145–151.

Winans, S. S., and Scalia, F. (1970). Amygdaloid nucleus: new afferent input from the vomeronasal organ. *Science* 170, 330–332.

Wong, S. T., Trinh, K., Hacker, B., Chan, G. C., Lowe, G., Gaggar, A., et al. (2000). Disruptionof the type III adenylyl ciclase gene leads to peripheral and behavioral anosmia intransgenic mice. *Neuron* 27, 487–497.

Woodley, S. (2010). Pheromonal communication in amphibians. *J. Comp. Physiol. A Neuroethol. Sens. Neural Behav. Physiol.* 196, 713–727.

Wray, S. (2010). From nose to brain: development of gonadotrophin-releasing hormone-1 neurones. *J. Neuroendocrinol.* 22, 743–753.

Wray, S., Grant, P., and Gainer, H. (1989). Evidence that cells expressing luteinizing hormone-releasing hormone mRNA in the mouse are derived from progenitor cells in the olfactory placode. *Proc. Natl. Acad. Sci. U.S.A.* 86, 8132–8136.

Wu, W., Wong, K., Chen, J., Jiang, Z., Dupuis, S., Wu, J. Y., et al. (1999). Directional guidance of neuronal migration in the olfactory system by the protein Slit. *Nature* 400, 331–336.

Xia, J., Broad, K. D., Emson, P. C., and Keverne, E. B. (2010). Epigenetic modification of vomeronasal (V2r) precursor neurons by histone deacetylation. *Neuroscience* 169, 1462–1472.

Yoon, H., Enquist, L. W., and Dulac, C. (2005). Olfactory inputs to hypothalamic neurons controlling reproduction and fertility. *Cell* 123, 669–682.

Young, J. M., Massa, H. F., Hsu, L., and Trask, B. J. (2010). Extreme variability among mammalian V1R gene families. *Genome Res.* 20, 10–18.

Young, J. M., and Trask, B. J. (2007). V2R gene families degenerated in primates, dog and cow, but expanded in opossum. *Trends Genet.* 23, 212–215.

Zelenitsky, D. K., Therrien, F. O., Ridgely, R. C., McGee, A. R., and Witmer, L. M. (2011). Evolution of olfaction in non-avian theropod dinosaurs and birds. *Proc. Biol. Sci.* 278, 3625–3634.

Zhang, J., and Webb, D. M. (2003). Evolutionary deterioration of the vomeronasal pheromone transduction pathway in catarrhine primates. *Proc. Natl. Acad. Sci. U.S.A.* 100, 8337–8341.

Zhao, H., Xu, D., Zhang, S., and Zhang, J. (2011). Widespread losses of vomeronasal signal transduction in bats. *Mol. Biol. Evol.* 28, 7–12.

Zhu, M., and Ahlberg, P. E. (2004). The origin of the internal nostril of tetrapods. *Nature* 432, 94–97.

Zou, D.-J., Firestein, P., Rivers, A., Mathews, G., Kim, A., Greer, C. A., et al. (2004). Postnatal refinement of peripheral olfactory projections. *Science* 304, 1976–1979.

Zufall, F., Ukhanov, K., Lucas, P., Liman, E. R., and Leinders-Zufall, T. (2005). Neurobiology of TRPC2: from gene to behavior. *Pflugers Arch.* 451, 61–71.

Zuri, I., and Halpern, M. (2003). Differential effects of lesions of the vomeronasal and olfactory nerves on garter snake (*Thamnophis sirtalis*) responses to airborne chemical stimuli. *Behav. Neurosci.* 117, 169–183.

Conflict of Interest Statement: The authors declare that the research was conducted in the absence of any commercial or financial relationships that could be construed as a potential conflict of interest.

Received: 25 May 2012; accepted: 26 November 2012; published online: 24 December 2012.

Citation: Suárez R, García-González D and de Castro F (2012) Mutual influences between the main olfactory and vomeronasal systems in development and evolution. Front. Neuroanat. ***6****:50. doi: 10.3389/fnana.2012.00050*

frontiers in
NEUROANATOMY

REVIEW ARTICLE
published: 19 September 2012
doi: 10.3389/fnana.2012.00039

The main but not the accessory olfactory system is involved in the processing of socially relevant chemosignals in ungulates

Matthieu Keller [1,2,3]* ***and Frédéric Lévy*** [1,2,3]*

[1] *INRA, UMR 85 Physiologie de la Reproduction et des Comportements, Nouzilly, France*
[2] *CNRS, UMR 7247 Physiologie de la Reproduction et des Comportements, Nouzilly, France*
[3] *Université François Rabelais de Tours, Tours, France*

Edited by:
Micheal Baum, Boston University, USA

Reviewed by:
Wayne Korzan, Boston University, USA
Peter Brennan, University of Bristol, UK

****Correspondence:***
Matthieu Keller and Frédéric Lévy, Laboratoire de Physiologie de la Reproduction et des Comportements, UMR 7247 INRA/CNRS/Université de Tours, 37380 Nouzilly, France.
e-mail: mkeller@tours.inra.fr; levy@tours.inra.fr

Ungulates like sheep and goats have, like many other mammalian species, two complementary olfactory systems. The relative role played by these two systems has long been of interest regarding the sensory control of social behavior. The study of ungulate social behavior could represent a complimentary alternative to rodent studies because they live in a more natural environment and their social behaviors depend heavily on olfaction. In addition, the relative size of the main olfactory bulb (MOB) [in comparison to the accessory olfactory bulb (AOB)] is more developed than in many other lissencephalic species like rodents. In this review, we present data showing a clear involvement of the main olfactory system in two well-characterized social situations under olfactory control in ungulates, namely maternal behavior and offspring recognition at birth and the reactivation of the gonadotropic axis of females exposed to males during the anestrous season. In conclusion, we discuss the apparent discrepancy between the absence of evidence for a role of the vomeronasal system in ungulate social behavior and the existence of a developed accessory olfactory system in these species.

Keywords: maternal behavior, sociosexual interactions, olfactory systems, male effect, olfactory learning, vomeronasal organ

INTRODUCTION

The sense of smell is of primary importance for social recognition among mammals and is mediated by the main and the accessory olfactory systems. These olfactory systems differ both in their organization and in their function. The main olfactory system is involved in the processing of volatile odors detected at the level of the main olfactory epithelium in the nasal cavity. Sensory neurons send axons to glomerular cell layer of the main olfactory bulb (MOB) where they synapse with dendrites of mitral and tufted cells. The olfactory information is then conveyed to several primary olfactory structures including the anterior olfactory nucleus, the olfactory tubercle, the piriform cortex, the posterolateral cortical amygdala, or the entorhinal cortex (Petrulis, 2009). By contrast, the accessory olfactory system is involved in the detection of non-volatile odors through receptors localized in the epithelium of the vomeronasal organ (VNO). These receptors synapse onto mitral cells of the accessory olfactory bulb (AOB) which then project mainly to the medial amygdala (Halpern and Martínez-Marcos, 2003). The olfactory information then reaches the hypothalamus at the level of various structures including the medial preoptic area or the bed nucleus of the stria terminalis (Scalia and Winans, 1975).

Although the processing of olfactory information between both systems is largely independent, many levels of convergence are found between them, for example, directly at the level of the olfactory bulb (Larriva-Sahd, 2008) or more downstream at the level of the amygdala (Licht and Meredith, 1987; Kang et al., 2009). Therefore, a recurrent problem in olfactory functional studies is to elucidate the role played by each olfactory system, as well as their interactions, in the detection of olfactory information and in the regulation of social behavior (Keller et al., 2009). For example in mice, the main olfactory system can respond to 2-heptanone, a molecule known to participate to mouse social communication, but this chemosignal also activates the accessory olfactory system (Xu et al., 2005). Conversely, volatile pheromones like farnesene or dimethylpyrazine, known to be detected by the main olfactory system can also trigger cellular activation in the mice vomeronasal epithelium (Leinders-Zufall et al., 2000).

Most of our current knowledge on the involvement of the main and the accessory olfactory systems in the regulation of behavior comes from studies using very few species, mostly mice and rats living in artificial laboratory environment. However, given the wide variety of organization of both olfactory systems (Mesiami and Bhatnagar, 1998), it is likely that the respective roles played by both olfactory systems vary across mammalian species. Studying the olfactory control of social behavior in ungulates (especially sheep and goat) could represent a complimentary alternative to rodent studies because ungulates, even farm animals like sheep, live in a more natural environment and their social behaviors depend heavily on olfaction (Gelez and Fabre-Nys, 2004; Lévy et al., 2004). In addition, ungulates constitute an

additional interesting model because the relative size of the MOB (in comparison to the AOB) is also more developed than in many other lissencephalic species like rodents.

In this review, we highlight the role of both olfactory systems in two well-studied social situations in sheep and goats, maternal behavior and sexual behavior (the so called "male effect") and we then discuss the general involvement of both systems in the regulation of ungulates social behavior and in comparison to rodents.

OLFACTORY SYSTEMS INVOLVED IN MATERNAL BEHAVIOR

In sheep, the establishment of maternal behavior is under the major influence of amniotic fluids which cover the lamb at birth. An important shift toward amniotic fluid is observed across pregnancy and parturition: while repelled by amniotic fluid throughout pregnancy, ewes become highly attracted to amniotic fluid around parturition (Lévy et al., 1983). This attraction mediates the attraction to the newborn because parturient ewes are more attracted to a model lamb smeared with amniotic fluid than the same model without amniotic fluid (Vince et al., 1985). In addition, when newborn lambs are washed to eliminate amniotic fluids at birth, maternal behavior is often disrupted, especially in inexperienced females (Lévy and Poindron, 1987). This rapid shift toward amniotic fluid is mediated by chemosensory stimuli. Indeed, when testing females in a context where the attraction/repulsion to amniotic fluid was not dependent on the presence of the lamb (test of food choice between two troughs containing food where one troughs where one trough was contaminated with amniotic fluid), it has been shown that females receiving an injection of zinc sulfate in the main olfactory cavity which destroys the main olfactory epithelium are neither repelled by nor clearly attracted to amniotic fluid (Lévy et al., 1983). By contrast, vomeronasal nerve section does not affect these attraction–repulsion responses to amniotic fluid (Lévy et al., 1995).

In sheep, the respective roles of the main and accessory olfactory systems to the display of maternal behavior were investigated in primiparous females. Anosmic mothers spent less time licking their neonates and emitted fewer maternal bleats (Lévy et al., 1995). On the other hand, mothers with only lesions of the VNO showed little disturbance of maternal care, thus underlying the importance of the main olfactory system in the establishment of maternal behavior at parturition.

In addition to the strict expression of maternal care, the establishment of a selective bond within the first few hours after parturition represents one of the essential characteristics of maternal behavior in precocial species such as ungulates. Numerous studies consistently indicate that olfaction plays a primary role in ewes' selective acceptance of lambs for nursing (Poindron and Le Neindre, 1980; Poindron et al., 1993). When females were rendered hyposmic through the use of zinc sulfate to destroy the olfactory epithelium, (Poindron, 1976; Romeyer et al., 1994; Lévy et al., 1995) or by sectioning the olfactory nerves (Morgan et al., 1975), females show no selective preference for their own young and nursed alien young indiscriminately. Similar results have been obtained in goats (Romeyer et al., 1994; Poindron et al., 2007). By contrast, the accessory olfactory system appears not to be involved in offspring recognition since the section of the accessory olfactory nerves does not induce deficits on the establishment of maternal selectivity in sheep (Lévy et al., 1995).

Ewes develop a selective bond with their newborn offspring, even when direct physical contact is prevented, providing that they have access to the lamb's salient odor (Poindron and Le Neindre, 1980; Romeyer et al., 1993; Otal et al., 2009), thus suggesting that lamb's olfactory signature is partly volatile. The recognizable odor profile of a lamb reflects a complex mosaic of chemical by-products of bodily processes. Indeed, a list of 133 volatile organic compounds associated with the wool of Döhne Merino lambs that are presumably involved in offspring recognition has been recently identified (Burger et al., 2011). Quantitative analysis and comparison of odor profiles reveal that the wool volatiles of twins are remarkably similar but that they differ from those of other twins or non-twin lambs. Unfortunately, when alien lambs are dressed in jackets sprayed with synthetic mixtures formulated to match the chemical composition of the scents of the ewes' own lambs, ewes reject these alien lambs (Burger et al., 2011).

The functional role of the MOB has been confirmed using various pharmacological, neurochemical, and electrophysiological approaches. Electrophysiological recordings from MOB mitral cells were first performed in awake ewes before and after birth (Kendrick et al., 1992). During pregnancy, none of the MOB mitral cells respond to lamb related odors (lamb, amniotic fluids…), but they respond to food odors. After birth, there is a noticeable increase in the number of mitral cells that responded to lamb odors, suggesting that the change in salience of the lamb odor that occurs at parturition is mediated by a shift in olfactory cell responsivity. Interestingly, among these MOB mitral cells, a small propotion responded preferentially to the odor of the familiar lamb, showing that already at the level of the MOB, a coding for the familiar lamb odor takes place.

Microdialysis analyses reveal that these changes in electrical properties of MOB mitral cells at parturition are the consequences of changes in the release of two neurotransmitters, the inhibitory gamma-amino-butyric-acid (GABA) and the excitatory glutamate within the MOB. Once ewes establish a selective bond with their lambs after parturition, the odors of familiar lambs, but not those of unfamiliar ones, increase the release of both transmitters. Infusion of the GABAa receptor antagonist bicuculline in the MOB prevents lamb recognition once it has been formed. Therefore, it is hypothesized that the general increase of GABA refines the olfactory signal by inhibiting MOB mitral cells with the exception of those processing the odor of the familiar lamb.

A dramatic increase of noradrenaline release also occurs during the learning of lamb odor (Lévy et al., 1993). Lesions of noradrenergic projections to the MOB or direct infusions of ß-adrenergic antagonist reduce the number of ewes developing the olfactory memory, without disrupting maternal care to the lamb (Pissonnier et al., 1985; Lévy et al., 1990). Contrary to the inhibitory effects of GABA on MOB mitral cell activity, the release of noradrenaline at birth induces the disinhibition of MOB mitral cells, thus allowing potentiation of the glutamatergic system by the retrograde messenger, nitric oxide (Kendrick et al., 1997).

In addition to these neurochemical changes, olfactory neurogenesis could provide another mechanism through which olfaction can contribute to lamb recognition. The olfactory bulb is a brain region where new neurons are continuously added during adult life. Production of new cells occurs at the level of the sub-ventricular zone (SVZ; Lois and Alvarez-Buylla, 1994; Doetsch et al., 1997, 1999) which contains neuronal stem cells that generate neuroblasts which then migrate through the rostral migratory stream toward the MOB. Once in the MOB, neuroblasts migrate radially in the different layers of the MOB, especially in the granular cell layer and to a lower extent in the periglomerular cell layer where these cells start to differentiate into mature GABAergic neurons expressing specific phenotypic markers such as NeuN (Lledo et al., 2006). During maturation, it is noticeable that around 50% of new cells die while the remaining half survives and is integrated into the olfactory network. This survival is highly regulated by both external and internal factors (Lledo and Saghatelyan, 2005). In sheep, as in rodents, neural stem cells proliferate on the margins of the SVZ and a rostral migratory stream is evidenced from the SVZ up to the MOB consisting of neuroblasts which form chain-like structures. The neuroblasts differentiate into mainly granular neurons once they have reached the MOB (Brus et al., 2010, 2012). Unlike the SVZ of rodents, the SVZ of sheep is particularly expanded to the open olfactory ventricle in the MOB (Luzzati et al., 2003; Brus et al., 2010), suggesting that the migration pathway of adult-born cells follows this ventricle up the MOB. In addition, the time required for maturation of adult-born cells in the sheep MOB is around four months, much longer than that of rodents (Brus et al., 2012).

The capacity of the olfactory system to generate new interneurons is thought to play an important function in social situations where olfaction plays a pivotal role (Gheusi et al., 2009; Lévy et al., 2011a). In the context of maternal behavior in sheep, regulation of neurogenesis has been reported at the time of parturition and according to mother-young interactions. Mothers having interactions with their lamb for 2 days exhibit less cell proliferation in the SVZ and fewer neuroblasts in the MOB in comparison to non-pregnant females (Brus et al., 2010; Lévy et al., 2011b). Although these results are correlational by nature, we hypothesize that this down-regulation of neurogenesis could facilitate learning of lamb odor by decreasing cell competition and favoring maturation of surviving new neurons. Future work should validate this hypothesis by using more functional approaches including for example the use of anti-mitotic drugs such as Arabinofuranosyl Cytidine (ara-C) and examine the behavioral consequences of the blockade of adult olfactory neurogenesis.

Downstream to the level of the MOB, the identification of activated brain regions during olfactory bonding confirms the importance of the main olfactory system. Indeed, a comparison of the c-fos mRNA expression in mothers exposed to a lamb after parturition to non-gestant females receiving an artificial vaginocervical stimulation (mimicking the expulsion of the fetus) without being in contact with a lamb has been performed. It showed an increase in Fos expression that was mainly restricted to the main olfactory processing regions, i.e., the MOB, the piriform cortex, the frontal medial cortex and the orbitofrontal cortex in females exposed to lambs (Da Costa et al., 1997). Similar results were obtained using Fos immunocytochemistry after exposing intact selective mothers to their lamb and comparing them to anosmic mothers showing no sign of individual lamb recognition (Keller et al., 2004a).

Because the quantification of Fos expression is only a correlational method, the functional role of some brain structures showing Fos activation during the formation of olfactory lamb memory, were explored by using reversible pharmacological manipulation, revealing an important role for both the medial and the cortical nuclei of the amygdala (Keller et al., 2004b; **Figure 1**), which receive olfactory inputs from the MOB (Meurisse et al., 2009). Infusion of the anaesthetic lidocaïne, during the first 8 h post-partum, in either of these nuclei prevents animals from learning to discriminate their own lamb from an alien lamb and hence, both are permitted to suckle. This effect does not result from a disturbance of maternal acceptance or from an inability of memory retrieval.

Taken together, these results lead to the conclusion that the main olfactory system is involved in the control of lamb recognition at parturition. However, results showing that the AOB shows zif268 (an immediate early gene used as a marker of cellular activation) activation around parturition (Keller, 2003) and that the cauterization of the VNO entrance impairs maternal selectivity (Booth and Katz, 2000) raise the question of a possible involvement of the accessory olfactory system in offspring recognition. Because activation of AOB neurons requires a direct contact with the odorant source (Luo et al., 2003), and ewes exposed to olfactory cues but without any physical contact with the lamb develop a selective bond, the involvement of AOB in maternal selectivity is unlikely. The fact that the VNO can be activated by small volatile chemosignals (Leinders-Zufall et al., 2000; Trinh and Storm, 2003) prompts a more precise comparison of the effects of vomeronasal nerves section (Lévy et al., 1995) to those of cauterization of the vomeronasal duct (Booth and Katz, 2000). These authors also report that zinc sulfate infusion is ineffective in disrupting selectivity (Booth and Katz, 2000). However, regarding the main olfactory system, this discrepancy is probably due to methodological differences and to the small amounts of zinc sulfate solution used by Booth and Katz. Indeed, the application of around 2 mL of 1.5% ZnSO4 solution per nostril induces incomplete lesions of the main olfactory epithelium in many animals (in comparison with 50 mL of 1.5% ZnSO4 used by Poindron et al.), therefore failing to induce anosmia in an reliable way. This is, however, no longer the case when using a higher concentration of zinc sulfate (2.5%, Poindron et al., 2003).

OLFACTORY SYSTEMS INVOLVED IN THE MALE EFFECT

In ungulates, the introduction of a male among seasonally anoestrous females results in activation of LH secretion (short-term response) leading later to ovulation and sexual receptivity (long-term response; Delgadillo et al., 2009). This phenomenon is commonly known as the "male effect" and is frequently used to advance and synchronize reproduction in sheep and goats. Contact with the male is not necessary to observe the reactivation of the gonadotropic axis since the short-term response can be fully mimicked by exposing the females to the male odor (Knight and Lynch, 1980).

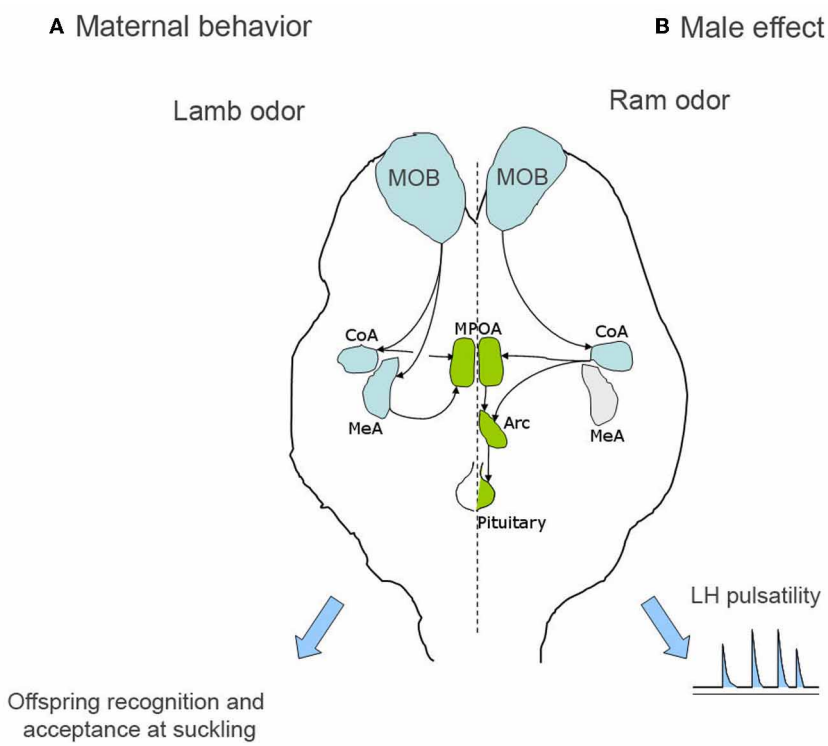

FIGURE 1 | Simplified representation of the processing of olfactory information in the case of both offspring recognition and male effect in sheep. (A) In the case of offspring recognition, lamb odor is processed by the main olfactory bulb and then by both the medial and cortical nuclei of the amygdala, before to reach the medial preoptic area, which is involved in the expression of maternal care and offspring acceptance at suckling. **(B)** In the case of the male effect, the main olfactory bulb is also involved but then only the cortical amygdala seems to be in charge of the processing of male odor. The final output is the GnRH pulse generator at least partly localized in the arcuate nucleus which controls LH pulsatility and the reactivation of the gonadotrope axis. Arc, arcuate nucleus; CoA, cortical amygdala; MeA, medial amygdala; MOB, main olfactory bulb; MPOA, medial preoptic area.

The chemosignal responsible for the reactivation of the female gonadotropic axis seems to be a mixture of various compounds which have only been partially identified. It has been shown that the biological activity of the chemosignal requires the simultaneous presence of compound retained in both acid and neutral fractions (Cohen-Tannoudji et al., 1994). Recent work has focused on identification of the male odor in goats using changes in multiple unit activity as a "real-time" bioassay of neural activity in female goats (Hamada et al., 1996). This approach has yielded important perspectives on the nature of the male odor in this species: (1) odor production is dependent upon testosterone and is localized to the head, neck, and shoulders of the male (Hamada et al., 1996; Iwata et al., 2000; Wakabayashi et al., 2000); (2) the odorant activity resides in the lipid fraction of fleece extract (Okamura and Mori, 2005); (3) fleece odor from male sheep induces multiple unit electrophysiological activity and an associated increase in LH secretion in female goats (Ichimaru et al., 2008); and (4) 4 ethyloctanoic acid, the chemical responsible for the strong odor of male goats, elicit LH activity only when left for several months at room temperature (Iwata et al., 2003), suggesting a bacterial fermentation of precursors.

The role of the main and the accessory olfactory systems have been evaluated through lesioning or inactivating different regions of the main or the accessory olfactory pathways. Destruction of the main olfactory epithelium through intranasal administration of zinc sulfate or inactivation of the cortical nucleus of the amygdala by infusion of the anaesthetic lidocaine completely blocks the neuroendocrine response to ram odor (Gelez and Fabre-Nys, 2004, 2006b; Gelez et al., 2004; **Figure 1**). By contrast, lesion of the VNO or inactivation of the medial nucleus of the amygdala does not disrupt the response of females (Cohen-Tannoudji et al., 1989; Gelez and Fabre-Nys, 2006b).

Correlational studies using Fos immunocytochemistry to reveal central activations triggered by male odors support the view that the main olfactory system primarily conveys the male odor. In sheep, when comparing groups exposed to a male, male fleece, female fleece or no odor, the male or its odor significantly increases Fos expression in the main olfactory system, especially the MOB and the cortical nucleus of the amygdala (Gelez and Fabre-Nys, 2006a). However, the AOB, but no downstream structures, express Fos immunoreactivity following exposure to the ram odor. The AOB could play a minor role in the detection of the ram odor by activating the cortical nucleus of the amygdala through their reciprocal connections (Meurisse et al., 2009).

In goats, neuroendocrine activations by male odor involve the kisspeptin system in the arcuate nucleus of the hypothalamus (Hamada et al., 1996; Murata et al., 2009, 2011; Okamura et al.,

2010). These kisspeptin cells are thought to be the intrinsic source of the GnRH pulse generator which consequently leads to LH release and ovulation. However, the olfactory system involved in the modulation of kisspeptin neurons has not been explored in the goat. The activation of the gonadotrope axis by male odor is confirmed by the fact that at the downstream stage, exposure to male odor is correlated with Fos activation of GnRH neurons in sheep (Gelez and Fabre-Nys, 2006a).

In summary, it has been shown that in sheep, contrary to many other species, the main olfactory system is primarily involved in the processing of the olfactory signal emanating from the male and that mediates a physiological response, while the accessory olfactory system seems to be less engaged. This is in contrast to rodents, where pheromonal cues are usually processed by the vomeronasal system (Keller et al., 2009). For example, sexual partner odor induces Fos activation in the AOB rather than the MOB in mice (Halem et al., 2001). In the female rat, removal of the VNO blocks the neuroendocrine response induced by male urine (Beltramino and Taleisnik, 1983). To the best of our knowledge, the few examples in which mammalian pheromonal signals are detected and processed by the main olfactory system relates to behavioral responses rather than physiological effects. This is the case for the rabbit mammary pheromone that induces the nipple search behavior (Hudson and Distel, 1983; Charra et al., 2012) and for the chemosignals contained in boar saliva that elicit receptivity posture in female pigs (Dorries et al., 1997).

A ROLE FOR VOMERONASAL OLFACTION IN UNGULATES?

The data presented in the context of maternal behavior as well as those related to the male effect clearly support a key role for the main olfactory system in ungulate social behavior. Evidence showing an involvement of the vomeronasal system is scarce and the only experiment claiming a role of the VNO in sheep offspring recognition has raised methodological concerns.

However, ungulates are one of the animal taxa where a specific olfactory behavior that is thought to be dependent upon the vomeronasal system, namely flehmen response, is widely reported (Melese-d'Hospital and Hart, 1985). This behavior is highly expressed at the time of mother–young interactions at birth and during sexual encounters. Indeed, flehmen behavior is evoked most readily by olfactory investigation of urine, vaginal, or amniotic fluid secretions, and is believed to be involved in the transport of fluid-borne chemical stimuli, such as sexual odors, from the oral cavity to the VNO (Melese-d'Hospital and Hart, 1985).

At the neuroanatomical level, the VNO, the AOB, and the "vomeronasal" amygdala have been identified and are quite well developed in many wild and farm ungulate species (Kratzing, 1971; Salazar et al., 2007; Vedin et al., 2010). Both VNO and AOB complete their morphological development around the last third of the gestation period (Salazar et al., 2003), and a specific lectin for oligomeric N-acetylglucosamine labels the sensory epithelium of the VNO, the vomeronasal nerves, and the nervous and glomerular layers of the AOB before birth, thus suggesting that the vomeronasal system may be able to function at or even before birth (whereas in rodents this is precluded by the AOB not completing its development before birth).

As in other species, in sheep the chemosignals are thought to contact vomeronasal receptors in the VNO epithelium through a pumping mechanism (Meredith et al., 1980; Melese-d'Hospital and Hart, 1985). The morphological features of the vomeronasal arteries and veins together with the existence of large autonomic and sensory innervations suggest that these vessels function similarly to erectile tissue (Salazar et al., 1998). The VNO sensory epithelium of sheep was studied at the morphological level using both optical and electronic microscopy (Kratzing, 1971) and showed only slight differences to that of rodents. However, if the vomeronasal system of ungulates seems to be perfectly functional, it is striking to notice that at the molecular level its importance seems to be quite reduced. Indeed, the ratio of the volume of the vomeronasal epithelium to that of the whole VNO in the goat is 8% in comparison to that found in the mouse (Wakabayashi et al., 2002). The size of goat V1R gene family is also smaller than that of rodent V1R gene families (Wakabayashi et al., 2002). In addition, most goat V2R gene products may not function as receptors since the V2R genes have multiple termination codons within their coding sequences (Wakabayashi et al., 2002). As a whole, the possibility exists that the VNO has evolved so that it has lost part of its role in the detection of social odors in ungulates and therefore the main olfactory system contributes mainly to the discrimination of these odors. Interestingly, the expression of one gene receptor (gV1ra1) of the V1R receptor family, a family of genes which is usually expressed in the VNO of rodents, has been found to be expressed in the main olfactory epithelium in goat (Wakabayashi et al., 2002, 2007).

The downstream organization of the vomeronasal system also seems to be perfectly functional, even if some slight differences with rodents can be noticed. First, the respective zone to zone projection from the apical and basal sensory epithelium of the VNO to the anterior and posterior part of the AOB, typical in rodents, is not present in adult sheep (Salazar et al., 2007) and goats (Takigami et al., 2000). With regard to the sheep AOB, its size seems to be relatively small in comparison to the MOB (Mesiami and Bhatnagar, 1998), and one of the AOB most prominent anatomical features is the scarce population of mitral/tufted cells and their dispersion (Salazar et al., 2007). A morphological consequence is that there is no clear presence of a classical plexiform layer in the stratification of the sheep AOB.

Finally, at the level of the central projections of the vomeronasal system, it seems that the vomeronasal amygdala of the sheep is as extensive as that of rodents (Jansen et al., 1998; Lévy et al., 1999) and the existence of vomeronasal projections to the medial amygdala has been documented (Jansen et al., 1998; Meurisse et al., 2009) and suggest a role of the vomeronasal system in ungulate social behavior.

In conclusion, the current knowledge on the regulation of social behavior by the accessory olfactory system leads to an apparent contradiction. Indeed, neuroanatomical characterizations suggest that despite a reduced relative size, the vomeronasal system seems to be perfectly functional. By contrast, the behavioral evidence regarding its function in social olfaction is scarce, therefore advocating for further investigations in this area. Particularly, the use of other behavioral situations than the ones

explored so far could lead to a re-evaluation of the role of the vomeronasal olfaction in the control of social behavior in ungulates. For example, it is likely that vomeronasal olfaction could play a more developed role in wild ungulates such as antelopes or moose than in domesticated species (Deutsch and Nefdt, 1992; Vedin et al., 2010).

ACKNOWLEDGMENTS

During the preparation of this manuscript, we were supported by grants from the French National Research Agency (ANR) and from the INRA/Pasteur Institute Transversal Research Program. We thank Laura Szymanski for kindly correcting the English of our manuscript.

REFERENCES

Beltramino, C., and Taleisnik, S. (1983). Release of LH in the female rat by olfactory stimuli. Effect of the removal of the vomeronasal organs or lesioning of the accessory olfactory bulbs. *Neuroendocrinology* 36, 53–58.

Booth, K. K., and Katz, L. S. (2000). Role of the vomeronasal organ in neonatal offspring recognition in sheep. *Biol. Reprod.* 63, 953–958.

Brus, M., Meurisse, M., Franceschini, I., Keller, M., and Lévy, F. (2010). Evidence for cell proliferation and its downregulation by parturition and interaction with the young in the sheep brain. *Horm. Behav.* 58, 737–746.

Brus, M., Meurisse, M., Gheusi, G., Keller, M., Lledo, P. M., and Lévy, F. (2012). Dynamic of olfactory and hippocampal neurogenesis in the sheep. *J. Comp. Neurol.* doi: 10.1002/cne.23169. [Epub a head of print].

Burger, B. V., Viviers, M. Z., Le Roux, N. J., Morris, J., Bekker, J. P., and Le Roux, M. (2011). Olfactory cue mediated neonatal recognition in sheep, Ovis aries. *J. Chem. Ecol.* 37, 1150–1163.

Charra, R., Datiche, F., Casthano, A., Gigot, V., Schaal, B., and Coureaud, G. (2012). Brain processing of the mammary pheromone in newborn rabbits. *Behav. Brain Res.* 226, 179–188.

Cohen-Tannoudji, J., Einhorn, J., and Signoret, J. P. (1994). Ram sexual pheromone: first approach of chemical identification. *Physiol. Behav.* 56, 955–961.

Cohen-Tannoudji, J., Lavenet, C., Locatelli, A., Tillet, Y., and Signoret, J. P. (1989). Non-involvement of the accessory olfactory system in the LH response of anoestrous ewes to male odour. *J. Reprod. Fertil.* 86, 135–144.

Da Costa, A. P., Broad, K. D., and Kendrick, K. M. (1997). Olfactory memory and maternal behaviour-induced changes in c-fos and zif/268 mRNA expression in the sheep brain. *Brain Res. Mol. Brain Res.* 46, 63–76.

Delgadillo, J. A., Gelez, H., Ungerfeld, R., Hawken, P. A., and Martin, G. B. (2009). The 'male effect' in sheep and goats–revisiting the dogmas. *Behav. Brain Res.* 200, 304–314.

Deutsch, J. C., and Nefdt, R. J. (1992). Olfactory cues influence female choice in two lek-breeding antelopes. *Nature* 356, 596–598.

Doetsch, F., Caillé, I., Lim, D. A., García-Verdugo, J. M., and Alvarez-Buylla, A. (1999). Subventricular zone astrocytes are neural stem cells in the adult mammalian brain. *Cell* 97, 703–716.

Doetsch, F., García-Verdugo, J. M., and Alvarez-Buylla, A. (1997). Cellular composition and three-dimensional organization of the subventricular germinal zone in the adult mammalian brain. *J. Neurosci.* 17, 5046–5061.

Dorries, K. M., Adkins-Regan, E., and Halpern, B. P. (1997). Sensitivity and behavioral responses to the pheromone androstenone are not mediated by the vomeronasal organ in domestic pigs. *Brain Behav. Evol.* 49, 53–62.

Gelez, H., Archer, E., Chesneau, D., Magallon, T., and Fabre-Nys, C. (2004). Inactivation of the olfactory amygdala prevents the endocrine response to male odour in anoestrus ewes. *Eur. J. Neurosci.* 19, 1581–1590.

Gelez, H., and Fabre-Nys, C. (2004). The "male effect" in sheep and goats: a review of the respective roles of the two olfactory systems. *Horm. Behav.* 46, 257–271.

Gelez, H., and Fabre-Nys, C. (2006a). Neural pathways involved in the endocrine response of anestrous ewes to the male or its odor. *Neuroscience* 140, 791–800.

Gelez, H., and Fabre-Nys, C. (2006b). Role of the olfactory systems and importance of learning in the ewes' response to rams or their odors. *Reprod. Nutr. Dev.* 46, 401–415.

Gheusi, G., Ortega-Perez, I., Murray, K., and Lledo, P. M. (2009). A niche for adult neurogenesis in social behavior. *Behav. Brain Res.* 200, 315–322.

Halem, H. A., Baum, M. J., and Cherry, J. A. (2001). Sex difference and steroid modulation of pheromone-induced immediate early genes in the two zones of the mouse accessory olfactory system. *J. Neurosci.* 21, 2474–2480.

Halpern, M., and Martínez-Marcos, A. (2003). Structure and function of the vomeronasal system: an update. *Prog. Neurobiol.* 70, 245–318.

Hamada, T., Nakajima, M., Takeuchi, Y., and Mori, Y. (1996). Pheromone-induced stimulation of hypothalamic gonadotropin-releasing hormone pulse generator in ovariectomized, estrogen-primed goats. *Neuroendocrinology* 64, 313–319.

Hudson, R., and Distel, H. (1983). Pheromonal release of suckling in rabbits does not depend on the vomeronasal organ. *Physiol. Behav.* 37, 123–128.

Ichimaru, T., Mogi, K., Ohkura, S., Mori, Y., and Okamura H. (2008). Exposure to ram wool stimulates gonadotropin-releasing hormone pulse generator activity in the female goat. *Anim. Reprod. Sci.* 106, 361–368.

Iwata, E., Kikusui, T., Takeuchi, Y., and Mori, Y. (2003). Substances derived from 4-ethyl octanoic acid account for primer pheromone activity for the "male effect" in goats. *J. Vet. Med. Sci.* 65, 1019–1021.

Iwata, E., Wakabayashi, Y., Kakuma, Y., Kikusui, T., Takeuchi, Y., and Mori, Y. (2000). Testosterone-dependent primer pheromone production in the sebaceous gland of male goat. *Biol. Reprod.* 62, 806–810.

Jansen, H. T., Iwamoto, G. A., and Jackson, G. L. (1998). Central connections of the ovine olfactory bulb formation identified using wheat germ agglutinin-conjugated horseradish peroxidase. *Brain Res. Bull.* 45, 27–39.

Kang, N., Baum, M. J., and Cherry, J. A. (2009). A direct main olfactory bulb projection to the 'vomeronasal' amygdala in female mice selectively responds to volatile pheromones from males. *Eur. J. Neurosci.* 29, 624–634.

Keller, M. (2003). *Processus D'acquisition et de Consolidation Impliqués Dans la Mémorisation des Caractéristiques Multisensorielles du Jeune par la Brebis. Approches Comportementales et Neurobiologiques*. PhD dissertation, Paris XIII University.

Keller, M., Baum, M., Brock, O., Brennan, P. A., and Bakker, J. (2009). The main and the accessory olfactory systems interact in the control of mate recognition and sexual behavior. *Behav. Brain Res.* 200, 268–276.

Keller, M., Meurisse, M., and Lévy, F. (2004a). Mapping the neural substrates involved in maternal responsiveness and lamb olfactory memory in parturient ewes using Fos imaging. *Behav. Neurosci.* 118, 1274–1284.

Keller, M., Perrin, G., Meurisse, M., Ferreira, G., and Lévy, F. (2004b). Cortical and medial amygdala are both involved in the formation of olfactory offspring memory in sheep. *Eur. J. Neurosci.* 20, 3433–3441.

Kendrick, K. M., Guevara-Guzman, R., Zorrilla, J., Hinton, M. R., Broad, K. D., Mimmack, M., and Ohkura, S. (1997). Formation of olfactory memories mediated by nitric oxide. *Nature* 388, 670–674.

Kendrick, K. M., Lévy, F., and Keverne, E. B. (1992). Changes in the sensory processing of olfactory signals induced by birth in sheep. *Science* 256, 833–836.

Knight, T. W., and Lynch, P. R. (1980). The pheromones that stimulate ovulation in the ewe. *Anim. Reprod. Sci.* 3, 133–136.

Kratzing, J. (1971). The structure of the vomeronasal organ in the sheep. *J. Anat.* 108, 247–260.

Larriva-Sahd, J. (2008). The accessory olfactory bulb in the adult rat: a cytological study of its cell types, neuropil, neuronal modules, and interactions with the main olfactory system. *J. Comp. Neurol.* 510, 309–350.

Leinders-Zufall, T., Lane, A. P., Puche, A. C., Ma, W., Novotny, M. V., Shipley, M. T., and Zufall, F. (2000). Ultrasensitive pheromone detection

by mammalian vomeronasal neurons. *Nature* 405, 792–796.

Lévy, F., Cornilleau, F., Keller, M., Jouaneau, M., Meurisse, M., and Brus, M. (2011a). *Adult Olfactory Neurogenesis is Down-Regulated by Parturition and Interactions with Young*. 10th Meeting of the French Society for Neuroscience, May 24–27, Marseille, France.

Lévy, F., Gheusi, G., and Keller, M. (2011b). Plasticity of the parental brain: a case for neurogenesis. *J. Neuroendocrinol.* 23, 984–993.

Lévy, F., Gervais, R., Kinderman, U., and Orgeur, P. (1990). Importance of b-noradrenergic receptors in the olfactory bulb of sheep for recognition of lambs. *Behav. Neurosci.* 104, 464–469.

Lévy, F., Guevara-Guzman, R., Hinton, M. R., Kendrick, K. M., and Keverne, E. B. (1993). Effects of parturition and maternal experience on noradrenaline and acetylcholine release in the olfactory bulb of sheep. *Behav. Neurosci.* 107, 662–668.

Lévy, F., Keller, M., and Poindron, P. (2004). Olfactory regulation of maternal behavior in mammals. *Horm. Behav.* 46, 284–302.

Lévy, F., Locatelli, A., Piketty, V., Tillet, Y., and Poindron, P. (1995). Involvement of the main but not the accessory olfactory system in maternal behavior of primiparous and multiparous ewes. *Physiol. Behav.* 57, 97–104.

Lévy, F., Meurisse, M., Ferreira, G., Thibault, J., and Tillet, Y. (1999). Afferents to the rostral olfactory bulb in sheep with special emphasis on the cholinergic, noradrenergic and serotonergic connections. *J. Chem. Neuroanat.* 16, 245–263.

Lévy, F., and Poindron, P. (1987). The importance of amniotic fluids for the establishment of maternal behavior in experienced and non-experienced ewes. *Anim. Behav.* 35, 1188–1192.

Lévy, F., Poindron, P., and Le Neindre, P. (1983). Attraction and repulsion by amniotic fluids and their olfactory control in the ewe around parturition. *Physiol. Behav.* 31, 687–692.

Licht, G., and Meredith, M. (1987). Convergence of main and accessory olfactory pathways onto single neurons in the hamster amygdala. *Exp. Brain Res.* 69, 7–18.

Lledo, P. M., Alonso, M., and Grubb, M. S. (2006). Adult neurogenesis and functional plasticity in neuronal circuits. *Nat. Rev. Neurosci.* 7, 179–193.

Lledo, P. M., and Saghatelyan, A. (2005). Integrating new neurons into the adult olfactory bulb: joining the network, life-death decisions, and the effects of sensory experience. *Trends Neurosci.* 28, 248–254.

Lois, C., and Alvarez-Buylla, A. (1994). Long-distance neuronal migration in the adult mammalian brain. *Science* 264, 1145–1148.

Luo, M., Fee, M. S., and Katz, L. C. (2003). Encoding pheromonal signals in the accessory olfactory bulb of behaving mice. *Science* 299, 196–201.

Luzzati, F., Peretto, P., Aimar, P., Ponti, G., Fasolo, A., and Bonfanti, L. (2003). Glia-independent chains of neuroblasts through the subcortical parenchyma of the adult rabbit brain. *Proc. Natl. Acad. Sci. U.S.A.* 100, 13036–13041.

Melese-d'Hospital, P. Y., and Hart, B. L. (1985). Vomeronasal organ cannulation in male goats: evidence for transport of fluid from oral cavity to vomeronasal organ during flehmen. *Physiol. Behav.* 35, 941–944.

Meredith, M., Marques, D. M., O'Connell, R. O., and Stern, F. L. (1980). Vomeronasal pump: significance for male hamster sexual behavior. *Science* 207, 1224–1226.

Mesiami, E., and Bhatnagar, K. P. (1998). Structure and diversity in mammalian accessory olfactory bulb. *Microsc. Res. Tech.* 43, 476–499.

Meurisse, M., Chaillou, E., and Lévy, F. (2009). Afferent and efferent connections of the cortical and medial nuclei of the amygdala in sheep. *J. Chem. Neuroanat.* 37, 87–97.

Morgan, P. D., Boundy, C. A. P., Arnold, G. W., and Lindsay, D. R. (1975). The roles played by the senses of the ewe in the location and recognition of lambs. *Appl. Anim. Ethol.* 1, 139–150.

Murata, K., Wakabayashi, Y., Kitago, M., Ohara, H., Watanabe, H., Tamogami, S., Warita, Y., Yamagishi, K., Ichikawa, M., Takeuchi, Y., Okamura, H., and Mori, Y. (2009). Modulation of gonadotrophin-releasing hormone pulse generator activity by the pheromone in small ruminants. *J. Neuroendocrinol.* 4, 346–350.

Murata, K., Wakabayashi, Y., Sakamoto, K., Tanaka, T., Takeuchi, Y., Mori, Y., and Okamura, H. (2011). Effects of brief exposure of male pheromone on multiple-unit activity at close proximity to kisspeptin neurons in the goat arcuate nucleus. *J. Reprod. Dev.* 57, 197–202.

Okamura, H., and Mori, Y. (2005). Characterization of the primer pheromone molecules responsible for the "male effect" in ruminant species. *Chem. Senses* 30(Suppl. 1) i140–i141.

Okamura, H., Murata, K., Sakamoto, K., Wakabayashi, Y., Ohkura, S., Takeuchi, Y., and Mori, Y. (2010). Male effect pheromone tickles the gonadotrophin-releasing hormone pulse generator. *J. Neuroendocrinol.* 22, 825–832.

Otal, J., Lévy, F., Cornilleau, F., Moussu, M., Keller, M., and Poindron, P. (2009). Preventing physical contact between parturient ewes and their neonate differentially impairs the development of maternal responsiveness and selectivity depending on maternal experience. *Appl. Anim. Behav. Sci.* 120, 140–149.

Petrulis, A. (2009). Neural mechanisms of individual and sexual recognition in Syrian hamsters (*Mesocricetus auratus*). *Behav. Brain Res.* 200, 260–267.

Pissonnier, D., Thiery, J. C., Fabre-Nys, P., Poindron, P., and Keverne, E. B. (1985). The importance of olfactory bulb noradrenalin for maternal recognition in sheep. *Physiol. Behav.* 35, 361–363.

Poindron, P. (1976). Mother–young relationships in intact or anosmic ewes at the time of suckling. *Biol. Behav.* 2, 161–177.

Poindron, P., and Le Neindre, P. (1980). "Endocrine and sensory regulation of maternal behavior in the ewe," in *Advances in the Study of Behavior, Vol. 11,* eds J. S. Rosenblatt, R. A. Hinde, and C. Beer (New York, NY: Academic Press), 75–119.

Poindron, P., Lévy, F., and Keller, M. (2007). Maternal responsiveness and maternal selectivity in domestic sheep and goats: the two facets of maternal attachment. *Dev. Psychobiol.* 49, 54–70.

Poindron, P., Nowak, R., Lévy, F., Porter, R. H., and Schaal, B. (1993). Development of exclusive mother-young bonding in sheep and goats. *Oxf. Rev. Reprod. Biol.* 15, 311–364.

Poindron, P., Serafin, N., Terrazas, A., Hernandez, H., Meurisse, M., Houot, B., Larriva, J., and Lévy, F. (2003). Comparison of the effects of two methods of main olfactory system impairment on olfactory discrimination and selective nursing of lambs by ewes. 35th Annual General Meeting of the European Brain and Beahviour Society. *Acta Neurobiol. Exp.* 63, 48. (supplement).

Romeyer, A., Poindron, P., and Orgeur, P. (1994). Olfaction mediates the establishment of selective bonding in goats. *Physiol. Behav.* 56, 693–700.

Romeyer, A., Porter, R. H., Lévy, F., Nowak, R., Orgeur, P., and Poindron, P. (1993). Maternal labelling is not necessary for the establishment of discrimination between kids by recently parturient goats. *Anim. Behav.* 46, 705–712.

Salazar, I., Lombardero, M., Alemañ, N., and Sánchez Quinteiro, P. (2003). Development of the vomeronasal receptor epithelium and the accessory olfactory bulb in sheep. *Microsc. Res. Tech.* 61, 438–447.

Salazar, I., Lombardero, M., Sánchez-Quinteiro, P., Roel, P., and Cifuentes, J. M. (1998). Origin and regional distribution of the arterial vessels of the vomeronasal organ in the sheep. A methodological investigation with scanning electron microscopy and cutting-grinding technique. *Ann. Anat.* 180, 181–187.

Salazar, I., Quinteiro, P. S., Alemañ, N., Cifuentes, J. M., and Troconiz, P. F. (2007). Diversity of the vomeronasal system in mammals: the singularities of the sheep model. *Microsc. Res. Tech.* 70, 752–762.

Scalia, F., and Winans, S. S. (1975). The differential projections of the olfactory bulb and accessory olfactory bulb in mammals. *J. Comp. Neurol.* 161, 31–55.

Takigami, S., Mori, Y., and Ichikawa, M. (2000). Projection pattern of vomeronasal neurons to the accessory olfactory bulb in goats. *Chem. Senses* 25, 387–393.

Trinh, K., and Storm, D. R. (2003). Vomeronasal organdetects odorants inabsence of signaling through main olfactory epithelium. *Nat. Neurosci.* 6, 519–525.

Vedin, V., Eriksson, B., and Berghard, A. (2010). Organization of the chemosensory neuroepithelium of the vomeronasal organ of the Scandinavian moose Alces alces. *Brain Res.* 1306, 53–61.

Vince, M. A., Lynch, J. J., Mottershead, B., Green, G., and Elwin, R. (1985). Sensory factors involved in immediately postnatal ewe/lamb bonding. *Behaviour* 94, 60–84.

Wakabayashi, Y., Iwata, E., Kikusui, T., Takeuchi, Y., and Mori, Y. (2000). Regional differences of pheromone production in the sebaceous glands of castrated goats treated with testosterone. *J. Vet. Med. Sci.* 62, 1067–1072.

Wakabayashi, Y., Mori, Y., Ichikawa, M., Yazaki, K., and Hagino-Yamagishi, K. (2002). A putative pheromone receptor gene is expressed in two distinct olfactory organs in goats. *Chem Senses* 27, 207–213.

Wakabayashi, Y., Ohkura, S., Okamura, H., Mori, Y., and Ichikawa, M.

(2007). Expression of a vomeronasal receptor gene (V1r) and G protein alpha subunits in goat, Capra hircus, olfactory receptor neurons. *J. Comp. Neurol.* 503, 371–380.

Xu, F., Schaefer, M., Kida, I., Schafer, J., Liu, N., Rothman, D. L., Hyder, F., Restrepo, D., and Shepherd, G. M. (2005). Simultaneous activation of mouse main and accessory olfactory bulbs by odors or pheromones. *J. Comp. Neurol.* 489, 491–500.

Conflict of Interest Statement: The authors declare that the research was conducted in the absence of any commercial or financial relationships that could be construed as a potential conflict of interest.

Received: 07 June 2012; paper pending published: 26 June 2012; accepted: 30 August 2012; published online: 19 September 2012.

*Citation: Keller M and Lévy F (2012) The main but not the accessory olfactory system is involved in the processing of socially relevant chemosignals in ungulates. Front. Neuroanat. **6**:39. doi: 10.3389/fnana.2012.00039*